Fifth International Oil Sands Tailings Conference

Lake Louise, Alberta, Canada: December 4-7, 2016

U of A Geotechnical Centre

IOSTC

FIFTH INTERNATIONAL

OIL SANDS

TAILINGS CONFERENCE

Lake Louise, Alberta
Canada

December 2016

Proceedings of the Fifth International Oil Sands Tailings Conference

4-7 December 2016, Lake Louise, Alberta, Canada

Fifth International Oil Sands Tailings Conference

Edited by

David C. Sego, G. Ward Wilson & Nicholas A. Beier

University of Alberta Geotechnical Centre and
Oil Sands Tailings Research Facility

University of Alberta Geotechnical Centre Edmonton, Alberta, Canada

Published by: University of Alberta, Dept. of Civil & Environmental Engineering

ISBN 978-1-55195-326-7
Printed in Canada

FORWARD

It is with great pleasure that we present the **Fifth International Oil Sands Tailings Conference 2016 (IOSTC'16)**. There have been several sweeping changes in the management of oil sands tailings since the First International Oil Sands Tailings Conference held in 2008 (**IOSTC'08**), which offered an industrial and regulatory perspective on the needs for tailings research and management. In response to Directive 74 issued by the Energy Resources Conservation Board (ERCB, now Alberta Energy Regulator (AER)) in 2009, **IOSTC'10** focused on presenting technologies and approaches to meet the provincial regulator's tailings criteria and requirements for the oil sands industry. Two years later, **IOSTC'12** provided a venue to present the Oil Sands Tailings Technology Deployment Road Map prepared by the Consortium of Tailings Management Consultants (CMTC) on behalf of Alberta Innovates – Environment and Energy Solutions (AI-EES) and the Oil Sands Tailings Consortium (OSTC, now Canada's Oil Sands Innovation Alliance (COSIA)). At **IOSTC'14**, Alan Fair provided observation on the development of tailings management from his 30-year career in the oil sands industry and the research program from the **NSERC/COSIA Senior Industrial Research Chair in Oil Sands Tailings Geotechnique** held by Dr. G. Ward Wilson at the University of Alberta was presented**.**

The aim of **IOSTC'16** is to provide a further exchange of information between the people responsible for managing the oil sands tailings: researchers and providers of tailings management services who have experience with this industry. This year's conference will have special keynote addresses from AER and the oil sands companies. The AER will outline the current approach to fluid tailings management regulation and associated tailings containment facilities. The oil sands companies will outline their path forward to meet the requirements of the Oil Sands Tailings Management Plan recently put forward by the Government of Alberta. **IOSTC'16** has received strong support by the authors who have submitted a significant number of manuscripts, the exhibitors who continue to support the conference in these trying economic times and most importantly by our sponsors who recognize the important contribution of this conference to meeting the challenges presented by oil sands tailings to the environment and the viability of this most important Alberta industry.

We want to personally thank members of the OSTRF for their encouragement and support. The conference would not have been possible without the dedication of Elena Zabolotnii, Vivian Giang and especially Sally Petaske who provided so much assistance and leadership.

The technical challenges associated with mature fine tailings (MFT) require novel and innovative approaches to ensure the sustainable development and environmental stewardship of Alberta's vast oil sands. It was with this in mind that the session themes and manuscripts were selected for presentation and inclusion in the proceedings. We want to thank our professional colleagues who willingly contributed their technical knowledge, experiences and especially their time to write the manuscripts that make the proceedings of this conference. May you find further insights to enhance your understanding of the current state-of-practice in oil sands tailings management through **IOSTC'16**.

David C. Sego, Nicholas A. Beier and G. Ward Wilson
Co-Chairs, IOSTC 2016 Organizing Committee

Thank you to the following sponsors for their support in making the Fifth International Oil Sands Tailings Conference a huge success:

PLATINUM SPONSORS:

GOLD SPONSORS:

Alfa Laval Inc.

SILVER SPONSORS:

TABLE OF CONTENTS

SESSION B-1: RECLAMATION

SESSION B-2: CHEMICAL INTERACTIONS

SESSION C-1: TAILINGS PROPERTIES AND MEASUREMENTS

SESSION C-2: CHEMICAL INTERACTIONS (2)

SESSION D: TAILINGS DEWATERING

SESSION E: TAILINGS PROPERTIES AND MEASUREMENTS (2)

SESSION F: TAILINGS MANAGEMENT (2)

SESSION G: TAILINGS BEHAVIOUR

Keynote

Presentation

TAILINGS TREATMENT APPROACHES AT KEARL – AN UPDATE

Paul Cavanagh
Imperial, Calgary, Canada

The Kearl tailings plans are currently under review with the Alberta Energy Regulator (AER) and are not approved. This submission is for information only, and without the opportunity for follow-up questions, to maintain the integrity of the regulatory approval process.

ABSTRACT

The objective of the Tailings Management Framework (TMF) is to minimize fluid tailings accumulation and have fluid tailings ready to reclaim in an acceptable timeframe. The TMF considers this objective will be accomplished through the use of progressive treatment of tailings and reclamation while balancing environmental, social and economic needs.

The Kearl project started production in 2013 and has a projected end of mine life of about 2060. At Kearl, today, it is considered that alignment with the TMF objectives and achievement of expectations will be achieved by employing several complimentary strategies and technologies:

- Design with the end in mind to create a sustainable closure landscape;
- Treat tailings prior to accumulating large volumes of fluid tailings, including flotation tailings (FLT) and fluid fine tailings (FFT);
- Deposit treated tailings in their final landscape position for progressive reclamation; and
- Construct a single external tailings area.

The proposed treatment processes at Kearl were designed with flexibility as a primary component to accommodate changes in material properties, technologies, and closure objectives. The base system comprises thickeners with secondary in-line flocculent injection to produce thickened tailings that are hydraulically placed in thick multi-layer deposits, which can then be capped and reclaimed as terrestrial, wetlands or aquatic surfaces.

This paper describes the chosen tailings treatment technologies at Kearl and assesses the strengths, opportunities and challenges in managing the interconnected tailings, business and regulatory processes. The implications of balancing business, environmental, and social needs, while pursuing the principal objectives of fluid tailings reduction and timely reclamation are discussed. Some areas for further research are suggested.

INTRODUCTION

Imperial Oil Resources Ventures Limited (IOL) and ExxonMobil (EM) are joint owners of the Kearl Oil Sands Project (KOSP) located about 40 km northeast of Fort McKay, Alberta. IOL is the operator of the asset, which includes an open pit mine, bitumen extraction facilities, and storage areas for overburden, reclamation and tailings materials.

This paper describes the chosen tailings treatment technologies at Kearl and assesses the strengths, opportunities and challenges in managing the interconnected tailings, business and regulatory processes. The implications of balancing business, environmental, and social needs, while pursuing the principal objectives of fluid tailings reduction and timely reclamation are discussed. Some areas for further research are suggested.

REGULATORY CONTEXT

In 2015 the Government of Alberta (GoA) released the Tailings Management Framework for the Mineable Athabasca Oil Sands (TMF)[1], which provides policy direction for the responsible development of the oil sands. The TMF seeks to balance environmental protection and the associated risk of increasing fluid tailings volumes and provides two principal objectives: to reduce the amount of fluid tailings on the landscape more quickly; and to have tailings ready to reclaim in an acceptable timeframe.

Following the release of the TMF, in part to provide consistent direction to oil sands mine operators, the Alberta Energy Regulator (AER) suspended regulatory Directive 074 (D074)[2] in early 2015 and released a new regulatory Directive 085 (D085)[3] in mid-2016. The D074 objectives and criteria were focused on accelerated fines capture and achieving early reclaimable landscapes using prescriptive implementation strategies and measures of success based on volumes of fines and deposit strength. The TMF and D085 provide policy and implementation direction to limit accumulation of fluid tailings on the landscape and have deposits ready to reclaim in an acceptable time. There is flexibility for site-specific tailings treatment and performance measurement providing the two principal regulatory objectives are on a trajectory to being achieved.

TAILINGS PLAN BACKGROUND

A simplified process flow diagram and conceptual deposit configuration for the KTMP prior to startup is shown on Figure 1 and Figure 2, respectively. The objectives of the Kearl Tailings Management Plan (KTMP) at that time were:

- Early treatment to minimize accumulation of MFT
- Significantly reduced footprint for External Tailings Areas (ETAs)
- Early trafficable landscape and progressive reclamation
- Maximize water recycle and reduce fresh water import
- Allow development of reliable and sustainable operation with environmentally sound design and processes.

Prior to Kearl startup, the treatment methods, components and technologies in the KTMP included:

- Thickeners to treat K1 and K2 FT and recycled MFT from the West ETA
- Interlayered sand and thickened tailings in the East ETA from 2016 to 2023 (See Figure 2)
- Thickened TSRU tailings placed in pit, in thin lifts, starting in about 2018
- In pit deposition of CST and thickened FT would commence in about 2023
- End pit lakes will be used at the end of mine life

The KOSP started producing bitumen in 2013 with a projected end of mine life of about 2060. The KOSP started its initial ore processing train (K1) followed by a second train (K2) in mid-2015. Kearl tailings are being deposited northeast of the plant site in the external tailings area (ETA), which is divided into east and west deposition areas, as shown on Figure 3. During 2013 and 2014 we learned that the FLT stream from K1 had significantly different properties from those assumed in the thickener design basis and that the interlayered thin lift tailings deposit, while offering the potential benefit of significantly reduced time required for consolidation, would not be as constructible as originally envisioned. We also learned that we needed to develop a more flexible and comprehensive adaptive management strategy to achieve the desired outcomes.

In 2014 and 2015, the KTMP and thickening process was modified to include additional facilities such as a mix box downstream of the thickeners and inline secondary re-flocculation. The geometry of the East ETA thickened tailings deposit was modified to a multi-lift deep deposit in a thickened tailings containment area (TTCA) and a conceptual closure landform design (Figure 4) that is complementary to, and consistent with, the expected behavior of the multi-layer, deep TT deposit was developed. The plan and cross-section of the TTCA are shown on Figures 5 and 6, respectively. Tailings will be deposited in pit starting as early as 2018 (for some streams).

The key objectives for managing tailings at Kearl in the updated (2016)[4] are to:

- Minimize long-term environmental effects;
- Minimize the accumulation of fluid tailings (FT);
- Maximize water recovery from tailings for reuse in the plant; and
- Minimize the land footprint required for tailings management.

Achievement of tailings treatment, regulatory and business objectives is expected through the use of several complimentary strategies:

- Design with the end in mind to create a sustainable closure landscape;
- Treat tailings prior to accumulating large volumes of fluid tailings, including flotation tailings (FLT) and fluid fine tailings (FFT);
- Deposit treated tailings in their final landscape position for progressive reclamation; and
- Construct a single external tailings area.

The updated KTMP now:

- Integrates mine, reclamation, and closure planning–designing with the end in mind;

- Treats tailings prior to accumulating large volumes of fluid tailings;
- Minimizes land disturbance by using a single external tailings area;
- Aligns with the objective and outcomes of the TMF;
- Addresses the application requirements for Directive 085;
- Incorporates knowledge and experience gained since the start-up of production; and
- Benefits from collaborative industry forums such as COSIA.

Currently, coarse sand tailings (CST) from K1, all FLT, and the tailings solvent recovery unit (TSRU) tailings are being deposited in the West ETA, which contains a process water pond for re-use in the plant. The East ETA containment dykes are constructed with CST from K2 with process water runoff being collected and transferred to the West ETA. Fluid fine tailings (FFT) have started to accumulate beneath the process water recycle pond in the West ETA, with a current volume of about 5 million cubic meters. Commissioning and startup of the thickening process is underway with the first thickened tailings deposited from the south slope of the TTCA panels, as shown of Figure 7, expected in the East ETA in late 2016 or early 2017. The D085 compliant KTMP was submitted for regulatory approval on November 1, 2016.

PATH FORWARD AND KEY GUIDING PRINCIPLES

In 2012, the KTMP and proposed treatment processes were conceived within the business and regulatory setting of the day using assumed input parameters. Since that time, the focus and rate of development of the KTMP has changed for several reasons:

- Economic conditions associated with changing commodity prices
- Changing social and environmental expectations and regulatory requirements
- Uncertainties with the thickening process and deposit performance

In the face of these stark realities, it was appropriate to pause, reflect and embrace some key guiding principles that could ultimately lead to successful outcomes, such as:

- **Aligned objectives are not the same as results.** It is considered that the objectives of the KTMP, the TMF and D085 are aligned. However, aligned objectives, while an important first step, is not the same as achieving results.
- **Need outcome certainty and process flexibility.** There is heightened need for confidence in the performance of the tailings deposits and for flexibility in the process toward achieving required outcomes. The regulatory policies and requirements in the TMF and D085 seek to promote consistent industry outcomes and allow for flexibility in the management of technical and operational uncertainties.
- **Increased focus on defining desired outcomes.** Since 2012, there has been increased focus on expected outcomes and requirements of the end landscape, which must be consistent with deposit performance and the management of technical uncertainties.
- **Adapting is key.** Success of the KTMP relies greatly on the use of adaptation and continuous improvement as illustrated in Figure 8. For example, the updated KTMP and facilities were adapted, designed and built using IOL research and the research, innovation and experience developed by, or in collaboration with, others from available technology or industry sources (e.g.; Canada's Oil Sands Innovation Alliance (COSIA)).

In order to keep pace with changing expectations and manage uncertainty in a low commodity price environment, it is unlikely, due to challenges such as scaling up from a laboratory data or pilot facilities to full commercial scale and other challenges, that we would be able to adequately quantify the commercial characteristics and parameters without having at least some production run time and deposit observations at full scale. Clearer end targets and increased process flexibility should result is less overall cost and risk than relying on small scale data and deterministic designs and solutions.

TECHNICAL CHALLENGES

Today, our approach is more flexible and less deterministic than before but, as they say, there's good news and bad news. We can change or adjust our plans and facilities, the main questions being: why change and change to what? Through the development of the KTMP we have identified several issues with technical, operability and the desired outcomes that need to be overcome, such as:

- Feed variability and process control (instrumentation)
- Floc degradation from pipe or deposit shear
- Mixing of materials in the pipes and deposit
- Deposit flow, segregation, freezing, and consolidation
- Deposit and closure landscape compatibility
- Landscape requirements, and
- Dam closure and de-licensing.

There are also some unique opportunities and conditions, as would be expected at each oil sands mine, which the KTMP seeks to leverage to achieve business and regulatory objectives. For example, the issues of feed variability and deposit segregation are, for Kearl, in a context of low fines content ore where we currently have lower than expected fines and solids (but relatively high variability) flowing into the thickener and low accumulated FFT in the West ETA. These conditions have some positive attributes but might also be temporary, make thickener and in-line re-flocculation operation difficult, and would almost certainly result in higher sand accumulation and fines segregation in the East ETA deposit.

Success, therefore, depends on the ability to monitor and adjust as conditions change and the facilities operate. We are certain that feed variability exists and that segregation in the deposit will occur but accurate characterization of feed properties and eventual distribution of the fines in the deposit are notoriously difficult to quantify, such that using deterministic design and operation strategies are not practical to predict impacts on landforms and containment. However, we can increase the likelihood of meeting performance expectations by adopting the following adaptive approaches:

- Define the range of landforms and self-sustaining eco-systems that would fit into the public mandate for establishing an "equivalent land capability",
- Use the treatment process to improve key characteristics and manage outcomes, and
- Manage risks by incorporating appropriate flexibility and safeguards into the design, construction, operation, and closure of structures.

If done appropriately this should result in treatment processes and deposition plans that are less sensitive to the accurate understanding and management of feed variability and deposit segregation in order to achieve landform performance and dam de-licensing requirements.

To these ends, the potential scope or impact of the identified technical challenges and uncertainties of thickening, deposit performance, and construction and closure of the ETA were assessed. For example, the East ETA dyke designs can accommodate either "wet" or "dry" East ETA pond configurations and deposition strategies and the treated deposits will be placed in a thickened tailings containment area (TTCA) within the East ETA surrounded by "extra-large" sand containment dykes.

In other examples, assessment of the potential effects of snowfall on the accumulation of frozen layers in the deposit during winter and different capping approaches were undertaken to understand the risks and to develop a level of confidence that we could construct and cap the deposit. These assessments were not carried out so much to develop definitive designs or operating strategies, but rather to assess input parameters, factors or requirements for successful development of the deposit and compatibility with subsequent construction and reclamation approaches.

A similar approach was extended to assess the potential for de-commissioning and de-licensing of the ETA. We assessed longer-term risks associated with the ETA landform in comparison with potential failure modes using risk-based approaches similar to that suggested in the De-licensing of Oil Sands Tailings Dams Technical Guidance Document[5]. The results indicate that de-licensing could be achieved by reducing risk to reasonably practical levels notwithstanding that the work was preliminary and only based on what we know today, and would require additional assessment and a regulatory framework that incorporates risk-informed or risk-based approaches in order to de-license the ETA.

POTENTIAL MITIGATIONS

It is often difficult to predict the operability and reliability of large, complex processes and their expected performance using data from small-scale investigations or information from different operational or investigational context. This is particularly apparent with a fit-for-purpose process designed to achieve site-specific targets.

On the basis of work completed to date, and without necessarily a comprehensive understanding of individual technical issues and challenges or how they interact with each other at commercial scale, it was concluded that it should be possible to construct, cap, close and de-license the thickened tailings deposit and enclosing structures providing that appropriate monitoring and mitigation strategies were included in the commercial scheme, as appropriate or required.

Various mitigation strategies and options to augment the base scheme could be implemented in the different stages of development depending on the specific issues that need to be addressed and their potential impact to the closure. The following is a summary of several mitigation strategies that have been investigated and could be considered to address potential issues and challenges at Kearl:

- Amend feed properties:
    - Hydrocyclones
    - Slipstream CST (KIMR)
- Adjust chemical and/or dose
- Enhance secondary injection and mixing
    - Utilize dynamic mixers
    - Change mixing locations
- Deposit amendments
    - Change number and location of discharge points
    - Subaqueous deposition
    - Drainage layers in the deposit
    - Wick drains or surface drying (for capping)
- Alternative capping and landforms
    - Proto-bog (allows settlement)
    - Domed surface (accounts for settlement)
- Additional TTCA
    - Construct new external TTCA
    - Convert entire ETA to wet facility

Some advantages of the Kearl development include very small amount of legacy MFT and the available time to assess and understand the deposit, landform and de-licensing requirements before selecting construction methods, cover designs and closure strategies. However, the new facility does not have a lot of run-time on which to base tailings treatment and mitigation decisions and changes and/or mitigations to the plans should be expected.

AREAS OF RESEARCH

Based on the assembled plans and potential mitigation strategies, the following areas of research that would be considered aligned with, and beneficial for, the needs of Kearl going forward are:

- Technical or process uncertainties:
    - Pilot to commercial scale-up (develop empirical models)
    - Pipe and deposit floc shear/degradation
    - Pipe and deposit mixing
    - Deposit segregation and flow
    - Enhanced fines beach capture
    - Sub-aqueous deposition
    - Deposit Freeze/Thaw
    - Centrifuge testing of tailings
    - Instrumentation
- End target uncertainties:
    - Risk management in regulatory framework
    - Deposit/landscape characteristics and compatibility
    - Mine water release criteria
    - End pit lakes

CONCLUSIONS

There is opportunity for measured, strategic responses to the changing performance expectations while maintaining necessary progress toward closure and de-licensing of facilities. Each mine in the oil sands is unique and will require tailored processes and targets for tailings treatment that consider site-specific conditions, performance requirements and available timelines. Flexibility in the design, monitoring and mitigation strategies is critical to success.

At Kearl, we have chosen to assemble existing complimentary technologies to take advantage of specific site conditions in an attempt to:

- Intercept and treat constituent materials before they contribute to fluid tailings growth;
- Recycle and treat fluid tailings prior to developing mature fine tailings; and
- Progressively reclaim treated deposits.

There are still unanswered technical and process related questions that will need to be addressed as we progress toward closure and de-licensing of tailings facilities.

However, we consider that success can be achieved at Kearl and within the broader industry by embracing the principles that outcome certainty can be achieved with aligned objectives, well-defined outcomes, process flexibility and adaptive approaches. The new regulatory direction, technology sharing through COSIA and IOSTC, and the commitment to manage tailings responsibly are all important components to achieving those desired outcomes.

Key areas that require continued and simultaneous active research and development include refined definitions of desired outcomes, developing and commercializing appropriate methods and technologies to achieve those outcomes, and implementation through flexible and adaptive systems.

REFERENCES

1. Lower Athabasca Region – Tailings Management Framework for the Mineable Athabasca Oil Sands. Government of Alberta, March 13, 2015.

2. Directive 074: Tailings Performance Criteria and Requirements for Oil Sands Mining Schemes. Alberta Energy Regulator, February 3, 2009.

3. Directive 085: Fluid Tailings Management for Oil Sands Mining Projects. Alberta Energy Regulator, July 14, 2016.

4. Kearl Oil Sands Tailings Management Plan. Imperial Oil Resources Ventures Limited, November 1, 2016.

5. Oil Sands Tailings Dam Committee. 2014. De-licensing of Oil Sands Tailings Dams, Technical Guidance Document. March 2014.

FIGURES

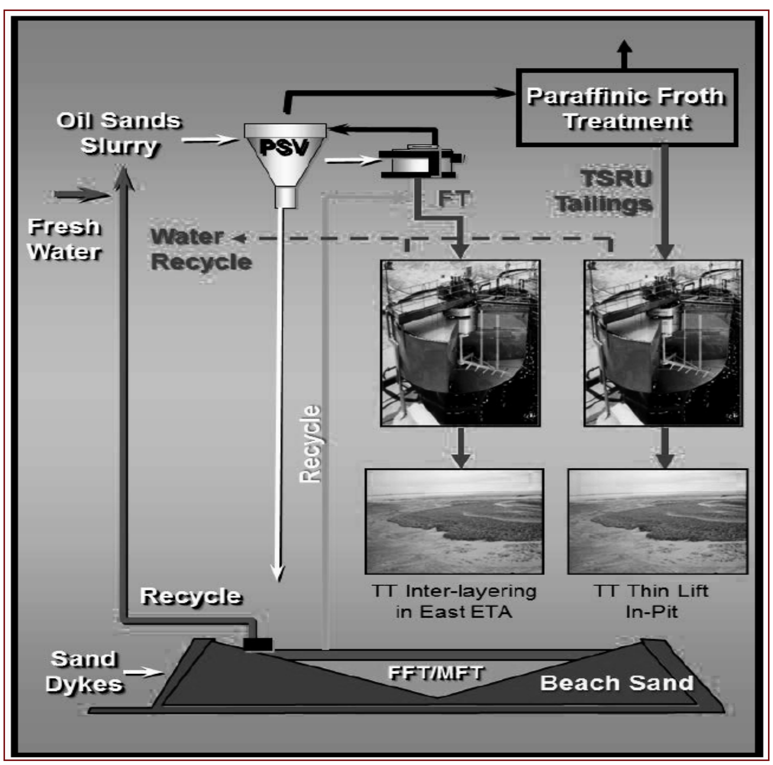

Figure 1. 2012 Kearl Tailings Deposition Process Flow Diagram

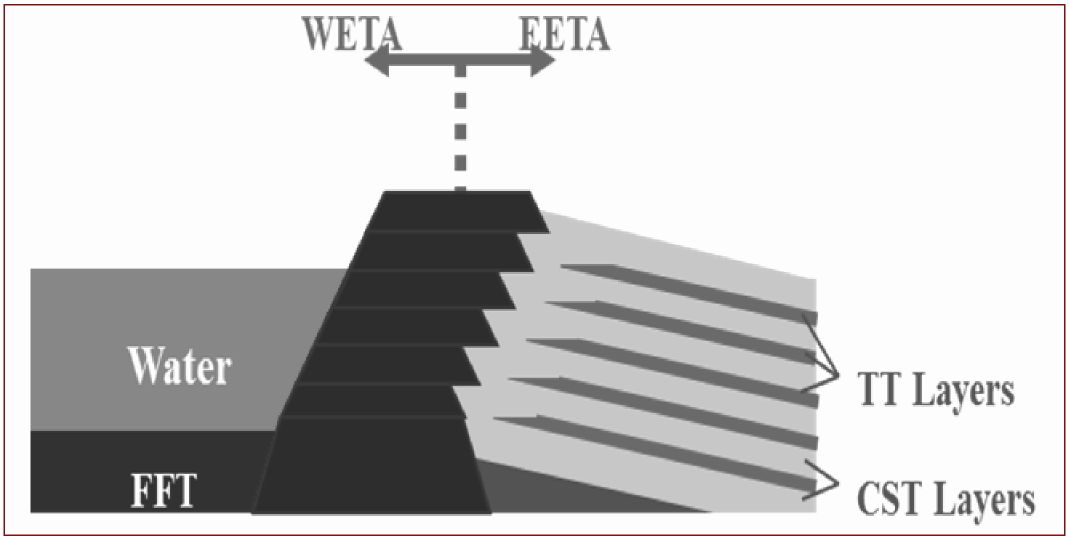

Figure 2. Kearl External Tailings Area

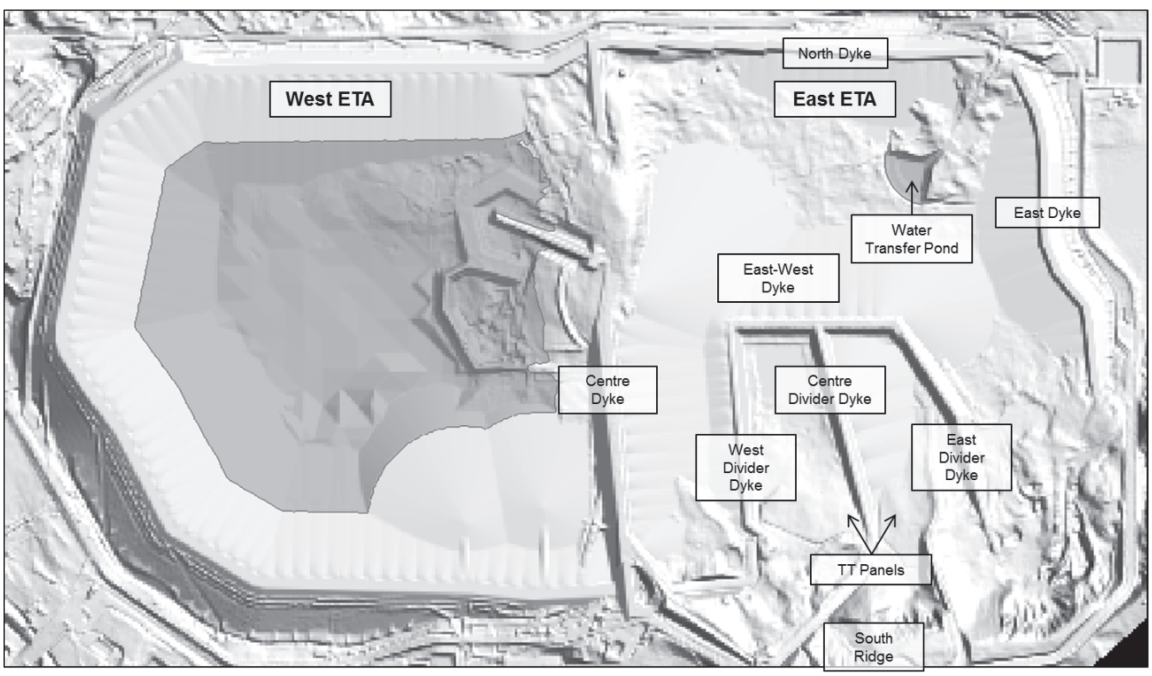

Figure 3. Kearl Interlayered Deposit East ETA

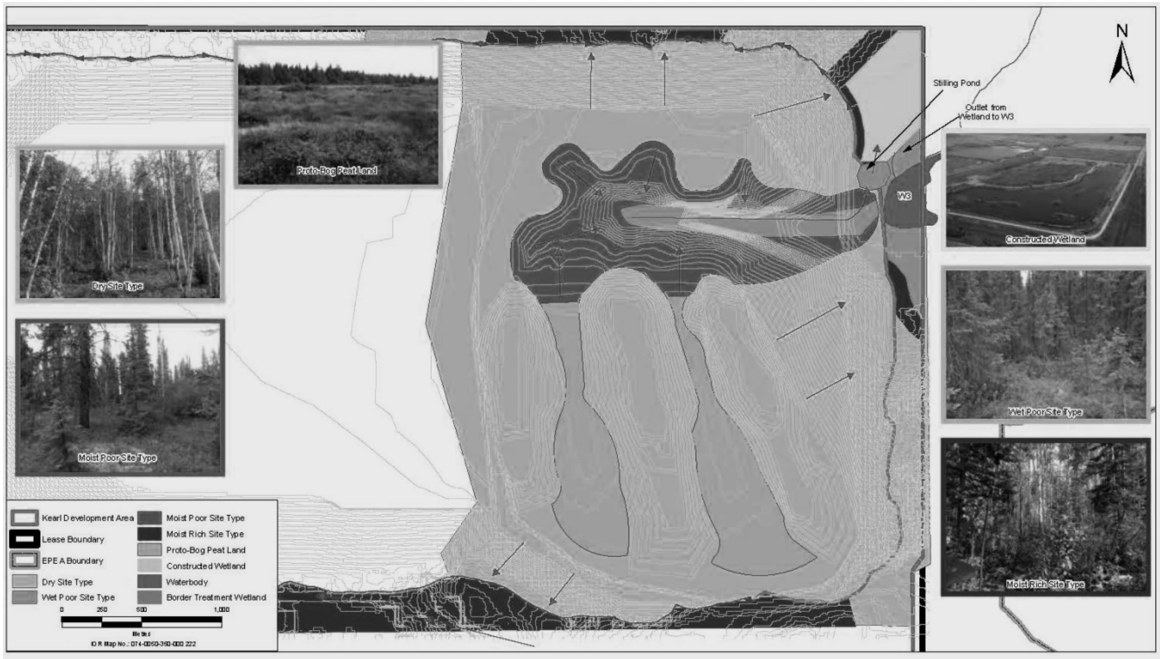

Figure 4. Conceptual Closure Landscape East ETA

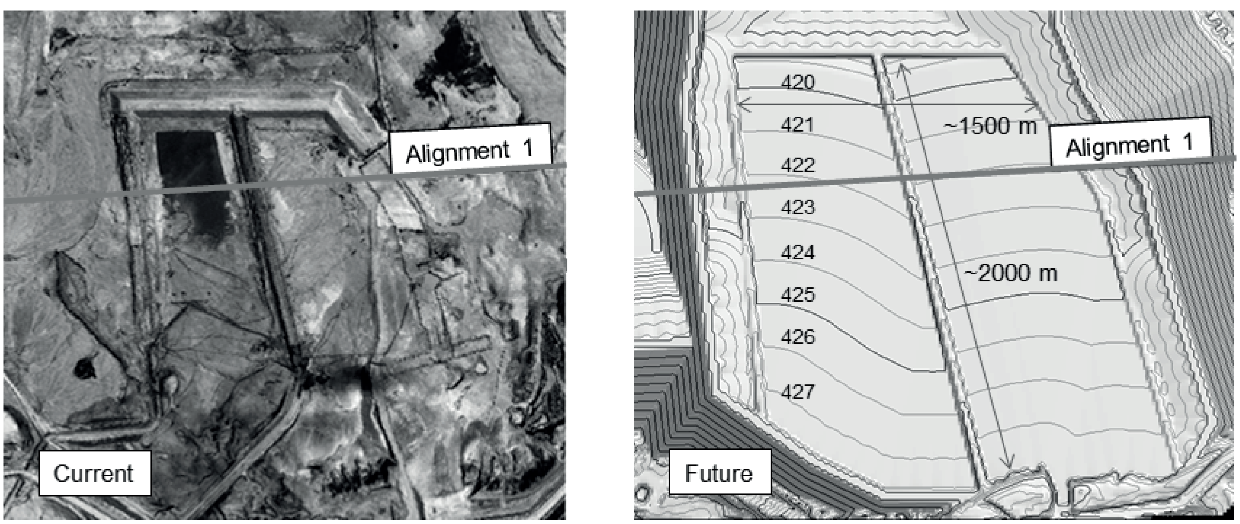

Figure 5. Plan View of East ETA Thickened Tailings Containment Area

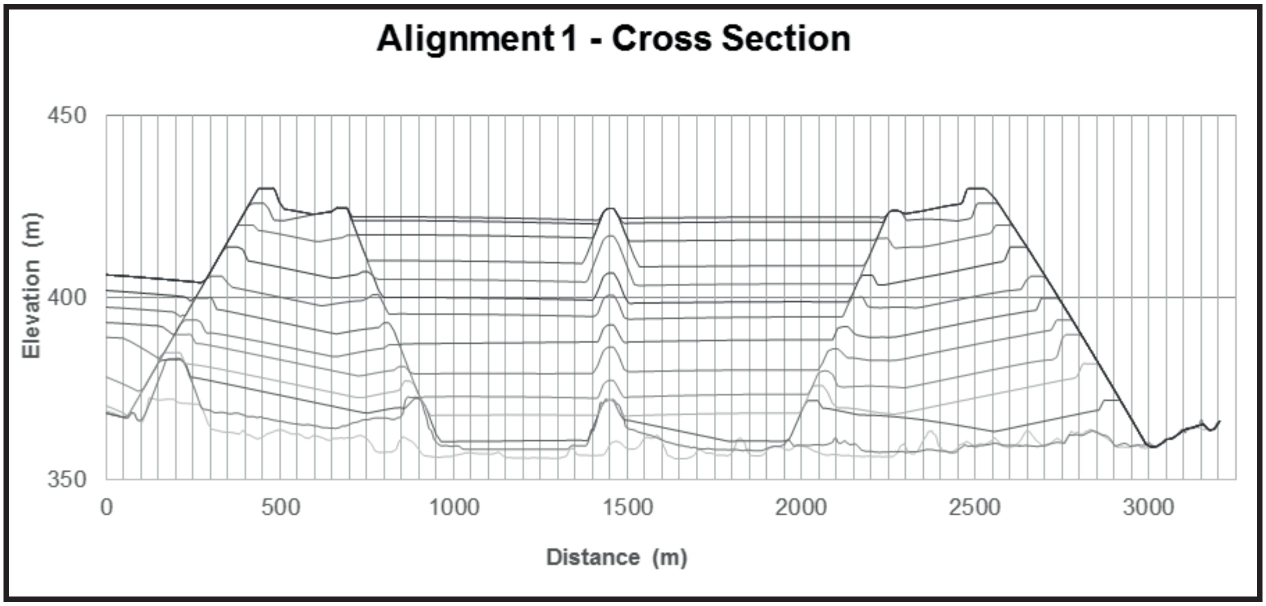

Figure 6. Cross Section of East ETA Thickened Tailings Containment Area

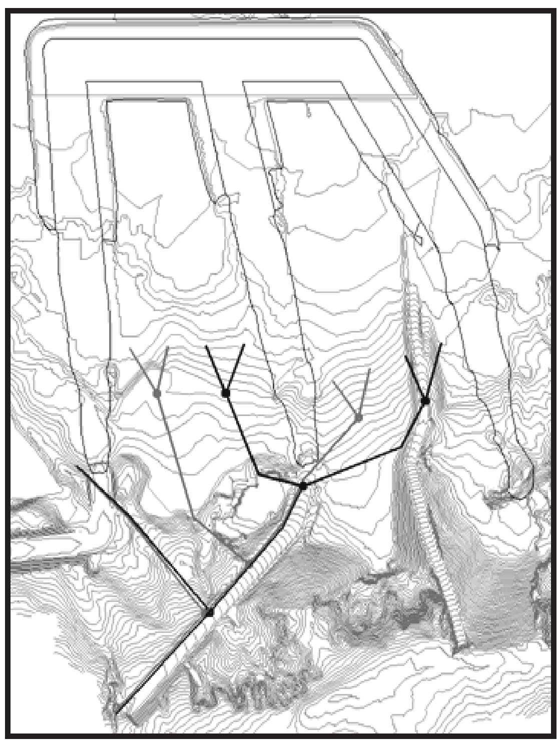

Figure 7. Conceptual Piping Layout Thickened Tailings Containment Area

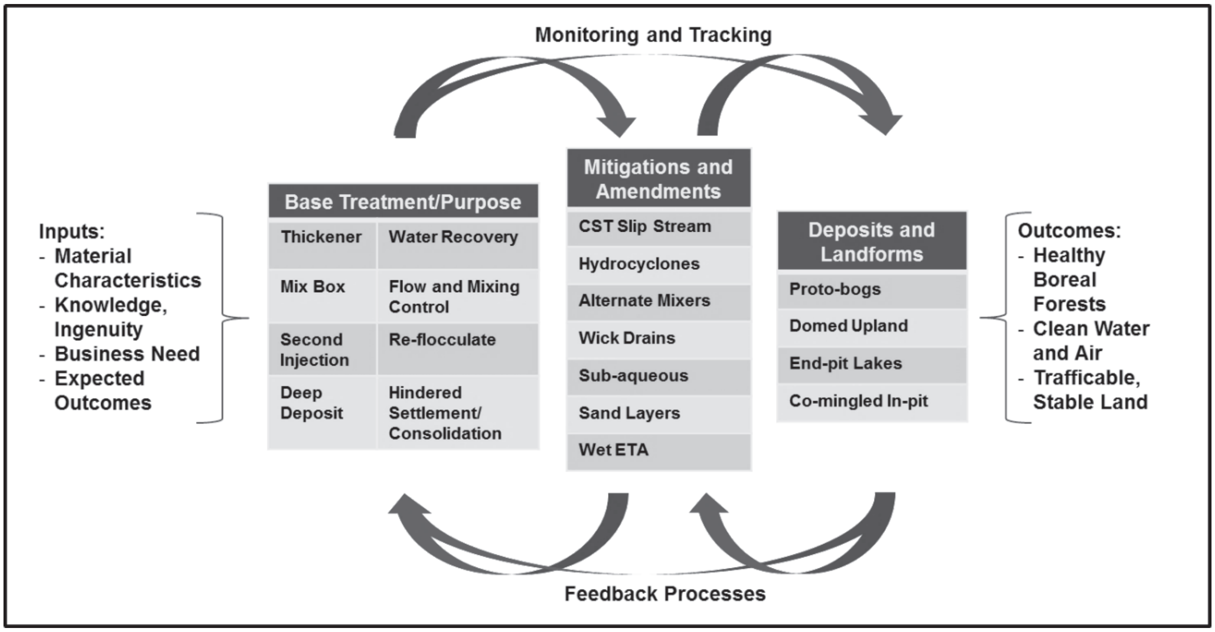

Figure 8. Tailings Management Processes

Session A-1

Tailings Modelling and Behaviour

CONSOLIDATION-DESICCATION IN OIL SANDS FINE TAILINGS AND THE UNSATCON MODEL

Paul Simms and Shunchao Qi
Carleton University, Ottawa, Canada

ABSTRACT

Models that have the ability to simulate desiccation and large strain consolidation are from time to time employed to predict post-deposition densification of subaerially deposited tailings. Most models employ a relatively simple treatment of the unsaturated zone to achieve workable coupling. This paper presents a piecewise-linear formulation for coupling large strain consolidation and unsaturated flow using a mass conservative and non-iterative solution. The model also incorporates stress history effects (hardening) on both the consolidation behaviour and on the desiccation behaviour, as well as wet-dry hysteresis, which allows for reasonable simulation of multilayer deposition scenarios. The model is tested against several previously published laboratory and field cases of combined consolidation and desiccation on both oil sands and hard rock tailings, including cases from Shell's AFD trials, and mesocale "Drybox" laboratory simulations of multilayer deposition of thickened gold tailings, and in-line flocculated mature fine tailings, some of which have been previously presented in the IOSTC series. Advantages and limitation of the model are discussed.

INTRODUCTION

Surface processes such as evaporation or freeze-thaw can contribute to dewatering and / or surface stabilization in a range of tailings deposition scenarios. In scenarios involving successive placement of lifts, such as Suncor's Tailings Reduction Operations (TRO) or Shell's Atmospheric Fine Drying (AFD) trials, it is expected that surface process will contribute substantially to dewatering. In deep deposits, surface processes may contribute to densification or strength gain in top few metres, and the crust may facilitate trafficability and therefore other reclamation or dewatering activities. Knowledge of the interplay between unsaturated flow and consolidation is also required to correctly interpret data from field trials, and correctly extrapolate strength–density relationships, as strength data from the near surface may be biased by stress history effects from desiccation. Operators are also concerned that desiccation may actually inhibit consolidation in a deep deposit. Therefore, the ability to correctly simulate the coupled desiccation-consolidation process is important to oil sands tailings management in a number of ways.

The present paper focuses on the development on a new model that simulates desiccation-consolidation in a complete way, relative to commonly used approaches. The first part of the paper summarizes model development, which is is given more completely in other sources (Qi et al 2016 a,b, and c). The second part of the paper compares the predictions of the model to field and laboratory data, discusses the advantages and limitations of this model, and how it should or could be used appropriately to assist tailings deposition planning,

THEORY

Tailings dewater due to several processes. Some type of tailings, such as in-like flocculated MFT, may undergo rapid dewatering due to the action of the polymer of immediately after deposition, through the aggregation of particles and subsequent sedimentation. Some consider this process to be independent of effective stress: Jeerivapoolvarn (2010) modeled the transition from sedimentation to consolidation of oil sands fine tailings using a void ratio based parameter to gradually apply effective stress. In the authors' model, the post-rapid dewatering phase is the initial condition, and so sedimentation is not calculated independently from consolidation.

Thixotropy and creep have been shown to strongly influence the dewatering behaviour of MFT over the timescale of years (Jeeravipoolvarn et al. (2009). It is quite likely that thixotropy will play a role in the long-term dewatering behaviour of new tailings technologies (in-line flocculation, centrifuge, thickening), however, in this paper we focus on the correct coupling between desiccation and consolidation, leaving the addition of thixotropy to later work or to others.

The initial dewatering behaviour of any tailings deposit will be dominated by large strain consolidation (Figure 1). Depending on climate, layer thickness, the consolidation properties, and whether the geometry of the impoundment will allow for runoff or retain surface water, at some point surface will be removed or evaporated, and desiccation through evaporation will start. The unsaturated zone will progress downwards into the tailings, and will influence dewatering through changes in volume change and permeability behaviour. The rate of evaporation at the surface is governed by a number of factors, including salinity and cracking (Simms et al. 2016, Rozina et al. 2015, Innocent-Bernard et al. 2014).

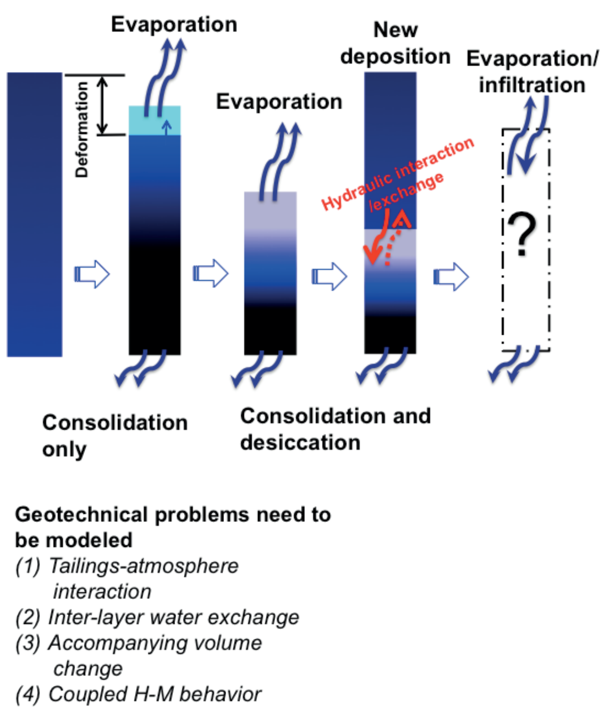

Figure 1. Conceptual model for multilayer deposition

For a single deposit, dewatering proceeds monotonically, and the the loading-unloading or wet/dry hysteresis need not be considered. However, if another layer of tailings is added, or if rainfall occurs, then the stress history of the tailings must be considered. The underlying tailings will not swell back to their initial condition: they exhibit hysteresis in both their volume change – stress state and in their water content -stress state relationships. To properly model multilayer deposition, both types of hysteresis should be considered.

MODEL FORMULATION

The formulation uses constitutive equations for void ratio and hydraulic conductivity as functions of vertical effective stress in the saturated zone, and three-dimensional constitutive surfaces (equation with two dependent variables) for void ratio, hydraulic conductivity, and additionally water content for the unsaturated zone, that depend on both total net normal stress and matric suction. The constitutive equations for the saturated zone are power functions that are typically used for large strain consolidation analysis:

$$e = C_1(\sigma')^{C_2} \tag{1}$$

$$k = H_1 e^{H_2} \tag{2}$$

where e, k, and σ' are the void ratio, hydraulic conductivity, and vertical effective stress, while C_1 and C_2 and H_1 and H_2 are parameters.

When regions of soil (or tailings) become unsaturated, the hydro-mechanical behaviour of the soil can be described using constitutive equations that depend on two dependent variables: total stress and matric suction (Vu and Fredlund 2004). Many researchers prefer to avoid the complexity of using these equations, and have attempted to extend the effective stress equations to unsaturated conditions, usually introducing some dependency on degree of saturation. This, however, is problematic, as changes in effective stress can occur through both changes in total stress and matric suction. For example, increasing the effective stress by increasing suction tends to desaturate soil or tailings, while increasing effective stress by the same amount but by increasing total stress tends to increase the degree of saturation.

A number of formulations exist for describing the constitutive surfaces for unsaturated soils, with varying degrees of complexity (for example, but not exhaustively (e.g. Vaunat et al. 2000; Wheeler et al. 2003;, Vu and Fredlund 2004.. The functions proposed by Vu and Fredlund (2004) are adopted: The functions for void ratio, water content (geotechnical) and hydraulic conductivity are:

$$e = a + b\log\left[\frac{1 + c(\sigma - u_a) + d(u_a - u_w)}{1 + f(\sigma - u_a) + g(u_a - u_w)}\right] \quad (3)$$

$$w = A + B\log\left[\frac{1 + C(\sigma - u_a) + D(u_a - u_w)}{1 + F(\sigma - u_a) + G(u_a - u_w)}\right] \quad (4)$$

$$k = \frac{H_1 e^{H_2}}{1 + m[(u_a - u_w)/(\rho_w g)]^n} \quad (5)$$

where, *w* is water content, r_w is the unit weight of water, *m* and *n* are two material parameters accounting for the effect of suction on the hydraulic conductivity, *a*, *b*, *c*, *d*, *f*, *g* and *A*, *B*, *C*, *D*, *F*, *G* are empirical material parameters for void ratio and water content constitutive relationships, respectively.

Though the number of parameters in the constitutive surfaces is high, the surface must allow a wide range of flexibility in the shape, which is essential since the void ratio and water content may be quite high at low stress and suction level and decrease dramatically with a slight increase in stress or suction. Additionally, these parameters are well-constrained by data measured in the extreme planes of the constitutive surfaces, when either suction or total stress approaches zero. In the case of zero suction, for example, *d* and *g* vanish, and the remaining terms may be found by fitting the constitutive equation to measured void ratio-effective stress data from conventional large strain consolidation tests, while in the opposite plane the remaining data can be obtained using data from a conventional soil-water characteristic curve test. Therefore, the necessary parameters may be found by relatively conventional test procedures.

The solution method is evolved from the piecewise-linear solution of large strain consolidation developed by Fox and Berles (1997). Water flow and deformation and solved using a finite difference solution to water flow, in which constant mass of solids is preserved at each node, but the mass of water may vary:

$$w_j^{(i)} M_{s,j}^{(0)} = w_j^{(i-1)} M_{s,j}^{(0)} - [(v_j^{(i-1)} - v_{j+1}^{(i-1)})\Delta t^{(i-1)}]\rho_w \quad (6)$$

where (i) denotes time step, (j) denotes a node, M_s is the mass of solids at each node, which does not change with time, and v is the darcy velocity. Under saturated conditions, e=wGs, total stress is the sum of overlying mass (sum of solid and water mass of overlying nodes) and pore-water pressure can be computed using Equation 1. If the pore-water pressure calculated from Equation 1 is negative, then the element is now consider unsaturated, and the water content, suction, and void are sequentially recalculated as described above using Equations 6, 4, and 3. Conversely, if the pore-water pressure becomes positive when an element at a node is considered initially unsaturated, the element subsequently is considered to be saturated and Equations 1 and 2 are employed. This transition is necessary, as Equations 3 and 4 are not applicable when pore-water pressures are positive.

Further details on theory and implementation are described in Qi et al. 2016a.

Stress History Formulation

Single layer deposition only involves monotonic change in the two strain variables of unsaturated soils. However, multi-layer deposition involves a significant amount of irrecoverable volumetric strain if the stress or suction decrease from the maximum level that a soil has ever been subjected. This is particular true if the deposit has a high initial void ratio and reached its shrinkage limit under the effect of evaporation - it cannot rebound to its initial state upon rewetting by the water from the newly deposited layer.

To simulate the unloading behaviour, an elastic plane (surface) is defined in the void ratio-stress-suction space to track recoverable volumetric strain, as shown in Figure 2. This surface is an extension of the rebound line, more generally the yield surface, in classical Cam-Clay Model for saturated soils. The virgin (plastic) consolidation and rebound (elastic) lines become three-dimensional surfaces for unsaturated soils due to use of two stress state variables. The plastic surface (Eq. 3) is stationary while the location of elastic surface depends on the current state of soil:

$$e^e = C_1 - \kappa \ln(\sigma - u_a) - \kappa_{ss} \ln[(u_a - u_w) + 1] \quad (7)$$

Where, *e* is void ratio, e^e is elastic void ratio, $(\sigma - u_a)$ is net stress, $(u_a - u_w)$ is matric suction, σ is the total stress, u_a is the pore-air pressure (usually assumed to be zero in nature) and u_w is the pore-water pressure. *The symbols* κ and κ_{ss} are the slopes of rebounding plane with net stress and suction, respectively. The value of C_1 determines the location of elastic rebound surface and is calculated from the current state of the soils. The shape of this surface is among the simplest possible, and has several advantages including smooth transition to the log-liner slope adopted by many saturated soil models (e.g. Cam Clay). This surface is used several formulations of unsaturated soil models (Zhang and Lytton 2009, Alonso et al. 1990). The constitutive surfaces are shown conceptually in Figure 2.

The other variable, water content, also exhibits hysteric behaviour, including volume change and hydraulic hysteresis. The soil-water characteristic curve is known to change with vold ratio, as well as exhibiting wet-dry hysteresis: Some researchers (Wheeler et al. 2003, Sheng et al. 2008) suggested that this behaviour can be modelled in the same framework of elasto-plasticity: their approach is adopted in the model. The void ratio and path dependent soil-water characteristic curve can be defined by the following equations, which define planes in long-linear degree of saturation – matric suction – void ratio space: These surfaces are mathematically described using

$$S = 1 - \kappa_s \ln[(u_a - u_w) + 1] \quad (8)$$

$$S = \kappa_s \ln(10^6 + 1) - \kappa_s \ln[(u_a - u_w) + 1] \quad (9)$$

$$S = C_{drying} - \lambda_{se} e - \lambda_{sr} \ln[(u_a - u_w) + 1] \quad (10)$$

$$S = C_{wetting} - \lambda_{se} e - \lambda_{sr} \ln[(u_a - u_w) + 1] \quad (11)$$

$$S = C_{scanning} - \lambda_{se} e - \kappa_s \ln[(u_a - u_w) + 1] \quad (12)$$

in which, Eq. (8) and (9) describe the main (drying and wetting) surfaces at suction lower than the air-entry value and higher than the residual water content, which are assumed not to change with void ratio. Eq. (10) and (11) describe the ma in surfaces at intermediate suctions for drying and wetting paths, respectively, and are void ratio dependent. Eq. (12) describes what happens when wetting occurs following drying to a point greater than the air-entry value, but less than the residual water content: the slope is parallel to the surfaces defined by (8) and (9), but the location depends on stress history, which is tracked through $C_{scanning}$.. S is the degree of saturation. All surface parameters can be determined from soil water characteristic curve tests, except that the value of $C_{scanning}$ is calculated from current soils' state. These surfaces are also shown in Figure 2.

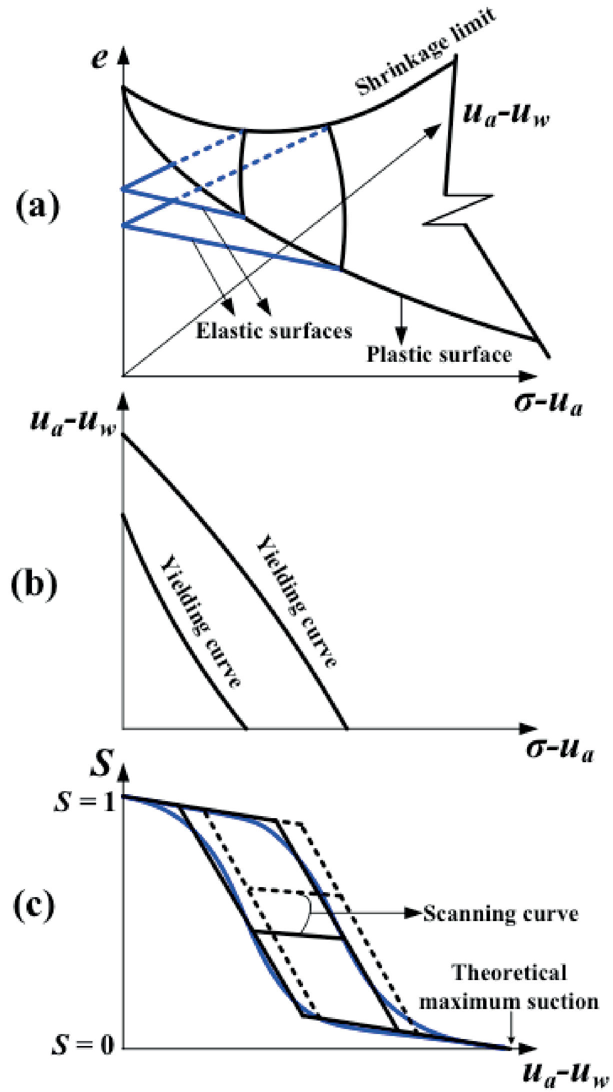

Figure 2. Elasto-Plastic constitutive surfaces in UNSATCON

Although the hydraulic behaviour may be better described using surfaces extended from an *S*-type curve based on the experimental observation (e.g. Fredlund and Xing, 1994; Tsiampousi et al. 2013), the modelling results presented later show this void ratio-dependent soil water retention model selected in our study (consisting of several planes in *S*-*e*-(u_a-u_w+1) space) appears to be sufficient to simulate the test case, and is certainly easier to implement than a S-type curve.

Further details on implementation of the elasto-plastic aspects of the model, are given in Qi et al. (2016 c).

TEST CASES

Monotonic dewatering

Two monotonic cases on in-line flocculated tailings were presented in Qi et al. (2016b). The first was a laboratory column test (Soleimani et al. 2014) and the second were results from simulation of one of the test cells at Shell AFD trials (Dunmola et al. 2013). A subset of the results from the second case, the field trial, are shown below. Figure 3 shows the predicted solids content, void ratio, degree of saturation and pore-water pressure.

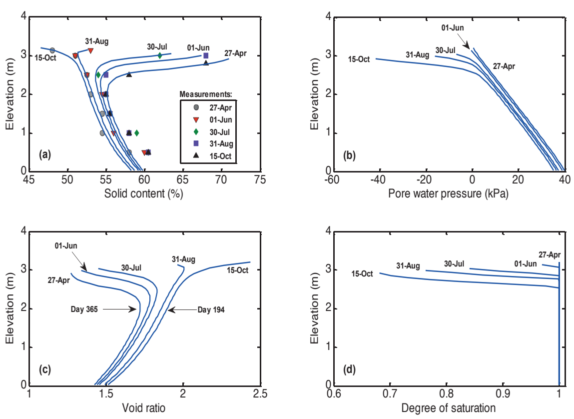

Figure 3. Simulation of field trial deposition of in-line flocculated mature fine tailings

Figure 4 shows the stress paths for two nodes during the simulation of the AFD trial, corresponding to two initial elevations. This shows the model's capability to simultaneously model saturated and unsaturated behaviour, and that indeed calculated void ratios follow the inputed constitutive surface.

Figure 5 shows the advantage of truly incorporating unsaturated flow in terms of improved realism of volume change near the soil surface, The model's out (UA) is compared to a purely saturated analysis (SA), and two saturated analysis that include evaporation and also two different limiting value of suction of the soil surface (QUA). The QUA type of quasi-unsaturated analysis is used in some models to approximate unsaturated behaviour, by limiting suction so as to impose a maximum value of effective stress at the surface, and therefore to replicate the minimum void ratio at the shrinkage limit. This, however, as shown in Figure 5, either causes an underestimate of actual evaporation, or over-privileges dewatering in terms of volume change very near the surface. In the UA analysis, the shrinkage limit is correctly simulated, and the evaporation is partly satisfied by water from de-saturation, not just volume change.

Multilayer deposition (de-watering and re-watering)

Two cases are presented. The first case is from the published multilayer deposition experiment on thickened gold tailings (Daliri et al. 2016). The second is from a multilayer deposition experiment on simulated in-line flocculated tailings (Rozina et al. 2015). The tailings used in Daliri et al. (2016) have been studied extensively (Al-Tarhouni et al. 2011, Fisseha et al. 2010, Mizani et al. 2013). Parameters for the constitutive surfaces are given in Table 1.

Tailings were deposited in layers ranging from 0.14 to 0.18 m in initial thickness at a void ratio of 1.1, into a 1 m by 0.7 m instrumented Plexiglas box reinforced with steel bars. Evaporation and drainage were directly measured using a tipping bucket and by the box' weight, as the whole box sits on load cells. More detail on the experiment can be found in Daliri et al. (2016).

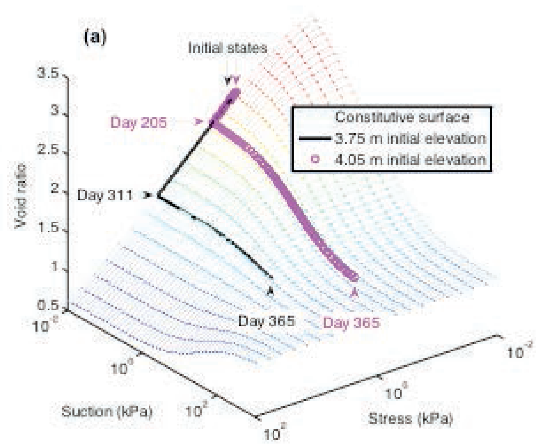

Figure 4. Void ratio stress paths for two initial elevations

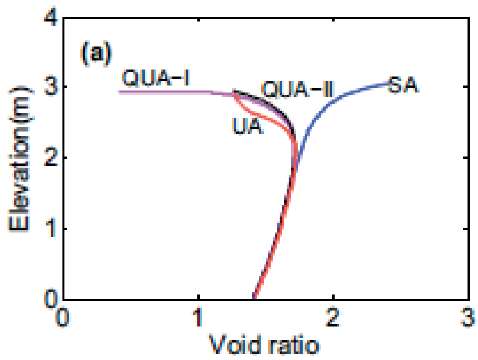

(a)

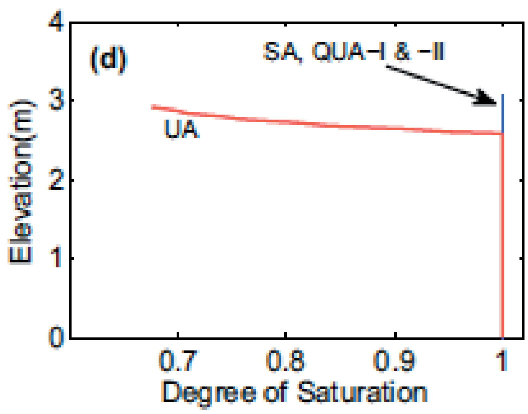

(b)

Figure 5. Performance of model compared to models without true unsaturated flow coupling. SA denotes saturated only analysis, QUA denotes saturated analysis with evaporation, where different maximum values of suction (1000 kPa, 10 kPa) are assigned to the surface node

Measured and modelled average layer GWC and pore-water pressure at various depths are presented in Figures 6 and 7, while depth profiles of void ratio are shown in Figure 8. Agreement between average layer GWC, and the pore-water pressure sensors are quite good: the deviation with the pore-water pressures in some cases for suction values in excess of 100 kPa is explained by cavitation of those sensors. The tailings water content in the old layer rebounds to a value close to saturation at the shrinkage limit. In fact, the void ratio at the top of the old layer somewhat decreases below the shrinkage limit rather than swelling (Figure 8). This is explained by the increase in total stress and that the slope of the elastic surface is larger along the new normal stress axis. The second layer indeed remains on the elastic surface for the remainder of the simulation, as the suction does not return to its original value, and the new pre-consolidation pressure (the projection of the elastic surface on the net normal stress – void ratio plane) is about 300 kPa, as shown in Figure 9.

Some preliminary results are also presented from an analysis of a three layer drying box test that was presented by Rozina et al. (2015). The same plastic surface and water-retention data used in modelling the field AFD trial (Qi et al. 2016b) were used to analyze the drying box experiment. The slopes of the elastic surface are calculated from consolidation data (Gholami and Simms 2015). As with the gold tailings, evaporation and drainage are measured and directly applied as boundary conditions. The initial heights of each layer are 0.31, 0.33, and 0.32 cm respectively.

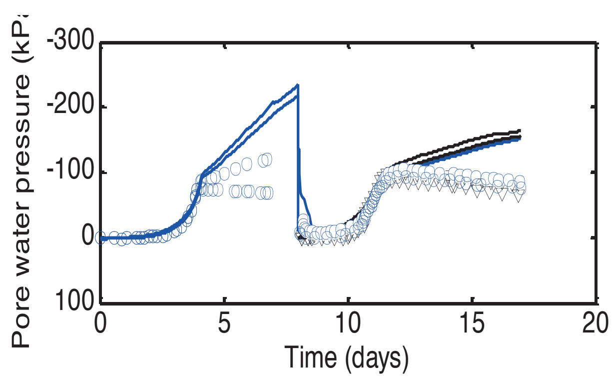

Figure 6. Modelled pore-water in first two layers from Daliri et al. (2016)

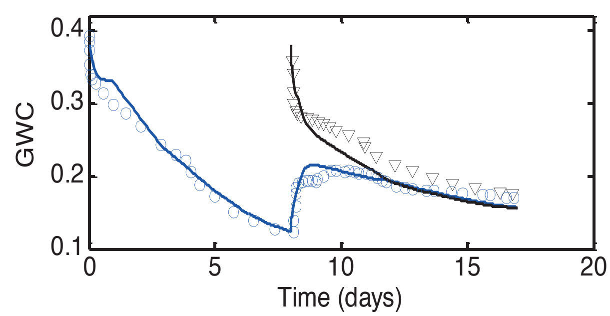

Figure 7. Modelled average GWC in each layer in first two layers from Daliri et al. (2016)

Table 1. Parameters for constitutive relationships for Daliri et al. (2016)

Volume change behaviour								
Parameters	a	b	C	d	F	g	κ_s	κ_{ss}
Value	1.2	0.166	0.004	0.02	35.9	41	0.015	0.0015
Elastic surface	κ	κ_{ss}						
	0.015	0.0015						
Water retention behaviour								
Parameters	C_{drying}	$C_{wetting}$	λ_{se}	λ_{sr}	κ_s			
Value	3.1	2.65	0.6	0.4	0.028			
Water hydraulic conductivity								
Parameters	H_1	H_2	M					
Value	3×10^{-7}	7.1057	0.75					

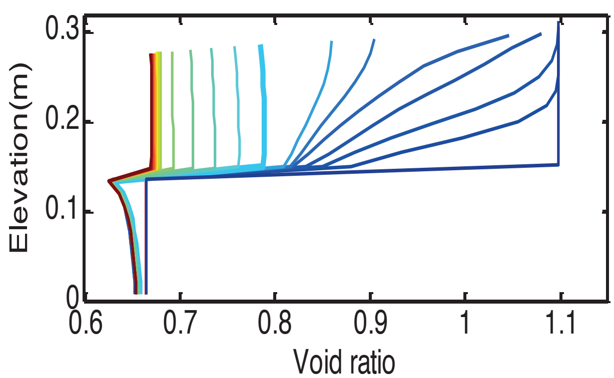

Figure 8. Void ratio in two layers after placement of the second layer in Daliri et al. (2016)

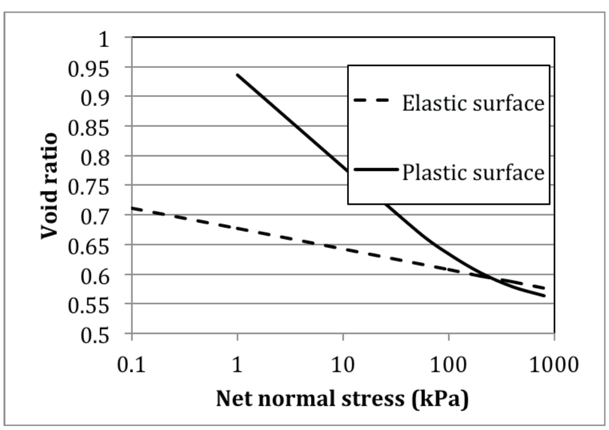

Figure 9. Projection of elastic and plastic surfaces in net normal stress-void ratio axis, after desiccation to 200 kPa matric suction

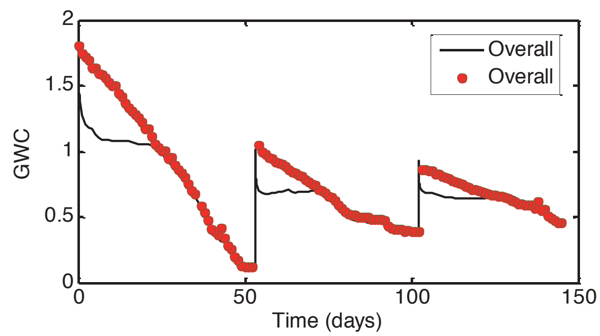

Figure 10. Overall GWC in three layer drying box test on in-line flocculated MFT

As shown in 'Figure 10, the overall rate of dewatering is reproduced by the model, though this is simply a test of mass conservatism, as the boundary conditions are known. The deviation of the predictions from the measurements after the placement of each new lift is due to the presence of supernatant water, the mass of which is included in the total measured mass.

Figure 11 shows the change in void ratio and degree of saturation after addition of layer 2. Similar to the gold tailings, the void ratio of the bottom layer does not appreciably change. Different from the gold tailings, the resaturation process is slower, and in fact, the underlying tailings continue to absorb water from the fresh layer for the simulated time (60 days). The shape of the profile at 60 days is similar to the measured profile of gravimetric water content taken from a core sample (Figure 12). The lower hydraulic conductivity of the polymer amended MFT delays the resaturation of the previously desiccated layer.

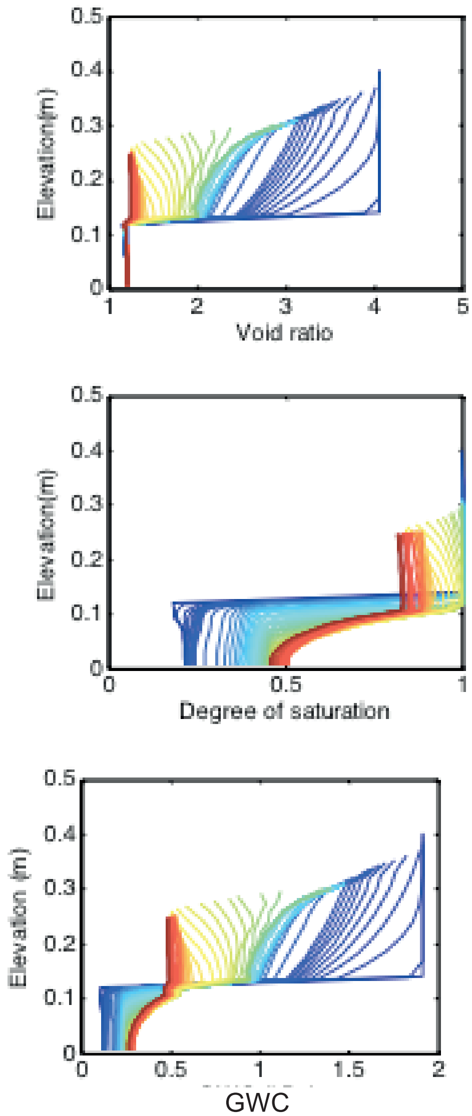

Figure 11. Void ratio, degree of saturation profile, and GWC after deposition of second layer for in-line flocculated MFT

APPLICATION AND LIMITATIONS

The model has several advantages that have been discussed in this paper, including, greater realism of dewatering predictions near the ground surface, ability to handle stress history effects, which are essential to model multilayer deposition, and the ability to simultaneously model saturated and unsaturated processes at different depths. Not shown in this paper is that the model is extremely fast – for example, simulation of the 3 layer drying

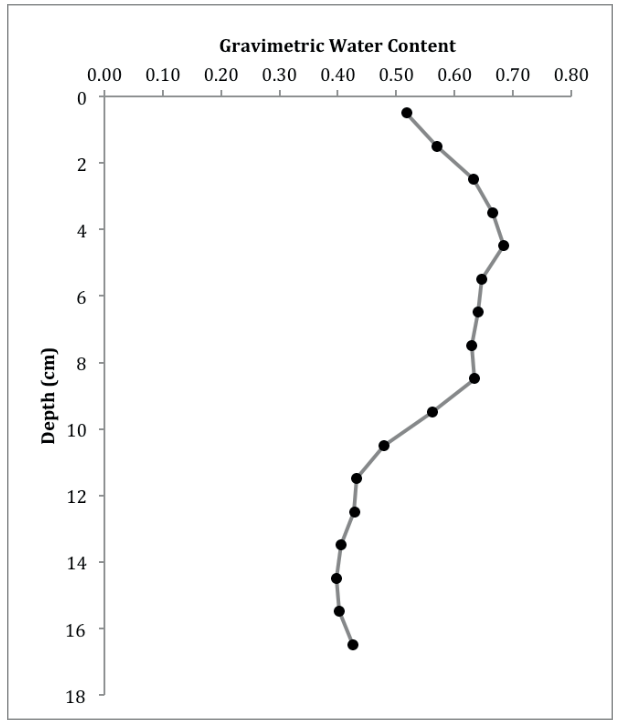

Figure 12. Measured data from core sample taken 60 days after placement of second layer

box experiment on in-line flocculated tailings takes less than 5 minutes. This is due to the explicit nature of the formulation (either no or only 1 iteration at a point in space per time step), and the simpler treatment of large strain consolidation afforded by the piecewise-linear formulation.

The model presently does not include any sort of predictive capacity for evaporation. Evaporation in oil sands tailings is complex due to the action of cracks and osmotic suction, thought several studies suggest that evaporation in freshly placed tailings is often higher than what would be predicted by conventional unsaturated flow codes with soil-atmospheric coupling (Simms et al. 2016).

Oil sands tailings exhibit significant cracking. This model is 1D and does not specifically simulate the influence of the 3D boundary condition on dewatering or rewetting. The model would be conservative with respect to dewatering, but potentially non-conservative with respect to wetting due to rain However, as shown in the paper, the irrecoverable volume change occurring after initial drying or due to consolidation is such that the threat of rewetting to overall dewatering efficiency is lower than perhaps anticipated by some.

The model does not simulate thixotropy (creep), which likely plays an influence in long-term dewatering of the various new types of oil sands tailings.

REFERENCES

Al-Tarhouni, M., Simms, P., and Sivathayalan, S. 2011. Cycic behaviour of reconstituted and desiccated-rewet samples of thickened gold tailings in simple shear. Canadian Geotechnical Journal, 48(7): 1044-1060

Alonso, E. E., Gens, A., & Josa, A. 1990. Constitutive model for partially saturated soils. Géotechnique, 40(3), 405-430.

Daliri, F. Simms, P. Sivathayalan, S. 2016. Shear and dewatering behaviour of high density gold tailings in a laboratory simulation of multi-layer deposition. Canadian Geotechnical Journal, 2016, 53(8): 1246-1257

Dunmola, A., Cote, C., Freeman, G., Kolstad D., Song, J., and Masala S. 2013. Dewatering and shear strength performance of in-line flocculated mature fine tailings under different depositional schemes. Proceeding of Tailings and Mine Waste 2013 November 3rd-6th 2013, Banff, Alberta p5 - 14.

Fisseha, B., Bryan, R, and Simms, P. 2010. Evaporation, unsaturated flow, and salt accumulation in multilayer deposits of a gold “paste” tailings. ASCE Journal of Geotechnical and Geoenvironmental Engineering, DOI:10.1061/(ASCE)GT.1943-5606.0000367

Fox, P. J., & Berles, J. D. 1997) CS2: A piecewise-linear model for large strain consolidation. International Journal for Numerical and Analytical Methods in Geomechanics, 21(7), 453-475

Fredlund, D. G., & Xing, A. (1994). Equations for the soil-water characteristic curve. *Canadian geotechnical journal*, *31*(4), 521-532.

Gholami, M., Simms, P. 2015. Shear strength and consolidation behaviour of raw and polymer amended oil sand fine tailings evaluated in simple shear and triaxial devices. Proceedings of GeoQuebec: 68th Canadian Geotechnical conference. Electronic proceedings.

Innocent-Bernard, T**.**, Simms, P. , Xiaoli, Y., Sedgwick, A. 2014. Multilayer Deposition of Two Batches of Thickened Oil Sands Tailings: Experiments and modeling. International Oil Sands Tailings Conference, December 7th-10th, 2014, Lake Louise, Alberta.

Jeeravipoolvarn,S., Scott, J.D., Chalaturnyk. R.J. 10 m standpipe tests on oil sands tailings: long-term experimental results and prediction. Candian Geotechnical Journal, 46:875-888.

Mizani, S., He., X., and Simms, P. 2013. Application of lubrication theory to modeling stack geometry of thickened mine tailings. Journal of Non-Newtonian Fluid Mechanics, 198 (59–70).

Qi, S, Daliri, F. Simms, P, Vanapalli, S. Coupled unsaturated flow–large strain consolidation with stress history. Submitted to Geotechnique, September 2016.

Qi, S., Simms, P., and Vanapalli, S. (2016). Piecewise-Linear Formulation of Coupled Large Strain Consolidation and Unsaturated Flow. I: Model Development and Implementation. ASCE Journal of Geotechical and Geoenvironmental Engineering. In Press.

Qi, S., Simms, P.,Vanapalli, S. , and Soleimani, S. (2016). Piecewise-Linear Formulation of Coupled Large Strain Consolidation and Unsaturated Flow. II Model Calibration and Testing. ASCE Journal of Geotechnical and Geoenvironmental Engineering. In Press.

Rozina, E. Mizani, S., Malek, M., Sanchez, M., Simms, P. 2015. Desiccation and Consolidation in a laboratory simulation of multilayer deposition of oil sand fine tailings. Paste 2015 Cairns, Australia, May 5th-7th 2015, pp. 81-93.

Sheng, D., Fredlund, D. G., & Gens, A. 2008. A new modelling approach for unsaturated soils using independent stress variables. Canadian Geotechnical Journal, *45*(4), 511-534.

Simms, P., Soleimani, S., Mizani,S., Daliri,F., Dunmola,A. , Rozina, E. and Innocent-Bernard, T. 2016. Cracking, salinity, and evaporation in mesoscale drying experiments on three types of mine tailings. Submitted to Environmental Geotechnics. August 2016.

Soleimani, S., Simms, P, Gholami, M. 2014. Desiccation-consolidation modeling and strength testing using simple shear of polymer-amended MFT. International Oil Sands Tailings Conference, December 7th-10th, 2014, Lake Louise, Alberta.

Tsiampousi, A., Zdravkovic, L., & Potts, D. M. 2013. A three-dimensional hysteretic soil-water retention curve. Geotechnique, 63(2), 155.

Vu, H. Q., & Fredlund, D. G. 2004. The prediction of one-, two-, and three-dimensional heave in expansive soils. Canadian Geotechnical Journal, *41*(4), 713-737.

Wheeler, S. J., Sharma, R. S., & Buisson, M. S. R. 2003. Coupling of hydraulic hysteresis and stress–strain behaviour in unsaturated soils. Géotechnique, 53(1), 41-54.

Zhang, X., & Lytton, R. L. 2009. Modified state-surface approach to the study of unsaturated soil behavior. Part I: Basic concept. Canadian Geotechnical Journal, 46(5), 536-552.

CONSOLIDATION AND ATMOSPHERIC DRYING OF FINE OIL SAND TAILINGS: COMPARISON OF BLIND SIMULATIONS AND FIELD SCALE RESULTS

Philip J. Vardon[1], Yutian Yao[1], L.A. van Paassen[1] and A. Frits van Tol[1,2]
[1]Delft University of Technology, Delft, the Netherlands
[2]Deltares, Delft, the Netherlands

ABSTRACT

This paper presents a comparison between blind predictions of field tests of atmospheric drying of mature fine tailings (MFT) presented in IOSTC 2014 and field results. The numerical simulation of the consolidation and atmospheric drying of self-weight consolidating fine material is challenging and requires significant knowledge of the material, climate and the interaction between the two. This paper presents the outcome of a study which developed a numerical model, undertook material characterization and predicted the behaviour of full scale field tests undertaken in Shell Canada's Muskeg River Mine near Fort McMurray, Alberta. The blind predictions were published in IOSTC 2014. A comparison between the observed and simulated behaviour in terms of settlement and void ratio yields a number of conclusions regarding the model: (i) all of the major observed features can be predicted by the numerical model; (ii) the quantification of the behaviour is well represented; (iii) due to the fast initial consolidation, the amount of material recorded as being deposited was underestimated; (iv) significant shear strength development requires a void ratio reduction which either requires a significant overburden or atmospheric drying.

INTRODUCTION

Mature fine tailings (MFT) are the fine tailings that arise from initial disposal of the tailings in settling ponds, where the dense solids with a large particle size (i.e. sands) settle to the bottom, water without solids remains at the top and can be recycled. The remaining middle layer is composed of the fine particles and a high water content, known as MFT. These tailings suffer from high volume, extremely low shear strength and extremely long settling times.

A number of techniques have been developed to deal with such tailings, one of which is flocculation, via addition of a chemical flocculent, and atmospheric drying in layers.

Shell Canada have investigated this possibility resulting in a proposed flocculent and a series of field scale tests at the Muskeg River Mine near Fort McMurray, Alberta. Delft University of Technology has supported this work via an experimental and numerical project, with a summary of the experimental work presented in this conference (Yao et al., 2016) and previously (Yao et al., 2012, 2014). The numerical model was originally presented by van der Meulen et al. (2012) and further developed and validated by Vardon et al. (2014), including blind predictions of the behaviour of the field tests. Some further theoretical analyses were undertaken looking at the most efficient method of layering, to yield the most reduction in volume and even density (Vardon et al., 2015).

This paper presents the results of a comparison between the blind predictions presented by Vardon et al. (2014) and the results of the field tests. Additional simulations were undertaken where deviations were found to investigate the causes of the deviations. The numerical model and the field tests are initially briefly outlined as background to the results.

NUMERICAL MODEL

Governing equations

While consolidation is typically, and generally, solved using two coupled equations (e.g. Biot 1941), the self-weight consolidation of deposited liquid material is mostly driven by shrinkage and is typically stored in deposits which are much wider than deep and therefore can be considered 1D. Therefore, in this work, a 1D model where the hydraulic behaviour is primarily solved is appropriate. The deformation is then calculated in a second step, based on the results of the hydraulic model.

The governing equation is therefore based upon the conservation of water mass and utilizes Darcy's Law to calculate the water flow. The water potential includes the following components:

- Elevation
- Overburden
- Suction/pressure.

The equation solved (after Kim et al., 1992) is:

$$\frac{\partial \Theta}{\partial \mathrm{t}} = \frac{\partial}{\partial z}\left[K \frac{\partial}{\partial z}(\varphi + z + \Omega)\right] \quad (1)$$

where Θ is the volumetric water content (V_w/V_t), t is time, z is the elevation, K is the hydraulic conductivity, φ is the water potential, i.e. the suction or the pressure, and Ω is the overburden component.

By expanding the spatial differential of the water potential, i.e. the part inside the square bracket of eq. (1) and ignoring any surcharge, yields:

$$\frac{\partial \theta}{\partial \mathrm{t}} = \frac{\partial}{\partial z}\left[K\left(\begin{array}{c}\frac{\partial \varphi}{\partial \theta} \cdot \frac{\partial \theta}{\partial z} + 1 + \\ \gamma \frac{\partial e}{\partial \theta} + \frac{\partial^2 e}{\partial \theta^2} \int_{z_0}^{z} \gamma \, \mathrm{d}z \cdot \frac{\partial \theta}{\partial z}\end{array}\right)\right] \quad (2)$$

where θ is the water ratio (V_w/V_s), e is the void ratio (V_v/V_s) and γ is the volumetric weight of the material. The water content is related to the water ratio as $\Theta = \theta/(1+e)$.

Two sets of coordinates have been defined: Cartesian coordinates, where z is the vertical coordinate in real space, and Lagrangian coordinates, where the same solid material always has the same position, and m is the vertical coordinate, defined as $\mathrm{d}m = \mathrm{d}z/(1+\mathrm{e})$. This is useful to understand how the material evolves.

At each position in the soil column and in time $\partial\varphi/\partial\theta$ can be calculated from the Soil Water Retention Curve, and $\partial \mathrm{e}/\partial\theta$ and $\partial^2 e/\partial\theta^2$ can be calculated from the shrinkage curve. K changes as the void ratio changes, so must also be updated.

Boundary conditions

To simulate both consolidation behaviour and evaporation (and precipitation) a competitive boundary condition has been incorporated at the top surface. Potential evaporation, rainfall, permeability restricted flow and consolidation driven flow are all calculated and the dominant mechanism used as a flux boundary condition.

FIELD TESTS

Three field tests were undertaken, the first termed the '*Deep stack*', where only a single layer was deposited, the second termed '*Thick multi-lift*' where three thick layers (lifts) were deposited and the third termed '*Thin multi-lift*' where seven thin layers were deposited. Approximately the same amount of material was deposited in each test. Table 1 gives the layer thicknesses for each test and layer.

Table 1. Field test layer thicknesses for the three field tests

Test	Lift	Days from start	Reported layer thicknesses (cm)	Post-analysis layer thicknesses (cm)
Deep stack	1	0	450.0	480.0
Thick multi-lift	1	0	100.0	130.0
	2	257	180.0	230.0
	3	346	130.0	150.0
Thin multi-lift	1	0	90.0	100.0
	2	37	50.0	80.0
	3	257	50.0	60.0
	4	290	50.0	50.0
	5	317	60.0	60.0
	6	346	110.0	130.0
	7	365	40.0	50.0

RESULTS

The analyses were undertaken with the material parameters as reported in Vardon et al. (2014), determined based upon the experimental work presented in Yao et al. (2012, 2014).

The atmospheric drying is the critical forcing parameter, so has been reproduced here in Figure 1. Via an initial sensitivity analysis it was found that averaging the precipitation and evaporation potential monthly gave good results and allowed the numerical model to run efficiently. The model run time was between 30 secs and 5 minutes, and was variable on the non-linearity of the fluxes and the steepness of the gradients in the system.

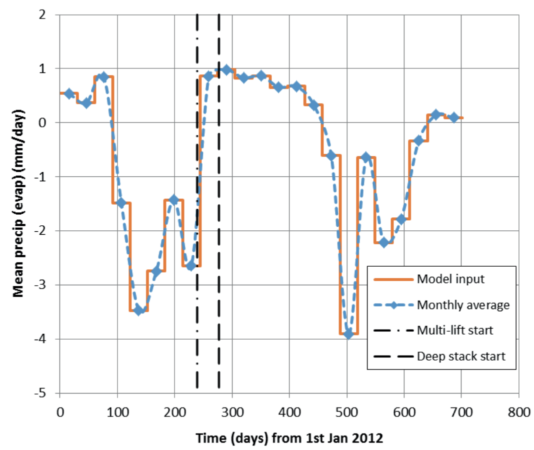

Figure 1. Mean precipitation averaged per month. Negative mean precipitation is equal to evaporation potential.

Initial results

The initial results of the Deep Stack simulation are presented in Figure 2. The solid squares are the experimental results and the blue lines the numerical simulations. In Figure 2(a) the depth is shown, with the series of blue lines every 40cm initially (shown in Figure 17 of Vardon et al., 2014). The gaps in experimental data are due to snow cover where the surface could not be observed. The results show excellent agreement with the trend of displacement, in particular at the start and where the gradients change due to evaporation, e.g. between 260 and 300 days, with an 8% underestimation of final depth.

The void ratio profiles are presented in Figure 2(b), with the time series progressing from the right of the figure to the left. The experimental profile at 374 days is overlain the results. In comparison the final numerical situation is the most left dotted red line. In general, excellent agreement between the experimental and numerical prediction was found. A dense crust is shown in both the experimental and numerical results starting from approximately 2m above the base until the surface. The numerical results show a slight overestimation of the void ratio at the base of the stack.

It is also useful to present the results in terms of material level coordinates, i.e. the same solid material always has the same coordinate, as this allows an understanding of the history of the material. This is also how the results were presented in Vardon et al. (2014). However, when this was undertaken, shown in Figure 3 (numerical results from Figure 15, Vardon et al., 2014), it was clear that there was more solid material recorded in the experiments than in the numerical model, by approximately 7%. It is hypothesized that this was the cause for the underestimation of the final stack depth. It is also thought likely as the very sharp gradient in the early part of the experiment would make the amount of material deposited very difficult to control. This same trend was observed in the *Thick multi-lift* and the *Thin multi-lift*, but increasing with each lift. These results are shown in Appendix I.

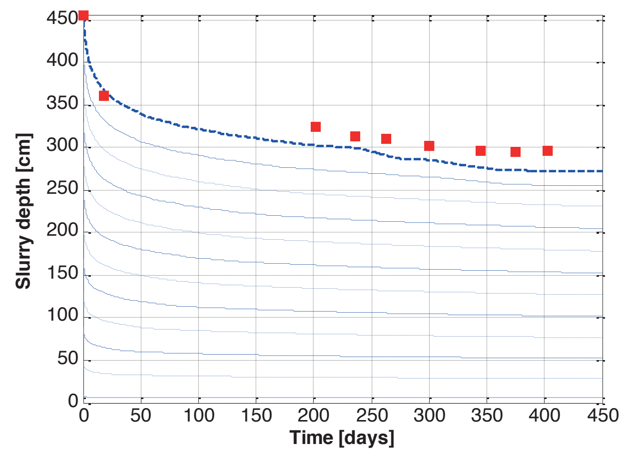

(a) Temporal evolution of the depth

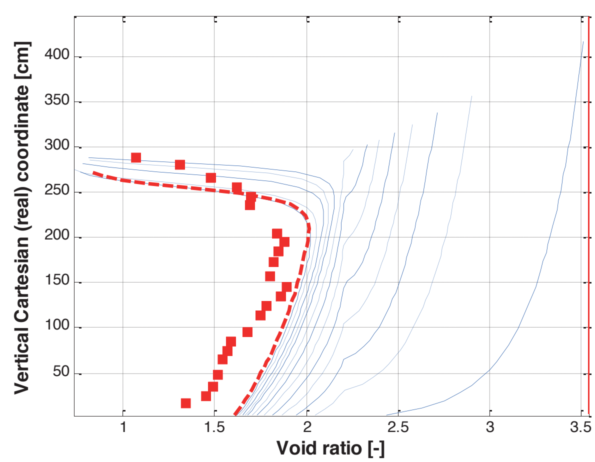

(b) Void ratio profiles, with 374 day experimental profile (squares). Final numerical result (thick dotted line) is 450 days.

Figure 2. Comparison of the results of the *Deep stack* numerical simulation against the experimental results

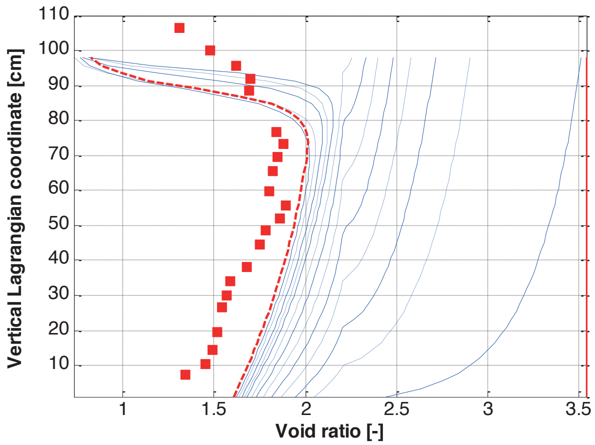

Figure 3. Comparison of the results of the *Deep stack* numerical simulation against the experimental results in material level (Lagrangian) coordinates.

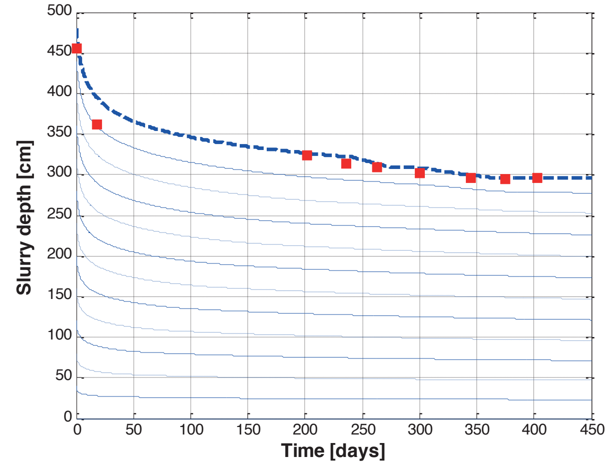

(a) Temporal evolution of the depth

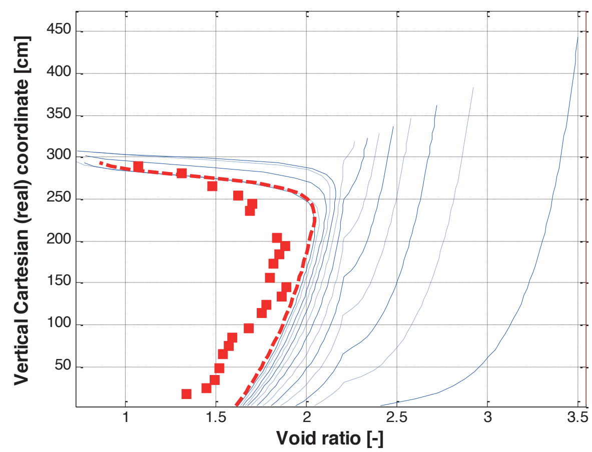

(b) Void ratio profiles, with 374 day experimental profile (squares). Final numerical result (thick dotted line) is 450 days.

Figure 4. Comparison of the results of the *Deep stack* updated numerical simulation against the experimental results

Updated results with additional material

Following the conclusions that in general the trends and material behaviour seemed to be well represented, but that there was additional material deposited, a series of additional simulations were undertaken.

The simulations were identical (material parameters and boundary conditions) with the exception of addition material. The amount of additional material was calculated from the void ratio measurements, as the layering was clear (e.g. see Figure A1(b)). The updated layer thicknesses are shown in the last column of Table 1.

The results are presented below. In Figure 4 for the *Deep Stack*, in Figures 5 and 6 for the *Thick multi-stack* and in Figure 7 for the *Thin multi-stack.*

In Figure 4(a), it is seen that the additional material only affects slightly the match of the results initially, and it matches excellently later in the analysis. In Figure 4(b) the void ratio matches well in the entire thickness of the stack, although there is a slight underestimation of the reduction of void ratio at the base of the stack until the evaporative 'crust'.

In Figure 5 substantial qualitative and quantitative agreement are observed. In particular, the overall depth reduction is well matched in each layer, the void ratio is well represented throughout. Note that in the top layer the final numerical results are late than the experimentally recorded result, and the switch between consolidation and evaporative behaviour is well represented.

It is noticed that the void ratio at the top of the top of the second layer is under-predicted. It is hypothesized that the reason for this difference is that this crust starts to develop just at the end of the period where the second layer is exposed to the atmosphere, due to elevated evaporative fluxes and reduced consolidation fluxes. During this time, there is a competition between the evaporative and consolidation boundary condition and the model is then sensitive to small changes in these values. This is shown in Figure 6, where the water fluxes are shown. The black box highlights the time where the crust in the second layer is formed. The consolidation flux (the smoothly decreasing line) and the evaporative fluxes (the steady line) in this period are almost equal and therefore the crust formation is sensitive to these changes.

To increase the depth of the crust and take advantage of the evaporative behaviour, the deposition could be delayed (e.g. as suggested by Vardon et al., 2015).

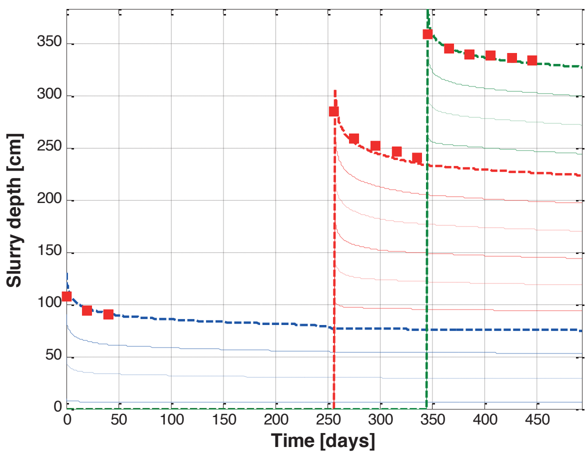

(a) Temporal evolution of the depth

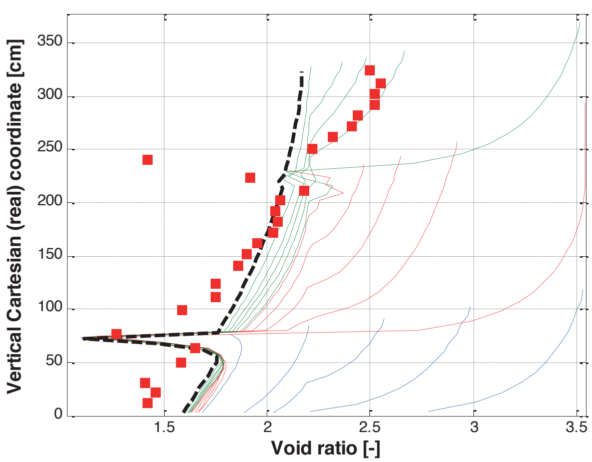

(b) Void ratio profiles, with 412 day experimental profile (squares). Final numerical result (thick dotted line) is 450 days.

Figure 5. Comparison of the results of the *Thick multi-stack* updated numerical simulation against the experimental results

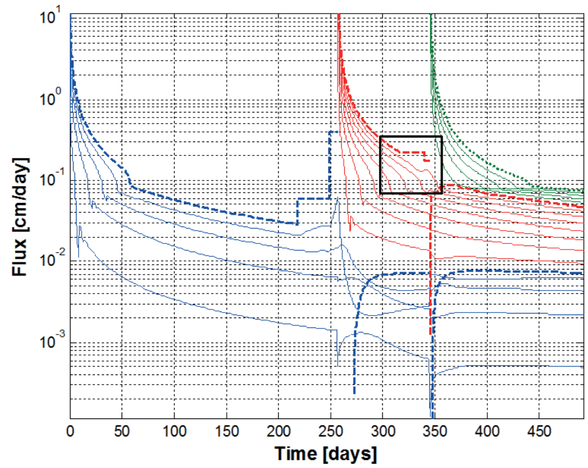

Figure 6. Water flux evolution for the *Thick multi-stack*

In Figure 7, again substantial qualitative and quantitative agreement are observed, however there are more differences than in the prior two simulations.

The overall depth reduction is well matched, the void ratio is well represented, in particular, quantitatively in the lowest three layers and qualitatively in the upper four and the switch between consolidation and evaporative behaviour is well represented. The main differences which can be observed are that in the later stages there is some overestimation of height reduction and there is overestimation of reduction in void ratio in the upper layers.

In this test, mostly a new layer was added when the soil was still significantly consolidating, with the exception of the second layer, where the void ratio results match well the experimental results. It is hypothesised that this makes the model sensitive to variations in initial water content, the deposition process, averaging of climatic data and the behaviour of the material in very wet conditions, where settling of particles may occur (as opposed to consolidation behaviour).

RESULTS DISCUSSION

In general, the qualitative and quantitative predictions of the numerical model are in close agreement with the experimental results.

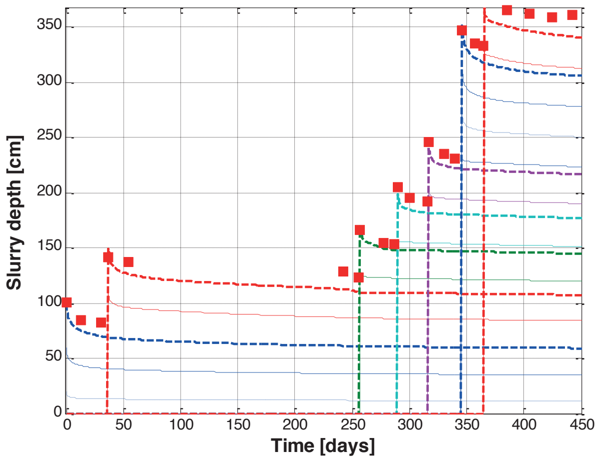

(a) Temporal evolution of the depth

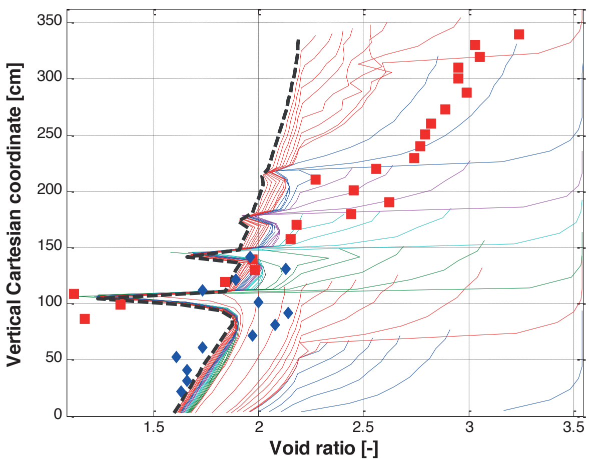

(b) Void ratio profiles, with 276 day experimental profile (diamonds) and 412 day experimental profile (squares). Final numerical result (thick dotted line) is 450 days.

Figure 7. Comparison of the results of the *Thin multi-stack* updated numerical simulation against the experimental results

In particular, it can be seen that:

- The general settlement rates and amounts are in good agreement.
- The rates of settlement in time are very closely matching. Specifically, both the typical consolidation curve at the beginning of each layer, and the times where high evaporation are expected, are well represented.
- The void ratio (therefore material density) distribution is well predicted. Both the general trend of denser material at the base and the denser layers due to evaporation are well predicted.

It was expected to have deviation of the results from the experiments in the periods where significant snow cover was seen. However, based on the settlement gradients, while some evidence is apparent, significant deviation is not seen. Possible reasons include: limited frost depth due to the isolating snow cover, or excess pore pressures building up near the surface which can quickly dissipate when ice and snow melts or warmer water flowing out of the soil (from depths where the soil is unfrozen) due to consolidation.

Where the model has the most layers, especially within a relatively short period of time the model results deviates most from the experimental results. This coincides with the initial deposition and the surface boundary having the most uncertainties, e.g. the settlement behaviour prior to consolidation, the impact of snow and ice cover, cracks, runoff and the impact of using monthly averaged weather data.

DEPOSITION REQUIREMENTS

The ability to numerically simulate the behaviour of atmospheric drying of MFT gives the ability to test various strategies numerically (e.g. Vardon et al., 2015). However, the objective should be clear. The problems of volume reduction, can mostly be solved via flocculation and consolidation processes, with the majority of the reduction in stack height coming from this process, see Figure 5 in combination with Figure 6. Evaporation allows additional reductions of water content, and more limited reductions in void ratios, however it is this final reduction in void ratio which gives significant strength gain. Therefore, timing the layer deposition, so that consolidation processes dominate in times of low evaporation potential and evaporation processes are dominant when there are high evaporation potentials, allows both volume reduction and strength gain to be maximized.

The currently withdrawn directive on how tailings should be disposed of, known as D074 (ERCB, 2009), however, had strength based requirements. A methodology to translate results here into strength-based requirements is proposed. This can be useful to meet future regulations or can be input into stability or liability calculations.

Locat and Demers (1988) proposed a relationship for the remoulded shear strength (converted to kPa from Pa in the paper):

$$c_u = \left(1.167/_{LI}\right)^{2.44} \quad (3)$$

where c_u is the remoulded undrained shear strength and *LI* is the liquidity index. *LI* is in turn defined as:

$$LI = \frac{w-LL}{LL-PL} \quad (4)$$

where *w* is the geotechnical water content (mass water / mass solids), *LL* is the Liquid Limit and *PL* is the Plastic Limit. The *LL* and *PL* were determined by Yao et al. (2012) as 66.5 and 22.7 respectively.

Equation (3) and experimentally determined residual strength from the field tests are shown on Figure 8.

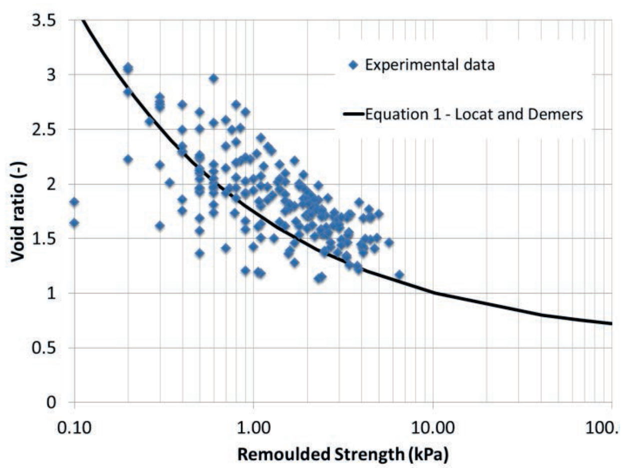

Figure 8. Remoulded undrained shear strength. Blue diamonds are measured data from the Shell field tests (all data aggregated), the solid black line is the proposed relationship from Locat and Demers (1988) (Equation 3).

For the peak strength, the appropriate shear strength for stability analysis, a relationship of the same form, is suggested, with the coefficient and exponent calibrated against experimental evidence, at a reasonable lower bound. The relationship proposed is:

$$c_u = \left(1.5/_{LI}\right)^{4.0} \quad (5)$$

This relationship, against experimentally determined values is shown in Figure 9.

From this figure, to meet the requirements that were set in D074, a void ratio of below 1.5 would be required. From the results presented, this is only reached at the base of some of the stacks and in the crusts, i.e. the material which has dried significantly due to evaporation.

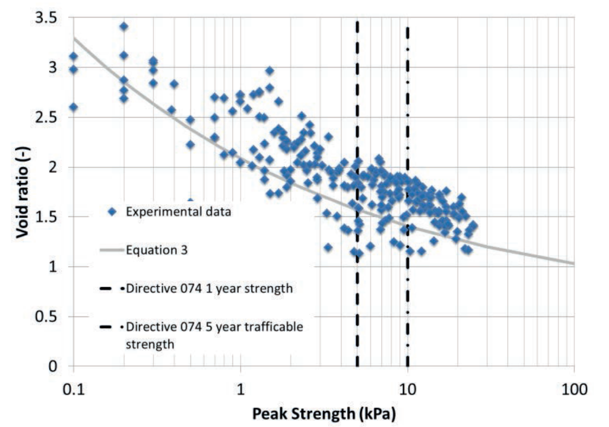

Figure 9. Undrained shear strength. Blue diamonds are measured data from the Shell field tests (all data aggregated) and the grey line is a proposed relationship based upon the experimental data (Equation 5). The vertical lines are the strengths indicated by Directive 074 (ERCB 2009).

To enable the atmospheric drying to achieve maximum volume reduction or maximum strength, evaporative fluxes need to be required to win the boundary condition competition. The requires the consolidation fluxes to be lower than the evaporative fluxes in the periods of time where the potential evaporation is high, i.e. during the summer. The layer size can be tuned so that during the autumn periods, material could be deposited and allowed to consolidate, yielding the majority of the volume reduction and then in the summer allowed to form a crust. Depending on the exact requirements the depth of the layer can be tuned either based on the consolidation behaviour or the drying behaviour (or a combination).

CONCLUSIONS

The results of the predictive numerical modelling investigation of field tests presented in Vardon et al. (2014) were compared to the experimental results. The model has been shown to be able to predict both qualitatively and quantitatively the behaviour of MFT under AFD field tests.

Initial modelling, based on information received prior to modelling, suggested that more (solid) material was deposited than indicated. Subsequent simulations with additional material yielded improved results, which were able to reproduce almost all features in both a quantitative and qualitative manner. Therefore the model is considered validated in this case.

In addition, a method to predict the strength behaviour based on the void ratio has been initially examined, indicating a method to assess compliance with future regulations or to assess the ongoing changes in stability.

Timing the layer deposition so that consolidation processes dominate first, and volume reduction is maximized, and then afterwards evaporation processes dominate to increase strength (and further reduce volumes) provides an optimal solution. This model allows the numerical investigation of such scenarios to provide optimal solutions which also satisfy regulations.

ACKNOWLEDGEMENTS

Funding for this work and field data were provided by Shell Canada. This support is gratefully acknowledged.

REFERENCES

ERCB (2009). Directive 074, Tailings Performance Criteria and Requirements for Oil Sands Mining Schemes, Energy Resources Conservation Board of Alberta.

Locat, J. and Demers, D. (1988). Viscosity, yield stress, remoulded strength, and liquididity index relationships for sensitive clays. Canadian Geotechnical Journal, **25**(4), 799-806.

van der Meulen, J., van Tol, F., van Paassen, L. and Heimovaara, T. (2012). Numerical modeling of drying and consolidation of fine sediments and tailings. IOSTC 2012, 399-409.

Vardon, P.J., Nijssen, T., Yao, Y. and van Tol, A.F. (2014). Numerical simulation of fine oil sand tailings drying in test cells. IOSTC 2014, 59-69.

Vardon, P.J., Yao, Y., van Paassen, L. and van Tol, A.F., (2015). The use of a large-strain consolidation model to optimise multilift tailing deposits. Proceedings of the Tailings and Mine Waste Management for the 21st Century, 263-270, Sydney.

Yao, Y., van Tol, A.F. and van Paassen, L. (2012). The effect of flocculant on the geotechnical properties of mature fine tailings: an experimental study. IOSTC 2012, 391-398.

Yao, Y., van Tol, A.F., van Paassen, L. and Vardon, P.J. (2014). Shrinkage and swelling properties of flocculated mature fine tailings. IOSTC 2014, 27-35.

Yao, Y., van Tol, A.F., van Paassen, L.A. and Vardon, P.J. (2016). Dewatering Behaviour of Fine Oil Sands Tailings: A Summary of Laboratory Results. Submitted to IOSTC 2016.

APPENDIX I

Original numerical predictions against the experimentally recorded results.

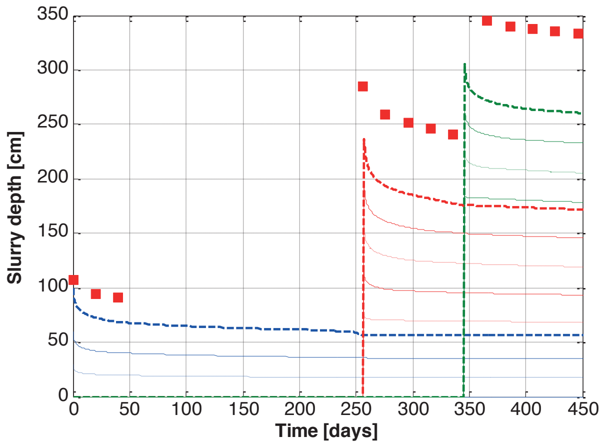

(a) Temporal evolution of the depth. (Numerical results from Figure 17, Vardon et al., 2014).

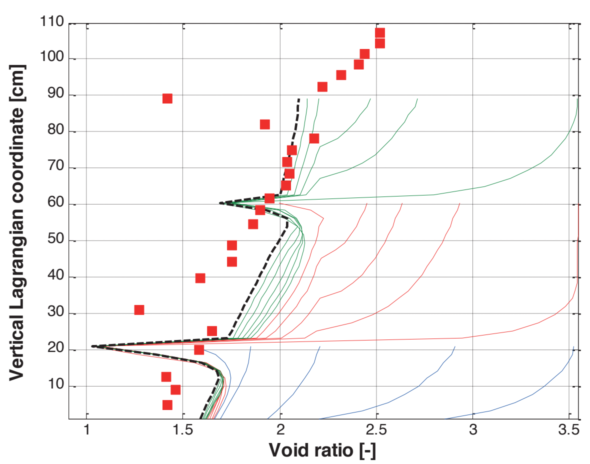

(b) Void ratio profiles in material level (Lagrangian) coordinates with 412 day experimental profile (squares). Final numerical result (thick dotted line) is 450 days. (Numerical results from Figure 19, Vardon et al., 2014)

Figure A1. Comparison of the results of the *Thick Multi-stack* numerical simulation against the experimental results

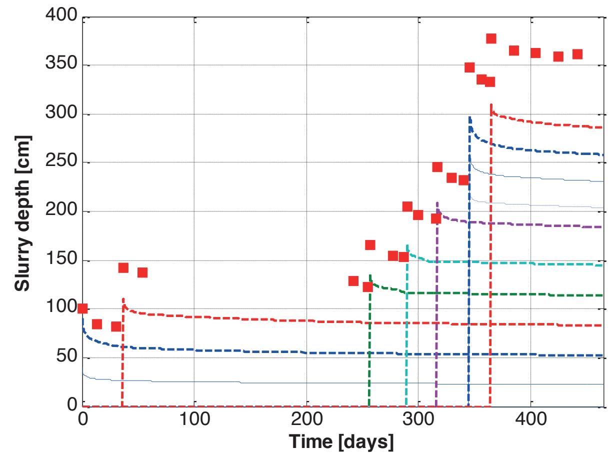

(a) Temporal evolution of the depth

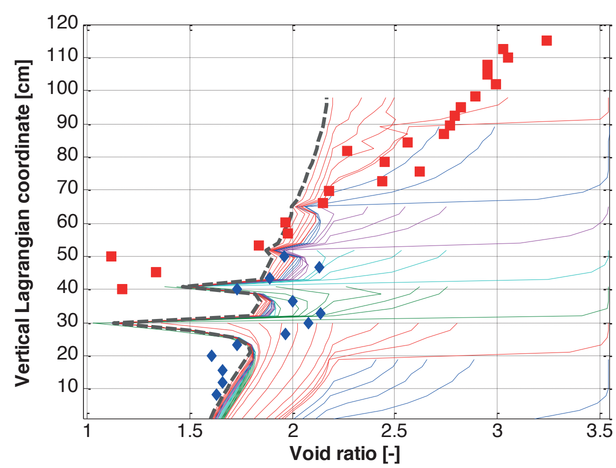

(b) Void ratio profiles in material level (Lagrangian) coordinates with 276 day experimental results (diamonds) and 412 day experimental profile (squares). Final numerical result (thick dotted line) is 450 days. (Numerical results from Figure 21, Vardon et al., 2014).

Figure A2. Comparison of the results of the *Thin Multi-stack* numerical simulation against the experimental results

OPTIMIZING TAILINGS DEPOSITION TO MAXIMIZE FINES CAPTURE: LATEST ADVANCE IN PREDICTIVE MODELING TOOLS

L. Sittoni[1], A.M. Talmon[1,2], J.L.J. Hanssen[1], H. van Es[1,2], J.A.Th.M. van Kester[1], R.E. Uittenbogaard[1], J.C. Winterwerp[1,2] and C. van Rhee[2]
[1]Deltares, The Netherlands
[2]Delft University of Technology, The Netherlands

ABSTRACT

Improving the understanding and predictability of tailings or slurry deposition reduces the risk, the liability and the cost of mining, dredging, and land reclamation activities. Some of the key questions refer to: deposition behavior; beach slopes and geometry; segregation of coarse and fine fractions.

In this paper we discuss flow and sand segregating behavior of fines and mixed tailings when flowing down a beach. We present preliminary numerical simulations performed with a new special module of Delft3D dedicates to tailings and non-Newtonian flow deposition, which includes slurry rheology and shear-induced sand settling processes. Delft3D is an open source numerical modeling suite developed and maintained by Deltares used world-wide for coastal, riverine and morphological studies. The tailings module is being thoroughly tested against analytical solutions and laboratory experiments. The model captures typical non-Newtonian plug-flow velocity profile, sand settling behavior and the formation of a slow-flowing sand rich gelled bed layer near the beach – slurry interface. Particle size (or sand to fines ratio) distribution and flow characteristics will be presented for different tailings of varying density and sand content, when flowing along a beach. When applicable, the results will be presented in sand to fine ratio to estimate sand capture along the deposit.

This model proves to be a useful tool to improve understanding of flow and segregating behavior of tailings and slurries. This model is especially beneficial to study how variation in critical parameters, such as rheological parameters, solids content, particles size distribution and flow rates influence deposition.

INTRODUCTION

Understanding and predicting the deposition behavior of tailings or slurries is critical for the mining and dredging industry, as well as for land reclamation and coastal or inland safety. Thousands of cubic meters of tailings are produced and deposited in tailings basins every day; land is being reclaimed for human developments or coastal protection at faster pace and in more remote areas; mud slides, caused by natural disaster or manmade structure failures, kill people every year. Yet, the understanding of tailings and slurries flow and depositional behavior, as well as comprehensive and validated tools to evaluate different management or protection scenarios are lacking. Deltares has set improving understanding and prediction of tailings and slurry deposition behavior as a key topic in its strategic agenda. This includes theoretical, laboratory and numerical enhancement activities.

This paper specifically focuses on the latest advance in numerical prediction of tailings deposition and sand segregation in beach above water environment. This project is a collaborative effort between Deltares, the Canadian Oil Sands Innovation Alliance (COSIA) and the Dutch Government sponsored program Topconsortium voor Kennis en Innovatie (TKI) Deltatechnologie, which promotes private – public research and development of socially impacting innovative technologies.

As part of this project, the numerical open-source software Delft3D[1], which is developed and maintained by Deltares, is being upgraded to simulate non-Newtonian fines dominated flow and sand settling behavior in non-Newtonian carrier fluids. Delft3D, in the currently open source version, includes 3D shallow water hydrodynamics (i.e. no vertical acceleration), sediment transport and water quality processes. Delft3D has been implemented to simulate delta deposits in alluvial environment,

[1] https://oss.deltares.nl/web/delft3d

with good agreement between observed and simulated deposition characteristics, i.e. geometry and grain size distribution (van der Vegt et al. 2015) and slopes (Sheets, et al. 2014). The strategy is to build on the robust and tested numerical engine, the physical processes, and the experience of Delft3D, towards the specific processes of tailings deposition behavior.

The end objective of this exercise is to provide the community with a numerical tool which is capable of predicting flow behavior and particles size distribution (i.e. fines capture) in 3D of a wide range of tailings and slurries, from diluted sand dominated tailings, to thick fine dominated non-segregating slurries. In this paper we will present the recent advance towards this objective and a strategy forward.

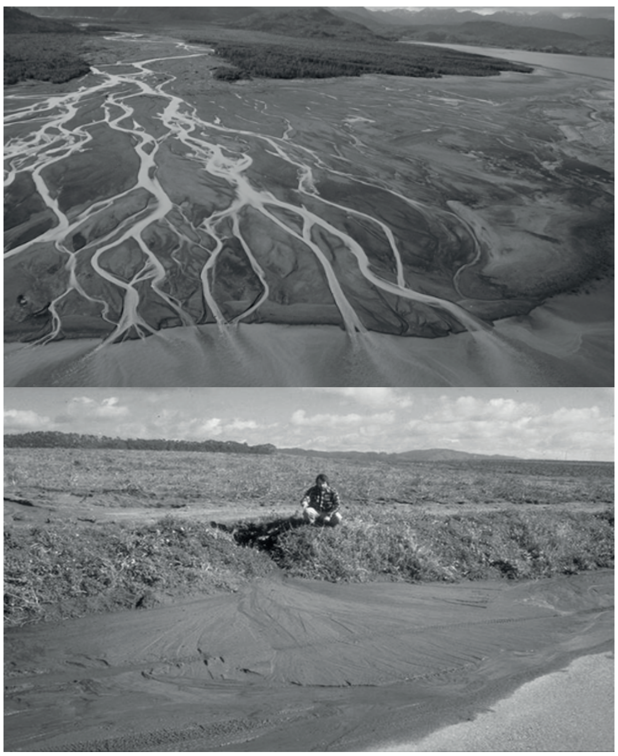

Figure 1. Natural deltas at different scales. Top: Kachemak Bay in Alaska. Source Flickr – NOAA; Bottom: Runoff from cultivated field near Pigeon Point, CA. Source: Gary Parker e-book morphodynamic

DELTAS AND BEACHES

Tailings or dredge material beaches have similar morphological features as natural deltas, even though the spatial scale may differ by few orders of magnitude. At very different scales, natural deltas have indeed similar features, i.e. channel pattern,

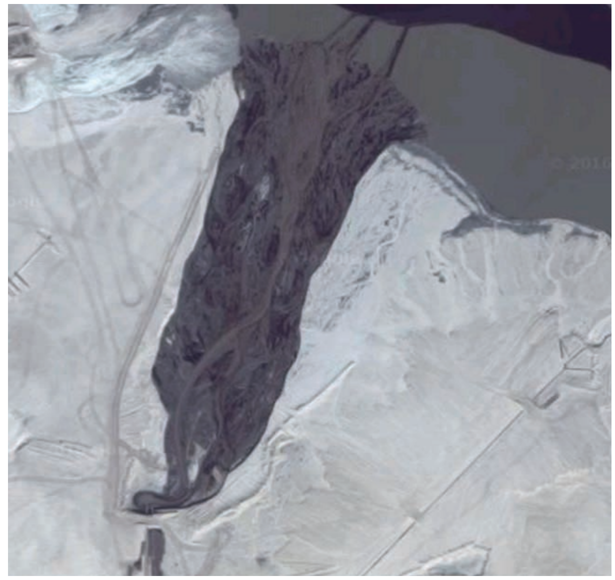

Figure 2. Sand dominated diluted tailings stream from oil sands external facility. Source: Google maps

Figure 3. Fines dominated thick tailings beach, with long single channel and expanding flow. Source: B. Pirouz, ATC Williams, Australia

delta geometry, slope. Figure 1 depicts the river delta of the Kachemak River in Alaska compared with the delta formed by cultivated field runoff. The first has extent on the order of one kilometer, the second in the order of few meters.

Tailings or dredge material beaches present similar morphological features as natural deltas, where the input river is the end of a pipeline. Figure 2 shows a picture of an oil sands external facility beach, which is very comparable in morphological features to the natural deltas of Figure 1. Yet, tailings beaches may differ from natural deltas by solids densities and when fine dominated. Mining and dredging industry is indeed transitioning toward higher solids density slurries often dominated by fines (e.g. flocculated tailings, thicken tailings or non-segregating tailings). Fine dominated tailings beaches show different morphological features with less, long and stable channels terminating in flow widening lobes (Figure 3).

TAILINGS SPECIFIC PROCESSES

Diluted sand dominated deltas are driven by typical alluvial processes that are rather well understood and implemented in numerical models such as Delft3D (van der Vegt et al. 2015). High solids concentration typical of tailings or slurry streams, and large quantity of fines induce specific tailings processes. Thick and flocculated tailings shows higher viscosity towards non-Newtonian, near-laminar or completely laminar behavior, where sand settles depending on the rheology of the carrier fluid (i.e. water plus fines) and flow regime. Settled sand form a high sand concentration layer near the bed. This layer is not static, but flows at lower velocity due to the increase viscosity induced by higher sand concentration. We call this layer gelled bed (Sisson et al., 2012). These tailings also show relatively rapid change of characteristic with time due to dewatering and thixotropy. These processes are detectable in 1D vertical or 2D vertical (e.g. a cross section along a beach). In 3D, channel width and avulsion (i.e. change in course) are likely determined by tailings rheology and sand segregation (Pirouz et al., 2013). While 2D processes have been documented, 3D behavior is still poorly understood and demand for further research.

In this paper we focus on rheology and sand settling processes, leaving thixotropy and 3D to a later stage. The theoretical framework to describe sand-fines slurry flow and segregation behavior includes a dual rheology approach (Spelay 2007, Talmon et al. 2014). The rheology of the sand-mud mixture is quantified for flow momentum simulations. The rheological parameters (inherent viscosity, Thomas 2010) of the carrier fluid (fines+water only) determine sand segregation (e.g. settling of coarse particles within the carrier fluid), which includes shear induced settling.

Three different existing rheological formulations which are traditionally utilized in different fields, i.e., industrial concentrates, tailings and fluid mud flow in natural environments, are compared and included in Delft3D. The implemented formulation utilizes Bingham-type model concept:

$$\tau = \tau_y + \mu\gamma \qquad (1)$$

where τ is the shear stress, τ_y the yield stress, μ the plastic viscosity and $\bar{\gamma}$ the shear rate. More details on the theoretical description of the rheological models can be found in Talmon et al. (2016) and Hanssen (2016).

The shear induced hindered settling of a sand particle in a non-Newtonian flow can be described as:

$$w_{s,eff} = w_{s,0}(1-k\phi_{sol})^n = \alpha\frac{(\rho_s-\rho_{cf})gd^2}{18\mu_{apparent-cf}}(1-k\phi_{sol})^n$$

Where $w_{s,eff}$ is the effective settling velocity, $w_{s,0}$ is the non-hindered settling velocity, ϕ_{sol} is the volumetric concentration of solids, α a calibration parameter, ρ_s the density of sand particles, ρ_{cf} the density of the carrier fluid, d is the sand diameter and μ the apparent viscosity. The parameters k and n are determined empirically (Pennekamp et al., 2010; Sisson et al., 2012; and Spelay, 2007). The formula is verified with shear cell data in the work of Pennekamp et al. (2010). Confirmation is also found in shear cell tests by Sisson et al., 2012 and Talmon et al., 2014.

NUMERICAL APPLICATION TO OIL SANDS TAILINGS

The three rheological analytical models and the sand settling relations were implemented in Delft3D, and verified in 1DV mode against theoretical derivations (Slatter and Williams, 2013) and experimental observations (Spelay 2007, Pirouz 2013). Details of numerical implementation and testing can be found in Hanssen (2016).

Upon verification against experimental data, the model was applied in 1DV to two typical oil sands tailings streams: low sand, high carrier fluid viscosity thickened tailings (TT), and high sand lower carrier fluid viscosity tailings streams (NST). Rheological parameters are assumed as typical tailings data to verify behavior, and are not referring to specific tailings. Table 1 reports the characteristics of the two streams.

Table 1. Characteristic of conceptual oil sands tailings mixtures

	Cs_w*	SFR	τ_y	ρ
	%	-	Pa	kg/m^3
TT	40	0.25	40	1,330
NST	67.5	5	20	1,725

* Solids content by weight

The 1DV simulations were run to approximate simulation of tailings flow down a 1 km 1% slope at a constant 1 m^3/s flow rate and constant tailings discharge characteristics. Two fractions were included in the model: fines and sand, in addition to water. Water and fines form the carrier fluid, which in the model is not allowed to change its properties with time (i.e. zero settling of fines, no dewatering, no thixotropy). Tailings flow down a slope is a 3D process by definition, therefore 1DV simulations represents an approximation of a cross section along a beach, in one single profile that evolves in time following the flow.

Figure 4 and Figure 5 show the results of the 1DV simulations. A uniform mixture was discharged from the hypothetical pipe, and let run down the slope. The velocity (left) and sand to fines ratio (SFR, right) profiles are depicted at 100 m, 500 m, and 1,000 m along the slope. The three lines represent the three different rheological models (Hanssen 2016).

The TT simulations show a typical non-Newtonian plug-flow like velocity profile, with a sheared zone that extends for the lowest 25% to 30% of the flow. Sand settling is a function of the shear rate. The SFR profile shows decrease in sand concentration in the shear zone, and increase near the bed. Sand depletion in the shear zone and accumulation near the bed increases away from the discharge point. Flow velocity diminishes as sand concentration increases due to increase in mixture viscosity. However, even if much slower, the sand rich layer does not build a sand skeleton and continues to flow. This is consistent with the findings of Talmon (2010). Again, the three rheological models influence the sand settling behavior. The three models show rather different sand settling behavior, especially Model 1 (dashed line) from Model 2 (solid line) and Model 3 (dotted line). Model 1 is based on the Herschel-Bulkley rheological model, with exponent of the shear rate (Eqn 1) between zero and one. This model produces a less thick sheared region with locally higher shear rates. This causes a thinner layer where sand settles faster, yielding to lower sand concentration and sharper gradients. At this moment which rheological model is the most accurate for sand segregation is uncertain and under investigation. Verification likely requires specific high resolution data to be collected. Independently on the rheological models, all simulations show consistent behavior in line with theoretical expectations and experimental observations.

The NST simulation was run for a single rheological model only. This simulation shows different and, at first sight, counterintuitive behavior. The flow profile still displays a non-Newtonian plug flow profile. Since sand is only settling in the sheared velocity profile and no sand is supplied from the plug, the sand concentration directly under the plug decreases strongly. This allows for a greater velocity gradient. The sharp decrease of sand concentration at the bottom of the plug only occurs only at high sand concentrations because of a greater sensitivity of rheological parameters to sand.

As soon as sand settles, it packs up immediately with sharp increase mixture viscosity and decrease in flow velocity. The settled material comes to a halt. This is not too different from the TT simulations with Model 1, which expressed the largest sand concentration gradients. Because of the initially large sand concentration, additional sand accumulation near the bed is limited.

The last observation relates to flow velocity, which is lower in the TT case than the NST case. This is because in these concept simulations a rather viscous carrier fluid is imposed. The TT having a larger fraction of carrier fluid compared with the sand rich NST, the TT ends up with stronger mixture rheology, even at lower sand content. Rheology values where chosen in this study to highlight this behavior. This may not be the case in actual oil sands tailings.

As depicted in Figure 4 and Figure 5, this model can compute SFR profile, or average SFR if averaged, along any cross section. By comparing SFR along the beach with input SFR, fines capture can be estimated.

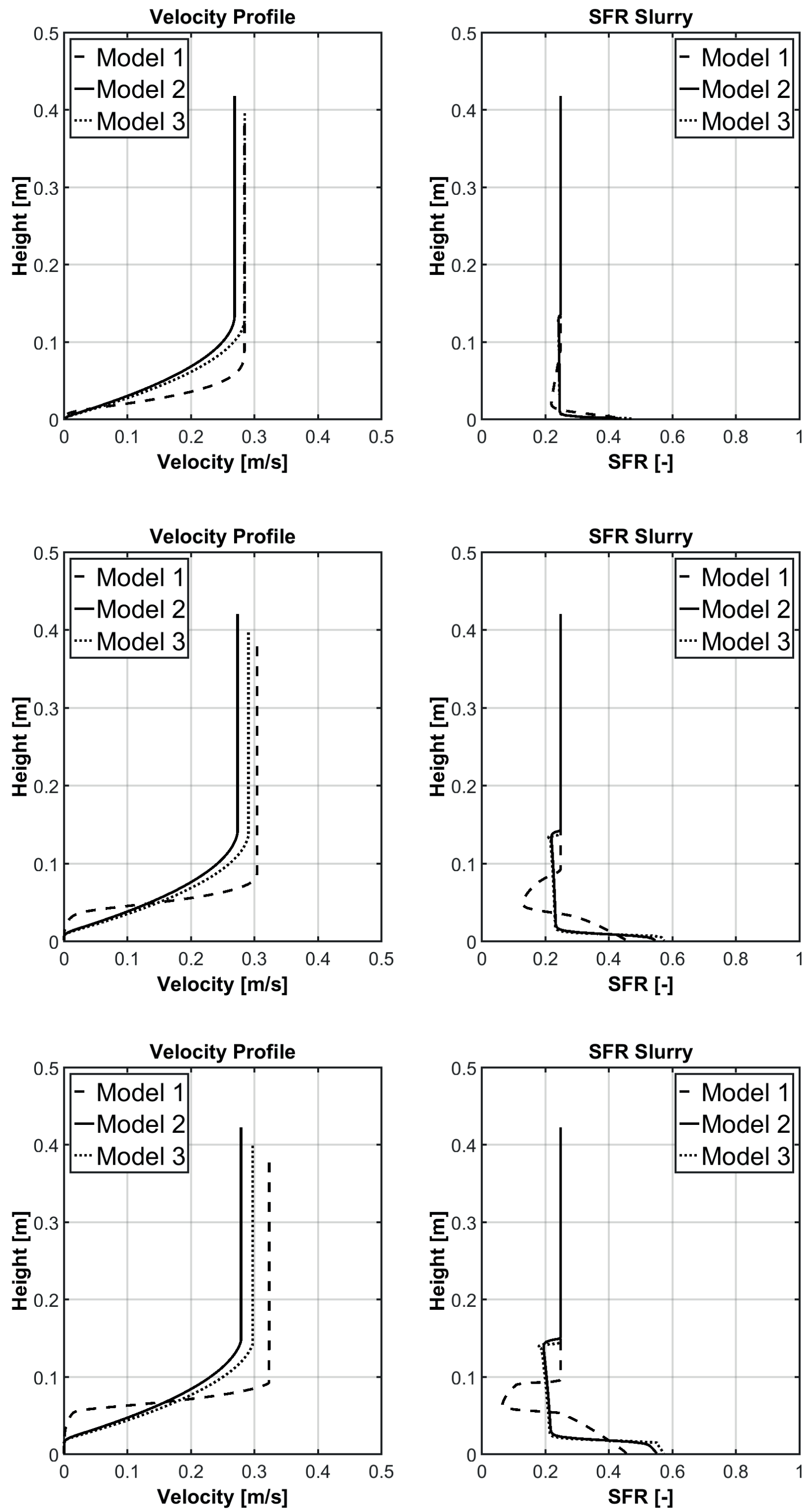

Figure 4. Results of concept TT simulations down a 1 km beach, after 100 m (top), 500 m (middle) and 1,000 (bottom). Left plots: velocity profile; right plots: SFR profiles. Three lines indicate three different rheological models.

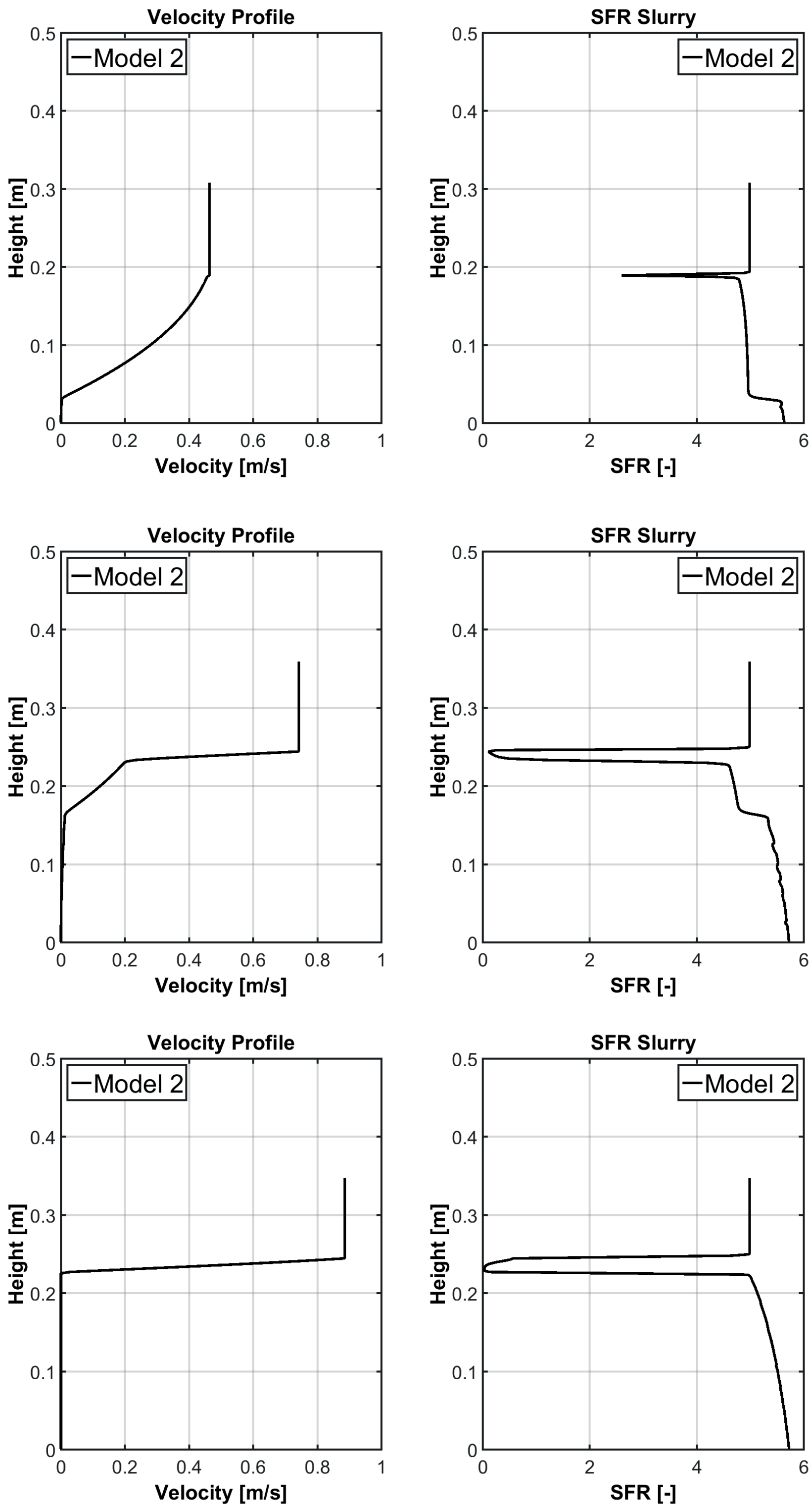

Figure 5. **Results of concept NST simulations down a 1 km beach, after 100 m (top), 500 m (middle) and 1,000 (bottom). Left plots: velocity profile; right plots: SFR.**

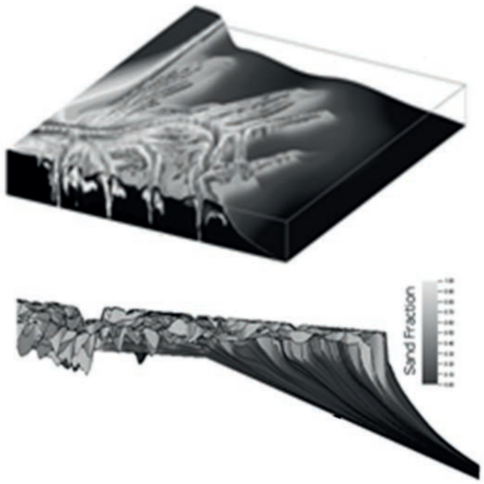

Figure 6. **Re-drawn from van der Vegt et al. (2015), Delft3D simulations of alluvial delta. Topography and bathymetry (top), where gray scale represents elevation; and cross section across the deposit (bottom), where gray scale represent fraction of fines (dark) and sand (light). Interesting to notice how most fines are trapped in the beach below water (BBW) section of the deposit, in line with fines capture observation in oil sands tailings beaches.**

STEPS FORWARD TOWARDS 3D BEACH DEPOSITION PREDICTION

The latest numerical enhancement described in the previous section refer to upgrading Delft3D to simulate high solids content and thick non-Newtonian tailings, so to cover a wide spectrum of tailings properties.

Full 3D delta (or tailings beaches) simulations for alluvial systems or diluted whole tails are already possible in Delft3D open source. Delft3D includes also a full deposit stratigraphy scheme which allows keeping track of the deposited particle size distribution, as well as erosion and deposition functions with direct feedback to the morphology (Figure 6).

At the time of writing, the expanded Delft3D with the formulations described in the section above is being tested in 2DV mode (e.g. a beach cross section), and compared to oil sands fines capture data.

The strategy forward toward full simulation of 3D tailings deposition behavior has multiple possible paths, and can be steered by industry needs. This does not limit to numerical enhancement and simulation, but it is necessarily coupled with theoretical advance and laboratory or, better, pilot of field observations.

A logical path forward after testing in 2DV is to attempt 3D simulations (already within the capability of Delft3D), and to compare those to pilot or field observations. We especially expect channel width, erosion / deposition and avulsion patterns to be driving mechanisms for determining beach slope and deposit characteristics. Similarly, deposition of coarse tailings within existing fluid tailings basins represents another interesting application for which the upgraded Delft3D may be an ideal tool. In this case focus should be on 2DV processes, especially vertical mixing. If interaction with different tailings streams or co-disposal at different time intervals is the focus, dewatering and thixotropy may need to be included, driving development in this direction.

CONCLUSIONS

This paper described the most recent advance in simulating tailings and slurry flow deposition behavior for a wide range of tailings properties. The philosophy of this study is to enhance the capabilities of an existing tool, Delft3D, which is open source and used daily by thousands of people worldwide in engineering projects.

Latest results in 1DV mode were presented in this paper with direct conceptual application to typical oil sands tailings. The model reproduced non-Newtonian sand segregating behavior in agreement with theoretical expectation and laboratory observations. In depth testing and validation in 1DV and 2DV are on-going at the time of writing this paper.

Open source Delft3D has proven to be able to simulate alluvial deltas of high-level of complexity. This tailings and slurry extension has so far revealed to be adequate to simulate fundamental tailings and slurries deposition processes in 1DV. Especially this model proved to be a useful tool to show how changes in rheological parameters and sand content influence variation, sometimes pronounced, in flow and sand settling behavior, therefore implication to SFR and fines capture. As all models, this model is a tool with physically based assumptions and approximation, which, in this specific case, helps physical understanding and evaluation of possible tailings management scenarios. Therefore, it should be best utilized not alone, but aside to rheological and field tests, so to couple understanding, observations and predictions.

Here we have proposed different strategies for applications, which follow practical opportunities in line with specific industry needs. Indeed, while development never ends, the authors believe that each next step cannot be limited to numerical enhancement. An existing tool, such as the one presented in this paper, needs to be validated against pilot of field data designed for a specific application, judged on degree of accuracy, utilized accordingly, and further developed as necessary. Therefore, when properly calibrated against actual data from specific applications, this model can be utilized to evaluate different scenarios, technologies and aid tailings management decisions.

REFERENCES

Hanssen, J. L. J., 2016. Towards improving prediction of non-Newtonian settling slurries with Delft3D: theoretical development and validation in 1DV. MSc thesis Delft Technical University of Technology.

Pennekamp, J. G. S., Talmon, A. M., & van Kesteren, W. G. M. 2010. Determination of Non-Segregating Tailings Conditions. In 19th World dredging congress (pp. 848–858).

Pirouz, B., Seddon, K., Pavissich, C., Williams, P., & Echevarria, J. 2013. Flow through tilt flume testing for beach slope evaluation at. In Paste 2013 (pp. 457–472).

Sisson, R., Lacoste-bouchet, P., Vera, M., Costello, M., Hedblom, E., Sheets, B., Nesler, D. Solseng, P., Fandrey, A., van Kesteren W.G.M., Talmon, A., Sittoni, L. 2012. An analytical model for tailings deposition developed from pilot scale testing. In 3rd International oil Sand Tailings Conference.

Slatter, P. T., & Williams, A. T. C. 2013. Analysis and flow behaviour prediction of paste material in sheet flow. In Paste 2013 (pp. 473–480).

Sheets B., Wagner T., Swenson J., Horton J., Langseth J., Sittoni L., Walstra D.J.R., Winterwerp J.C, Uittenbogaard R., van Kester J., Talmon A.M., 2004. Muddy river deltas as analogues for oil sand tailings beaches: improving fines capture and operational efficiency with tailings beach deposition modeling. Proc. 4th Int. Oil Sand Tailings Conference, IOSTC (eds. D. Sego, G.W. Wilson and N. Beier), Lake Louise, Canada, pp.397-405.

Spelay, R. B. R. 2007. Solids transport in laminar, open channel flow of non-newtonian slurries . PhD thesis at University of Saskatchewan

Talmon, A.M. ,2010, Regarding “Are tube viscometer data valid for suspension flows” [Letter to the editor], Korea-Australia Rheology Journal, Vol. 22(3), pp.169-171.

Talmon, A.M., Hanssen, J. L. J., Winterwerp, J.C., Sittoni, L., van Rhee, C., 2016. Implementation of tailings rheology in a predictive open-channel beaching model. PASTE 2016, Santiago del Chile.

Talmon, A. M., van Kesteren, W. G. M., Sittoni, L., & Hedblom, E. P. 2014. Shear cell tests for quantification of tailings segregation. Canadian Journal of Chemical Engineering, 92(2), 362 373.

Thomas A.D, 2010, Method of determining the inherent viscosity of a slurry and other rheological trends as illustrated by a data bank of over 200 different slurries, 18th Hydrotransport conference, Rio de Janeiro, Brazil, 325 340.

Vegt H. van der,. Storms J. E.A., Walstra D. J. R, Howes, N.C. 2015. Analysis tools to quantify the variability in deltaic geological models using Delft3D simulation results. 2nd EAGE Conference on Forward Modelling of Sedimentary Systems.

LARGE-STRAIN CONSOLIDATION MODELING TO DETERMINE REPRESENTATIVE TAILINGS CONSOLIDATION PROPERTIES FROM TWO MESO-SCALE COLUMN TESTS

Jason Stianson[1], Robert Mahood[2], Delwyn G. Fredlund[1] and Josh Sun[1]
[1]Golder Associates Ltd.
[2]Shell Canada Energy

ABSTRACT

Shell Canada Energy has undertaken a technology development project that involved the use of column tests, or geocolulmns, to study large-strain consolidation of flocculated oil sand tailings. The tests were initiated in 2014 and involved columns that were 3 m high with 0.6 m in diameter. Tailings in the two columns analyzed were treated with a dewatering amendment known as XUR and partially-hydrolyzed polyacrylamide (HPAM), respectively. Large-strain consolidation modeling was used to back-analyze the self-weight consolidation behaviour of the tailings and thereby determine representative consolidation property functions; namely, hydraulic conductivity and compressibility properties. This paper presents the modeling steps used to ascertain representative consolidation properties of the amended oil sand tailings.

INTRODUCTION

Shell Canada Energy (Shell) is conducting an integrated program of consolidation testing using various size specimens and spanning a range of effective stresses and overall sample volumes (Figure 1). Tests include graduated cylinders (0.15-0.4 m high by 58 mm diameter), large-strain consolidometers (0.1 m high by 150 mm diameter), geocolumns (3 m high by 0.6 m diameter), casings (10 m high by 2.75 m diameter), test cells (5 m deep by ~2,500 m^2), and beam centrifuge. The intention is to back-analyze the measured consolidation response and determine representative compressibility and hydraulic conductivity relationships from each type of test (i.e., tests were conducted at different scales of samples but on the same type of treated tailings.). The results are used to develop representative compressibility and hydraulic conductivity relationships that are applicable for the design of full-scale, commercial reclamation of tailings.

This paper provides a summary of the first phase of large-strain consolidation modelling being conducted by Golder Associates Ltd. (Golder), focusing on the back-analysis of two of the geocolumn tests being conducted by Shell. The large-strain consolidation modelling considered the period of self-weight consolidation which extended over a period of approximately two years from deposition to March 29, 2016 (Note: GC1 deposition on August 14, 2014 and GC2 deposition on July 30, 2014). After self-weight consolidation is complete, Shell will use a custom built load frame to apply increasing pressure increments to further consolidate the tailings. Back-analysis modelling will be updated after the completion of each pressure increment, and with time, include other datasets from a casing pilot project (Stianson et al. 2016) and other lab and field data.

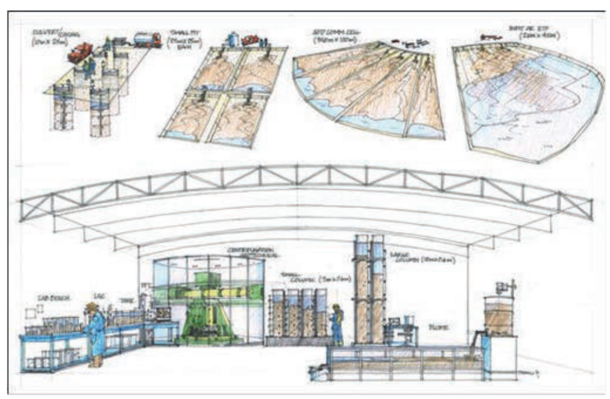

Figure 1. Steps in the Shell tailings technology evaluation program

GEOCOLUMNS

Shell initiated three 3 m high by 0.6 m diameter column tests in Q3 of 2014 to study the large-strain consolidation behaviour of oil sand tailings amended with two different chemicals. The column tests have been named Geocolumn 1, 2, and 3 (with acronyms GC1, GC2, and GC3) (Figure 2). Tailings in GC1 were treated with

HPAM 3338 (HPAM) while tailings in GC2 and GC3 were treated with a Dow amendment known as XUR.

The HPAM and XUR treatment levels were 1,000 parts per million (ppm) and 1,900 ppm of dry polymer weight per dry weight of FFT solids, respectively and applied using a flow rate of approximately 2 USGPM and 10 USGPM respectively (Poindexter et al. 2015).

Figure 2. Picture of Geocolumn 1, 2 and 3

The tailings in GC1 and GC2 were poured in one lift to a height of approximately 2.75 m. The columns have been monitored for approximately two years under self-weight consolidation conditions. Monitoring has included: 1) pore-water pressure measurements using external transducers installed along the profile of the column (Figure 3), and 2) visual measurements to track the tailings water interface or mudline settlement. The increase in average tailings solids content was calculated based on mudline measurements. At the time of this paper in 2016, Shell plans to collect sample and measure solids content profiles. The elevation of pressure transducers installed on the sides of GC1 and GC2 are presented in Table 1. Supporting laboratory tests were also undertaken to measure the index properties of the as-placed tailings in each geocolumn (Table 2).

Table 1. Summary of transducers installed on GC1 and GC2

GC1		GC2	
Transducer	Elevation	Transducer	Elevation
PT1	0	PT1	0
PT2	0.335	PT2	0.335
PT3	0.585	PT3	0.585
PT4	0.835	PT4	0.835
PT5	1.085	PT5	1.085
PT6	1.585	PT6	1.585
PT7	2.085	PT7	2.085

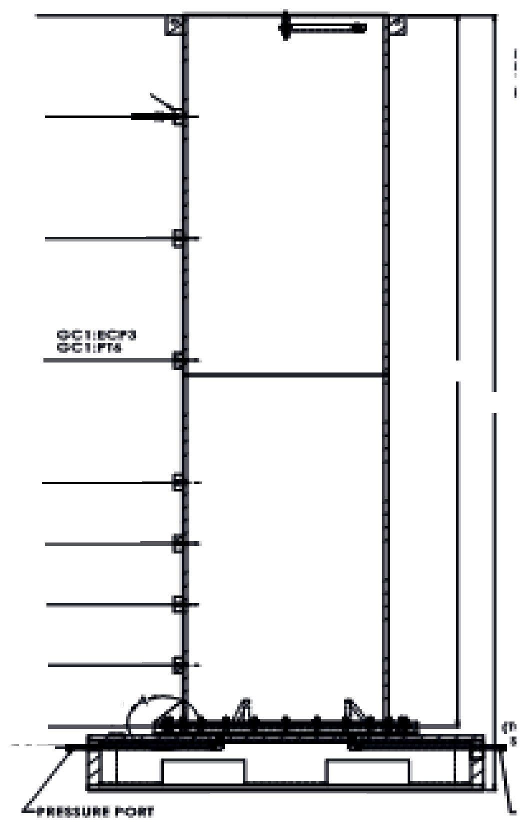

Figure 3. Drawing of the Geocolumn 1 and the location of the pressure transducers

Table 2. Summary of as-placed tailings index properties

Geocolumn	Solids Content (%)	Bitumen (%)	Specific Gravity	MBI	PSD < 44 μm (%)	Yield Stress (kPa)	Liquid Limit (%)	Plastic Limit (%)	Plasticity Index (%)
1	32.3	2.82	2.17	7.0	90.2	261.5	46	20	26
2	31.0	2.86	2.24	7.0	89.5	48.0	48	23	25
3 (Pour 1)	28.3	2.49	2.28	6.8	89.6	60.2	48	28	20
3 (Pour 2)	28.8	2.53	2.24	6.6	88.9	35.7	47	26	21

DATA ANALYSIS AND INITIAL CONDITIONS

The monitoring data for GC1 and GC2 was post-processed to assess the initial period of sedimentation, the degree of consolidation, and estimate initial consolidation properties (i.e., hydraulic conductivity and compressibility) to serve as the starting point for the overall consolidation modeling approach.

Sedimentation to Consolidation Transition

The transition solids content (TSC) was considered to mark the end of sedimentation, the beginning of consolidation, and the starting point for large-strain consolidation modeling. The TSC was evaluated using two different approaches, one approach based on settling tests conducted in graduated cylinders and a second approach based on the velocity of the settling front observed in GC1 and GC2.

The graduated cylinder settling tests recognize that the TSC will occur at the mudline in a full-scale operation and corresponds to the solids content at the surface of the deposit where the effective stress is near to zero. A series of three small scale settling tests were conducted in graduated cylinders to estimate the TSC. Settling tests were conducted in 1,000 ml, 500 ml, and 250 ml size cylinders; namely, samples of decreasing volume and in turn decreasing effective stress levels. The average solids content and sample volume was calculated based on settled tailings height in each cylinder. A graph of solids content versus sample volume was prepared and linear extrapolation was used to estimate the solids content for a sample of zero volume (Figure 4). In other words, a sample with zero effective stress simulating an infinitely thin layer at the tailings surface.

The TSC for GC1 was estimated to be 33.5% and is about 1% higher than the deposition solids content of 32.3% (i.e. corresponding to a tailings height of 2.61 m and void ratio of 4.3). There is some scatter in the solids content data from the three cylinder tests on GC1 material making it difficult to interpret a straight line fit through the data. The GC2 TSC was estimated to be 39.8% and is about 9% higher than the deposition solids content of 31%. The solids content data from the three cylinder tests on GC2 material appear to provide a reasonable fit along a straight line.

The second method of determining the TSC is based on the approach described by Pane and Schiffman (1997) where sedimentation is identified when the velocity of the settling front is constant. The incremental settling velocity (υ_{si}) of the tailings surface is determined from the settlement data according to Eq. [1].

$$\upsilon_{si} = \frac{h_2 - h_1}{t_2 - t_1} \qquad [1]$$

where, h_1 is the height of the sample at time t_1, h_2 is the height of the sample at time t_2. The resulting settling velocity versus time relationships for GC1 and GC2 are presented in Figure 5.

The TSC for GC1 was estimated to be 34.3% occurring at an elapsed time of about 60 minutes after deposition, at a tailings height of about 2.55 m, and void ratio near 4.2. The TSC for GC2 was estimated to be 40.2% occurring at an elapsed time of about 510 minutes (i.e., 8.5 hours) and at a tailings height of about 1.97 m. The TSCs evaluated from the settling velocity of GC1 and GC2 appear to be similar to the values estimated from separate cylinder tests.

Initial Consolidation Properties

Back analysis modeling involves an iterative approach where initial consolidation property functions are estimated and then adjusted until the model provides a reasonable match to measured data. The efficiency of the procedure can be increased if initial consolidation property estimates are reasonable. The following sections highlight how initial consolidation properties can be estimated using settlement data, pore-water pressure measurements, and supporting laboratory measurements.

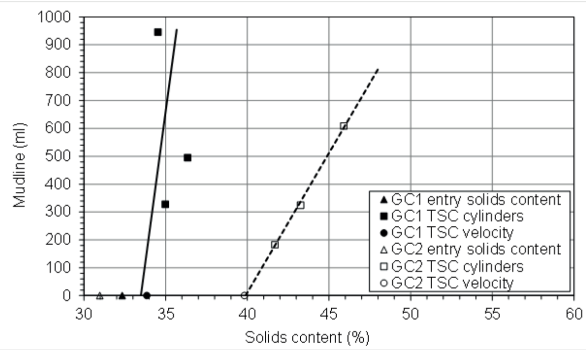

Figure 4. GC1 and GC2 sedimentation graduated cylinders

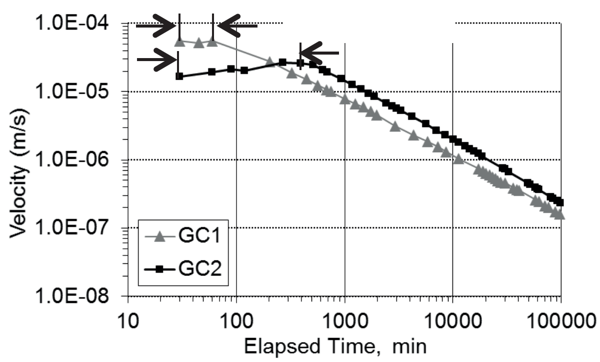

Figure 5. GC1 and GC2 sedimentation velocity

Initial Hydraulic conductivity

Settlement data was used to estimate tailings hydraulic conductivity for a series of average void ratio conditions. The initial velocity of the settling front was used to compute an equivalent hydraulic conductivity during sedimentation (i.e., over the high void ratio range) and the Casagrande and Taylor construction procedures were used to estimate tailings hydraulic conductivity during self-weight consolidation at average void ratios. The estimated hydraulic conductivity values were compared to existing measurements on fluid fine tailings (FFT) which represent the lower bound hydraulic conductivity for tailings that have not been flocculated.

The initial settling velocity of the GC1 and GC2 tailings (Figure 5) was used to calculate an equivalent hydraulic conductivity during sedimentation according to the procedure described by Pane and Schiffman (1997). The equivalent hydraulic conductivity, *k*, was computed using Eq. [2]:

$$k(e_o) = \frac{v_{si_{avg}}(1+e_o)}{G_s - 1} \qquad [2]$$

where, e_o is the initial void ratio, G_s is the specific gravity, and $v_{si_{avg}}$ is the average initial settling velocity of the solids (i.e., 5.6x10^{-5} m/s for GC1 and 2.6x10^{-5} m/s for GC2). The approach is considered valid, "*only as long as there is suspension of the initial porosity at the sediment-water interface, that is, as long as the surface settling velocity is constant.*" The resulting equivalent hydraulic conductivity values for GC1 and GC2 were computed to be 2.6x10^{-4} m/s and 1.2x10^{-4} m/s, respectively. The values have been plotted in Figure 6 representing the upper bound hydraulic conductivity over the range of void ratio where sedimentation occurs.

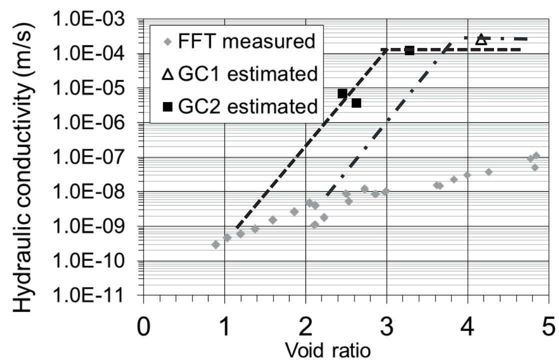

Figure 6. Initial estimates of hydraulic conductivity calculated based on settlement measurements

The hydraulic conductivity during self-weight consolidation was calculated using Eq. [3]:

$$k = \frac{C_v \alpha_v \gamma_w}{1+e} \qquad [3]$$

where, a_v is the coefficient of compressibility (i.e., $\Delta e/\Delta\sigma'$), γ_w is the unit weight, *e* is the average void ratio, and C_v is the coefficient of consolidation (i.e., Eq. [4] for Casagrande's method and Eq. [5] for Taylors method.).

$$C_v = \frac{TH^2}{t_{50}} \quad [4]$$

$$C_v = \frac{TH^2}{t_{90}} \quad [5]$$

The calculation parameters and estimated GC2 hydraulic conductivity values for both methods are listed in Table 3. The corresponding Casagrande and Taylor construction of the settlement data used to determine t_{90} and t_{50} are presented in Figure 7 and Figure 8, respectively. The self-weight consolidation of GC1 did not progress to the same degree which indicated the hydraulic conductivity was less than GC2 and precluded the completion of similar construction analysis.

The estimated hydraulic conductivity values for GC2 are plotted in Figure 6 and provide an estimate of the hydraulic conductivity as the tailings consolidate to lower void ratios and approach the hydraulic conductivity of FFT.

Table 3. GC2 Casagrande and Taylor parameters

Parameter	Taylor	Casagrande
t90 Taylor t50 Casagrande	4.1	2.2
H (cm)	177.6	167.3
C_v (cm^2/s)	7.46E-2	2.89E-2
a_v (/kPa)	0.329	0.470
e (average)	2.46	2.63
k (m/s)	6.97E-6	3.67E-6

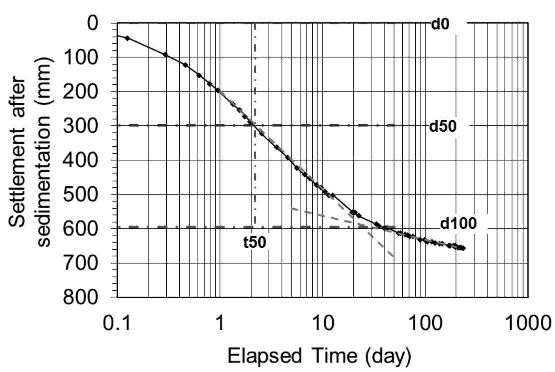

Figure 7. Casagrande construction of GC2 settlement data

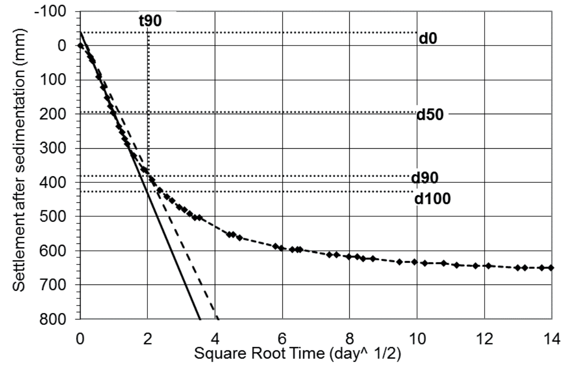

Figure 8. Taylor construction of GC2 settlement data

Initial Compressibility

Initial tailings compressibility data was estimated based on the average void ratios computed from settlement and average effective stresses computed from pore-water pressure measurements. The average void ratio and effective stress data points are compared to measured FFT compressibility data in Figure 9. The end of deposition and end of sedimentation void ratios are plotted along the y-axis to indicate that the effective stress is assumed to be near to zero. The remaining compressibility data appears to be similar to measurements on raw FFT.

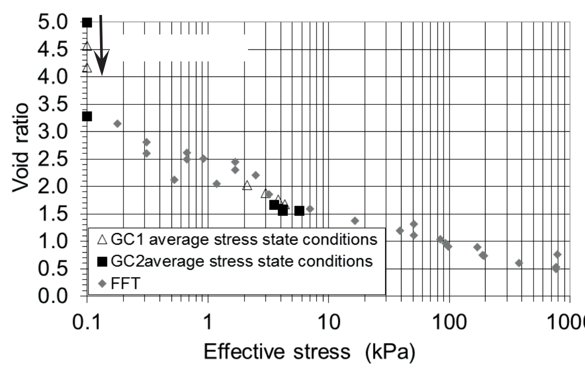

Figure 9. Initial estimates of compressibility based on measured settlement

Degree of Settlement versus Degree of Excess Pore-Water Pressure Dissipation

A new method was developed for evaluating the consolidation performance of a column test through the development of a normalized presentation of settlement and pore-water pressure data into one graph. The method is based on the relationship between degree of settlement (percent) and degree of excess pore-water pressure dissipation (percent). The degree of settlement was calculated using Eq. [6]:

$$(h_i - h_t)/(h_i - h_f) * 100\% \qquad [6]$$

where h_i *is* the initial tailings height, h_t is the tailings height at time (t), and h_f is the final tailings height when the degree of consolidation is 100% (e.g., initially determined by running the consolidation models for an extended period of time and verified once self-weight consolidation is complete.).

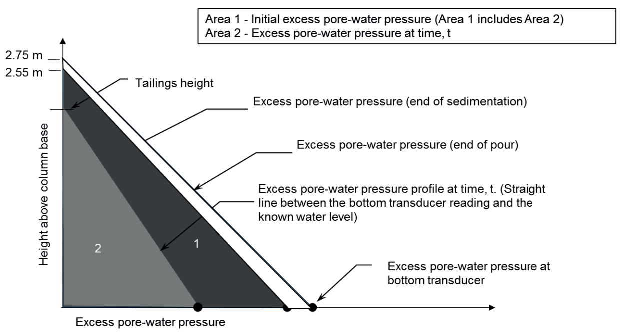

Figure 10. Schematic illustrating the calculation of percent excess pore-water pressure dissipation

The degree of excess pore-water pressure dissipation was calculated following the approach sketched in Figure 10; namely, Area 1 (darker) minus Area 2 (lighter) divided by Area 1 (i.e., [Area 1-Area 2]/Area 1). The initial pore-water pressure used to compute Area 1 corresponds to measurements collected immediately following the tailings pour (i.e., when the tailings height was approximately 2.75 m). There appeared to be some delay in the transducer response which coupled with some early dissipation of excess pore-water pressure meant that pore-water pressure readings did not always increase to the maximum anticipated values (i.e., equal to the bulk unit weight of the tailings multiplied by the deposited tailings height.). The lower pore-water pressure readings can result in higher initial excess pore-water pressure dissipation percentages.

CONSOLIDATION MODELING

The modeling approach utilized an iterative procedure where initial compressibility and hydraulic conductivity properties were modified to achieve a reasonable match between the measured and simulated response. The measured settlement versus time and incremental excess pore-water pressure profiles were used as the primary measurements for model calibration. In addition, the coefficient of determination, R-squared, (R^2), was used as a statistical tool to evaluate how closely the modelled results matched the measured data for a particular set of consolidation properties. Separate R^2 values were computed for the settlement and pore-water pressure data. The overall R^2 value for the modeling scenario was computed by multiplying the R^2 from the computed settlements by the R^2 from the computed pore-water pressures to give an overall R^2. Representative consolidation properties are considered to correspond to the modeling scenario with the highest R^2 value.

One-dimensional large-strain consolidation modeling was conducted with FS Consol version 3.49 (GWP Geo Software Inc. 2014). The model is formulated based on Gibson's (1967) finite strain consolidation theory.

Modeling Parameters

The governing modeling parameters are presented in Table 4 including the tailings properties, geometry, and boundary conditions. Properties are compared for the end of deposition, end of sedimentation, and end of primary consolidation. The end of sedimentation parameters were used as the initial model conditions. The tailings height estimated at the end of primary consolidation is provided to indicate the final settlement that was used to compute the degree of settlement.

GC1 Model

GC1 consolidation properties were calibrated based on measured settlement and pore-water pressure over a 593 day period from August 14, 2014 to March 29, 2016. Figure 11 provides a comparison between the measured and modelled settlement for GC1. The R^2 value for the comparison is 0.978.

Table 4. Summary of GC1 and GC2 model parameters

Type	Parameter	GC1	GC2
Tailings (end of deposition)	Height (m)	2.75	2.75
	Solids content	32.3%	31.0%
	Void ratio	4.57	5.00
	Unit weight (kN/m^3)	11.9	11.8
Tailings (end of sedimentation initial model conditions)	Height (m)	2.55	1.97
	Solids content	34.3%	40.2%
	Void ratio	4.16	3.3
	Unit weight (kN/m3)	12.2	12.7
	Specific gravity	2.17	2.24
Tailings (end of primary consolidation)	Height (m)	1.64 m	1.30 m
Boundary Conditions	Top of tailings	Constant head 2.75 m	Constant head 2.74 m
	Bottom of tailings	Zero flux	Zero flux

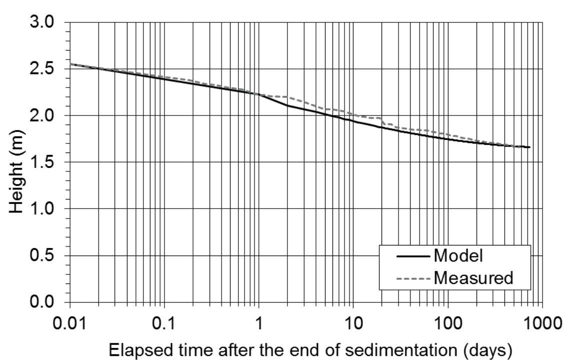

Figure 11. GC1 settlement comparison

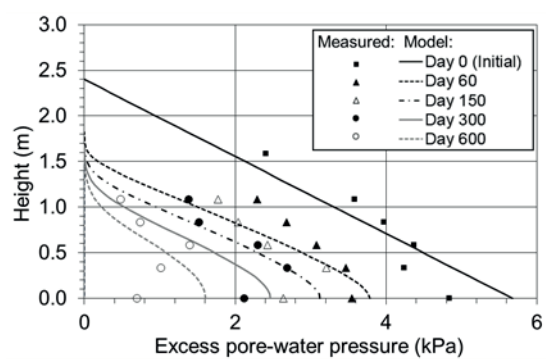

Figure 12. GC1 excess pore-water pressure comparison

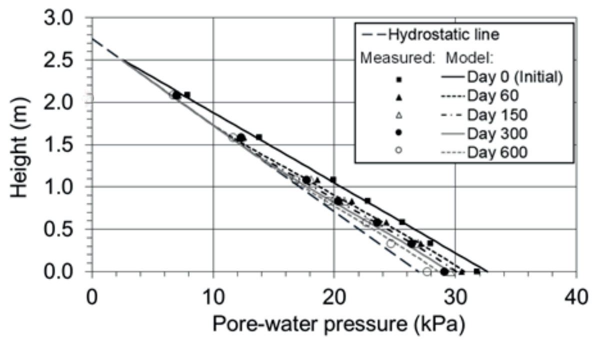

Figure 13. GC1 pore-water pressure comparison

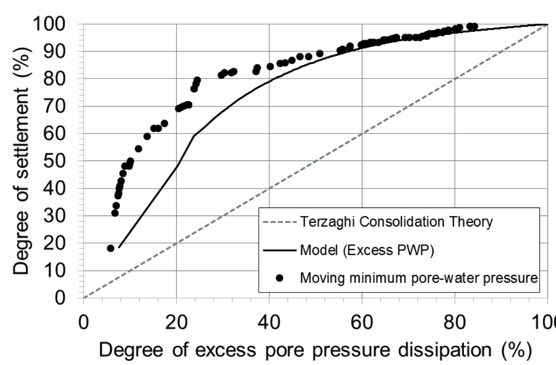

Figure 14. GC1 degree of settlement versus degree of excess pore-water pressure dissipation

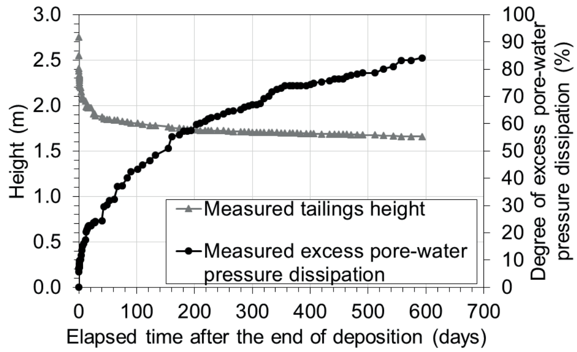

Figure 15. GC1 settlement and degree of excess pore-water pressure dissipation

Figure 12 and Figure 13 provide comparisons between the measured and modelled GC1 excess pore-water pressure profiles and pore-water pressure profiles, respectively. The R^2 value for the pore-water pressure comparison was computed to be 0.988 (i.e., Figure 13).

The degree of settlement versus degree of excess pore-water pressure dissipation relationship is presented in Figure 14. The measured data and model results do not start at the origin illustrating that the period of sedimentation was accounted for although not modelled in detail. It should be noted that the comparison is particularly sensitive during the initial stages of modeling since 70% of the settlement and 20% of the excess pore-water pressure dissipation occurs of the first 20 days of modelling. The data also highlights that GC1 has likely not reached 100% excess pore-water pressure dissipation.

Figure 15 present the relationship between settlement and excess pore-water pressure dissipation in terms of time. The results illustrate that a large portion of the settlement occurs in a short period of time while the excess pore-water pressure requires more time to dissipate. For example, 90% of the settlement corresponds to about 50% excess pore-water pressure dissipation and occurs in about 154 days. The results demonstrate that settlement progresses faster than dissipation of excess pore-water pressure which is significant since tailings management regulations are described in terms of volume (i.e., settlement.).

GC2 Model

GC2 consolidation properties were calibrated based on measured settlement and pore-water pressure over a 608 day period from July 30, 2014 to March 29, 2016. Figure 16 provides a comparison between the measured and modelled settlement for GC2. The R^2 value for the comparison is 0.983.

Figure 17 compares the modelled excess pore-water pressure response to the response computed from the GC2 transducers and Figure 18 compares the modelled and measured pore-water pressure profiles. The R^2 value for the pore-water pressure comparison is 0.986.

The overall 2016 model resulted in an R^2 value of 0.969 considering all the measured data up to March 29, 2016. The model results seem to provide a reasonable agreement with the settlement data, capture the initial and final excess pore-water pressure, but results in faster dissipation of excess pore-water pressure for intermediate time increments. More emphasis was placed on calibrating to the settlement measurements since pore-water pressure measurements proved challenging and showed greater fluctuations over time.

The degree of settlement versus degree of excess pore-water pressure dissipation relationship is presented in Figure 19. Similar to GC1, the measured data and the model results do not start at the origin illustrating that the period of sedimentation was accounted for although not modelled in detail. Both the measured and modelled data seem to confirm that GC2 consolidation is nearly complete.

Figure 20 presents the relationship between settlement and excess pore-water pressure dissipation versus time. The results are similar to GC1 illustrating that a large portion of the settlement occurs in a short period of time while the excess pore-water pressure requires more time to dissipate. For example, 90% of the settlement corresponds to about 60% excess pore-water pressure dissipation and occurred in about 13 days.

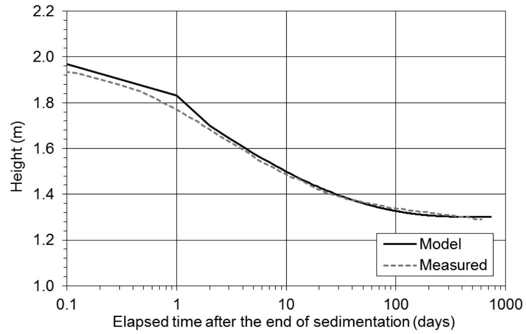

Figure 16. GC2 settlement comparison

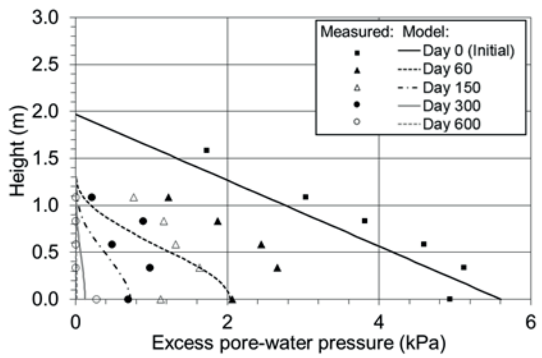

Figure 17. GC2 excess pore-water pressure comparison

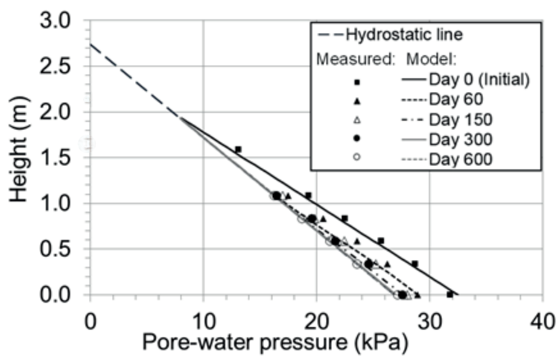

Figure 18. GC2 pore-water pressure comparison

CALIBRATED CONSOLIDATION PROPERTIES

The back-analysis approach was used in the assessment of representative tailings properties. Initial consolidation properties were selected based on: i) laboratory testing results on related materials, ii) results from a 2015 modeling study on the geocolumns and iii) compressibility and hydraulic conductivity data computed from the column measurements (e.g., settlement, construction procedures and stress state profiles). Initial hydraulic and compressibility fits were then adjusted after evaluating how well initial modeling results compared to the measured data. In other words, the hydraulic conductivity fit was shifted up or down to increase or reduce the rate of settlement and excess pore-water pressure dissipation and the closeness of the "model fit" was assessed.

The GC1 and GC2 compressibility and hydraulic conductivity functions are presented in Figure 21 and Figure 22, respectively. The compressibility data shows that the height of the geocolumns allowed the tailings properties to be calibrated up to an effective stress near 6 kPa and to a minimum void ratio near 1.5, under self-weight consolidation.

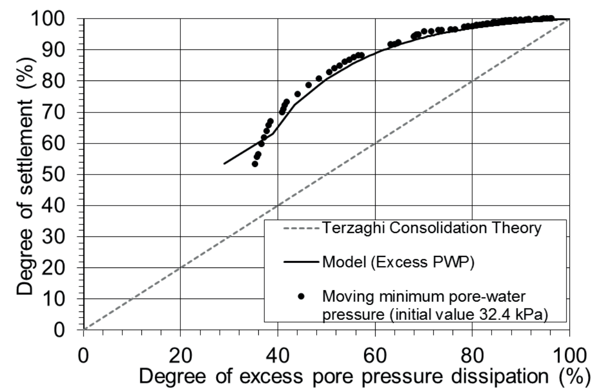

Figure 19. GC2 degree of settlement versus degree of excess pore-water pressure dissipation

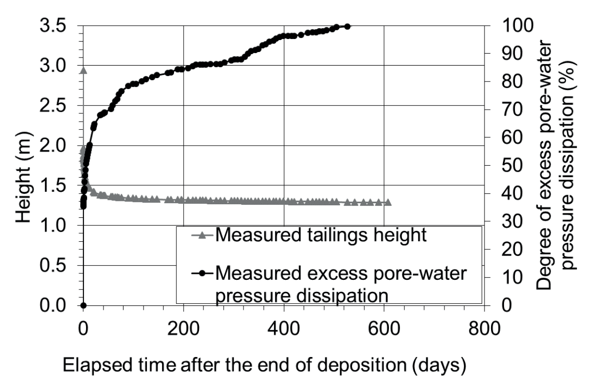

Figure 20. GC2 tailings height and degree of excess pore-water pressure dissipation

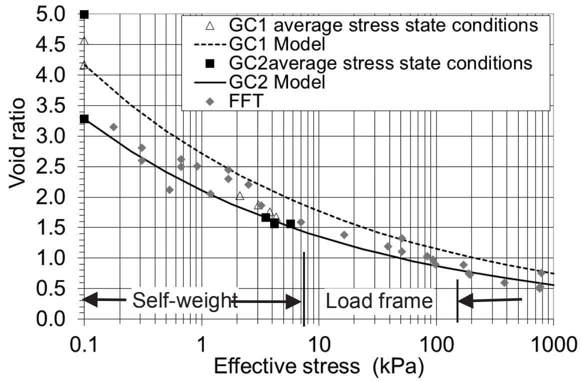

Figure 21. GC1 and GC2 compressibility

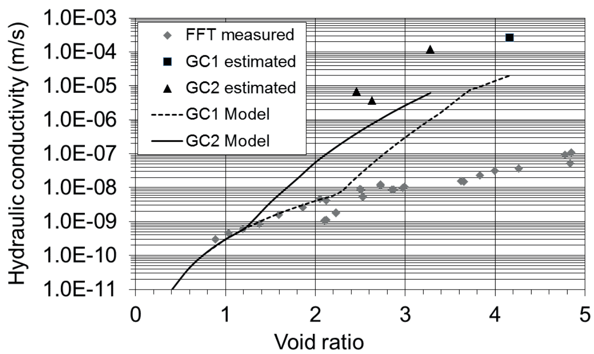

Figure 22. GC1 and GC2 compressibility

The hydraulic properties of the flocculated tailings show the most significant deviation from the properties of raw FFT and result in the following observations:

- The hydraulic conductivity shows the greatest difference over high void ratios with the values for flocculated tailings being two to three orders of magnitude higher than raw FFT.
- The hydraulic conductivity of the flocculated material decreases as consolidation progresses and eventually approaches similar values as FFT.
- The GC2 tailings flocculated with HPAM appear to approach FFT hydraulic conductivity levels near a void ratio of 2.3 and the GC2 tailings flocculted with XUR approach FFT values at a lower void ratio near 1.4.

FUTURE WORK

Ongoing and planned work will involve physical sampling of the tailings to validate assumed solids content, release water characterization and a series of loading stages applied with a load frame (Figure 23). The load frame will be used to increase the effective stress to between 100 kPa to 200 kPa. The maximum stress will be dictated by the strength of the acrylic columns. Specialized soft soil samplers and vane shear devices will be used to measure profiles of solids content and undrained shear strength in between loading increments.

Figure 23. GC1 and GC2 load frame assembly

CONCLUSION

The following conclusions are provided after evaluating the GC1 and GC2 monitoring data and conducting back analysis consolidation modeling of self-weight consolidation which extended for approximately 600 days.

- Two approaches were introduced to determine the transition solids content (TSC) between sedimentation and consolidation; one based on the interpretation of solids content from a series of separate graduated cylinder settling tests and the other based on an assessment of settling velocity of the tailings in the geocolumn. The two procedures are based on different approaches but appeared to result in similar solids content values (within 1%) defining the transition from sedimentation to consolidation. The transition solids contents were used to define the initial conditions for the start of consolidation modeling.
- Settlement data can be used to evaluate the transition from sedimentation to consolidation,

the equivalent hydraulic conductivity corresponding to the period of sedimentation, the end of primary consolidation, and average hydraulic conductivity during settlement (e.g., using the Casagrande and Taylor constructions.). The initial hydraulic conductivity estimates were used to guide the selection of reasonable consolidation properties for the start of back analysis modeling.

- A new approach was introduced for interpreting consolidation performance based on the relationship between degree of settlement and degree of excess pore-water pressure dissipation. The approach is shown to provide a meaningful means of highlighting various aspects of the consolidation process including, i) illustrating the differences between large-strain consolidation and small-strain Terzaghi consolidation theory, ii) considering the interpretation of degree of consolidation either in terms of settlement (i.e., volume) or dissipation of excess pore-water pressure, and iii) estimating whether primary consolidation is complete for a particular stage of testing.
- The hydraulic conductivity of the flocculated tailings was shown to have the greatest increase in the high void range (by two to three orders of magnitude). It was also shown that the hydraulic conductivity of the flocculated tailings would decrease and eventually reach similar levels as raw FFT as consolidation progressed.
- Customized load frames will be used to extend the characterization of tailings consolidation to higher levels of effective stress in the order of 100 kPa to 200 kPa.
- The calibrated consolidation properties represent a valuable asset that can be used to determine the performance of full scale deposits.

ACKNOWLEDGEMENTS

David Carrier is thanked for his many insights and specific improvements including the use of graduated cylinders to provide transition solids content, as well as the graphical and normalized presentation of settlement and pore water pressure data.

Ian Mountain and Brendan Mahe, Shell Technology Development Technologists, who were responsible for the actual geocolumn pouring. Shana Abdul Salam and Laura Li, Shell Technology Development interns in 2014 and 2015 respectively, who managed data compilation and reporting for the geocolumns

REFERENCES

Gibson, R.E., England, G.. & Hussey, M.J.., 1967. The theory of one-dimensional consolidation of saturated clays. I. Finite non-linear consolidation of thin homogeneous layers. Geotechnique, 17(3), pp.261–273.

GWP Geo Software Inc., 2014. Finite Strain Consolidation for Windows (FSConsol) 3.49 ed., Edmonton, Alberta: GWP Geo Software Inc.

Pane, V., Schiffman, R.L., 1997. The permeability of clay suspensions. Geotechnique 47, 273–288.

Poindexter, M. K.; Gillis, P. A.; Moore, J. S.; Tubbs, J.; Mahood, R. & Freeman, G. (2015), Geotechnical Column Evaluation of New Flocculant Technology for Dewatering Oil Sands Mature Fine Tailings, *in* Tailings and Mine Waste.

Stianson, J., Mahood, R., Thomas, D., Song, J., Li, (2016) A Shell Tailings Consolidation Casing Experimental Pilot Project (TCCEPP), in International Oil Sand Tailings Conference Proceedings.

FIELD PILOT PERFORMANCE RESULTS FOR FLOCCULATED FLUID FINE TAILINGS UNDER THREE DEPOSITIONAL VARIATIONS

Dale Kolstad[1], Ben Borree[1], Jason Song[2] and Robert Mahood[3]
[1] Barr Engineering Co.
[2]O'Kane Consultants Inc.
[3]Shell Canada Energy

ABSTRACT

A field pilot applying Shell's atmospheric fines drying (AFD) process for oil sands mature fine tailings (MFT) management was conducted at Shell Canada's Muskeg River Mine (MRM) between 2012 and 2015. The pilot assessed the dewatering and strength gain performance of treated MFT under three depositional variations; thin (0.5 m) multiple-lifts, thick (1.3 m) multiple-lifts, and a single lift deep (4.5 m) deposit. The rate and magnitude of deposit dewatering and densification – including relative contributions from flocculation and sedimentation (initial dewatering), self-weight-consolidation, evaporative drying, down-drainage, and freeze-thaw consolidation – were assessed through a combination of methods: modeling, laboratory and field measurements, and calculations leveraging more than 700 in situ instrument probes and 300 sample test results. The pilot was designed to address a specific Regulatory objective of ERCB Directive 74, namely short term strength gain.

Results indicate that initial dewatering performance is sensitive to the treated tailings properties; with subsequent dewatering influenced by deposition cycle time, environmental conditions, and site hydrogeological setting. All test deposits dewatered to similar solids content - 60% average - but the deep deposit exhibited higher peak shear strengths and more effective stress after 2 years. Despite significant densification of the treated MFT, none of the depositional approaches achieved the nominal, target end-states of 70 to 75% fines over fines plus water (FOFW) [COSIA, 2014] desired to provide stable, soil-like material for incorporation into a terrestrial reclamation landscape. Enhanced dewatering methods consisting of surcharging/capping, sand layering, wick drains, rim ditching, or others could be considered to advance these materials toward target end-states.

INTRODUCTION

Background

Shell has been using the AFD technology at their Muskeg River Mine (MRM) to recover mature fines tailings (MFT) from their external tailings facility (ETF), dewater the material in drying cells, and finally relocate the material to dedicated disposal areas (DDAs) or waste dumps. The AFD technology started as a field pilot in 2010 and then continued to a commercial scale at MRM beginning in 2012.

The AFD technology is based on rapid water release by flocculating the MFT followed by atmospheric drying to dewater and densify the formed deposits. The technology is based on thin lifts of treated MFT being placed inside sloped cells, where produced water is removed via a perimeter drainage ditch (Dunmola et. al, 2013).

The AFD process uses an in-line flocculation approach where MFT is treated with anionic polyacrylamide (A-PAM) polymer immediately prior to discharge into earthen mixing boxes, followed by flow and deposition into the drying cells. Additional details on Shell's AFD technology and field pilot are provided in the 2012 IOSTC AFD test cell paper (Kolstad et. al, 2012).

Field Pilot

A field pilot applying Shell's AFD process was conducted between 2012 and 2015. The pilot assessed the dewatering, densification, effective stress, and strength performance of treated MFT under three depositional approaches—thin multiple-lifts (Thin ML), thick multiple-lifts (Thick ML), and a single lift deep deposit (Deep Stack)—were investigated. The Thin ML deposit consisted of seven lifts of treated MFT deposited over the course of one year (August 2012 to August 2013), were deposited on an approximate 30 day cycle (excluding winter suspension), and averaged approximately 0.6m in thickness. The Thick ML deposit consisted of three thick lifts of treated MFT deposited over the same time period on an approximate 90-day cycle, and averaged 1.4m in thickness. The Deep Stack deposit consisted of one 4.5-metre-thick lift of treated MFT placed in a continuous pour in early October 2012. Surface water was removed from the field test cells following the initial dewatering, following significant precipitation events, and following snow melt in an effort to enhance the benefits of evaporative drying and freeze-thaw processes.

Each depositional approach was discharged into 1% to 2% sloped field test cells. The three field test cells had a footprint and top sectional area of approximately 2,000 m^2 to 3,000 m^2 each and a depth between 4 metres and 5 metres. Approximately 6,000 m^3 to 10,000 m^3 of tailings were placed into each cell. The perimeter berms were constructed using lean oil sands (LOS), and the foundations were excavated into the upper McMurray Formation [UM] unit.

The saturated hydraulic conductivity of the cell foundations were tested with a Guelph Permeameter. Permeability of foundation material was found to range from 5 x 10^{-6} to 1 x 10^{-7} m/s for the locations tested. This is on the high end of the expected permeability range compared to fine tailings (COSIA, 2012), and thus, the foundation material was not expected to limit under-drainage from the deposits. However, the presence of shallow groundwater near the cell foundations likely reduced its magnitude.

The field test cells were instrumented with over 700 probes mounted on several posts (Figure 1) located throughout the three field test cells to provide profiles of pore-water pressure and volumetric water content (VWC), total pressure at the base of the deposit, surface temperature and albedo, tailings temperature, and settlement. Tailings VWC values were obtained by converting the TDR readings using a material-specific TDR calibration equation for the tailings deposited in the test cells (Song, 2014).

Collection of treated MFT cores for geotechnical parameter analysis, which is termed profiling herein, were performed in close proximity to the instrumentation posts in an effort to align the instrumentation and physical testing datasets. During the course of the three year investigation, eight profiling events were completed.

Figure 1. Instrumentation posts in the Thin ML test cell

An automated meteorological station was installed in the area of the test cells to measure atmospheric conditions. Data was collected on an hourly basis over the three year monitoring period. Observed precipitation and calculated site potential evaporation (PE) over the monitoring period were relatively similar to and consistent with the long-term climate database for northern Alberta (Song et al, 2011).

MFT Feed and Treated MFT Characteristics

Samples of MFT and treated MFT were collected during deposition and post deposition to characterize and assess the composition of the material.

MFT was collected from spigots on the MFT pipeline and treated MFT was collected by excavator bucket from the mixing box during deposition. The recently treated MFT was tested during deposition for key performance indicators (KPIs) of the AFD process, including filtration constant, yield stress, and index properties. Index properties included water content, density, and methylene blue index (MBI). KPIs established by Shell for the AFD process includes yield stress greater than 150 Pa and / or filtration constant greater than 1. KPI criteria were established based on initial dewatering performance.

KPIs were met in the following: the entirety of the Deep Stack, two of the three Thick ML layers (1 and 2), and three of the 7 Thin ML layers (1, 2 and 4). The layers that did not meet KPIs had yield stress of 118 Pa and filtration constant of 0.4 on average. In general, material that did not meet KPIs had relatively higher MBI values (29.8 b/kg versus 25.8 g/kg on average), which could be indicative of poor mixing of flocculant solution and/or more clay-rich MFT. Under-dosing with flocculant solution is not a suspected cause for the material failing KPIs because all material was dosed at or above the target setting and KPI values did not correlate well with dosing values.

Post deposition samples include treated MFT collected by coring from floating docks deployed around the perimeter of the test cells. Laboratory testing was completed to characterize the treated MFT and is provided in Table 1. Specific gravity testing was completed on bituminous samples.

Table 1. Field Test Cell Deposit Characteristics

Deposit	# Lifts/Avg Lift Thickness (m)	Feed Solids Content (% total mass)	Fines (<44 um) by mass (%)	Average Bitumen (% by mass)
Thin ML	7 / 0.6	38	86	4.4
Thick ML	3 / 1.4	38	86	4.7
Deep Stack	1 / 4.5	37	91	6.2
Deposit	**MBI (g MB/kg solids)**		**Liquid Limit (%)**	**Specific Gravity**
Thin ML	28.0		60.3	2.28
Thick ML	28.4		56.7	2.25
Deep Stack	24.9		57.5	2.16

The field test deposits are fines-dominated tailings and generally resemble Thin-Layered Fines-Dominated Deposits and Deep Fines-Dominated Deposits (F-2) as defined by COSIA (COSIA, 2014). Figure 2 shows the initial and final geotechnical index results for the test deposits.

In general, the results are in the range expected for these deposit types, however the recently treated MFT was on the high end of the anticipated solids content range for MFT and much of the treated MFT deposit – namely the mid portion; see Figure 7b – has solids contents that are still considered to be in the early dewatering phase after the three year monitoring period.

A suite of laboratory consolidation testing was conducted to assess the compressibility and hydraulic conductivity as functions of vertical effective stress and void ratio, respectively. Tests included seepage induced consolidation (SIC), large strain consolidation (LSC) and oedometeric compression tests following ASTM 2435.

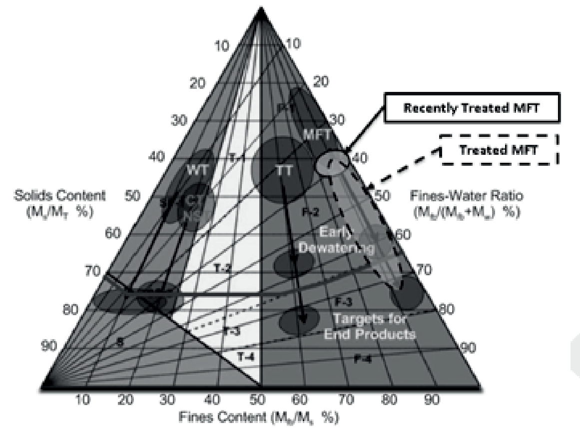

Figure 2. Representation of field test cell deposits following proposed Unified Oil Sands Tailings Classification System (UOSTCS)

SIC test samples were prepared in the lab using MFT samples collected in 2012, during Deep Stack and early ML depositions, and a range of flocculant doses in an effort to bracket anticipated field treated MFT behaviour. Derived compressibility and hydraulic conductivity curves from SIC results following finite strain nonlinear consolidation theory (Abu-Hejleh and Znidarcic, 1992) are depicted in Figures 3 and 4, respectively.

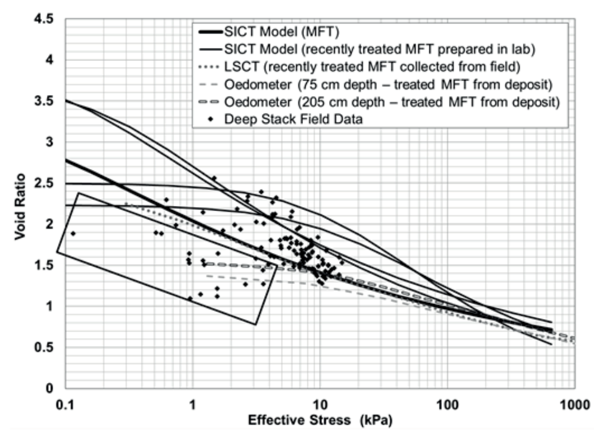

Figure 3. SIC, LSC, and odeometer compressibility results

LSC tests were conducted on one recently treated MFT sample collected during deposition from the mixing box of the Deep Stack. The material was subjected to a loading history during transport which presumably resulted in a modified treated MFT structure and material state than recently treated material prepared in the lab (SIC testing). Additional sample disturbance may have resulted from the material mixing /homogenizing and transfer approach used to prepare samples from the pails into consolidometer test specimens. Constant head hydraulic conductivity tests were conducted in the consolidometer at select stress intervals and are depicted as squares in Figure 4. For simplicity, only data from the Deep Stack is presented. Oedometer testing was completed on two relatively undisturbed samples collected from various locations and depths within the Deep Stack. Tests were conducted using a load increment ratio (LIR) of one over 24 hours. Oedometer tests were conducted by loading the specimen well beyond its pre-consolidation stress to a maximum stress sufficient to define the virgin compression line.

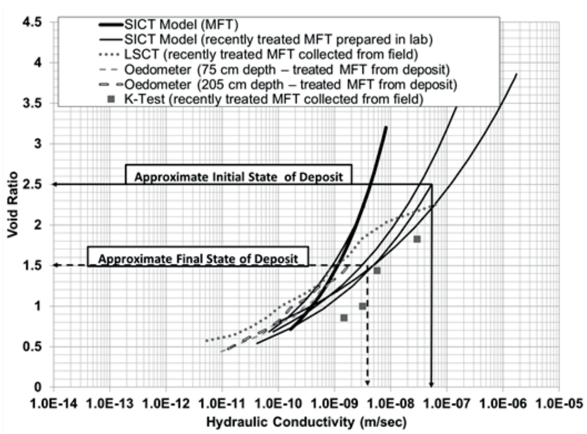

Figure 4. SIC, LSC, and odeometer hydraulic conductivity results

One sample was collected from a depth (75 cm) where the material experienced at least one freeze/thaw cycle and exhibited overconsolidation properties up to approximately 14 kPa (pre-consolidation stress). The other specimen collected at greater depth (205 cm) behaved overconsolidated up to the in-situ effective stress at the time of sampling (~15 kPa). Figure 3 also shows the effective stresses calculated for the Deep Stack deposit in comparison with compressibility curves from consolidation testing (squares). The majority of the Deep Stack with 3 kPa effective stress and greater appears to follow the envelope of consolidation curves. Samples with low void ratios and effective stresses were collected from the upper 100 cm of the deposit and would have been subjected to freeze/thaw and drying mechanisms as denoted by the box in Figure 3. These mechanisms would cause an overconsolidated response up to the pre-consolidation pressure and align reasonably well with the oedometer test specimen at 75 cm depth collected from this portion of the deposit.

DEPOSIT PERFORMANCE

Tailings Dewatering

The treated MFT dewatered through a combination of flocculation, sedimentation, consolidation phenomena, and evaporative drying as illustrated in Figure 5. Upon deposition into the cell and for several days after filling, the treated MFT rapidly released water (called “produced water”) due to the flocculation and sedimentation processes up to the transition solids content and the beginning of self-weight consolidation (phenomenon described in Ito and Azam, 2013); this is collectively referred to as the initial dewatering phase. The deposits further dewatered through self-weight consolidation with double drainage, freeze-thaw consolidation, and evaporative drying. These mechanisms occur within and at the boundaries of the deposit itself and generate water that can only be removed from the field test cell by run-off, actual evaporation (AE), and under-drainage.

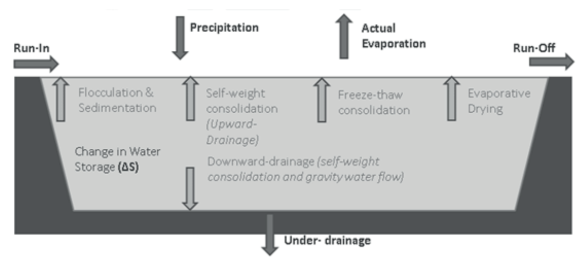

Figure 5. Tailings dewatering mechanisms and field test cell water balance elements

Water removed by runoff includes the produced water from the initial dewatering phase and potentially includes water released from additional self-weight consolidation and freeze-thaw consolidation. Runoff water was removed from the test cell by pumping from low spots (sumps) on the deposit surface. Water removed by AE includes water migrating to the surface from self-weight consolidation, freeze-thaw consolidation, and evaporative drying. Due to the short-term duration of initial dewatering, it was assumed that all of the produced water ran-off and that essentially no water was lost to evaporation or under-drainage. Water removed by under-drainage includes water migrating downward to the base from self-weight consolidation. The water balance was determined by analyzing elements contributing water to, or removing water from, the field test cells.

Dewatering Mechanisms Contributing to Tailings Solids Content Gain

To approximate single drainage self-weight consolidation (self-weight consolidation with drainage in upward direction), modelling was completed by Shell's consultant using an existing FS Consol model. The model was run from the end of the initial dewatering phase for each field test cell's first layer to the end of the three year monitoring period. Model assumptions included: no water cap on the tailings deposit surface, no drying at the tailings surface, no under-drainage at the tailings base, and no freeze-thaw in the upper layer.

Results from consolidation modelling and coring were used to quantify dewatering mechanisms contributing to deposit solids content gain. The quantification of dewatering mechanisms from a solids content increase perspective is provided to help understand the relative contribution of each dewatering mechanism to the densification of the deposit.

The increases in solids content by the tailings dewatering mechanisms for each test deposit over the three-year monitoring period are illustrated in Figure 6.

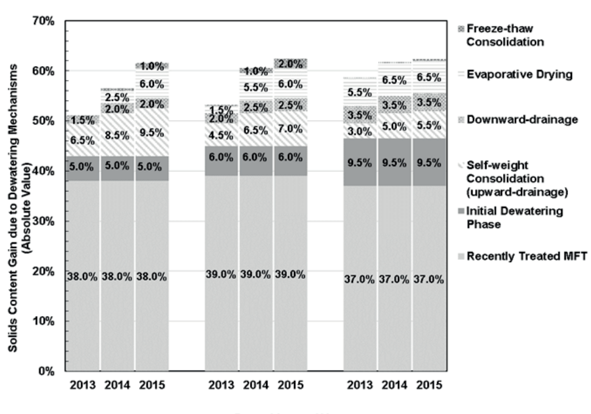

Figure 6. Solids content gain by dewatering mechanism

Solids content increases from dewatering are denoted in terms of absolute values. The increases in total solids content for the deposits over the monitoring period in comparison to initial treated MFT SC are 23.5%, 23.5%, and 25% for the Thin ML, Thick ML, and Deep Stack, respectively.

Treatment of the MFT with the flocculant solution adds water to the deposited slurry, but a volume of water in excess of that added is typically removed during the initial dewatering phase. The impact of initial dewatering was greatest in the Deep Stack, which had a solids content increase of 9.5% in relation to the initial treated MFT. The Thick and Thin ML had solids content increases of 6% and 5%, respectively. The initial dewatering period lasted between 5 and 17 days for the layers deposited. Initial dewatering performance results aligned with the process KPIs, further emphasizing the importance of this aspect of the technology, especially to meet early dewatering goals.

Downward drainage solids content increases were calculated to be between 2% and 3.5% to the deposits over the three-year monitoring period. The gain was most significant in the Deep Stack deposit—presumably due to the relatively higher permeability in the lower portion of the deposit when the driving head was the highest compared to the ML cells. Downward drainage was expected to decrease in all deposits with time as the tailings permeability reduced, excess pore-water pressure (PWP) dissipated, and the piezometric surface fell. In general, downward drainage appears to have significantly decreased within one year of pouring in all field test cell deposits as the lower portion of the deposits densified and permeability was reduced.

Based on field measurements obtained between August 2012 and October 2015, the average AE over PE ratio (AE/PE) for the AFD deposits in all three field test cells was approximately 0.7. The solids content increases in the test cells as a result of evaporative drying were relatively consistent, ranging between 6% and 6.5% over the monitoring period. However, the impact of evaporative energy on the deposit densification varied in response to the depositional history.

Evaporative drying from the tailings deposit was negligible in the Thin ML cell during the first year and was limited in the second year due to the routine presence of water at the tailings surface as the result of frequent layer deposition. This surface water consumed most of the available evaporation energy, and thus only thin crusts were developed. In contrast, the Deep Stack deposit experienced primarily self-weight consolidation for approximately the first seven months after deposition when evaporation potential was low, and then evaporation increased over the summer leading to formation of a significant (approximately 40 cm) crust. The ML cells did, however, achieve higher solids content increase from the combination of evaporative drying and self-weight consolidation than the Deep Stack cell did, indicating that multiple lift placements can benefit substantially from exposure to evaporative energy.

Freeze-thaw consolidation provided minimal solids content increase (<1%) to the Deep Stack deposit, and between 1% and 2% to the ML deposits with respect to the entire deposit. The frost depth was between 0.2 m and 0.3 m in the first year for all deposits due to recent pouring and high water contents at the on-set of freezing. The frost depth increased significantly to 0.8 m to 0.9 m in the second year in the ML cells when pouring was terminated earlier in the late summer than the previous year. Slightly lower frost depths of 0.6 m to 0.7 m were measured in the third year. The frost depth was not substantially different among the three field test cells, although the calculated water volume removed from freeze-thaw consolidation in the second and third years was much smaller in the Deep Stack cell due to water depletion from preceding self-weight consolidation and drying processes. Though, freeze-thaw contributed up to 10% SC gain in the frozen layer, the benefit of freeze-thaw consolidation is limited for the entirety of layered deposits unless the layering program is modified to exploit this mechanism.

An increase in solids content due to upward drainage of between 5.5% and 9.5% was determined from numerical modelling of self-weight consolidation and was most significant in the Thin ML deposit. The relatively better performance of the Thin ML and, to a lesser extent, Thick ML compared to the Deep Stack is suspected to be due to more water being available for removal from within the deposits following initial dewatering and slightly higher specific gravity material driving consolidation in these deposits. For simplicity, the numerical model used the same consolidation parameters for the deposits in the ML cells and Deep Stack cell, but used the different measured specific gravities. The self-weight consolidation modelling approach may have overestimated the solids content increases for the ML cells based on the observation that the modelled profile had higher solids content in some portions of the tailings deposits than those measured by coring samples on an annual basis. At the end of the monitoring period, excess PWP remained in all three deposits, with the highest PWP remaining in the Thin ML. Thus, additional self-weight consolidation is expected beyond what has been calculated to date.

Field Deposit Solids Content Gain, Densification, Effective Stress Development, and Strength Gain

The geotechnical performance varied between the deposits as the result of the layering approach and dewatering performance. The solids content profiles for the deposits are illustrated in Figure 7 with the Deep Stack, Thick ML, and Thin ML shown as solid, dashed, and dotted lines, respectively.

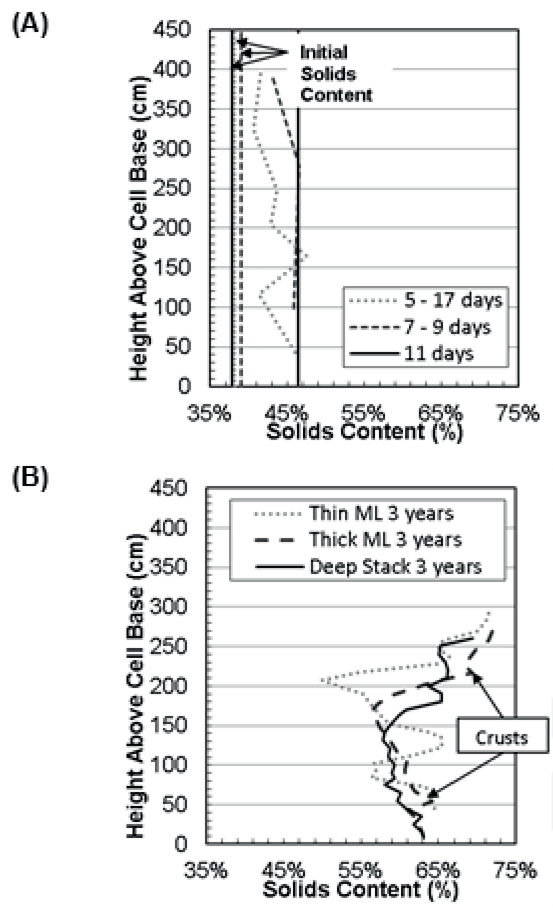

Figure 7. Initial (7a) and Final (7b) solids content in field test cell deposits. Exemplifies buried crusts in layers 1 and 2 of the Thick deposit.

The three deposit configurations ended with a similar average solids content of 62%, but the profiles are different as the result of variable dewatering. The Deep Stack has a characteristic 'C' shape that would be expected as the result of down-drainage and evaporation impact in the upper one metre of the deposit. By comparison, the ML deposits have both higher solids content crusts and densified layers and lower solids content regions that resulted from incomplete consolidation or drying prior to subsequent lift placement. The presence of crusts is illustrated in Figure 7b for the surface of buried layers 1 and 2 of the Thick deposit. The crusts in the ML cells, though relatively thin, appear to have created low permeability zones that impeded drainage and relief of excess PWP generated by progressive layering. The excess PWP dissipation was compared at approximately the same elevation in the center of the Deep Stack and second lift of the Thick ML deposit over a two year monitoring period. Excess PWP dissipation was found to be approximately 150 percent faster in the Deep Stack relative to the Thick ML cell.

Solids contents in the crust approached 75% with peak shear strengths over 20 kPa. The buried crusts in the ML cells rewetted but retained relatively higher solids content intervals within the deposit profile as stacking continued. With time, they became less distinguishable, and the deposit began to behave as a more uniform deposit. This is more obvious with the Thick ML deposit as shown in Figure 7b.

The total settlement for each cell is summarized in Table 2. Nearly half of the settlement occurred during the initial dewatering phase. Normalized settlement, which is normalized to total deposited thickness, is relatively equal between the field test cells; however, comparisons should consider that there were varying deposition histories and consolidation states between the deposits. Pore-water pressures remain greater in the ML field test cells and thus, there is a greater potential for additional settlement in those cells.

Figures 8A and 8B show the peak shear strength and remoulded shear strength profiles of the three test deposits at the end of the monitoring period. In Figure 8, the Deep Stack, Thick ML, and Thin ML are shown as solid, dashed, and dotted lines, respectively. Strength measurements were collected with an electronic field vane generally following ASTM D 2573.

The Deep Stack profile was between 17 kPa and 24 kPa in three years. The Thick ML and Thin ML deposit profiles had strengths generally between 5 kPa and 25 kPa after three years. Strength gain from evaporation, under-drainage, and consolidation is evident with the highest strengths observed close to the surface and base of the completed deposits. As expected, peak shear strength correlated positively with solids content and effective stress development, with rapid gains of strength observed when the material surpassed the liquid limit; generally about 55% to 60% solids content.

Table 2. Settlement performance of field test cells

	Cell	Deep Stack	Thick ML	Thin ML
Total	Settlement (cm)	189	198	193
	Thickness (cm)	455	415	446
	Normalized Settlement (cm/cm)	0.42	0.48	0.43

(A)

(B)

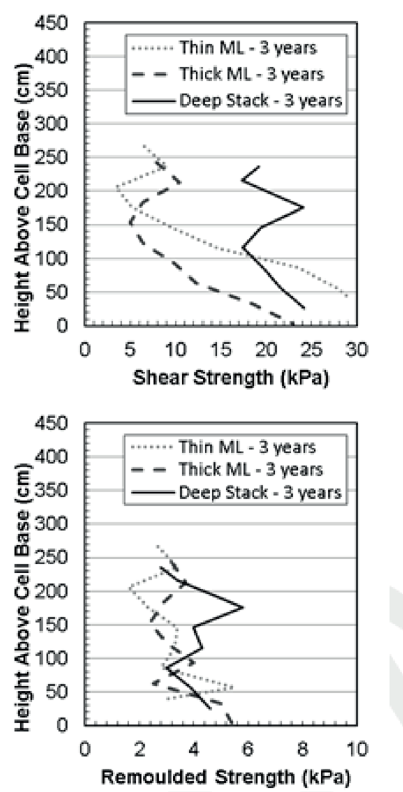

Figure 8. Peak (A) and remoulded (B) strengths in field test cell deposits

The sensitivity of the material is also noteworthy. The average sensitivity for all test deposits was approximately four, meaning that when remoulded, the treated MFT retain approximately one-fourth of the peak shear strength. This has implications for tailings management processes that would include disturbance of the formed deposits such as removal and placement in another location.

CONCLUSIONS

Based on the results of this field pilot, the following conclusions were drawn:

- Producing material meeting design specifications and deep stacking—to exploit the enhanced drainage attributed to a larger driving head and initially higher permeable material—is a superior approach to multiple thin lift deposits focused on short-term (one year or less) dewatering and strength gain performance.
- Multiple lift approaches can be more beneficial than deep stacking if allowed sufficient time to dissipate their excess pore-water pressure (PWP) and thoroughly dry or freeze-thaw consolidate prior to subsequent lift placement.
- For preliminary tailings management process planning at the commercial scale, solids content (SC) increase of 5% to 10% can be expected from initial dewatering, with the higher value achievable with material meeting or exceeding KPIs. Improved mixing of flocculant solution with MFT and/or selective harvesting of less clay-rich MFT may improve treated MFT KPI results and early dewatering behaviour and should be further investigated.
- An annual AE/PE ratio of 0.7 can be used for preliminary planning of treated MFT densification due to surface evaporation following removal of surface water. For 4- to 5-metre-deep deposits, the benefit of evaporative drying is highest over the first two drying seasons and then diminishes in subsequent seasons.
- Under-drainage improved water removal from the field test cells, but its contribution to commercial deposits depends on the regional hydrogeological setting and the properties of the tailings and foundation material. Minimal under-drainage should be anticipated for layered deposits greater than 4 metres deep after the first year due to the reduced permeability of the compressed tailings at the bottom of the stack.
- Freeze-thaw consolidation will provide only a minimal solids content increase (likely less than 2%) unless the layering program is modified to exploit this mechanism. The relative benefit of surface densification process, freeze-thaw and evaporation dewatering mechanisms, have limited potential to improve overall deposit density as deposits get thicker.
- For 4 to 5-metre-deep deposits, densification to about 60% average solids content and peak shear strengths greater than 5 kPa can be anticipated after two years regardless of the depositional approach. However, completion of primary consolidation will take longer than two years and enhanced dewatering methods consisting of surcharging/capping, sand layering, wick drains, rim ditching, or others could be considered to accelerate achievement of target end-states.
- The operational cycle time will be greater than 30 days for thin lifts and greater than 90 days for thick lifts to consolidate and allow drying of the material adequately to mitigate trapping of excess porewater pressure intra-lift. The cycle time should be established based on predictive modelling and optimized based on field performance monitoring.
- Remoulded shear strengths of approximately one-fourth of the peak undrained shear strength should be anticipated for treated MFT based on material performance.

REFERENCES

Abu-Hejleh, A.N., and Znidarcic, D., 1992, User Manual for Computer Program SICTA, Prepared for Florida Institute of Phosphate Research, University of Colorado, Boulder, 122 pp.

COSIA, 2012. Technical Guide for Fluid Fine Tailings Management.

COSIA, 2014. Guidelines for Performance Management of Oil Sands Fluid Fine Tailings Deposits to Meet Closure Commitments.

Dunmola, A., Cote, C., Freeman, G., Kolstad, D., Song, J., and Masala, S. Dewatering and Shear Strength Performance of in-line Flocculated Mature Fine Tailings under Different Depositional Schemes. Tailings and Mine Waste Conference 2013, pg. 5-14. Print.

Ito, M. and Azam, S. Large-strain Consolidation Modeling of Mine Waste Tailings. Environmental Systems Research. 2013.

Kolstad, D., Dunmola, A., Dhadli, N., O'Kane, M. Song, J., Masala, S .Towards the Improvement in Geotechnical Performance of Atmospheric Fines Drying (AFD) Deposits at Shell's Muskeg River Mine. International Oil Sands Tailings Conference 2012, pg. 157-167. Print.

Song, Q., O'Kane M., and Matthews, J. 2011. Deposition Thickness and Evaporative Drying for Oil Sands Tailings in Northern Alberta. Mine Closure 2011 – A.B. Fourie, M. Tibbett and A. Beersing (eds.), Australian Centre for Geomechanics, Perth, Australia. September 19-21, 2011, Lake Louis, Alberta, Canada.

Song, Q. O'Kane, M., Mahood, R., Cote, C, and Kolstad, D. Time Domain Reflectometry (TDR) Sensors- Application to Flocculated Mature Fine Tailings Performance Monitoring. International Oil Sands Tailings Conference 2014. pg. 499-508. Print.

THIXOTROPIC EFFECTS ON THE RHEOLOGY OF POLYMER AMENDED MATURE FINE TAILINGS: IMPLICATIONS FOR SURFACE DEPOSITION CONTROL

S. Mizani[1], P. Simms[1], G.W. Wilson[2] and N. Beier[2]
[1]Carleton University, Ottawa, Canada
[2]University of Alberta, Edmonton, Canada

ABSTRACT

Previous research has shown that the rheology of mature fine tailings treated with polymer shows shear and age dependent (thixotropic) behaviour associated with breaking and reformation of flocs. Which process is dominant depends on the shear rate, but it has been shown that reductions in yield stress due to high shear are reversible under low shear even when the tailings are still flowing. We show rheological measurements and quantitative analysis of SEM images that show how the fabric of the tailings can recover after shearing. These effects are evident in two large (6 m long) flume tests on in-line flocculated tailings conducted at the Oil Sands Tailings Research Facility. Two different deposition rates were used in the experiments. The fast deposition experiment could be modelled ignoring ageing effects, The slow deposition experiment exhibited two characteristics seen in field deposits of high density tailings: a varying slope that was steepest near the deposition point, and channel flow. Thixotropic behaviour therefore has important implications for surface deposition control.

INTRODUCTION

Several technologies that reduce water content in oil sands fine tailings prior to deposition are currently being trialed or even used at the commercial scale in the oil sands industry. One such technology is in-line flocculation, whereby polymer is injected into a pipeline flowing with fresh fluid fine tailings or reclaimed MFT. Application of the polymer flocculates the particles, and induces relatively rapid dewatering, such to that the tailings exhibit a yield stress almost immediately after they exit the pipeline and will stack. Stack-ability allows for placement in lifts, which can facilitate further dewatering through surface processes such as evaporation or freeze-thaw. In-line flocculation has been implemented at the commercial scale (Wells et al 2011, Caldwell et al. 2014, Matthews et al. 2011, Dunmola et al. 2013).

Operators of in-line flocculation technologies are concerned with the sensitivity of the polymer-created flocs to shear. Flocs could be destroyed by shear during transport or during deposition, which could reduce both the yield stress and the dewatering potential of the tailings. This was thought to be especially true when anionic polymers were employed; however, Mizani et al. (2013b, 2014) found that that while indeed the rheology of the tailings is degraded by high shear, this degradation is reversible, and that the tailings can re-flocculate, even while still flowing at relatively low shear rates, as might occur as tailings flow away from a deposition point. This begs the question as how best to manage deposition so as to maximize the recovery phenomenon.

Shear sensitivity and ageing (or thixotropy) has been studied using ideal clay suspensions, and rheological models accounting for ageing and shear sensitivity have been developed (E.G. Coussot et al. 2002). In such models, the viscosity decreases rapidly upon shearing and increases slowly when left at rest or under lower stress levels, for ideal clay suspensions Variable yield stress, hysteresis, jamming and avalanche of various non-Newtonian fluids have been shown to originate from this type of rheology (Alexandrou et. al 2009, Bonn et. al 2004, Moller et.al 2009 and Hewitt and Balmforth 2013).

Only a limited number of studies have incorporated these models into predictions of changing geometry of fluid. Computational works by Coussot et al. 2005 and Hewitt and Balmforth 2013 simulate the release of a finite volume of thixotropic material released from rest. There has been no attempt to model the changing geometry of thixotropic material following deposition during continuous pumping, as would be applicable to tailings deposition.

In order to improve understanding of these phenomena in oil sands tailings, and to help develop predictive tools to assist tailings deposition planning, a number of experiments were conducted using simulated in-line flocculated tailings. The largest of these tests were performed at OSTRF. Static mixers were used to create in-line flocculated tailings that were subsequently deposited in 6 m long flumes at different flow rates. The goal of this paper is to present these experiments, along with rheometry data and SEM image analysus used to interpret the results.

MATERIALS AND METHODS

Tailings properties

MFT samples used in this study were obtained from Shell Canada's Muskeg River Mine. MFT were delivered to Carleton University at 35% solids content (mass of solids / total mass). The specific gravity (solid phase density) was 2.2 g / cm^3 using ASTM D854 (2000). The particle size distribution of tailings was established by the combination of sieve (wet technique) and hydrometer analyses results based on ASTM D 422-63 (2002). The D10, D50, D60 are 0.8, 6.4, 11.1(microns). Geotechnical parameters Liquid Limit (LL), and Plastic Limit (PL) were 55%, 27% respectively (ASTM D4318, 2000). Mineralogical composition was: Quartz 30.3, Kaolinite 28.5%, Illite 19%, Rutile 0.5% and Amorphous 23.6%. Semi-quantitative amounts of clay minerals in the < 2 μm size fraction was: 70% Kaolinite and 30% Illite. The electrical conductivity of the pore-water is about 1.6 mS/cm, and is dominated by Na (320mg/L), Cl (130mg/L), and CO_3 (377mg/L) species. Results from Methylene Blue Index (MBI) test conducted on four different samples showed an average value of 4.03 (meq/100g), corresponding to an average clay percentage of 29.64%.

A high molecular weight anionic polymer, A3338, was used as a flocculant for fast dewatering of MFT samples and was added to the MFT as a 0.4% solution using a mixing protocol developed by Mizani et al. (2013b), designed to generate tailings with similar rheology as observed in field trials of in-line flocculation. A3338 is a branched polymer, with an average molecular weight of 18×106 g/mol, supplied by the company SNF.

Rheometry

All rheometry data were obtained using an Anton Paar Physica MCR Rheometer employing an air mounted vane fixture. Due to shear sensitivity of flocculated MFT, vane fixtures were chosen as it can be immersed directly into the sample with minimal disturbance. The vane fixture has been shown to have certain advantages for concentrated suspensions, including elimination off wall slip and minimization of the particle size effect (Nguyen et al. 2006).

The vane consists of four thin blades arranged around a central shaft, of height 40 mm and diameter of 22 mm. 30 minutes after mixing of the sample to the target floc dosage, the sample was poured into a cylindrical sample holder (part number CC27) with a diameter of 28.92 mm. Sample heights were approximately 8cm, submerging the vane by 20 to 10 mm.

Select samples were transferred to a scanning electron microscope. Small surface samples (~ 1 cm depth, less than 50 g) were spooned into the SEM sample holder. Samples were tested under low vacuum (ESEM) to produce images. Images were analyzed for pore-size distribution using the ImageJ freeware (www.imagJ.net). Thresholding is the key parameter in image analysis for defining what section of an image constitute pore-space, as a black and white image is constructed from the greyscale image. Thresholding was done by eye and by an optimization technique that identified a threshold at which sensitivity of the produced image to variation around that value threshold was minimized.

Large flume tests

These tests were conducted using OSTRF's 6 m long by 0.6 m wide flume. Tailing were deposited in the flume through a 1 inch diameter pipe, where MFT was fed from a holding tank using a progressive cavitation pump (43 L/min full scale). A 0.4% polymer solution was injected inline using a flex pro pump model A4, with a smaller capacity of (3 L/min full scale). A branched anionic polymer supplied by SNF was used for all tests, at a dosage of 850 ppm flocculant per mass of dry tailings.

The polymer solution was injected immediately before a series of static mixers. The deposition speed was varied while changing the number of elements in the static mixers (at higher flow rates less mixing is required) such that mixing energy remains constant for all tests. The tailings and floc solution were stirred continuously (using an impeller installed in the tank) during deposition process, to prevent any settlement.

Two tests were done using different flow rates:

The *Fast pour* was performed using a speed of 36L/min, which was the highest possible speed using this setup. The total deposition time was 21 minutes and 17 seconds. A total of 14.7 kg release water was collected at the end of deposition

The Slow Pour was performed using a speed of 10 L/min. The total deposition time was 62 minutes, a total of 52.6 kg of release water was collected at the end of deposition.

Non-contact ultrasonic displacement sensors were positioned over the middle of the flume to dynamically record changes in the deposit profile.

Analysis

The rheomery data was analysed using the Hewitt model, a viscosity bifurcation model. The Hewitt model (Hewitt and Balmforth 2013) is defined by the following two equations. The first describes how the structure, λ, changes due to ageing and shear:

$$\frac{d\lambda}{dt} = \frac{(\lambda_{\max} - \lambda)\chi}{\theta} - \alpha \dot{\gamma} \lambda \quad (1)$$

Where θ controls the rate of thixotropic ageing, α controls the rate of de-structuring due to shear, γ is the shear rate. Limiting the λ_{max} to unity representing the fully structured state , λ<1 would then represent a material that is de-structured to some degree. Hewitt defined viscosity as a function of structure in the following form:

$$\mu = \frac{\mu_0}{(1-\lambda)(1-\beta\lambda)} \quad (2)$$

Where μ_0 is a constant reference viscosity (Hewitt 2012), χ is a function of settling rate and β is a constant. As with other viscosity bifurcation models, models, yield stress behaviour is emergent from this model in the form of rapid increase in viscosity. In Hewitt's model, there are two critical stresses, $T_{low} = 4\beta\ \mu_0 / (\alpha T)$ and $T_{high} = 1/(1-\beta)\ \mu_0 / (\alpha T)$. For a full structured material, the structure will not decrease below applied stresses of T_{high}, where for a fully destructed material (λ=0), the material will not rapidly increase in viscosity and therefore manifest yield stress behavior unless the shear stress is below T_{low}. For intermediate values of initial structure, the stress at which yield is manifested depends on the shear history. The implications are that the yield stress corresponding to flow initiation can be much higher than the yield stress corresponding to flow stoppage.

RESULTS

Select Rheometry results for MFT dosed with 850 ppm polymer

Rheometry results on similarly prepared tailings has been presented in Mizani and Simms (2014) and Mizani et al. (2013b), we present select results here to illustrate the viscosity bifurcation behaviour, as well as to demonstrate the role of recovery on the properties of the material.

Figures 1 and 2 present controlled stress rheology fitted with the Hewitt model. The first figure shows results from samples that have rested for 30 minutes after preparation before shearing at different constant stress rates. It can be seen that there exists a critical stress, approximately at 400 Pa, below which the viscosity of the material rapidly increases, but above which the viscosity degrades to about 0.2 PaS. The Hewitt model replicates the viscosity bifurcation phenomenon, but the time the material takes to reacts is somewhat longer than predicted by the model, or in other words, the time until the equilibrium state is reached (either near infinite viscosity or residual viscosity is longer in reality than predicted by the model.

Figure 2 shows a constant decreasing stress, in which each stress is held for 5 s. This kind of test is done to simulate the stress conditions that might exist as tailings slow to rest in the field. Both modelled and real material show a jump in viscosity when the controlled stress drops to 50 Pa from 100 Pa. Therefore, each test shows a different yield stress depending on the shear history of the material, where the 400 Pa value corresponds the yield stress for shearing from rest, while the 50 Pa corresponds the value required to stop flow after the material has been substantially sheared.

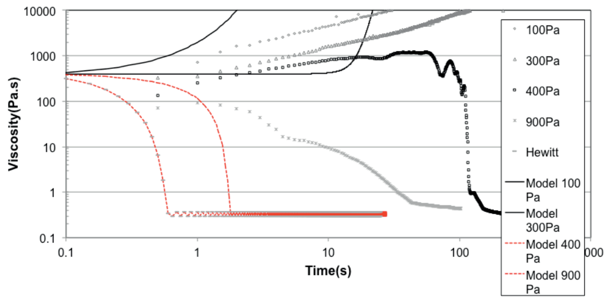

Figure 1. Measured and modelled viscosities under constant stress tests

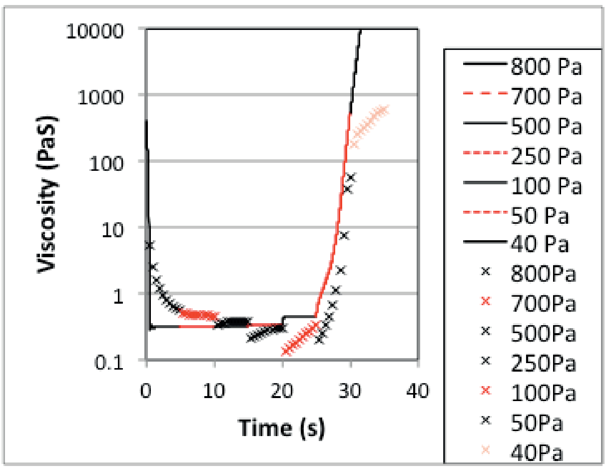

Figure 2. Measured and modelled viscosity in a controlled decreasing stress test

There is some debate about what happens to the flocs under shear when anionic polymers are used. The results in Figures 1 and 3 would suggest that floc disintegration is recoverable through the ageing process; however, the following results provide some more concrete evidence.

Figure 3 shows the elastic modulus determined by small-strain oscillatory rheometry before and at different times after shearing. The elastic modulus substantially drops after shearing, but then almost recovers to its pre-shearing level.

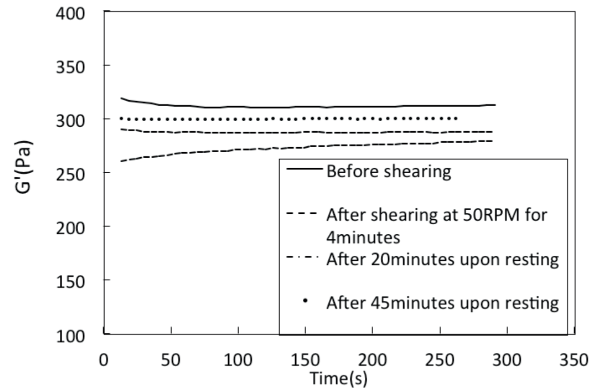

Figure 3. Elastic modulus measured by oscillatory rheometry before shearing and after shearing at various times

This recovery can be seen in image analysis of SEM images taken before, immediately after and then 45 minutes after shearing. Images of the tailings are tailing are shown in Figure 4. Qualitatively it can be seen that shearing has a definite affect on the fabric. Quantitatively, this can be tracked by pore-size analysis on the images, in Figure 5. It can be seen that shearing reduces the frequency of pores between 1 and 10 microns, but this substantially recovers within 45 minutes after shearing.

To summarize, the ability of the tailings to re-flocculate to some degree after shearing is demonstrated through the rheology results demonstrating recovery or ageing, the measurement of recovery in the elastic modulus measured by small-strain oscillatory rheometry, and by the analysis of SEM images.

Large scale flume test at OSTRF

The utility of the preceding observations to understanding deposition geometry can be observed in the large flume tests. Figure 6 and Figure 7 present data from flume deposition tests. The final profile of the faster deposition (36 l/ min) test can be fitted with simple lubrication theory based equations for resting profiles of a Bingham, using a value (60 Pa), which is close to the lower limit of yield stress from the Hewitt interpretation of the rheology (between 50 Pa and 100 Pa). The lubrication theory equations and their applicability to other tailings types are presented in Mizani et al. (2013a).

By contrast, the final profile of the slow pour cannot be fitted with lubrication theory. Up until 45 minutes, the transient profiles evolve as observed in the shorter duration tests. However, at this point, tailings no longer accumulate on the upper part of the slope, but rather flow down to near the toe. Indeed, height somewhat decreases on the upper part of the slope due to consolidation. The 45 minute profile itself can be fitted with the LT equation, but with the yield stress value of 400 Pa, close to the effective yield stress for an initially structured material (Figure 1) This suggests that at least part of the tailings near the bottom of the flume have come to a state equivalent to an initially fully structured state at rest.

A final note of interest is the formation of channel flow (flow changes from spreading to channel flow) observed at about 45 minutes, seen in Figure 8. Channel flows are flows of material in parabolic/circular narrow channel. This type of behaviour is regularly seen in most dewatered tailings deposits (Mizani et al. 2013). The channel flow mechanism persisted until the end of deposition and appears to have conveyed the bulk of the tailings to the toe-end of the deposit between 45 minutes and 65 minutes.

SUMMARY AND CONCLUSIONS

Oil sands fine tailings amended by an anionic polymer appear to exhibit viscosity bifurcation behaviour observed previously in ideal clay suspensions. Viscosity bifurcation implies that the viscosity and apparent yield stress of the tailings is controlled by competing process of de-structuring by shear, and recover of structure by ageing. Rheometry data of a particular polymer amended MFT can be reasonably well fit using the Hewitt model, a viscosity bifurcation model adopted from the literature. The implication of this phenomenon is that a range of apparent yield stresses can be manifested by the tailings, in this case ranging from a yield stress around 50 Pa for the when the material is sheared and then flows to a stop, or a yield stress of about 400 Pa corresponding the shear stress required to initiate flow in tailings that are fully structured. Implications of these observations are that the benefits are polymer flocculation are not necessarily destroyed when

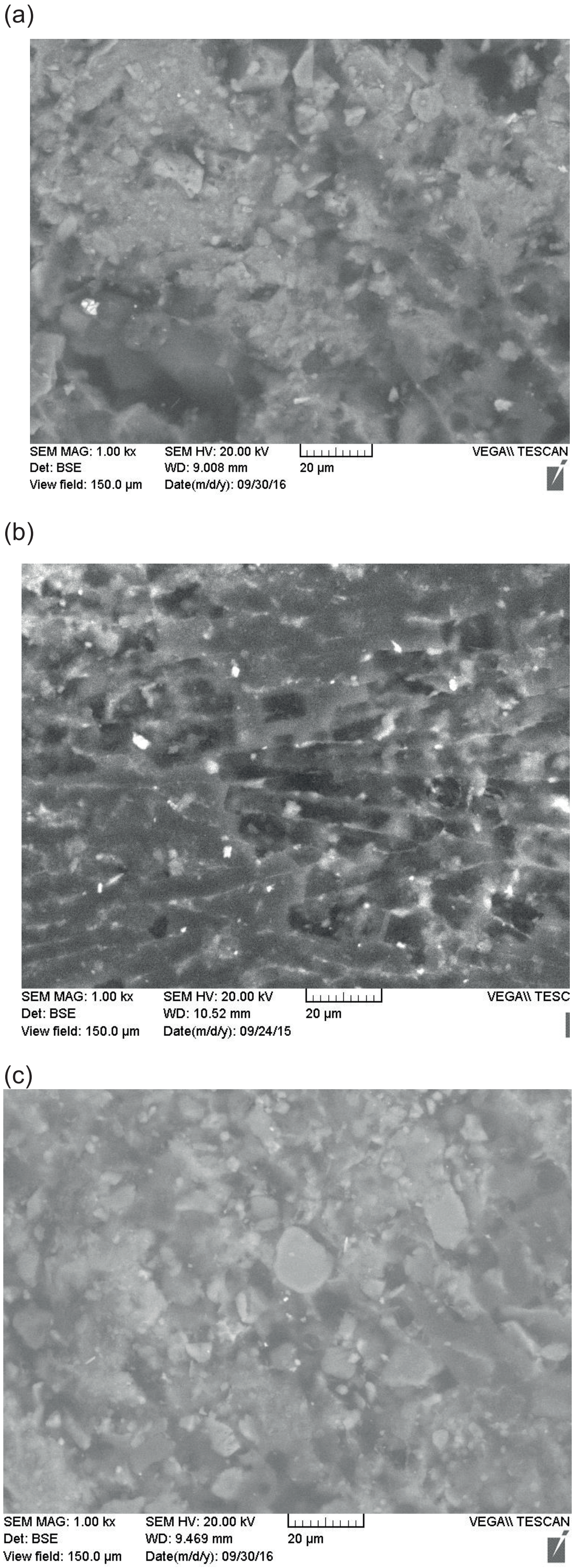

Figure 4. SEM images (a) before shearing, (b) immediately after shearing, and 45 minutes after shearing (c)

the material is sheared during transport or deposition.

Two relatively large flume tests were conducted at OSTRF to study the implications of this behaviour to deposition geometry. The two tests included a fast pour and a slow pour. While the fast pour could be modelled assuming a Bingham rheology with a yield stress of 60 Pa, the slpw pour could not. Evidence suggest that the slow pour was slow enough such that the yield stress of the tailings at the bottom of the flume began to manifest the yield stress corresponding to the fully structured state. This apparently may have contributed to the initiation of channel flow, and a concave profile (low slope near the toe) typical of most high density tailings deposited in the field.

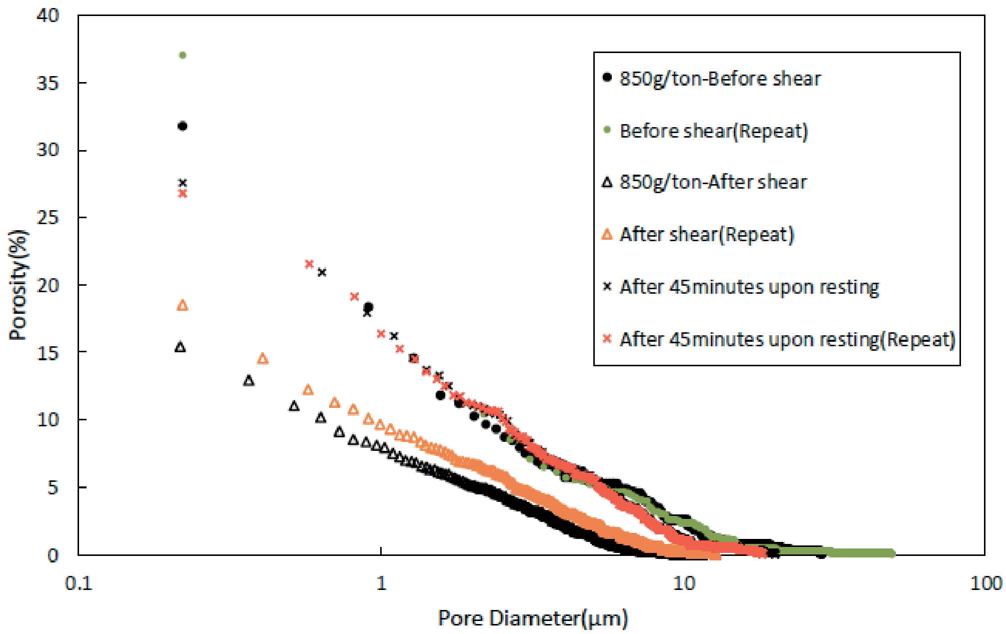

Figure 5. Pore-size distribution analysis of SEM images taken at different times before and after shearing

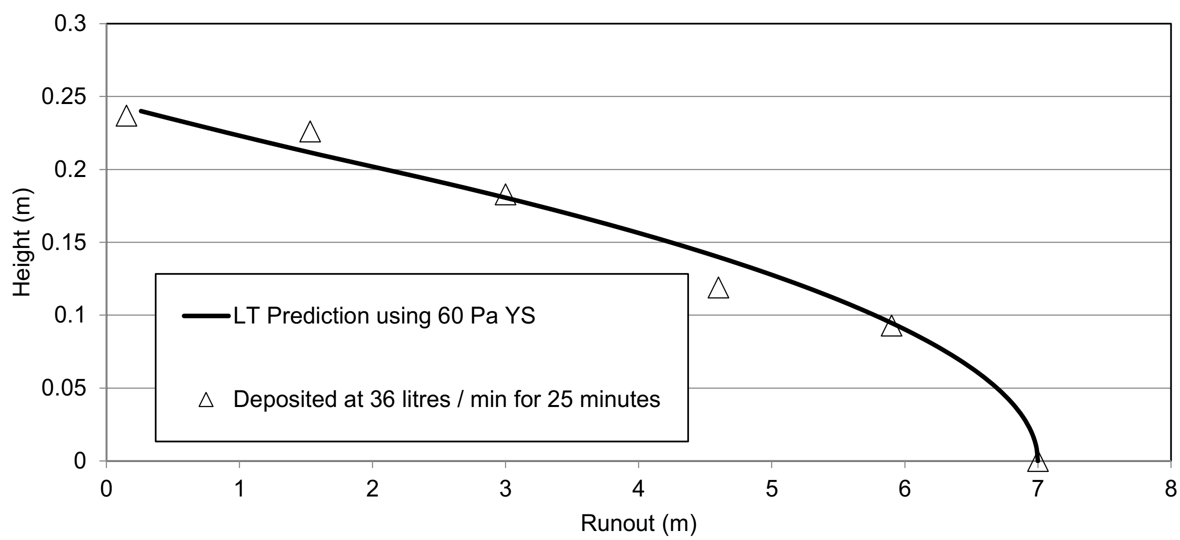

Figure 6. Flume deposition of 850 ppm tailings in a long flume (0.65 m wide) at 36 l/ min, fitted using 1D lubrication theory, yield stress of 60 Pa

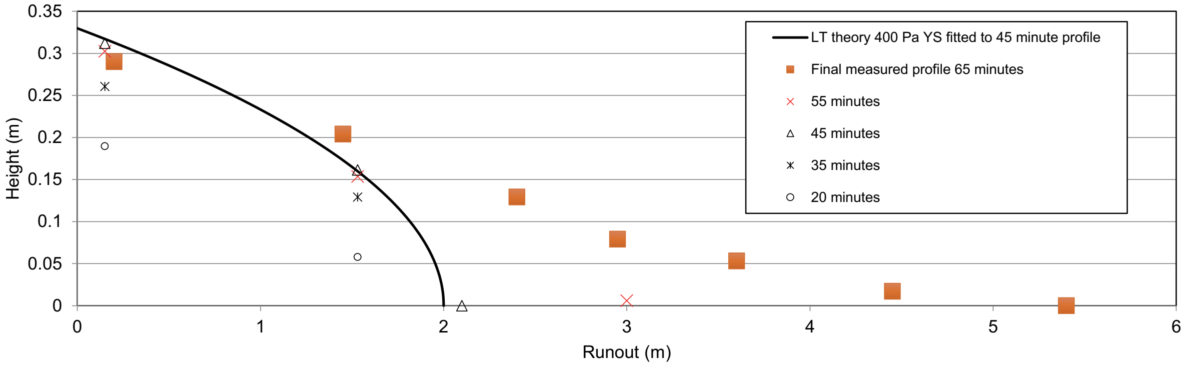

Figure 7. Flume deposition of 850 ppm tailings in a long flume (0.65 m wide) at 10 l/ min, the 45 minute profile fitted with 1D lubrication theory using 400 Pa YS

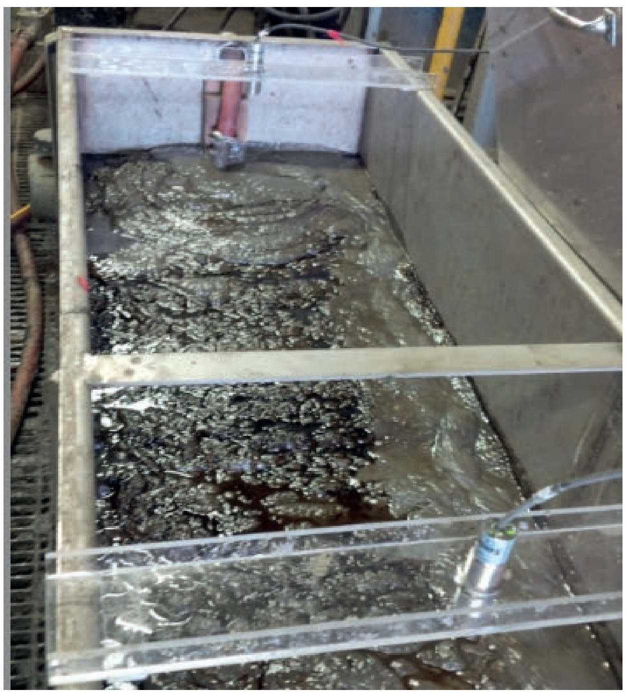

Figure 8. Channel ongoing at 45 minutes into the slow pour test

ACKNOWLEDGEMENTS

This research was funded by an NSERC CRD supported by COSIA, held by the second author. Support by staff at OSTRF and tailings supply by Shell Canada are gratefully acknowledged.

REFERENCES

Alexandrou AN, Constantinou N, and Georgiou G (2009) Shear rejuvenation, aging and shear banding in yield stress fluids, J. Non-Newtonian Fluid Mech 158: 6–17.

Bonn D, Tanaka H, Coussot P, and Meunier J (2004) Ageing, shear rejuvenation and avalanches in soft glassy materials, J. Phys.: Condens. Matter, 16: S4987–S4992.

Caldwell, J. Revington, A., McPhail, G., Charlebois, L. 2014 Optimised Seasonal Deposition for successful management of treated mature fine tailings. Proceeding of the 17th International Seminar on Paste and Thickened Tailings, Vancouver, Canada, June 2-5 2014

Coussot P, Nguyen QD, Huyun H T, and Bonn D. (2002). Avalanche behaviour in yield stress fluids. Phys. Rev. Lett. 88, 175501.

Dunmola, A., Cote, C., Freeman, G., Kolstad D., Song, J., and Masala S. 2013. Dewatering and shear strength performance of in-line flocculated mature fine tailings under different depositional schemes. Proceeding of Tailings and Mine Waste 2013 November 3rd-6th 2013, Banff, Alberta p5 - 14.

Hewitt DR, and Balmforth NJ (2013). Thixotropic gravity currents. Journal of fluid Mech. vol. 727: 56–82.

Matthews, J. G., Dhadli, N., House, P., & P. Simms. (2011). Field trials of thin-lift deposition of amended mature fine tailings at the Muskeg River Mine in Northern Alberta. Proceedings of the 14th

International Seminar on Paste and Thickened Tailings, R. Jewell and A. Fourie, eds., Australian Centre for Geomechanics, Crawley, Australia, 271–280.

Mizani S, and Simms P (2014) Geometry of polymer-amended fine tailings deposits: yield stress measurement and numerical modelling. International Conference on Oil Sand Tailings, Lake Louise, Alberta.

Mizani S, and Simms P (2016). Deposition Modelling of Amended Oil Sands Tailings Accounting for Thixotropy, in Proceedings 19th International Seminar on Paste and Thickened Tailings, Santiago, Chile.

Mizani S, He X, and Simms P (2013a) Application of lubrication theory to modeling stack geometry of high density mine tailings, Journal of Non-Newtonian Fluid Mechanics, Vol.198: 59–70.

Mizani S, Soleimani S, and Simms P (2013b) Effects of polymer dosage on dewaterability, rheology, and spreadability of polymer-amended MFT, in Proceedings 16th International Seminar on Paste and Thickened Tailings, Belo Horizonte, Brazil.

Moller P, Fall A, Chikkadi, V, Derks D, and Bonn D(2009) An attempt to categorize yield stress fluid behaviour, Phil. Trans. R. Soc. A, 367:5139– 5155.

Nguyen QD, Akroyd T, De Kee DC, and Zhu L (2006) Yield stress measurements in suspensions: an inter -laboratory study. Korea-Australia Rheology Journal, 18, No (1): 15-24.

Wells, P. S., Revington, A., & Omotoso, O. (2011). Mature fine tailings drying– technology update. Proceedings of the 14th International Seminar on Paste and Thickened Tailings, R. Jewell and A. Fourie, eds., Australian Centre for Geomechanics, Crawley, Australia, 155–166.

Session A-2

Tailings Management

IN SITU DEPOSITION OF TREATED TAILINGS

Trong Dang-Vu[1], Howard Keele[2], Pierre Lacoste-Bouchet[2], Reza Salehi[2], Aref Najafi[2], Colin Klein[1], Ajith Nelson[1] and Scott Ramey[1]
[1]SNF Energy Services, Canada
[2]Canadian Natural Resources Limited, Canada

ABSTRACT

A new polymer assisted tailings treatment technology has been developed by Canadian Natural Resources Limited (Canadian Natural) and SNF Energy Services. This technology consists of lifting, treating mature fine tailings (MFT) with polymer, redepositing treated MFT under water and capping with a layer of non-segregating tailings (NST). This process avoids costly material re-handling and minimizing the tailings operation footprint while remaining flexible to changing conditions. The obtained results showed that polymer addition prevented segregation and penetrating of capping layer (NST) into MFT (fingering). The dual polymer treated MFT tolerated thicker layer of NST and produced better consolidation as compared to single polymer treated MFT.

INTRODUCTION

Canadian Natural Resources Limited (Canadian Natural) has, for several years, investigated new technologies for the treatment of mature fine tailings (MFT) at the Horizon mine site. The challenges of MFT storage, disposal and handling are numerous and costly. Canadian Natural and SNF Energy Services have developed a new chemically assisted tailings treatment technology focused on controlled deposition characteristics, at greatly reduced cost of operation. This process will avoid costly material re-handling and minimizing the tailings operation footprint while remaining flexible to changing conditions. This process will lift, treat and redeposit solids without leaving the confines of the tailings structure. This deposit will later be capped by a layer of non-segregating tailings (NST) to assist with further dewatering, gaining strength with time and maintaining deposit integrity.

To support the concept and prove the feasibility of this approach a series of bench scale tests were conducted. This paper summarizes the preliminary findings to support the proof of concept.

EXPERIMENTAL METHODS

Samples of MFT and process water were obtained from Canadian Natural and their characterization was given in Table 1. The solids content of the MFT and process water was measured by moisture balance. Fines content was determined using wet sieving while clay content was quantified by MBI method. Two SNF's polymers were used: one anionic and one cationic and their properties were given in Table 2. Polymer solutions were prepared at a concentration of 0.4 wt.% using the supplied process water.

For each test, 200 g samples of MFT were flocculated using anionic polymer (single polymer treatment), anionic and cationic polymers (dual polymer treatment) or left untreated (blank/control). These MFT samples were poured into 1 L graduated cylinders and the consolidation of the treated and untreated MFT samples was observed over time while the solids content was calculated based on the observed volumes. To investigate the impact of water and NST layer capping on consolation, some cylinders were pre-filled with 500 mL of process water prior to MFT addition while other was capped with additional 100 g or 800 g of sand. These experiments are summarized in Table 3.

The polymer dosages were used at 2100 g/t of anionic for single polymer treatment and 2100 g/t of anionic and 600 g/t of cationic polymers for dual polymer treatment. Due to the addition of water from polymer solution the initial solids content of treated samples decreased slightly, as summarized in Table 4.

RESULTS AND DISCUSSION

Effect of Water Capping

Figure 1 shows single and dual treated samples with and without water capping. There was very little difference in consolidation between samples that were capped with water and those that were not.

After 5 days the single treated sample with no water cap reached 27.1 wt.% while the water capped sample reached 28.5 wt.%. Similarly for the dual treated samples, the un-capped sample gained 23.6 wt.% while the capped sample reached 23.1 wt.%. Improvement of consolidation with water cap was insignificant.

Effect of Polymer on Consolidation of Subaqueous Deposit

Figures 2 and 3 show samples capped with water after 1 day and 5 days, respectively. The untreated MFT was dispersed to some extent and with time it gradually began settling to original volume, as shown in Figures 2a and 3a. The approximate solids content of the sample after 5 days was 19.5 wt.% and it was significantly lower than the initial solids content. When flocculated with either the single or dual polymer, the samples were not dispersed during subaqueous deposition and gradually consolidated. After 5 days these samples reached 28.5 wt.% and 27.1 wt.% respectively. It indicates that polymer addition significantly improved consolidation of treated MFT as compared to untreated MFT. However, the water cap did not appear to increase solids content of treated MFT from the initial solids content of the MFT. Additional compaction is required to increase the solids content of the treated MFT. It can also be seen in Figures 2 and 3 that the dual polymer treatment produced very clean water layer while both no polymer and single treatments gave muddy water. This shows a very high fines capture and minimal segregation of sample treated with dual polymer.

Synergy Effect of Polymer Addition and Sand Capping

The synergy effects are shown in Figures 4 through 7. Figures 4 shows treated and untreated samples capped with additional 100g of sand. As shown in Figure 4a, the added sand penetrated (fingered) into untreated MFT layer, causing significant re-dispersion of MFT into water. No clear mud line was observed for the duration of the test. The treated samples, however, showed three distinctive layers of water, sand and treated MFT, as presented in Figures 4b ad 4c. Furthermore, water layer for dual treatment was cleanest as compared to those for no polymer and single treatments.

Figure 5 shows samples capped with 800g of sand after 5 days. Similarly to previous tests, the untreated MFT sample was dispersed by the sand addition and a portion of it settled on top of the sand layer, effectively creating a layer of un-capped MFT. In the case of the treated samples, it can also be seen that the additional weight of the larger sand cap significantly enhanced the consolidation of both samples. Dual polymer treatment gave the cleanest water.

Consolidation of treated MFT was quantitatively illustrated in Figure 6. For both single and dual treatments, consolidation increased with increasing in mass of added sand. For single polymer treated sample, solids content increased to 35.9 wt.% with 100g sand addition and reached 46.4 wt.% with 800g of sand addition. For dual polymer treated sample, solids content increased to 31.7 wt.% with 100g of sand and reached 48.2 wt.% with 800g of sand.

Figure 6 also shows that with lower mass of sand (no sand and 100g of sand), single polymer treatment consolidated better than dual polymer treatment (blue and red columns); however, with higher mass of sand (800g of sand) dual polymer treatment gave a higher consolidation than single treatment (green columns).

Long term consolidation of the sand capped samples is shown in Figure 7. The samples continue consolidating for about 120 days after which their consolidation rate starts leveling out. The dual treated sample capped with 800g of sand showed the highest consolidation, reaching 55.7 wt.%, while the single treated sample reached 48.4 wt.%. For samples capped with 100g of sand the trend was reversed with the single treated sample reaching 38.3 wt.% and the dual treated sample getting 34.7 wt.%. The reason for this difference can be attributed to the properties of the flocs produced by the single and dual polymer treatments. The dual polymer treatment produces stronger, more porous flocs that do not consolidate as easily under low pressures (lower mass of capping sand), leading to lower consolidation than samples not capped with sand or capped with only 100g of sand. However, the more porous structure of the flocs allows them to release more water and hence consolidate more when under higher pressures as compared to the weaker flocs produced by the single polymer treatment.

CONCLUSIONS

The conclusions of this work can be summarized as follows:

- Polymer treatment prevents dispersion of MFT not only during sub-aqueous deposition but also capping with sand
- When capped with a sufficient mass of sand, dual polymer treated MFT consolidated best, giving the highest solids content of 55 wt.% solids in 4 months
- Dual polymer treatment outperformed single polymer treatment with a larger sand cap, while single polymer showed superior consolidation with a smaller sand cap
- Water capping does not enhance the consolidation of MFT

Based on these findings, the next steps will be to determine the optimum polymer dosages for this application. Also, more tests will need to be conducted to determine the optimum thickness of the sand layer. This will allow larger scale testing to be conducted.

ACKNOWLEDGEMENTS

The authors wish to thank SNF and CNRL for permission to publish this work. The authors also wish to thank SNF Energy Services staff during performing the test.

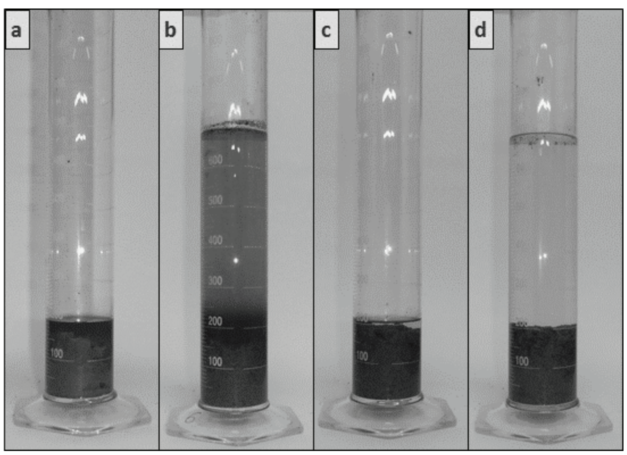

Figure 1. Treated samples after 5 days: a) single polymer no water cap, b) single polymer with 500 mL water, c) dual polymer no water, d) dual polymer with 500mL water

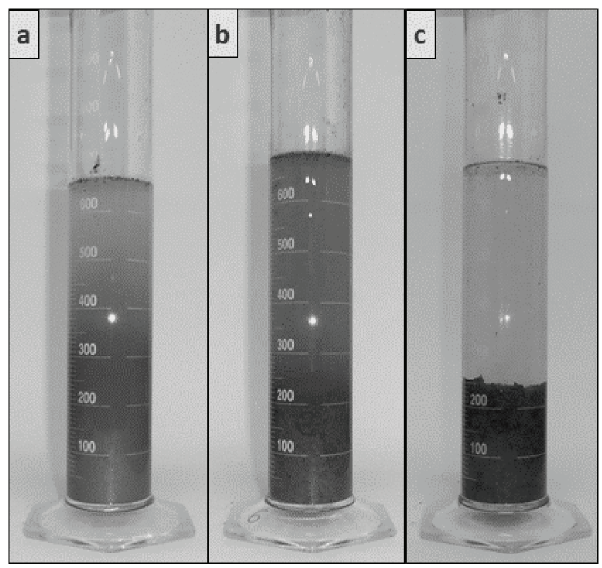

Figure 2. Water capped MFT after 1 day: a) untreated, b) single treatment, c) dual treatment

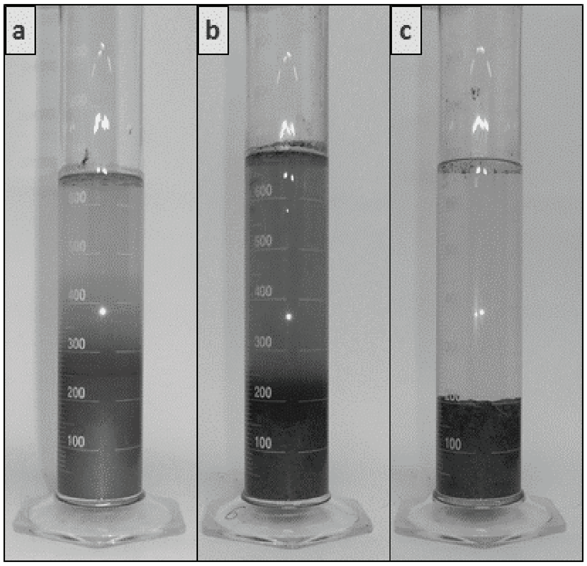

Figure 3. **Water capped MFT after 5 days: a) untreated, b) single treatment, c) dual treatment**

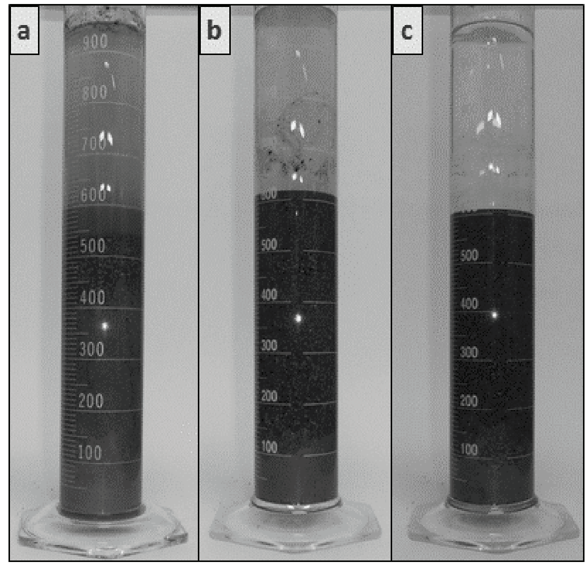

Figure 5. **Samples capped with 800g sand after 5 days: a) untreated, b) single treatment, c) dual treatment**

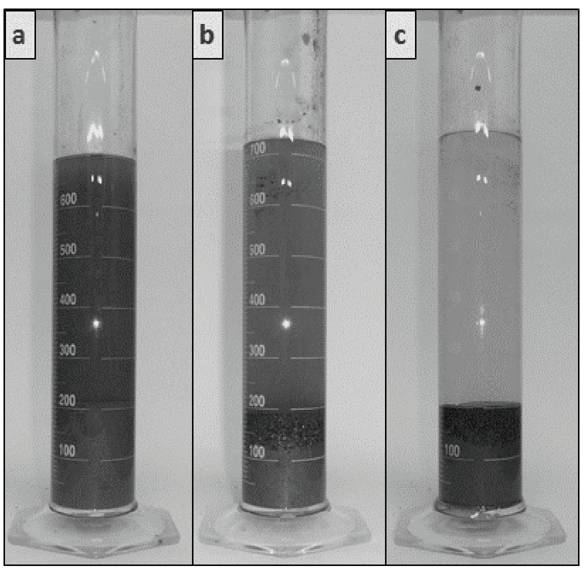

Figure 4. **Samples capped with water and 100g sand after 5 days: a) untreated, b) single treatment, c) dual treatment**

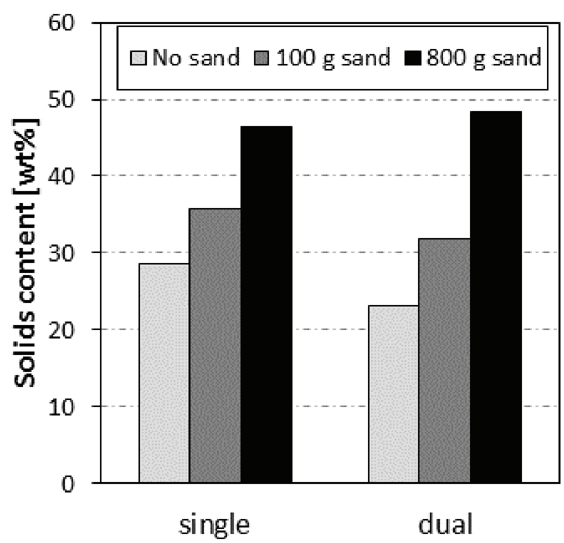

Figure 6. **Consolidation of treated MFT after 6 days**

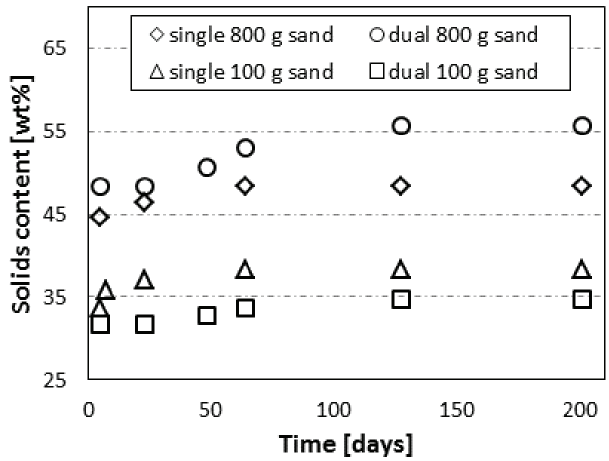

Figure 7. Consolidation of treated, sand capped MFT over time

Table 1. Characterization of MFT and process water samples

Sample	Solids content [wt.%]	Fines content [%]	Clay content [%]	pH
MFT	27.7	100	93.0	7.6
Process water	0.2	N/A	N/A	8.4

Table 2. Properties of the tested polymers

	Anionic polymer	Cationic polymer
Chemistry	Polyacrylamide	Polyacrylamide
Molecular weight	High	Very low
Charge density	Medium	Very high

Table 3. Experimental conditions

No	Polymer treatment	Water capping [mL]	Sand capping [g]	Remark
1	No	No	No	Control
2	No	500	No	Effect of water capping
3	No	500	500	Effect of sand capping
4	Single	none	none	Control single treatment
5	Single	500	none	Effect of water capping for single treatment
6	Single	500	100	Effect of NST capping for single treatment
7	Single	500	800	Effect of NST capping for single treatment
8	Dual	none	none	Control dual treatment
9	Dual	500	none	Effect of water capping for dual treatment
10	Dual	500	100	Effect of NST capping for dual treatment
11	Dual	500	800	Effect of NST capping for dual treatment

Table 4. Polymer dosages and resulting solids contents of treated MFT

Treatment	Anionic polymer dosage [g/t]	Anionic polymer dosage [g/t]	Volume Added [mL]	Treated MFT solids content [wt.%]
Single	2100	-	29.1	24.2
Dual	2100	600	37.4	23.3

INTERBEDDED SAND LAYERS (ISL) CONCEPT FOR DEEP FINES-DOMINATED TAILINGS DEPOSITS

Srboljub Masala[1], Silawat Jeeravipoolvarn[1], Reza Nik[2] and Robert Donahue[2]
[1]Thurber Engineering, Calgary, Canada
[2]Shell Canada Energy, Calgary, Canada

ABSTRACT

Deep deposits of dominantly fine tailings provide one option for fine tailings management in the oil sands. The objectives are to have a high fines-capture efficiency in a relatively small footprint without the need for re-handling of the deposited material. The challenges of this particular tailings management approach are long consolidation times, large deformations, slow rates of strength development, and extended monitoring before and after reclamation activities. Interbedded layers of coarser materials acting as horizontal drains have shown beneficial effects on consolidation of dredged deposits, clay fill embankments, water-retaining dams, etc.

Shell Canada Energy (Shell) with support from Thurber Engineering has started an evaluation program to assess the potential for interbedded sand layers (ISL) to accelerate consolidation of deep fines-dominated deposits. The first phase of this program was a desktop study with the goals to develop representative models and identify critical influential parameters. This paper will present the methodology and results of this study showing the parametric variation of sand layer thickness and length and the contrast in hydraulic conductivity between sand and fine tailings.

INTRODUCTION

Shell Canada Energy Ltd. (Shell) with support from Thurber Engineering Ltd. (Thurber) is evaluating the effectiveness of Interbedded Sand Layers (ISL) concept in accelerating consolidation of deep fines-dominated tailings deposits. The interbedded sand layers are intended to: (a) shorten the drainage paths and reduce the total consolidation time for the deposit; and (b) provide drainage pathways for quick drainage of consolidation-released water out of the deposit. This concept is widely used in civil engineering projects such as dredged fill structures or environmental projects including capping of hazardous waste, but it has received increased attention in the oil sands industry only recently.

Project framework

The study was planned with three phases. The goal of the first phase – Desktop Study – was to conduct a theoretical / numerical investigation of the feasibility and applicability of the ISL concept for accelerated consolidation of oil sands tailings in deep ponds. It also served as a gate to the next two phases that would explore practical aspects of the ISL deposit application and eventually lead to a large field-scale demonstration experiment.

The objectives of Phase 1 were the following:

- To evaluate the effectiveness of interbedded sand layers in reducing the overall consolidation time of a deep fines-dominated tailings deposit;
- To interrogate the key model variables and better understand their relative contribution and influence on the consolidation performance of the deposit;
- To specifically investigate two deposit cases specified by Shell: a low solids content in-line flocculated tailings (ILFT) and a high solids content centrifuge cake (CC);
- To establish the basis for comparison of different scenarios using selected performance parameters;
- To flag the uncertainties in the performed analyses and potential risks for commercial-scale applications and provide suggestions for the next two phases of investigation.

LITERATURE REVIEW

An introductory stage of Phase 1 was a literature review focused on the three topics relevant for the ISL concept study: theoretical approaches to modelling and simulation, analytical and numerical solutions, and applications (case histories or large-scale tests).

First theoretical approaches to consolidation of stratified natural soils or human-made layered soil structures date back to the middle of the 20th century, taking as the basis Terzaghi's small strain one-dimensional (1D) theory or its expanded 2/3D version by Rendulic (Terzaghi, 1943). High levels of sophistication were reached relatively early, dealing with complex problems of combined drainage systems consisting of vertical (wick drains) and horizontal (sand blankets) drainage elements. In the last two-three decades the modelling becomes increasingly based on the finite strain consolidation theory, limited to 1D conditions (vertical deformation and water flow). A great number of analytical 1D models were found in the literature, typically dealing with a pair of fine- and coarse-grained layers, or a multiple of them, subject to a variety of boundary conditions. These papers were not considered because of an early decision in this project to turn to a multidimensional consolidation analysis (explained in the next section).

A problem theoretically similar to the ISL concept was addressed by Gibson and Shefford (1968) which looked to establish rational design criteria for horizontal drainage layers in embankment structures. Their analysis was based on the small strain linear 2D solution for the pore water pressure in a double-drained clay layer with a surcharge load increasing at a constant rate with time. Their conclusions were biased to the particular design requirements of the embankment and may not be suitable to a tailings interlayer sand drainage application. They concluded that for a drain to be fully effective it should have a hydraulic conductivity at least 10^6 times that of the surrounding clay fill, although an acceptable efficiency could be achieved with the sand/clay hydraulic conductivity ratio of about $3x10^4$. These conclusions were driven by the specifics of embankment structural features and construction requirements, primarily the need for early stability. They did not take into account the factor of time which becomes prominent in the case of a tailings pond, when the deposit stability is not an issue during deposition and the filling times are long; in tailings ponds, drainage layers can eventually achieve high efficiencies given enough time.

The main result of this part of literature review was clear identification of three principal influences: layer thickness, length and hydraulic conductivity, including both sand and clay components, and the need to investigate their interrelationships through a clear and simple model.

The most relevant paper discussing assessment of theoretical concept of horizontal drainage layers in civil structures was by Sills (1974). Three examples of constructed soil structures – two fill dams and one road embankment – were analyzed using the Gibson-Shefford approach, with two of them confirming its validity. However, these examples were not directly applicable to the ISL concept because for two of them the drain-to-fill hydraulic conductivity ratios were much higher than anticipated in the ISL deposit problem, while for the third the hydraulic conductivity ratio was much lower. The times of construction were, relatively, either too short or too long, so that calculated drainage efficiency factors were extreme, and the answers obtained were essentially black or white. Nevertheless, the paper provided examples of successful construction of embankments of low hydraulic conductivity clay fill using sand blanket drainage.

MODELLING

Essential phenomenology to incorporate in modelling

Preliminary considerations of the theoretical problem in the ISL concept background showed that deformation in an ISL deposit is dominated by the consolidation settlement of fine tailings layers and is mostly vertical. The water flow pattern in an ISL deposit is multi-directional: it is essentially vertical in the fine tailings layers, but prevailingly horizontal in the sand layers (Figure 1). To realistically simulate behaviour of such a system, these relevant physical aspects had to be incorporated in any analytical model.

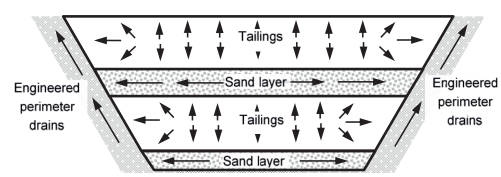

Figure 1. ISL Concept Configuration

The ISL flow pattern assumption was corroborated by a preliminary analysis of a steady-state flow through a single sand layer with various aspect ratios (the layer length-to-thickness ratio or L/t) gradually increasing from L/t = 2 to 100. The layer was subject to variable influx distributions from both top and bottom, with one lateral side sealed, with the no-flow boundary condition (BC), and the other free-draining, with zero excess pore pressure. Isotropic and anisotropic hydraulic conductivities were used, with the anisotropy ratio k_h/k_v up to 10. This was very similar to the conditions of the sand layers in the subsequent ISL consolidation analyses.

The analysis showed that the aspect ratio of L/t = 10 may be adopted as a lower limit of validity for the ISL flow pattern with the isotropic hydraulic conductivity, while the limit is a little higher – L/t = 20 – with the anisotropic hydraulic conductivity. Since the practical L/t aspect ratios were an order or magnitude higher in our ISL concept analyses it was concluded that the simplifying assumptions were justified and safe to use.

The effect of BCs for the fine tailings layer was investigated by comparing the ISL consolidation cases with free-drained and impervious ends. The flow rate through the lateral boundary (in the horizontal direction) was negligible compared to the flow rate to sand drains (in the vertical direction).

Model development

The multidimensional nature of water flow in the ISL problem clearly indicated the need to abandon 1D models that have been a common approach for the consolidation analyses of oil sands tailings deposits, and to adopt in this analysis two- or three dimensional models. Unfortunately, this requirement severely reduced the spectrum of available software for the ISL analyses and we found that the remaining software options would take us far beyond the current scope and budget. All that necessitated development of custom models for the ISL deposit analyses.

Production of theoretically rigorous software that would satisfy the stated requirement for problem multi-dimensionality and incorporate essential physics as well as highly desirable features such as the finite strain formulation of consolidation process, non-linearity of material properties, heterogeneity (layering), etc. in parallel with stability and efficiency of its numerical implementation was not achievable within the budget and time constraints. We decided to develop several custom models (with their own particular sets of assumptions) that would be capable of incorporating the salient features of physical behavior and then use engineering judgment for interpretation of their results. Two custom models are presented.

Model 1

Model 1 was based on a rigorous theory for multi-dimensional consolidation problem by Terzaghi-Rendulic:

$$\frac{\partial u}{\partial t} = c_x \frac{\partial^2 u}{\partial x^2} + c_y \frac{\partial^2 u}{\partial y^2} + B \frac{dp}{dt} \qquad \text{[Eq. 1]}$$

where u is the excess pore pressure that is a function of two space coordinates (x,y) and the time t, and c_x and c_y are the coefficients of consolidation in the directions of spatial coordinates, expressed by equations of the type:

$$c_x = \frac{k_x}{m_x \gamma_w} \qquad \text{[Eq. 2]}$$

where k is the hydraulic conductivity, m is the coefficient of volume change, and γ_w is the unit weight of water. The last term in Equation 1 represents the rate of generation of excess pore pressure caused by increasing weight of deposited material above the analyzed layer due to pond filling, with B being the Skempton pore pressure coefficient, adopted as B=1 in further derivations, and p the overburden pressure.

The drawbacks of this theory were the small strain formulation and linearization of material properties (the coefficient of consolidation as the only material parameter, combining hydraulic conductivity and compressibility into a single number). Its strengths were a clear theoretical basis, tested and proven over decades, and a rigorous treatment of water flow in 2D plain strain conditions without any simplifying assumptions (the flow was allowed in both spatial directions in both fine tailings and sand layer). Furthermore, Model 1 allowed implementation of a numerical solution without numerical instability or other computational issues.

In this method, the ISL deposit was analyzed using the “stacking approach” in which a representative “building block” of a periodic structure is extracted and subject to boundary conditions (BCs) equivalent to those that would be experienced by the block if it were in a real structure. In this case, the building block was a sequence of tailings layers that can be placed over one year of deposition – a “sandwich” consisting of one fine tailings layer between two sand half-layers (Figure 2).

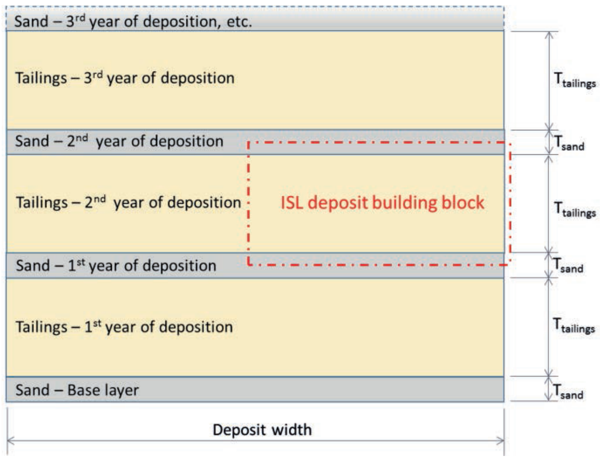

Figure 2. Periodic structure of an ISL deposit with Model 1 building block

This sand-tailings sandwich was adopted as the model geometry (Figure 3). In the analysis, it was subjected to gradually increasing surcharge load equivalent to the effective stress due to the weight of overburden (the material placed during pond filling). The overburden weight included buoyancy because of the assumption that the material was placed fully saturated and that the phreatic surface was kept at the top of tailings throughout analysis.

The self-weight was neglected. It caused certain differences during the first year of deposition, but they quickly decreased with time.

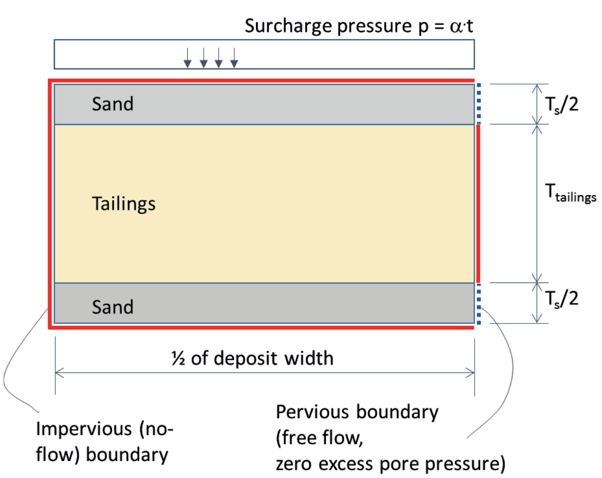

Figure 3. Model 1 geometry and BCs

Temporal evolution of the ISL Model 1 was approximated through the post-processing approach by "stacking" of the calculated model states for consecutive years; it required multiple analyses of the same model setup with a slightly varying input.

The stated problem was analyzed using the FlexPDE version 6, a finite element method (FEM) software for solving general partial differential equations (PDE).

Model 2

Model 2 was formulated as an axially symmetric problem (Figure 4) and incorporated the 1D finite strain formulation by Gibson et al. (1967) and material non-linearity (compressibility and hydraulic conductivity as functions of void ratio), but had to make a simplifying assumption about the water flow in sand layer through a "volume averaging" procedure. The volume-averaged flow length L=R/3 – the average flow distance of consolidation-released water within the sand layer, from the axis of symmetry to the perimeter – was calculated by averaging uniform flow rates over the horizontal contact area of the sand and fine tailings layers.

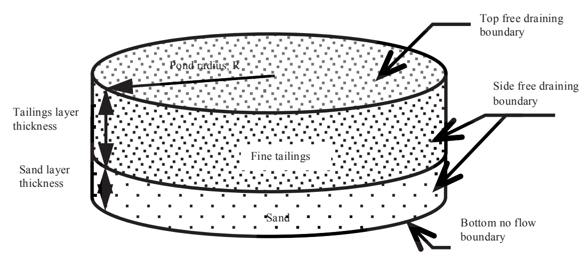

Figure 4. ISL layer configuration for Model 2

PARAMETRIC ANALYSIS

Literature review and preliminary analyses identified three critical parameters for the ISL deposit performance:

- Sand-to-tailings hydraulic conductivity ratio, or the consolidation properties of the materials in general;
- Sand-to-tailings layer thickness, or the ISL deposit configuration;
- Layer length, or the ISL deposit area.

Parametric analysis matrix

The above mentioned parameters had to be varied in the parametric analysis. It was decided to assign only two values to each parameter, to keep the total size of a full parametric analysis matrix at reasonable 8 cases. All other input data were kept constant in order to make the results comparable.

The fine tailings material was represented by two tailings types specified by Shell:

- Centrifuge Cake (CC), and
- In-Line Flocculated Tailings (ILFT).

Four analyses were performed for each tailings material, with:

- Two combinations of sand-to-fine tailings (S:F) layer thicknesses: S:F = 1 m:7 m and 2 m:6 m, and
- Two values of layer lengths in the models: 200 m and 500 m. It should be noted that a layer length in the model is a half of the actual pond width (in Model 1) or diameter (in Models 2 and 3) because the models are symmetric. In this case, 200m and 500 m correspond to the ponds of 400 m and 1 km in width or diameter.

The results of parametric analyses were compared to each other, for assessment of relative performance of different realizations of an ISL deposit for various tailings types and deposit sizes and configurations. However, it was also necessary to compare the overall ISL consolidation performance (i.e. the impact of horizontal drainage layers) to the performance of the same deposits without horizontal drainage – the "reference cases". The reference cases were the same CC and ILFT deposits, but homogeneous – without sand layers. They were analyzed using a common 1D software package for large strain consolidation simulations since the water flow occurred only in vertical direction. Underdrainage was allowed in these simulations for consistency with the ISL cases which all were double-drained. Underdrainage effect were limited to the bottom 10–15% of the deposit and were practically inconsequential.

Performance criteria

The parametric analysis output was specified in a way that allowed comparative performance assessment of the analyzed ISL configurations. The selected performance criteria were the following:

- Average degrees of consolidation for settlements U_s and excess pore pressure dissipation U_{ppe} at the end of pond filling (EOF)
- Average solids content and void ratio at EOF
- Solids storage efficiency (SSE) and fines storage efficiency (FSE) at EOF (The SSE and FSE are defined as the masses of dry solids and fines per unit volume of deposit in the ultimate, consolidated state, with fully dissipated pore pressures.)
- Times to reach U_s = 90% and U_{ppe} = 90%
- Differential settlement from EOF to a 100% consolidation.

Input data

The input consisted of several sets of data describing:

- Pond geometry and deposit configuration
- Initial and boundary conditions
- Tailings management schedule (filling rates and total filling times)
- Physical and geotechnical index properties of tailings, and
- Consolidation properties – hydraulic conductivity and compressibility – of tailings.

It should be noted here that the pond shape was kept prismatic / cylindrical (with vertical sides) to avoid introducing additional influences of: (a) the pond surface area variation with tailings elevation, (b) the resulting decrease of tailings rates of rise (RoR) and layer thicknesses over time (with constant tailings production over the pond filling period) and (c) the associated increases in drainage lengths and resident times in sand layers.

The tailings management schedule assumed an annual fine tailings production rate of 3.6 million tonnes of dry solids per year. The adopted RoR = 8 m and 9 years of deposition were kept constant for comparison purposes. The layer thicknesses were nominal values – they did not include consolidation settlement during deposition.

The physical and geotechnical properties of two analyzed tailings types were fixed – no parametric variation was performed. The consolidation properties for fine tailings (Figures 5 and 6) were based on relatively scarce laboratory experimental data, while the hydraulic conductivity of sand was based on field data from literature (McKenna et al. 2010) and was kept constant in the analysis.

The CC material was a "more critical" one as it was more compressible than ILFT and its hydraulic conductivity, besides being initially lower, also decreased faster with the stress increase (pond elevation).

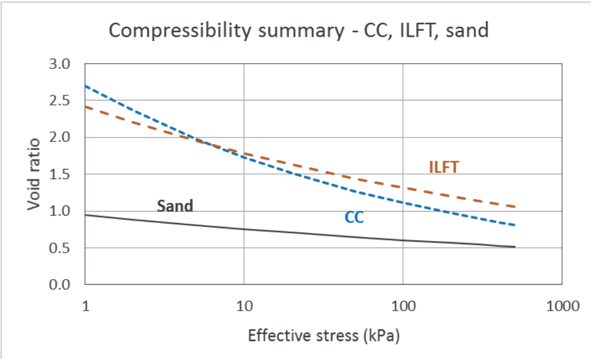

Figure 5. Compressibility functions

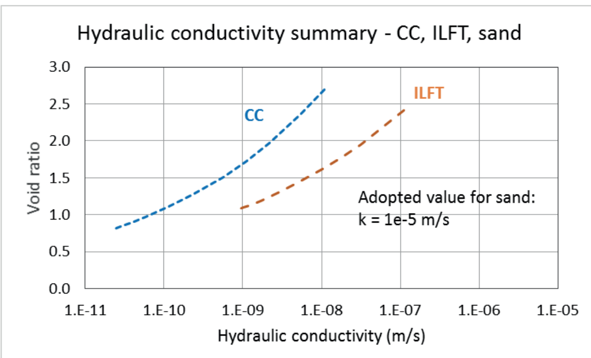

Figure 6. Hydraulic conductivity functions

Model 1 required as input the coefficients of consolidation c_v for sand and fine tailings, which were calculated using the compressibility and hydraulic conductivity functions from Figures 6 and 7. The calculated c_v values were also highly nonlinear functions of stress / void ratio, spanning 1-3 orders of magnitude (Figure 7). This precluded selecting average c_v values for the calculations with Model 1; the ranges of variation were used instead. Model 1 simulations therefore represented a kind of sensitivity analysis for the only material parameter c_v.

The use of c_v ranges implied a specific approach to the analysis outcomes and their interpretation. The minimum values of c_v were associated with the low stress range; the maximum values of c_v with the high stress range. In reality, the actual behaviour would be situated within the band bound by the simulated responses for the limiting values, the minimum and maximum c_v. It can be anticipated that the actual ISL deposit response would be closer to the simulated response for minimum c_v in the early stages of the consolidation, when effective stresses are relatively small; i.e. during filling and immediately after it. As consolidation progressed and the effective stresses increased, the actual response would move toward the simulated results for the maximum c_v.

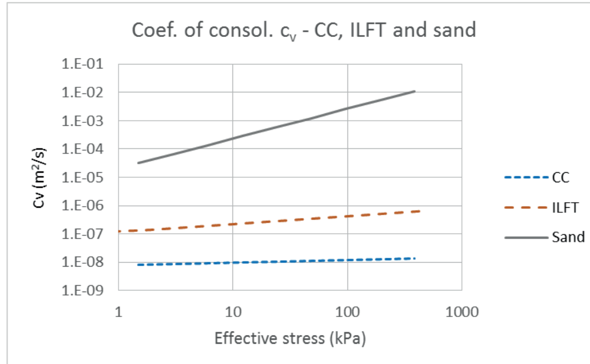

Figure 7. Ranges of variation of calculated c_v for CC, ILFT and sand

Effects not included in analysis

Time-dependent volumetric deformation during consolidation (creep) was not included. It was assessed to be a secondary effect in this analysis.

Environmental effects like freeze-thaw compression (that may increase settlements) and drying (resulting in reduction in hydraulic conductivity and compressibility in surface zone, and creation of non-homogeneities in the fine tailing layers) were not included. It was assumed that they would not take place under the operational conditions of a deep pond.

Potential scale-dependent influences on the tailings consolidation properties were neglected. A proper estimate of possible changes in the materials properties that were determined by laboratory testing when extrapolated to the field, to make them representative for a commercial-scale deposit, is critical, particularly for the hydraulic conductivity of sand in drainage layers.

SUMMARY OF RESULTS

Consolidation – settlements and pore pressure dissipation rates

Overall, this study showed that the ISL deposits consolidate more rapidly than the reference cases of homogeneous deposits of the same tailings without drainage layers. From the analyzed example of Shell's CC, the ISL concept is capable of producing dramatic increases in the consolidation rates of tailings deposits, thereby reducing the duration of consolidation from several hundred years to several decades, which fits it into a common mine lifetime. Figures 8 and 9 present the case of a 1 km wide pond; the data for a 400 m wide pond showed even faster consolidation. The coefficient of consolidation, mostly driven by the hydraulic conductivity ratio, is the dominant factor, with a significant contribution of the drainage layers (sand) thickness. For comparison, over a hundred years needed for the minimum c_v CC case to reach 90% of pore pressure dissipation, the reference case barely goes over 15% of the average pore pressure dissipation.

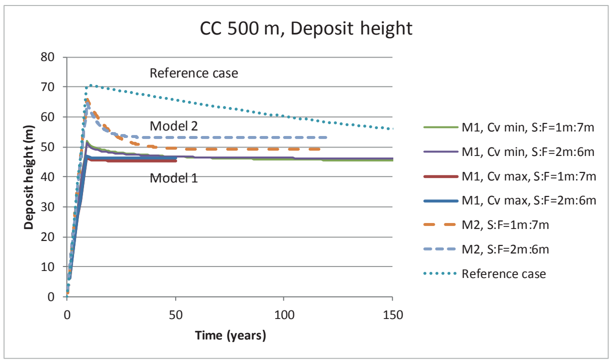

Figure 8. CC, 500 m long layers, deposit height (M1 = Model 1, M2 = Model 2)

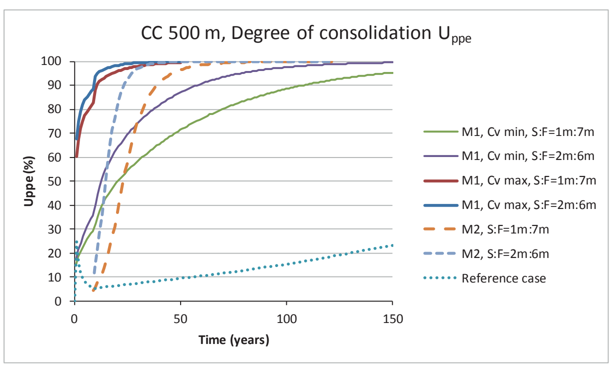

Figure 9. CC, 500 m long layers, U_{ppe} (M1 = Model 1, M2 = Model 2)

On the other hand, the ISL impact will depend in practice on the tailings treated: the effect of horizontal drainage can be quite modest in the case of relatively permeable materials like ILFT. Figures 10 and 11 show the case of a 400 m wide pond filled with ILFT. Obviously, there is an appreciable difference between the two cases of minimum and maximum c_v, which partially clouds the issue. However, even when the minimum c_v values are assumed representative, horizontal drainage layers do not significantly improve consolidation relative to the reference case ILFT deposit which drains only in vertical direction. For such a material, a different management concept should be considered. (As a caveat, this does not mean that a better performance of the ISL ILFT deposit cannot be obtained by optimization of fixed parameters in this analysis – RoR, layer thickness, etc. The optimization was not the goal of this work.) The remaining text will therefore focus on the CC material.

As a rule of thumb, the effect of horizontal drainage fades in the case of materials of high hydraulic conductivity. In such cases, the absolute flow capacity of sand layers as drainage conduits becomes critical because of huge amounts of consolidation-released water that have to be evacuated from the deposit. The length of drains, i.e. the pond size, becomes dominant: the longer the drain, the longer the flow time through drain.

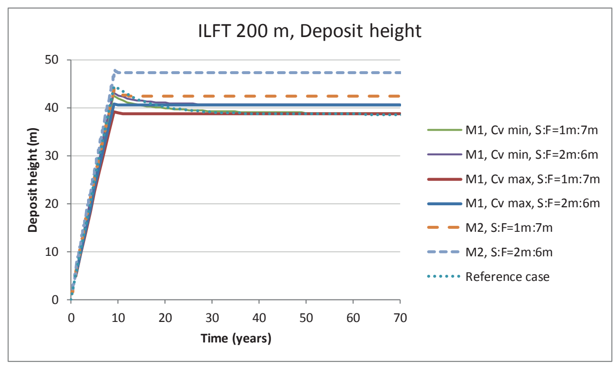

Figure 10. ILFT, 200 m long layers, deposit height (M1 = Model 1, M2 = Model 2)

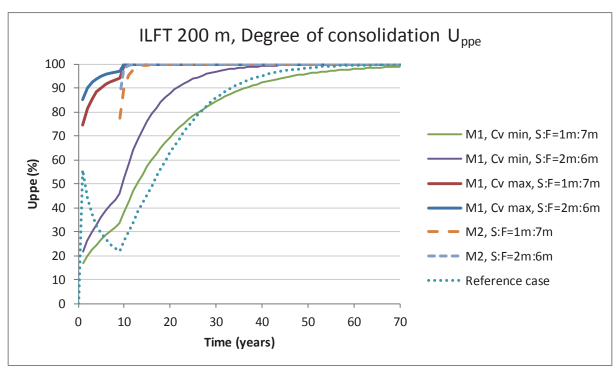

Figure 11. ILFT, 200 m long layers, U_{ppe} (M1 = Model 1, M2 = Model 2)

Post-deposition settlements

It is important to notice that the post-depositional settlements are much smaller with the ISL deposit than with a homogeneous deposit – the reference case, and it is valid for both CC and ILFT (Figures 9 and 11). This is very beneficial for reclamation design as it reduces the amount of material and work required, and increases the predictability of behaviour of final landscape design solutions.

Small post-depositional settlements also increase the storage efficiency of a tailings pond footprint area in the ISL concept and makes its lifetime longer. Both CC and ILFT solids and fines storage efficiencies (SSE and FSE) are consistently higher for the ISL deposits than the reference cases (Table 1).

DISCUSSION

Relative influences of three principal performance factors

They are possibly best graphically illustrated in Figures 12 to 14, presenting in parallel the excess pore pressure profiles at EOF and at selected times afterwards for four analyzed cases of CC in the Model 1 parametric analysis. The profiles plotted are for the vertical section in the middle of the pond (the axis of symmetry), where the pore pressure dissipation is the slowest.

The coefficients of consolidation varied from 0.324 to 0.435 m^2/year for CC and from approximately 19,000 to 355,000 m^2/year for sand. The high variation in the sand c_v is due to its compressibility as the hydraulic conductivity was adopted constant.

With smaller pond areas and shorter drainage layers (Figure 12) the effect of conductivity of drain layers (sand) is dominant over the thickness of drains – notice almost no difference between the lines for 1 m and 2 m thickness at either Min or Max c_v in the figure. The pore pressure in sand, relative to fine tailings, is very low in all four cases, indicating high drain efficiency from the start of pond filling.

For larger ponds and longer drainage layers (Figure 14) the drainage efficiency of sand layers quickly deteriorates for the case of Min c_v. The pore pressure in sand is only slightly different than in the fine tailings layers, revealing low drainage efficiency during deposition. On a side note, the drains are still highly efficient, right from the beginning of deposition, for the Max c_v case.

The value of c_v as the sole material parameter in this analysis becomes clear when pore pressure dissipation over time is inspected (Figures 13 and 14). The ratio of maximum pore pressures in fine tailings and in sand, for both Min and Max c_v, progressively increases with time, confirming much faster consolidation rate for the higher c_v material. The 2 m thick sand layer case (not shown) reveals even faster consolidation rate.

The drainage layer length seems to be an amplifying factor when the coefficient of consolidation is low (Figure 14). For the 500 m long drains, the pore pressures in fine layers are significantly higher for the same time instants than for the 200 m long drains. At the same time, the Max c_v performance is still acceptable.

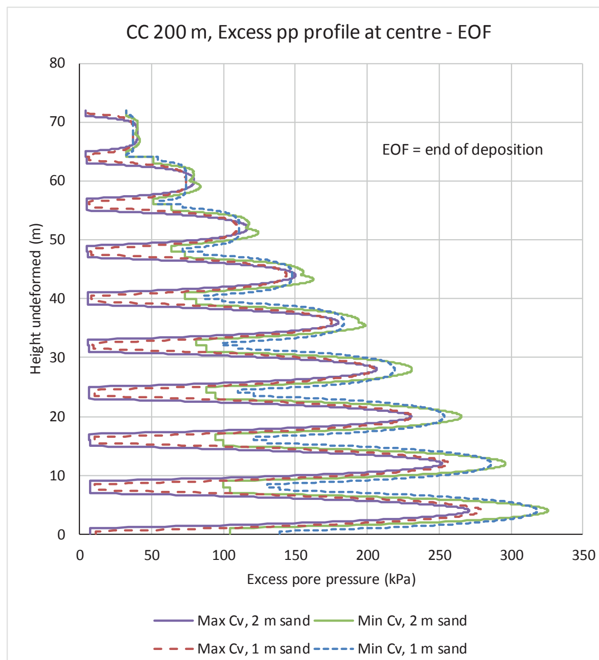

Figure 12. CC, L = 200 m long layers, excess pore pressure profiles at EOF

Potential application issues

The following are considered open problems for execution and maintenance of an ISL deposit, to be addressed in further work:

- Construction of drainage layers in an operating pond (sand delivery to pond interior)

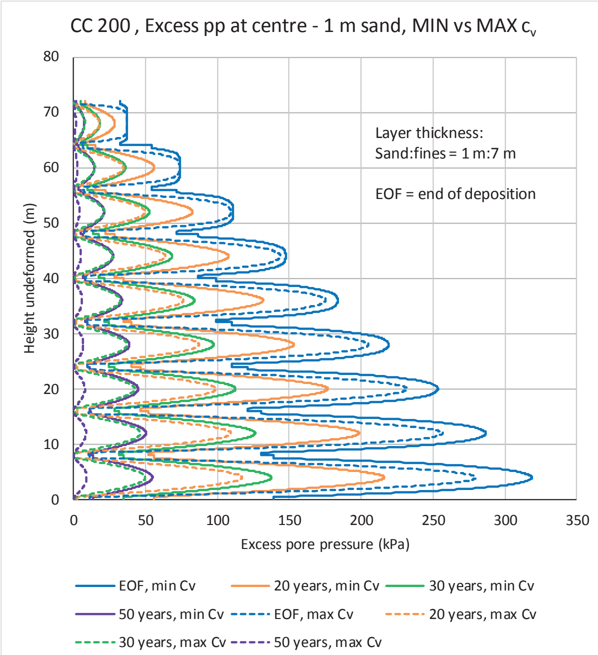

Figure 13. CC, L = 200 m, excess pore pressure profiles over time (EOF, 20, 30 and 50 years)

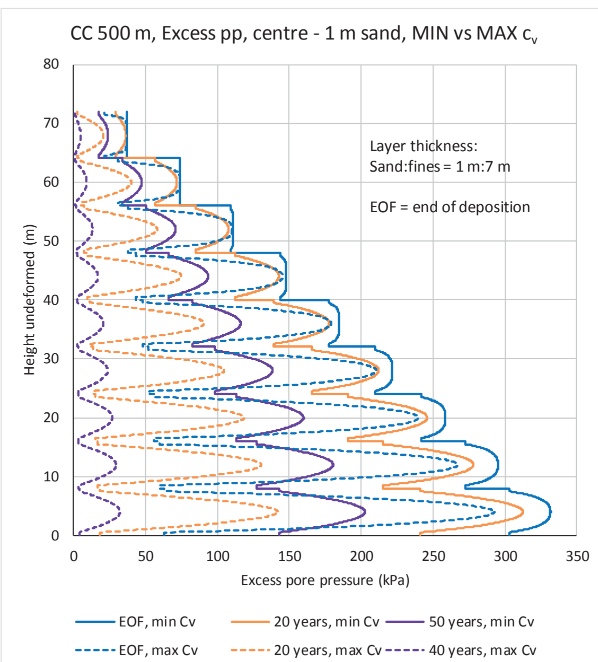

Figure 14. CC, L = 500 m, excess pore pressure profiles over time (EOF, 20 and 50 years)

- Construction of engineered perimeter drains
- Environmental effects: Impact of freeze/thaw, and drying densification of the treated fines tailings on sand drain effectiveness
- Performance monitoring (measurement types, instrumentation, locations, etc.).

CONCLUSIONS

Numerical analysis results indicate that ISL deposits consolidate more rapidly than the reference cases of homogeneous deposits of the same tailings without drainage layers. In particular, significant improvement on the rate of consolidation was obtained when analyzing low-hydraulic conductivity tailings such as centrifuge cake.

The three critical performance factors for the ISL concept from previous studies were confirmed:

- Hydraulic conductivity of sand, actually the ratio of hydraulic conductivities of sand and fine tailings;
- Drain length, or a representative length for the pond area; and
- Sand thickness, actually the ratio of thicknesses of fine tailings and sand layers.

Relative contribution of these three critical factors is not fixed nor easily predictable, but changes in a complex manner, depending on their absolute magnitudes. For example, with a high hydraulic conductivity of sand the impact of layer length is (relatively) reduced. When a pond becomes larger and the drains longer, the hydraulic conductivity effect is subdued. The thickness of sand layers seems, relatively, the least important of the three.

This analysis fixed the values of some parameters that may become critical to successful execution under certain circumstances, such as: material properties, filling rate, pond size and geometry, etc. Optimization prospects with moderate adjustments of some parameters were demonstrated.

It is recommended to expand the described analyses by including the following factors:

- Variation of factors that were kept constant in the performed analysis, aiming at understanding of their interaction and perceiving the domain of applicability of the ISL concept;

- Effects of filling rate and real pond geometry with sloping sides;
- Desired features – multidimensional flow, finite strain theory, non-linear material properties - into a comprehensive model;
- Reliable public or literature data on theoretical and empirical examples of layered soil structures for validation and verification purposes.
- Delineation of the application limits for various oil sands tailings types and possible synergies with other tailings management strategies and current practices.
- The following laboratory and field-scale investigations are recommended to increase the reliability of input data:
- More laboratory consolidation testing on investigated tailings;
- Analyses of tailings deposit data from pond surveys and, if available, dedicated field investigation programs, to improve understanding of settling behavior and data reliability for sand and fine tailings under field conditions;
- Collecting public and literature data on civil and mining projects implementing horizontal drainage layers for validation and verification purposes.

The following are questions related to further planning and execution of ISL staged investigation program:

- Investigate potential methods for construction of ISL deposits, especially hydraulic delivery of materials from the perimeter into the interior of tailings ponds under usual operational conditions, including field-scale trial depositions with planned materials;
- Investigate process control and steering at the commercial scale, based on monitoring in the field and feedback to the operations.

REFERENCES

Gibson, R.E., England, G.L. and Hussey M.J.L. 1967. The Theory of One-dimensional Consolidation of Saturated Clays. I. Finite Non-linear Consolidation of Thin Homogeneous Layers. Géotechnique, 17(3): 261–273.

Gibson, R.E. and Shefford, G.C. 1968. The efficiency of horizontal drainage layers for accelerating consolidation of clay embankments. Geotechnique 18, No. 3, 327-335.

McKenna, G., Biggar, K., Kyaw, S.M., and Journault, J. 2010. Oil sands tailings sand hydraulic conductivity. 2nd International oil sands tailings conference. December 5-8, 2010. Edmonton, AB, Canada, pp. 21-30.

Sills, G. C. 1974. An assessment, using three field studies, of the theoretical concept of the efficiency of drainage layers in an embankment. Geotechnique 24, No. 4, 467- 474.

Terzaghi, K. 1943. Theoretical Soil Mechanics. Wiley, New York.

Table 1. Performance criteria, CC, 500 m long layers

Model	Model 1				Model 2		Reference case
Layer thicknesses ratio sand: fines (m)	1:7		2:6		1:7	2:6	
	Min c_v	Max c_v	Min c_v	Max c_v			
EOF deposit height H (m)	52.0	46.4	51.4	46.9	66.0	64.6	70.0
EOF U_s (%)	75	96	80	97	29	44	11
EOF U_{ppe} (%)	29	83	36	88	5	12	5
EOF average void ratio e	1.3	1.1	1.1	1.0	2.1	1.9	2.4
EOF average solids content SC (%)	65	70	69	73	54	57	51
Solids storage efficiency SSE (t/m^3)	1.26		1.37		1.34	1.48	< 0.96
Fines storage efficiency FSE (t/m^3)	1.01		0.86		1.06	0.90	< 0.96
Time from SOF to U_s = 90% (years)	26	< EOF	15	< EOF	29	19	> 200
Time from SOF to U_{ppe} = 90% (years)	105	11	57	< EOF	39	24	> 200
Settlement from EOF to U_s = 100% (m)	6.7		5.2		16.8	11.5	> 17.4

SOF = start of filling

ON THE BENEFICIAL USE OF SOFT MUD – CASE STUDY MARKER WADDEN PROJECT

Thomas Vijverberg, Walter Jacobs, Roeland Lievens and Alexis Roels
Boskalis, Papendrecht, The Netherlands

ABSTRACT

The oil sands industry faces a number of challenges with regard to the handling of mature fine tailings:

1. Reclamation which is required from an environmental and regulatory perspective. Restoring the landscape in its original state is the main purpose.
2. Dewatering and strength development of mature fine tailings is rather slow.
3. Handling large volumes requires a cost-effective work method: limit use of additives, limit multiple operational rehandling steps, smart use of natural processes.

These challenges are also observed in land reclamation projects. This paper presents a case study of the Marker Wadden project in the Netherlands. This project shows that it is possible to reclaim large volumes of fine cohesive material in an economical way, using state-of-the-art design tools and monitoring techniques, allowing for an adaptive construction method. The scale of the project (300 – 500 ha) is comparable to typical oil sands ponds (diameter of ~2-4 km, 300 – 1000 ha).

In Lake Markermeer large quantities of fine sediment are present, due to which the ecological state of the lake is low. The main challenge in building this large nature reserve area with soft mud is to do this in an economical way, creating physical gradients, promoting biodiversity and enabling the catchment of fines.

Starting points of Boskalis' (design and construct contractor) design were:

- Make use of natural processes as much as possible;
- Smart design of operational work method, taking into account processes like: self-weight consolidation, crust formation, atmospheric drying and effect of vegetation;
- Apply state-of-the-art design tools: model, experiments, monitoring, adaptive management.

Soft mud exhibits highly varying characteristics at each project, but the design and construction principles as applied for the Marker Wadden project can also be applied to the oil sands industry for reclamations constructed from mature fine tailings. This makes the Marker Wadden project a good example of how to reclaim large deposits of soft mud in a proven, economical and safe manner.

INTRODUCTION

Lake Markermeer

Lake Markermeer is a large (680 km^2), shallow fresh water lake in the center of the Netherlands (Fig. 1). It is an artificial lake which was formerly part of the Zuiderzee (tidal bay). After the area was closed off with two dams it became a fresh water lake with unique ecological values (Natura2000 area).

Over the past decades, several ecological problems have arisen related to, amongst others, high turbid water (decrease in light penetration due to large quantities of fine sediment), decrease in biodiversity and change in nutrients (Vijverberg 2011 and De Lucas Pardo (2014)). Several solutions for these problems have been investigated within the research project 'Natuurlijker Markermeer IJmeer' (kennis.markermeerijmeer.nl).

One of the recommendations was to increase the habitat diversity. This diversity is rather limited now, due to the size and shallow character of the lake, and also the hard infrastructural elements at the borders (dikes). Nature reserve areas at the east side will enhance the diversity.

The Marker Wadden project (Fig. 1) was set up to develop such areas and to improve the ecology.

Figure 1. Location of Marker Wadden in Lake Markermeer (www.nos.nl)

Project Background

The Marker Wadden project is initiated by Nauurmonumenten (Dutch NGO). The basic idea is to build nature reserve islands with Holocene and soft fine clay material from the lake. By using this material, the total amount of fine sediments available in the lake for resuspension will reduce, improving the light climate. The islands are designed to be an ideal habitat for birds, because of the shelter and the typical vegetation (such as reed) that it provides. Figure 2 shows an artist's impression that was made by during the project tender phase.

Figure 2. Artist's impression of the Marker Wadden islands

For the first phase of the project (approximate size of 300 ha) a fixed budget was available. The tender question was to design an area that is as large as possible, staying for a fixed budget. Bids were predominantly evaluated on these criteria, besides some quality aspects.

The client also defined stringent project requirements with respect to final elevations of the area. Those requirements are challenging due to the difficulty to predict self-weight consolidation of the soft material, characterized by large volume variations which are rather sensitive to the varying local sediment characteristics (mud content, density, physico-chemical constituents, etc).

Strength requirements were also defined, in terms of goose accessibility. This is a rather unique requirement, as it focuses on future function rather than physical properties.

Boskalis[1], as main contractor, led the project team for this design and construct tender. The project team consists of many different disciplines like landscape architects, geotechnical engineers, specialist consultants for consolidation and crust formation, ecologists, etc.

All risks were carried by the main contractor, including the risks of the behavior of the soft mud. Special attention was paid to safety with respect of the floating equipment and the soft character of mud vs accessibility for personnel, equipment and visitors.

Relation with oil sands industry

Although the Marker Wadden Project has a different background, several similarities can be identified with the oil sands industry and the handling of mature fine tailings.

The project is an example of how to reclaim an area using large quantities of soft material for which dewatering and strength development is a rather slow process.

Also within the Marker Wadden project, a safe, proven and economical solution was required. The large volumes require a cost-effective approach and work method.

The spatial scale of the project (300 – 500 ha) is comparable to typical oil sands ponds (diameter of ~2-4 km, 300 – 1000 ha). Figure 3 shows an overview of the first two compartments during construction to give an impression of the scale.

Technically there are some differences between the Marker Wadden project and the oil sands industry. Due to the shallow water in Lake Markermeer, a layer of 5 m of soft material had to

[1] Royal Boskalis Westminster N.V. is a leading global services provider operating in the dredging, maritime infrastructure and maritime services sectors. www.boskalis.com

be reclaimed, whereas in tailing ponds 10's of meter needs to be filled up (old mining pits).

Furthermore, the explicit goal of Marker Wadden is to create a nature reserve. Mature fine tailings reclamation is required from an environmental and regulatory perspective. Restoring the landscape in its original state is the main purpose. In this sense the functional requirements are the same (nature development), however the 'accessibility-strength' is different.

This paper will show that design techniques and operational working methods used in the Marker Wadden project can also be implemented in the oil sands industry.

Figure 3. First two compartments during construction showing the scale of the project (© John Grundlach)

DESIGN OF THE MARKER WADDEN

General concept

The landscape design of the Marker Wadden was made by Vista Landscape Architects, as part of the Boskalis consortium during the tender.

This design was integrated (combination of disciplines) during a iterative design process allowing for a high-quality, economical design and operational work method (ensuring an optimal (fast) consolidation process and promote strength development).

Figure 4 shows a top view of the project with its characteristic features.

All material used for constructing the Marker Wadden (both sand and clay) was collected in the borrowing pit. Sand was dredged from deeper layers (up to 20 m), clay from the upper 10 m of the bed.

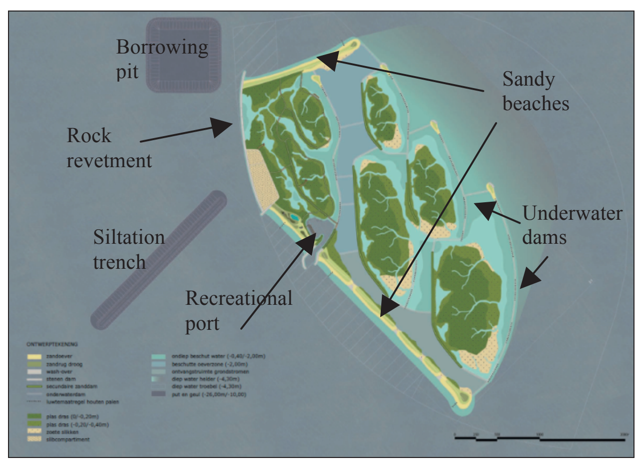

Figure 4. Design of the Marker Wadden with its characteristic features

The total area was divided in several smaller compartments, divided by bunds/dams.

Sand was used to create the sandy beaches (along the north and southwest shores), underwater dams at the east side and the compartment dams inside the area.

Beaches, dams and rock revetment were needed to protect the area from wave attack.

The main area (indicated in green in Fig. 4) was filled with Holocene clay. The process from filling of the compartments to final strength development is indicated schematically in Figure 5.

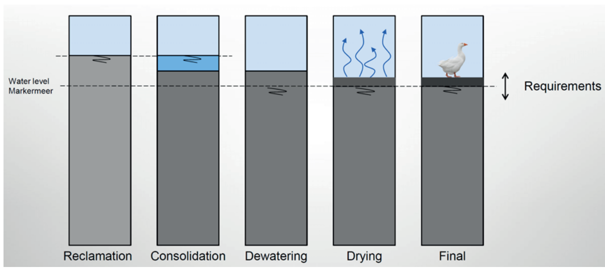

Figure 5. Process from reclamation to final strength

First, the compartments were reclaimed with a clay-water mixture. Immediately after reclamation, the clay sediment starts to settle and start to consolidate, forming a ‘clear’ water layer on top.

After some time, when consolidation of the bed has continued, the water layer on top was removed and drying of the bed started, forming a dry crust on top of the soft bed.

The weight of the crust on top of the soft material increases the rate of consolidation.

During the design phase, the consolidation process was modelled and estimations were made at what moment in time the final bed height will be achieved and also strength requirements will be met.

Testing and modelling of consolidation

The above mentioned process of consolidation and crust formation of the soft clay material is rather unique and experimental. Building with this type of material with the set requirements has not been done in projects before. For this reason different tests were executed during the design phase of the project.

Both laboratory tests and large scale container tests were executed by Boskalis together with universities to verify consolidation parameters, crust formation and monitoring techniques.

Settling column tests (Fig. 6) were performed in the Boskalis Geotechnical Lab to determine consolidation relations, i.e. compressibility and permeability relations that are required for consolidation modelling. Clay material from Lake Markermeer was tested to achieve the most relevant results for the project. More information about these tests can be found in Winterwerp and Van Kesteren (2004).

The main advantage of these tests is that they are quick and cheap. Therefore many tests can be done with varying parameters, such as initial density. These tests are therefore efficient for evaluating the sensitivity of the parameters.

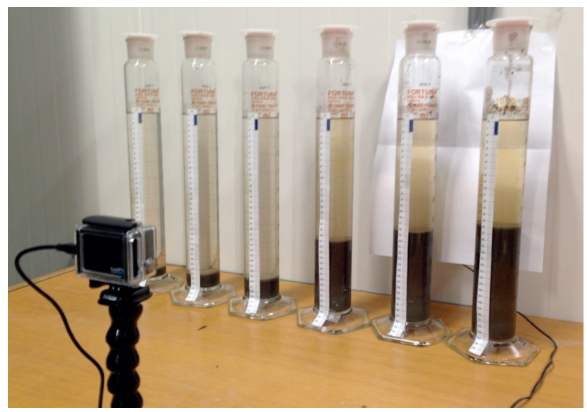

Figure 6. Setup of consolidation column tests

Additional to the column tests, Seepage Induced Consolidation (SIC) tests have been carried out at the Physical Laboratory at Deltares to determine the consolidation parameters. The tests have been executed on the same samples from Lake Markermeer in order to determine the consolidation relations. SIC tests are considered to be more accurate than column tests and give direct input parameters for numerical modelling of the consolidation process. More information about SIC tests can also be found in Winterwerp and Van Kesteren (2004).

Both the column tests and the SIC tests are small scale laboratory tests. To investigate if scale effects can play a role in these tests, large scale container tests were performed at the Boskalis head office.

Three containers (l x w = 5.9m x 2.3m and h = 1.9m), were filled with material from Lake

Markermeer (total volume of 24 m^3 per container). One container was filled completely at the start of the experiment. Two others were initially filled half and later an additional filling was carried out to test the effect of different filling strategies.

Several parameters were measured during the test period of about 6 months, amongst which: bed level development (Fig. 7), pore water pressures, bed density and bed characteristics (i.e. distribution of the sand-fine ratio over depth).

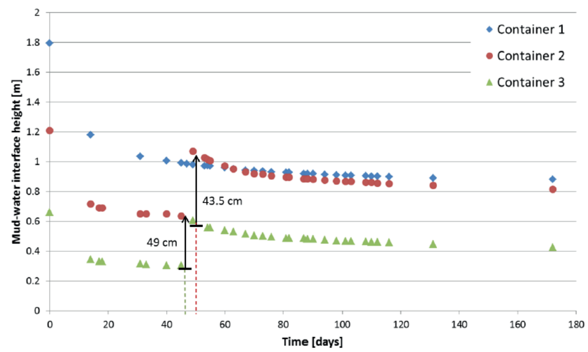

Figure 7. Bed level development during the container tests

Based on the numerical modelling and physical testing it was concluded that both input parameters of column tests and SIC tests can be used to describe the consolidation behavior in the containers. Also, the initial (local) density is a major input parameter that determines the consolidation results (Van Olphen, 2016).

In the design phase, many numerical modelling simulations were performed with DELCON. DELCON is a numerical, one dimensional finite strain model for self-weight consolidation of mud including a gas phase, and is developed by Deltares. As input, the model requires the constitutive relations between void ratio, permeability and effective stress. The DELCON model does not include creep effects.

The advantage of such a model is that many simulations can be carried out to test different filling strategies and determine the sensitivity of the outcomes for initial parameters. Fig. 8 shows a typical modelling result.

Based on model outcomes, the final bed heights and densities after construction period were estimated.

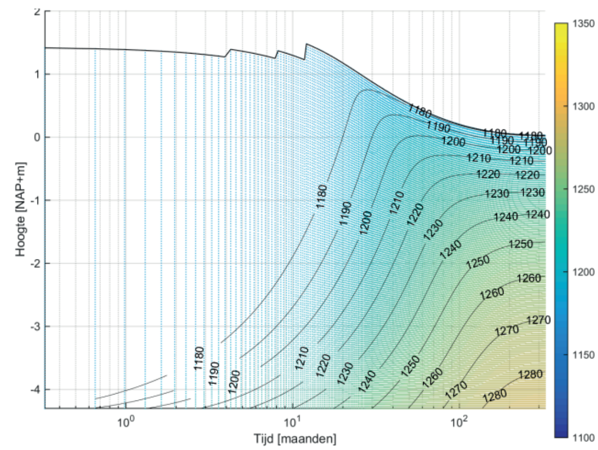

Figure 8. Typical result from numerical modelling: bed level and density development in time

Crust formation was modelled with a different model, developed by Delft University of Technology (Vardon et al 2015). Effect of crust formation on consolidation behavior was analyzed in terms of extra bed level lowering.

As can be concluded from above, Boskalis was supported by specialized consultants during the design. This was needed to produce a state-of-the-art design with the best available knowledge. As the contractor was in the lead, we were able to integrate planning, work method and costs as integral design parameters. This ensured that in the end an economical design was made that is also practical and safe to execute.

Construction method

In April 2016, Boskalis started the construction of the Marker Wadden. The main consideration during the design of the work method was that the largest cost driver, the Cutting Suction Dredger (used for its high production rates), has to operate and produce optimally. This is needed because the client asked for an area as large as possible for a fixed budget. This consideration is kept top of mind for the adaptive management as well.

An important decision had to be made: Focus on high production rates or focus on high production densities. Higher production rates results in a shorter construction time. However, consolidation towards higher densities to comply with client demands takes time. When producing higher densities much time is won in the process after construction towards the final consolidation state.

Because of the uncertainties in the consolidation, the focus was on high densities.

The area is constructed in a number of steps and layers, as indicated in Figure 9. First, small sandy bunds (1) of 1 – 1.5 m high were constructed. The area in between was filled with a clay-water mixture (2). Next, the sandy bunds were raised up to the water level, around 0 m (3), and in succession the area in between was filled again with a clay-water mixture (4).

Figure 9. **Top panel: indicative steps to construct the project. Lower panel: overview of construction of the sandy bunds and filling of the compartments. (© John Grundlach)**

The sandy bunds were then raised above the water level (visible in Fig. 9 lower panel) and sub compartments were created by intermediate bunds (5). The sub compartments enabled us to have different water levels and filling rates in the different compartments. Finally the clay mixture was pumped into the area above the lake level (6). After that, the consolidation process continued.

A state-of-the-art spreader pontoon was used to fill the compartments, allowing for the controlled installation of thin layers of soft mud. Figure 10 shows the pontoon in operation during the construction of Marker Wadden.

Figure 10. **Spreader pontoon in operation in the Marker Wadden (© John Grundlach)**

ADAPTIVE MANAGEMENT DURING CONSTRUCTION

Adaptive management was carried out during the construction phase. This was important to control the reclamation process by monitoring and predicting the soil behavior. The monitoring data was used to validate or correct our predictions, and to support execution by anticipating operational or requirement-related problems if the soil material behaves differently than expected. When necessary, the work method was adjusted.

This section shortly describes the activities carried out during the construction phase and the lessons learned.

Additional testing and field monitoring

During the design phase, consolidation tests were carried out on material from bottom of Lake Markermeer. Material was taken from vibrocores of up to 10m deep in the bottom, in order to represent as much as possible the actual material to dredge in execution.

Additional column tests and SIC tests were performed on material taken from the first filling layer of the compartments.

The material that is pumped into the compartments during construction is cut and hydraulically transported and has different characteristics. Due to bulking, the density in the compartments is lower than the consolidated clay from the Markermeer bed. Also, the clay floc characteristics might have changed during the dredging process, which was also observed by Van Olphen (2016).

To increase the accuracy in predicting consolidation behaviour of hydraulically reclaimed mud, additional tests were performed on the actual material from the compartments to determine the most representative parameters as input for the numerical modelling.

Field monitoring was carried out frequently (once or twice a week), to monitor the consolidation behavior of the material in the compartments.

Bed levels were measured with both a single beam echo sounder and a multi beam. In fact, the layer that is observed is a pycnocline between the water and the clay-mixture layer.

The survey was carried out on a fixed grid system to guarantee coverage of the area and to compare different surveys in time.

As shown in figure 11, it was anticipated that the echo sounder reflected at a density gradient between 1000 kg/m^3 and 1100 kg/m^3.

Density profiles from the fresh bed to the original bed were taken at various locations inside the compartments, using a MudBug device.

Before the Marker Wadden construction started, different systems to measure the density were tested. The MudBug performed best (Kleine Schaars, 2016). More information on this device can be found on the website www.muddensity.com.

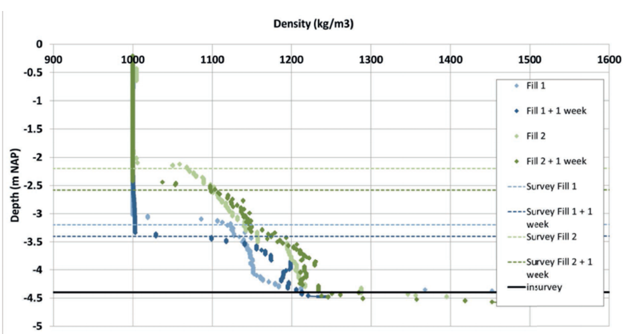

Figure 11. Typical MudBug result

Density profiles were measured directly following completion of a fill layer and then at regular intervals. These measurements give an idea about the initial density profile and the settlement/consolidation over time. Figure 11 shows typical results from the MudBug for the first 2 fill layers.

After the fourth filling layer (in which the mud mixture was pumped initially above the water level) the situation was 'at rest' for some months. The measurement frequency was reduced, which is in line with the reduced consolidation speed over time.

Observations and Lessons Learnt

The field measurements and additional lab tests improved the knowledge on the consolidation behavior of soft mud. The main lessons learnt are:

- Significant heterogeneity in density was found in the compartments, both horizontally as vertically. Close to the spreader pontoon denser layers were found than further away from the pontoon. The first filling layers had a lower average density than the filling layers at a later stage.
- Because of this, the consolidation behavior of the mixture changes in time and in space, which makes it difficult to predict. Frequent monitoring is therefore needed.
- In the first days after pumping the material in the compartments, the sediment in the mixture started to settle and a cleaner water layer was formed on top. After a few days the water on top could be allowed to flow out.

Based on the field measurements, numerical modelling with the DELCON software was updated to improve the consolidation prediction and determine the final bed levels.

Results of the numerical simulations were validated on the consolidation speed of the first weeks, measured in the field.

Within the analysis, 2D effects (heterogeneity in density) were taken into account by differentiating between the variations in layer thickness between different locations.

Implications for project execution

Field measurements, observations, numerical modelling updates and the lessons learnt increased our understanding in the consolidation behavior of the material during the construction.

Figure 12 shows a schematic picture of the uncertainty and certainty in time during the different project stages.

This ‘tilted funnel’ indicates that the accuracy of the analysis continuously increases as more understanding is gained on the material behavior.

Because of the knowledge gained during preparation and execution, combined with the integrated adaptive management process we were able to continuously optimize the work method to reduce the risk of not fulfilling the project requirements in terms of bed elevation and strength, as set by the client. The following construction method components could be adjusted: management of the compartments (size, number of filling layers and water levels), mixture density and production rates of the dredger, time interval between the filling layers.

Adaptations to the work method were chosen and implemented such that the main cost driver, the Cutter Suction Dredger, can maintain optimal production rates.

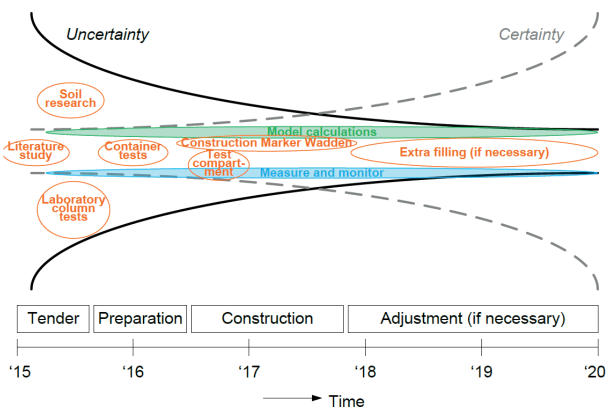

Figure 12. ‘Tilted funnel’ indicating the increase in understanding of the material behavior

MARKER WADDEN AS AN EXAMPLE FOR RECLAIMING OIL SANDS TAILINGS PONDS

The Marker Wadden project shows that it is possible to build a land reclamation with soft muddy material. The layers consolidate and the material gains strength.

Although fine material has been used before in land reclamations, it’s use is not straightforward. Often this material is considered to be unsuitable or waste material and chemical additives are needed to comply with strength requirements. Using additives makes it rather expensive and/or environmental unfriendly and can therefore not be applied on a large scale.

The Marker Wadden project shows that it is possible to build with soft material, without using these additives, multiple re-handling steps and/or mechanical ways like centrifuges to accelerate consolidation.

Because of this we think that the Marker Wadden project is a good example for reclamation using mature fine tailings in the oil sands industry.

At a first glance the two cases are rather different. However there are several similarities between the cases.

The principle of reclaiming large quantities of soft material at relatively low costs is applicable to both cases. Also the requirements are quite similar. The reclamation will not be used as a construction site, as nature development is one of the main drivers. This reduces the strength criteria and making a reclamation without additives possible.

Although characteristics of the soft clay material in the Markermeer are different from the oil sands tailings, the same physical processes occur. In principle, the processes of settling, self-weight consolidation, crust formation and atmospheric drying, and effect of vegetation are similar. Because of differences in sediment characteristics the behavior can deviate from project to project, however the same theory and tools can be used for predictions.

In both cases an integrated and iterative design process is needed, incorporating state-of-the-art design tools/engineering, operational experience and costs. This approach leads to realistic and cost-efficient projects, making optimal use of the contractors experience and operational knowhow.

For both cases a similar operational work method can be applied and adaptive management of operations is needed to continuously optimize that work method. The latter requires proper field monitoring and engineering involvement.

However due to the differences in reclamation depth (5 m in the Markermeer – 10’s of m in oil sands ponds) the work method from the Marker Wadden cannot be copied exactly to the oil tailing ponds. Reclaiming 10’s of meters with soft material without any acceleration measures would result in consolidation times of typically 100's -1000 years (Jacobs et al 2012). The consolidation time is proportional to the square of the layer height ($t \sim h^2$). These thick layers will take a long time to form sufficient dense layers.

Jacobs et al (2012) and Langseth et al (2015) describes a method of accelerating consolidation of mature fine tailings by the means of applying a surcharge of the soft layer by sand capping. Different types of capping methods are presented, as also shown in figure 13: a cap of sand and muskeg (a), with additional vertical drains (b) and a sandwich structure of alternating layers of tailings (~m's) and sand (~dm's) (c).

Using sand capping is a proven technique in multiple dredging projects and can simply be implemented in the work method that was used for the Marker Wadden project.

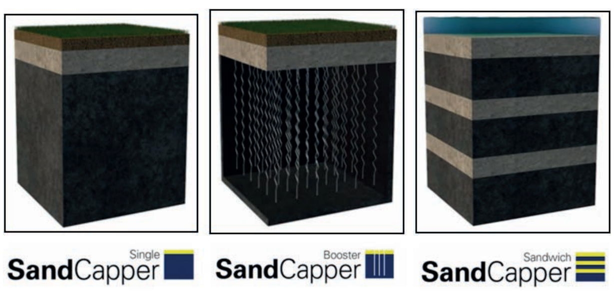

Figure 13. Sections of a schematized oil sands tailings pond with a cap of sand and muskeg (a), with additional vertical drains (b) and a sandwich structure of alternating layers of tailings (~m's) and sand (~dm's) (c) (Jacobs et al 2012)

Figure 9 already shows different filling layers of the compartments. Sand capping layers can be applied between those layers, resulting in a sandwich structure shown in Figure 13c. In this way the work method from the Marker Wadden can be scaled up to larger reclamation depths, without increasing the consolidation time intensively.

Jacobs et al (2012) stated that a strategy in which advanced engineering, dredging expertise and site-specific characteristics is required to design a sand cap and to ensure an efficient and safe work method.

The way Boskalis approached the Marker Wadden project is an example of such a strategy with state-of-the-art modelling tools, field and lab testing, and adaptive management.

CONCLUSIONS

The Marker Wadden project, as presented as case study in this paper, shows that it is possible to build a land reclamation with soft muddy material without the use of chemical additives, in an economical and safe way.

Boskalis – as main contractor – was in the lead for this innovative design and construct tender, based on quality and with a fixed budget.

State-of-the-art design tools were used combining laboratory testing, field testing, monitoring and numerical modelling with DELCON. These tools were used to gain an understanding that was used for design as well as for the adaptive management during construction.

A smart design of the operational work method was made taking into account self-weight consolidation, crust formation, atmospheric drying and effect of vegetation.

As the client requirements are strict, it was crucial to follow the consolidation behavior of the soft material in the compartments and adjust the work method. During construction, continuous monitoring was performed, and combined with the integrated adaptive management we were able to adjust the work method, when necessary. This reduced the risk of not fulfilling the project requirements in terms of bed elevation and strength. The following construction method components could be adjusted: management of the compartments (size, number of filling layers and water levels), mixture density and production rates of the dredger, time interval between the filling layers.

The Marker Wadden project can be considered as a good example for the oil sands industry how to reclaim large deposits of soft mud at a proven, economical and safe manner. There are several similarities between the two cases, mainly related to: (1) the principle of reclamation large quantities of soft material at relatively low costs, (2) the same physical processes (like self-weight consolidation, crust formation and atmospheric drying) occur and the same design tools are applicable, (3) an integrated and iterative design process is needed, incorporating state-of-the-art design tools/engineering, operational experience (adaptive management), cost and safety.

However due to the large reclamation depths in the mine tailing ponds (10's of meters), the construction method of Marker Wadden cannot by copied exactly. Sand capping layers in between the soft filling layers can be used to accelerate consolidation of mature fine tailings. This proven concept has been used before and is for example described in earlier papers such as Jacobs et al (2012).

REFERENCES

Beuth, L., Jacobs, W., Dykstra, C., (2014) Numerical Modeling of Hydraulic Sand Capping on Creeping Ultra-Soft Tailings. Proceedings of International Oil Sands Tailing Conference 2014.

De Lucas Pardo, A. (2014). Effect of biota in fine sediment transport processes: A study of lake Markermeer (Phd. thesis). TU Delft.

Jacobs, W., Dykstra, C., Kesteren, W. van (2012). In situ hydraulic capping of soft tailings. Proceedings of International Oil Sands Tailing Conference 2012.

Kleine Schaars, L.C. (2016). Meetsensor selectie project Marker Wadden. Bachelor thesis Hanzehogeschool Groningen.

Langseth, J., Luger, D. and Jacobs, W. 2015. Placement of Caps on Soft and Fluid Tailings. Tailings & Mine Waste 2015.

Olphen, E.J.C. (2016). Consolidation behaviour of soft cohesive soils, the correlation between different scale model tests - Case study of the Marker Wadden. MSc Thesis Delft University of Technology.

Vardon, P.J., van Paassen, L.A., van Tol, A.F.(2015). Sludge depot modelling for self-weight consolidation and atmospheric drying. TU Delft, 2015. GE/PJV/15.001.

Vijverberg, T., Winterwerp, J.C., Aarninkhof, S.G.J., Drost, H. (2011). Fine sediment dynamics in a shallow lake and implication for design of hydraulic works. Ocean Dynamics (2011) 61:187–202.

Wichman, B., Greeuw, G. (2016). Seepage Induced Consolidation test, Marker Wadden sediments. Final report 1221329-000-ZKS-0004. Deltares.

Winterwerp, J.C., van Kesteren, W.G. (2004). Introduction to the physics of cohesive sediment dynamics in the marine environment. Elsevier.

CO-DEPOSITION IN THE OIL SANDS: BLENDING OF FLUID FINE TAILINGS WITH OVERBURDEN

Ralph Burden and G. Ward Wilson
University of Alberta, Edmonton, Canada

ABSTRACT

Blending waste rock with fluid tailings to create a new material with favorable properties has been shown to be effective at conventional mines. In the oil sands, this "Co-disposal" technique has the potential to become a useful method of dewatering and reclaiming large volumes of MFT. Whilst other methods focus on increasing solids content by removing water, essentially here we are increasing solids content by adding solids. This is particularly promising due to the high water demand provided by the clay shale overburden materials; moisture is rapidly transferred from the MFT to the shale upon mixing, creating a stable homogenous material.

A theoretical model to characterize the behaviour of this complex material, enabling design of the geotechnical properties of mixtures and prediction of the behaviour of commercial-scale deposits, is required. This paper presents a review of the current theory of the design and characterization of "co-disposal" materials, and a review of previous studies investigating the properties of Clearwater shale-MFT mixes. Where appropriate, the theoretical approach is extended to include oil sands materials and its applicability to oil sands applications is discussed. Preliminary results from mixing trials aimed at verifying the conceptual model are also presented.

INTRODUCTION

Mines typically produce two waste streams; wet streams from the extraction process (such as MFT) and waste rock or overburden material. Research at conventional mines has shown that these materials can be blended to produce a new material consisting of a waste rock skeleton with fine tailings occupying the void spaces Wilson et al. (2008). This has been shown to have favorable properties; it combines the high shear strength and low compressibility of the waste rock skeleton with the water retention properties and low permeability of the tailings. In practice this reduces the total volume of waste storage required, reduces the need for containment of fine tailings and can mitigate the problem of oxidation that can be associated with waste rock dumps.

This paper discusses the application of this "co-deposition" technique to oil sands mining; mixing fluid tailings with Clearwater shale overburden. Dewatering of MFT remains a significant, largely unresolved challenge, and represents a barrier to reclamation and closure. Whilst most approaches currently in use or development aim to increase the solids content of the MFT by removing water, essentially here we are increasing the solids content by adding solids. This has great potential because of the high water demand of the overburden material. The Clearwater formation often has natural water contents below the plastic limit. Upon mixing, water is rapidly transferred from the MFT to the shale. Early indications have shown that this can create a stable material with shear strengths well in excess of 5 kPa, possibly eliminating the need for containment and having the potential to create dry post-closure landscapes.

LITERATURE REVIEW

A review of previous work relevant to this topic is given below. The first section gives a brief summary of the geological setting and geotechnical properties of oil sands overburden materials. The second section is a comprehensive treatment of previously published works on the properties of Clearwater shale – FFT mixtures. The final section deals with co-disposal of mine wastes in a more general sense, starting with a historical review and finishing with the state of the art.

Geological background: Oil sands overburden materials

The McMurray formation is overlain by Cretaceous clay shale of the Clearwater formation throughout the region. This forms the predominant overburden material on the west side of the river. On the east side, it is overlain by the primarily sandstone Grand Rapids formation and some glacial outwash deposits. On average, the Clearwater formation is around 75m deep (Conly, Crosley et al. 2002).

This paper deals exclusively with the blending of fine tailings with Clearwater shale overburden.

The Clearwater formation is well described and characterised in the literature (Isaac, Dusseault et al. 1982, O'Donnell and Jodrey 1984); only a brief summary is given here. It was deposited in a mixed marine and continental environment. It consists mainly of silts (around 50%), marine clay shales (around 44%) and some beach and shoreface sands (around 6%). The clay fraction is mainly composed of illite and smectite, with smaller quantities of kaolinite and chlorite. The Clearwater formation on Syncrude's lease was found to consist of 7 sub-layers, each readily identifiable by a distinct geophysical response. These are informally identified by Syncrude as KCW, A, B, C, D, E and F respectively.

Geotechnical properties of the Clearwater formation, after Lord and Isaac (1989) are summarised in Table 1.

Table 1. Geotechnical properties of the Clearwater formation measured both in-situ and inside dredged "lumps", after Lord and Isaac (1989)

	Clay content (%)	w (%)	Liquid limit (%)	Plastic limit (%)	Bulk density (kg/m^3)
Dredged "lumps"	43 - 64	17-25	64-79	22 - 28	1700 - 2000
In-situ	11 - 40	16-25	37 - 53	18 - 25	2070 - 2100

It is noteworthy that the in-situ moisture content of the Clearwater formation is generally at or below the plastic limit. This is significant because it implies that the shale has a high water demand; upon mixing it will draw the water out of the tailings, causing rapid dewatering and strength gain.

Previous studies on MFT-Clearwater shale mixtures

Several studies were carried out in the 1980s to investigate the properties of clay shale overburden lumps, or "balls", mixed with MFT or tailings pond water. The focus was on creating hydraulically placed overburden dumps rather than on tailings disposal, which at the time was not considered to be the priority area that it is today. However, the work is worthy of re-examining in this context.

During the summers of 1985 and 86, field scale trials were conducted on Syncrude's lease to assess the feasibility of creating stable, hydraulically placed overburden dumps using dredging techniques (Lord and Isaac 1989). 12,100 m^3 of Pleistocene lacustrine clay and 13,600 m^3 of KCC Clearwater shale, considered representative of the overburden materials found on the lease at the time, were dredged and deposited into test cells ranging from 1.5 to 6 m deep. The main focus was to determine the geotechnical properties of the deposits. We are mostly concerned here with the results from the Clearwater shale test cells, because that is the predominant overburden material at present and in the future. Both tailings pond water and MFT were used as transport fluids. The MFT had a solids content of approximately 30% and a bitumen content ranging between 2 and 3%. The final deposits had solids contents around 75%.

Density tests performed immediately upon deposition showed many air voids. However, tests performed after 20 days showed almost zero air voids with saturation in excess of 97%; this implies that the initial macro porosity was sealed off by swelling of the shale lumps. Unfortunately, no settlement data was published since all of the instrumentation was destroyed during deposition. The undrained shear strength was found to vary between 6 and 35 kPa; effective stress parameters were in the range φ'=20°-27° c'=0-10 kPa. Dissipation of excess pore pressure in response to surcharge loading was observed to be slow; only 10% dissipation in 100 days, irrespective of the transport fluid used.

Ash and Dusseault (1987) carried out laboratory tests on shale – MFT mixtures. Swedish drop cone tests on a 50/50 volumetric mix at 24 and 72 hours gave average undrained shear strengths of 30 and 33 kPa respectively. They also carried out "Nylon stocking" tests to study the moisture transfer process; shale lumps are lowered into an excess of tailings sludge for a specified time and then re-weighed. It was found that a steady state is reached in two to four days with a typical mass increase of 20%. To put this result in some perspective, if a 50/50 volumetric is assumed, and the same amount of swelling of the shale lumps is achieved, this would equate to an increase in the solids content of the sludge from 30 to 55%, corresponding to a significant amount of dewatering.

Mimura (1990) investigated the shear strength of the Clearwater shale "lump" structure, carrying out 42 CU tri-axial tests using a range of mixing fluids, confining stresses and "softening" durations. All of the tri-axial tests showed high cohesion intercepts (up to 62 kPa) and low friction angles (less than 8°). High positive pressures were measured during shearing, although unconsolidated shale lumps may have developed negative pressures. The mixing fluid had no significant impact on the strength, but mixes made with MFT were observed to have very slow consolidation times because of the low permeability. Six "Softening" tests were also carried out, were clay lumps were placed in a consolidation cell, which was topped up with pond water. The object was to determine the vertical confining stress at which the clay lump structure was no longer free draining. It was found that the lump structure deformed to a limiting void ratio of around 0.7 at around 60 kPa.

Co-disposal and design of waste rock – fine tailings blends

Co-disposal of waste rock and tailings in conventional mining has been around for a number of years. The earliest use is probably in underground backfills, often combined with a binder such as Portland cement (Brawner and Argall 1978). Pumped co-disposal has also been implemented successfully at several coal mines around the world, and has been shown to reduce the waste volumes and the need for containment (Williams 1997). Other approaches that have been demonstrated include layered co-disposal, or "co-mingling", which involves typically involvements placement of fine tailings layers inside a waste rock pile to act as a barrier to seepage or oxygen flux, and waste rock "inclusions": waste rock dykes placed build inside tailings ponds as the ponds are raised, to promote drainage and improve overall stability and seismic resistance. A good summary of these techniques is given by Bussiere (2007). More recent research at metal mines has focussed on producing homogenous blends to create an engineered material, known as "paste rock", which has favourable properties, combining the high strength and low compressibility of the waste rock with the low permeability and high water retention of the tailings (Wilson et al. 2008).

Wickland et al. (2006) present a theoretical basis for the design of waste rock and fine tailings blends, based upon classic particle packing theory examining the geometric arrangement of binary mixtures developed by Furnas (1928). A binary mixture is defined as a mixture of two different groups of uniformly sized particles. Theoretical treatments usually deal with ideal spheres; however, the concepts relate equally well to 2 groups of randomly shaped and sized particles with different mean diameters. The primary properties that influence the packing arrangement of a binary mixture are the particle size ratio, the mix ratio and the packing density of the individual components. A good review of particle packing theory in general and its application to design of mine waste blends is given by Wickland (2006).

Overall porosity reduces with an increase in particle size ratio; maximum packing density occurs at an infinite particle size ratio. This is probably representative of a mix of waste rock and fine tailings. Mixture ratio also has an important influence: maximum density occurs at a sweet spot when the pore space of the larger particles is "just filled" by the fine tailings. This is illustrated by Figure 1 below reprinted from Wickland (2006) after experimental studies by Furnas (1928), which shows porosity against mix ratio for a range of particle size ratios.

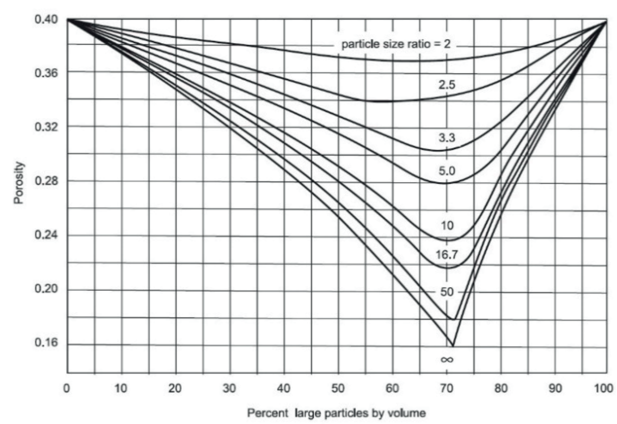

Figure 1. Porosity versus percent larger particles by volume for a binary mixture, including size ratio effects, after Furnas (1928) (Reprinted from Wickland 2006)

Figure 1 shows that the "just filled" point for an infinite particle size ratio occurs when the mix contains around 72% larger sized particles by volume. However, it should be noted that Figure 1 was generated based on an assumption about the porosities of the individual components. Hence, the exact position of the "just filled" point is dependent upon the porosities of the individual components of the blend; if the larger particle size had a lower porosity, the “just filled” point would be lower, and vice versa.

MIX DESIGN AND PHASE RELATIONSHIPS

This section attempts to take a similar approach to that of Wickland et al. (2006) in developing a conceptual model and a logical approach to mix design of waste rock – fine tailings blends, but specifically for the unique case of oil sands materials. The applicability of this approach to this case is discussed and where appropriate it is adapted and extended.

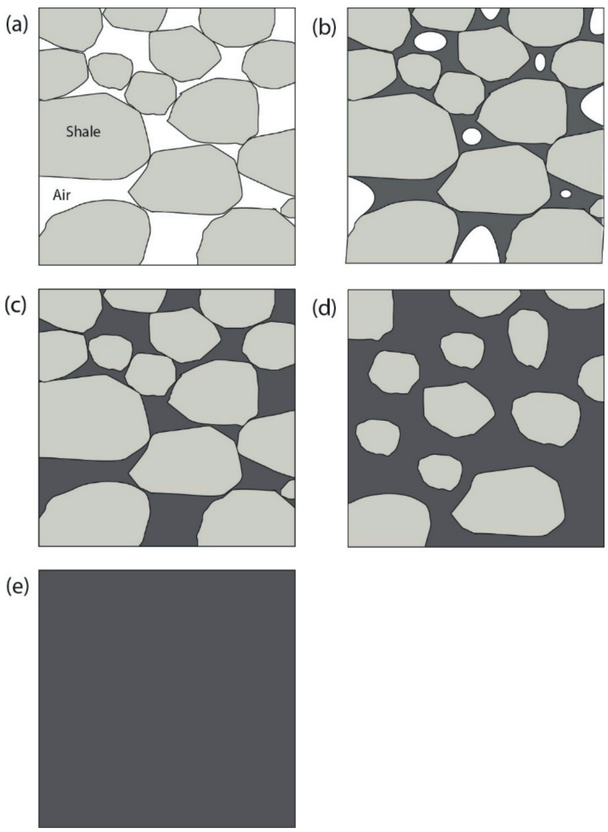

Figure 2. Particle structure configurations for Clearwater shale - FFT blends: (a) Shale lumps only; (b) Shale lump matrix partly filled with tailings; (c) "Just filled" condition; (d) "Floating" shale lumps in a tailings matrix; (e) Tailings only

Conceptual model

Waste rock – fine tailings blends can exist in 3 main configurations: a waste rock skeleton where the voids are partly filled with tailings, a tailings matrix with “floating” waste rock particles and the “just filled” case (Wickland et al. 2006). In the case of Clearwater shale – MFT blends, the “waste rock” particles can be likened to unsaturated shale “lumps”. This is shown schematically in Figure 2.

At the time of mixing, the shale lumps are unsaturated and contain shale solids, water and air voids. Figure 3 attempts to illustrate this schematically for the “floating” case (case (d) above).

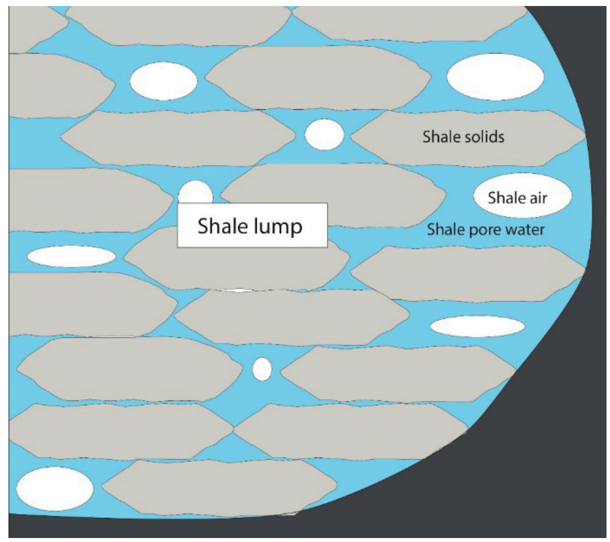

Figure 3. Schematic showing the internal structure of a Clearwater shale lump in the "floating" condition (represented by Figure 2 (d) above)

Figure 4 shows the phase diagram, and the notation used in this paper to describe the mass and volume of the respective phases.

The blend can be characterised using a *global void ratio*, defined as:

$$[1] \qquad e = \frac{Total\ volume\ of\ voids}{Total\ volume\ of\ solids}$$

Using the notation given in Figure 4, equation 1 becomes:

$$[1a] \qquad e = \frac{V_{sw}+V_{sa}+V_{tw}+V_{ta}+V_{ma}}{V_{ss}+V_{ts}+V_{sw}+V_{bit}}$$

In addition, we have the internal shale “lump” void ratio,

[2] $$e_s = \frac{V_{sw} + V_{sa}}{V_{ss}}$$

and the tailings void ratio,

[3] $$e_t = \frac{V_{tw} + V_{ta}}{V_{ts} + V_{bit}}$$

If e_s and e_t are known or assumed, it is possible calculate the *macro void ratio*, defined as

[4] $$e_m = \frac{V_t + V_{ma}}{V_s}$$

At initial conditions, it may be reasonable to assume that the internal void ratio of the intact shale lumps (e_s) is equal to the in-situ void ratio of the shale. It is convenient and often reasonable to assume that the tailings are fully saturated. However, experience has shown that the tailings often contain entrained air bubbles; this is particularly true in the case of centrifuge cakes, and this may be considered a separate air phase in the conceptual model. In summary, 3 air phases are proposed as follows: Air in the unsaturated shale pores (V_{sa}), occluded air in the fluid tailings (V_{ta}) and “macro” air voids (V_{ma}). The degree of saturation of the cake used for the present study was measured as 99.1 %.

Volume V	Shale volume V_s	Shale solids V_{ss}
		Shale water V_{sw}
		Shale air voids V_{sa}
	Tailings volume V_t	Mineral solids V_{ts}
		Bitumen V_{bit}
		Tailings water V_{tw}
		Tailings air voids V_{ta}
	Macro air voids V_{ma}	

Mass M	Shale mass M_s	Shale solids M_{ss}
		Shale water M_{sw}
	Tailings mass M_t	Mineral solids M_{ts}
		Bitumen M_{bit}
		Tailings water M_{tw}

Figure 4. Phase diagram for Clearwater shale - FFT blends

Mix design variables

In general terms, the principal design variables that govern the properties of shale – FFT blends are the mixture ratio, the lithology of the shale, the initial particle size distributions of the FFT and shale, the initial moisture contents of the FFT and shale and the bitumen content of the FFT. In addition, the “macro” particle size distribution, i.e. the size of the shale lumps, must also be considered.

Mixture ratio

In practical terms, the mixture ratio is the main design parameter that can be used to directly control the properties of the blend. Therefore, it is useful to develop a theoretical model that can predict the properties of a blend of a given mix ratio. Solids content (s or s_m) is widely used in the industry to characterise tailings. Given that gravimetric moisture content (w) and bitumen content (b) of the constituents of the blend can easily be measured, it is straightforward to calculate the mix ratio that will produce a blend of the desired final solids content. Bulk Mass Ratio (BMR) defined below, has been found to be a convenient parameter to produce blends in the lab.

[5] $$BMR = \frac{Bulk\ mass\ of\ shale\ (M_s)}{Bulk\ mass\ of\ tailings\ (M_t)}$$

Figure 6 shows the relationship between final solids content and BMR for a typical blend of centrifuge cake and Clearwater shale.

Wickland et al. (2006) proposed the mix ratio parameter R, defined as the ratio of waste rock to tailings by dry mass, as the primary design variable for waste rock and tailings blends. This is a useful parameter for defining mix ratio when investigating the relationship between the mix ratio and properties of the blend, since it is independent of variations in the properties of the original constituents of the mix, such as moisture content, bitumen content and void ratio. Note that for the purposes of this paper, R is defined as the ratio of dry shale soilds mass to dry tailings mineral solids and bitumen mass combined:

[6] $$R = \frac{M_{ss}}{M_{ts} + M_{bit}}$$

Relationships between R, BMR or final solids content (geotechnical (s) or mining (s_m) definitions)

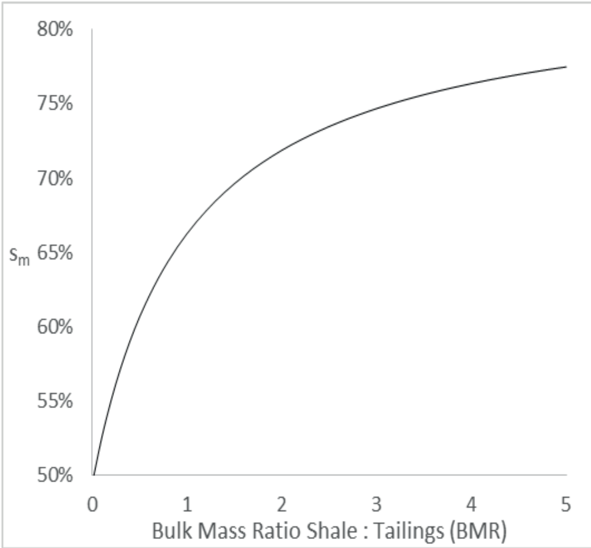

Figure 5. Bulk Mass Ratio (BMR) versus solids content (s_m) for a typical Clearwater shale – centrifuge cake blend, based on the following assumed parameters: w_{shale}=20%; w_{cake}=100%; b=3%

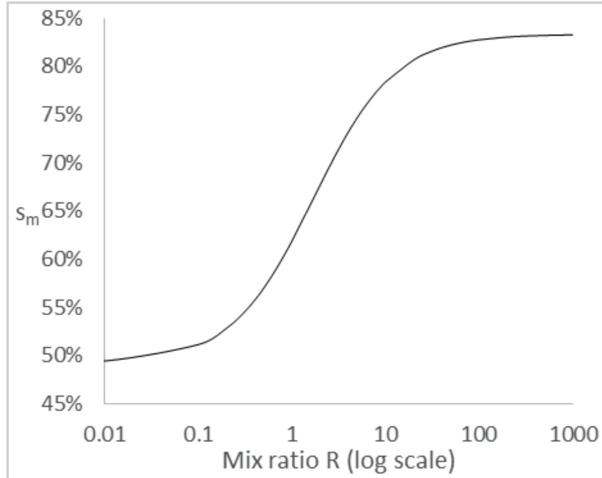

Figure 6. R versus solids content (s_m) for a typical Clearwater shale – centrifuge cake blend, based on the following assumed parameters: w_{shale}=20%; w_{cake}=100%; b=3%

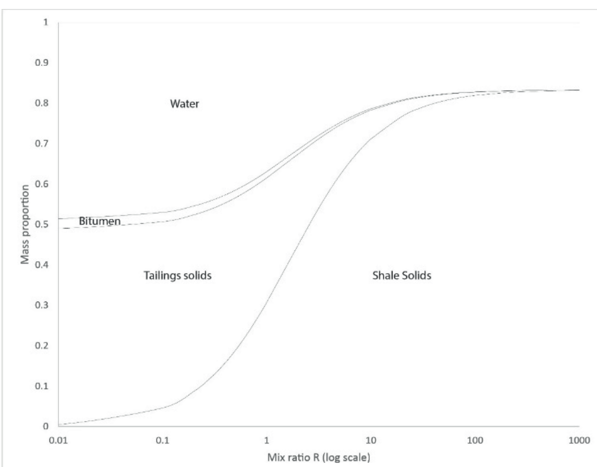

Figure 7. Mass proportion diagram for a typical Clearwater shale – centrifuge cake blend, based on the following assumed parameters: w_{shale}=20%; w_{cake}=100%; b=3%

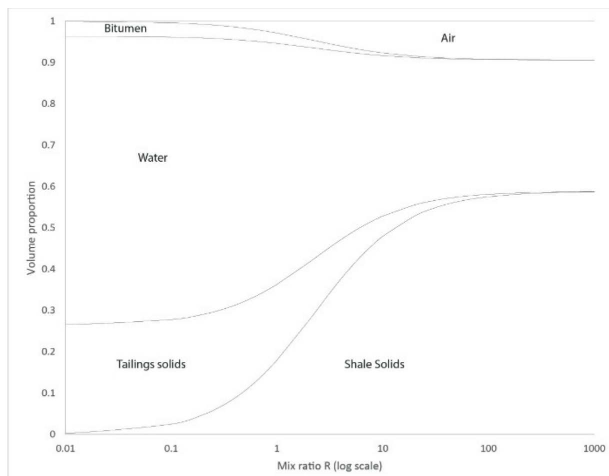

Figure 8. Volumetric proportion diagram for a typical Clearwater shale – centrifuge cake blend, based on the assumption of zero macro air voids and the following assumed parameters: e_s=0.7 w_{shale}=20%; w_{cake}=100%; b=3%

are easy to calculate when basic properties are known and these design variables can be used interchangeably. Figure 6 shows R against solids content for the same blend.

Figures 7 and 8, similar to those by Wickland et al. (2006), show the theoretically calculated mass proportion and volumetric proportion versus R for the same blend.

Figure 8 was generated for the condition where no “macro air voids” exist, i.e. all of the void space within the shale lump structure is filled with tailings (the “just filled” or “floating condition described above). The initial void ratio of the shale lumps (e_s) was assumed to be 0.7, and the tailings were assumed to be fully saturated.

It should be noted that the “zero macro air voids” assumption, upon which Figure 8 is based, represents a significant departure from the approach developed by Wickland et al. (2006). Classic binary mixture models usually assume a fixed macro void ratio for the waste skeleton; in this case the “just filled” point represents a “sweet spot” between “floating” waste rock particles on one side and unsaturated conditions on the other. Conversely, here we are assuming that shale – FFT blends can be readily compacted to the “just filled” point and can exist at a wide range of macro void ratios. Clearly, this assumption is not valid for the full range of mix ratios, but it may be reasonable for the range of mix ratios of interest.

Wickland et al. (2006) suggest that the “just filled” point represents the optimum mix ratio, and this theoretically occurs at around 72 % larger particles by volume, as shown in Figure 1. For a Clearwater shale - centrifuge cake blend, this would correspond to an R of around 5 or 74 % soilds. However, such a high solids content may not represent the most efficient mix ratio for tailings disposal. This suggests that for the range of mix ratios of interest, i.e. 68-72 % solids, the blend would be wet of the “just filled” point and said to be in the “floating” condition (Figure 2 (d)). There is a need for more experimental verification of properties of blends at a range of mix ratios, and this is an area of ongoing study.

MOISTURE TRANSFER PROCESS

Upon mixing, moisture will be transferred from the tailings into the shale. The shale lumps will swell, and the tailings will gain strength and stiffness as they lose water, effectively creating a new material with significantly different properties. This probably represents the biggest single difference between simple waste rock and oil sands overburden materials.

For the range of mix ratios of interest, the blends are generally assumed to consist of unsaturated shale lumps within a continuous phase of saturated fine tailings. In this case, porewater pressure in the interior of the shale lumps will most likely be highly negative, and the pore pressure in the tailings will most likely be close to zero. If we suppose, therefore, that the primary driving force behind the flow of water from the tailings to the shale lumps is the matric suction gradient between the two phases, then we should expect to see a significant increase in the suction in the tailings, starting immediately upon blending and continuing until some sort of equilibrium point is reached between the two materials. Furthermore, we might suppose that the position of the equilibrium point is defined by the mix ratio. This is because if a greater volume of shale lumps are available for a given volume of tailings, a greater volume of water will flow into them before equilibrium conditions are reached, and the tailings will ultimately have a lower moisture content and higher suction.

Mixing trial

To test this hypothesis, a simple laboratory test was carried out. KCA – centrifuge cake blends prepared at a range of solids contents were rapidly mixed and compacted by hand into a sealed container. The KCA lumps were passed through a No. 4 sieve prior to blending. The lid of the container consisted of a rubber stopper which was drilled out, and a UMS T-5 tensiometer connected to a DL-6 data logger was inserted through the hole forming an airtight seal. This allowed continuous measurement of matric suction without disturbing the sample. The container was placed in a water bath controlling temperature for the duration of the test. Figure below shows the development of matric suction (u_a-u_w) with respect to time for 65 and 70% solids content blends.

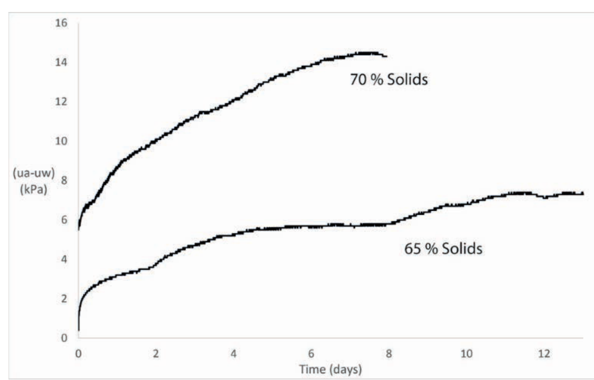

Figure 9. Matric suction development versus time for 65 and 70 % solids KCA – centrifuge cake blends

The data appears to match the hypothesis proposed above. It can be seen that the rate of increase is initially rapid and gradually reduces as the equilibrium point is reached. Equilibrium appears to be reached in around one to two weeks. While the results are encouraging in a general way, it is not apparent whether or not the shale lumps achieve 100% saturation, and if so, what happens to the air. Generally speaking, experience from simple laboratory mixing trials and compression tests has indicated that complete saturation is rarely, if ever achieved, and air remains entrained in the material. This effect is likely to be even more prevalent in field scale trials. Clearly, this is an extremely complex problem with many variables, and an area of ongoing study. There is a need for a more rigorous study of suction, pore pressure response and volume change for a range of mix ratios and loading conditions.

The influence of porewater chemistry

The water chemistry of the fine tailings and overburden has the potential to have a significant influence on the process of moisture transfer and swelling of the shale lump structure. Generally speaking, because the Clearwater formation was deposited in a largely marine environment, it is expected that the porewater will have a similar composition to seawater. This should result in rapid diffusion into the lump due to osmotic gradient, and consequent swelling, when the shale lumps are exposed to fresh water. Nevertheless, Lord and Isaac (1989) note that Clearwater shale has lower salinity than expected, and this combined with the salinity of the tailings water caused less dispersion and disintegration of the lump structure due to osmotic suction than previously thought.

CONCLUSIONS

Co-disposal of fine tailings and waste rock or overburden material is an emerging technology which has the potential to significantly improve the way mine waste is managed. In the oil sands this approach could offer an effective and economical means of dewatering MFT and managing the large volumes of fine tailings that have thus far proven problematic. The theoretical approach for design and characterisation of waste rock – fine tailings blends, developed by Wickland et al. (2006) has been extended to apply to oil sands materials. It is proposed that the mix ratio can be used as the principle parameter to control the properties of a blend, and that the conceptual model can be used to predict the properties of a blend of a given mix ratio. Upon mixing, water is transferred from the fine tailings to the shale lumps due to a matric suction gradient. There is a need for experimental verification of the applicability of the conceptual model to characterise these blends at a range of mix ratios. There is also a need for a rigorous study of the process of moisture transfer, and the suction, pore pressure response and volume change behaviour under a range of loading conditions.

REFERENCES

Ash, P. O. (1987). Improvement of oil sands tailings sludge disposal behaviour with overburden material.

Brawner, C. and J. Argall, GA (1978). Concepts and experience for subsurface storage of tailings. Proceedings of the 2nd International Tailings Symposium, Tailings Disposal Today, Denver, Colo.

Bussiere, B. (2007). "Colloquium 2004: Hydrogeotechnical properties of hard rock tailings from metal mines and emerging geoenvironmental disposal approaches." Canadian Geotechnical Journal **44**(9): 1019-1052.

Conly, F., R. Crosley and J. Headley (2002). "Characterizing sediment sources and natural hydrocarbon inputs in the lower Athabasca River, Canada." Journal of Environmental Engineering and Science **1**(3): 187-199.

Dusseault, M. B., Ash, P. O. (1987). Strength development in oil sands sludge/clay shale mixes for tailings disposal. UF/FIPR Symposium on Consolidation and Disposal of Phosphatic and Waste Clays. F. C. Townsend. Lakeland, Florida.

Furnas, C. C. (1928). The relations between specific volume, voids, and size composition in systems of broken solids of mixed sizes, US Department of Commerce, Bureau of Mines.

Isaac, B. A., M. B. Dusseault, G. D. Lobb and J. D. Root (1982). Characterization of the Lower Cretaceous overburden for oil sands surface mining within Syncrude Canada Ltd. Leases 17 and 22.

Lord, E. R. F. and B. A. A. Isaac (1989). "Geotechnical investigations of dredged overburden at the Syncrude oil sand mine in northern Alberta, Canada." Canadian Geotechnical Journal **26**(1): 132-153.

Mimura, D. W. (1990). Shear strength of hydraulically placed clay shale. MSc, University of Alberta.

O'Donnell, N. and J. Jodrey (1984). Geology of the Syncrude mine site and its application to sampling and grade control, Syncrude Canada Ltd., Edmonton, Alberta.

Wickland, B. E. (2006). Volume change and permeability of mixtures of waste rock and fine tailings, University of British Columbia.

Wickland, B. E., G. W. Wilson, D. Wijewickreme and B. Klein (2006). "Design and evaluation of mixtures of mine waste rock and tailings." Canadian Geotechnical Journal **43**(9): 928-945.

Williams, D. (1997). Effectiveness of co-disposing coal washery wastes. Proceedings of the 4th International Conference on Tailings and Mine Waste.

Wilson, G., B. Wickland and J. Miskolczi (2008). Design and performance of paste rock systems for improved mine waste management. Proceedings of the 1st International Seminar on Management of Rock Dumps, Stockpiles and Heap Leach Pads, Perth, Australia.

OVERVIEW OF HOLISTIC APPROACH TO OIL SANDS TAILINGS MANAGEMENT

Siba Patnayak and Saidul Alam
Advisian, Calgary, Canada

ABSTRACT

Development of tailings management plan for an oil sands operation is driven by the post-closure landform requirements and requires a holistic approach. The physical and chemical properties of the tailings produced must be understood. The long-term containment requirements, method of tailings deposition, water management plan, reclamation and closure objectives and regulatory requirements etc. should be taken into consideration while developing tailings management plans.

An overview of the holistic tailings management approach is presented in this paper with practical examples.

INTRODUCTION

Surface mining operations in northern Alberta oil sands use truck and shovel mining methods. Typically, ore is mined with electric and hydraulic shovels and transported by large trucks to the Ore Preparations Plants where the ore is crushed and conveyed to Slurry Preparation Plants (SPPs). At the SPPs, the ore is mixed with hot process water and slurry is produced. The slurry is processed in Extraction Plants to recover bitumen. Clark Hot Water Extraction process is widely used in the oil sands industry. Caustic is added in extraction process to disperse the ore. Bitumen being lighter than water floats above water and is extracted as froth. The extraction process produces waste by-product in slurry form called tailings that typically consist of sand, clay, silt, other mineral particles, residual hydrocarbons and process affected water. The tailings are conveyed to the desired disposal/storage locations primarily by large diameter pipelines.

Tailings are often toxic in nature and present risk to the environment during and after mining operation ceases. Therefore, tailings need to be managed responsibly in a manner to avoid harmful environmental consequences. Depending upon the characteristics of the tailings and closure and reclamation objectives, tailings may require treatment and/or dewatering prior to deposition.

In the oil sands operations, tailings are generally stored in either above ground tailings storage facilities (TSFs) or previously mined out pits. Some of world's largest TSFs exist in northern Alberta. The dyke encompassing Syncrude's Mildred Lake Settling Basin TSF is reported as the largest manmade earthen dyke in the world (Morgenstern 2001). The TSFs must be properly designed, operated and progressively closed and reclaimed to a stable, non-contaminating and ecologically self-sustaining landform to ensure there are no detrimental effects to the environment. A poorly designed or managed TSF can lead to adverse environmental impacts, higher risks to public health and safety and increased closure costs. Therefore, it is important to develop a holistic tailings management approach starting from the conceptual development stages. This paper outlines the key considerations that should be included while formulating a holistic tailings management approach.

CHARACTERISTICS OF OIL SANDS TAILINGS

Tailings generated from oil sands extraction process contain a higher percentage of fines and clay minerals compared to other kinds of mining. Tailings generated from the primary and secondary extraction process (froth treatment tailings) typically contain about 90% and 10% of the mineral soil (of the total tailings solids mass) respectively. Whole tailings (WT) generated by primary extraction process typically have solids concentrations ranging from 40 to 60% and fines content (particle size less than 44 μm) of 15 to 30% (Matthews et al. 2011). Froth treatment tailings stream primarily consists of fines particles, unrecovered bitumen, residual diluents (solvent) and process water.

When tailings slurry with high water content is discharged in a storage facility, the heavier particles settle near the discharge points forming a beach while the fines along with the runoff water flow away from the discharge points and form a fluid pond. Any fluid that contains more than 5% suspended solids (by mass) and has less than 5 kPa undrained shear strength is called fluid tailings or fluid fine tailings (AESRD 2015). In 2013, there were approximately 976 Mm^3 of fluid tailings contained within tailings ponds in Fort McMurray region (AESRD 2015). Conventionally deposited tailings generate suspension of fluid tailings with a solids concentration of less than 8% immediately upon deposition. The fines in the fluid pond remain in suspension for long period of time because the clay minerals (particle size less than 2 μm) within the fines hinder the settlement process due to physicochemical interaction and low self-weight of the clay particles. Some of the suspended fines slowly settle due to self-weight, forming a gradually increasing density profile with depth. After 2 to 3 years, the solids concentration at depth in the pond increases to about 30%, after which any significant increases in solids content is very slow (Matthews et al. 2011). Sedimentation and consolidation process further releases water from the tailings deposits and the solids content increases over time. The solids content of fluid tailings can vary from about 0.5% to as much as 60% by weight.

REGULATORY REQUIREMENTS FOR OIL SANDS TAILINGS MANAGEMENT

In 2009, the Energy Resources Conservation Board (ERCB) implemented Directive 074 for oil sands tailings management (ERCB, 2009). Directive 074 was based on the fines capture and shear strength of the tailings deposits. Directive 074 stipulated that tailings deposits must achieve an undrained shear strength of 5 kPa one year after the end of deposition. Directive 074 was inadequate to meet the overall intent of tailings management and hence was suspended in 2014. In March 2015, the Alberta Environment for Sustainable Resource Development (AESRD) released the Tailings Management Framework (TMF) for the Mineable Athabasca Oil Sands. The TMF provides direction to manage fluid tailings volumes during and after mine operation in order to decrease liability and environmental risk resulting from the accumulation of fluid tailings on the landscape (AESRD 2015). The TMF fills the gaps in Directive 074 by considering the full life cycle of oil sands mining operation. The TMF provides the basis for a holistic landscape management approach and encourages early initiatives for tailings management to reduce long-term liability. In response to the release of the TMF, the Alberta Energy Regulator (AER) released Directive 085 on July 14, 2016 (AER 2016). Directive 085 sets out the requirements for managing fluid tailings volumes for the oil sands mining projects and adopts a risk-based approach for tailings management. Directive 085 provides flexibility to the operator for developing site specific tailings management plans but at the same time, it holds operators accountable for managing tailings responsibly.

KEY ELEMENTS OF HOLISTIC TAILINGS MANAGEMENT APPROACH

Key elements of a holistic tailings management approach proposed in this paper include:

1. Understanding closure and reclamation objectives;
2. Understanding tailings characteristics;
3. Developing tailings technology and fluid tailings treatment plans;
4. Developing tailings deposition strategy;
5. Developing progressive closure and reclamation plans;
6. Developing performance monitoring and measurement plans; and
7. Adaptive management.

A flowchart depicting the relationships between these elements is presented in Figure 1.

For the oil sands operations in Alberta, the goal of closure and reclamation is to develop locally-common, self-sustaining boreal forest ecosystems in the closure landscape. Both the TMF and Directive 085 aim at achieving the following key closure and reclamation objectives:

- Meeting regulatory requirements;
- Meeting stakeholder's expectations; and
- Act towards responsible environmental management.

A responsible tailings management plan involves managing tailings in such a way that the volume of accumulated fluid tailings is minimized during operations to promote progressive closure and reclamation. It is expected that the reclaimed landscape will be composed of a variety of upland terrestrial ecosites, riparian shrubland ecosites, wetlands in drainage areas, and shrubland mixes along drainage channels (CNRL 2016). The reclaimed landscape may also have End Pit Lakes (EPLs). The reclaimed ecosites should be typical of the Athabasca Oil Sands Region and similar to pre-development conditions. Figure 2 illustrates a schematic view of closure landscape.

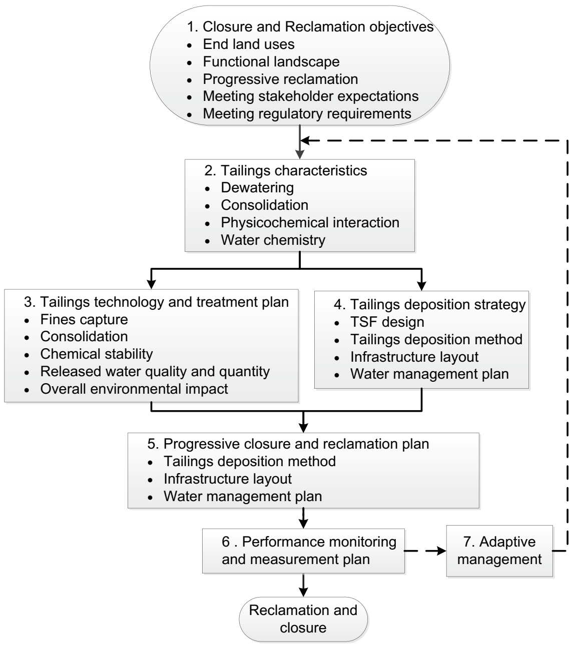

Figure 1. Flowchart Illustrating Key Elements of Holistic Tailings Management Approach Understanding Closure and Reclamation Objectives

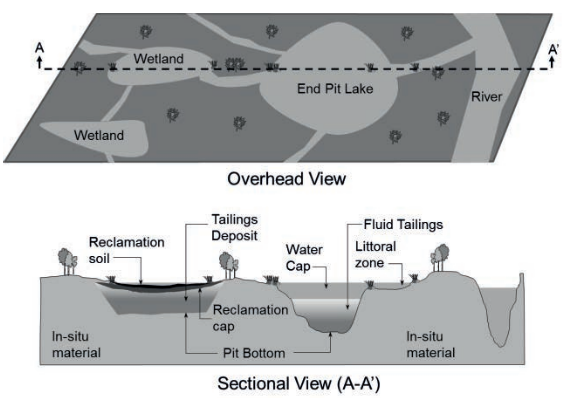

Figure 2. Schematic View of Closure Landscape

Understanding Tailings Characteristics

A holistic tailings management approach requires understanding of physical and chemical properties of the tailings that need to be managed. The dewatering and consolidation behaviour of tailings as well as the environmental factors determines the nature of closure landform. The tailings characteristics also govern the closure and reclamation schedule.

Oil sands tailings do not quite follow Terzaghi's conventional soil mechanics theory. This is because the conventional soil mechanics theory is based on infinitesimal strain, whereas tailings slurry with high water content undergoes large volume change (finite strain). Finite strain consolidation theory proposed by Gibson et al. (1967) is widely used to predict the settlement behaviour of tailings.

Several commercial software such as FSConsol and SVOffice are used to predict the consolidation behaviour. These modelling tools require material input parameters, which are determined from laboratory testing. Common laboratory bench scale testing include particle size distribution, atterberg limits, specific gravity, bitumen content, and large strain consolidation testing along with hydraulic conductivity measurements. Advanced laboratory tests such as soil water characteristic curve (SWCC) tests are carried out to analyze unsaturated tailings behaviour (Fredlund et al. 2011, Owolagba 2013).

Large scale column tests are commonly used to understand settlement and consolidation behavior of tailings. Column tests performed on oil sands tailings have been reported by Sun et al. (2014) and Scott et al. (2013). At the University of Alberta, Edmonton, Canada, 10 m tall column tests were conducted for 30 years using tailings originating from Syncrude's tailings ponds (Scott et al. 2013). Extensive bench scale laboratory tests were also conducted along with the column tests. The column test results were compared the settling behaviour predicted by the large strain consolidation models and then the applicability of the models to actual tailings ponds were evaluated. Jeeravipoolvarn (2005) showed that the large strain consolidation formulation developed by Gibson et al. (1967) over-predicts the settling behaviour of oil sands tailings in meso-scale testing (Figure 3).

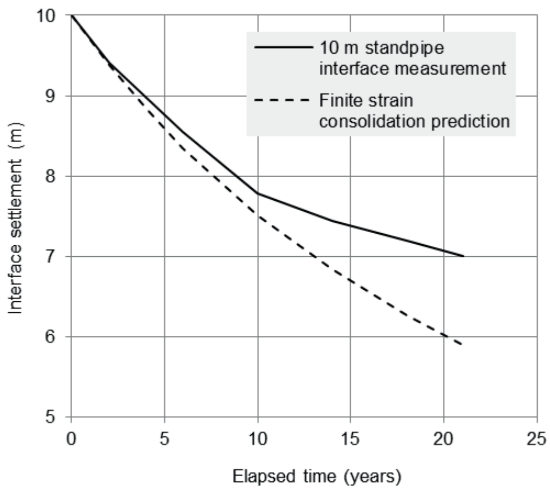

Figure 3. Observed and Predicted Consolidation of Oil Sands Tailings (after Jeeravipoolvarn 2005)

The inaccuracies in the prediction of consolidation behaviour are not necessarily due to limitations of the bench scale tests. Environmental factors such as freeze-thaw, desiccation and drying, precipitation, seepage, physicochemical interaction, variability in material properties between laboratory sample and field material and scale effect play significant role in making consolidation behaviour prediction difficult. The existing commercial software do not consider all these variables and often rely on assumptions. Therefore, the limitations associated with the commercial software should be taken into consideration while predicting consolidation behaviour. Similarly, the assumptions must be carefully chosen based on experience.

In cold regions, such as northern Alberta, the surface of the tailings deposits can freeze and inhibit upward movement of pore water. Therefore, the dewatering and consolidation behaviour of tailings deposits are expected to be different in the winter months compared to the summer months. Freeze-thaw consolidation tests should be carried out to assess the dewatering behaviour of tailings. Freeze-thaw consolidation tests on oil sands tailings have been reported by Zhang and Sego (2014), Proskin et al. (2010) and Proskin (1998). Commercial software such as TEMP/W (GeoStudio) and FTCD (Freeze-Thaw-Consolidation-Desiccation) can be used to perform freeze-thaw analyses. Under freezing temperature conditions intermittent deposition of tailings can result in formation of ice lenses within tailings deposits. Rate of tailings deposition can also impact the freeze-thaw behaviour. A typical plot of oil sands tailings consolidation behaviour for summer only operation is illustrated in Figure 4. This figure shows the average solids content of the deposit increases rapidly during the thaw strain period.

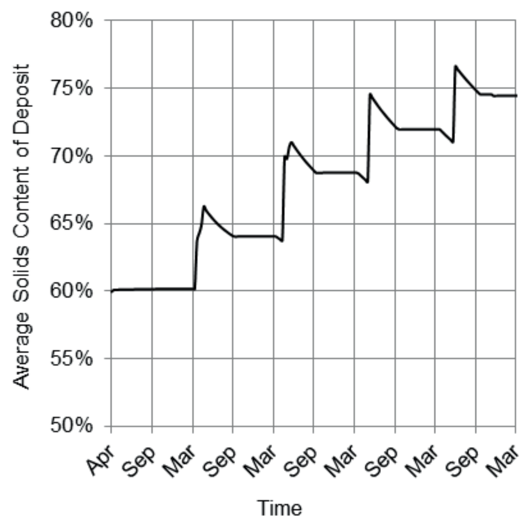

Figure 4. Average Solids Content of a Tailings Deposit During Summer Only Operation

In a tailings pond, the water content and void ratio of fluid tailings deposits generally decrease with depth. Near the surface of FT deposit, the void ratio can be so large that particle to particle contact may not exist. In this region, hindered sedimentation process governs the settling behaviour of the deposit and Terzaghi's effective stress principle may not be valid (Imai 1981). Tan (1995) suggested that the effective stress at large void ratio is derived from the physicochemical interaction and as such the effective stress may not control the deformation in a soil water system, such as fluid tailings. Hence, the clay water chemical interaction must be understood through proper characterization.

The sedimentation behaviour of clay rich fluid tailings deposits significantly depends on the water chemistry. Zeta potential test can be used as an indicator of fluid tailings sedimentation behaviour (Islam 2014).

Developing Tailings Technology and Fluid Tailings Treatment Plans

Any tailings treatment technology must aim at minimizing environmental risks during operation as well as meeting final closure and reclamation objectives. Key criteria for selecting tailings technologies include:

Fines capture

For conventional tailings deposits with beaches, enhancing the fines capture in the beaches is one of the key goals of any tailings technology. By capturing higher percentage of fines in the beaches the volume of fluid tailings in the tailings ponds decrease.

Fines capture of the treated tailings is evaluated by measuring the segregation behavior of the tailings mixture. Figure 5 is a ternary diagram and shows characteristics of oil sands tailings. The segregating-nonsegregating boundary defines the segregation or preferential settling of the solid particles. Above this line the coarse particles settle through the tailings slurry and therefore segregate while below the boundary no appreciable differential settling of the coarse particles takes place regardless of their concentration. Tailings can be rendered nonsegregating by increasing the solids content and/or fines content to below the segregation boundary or by the addition of lime, gypsum and synthetic polymers etc.

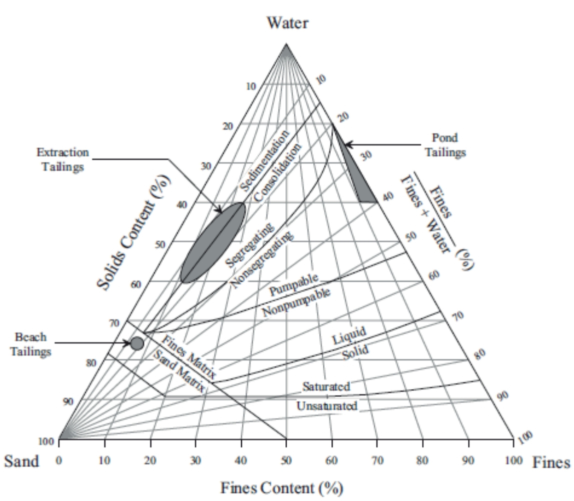

Figure 5. Typical Ternary Diagram Showing Boundary Zones of Oil Sands Tailings (after Azam and Scott 2005)

High water content tailings are often treated and dewatered (thickened) prior to deposition in a TSF. The thickening process increases the slurry density and reduces the potential for segregation.

Consolidation characteristics of tailings

Consolidation of tailings results in volume reduction and therefore, increases the life of TSF.

Settling/consolidation behaviour of tailings deposits also impacts the nature of closure landforms and progressive closure and reclamation schedule. Reduced post-infilling settlement and consolidation of the tailings deposits will reduce the deformation of the final landscape after reclamation. A typical consolidation curve for Composite Tailings (CT) is given in Figure 6. This shows the solids content increases rapidly up to 75% within few months after deposition after which the rate of consolidation significantly slows down.

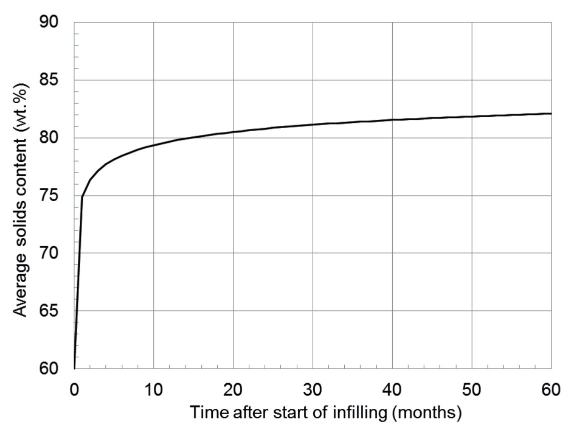

Figure 6. Typical Solids Content Plot for CT (modified from CNRL 2016)

Chemical stability

Chemical stability is an indication of the stability of the structural morphology of the treated tailings. Tailings technology must be designed to maximize the long-term stability of tailings deposits. Tailings treatment technologies often involve mixing of polymers and coagulants to the tailings slurry to enhance fines capture and/or accelerate dewatering and consolidation. The treated tailings should be stable to withstand the impact of shear during pipeline transportation. The chemical should also provide stability to the tailings deposits to meet the long-term performance goals. The geotechnical benefits of flocculation in dewatering oil sands tailings are described by Dunmola et al. (2013).

Quality and quantity of release water: A higher water release rate can enhance the ability to reuse process water in bitumen extraction process and therefore, can potentially reduce water intake from the environment.

The released water chemical composition is an important factor in technology selection process as it impacts the quality of recycle water. Technologies and/or chemicals with zero minimum impact on water chemistry are ranked higher in the evaluation process.

Overall environmental impact

Tailings technology should have minimum detrimental effect on the environment. The residual and net environmental risks of each tailings technology with respect to air, land, water quality and water use intensity must be assessed prior to technology selection.

Oil Sands Tailings Technology Deployment Roadmap Study was conducted by Canada's Oil Sands Innovation Alliance (COSIA) in collaboration with the oil sands industry to evaluate a suite of tailings treatment technologies (COSIA 2012a). The study was intended to identify tailings technologies that may reduce FT volumes and meet the goals of responsible tailings management. Alberta Innovates-Energy and Environment Solutions (AI-EES), in collaboration with the Oil Sands Tailings Consortium (OSTC), and Consortium of Tailings Management Consultants (CTMC) prepared a technology deployment roadmap to manage oil sands tailings.

Several technologies were identified for current and future application, of which a few have been implemented by the oil sands operators in Fort McMurray region (Table 1).

Selection of tailings technologies for a specific site depends upon several factors such as fines volume, sand to fines ratio (SFR) of the ore, availability of sand for the tailings treatment process, climatic condition and availability of land areas for tailings disposal. Some of these factors are briefly described below:

- CT and Non-segregated Tailings (NST) use WT or coarse sand tailings (CST) to capture fines. Therefore, availability of WT or CST is an important consideration for selecting technologies such as CT and/or NST. Syncrude and Suncor use mine waste (overburden and interburden) as well as tailings sand for construction of tailings dykes. Therefore, the availability of tailings sand to be used in tailings treatment process is limited. However, Canadian Natural Resources Ltd. (CNRL) uses only mine waste to construct tailings dykes and hence, majority of the WT can be used for the production of NST.
- Tailings technologies such as Suncor's Tailings Reduction Operation (TRO) and Shell's Atmospheric Fines Drying (AFD) require very large areas for disposing tailings in thin lifts and subsequent drying. Therefore, this type of technology may not be effective where large areas are not available for tailings disposal.
- Centrifuge technology has challenges related to transportation of dewatered tailings. This technology is also capital intensive and therefore, limits the volume of fines that can be treated.
- The EPL technology is proposed by oil sands operators to store fluid tailings in previously mined out pits. This technology is currently being demonstrated at a commercial scale at Syncrude's Base Mine Lake. The demonstration is planned to continue for 10 years. Since the EPL technology is not fully proven in the oil sands industry yet, Directive 085 requires operators to develop alternate technologies to mitigate the risks and uncertainties associated with the EPL technology.

Developing Tailings Deposition Strategy

Key considerations for developing a tailings management plan should include:

- design of TSF;
- selection of tailings deposition method;
- development of deposition plan and infrastructure layout; and
- water management plan.

Design of TSF

The following factors should be considered while designing TSFs:

1. Containment requirement

Design of TSF starts with identifying short-term and long-term containment requirements. Tailings mass balance models are used to forecast short-term and long-term tailings volumes based on ore production rates. In addition to tailings storage, excess water is often stored in the TSFs to meet overall site containment requirements. Current regulations require that the process affected water cannot be released into the environment without meeting the acceptable quality. Therefore, the overall storage requirements should be considered while estimating the TSF capacity. Requirements for possible future expansion of the TSF to meet potential production increase should also be considered. Site-wide water balance simulation is often carried out to estimate the containment requirements. A typical plot showing the estimation of containment requirement for an oil sands mining operation is shown in Figure 7.

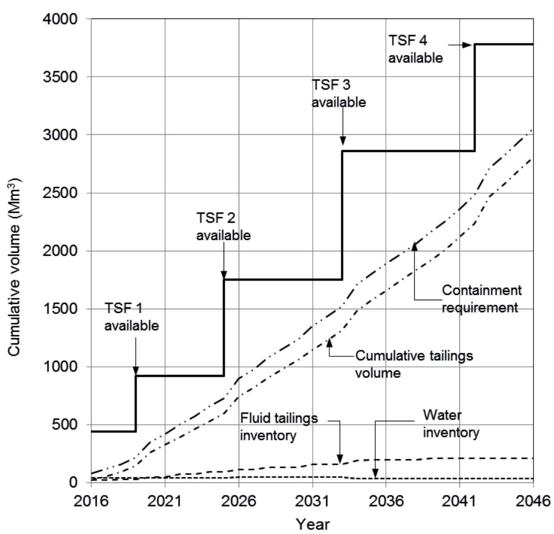

Figure 7. Typical Plot Showing Estimation of Containment Requirement

2. Location and topography

Both above ground and in-pit TSFs have been in use in the oil sands industry. Perimeter dykes and valley design (or variation of it) are most common for above ground TSFs. The design choice is primarily dependent upon natural topography, site conditions, and economic factors.

Location of the TSF is largely governed by the proximity to overburden mining or borrow source areas, proximity to extraction plant, presence of ore beneath the TSF footprint and proximity to environmental water bodies such as river.

3. Method of dyke construction

Tailings dykes are constructed either using mine waste or tailings sand. Because the costs are driven by the amount of fill material used in the dyke or embankment, major savings can be realized by using tailings sand for dyke construction. Some of the tailings dykes at Syncrude, Shell and Suncor sites have been constructed using tailings sand by “cell construction” method. CNRL however uses mine waste for dyke construction.

The dykes are built as downstream, upstream or centerline construction (Figure 8). Each of the dyke structure is constructed in successive lifts. Selection of a dyke design depends upon the availability of borrow material, footprint area and deposition plan. For example, if the dyke is planned to be constructed using “cell construction” method, then the downstream construction may not be practical.

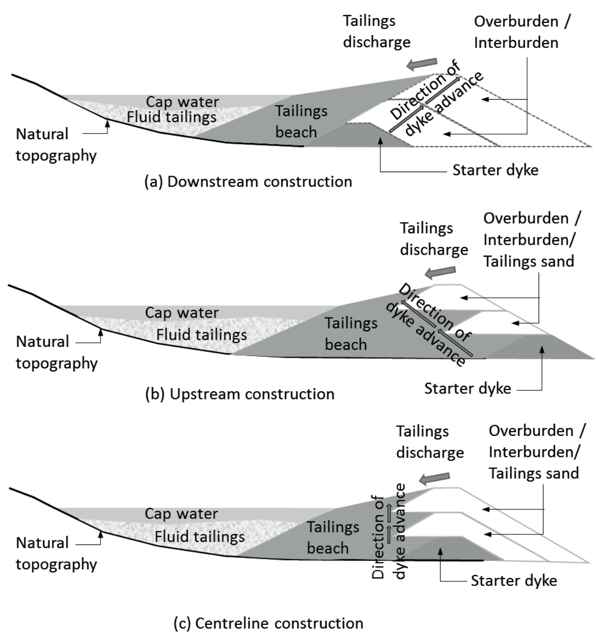

Figure 8. Upstream, Downstream and Centreline Dyke Construction

Generally, the footprint of dyke increases with downstream construction as the dyke gets higher. Upstream construction requires smaller footprint but it requires raising the dyke above the previously deposited tailings beaches. Dyke failures appear to be more common where upstream construction has been employed (LPSDP 2007). In the case of centerline or upstream dyke construction, seismic activity can potentially liquefy the foundation material (tailings beaches) and initiate failure.

The geotechnical designs of each tailings containment structures must meet regulatory requirements, such as Dam Safety Guidelines (CDA 2007) and other relevant industry standards. Understanding the site geology is paramount for any dyke design as the failure to understand the geological formation and the strength characteristics of foundation material at the site can cause serious consequence.

Risk based approach consisting of an observational method should be adopted for the design, construction and operation phases of the tailings structures. Adopting the observational method during construction and operation can provide performance data which will guide the operators for making timely modifications to the design, construction and operation of the containment structures.

Selection of Tailings Deposition Method

Tailings disposal methods that are currently being used in the oil sands industry can be broadly divided into two categories: (a) beaching or sub-aerial deposition, (b) sub-aqueous deposition (under water or under tailings).

The beaching or sub-aerial deposition is the most common deposition method used in the oil sands industry and has been used by all operators. This refers to a deposition scenario where tailings slurry is discharged from a point higher than the tailings elevation or pond level. This allows tailings to flow away from the deposition point followed by:

- release of water from the slurry matrix;
- increased slurry density and decreased flow velocity; and
- formation of tailings beaches.

Sub-aqueous deposition refers to a deposition scenario where the tailings discharge point is submerged under water or fluid tailings. The sub-aqueous deposition offers a low energy deposition environment and the settled tailings in such environment forms a steeper tailings beach below the fluid compared to the beach formed in sub-aerial deposition environment (Robertson and Wels 1999).

Sub-aqueous deposition systems are mostly preferred for reactive tailings. In this method, the water or fluid tailings cap prevents oxidation of reactive tailings to avoid acid mine drainage. In the oil sands industry, sub-aqueous deposition systems are used to reduce fines segregation. A tremie is an example of such deposition system and has been used by oil sands operators to reduce turbulence in tailings discharge pipe, which helps to prevent segregation of tailings.

Development of Deposition Plan and Infrastructure Layout

Development of deposition plans is one of the key elements of holistic tailings management approach. Volumetric deposition modelling software such as Muck3D can be used to simulate progression of tailings deposits over time. Deposition plans can be very useful in identifying tailings infrastructure requirements such as size and number of tailings pipelines, their location, number of discharge points and sequence of operation, future pipeline moves and location and size of water removal system etc.

Deposition modelling software use beach slope parameters. Oil sand tailings beach slopes can vary considerably (from nearly flat to 4%). Based on pond investigation surveys it has been reported that tailings form steeper beach slopes below water compared to beach above water (COSIA 2013). Generally, tailings slurry with lower water content tends to form steeper slope compared to tailings slurry with higher water content. Also, tailings slurry with lower water content may flow shorter distance on the beach compared to tailings with higher solids content. Utilization of TSF storage capacity can be significantly impacted by the beach slope parameters. Since the beach slopes vary considerably due to the variation in feed ore and nature of tailings treatment, it is important to carry out sensitivity analyses to assess the impact on TSF storage capacity. A typical plot showing impact of beach slope on utilization of TSF storage capacity is given in Figure 9.

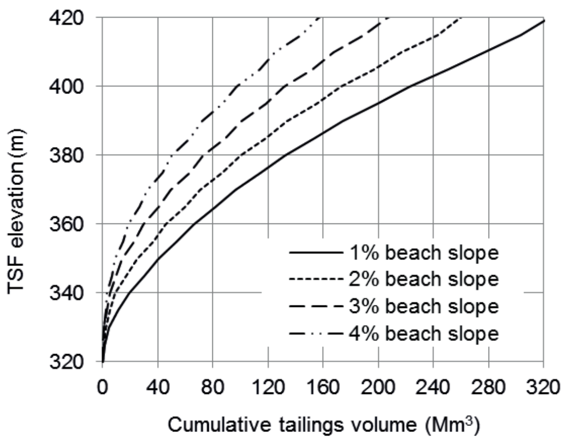

Figure 9. TSF Storage Capacities for Different Beach Slopes

Tailings deposited from the entire perimeter generally results in better utilization of TSF capacity. However, a perimeter discharge layout may require higher capital investment compared to discharge from part of the perimeter. Too many discharge points can be advantageous from storage utilization perspective but they can create operational complexities. On the other hand, too few deposition points can result in ineffective utilization of storage capacity. For a fixed TSF geometry and elevation, a typical plot showing the effect of number of deposition points on TSF storage capacity utilization is shown Figure 10. This figure shows that there is no significant gain in storage capacity utilization beyond nine discharge points.

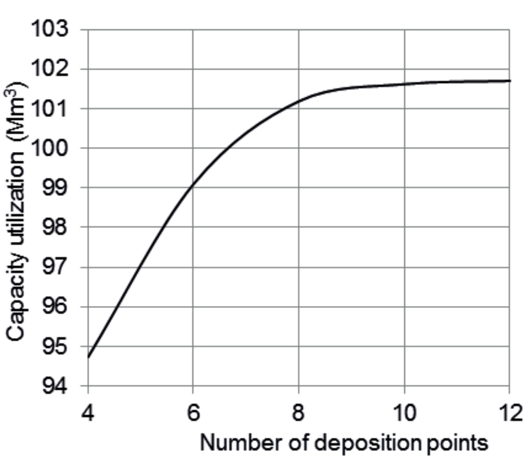

Figure 10. Storage Capacity Utilization vs. Number of Deposition Points

Tailings that does not meet the design specification (off-spec) should be managed separately from tailings meeting specification (on-spec). Therefore, it is important to develop on-spec and off-spec tailings management plans. A schematic showing on-spec and off-spec tailings management plan is shown in Figure 11. This figure illustrates that by depositing off-spec material at designated locations can potentially reduce beach erosion and resulting fines segregation in other parts of the deposits.

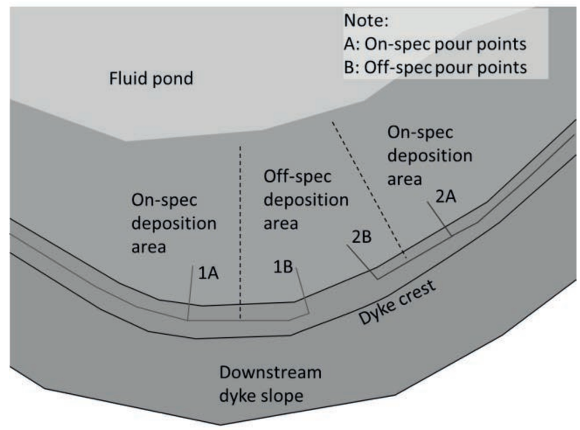

Figure 11. Schematic Showing On-spec and Off-spec Tailings Management

Water removal is a key consideration in tailings deposition planning as it has significant impact on tailings operations and capital/operating costs. Location of water removal systems such as barges and dredges depends on the volume of process water needs to be transferred, pipeline capacity, pumping distance, source of electricity etc. Analyses of deposition plans can be very helpful in identifying the location of release water pond for different discharge configurations.

Water Management Plan

Mikula (2012) reported that one barrel of bitumen generates about 1.5 barrel of tailings. Technological developments in ore processing over the years have significantly reduced the water usage in processing plants and thereby reducing the water withdrawal from the environment. Despite this, a significant volume of process water has been accumulated over the years in the Fort McMurray region (Guo 2010).

In order to manage the environmental water responsibly, the tailings management plan should focus on maximizing use of tailings release water in the extraction plants.

Developing Progressive Closure and Reclamation Plans

The closure and decommissioning of the tailings storage facilities should be carefully considered as part of the mine closure plan to ensure that appropriate public health and safety, community, and environmental criteria can be established for the design. Closure criteria for the tailings storage facilities should be reviewed in consultation with the community during the operating phase, and the tailings management strategy continuously updated.

Reclamation and closure planning is an iterative process that integrates the evolving mine and tailings planning processes (Figure 12). It is important to develop the closure and reclamation plans at the early stages of planning and continuously update them as the mine and tailings plan evolve.

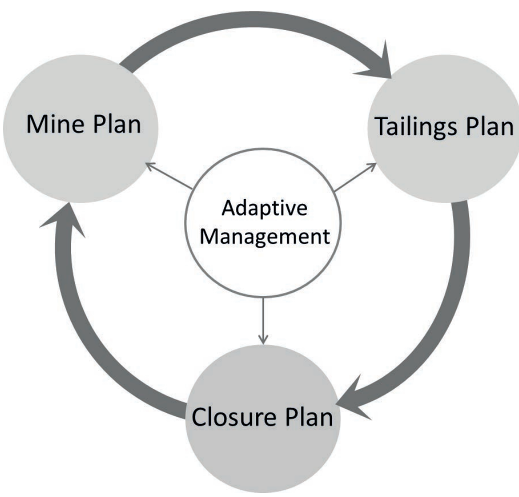

Figure 12. Iterative and Integrated Planning Process

Periodic status maps depicting progression of mining, tailings deposition and closure and reclamation should be created to ensure the closure and reclamation plan is always aligned with the mine and tailings deposition plans. Additionally, integrated schedule comprising of activities such as tailings deposition, capping, revegetation etc. should be developed for each TSF.

Developing Performance Monitoring and Measurement Plans

The main objective of the TMF is to minimize fluid tailings accumulation by treating them with suitable technologies and reclaiming the tailings deposits progressively during the life of the project in order to manage long-term liability and potential environmental risks. The TMF sets out indicators, targets, triggers and limits, based on forecasted fluid tailings volumes, for each site. Fluid tailings are considered to achieve ready to reclaim (RTR) state when they have been processed with a valid technology, placed in their final landscape position and meet performance criteria. The RTR criteria is intended to track the volume of treated fluid tailings during the operational phase of the deposit to ensure that the cumulative fluid tailings volume remains below the approved fluid tailings profile. The goal of the TMF and Directive 085 is to ensure that all legacy fluid tailings (generated prior to January 2015) achieve RTR status by the end of mine life and all new tailings (generated after January 2015) achieve RTR status within 10 years of end of mine life. A schematic showing the transition of fluid tailings deposits to RTR state is shown in Figure 13.

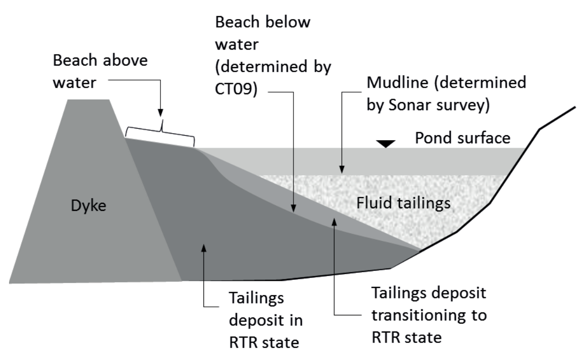

Figure 13. Schematic Illustrating Progression of Fluid Tailings Deposits to RTR State

In order to evaluate whether active treated tailings deposits are on a trajectory to meet TMF objectives, Directive 085 specifies two subobjectives that address different aspects of performance:

- Sub-objective 1: the deposit's physical properties are on a trajectory to support future stages of activity; and
- Sub-objective 2: to minimize the effect of the deposit has on surrounding environment and

to ensure that a locally common, diverse and self-sustaining ecosystem will be developed.

Oil sands operators are required to develop RTR criteria and measurement plans specific to their fluid tailings deposits. In response to Directive 085, Suncor and CNRL have already submitted their tailings management plans (as of September 30, 2016). The RTR criteria proposed by these operators are given in Table 2. It is expected that operators will continuously review and/or modify or develop additional RTR criteria, if required, when data, findings and lessons learned becomes available in the future.

Directive 085 provides guidance on fluid tailings volume measurement methods. Currently, oil sands operators conduct annual pond investigation program which typically include the following:

- Topographic survey (LiDAR or equivalent survey techniques) to determine the tailings beach surface and pond surface elevation;
- Sonar survey to determine the mud water interface;
- CT09 sounding (or similar techniques) to determine the pond bottom;
- Cone Penetration Test (CPT) for geotechnical characterization of tailings deposits;
- Sampling of water, fluid tailings and pond bottom and laboratory testing (includes particle size distribution, atterberg limit, dean stark, specific gravity, methylene blue index, large strain consolidation and water chemistry); and
- Groundwater and surface water monitoring.

Additional deposit specific measurements such as SFR of the deposit, tailings slurry density, water content of tailings deposits, pore water pressure etc. may be required in the future to assess the performance of fluid tailings deposits.

Adaptive Management

Adaptive management is a flexible decision making process which can be applied when dealing with uncertainties in tailings technology performance. This is a structured and iterative process that aims at reducing uncertainty over time via system monitoring. An adaptive management approach involves exploring alternate ways to meet management objectives, predicting the outcomes of alternatives based on the current state of knowledge, implementing one or more of these alternatives, monitoring to learn about the impacts of management actions, and then using the results to update knowledge and adjust management actions.

Existing and new tailings management technologies remain unproven, ranging from pilot scale development to commercial demonstration. At present, no technology can be considered "mature", in the sense that it has demonstrated an attainment of reclamation and closure criteria. Given the inherent challenges and learning curve as these technologies are validated at a commercial-scale, the design, operation and regulatory processes involved must accommodate an adaptive management approach to succeed. Key principles of adaptive management approach that can be applied to tailings management include:

- understanding tailings management objectives;
- predicting outcomes using new and existing tailings technologies;
- acknowledging inherent challenges and uncertainties associated with tailings technologies;
- improving understandings from experience and data collected from monitoring; and
- making use of lessons learned, management interventions and follow-up monitoring to promote understanding and improve subsequent decision making.

CONCLUSIONS

Development of tailings management plan for an oil sands operation is complex and is driven by the post-closure landform requirements. The long-term containment requirements, physical and chemical properties of tailings, method of tailings deposition, water management plan, reclamation and closure objectives, and regulatory requirements etc. should be taken into consideration while developing tailings management plans.

The TMF provides direction to manage fluid tailings volumes during and after mine operation in order to decrease liability and environmental risk resulting from the accumulation of fluid tailings on the landscape The main objective of the TMF is to minimize fluid tailings accumulation by treating them with suitable technologies and reclaiming the tailings deposits progressively during the life of the project. Oil sands operators are required to develop RTR performance criteria specific to their treated tailings deposits. The RTR criteria is intended to track the volume of treated fluid tailings during the operational phase of the deposit to ensure that the cumulative fluid tailings volume remains below the approved fluid tailings profile

Existing and new tailings management technologies remain unproven, ranging from pilot scale development to commercial demonstration. Given the inherent challenges and learning curve as these technologies are validated at a commercial-scale, the design, operation and regulatory processes involved must accommodate an adaptive management approach to succeed.

ACKNOWLEDGEMENT

The authors wish to thank Brad Hansen, Nicholas Payne and Christine Baine of Advisian for their support to prepare this manuscript.

REFERENCES

AER (Alberta Energy Regulator) (2016). Directive 085: Fluid Tailings Management for Oil Sands Mining Projects, Issued by Alberta Energy Regulator on July 14, 2016.

AESRD (Alberta Environment and Sustainable Resource Development) (2015). Lower Athabasca Region- Tailings Management Framework for the Minable Athabasca Oil Sands. Alberta Environment and Sustainable Resource Development. Government of Alberta. ISBN: 978-1-4601-2174-0 (online version), March 2015.

Azam, S. and Scott, J. D. (2005). Revisiting the Ternary Diagram for Tailings Characterization and Management. Geotechnical News. pp. 43-46.

CDA (Canadian Dam Association) (2007). Dam Safety Guidelines 2007, Published by Canadian Dam Association.

CNRL (Canadian Natural Resources Ltd.) (2016). Application for the Approval of Canadian Natural's Tailings Management Plan (TMP), submitted to Alberta Energy Regulator, September 23, 2016.

COSIA (Canada's Oil Sands Innovation Alliance) (2012a). Oil Sands Tailings Roadmap – Project Report – Volume 1 – Summary Report. Submitted to Alberta Innovates – Energy and Environment Solutions.

COSIA (Canada's Oil Sands Innovation Alliance) (2013). Beach Fines Capture Study. Submitted to Canada's Oil Sands Innovation Alliance, June 2013.

Dunmola, A., Dhadli, N., Freeman, G., Kolstad, D., Fasking, T., Song, J. and Langseth, J. (2013). Geotechnical Benefits of Flocculation in Dewatering Mature Fine Tailings, In Proceedings of 66th Canadian Geotechnical Conference 2013, Montreal, QC, Canada.

ERCB (Energy Resources Conservation Board) (2009). Directive 074: Tailings Performance Criteria and Requirements for Oil Sands Mining Schemes, Bulletin 2009 – 02, Issued by Energy Resources Conservation Board on February 2009.

Fredlund, D. G., Stone, J., Stianson, J. and Sedgwick, A. (2011). Determination of Water Storage and Permeability Functions for Oil Sands Tailings. In Proceedings of the Tailings and Mine Waste Conference 2011, Vancouver, Canada.

Gibson, R. E., England, G. L. and Hussey, M. J. L. (1967). The Theory of One-Dimensional Consolidation of Saturated Clays, Geotechnique, **17**, (3), 261–273.

Guo, Z. (2010). An Integrated Engineering Solution in Treating Tailings Pond Water from Alberta's Oil Sands Industry, In Proceedings of 2nd International Oil Sands Tailings Conference 2010, Edmonton, AB, Canada.

Imai, G. (1981). Experimental Studies on Sedimentation Mechanism and Sediment Formation of Clay Materials, Soils Found., **21**, (1), 7–20.

Imperial Oil (2016). Kearl Oil Sands Tailings Management Plan. Tailings Management Plan Submitted To Alberta Energy Regulator, November 2016.

Islam, S. (2014). Thickening of mature fine oil sands tailings. MSc Thesis, University of Western Ontario. London, ON, Canada.

Jeeravipoolvarn, S. (2005). Compression behaviour of thixotropic oil sands tailings. MASc Thesis, University of Alberta, Edmonton, AB, Canada.

LPSDP (2007). Leading Practice Sustainable Development Program for the Mining Industry, Handbook Published by The Australian

Government Department of Industry, Tourism and Resources. ISBN 0 642 272500 4.

Matthews, J.G., Dhadli, N., House, P. and Simms, P. (2011). Field Trials of Thin-Lift Deposition of Amended Mature Fine Tailings at the Muskeg River Mine in Northern Alberta. Proceedings of the 14th International Seminar on Paste and Thickened Tailings (Paste2011), Perth, Australia, 5-7 April 2011. Jewell, R.J. and Fourie, A.B. (eds.). Australian Centre for Geomechanics, Perth. pp. 271-280.

Mikula, R. J. (2012). Advances in Oil Sands Tailings Handling: Building the Base for Reclamation, In Restoration and Reclamation of Boreal Ecosystems: Attaining Sustainable Development, Vitt, D.H. and Bhatti, J.H. (eds), Cambridge University Press, 2012, pp. 103-122.

Morgenstern, N. (2001). Geotechnics and Mine Waste Management - Update: Seminar on safe tailings dam constructions. Gallivare, Swedish Mining Association, Natur Vards Verket, European Commission:.pp. 54-67.

Owolagba, J. O. (2013). Dewatering behavior of centrifuged oil sand fine tailings for surface deposition. PhD Thesis, Faculty of Graduate Studies and Research, University of Regina, Regina, SK, Canada.

Proskin, S. A. (1998). A geotechnical investigation of freeze-thaw dewatering of oil sands fine tailings. Ph.D Thesis, University of Alberta. Edmonton, AB, Canada.

Proskin, S. A., Sego, D. and Alostaz, M. (2010). Freeze–Thaw and Consolidation Tests on Suncor Mature Fine Tailings (MFT), Cold Reg. Sci. Technol., **63**, (3), 110–120.

Robertson, A. and C. Wels (1999). Cover placement on extremely weak, compressible tailings, Robertson GeoConsultants Inc., Vancouver, Canada.

Scott, J. D., Kabwe, L., Wilson G.W., Sorta, A. and Jeeravipoolvarn, S. (2013). Properties Which Affect the Consolidation Behaviour of Mature Fine Tailings, In Proceedings of the Tailings and Mine Waste Conference 2013, Banff, AB, Canada.

Shell (2016a). Jackpine Mine Fluid Tailings Management Plan. Tailings Management Plan Submitted To Alberta Energy Regulator, October 2016.

Shell (2016b). Muskeg River Mine Fluid Tailings Management Plan. Tailings Management Plan Submitted To Alberta Energy Regulator, October 2016.

Sun, R., R. Spelay, J. Kan and A. Goldszal, (2014). Column Consolidation Testing of Oil Sands Tailings, In Proceedings of the 4th International Oil Sands Tailings Conference 2014, Lake Louise, AB, Canada.

Suncor (2016). Suncor Base Plant Application for the Draft Tailings Directive. Tailings Management Plan Submitted To Alberta Energy Regulator, April 2016.

Syncrude (2016). Tailings Management Plan Application, Syncrude Aurora North Mine. Submitted To Alberta Energy Regulator, October 2016.

Tan, T.S. (1995). From Sedimentation to Consolidation: A Geotechnical Perspective, In Proceedings of International Conference on Compression and Consolidation of Clayey Soils, May, 1995, Hiroshima, Japan, Yoshikuni and Kusakabe (eds), Balkema, pp. 937-948.

Zhang, Y. and Sego, D. C. (2014). Freeze-Thaw Dewatering of Albian Mature Fine Tailings, CIM Journal **5**, (1), 48–63.

Table 1. Tailings Technologies Implemented or Proposed by Oil Sands Operators

Tailings Technology	Technology Description	Application
Composite Tailings (CT)	CT combines fluid fine tailings with gypsum and sand. Gypsum acts as a coagulant enabling the fines to bind to heavier sand particles. This mixture causes the tailings to settle more quickly and release water.	Syncrude, Suncor and Shell
Non-segregated Tailings (NST)	NST combines thickener underflow and cyclone underflow to make a non-segregating sand-and-fines mixture. Carbon dioxide (CO_2) is injected into the process as a rheology modifier to increase yield strength of the slurry and decrease the potential for mixture segregation (CNRL 2016).	CNRL
Tailings Reduction Operation (TRO)	TRO uses an in-line flocculation process in which mature fine tailings (MFT) is mixed with a polymer to accelerate dewatering. The polymer flocculant sticks to the clay particles in the MFT and helps them to bind together, allowing the clay to be separated from the water. The thickened MFT is then deposited in disposal areas specifically constructed for dewatering. The resulting material can be reclaimed in the same location where it was dried or transported to another location for final reclamation.	Suncor
Atmospheric Fines Drying (AFD)	Similar to TRO	Shell
Thickened Tailings(TT)	Thickened tailings are produced by separating the tailings stream with cyclones into a coarse sand underflow and a fine tailings overflow. The overflow, comprised primarily of water and fine particles, is then combined with a polymer in a thickener vessel to produce tailings that have about the same solids content as MFT. By thickening the overflow tailings stream to the approximate consistency of MFT as tailings are produced, rather than waiting for self-weight settling, water is released immediately for recycling.	Imperial Oil and Shell
Centrifuge	Centrifuges use centrifugal force to dewater MFT to desired solids content. MFT is harvested from the tailings pond and subsequently treated with flocculent and/or coagulant. The mixture is then pumped into the centrifuge. The process of spinning the mixture, aided by the coagulating agent, removes the water and causes the solids to bind together. The released water is returned to the tailings pond.	Syncrude and Shell
CO_2 injection	CO_2 is injected into the tailings process as a rheology modifier to increase yield strength of the slurry, decrease the potential for mixture segregation and enhance fines settlement.	CNRL
End Pit Lake (EPL)	The EPL technology involves storage of residual fluid tailings in previously mined out pits. The goal of EPL technology is to create a biologically active, self-sustaining and functional ecosystem and is expected to discharge water of acceptable quality to downstream aquatic environments.	Syncrude, Suncor, Shell, Imperial Oil and CNRL

Table 2. RTR Criteria Proposed by Oil Sands Operators

Operator	RTR Criteria		
	Tailings Technology	Sub-objective 1	Sub-objective 2
		Indicator(s)	Indicator(s)
Suncor (Suncor, 2016)	In-line flocculation of FT (e.g. TRO)	Primary: • Clay to water ratio (CWR)	• Measures are not clearly defined
CNRL (CNRL, 2016)	NST	Primary: • Solids content Additional: • Porewater pressure; • Effective stress; • Deposit SFR; and • Consolidation of NST deposit (monitored with LiDAR surveying or equivalent).	• Soil moisture; • Soil type and depth; • Soil chemistry; • Upland vegetation type, health and vigor; • Wetland vegetation type, health and vigor; • Total suspended solids; • Salinity; and • Light penetration.
Shell (Shell 2016a, Shell 2016b)	AFD, CT, TT and Centrifuge	• Solids content	• Groundwater monitoring and soil & water chemistry
Syncrude (Syncrude 2016)	CT and Centrifuge	• Solids content	• Groundwater monitoring, deposit water volume & chemistry, fugitive emissions
Imperial Oil (Imperial Oil 2016)	TT	• Solids content	• Groundwater & surface water monitoring, tailings water chemistry, stability and erosion

OIL SANDS TECHNOLOGY TO MEET THE CHALLENGES OF NEW WORLD SUSTAINABLE TAILINGS MANAGEMENT

Kevin Moran, John Oxenford and Scott Nelson
Titanium Corporation, Edmonton, Canada

ABSTRACT

Recent events are shaping the emerging environmental landscape for Canadian oil sands mining operations. The industry and provincial government will be stewarding towards a revised Tailings Management Framework (TMF) that includes the new Directive 85 and aims to sustainably control tailings volumes. The UN Paris Conference, Canadian government commitment/support and Alberta's Climate Change Leadership Plan (CCLP) to limit global CO_2e impacts will require oil sands miners to significantly reduce their greenhouse gas (GHG) emissions and intensities. Other air-borne emissions issues are being identified, including volatile organic compounds and secondary organic aerosols. Secondary extraction tailings, often referred to as froth treatment tailings, are a significant source of tailings management and air emissions issues.

Titanium Corporation has developed an 'end-to-end' suite of technologies to remediate oil sands froth treatment tailings, enabled via novel and innovative recovery of contained hydrocarbons, that offer important reductions to GHG and other emissions as well as avoidance of tailings ponds altogether. In addition, these CVW™ technologies offer fit-for-reuse water recovery, heat integration, pyrite and radioactive materials management as well as positive economics.

Implementation of the Company's CVW™ technologies allows for the reduction of more than 80% of fugitive methane and VOC emissions at oil sands mines. This represents a reduction in GHG emissions intensity by ~10% at mature sites, or up to 3-5 megatonnes of CO_2e annually across the industry by 2030, and is a significant contribution to the annual methane emissions reduction target set by the CCLP. Efficient tailings management performance is realized that may allow for direct deposition into a reclamation landscape. Titanium's technology is well aligned with the key tenets of the Alberta Directive 85 and can assist the industry in achieving important sustainability improvements that are consistent with advancing global expectations.

INTRODUCTION

Canada's oil sands represents an important source of unconventional oil. First commercially accessed by conventional mining technologies in 1967, the mining sector has grown to about one million barrels of daily production in 2015, and is forecast to reach 1.5 million barrels per day by 2030 (CAPP, 2016). Along with producing about 25% of Canada's oil, the mining operations create a sizable environmental impact. A visible aspect of this industry, that has received much public attention in recent years, are the oil sands tailings and tailings containment ponds.

These ponds hold tailings largely generated during bitumen production operations. The consolidation of tailings and management of tailings volumes is challenged in part by the formation of fluid fine tailings (FFT). FFT are comprised of sub 45 micron solids and will only sediment to about 30% solids concentration, after significant quiescent settling in ponds, precluding management towards a dry landscape. The industry is managing approximately 975 million m^3 of FFT in 22 tailings ponds, covering an area of 54,363 acres. In 2009, the Alberta Energy Regulator (AER) introduced Directive 74 to guide the industry's tailings management practices (AER, 2009). With an emphasis on fines capture, it required deposits to reach 5 kPa shear strength within a year for reclamation. In response, the industry has introduced a number of tailings management technologies; many of these were identified as high priority options by the OSTC and COSIA (Sobkowicz, 2012).

On the matter of air quality, the oil sands contributed about 22% of Alberta's 267 megatonnes of GHG emissions in 2013 (Leach et al., 2015a). Up to 10% of those emissions attributed to the mining sector, currently over one megatonne CO_2e annually, are emitted as fugitives from tailings ponds (Alberta Environment and Parks, 2015). In fact, the tailings pond methane emissions account for about 70% of fugitive GHG emissions at an oil sands mine. These values can be expected to increase with industry growth and maturation of microbial communities within tailings ponds that are responsible for methanogenic fermentation of naphtha or other process solvents (Holowenko et al., 2000; Siddique et al., 2007).

A primary source of pond GHG and VOC emissions has been identified as the process solvent, a naphtha or paraffin, that is employed in secondary extraction operations. A portion of this solvent is lost to froth treatment tailings as diluted bitumen due to inefficiencies in the extractive processes. The industry is limited to release no more than four barrels of process solvent per thousand barrels of dry bitumen produced. Data for this metric is reported on a monthly basis to the AER (Statistical Table 39); the industry average was ~3.3 bbl/kbbl for the period of 2011 to 2015.

In addition to containing all of the lost extraction solvent, froth treatment tailings, which can represent up to 10% of site-wide tailings (the balance coming from primary extraction), also hold a disproportionate amount of fine particulate solids (which contribute to FFT) and 25% of the lost bitumen. These tailings also concentrate radioactive minerals (Chow et al., 2013) and pyrite, a source of acid rock drainage (Kuznetsov et al., 2015).

In 2015, the Canadian Council of Academies examined the state of minable oil sands tailings management and identified future opportunities. They concluded that froth treatment tailings should be managed separately from extraction tailings, stating (Newell et al., 2015):

> *"Separation and effective treatment of froth tailings can address two important tailings problems: reduce fugitive emissions resulting from decomposing solvent that remains in froth tailings after treatment and keep out the most toxic elements that hinder the reclamation of tailings ponds."*

The Canadian Council of Academies report went on to highlight Titanium Corporation's unique solution to the management of froth treatment tailings – one that prevents emissions and generates revenue through the recovery of heavy minerals.

The Alberta government, newly elected in 2015 with a mandate to introduce meaningful environmental reforms, initiated a far reaching public consultation into GHG emissions. The resulting Climate Change Leadership Plan (CCLP), which set a course for GHG emissions management for the province (Leach et al., 2015b). The CCLP placed a cap on oil sands emissions, increased the carbon levy to $30 per tonne by 2017 and placed emphasis on methane emissions abatement, targeting a 45% reduction or 12 megatonnes annually.

The Alberta Energy Regulator engaged the industry and public in their recent Tailings Management Framework (Government of Alberta, 2015). The exercise was intended to revamp guidance of oil sands tailings management and replace Directive 74. After an extended consultation process, Directive 85 (AER, 2016) was released in July of this year. This new Directive emphasized that oil sands tailings should be 'ready-for-reclamation' in relation to inventory accounting, leaving to reasonable interpretation the means by which this may be demonstrated. In one of its key objectives, the Directive indicates that special handling of froth treatment tailings may be appropriate. Further, approaches were encouraged that would synergistically address related environmental issues, including gas emissions (GHG, VOC etc.) and acidification.

Titanium Corporation, with the support of industry and governments, has developed a unique and sustainable solution to manage oil sands froth treatment tailings. The CVW™ process incorporates emerging environmental and tailings management perspectives in remediation of these tailings, potentially leading to solutions that avoid pond deposition. It offers a unique opportunity in the delivery of positive economics through operational cost savings and the recovery of high quality hydrocarbons and valuable heavy minerals.

END-TO-END DRY RECLAMATION OF FROTH TREATMENT TAILINGS

Froth treatment tailings are generated during secondary extraction operations, designed to clean the produced bitumen froth in advance of upgrading and/or pipeline transportation, in oil sands mining bitumen production. The bitumen froth is mixed with a lighter hydrocarbon - naphtha or a paraffin blend - producing a diluted bitumen product from which water and solids are more easily separated in centrifugal or gravity separators. The resultant tailings contain a minimum of about 2% diluted bitumen and 15-20% solids (Chow et al., 2013), about 30% of which is fines.

While froth treatment tailings comprise only up to 10% of the bitumen production tailings, they represent both significant are enriched with both economic potential and environmental challenges. About 25% (or more) of the bitumen lost during bitumen production is contained in froth treatment tailings along with a significant amount of process solvent at about 10% mass relative to the lost bitumen. The hydrocarbons present challenges in tailings management (Chow et al., 2013) and the solvent contributes to fugitive GHG emissions (Siddique et al., 2007; Burkus et al., 2014).

Due to their hydrophobic nature, the solids fraction is enriched in heavy minerals, including the marketable valuables, zircon and minerals bearing titanium (Tipman et al., 1996, Ciu et al., 2003). As well, problematic minerals such as pyrite and monazite/xenotime are concentrated into the froth treatment tailings. Pyrite can be involved in acidification reactions with implications towards mine management and reclamation activities. Monazite/Xenotime contain radioactive elements, including uranium and thorium, which concentrate at the beach of the froth treatment tailings deposition sites at tailings ponds, potentially creating issues related to NORM management (Sobkowicz, 2012).

CVW™ Technology Overview

Titanium's 'Creating Value from Waste™,(CVW™) technology (**Figure 1**) is comprised of a number of processing modules, each focused on a specific function towards remediation and/or value creation.

A concentrator plant is designed for hydrocarbon recoveries, heavy minerals production and tailings/water management. Minerals separation is conducted in a separate facility. The CVW™ process has been designed to integrate with oil sands bitumen production operations requiring no change to existing processes.

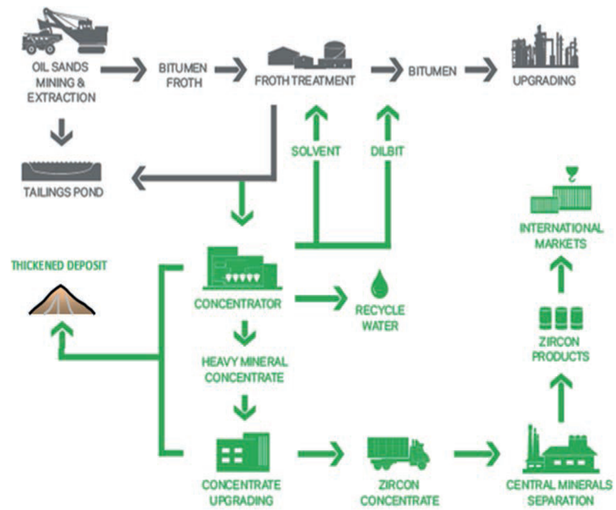

Figure 1. Integration of CVW™ technology at commercial oil sands mining operation

Tailings Hydrocarbon Removal and Recovery

The heart of the process lies in the ability to efficiently and effectively recover hydrocarbons from the tailings (Moran et al., 2015). This is achieved by first size classifying the froth treatment tailings, where hydrocarbons are segregated into a fines-dominated fraction that resembles mature fine tailings (CVW™ fluid fine tailings; **Figure 2**).

Bitumen is recovered from the CVW™ fluid fine tailings, and the corresponding heavy minerals rich coarse fraction (CVW™ Coarse Tailings; **Figure 2**), using flotation and solvent extraction to achieve recoveries of up to 90% of lost bitumen at coker-feed quality.

Process solvent is recovered from these raffinates using an advanced distillation operation that exploits their phase thermodynamics, achieving recoveries in excess of 95% (Moran et al., 2015; **Figure 3**). The resultant cleaned tailings contain residual solvent at less than 0.7 bbl/kbbl dry bitumen, representing an improvement of about 80% compared to current commercial technologies.

CVW™ technologies have been developed over a 12 year period, highlighted by an extensive commercial demonstration at CanmetENERGY's Froth Treatment Pilot Plant in Devon, AB between 2010-2013. The project, conducted with support from oil sands operators, Alberta Energy, SDTC and NRCan, was a large scale validation of fully integrated process modules. Following demonstration, CVW™ was ranked a 'priority' technology by the 2012 COSIA-sponsored Oil Sands Tailings Technology Road Map (Sobkowicz, 2012).

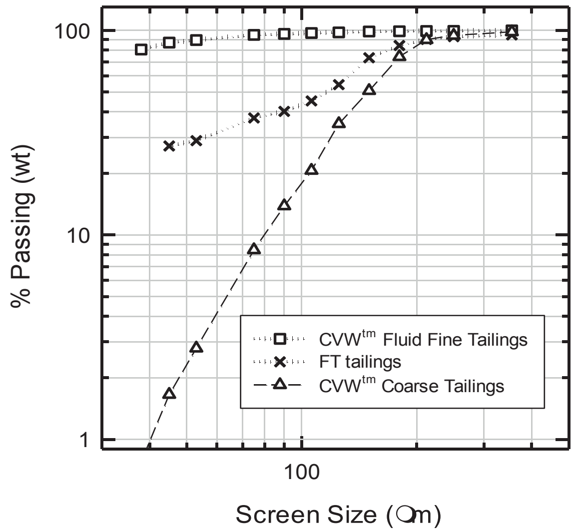

Figure 2. Particle size distributions of froth treatment tailings and CVW™ tailings

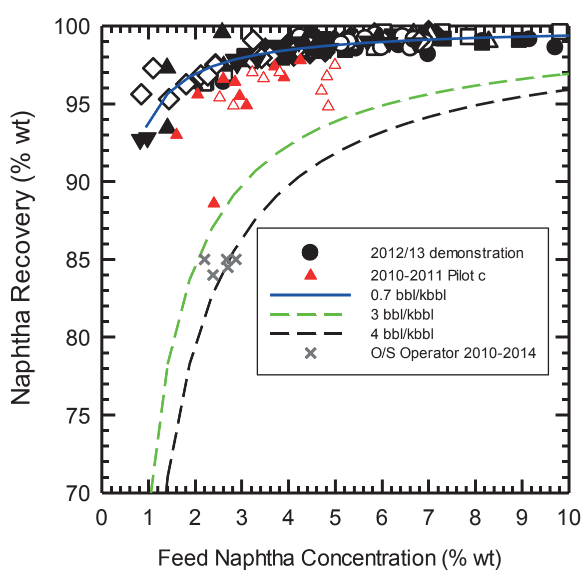

Figure 3. Solvent recovery from CVW™ tailings. (Data obtained from Titanium's demonstration pilots, 2010-13)

CVW™ technologies have been developed over a 12 year period, highlighted by an extensive commercial demonstration at CanmetENERGY's Froth Treatment Pilot Plant in Devon, AB between 2010-2013. The project, conducted with support from oil sands operators, Alberta Energy, SDTC and NRCan, was a large scale validation of fully integrated process modules. Following demonstration, CVW™ was ranked a 'priority' technology by the 2012 COSIA-sponsored Oil Sands Tailings Technology Road Map (Sobkowicz, 2012).

Thickening and Hot Water Recovery

Titanium's process tailings, including those CVW™ fine fluid tailings produced during bitumen recovery operations, are characterized, in part, by very low bitumen to solids ratio of ~0.01 - 0.03. These fluid fine tailings are hot, at about 95°C, having just been processed for naphtha recovery in Titanium's tailings distillation unit. Thickening of these tailings was conducted at CanmetENERGY as part of the Company's commercial demonstration pilots (2010-2013; **Figure 4**).

Figure 4. Thickening operation at the CanmetENERGY CVW™ pilot demonstration

Titanium's FFT, characterized by 77% - 95% fines particles, are highly amenable to both thickening and hot water recovery. The low relative hydrocarbon content of this FFT improves the efficacy of additives employed to promote flocculation. Hot water can then be collected from the thickener overflow.

The produced thickened slurry is comprised of up to 50% solids, representing a fines capture of over 99%. The thickening performance was achieved at significantly lower flocculant dosing, at 200-400 ppmw, compared to conventional fluid fine tailings. Up to 80% of the water contained in the CVW™ fluid fine tailings can be recovered at elevated temperature above 70°C. This recovered hot water, (characterized by low solids content <0.5%) is immediately fit-for-reuse as extraction process water. This heat integration opportunity creates GHG emissions reductions, of approximately 100,000 tonnes per year (per site) due to reduced natural gas consumption in bitumen production.

Thickened FFT - Ready to Reclaim Deposition

Consistent with Alberta's Tailings Management Framework and the Regulator's Directive 85, Titanium's CVW™ tailings remediation process provides "ready-to-reclaim" tailings deposition opportunities (Titanium Corporation, 2015).

Titanium's fluid fine tailings were subjected to a suite of conventional tailings management options during testing at CanmetENERGY (Mikula et al., 2010, 2011). These included technologies used to test conventional FFT, such as centrifugation, rim ditching and thin lift deposition. The CVW™ FFT responded very well (at low flocculant loading) to all tailings management options and the performance was attributed to the low hydrocarbon concentration.

The positive impacts of low bitumen concentrations on mature fine tailings consolidation reside in improved permeability/hydraulic conductivity. While the effect can be muted during sedimentation (Chow et al., 2013), it becomes significant as the solids concentrate, consolidate and develop significant shear strength, accelerating progress toward meeting reclamation standards identified by the industry's stakeholders.

There are several reasons for the improved FFT consolidation. Polymer flocculants are generally designed for ionic interactions with mineral matter; their efficacy will be reduced if the fine particles are coated with bitumen. Residual bitumen in FFT may contribute to an osmotic effect, leading to steric barriers, at advanced consolidation. Additionally, at high degrees of consolidation, colloidal interactions are negatively impacted if bitumen coatings confound the FFT.

Titanium's CVW™ FFT can produce a highly consolidated deposition, achieving solids concentrations in excess of 70% and shear strength of over 10 kPa (**Figure 5**). This performance compares well against conventional FFT, also shown in **Figure 5**, particularly in light of the low flocculant dosing utilized, about four times lower relative to conventional FFT treatments (Moran et al., 2016).

Directive 85 has some flexibility on metrics for the evaluation of tailings management performance, leaving sufficient demonstration to the operator. However, the use of depositional shear strength, cited as a key metric in Directive 74, remains the industry standard, at least with respect to thin lift deposition (Sobkowicz et al., 2014). Therefore, it remains an appropriate metric for the current evaluation, noting also that Titanium's FFT processed well across a range of conventional tailings management processes.

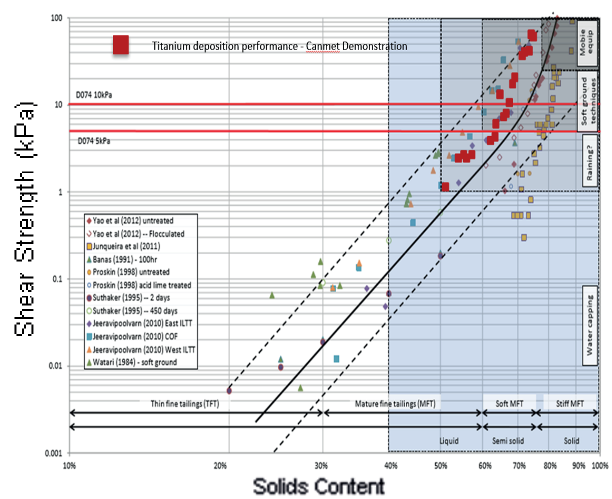

Figure 5. Performance of Titanium's FFT in thin lift processes. Adapted from Chow et al. (2013)

To better understand the performance of the CVW™ FFT towards final deposition, contextualizing in three phases - solids, fines and water - is effective in identifying the unique performance of the technology. This type of analysis was first introduced over thirty years ago by Syncrude and the University of Alberta (Scott and Cymerman, 1984), revisited a decade ago (Azam and Scott, 2005) and is now part of the COSIA lexicon (Dhadli et al., 2012). COSIA utilizes the ternary diagram to identify zones of FFT, in part using a solids-to-fines ratio (SFR), and classification of depositions. Note these tailing ternary diagrams do not reflect any hydrocarbon concentrations that may be present in the tailings.

As points of reference, select common tailings are represented on the ternary diagram (**Figure 6**). Extraction tailings (produced in the primary bitumen production operation involving water-based digestion of oil sands ore and gravity separation of a bitumen froth) are characterized by a solids content of 40-60% and fines content of 10-30%. Beached tailings (deposited onto the tailings pond beach at deposition) have high solids content with less than 10% fines. At the other end of the spectrum, Mature Fine Tailings (listed as 'Pond Tailings' in **Figure 6**; referred to as fluid fine tailings in the modern vernacular), are characterized by high fines content and about 30% solids. Mature Fine Tailings may contain over 5-10% of their mass in bitumen.

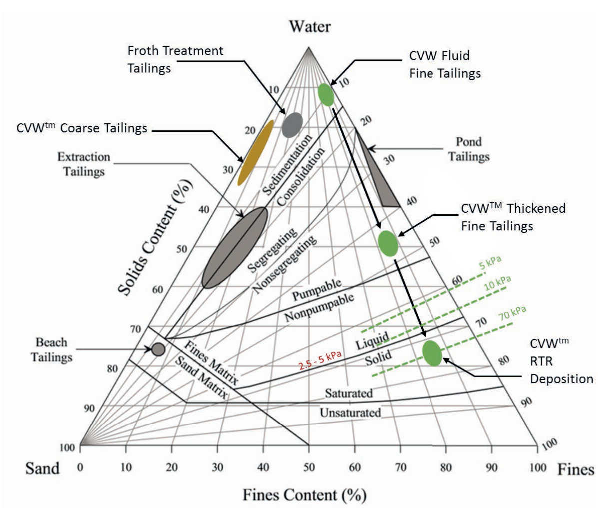

Figure 6. Ternary diagram depicting the phase and processing behaviour of tailings generated during oil sands bitumen production and CVW™ remediation of froth treatment tailings. (Adapted from Scott and Cymerman, 1984)

The 'phase' boundaries in **Figure 6**, often reflecting differences in processing behaviour, were ascertained through physical experimentation and have been generally accepted by the industry. In the fines-dominated region, where the sands-to-fines ratio (SFR) is less than one, a transition from sedimentation to consolidation is observed at a solids concentration of 15-25%. Further, the slurry thickens to a *pumpable* limit at just over 50% solids to about 62% at an SFR of one. Above 50% solids, a fines-dominant tailings slurry, characterized by a low SFR consistent with MFT, cannot be transported by pipeline, largely due to economic considerations. It is important to note that this boundary occurs at higher solids concentrations as the SFR increases.

The curve demarking a liquid/solids boundary in **Figure 6** represents a shear strength for conventional fines-dominated tailings of 2.5 - 5 kPa (Azam and Scott, 2005). This is the strength originally required by Directive 74 and now required for compliance with tailings management regulations. As with the 'pumpability' curve, the solids transition curve also occurs at higher solids concentrations with increasing SFR. Froth treatment tailings, generated during the secondary bitumen production operation (intended to clean the bitumen froth) are characterized by fines concentrations in the range of 30-40% and solids content of ~15-20%. They are characterized with a lower SFR than extraction tailings but still reside outside the 'fines-dominant' region. In Titanium Corporation's bitumen recovery process, the froth treatment tailings are first classified by particle size, forming a CVW™ fluid fine tailings stream that also contains the plurality of bitumen originally present in the froth treatment tailings. The remaining solids are processed to produce heavy minerals concentrate, resulting in coarse tailings generation; this stream (with bitumen removed) consolidates somewhat easily.

The CVW™ FFT, as indicated above, thicken readily at low flocculant dosing to form a thickened slurry at 50% solids. These tailings are very manageable for subsequent treatment as they remain within the fluid boundary and can be transported to a dedicated disposal area. The CVW™ thickened fluid tailings can then be subjected to a range of tailings management options, including thin lift deposition or centrifugation. All conventional tailings management options were tested by CanmetENERGY during Titanium's Integrated Demonstration Pilot (2010-2013; Mikula et al., 2010, 2011) and showed that solids concentrations of 75% can be achieved (c.f., **Figure 5**) at low flocculant dosing of 200-400 ppmw that achieves over 98% fines capture. Excellent depositional shear strengths were observed, reaching 5 kPa at about 60% solids, 10 kPa at 65% solids and 70 kPa at 75% solids (**Figure 6**). This performance exceeds standards set by Directive 85. In addition, the observed dewatering exceeds that of ‘conventional’ fluid fine tailings, with a 5 kPa strength at ~70% solids. The dramatic increase in deposition shear strength at lower solids contents is attributed to the low hydrocarbon concentrations in the CVW™ fluid fine tailings. CVW™ technology offers an ‘end-to-end’ solution for management of froth treatment tailings, providing “Ready to Reclaim” depositions while avoiding pond settling.

COMPLIMENTARY SUSTAINABLE BENEFITS TO CVW™ REMEDIATION

In addition to efficient dewatering of fluid fine tailings generated from froth treatment tailings, CVW™ offers a number of additional benefits to environmental performance and economic diversification. On environmental matters, the technology delivers significant air quality improvements, through GHG, VOC and Secondary Organic Aerosol (SOA) emissions reductions, and improved management of radioactives and pyrite while reducing negative impacts.

GHG, VOC and SOA Emissions Reductions

The ability of Titanium’s CVW™ technology to effectively remove (and recover) hydrocarbons from froth treatment tailings has direct tangible benefits in reducing harmful air-borne emissions. The recovery of hydrocarbons from froth treatment tailings, before they are allowed to enter a tailings impoundment, removes the substrate that is essential for the formation of methane, prevents flashing of lighter hydrocarbons into the environment and prevents the release of SOA precursors. Titanium’s CVW™ technology recovers 85% of the bitumen and over 95% of the process solvent (paraffin or naphtha) from froth treatment tailings, preventing the release of these harmful hydrocarbons into the environment.

The industry currently releases about 1.2 million barrels of process solvent into the environment from froth treatment tailings annually. With growth of the mining sector, this value could climb to 1.8 million barrels by 2030. Once released into tailings ponds, these solvents serve as a substrate for microbial fermentation to form methane. An Alberta Environment and Sustainable Resource Development model describing this methanogenesis (Burkus, 2014), modified to better reflect the nature of industrial process solvents, estimates that fugitive GHG emissions due to process naphthas in mature ponds are approximately one gram of carbon dioxide equivalents per megajoule of bitumen produced. This model correlates with recently released industry data (Alberta Environment and Parks, 2015) and University of Alberta measurements (Siddique et al., 2007). With industry growth and microbial community maturation, the fugitive release of methane from tailings ponds can reach three megatonnes annually by 2030 (**Figure 7**). Based on data from the University of California at Davis (Yeh et al., 2010), a recent Jacobs analysis (Keesom et al., 2012) estimates tailings pond emissions could reach five megatonnes by 2030.

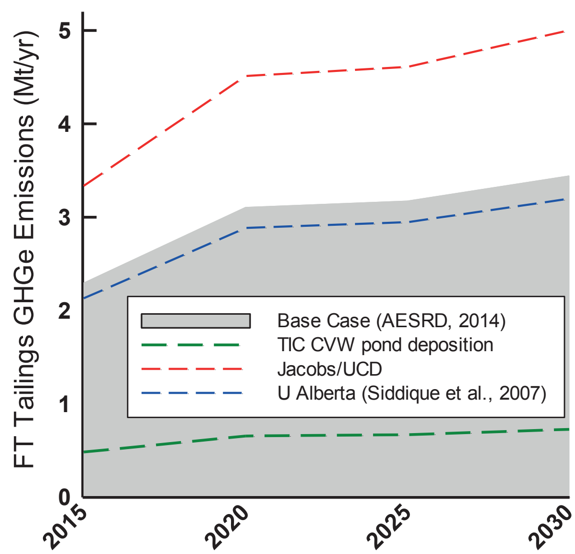

Figure 7. Estimated fugitive methane emissions from oil sands tailings ponds and impact of CVW™ technology

Titanium’s CVW™ technology would prevent up to 80% of these fugitive emissions, reducing pond-related emissions to less than one megatonne annually. Implementing CVW™ technology would make a significant contribution to Alberta’s commitment, made in the Climate Change Leadership plan, to reduce province-wide annual methane emissions by 12 megatonnes.

As froth treatment tailings are hot (~95°C) when they are placed into a tailings pond, a portion of the contained naphtha will flash off into the environment as volatile organic compounds. It is estimated that up to 20-30% of the contained naphtha may volatize, depending on the type of naphtha used. The Pembina Institute has published VOC emissions rates for oil sands producers (Dyer et al., 2008).

A value of 95 g/bbl bitumen produced has been used to estimate industry average emissions; results appear consistent with industry reporting. At current rates, the industry is emitting about 48 kt/yr; with growth, this value may reach almost 70 kt/yr by 2030 (**Figure 8**). Implementation of CVW™ technology to recover process naphthas prior to release into tailings ponds will prevent formation of VOC's, reducing site-based emissions by 30-50 kilotonnes annually.

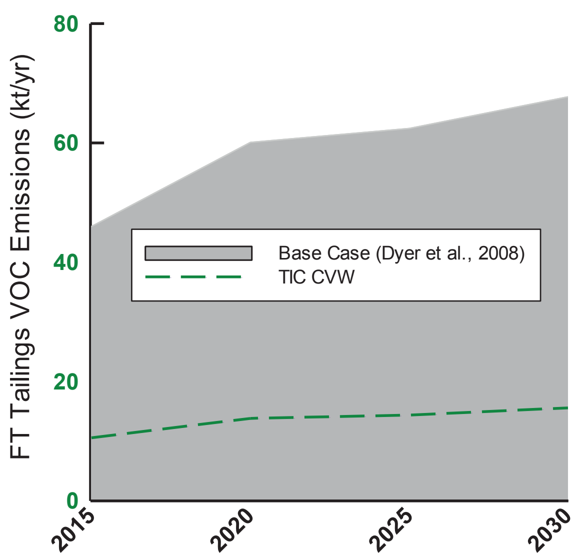

Figure 8. Estimated fugitive VOC emissions from froth treatment tailings and impact of CVW™ technology

Secondary organic aerosols (SOA) have recently been identified by Environment Canada as a health issue related to oil sands production (Liggio et al., 2016). These SOAs form from the release of intermediate- and semi-volatile hydrocarbons including bitumen sourced at the mine face and in tailings ponds. Hydrocarbons lost in froth treatment tailings, due to the elevated temperature and solvent diluted nature, may contribute disproportionately to SOA formation (Liggio, 2016). Preventing the release of hydrocarbons (CVW™) from froth treatment tailings will serve to address this emerging health concern.

Tailings Solids Management

Due to the nature of oil sands bitumen production operations, heavy minerals become concentrated in froth treatment tailings. Some of these minerals are enriched in radioactive elements, often reported as uranium and thorium isotopes. Under Canadian Naturally Occurring Radioactive Materials (NORM) guidelines (Tiefenbach et al., 2014), special management is required if radioactive concentrations of select isotopes exceed threshold values. Each isotope has a threshold value and the total radioactivity cannot exceed a 'sum of ratios' of one.

Oil sands froth treatment tailings, and the tailings beach on which they are deposited, concentrate radioactive bearing minerals. Typical froth treatment tailings, measured during Titanium's Integrated Demonstration Plant at CanmetENERGY, exceeded several individual NORM thresholds as well as the sum of ratios (**Figure 9**). In this graphic, radioactivity is measured as specific activity (Bq/g). Froth treatment tailings averaged a sum of ratios in excess of three, suggesting that specific management practices may be appropriate. In Titanium's CVW™ process, the fluid fine tailings and primary coarse tailings, comprised largely of silicas and quartz minerals, report to the 'concentrator tailings'. These represent the bulk (over 80% of the solids mass) of the produced tailings. Note that the radioactivity of these tailings is significantly reduced, with a sum of ratios reading less than one, indicating that specific NORM management is not required. The radioactivity contained in the froth treatment tailings becomes concentrated in the heavy minerals concentrate (sum of ratios over 10), an intermediate stream that bridges to the minerals production modules of the process. Within the minerals separation process, the radioactivity is concentrated into the dry tailings and product streams. The products, zircon and titanium-bearing minerals including leucoxene, are sold into global minerals markets, representing an important economic diversification opportunity for oil sands and Alberta, effectively diluting the radioactivity and associated exposure. The minerals separation tailings are less than 20% of the total tailings volume and can be managed more effectively (**Figure 10**).

In a similar vein, pyrite is also concentrated in froth treatment tailings and subsequently, into a stream of CVW™ minerals separation wet tailings. Since these tailings represent only 1% of the froth treatment tailings (**Figure 10**), pyrite can be managed cost effectively, addressing issues of acid rock drainage during active mining and reclamation.

SUMMARY

Titanium Corporation has developed a remediation technology for froth treatment tailings that significantly reduces GHG, VOC and SOA emissions by up to 80% while improving dewatering performance. CVW™ technology also provides opportunities to effectively manage both pyrite and radioactives and offers an 'end-to-end' solution for the management of froth treatment tailings that avoids deposition in tailings ponds.

CVW™ technology is well aligned with emerging leadership initiatives on tailings under Alberta's Energy Regulator's Directive 85, and will make a significant contribution to reducing climate changing GHG emissions and health harmful VOCs and SOAs. Implementation of the technology will make significant strides towards meeting methane reduction targets set in Alberta's Climate Change Leadership Plan and Canada's agreements with the United States.

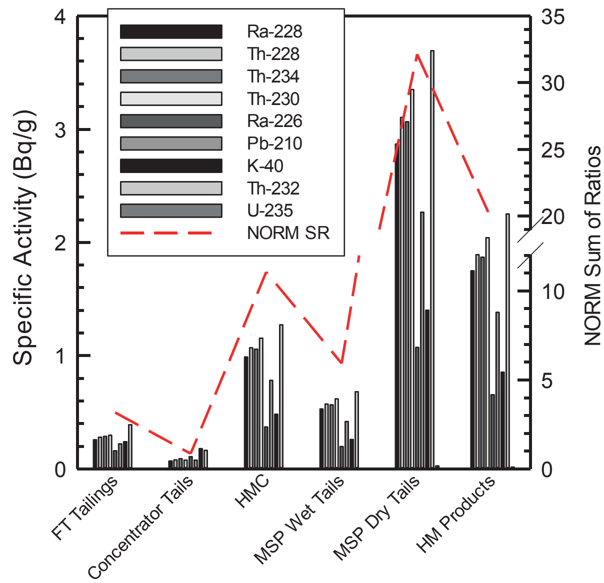

Figure 9. Specific radioactivity of isotopes within Froth treatment tailings and select CVW™ process streams

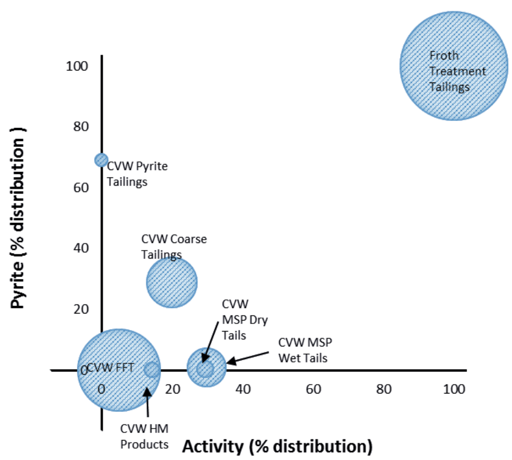

Figure 10. Relative distributions of radioactivity and pyrite in froth treatment tailings and select CVW™ tailings and products

REFERENCES

Alberta Energy Regulator (2009). "Directive 074: Tailings Performance Criteria and Requirements for Oil Sands Mining Schemes", AER, 16 pp.

Alberta Energy Regulator (2016). "Directive 085: Fluid Tailings Management for Oil Sands Mining Projects", AER, 54 pp.

Alberta Environment and Parks (2015). "Fugitive Emissions for SGER Oil Sands Facilities: 2011-2014", posted October 2, 2015, http://osip.alberta.ca/library/Dataset/Details/263, accessed September 13, 2016.

Azam, S. and J.D. Scott (2005). "Revisiting the Ternary Diagram for Tailings Characterization and Management", Geotechnical News, Dec., 43-46.

Burkus, Z., J. Wheler and S. Pletcher (2014). "GHG Emissions from Oil Sands Tailings Ponds: Overview and Modelling Based on Fermentable Substrates. Part I: Review of the Tailings Ponds Facts and Practices", Alberta Environment and Sustainable Resource Development, 24 pp.

Burkus, Z. (2014). "GHG Emissions from Oil Sands Tailings Ponds: Overview and Modelling Based on Fermentable Substrates. Part II: Modeling of GHG Emissions from Tailings Ponds Based on Fermentable Substrates", Alberta Environment and Sustainable Resource Development, 30 pp.

Canadian Association of Petroleum Producers (2016). "Crude Oil: Forecast, Markets and Transportation", CAPP, June, 42 pp.

Chow, R., G. McKenna, S.M.K Win and J. Journault (2013). "Recovery of Bitumen from Oil Sands Tailings Streams and Deposits: Potential Opportunities and Benefits", HOOS-16156-2013, Alberta Innovates Technology Futures, 75 pp.

Ciu, Z, Q. Liu, T.H. Etsell, J. Oxenford, and J. Coward (2003). "Heavy Minerals in the Athabasca Oil Sands Tailings - Potential and Recovery Processes", *Canadian Metallurgical Quarterly*, **42** (4), 383-392.

Dhadli, N., A. Fair, A. Hyndman, A. Langer, P. McEachern, S. Nadeau, A. Nickerson, F. Payne, B. Penner, B. Shaw and R. Sisson (2012). "Technical Guide for Fluid Fine Tailings Management", Oil Sands Tailings Consortium, COSIA, 131 pp.

Dyer, S., J. Moorhouse, K. Laufenberg and R. Powell (2008). "Under-Mining the Environment: The Oil Sands Report Card, Appendices 1-5", Pembina Institute, 44 pp.

Government of Alberta (2015). "Lower Athabasca Region - Tailings Management Framework for the Mineable Athabasca Oil Sands", Alberta Government, March, 58 pp.

Holowenko, F.M, M.D. MacKinnon and P.M. Fedorak (2000). "Methanogens and Sulfate-Reducing Bacteria in Oil Sands Fine Tailings Waste", *Can. J. Microbiol.*, **46**, 927-937.

Kuznetsov, P., A. Kuznetsova, J.M. Foght and T. Siddique (2015). "Oil Sands Thickened Froth Treatment Tailings Exhibit Acid Rock Drainage Potential During Evaporative Drying", Sci. Tot. Env., 505, 1-10.

Leach, A., G. Lambert, L. Coady, S. Cairns and A. Adams (2015a). "Climate Leadership: Discussion Document", Alberta Environment and Parks, 97 pp.

Leach, A., A. Adams, S. Cairns, L. Coady and G. Lambert (2015b). "Climate Leadership: Report to Minister", Alberta Environment and Parks, 57 pp.

Liggio, J. (2016). Personal communication with K. Moran, June 14, 2016.

Liggio, J., S. Li, K. Hayden, Y. Taha, C. Stroud, A. Darlington, B. Drollette, M. Gordon, P. Lee, P. Liu, A. Leithead, S.G. Moussa, D. Wang, J. O'Brien, R. L. Mittermeier, J.R. Brook, G. Lu, R.M. Staebler, Y. Han, T. Tokarek, H. Osthoff, P. Makar, J. Zhang, D. Plata and D. Gentner (2016). "Oil Sands Operations as a Large Source of Secondary Organic Aerosols", *Nature*, **534**, 91-94.

Keesom, B., J. Blieszner and S. Unnasch (2012). "EU Pathway Study: Life Cycle Assessment of Crude Oils in a European Context", Jacobs Consultancy, 80 pp.

Mikula, R., K. Dickson and J. Elias (2010). "Dewatering Treatment Options for Titanium Corporation Naphtha Froth Treatment Tailings: Final Report", CanmetENERGY, Division Report Devon, 2010-092-CF, 27 pp.

Mikula, R., K. Dickson and J. Elias (2011). "Dewatering Treatment Options for Titanium Corporation Paraffinic Froth Treatment Tailings: Final Report", CanmetENERGY, Division Report Devon, 2011-089-CF, 27 pp.

Moran, K., S. Nelson and J. Oxenford (2016). "New Oil Sands Technology to Meet the Challenges of Climate Change and Tailings Management", World Heavy Oil Congress, Paper 260, September 7-9, 14 pp.

Moran, K., J. Oxenford and S. Nelson (2015). "Reducing GHG and VOC Emissions from Froth Treatment Tailings Through the Innovative Capture of Contained Hydrocarbons", COSIA, Innovation Summit, Banff, AB, March 31-April 2.

Newell, E., S. Vaughn, M. Aubertin, J. Bergerson, I.D. Gates, M.R. Gray, J.Masliyah, G. McKenna, J. Nagendran, P. Painter, J. Peace and K. Percy (2015). "Technological Prospects for Reducing the

Environmental Footprint of Canadian Oil Sands", Canadian Council of Academies, 252 pp.

Scott, J.D. and G.J. Cymerman (1984). "Prediction of Viable Tailings Disposal Methods", Proceedings of the Symposium on Sedimentation and Consolidation Models: Prediction and Validation, San Francisco, American Society of Civil Engineers, 522-544.

Siddique, T., P.M. Fedorak, M.D. MacKinnon and J. M. Foght (2007). "Metabolism of BTEX and naphtha compounds to Methane in Oil Sands Tailings", *Environ. Sci. Technol.*, **41**, 2350-2356.

Sobkowicz, J. (2012). "Oil Sands Tailings Technology Deployment Roadmaps: Project Report - Volume 1, Project Summary", File 17-235-22, Thurber Engineering, 61 pp.

Sobkowicz, J., A. Hyndman, R. Dawson and B. Watts (2014). "Guidelines for Performance Management of Oil Sands Fluid Fine Tailings Deposits to Meet Closure Commitments", COSIA, 31 pp.

Tiefenbach, W., G. Hughes, C. Rodgerson, J. Chen, B. Theriault, C. Cuthill and R. Stacy (2014). "Canadian Guidelines for the Management of Naturally Occurring Radioactive Materials (NORM): Revised 2011", Health Canada, 70 pp.

Tipman, R., R. Healy, V. Plitt, A. Turak and R. McCosh (1996). "Minerals Developments Agreement: Co-Products Study", Final Report, Project No. Y248C, H.A. Simons, Ltd., 243 pp.

Titanium Corporation (2015). "Remediating Oil Sands Froth Treatment Tailings to Reduce Environmental Impacts and Create Economic Growth and Diversification for Alberta: Titanium Corporation's Submission to the AER Tailings Management Framework", Titanium Corp., 26 pp.

Yeh, S., S. M. Jordaan, A. R. Brandt and D. Keith (2010). Land Use Greenhouse Gas Emissions from Conventional Oil Production and Oil Sands", *Env. Sci. Tech.*, **44**(22), 8766-8772.

Session B-1

Reclamation

SHEAR STRENGTH AND DENSITY OF OIL SANDS FINE TAILINGS FOR RECLAMATION TO A BOREAL FOREST LANDSCAPE

Gord McKenna[1], Brent Mooder[1], Bill Burton[1] and Andy Jamieson[2]
BGC Engineering Inc, [1]Vancouver and [2]Calgary, Canada

ABSTRACT

The design goal for oil sands mine reclamation is widely recognized: to build reclaimed landforms that are capable of supporting a self-sustaining, locally common boreal forest. Less clear are appropriate design objectives for fine tailings deposits to economically and reliably achieve this goal in a timely manner. The climate limits open-water area to about 10% to 20% of each watershed to provide a positive water balance. The remaining 80% to 90% of each watershed must be reclaimed as terrestrial forest and peatlands with enough local relief to support the needs of vegetation.

Post-reclamation tailings deposit settlement and shear strength are key geotechnical landform design parameters. Existing tailings technologies are discussed, particularly for fine fluid tailings, and published properties are correlated to capping options and long-term settlement. Weak, low-density fine tailings deposits can be capped with water to form lakes and shallow-water wetlands. Fine tailings deposits that reach at least 70% to 80% solids prior to reclamation can be reclaimed as terrestrial landforms. Fine tailings dried to near their plastic limit (see Sharma & Bora 2003) can produce landforms constructed adopting standard geotechnical (dump construction) techniques. The large fluid fine tailings volumes and fine tailings deposit areas require tailings technologies that produce strong and dense tailings for most of the fine tailings deposits at each oil sands mine.

Selecting an appropriate suite of tailings technologies and tailings deposit designs requires reclamation design at the landscape and landform scales, collaboration amongst many disciplines, and recognition of the scale that technologies must work in oil sands mines.

INTRODUCTION

Oil sands mining in northeastern Alberta, Canada, generates large volumes of mining byproducts, particularly fine tailings. Stabilizing, capping, and reclaiming fine tailings deposits is difficult for several reasons: they have fluid-like strengths (COSIA 2012, 2014); they have low density and consolidate slowly, leading to metres to tens of metres of settlement over decades to centuries (eg Shaw et al 2010); and, as they consolidate, the tailings release oil sands process water (OSPW) which must be assimilated into and bioremediated by the reclaimed landscape (CEMA 2012, 2014).

This paper describes the shear strength and density of oil sands fine tailings required to allow reclaiming these fine tailings deposits to a boreal forest landscape. The paper addresses the following series of questions:

- What is the overall design goal for oil sands reclamation at the landform and landscape scales? How do reclamation design goals impact tailings technology selection?
- What proportions of upland forest, terrestrial wetlands, and open water are needed in a landscape to meet water quantity and quality objectives?
- What oil sands tailings types are in commercial use today? What are the densities and shear strengths at discharge and in the tailings deposits over time of these tailings types?
- What technologies are available to cap and reclaim fine tailings deposits as upland boreal forest? How strong and dense do the deposits need to be to support capping and reclamation of landforms? How much settlement can the reclaimed landscape tolerate?
- What tailings technologies are available to meet these requirements for upland tailings reclamation?

Oil sands mine operators will require a suite of tailings technologies for mines and reclaimed landscapes to be successful. Tailings technology selection is an integral aspect of oil sands reclamation, as the tailings form the majority of the substrates in the closure landscape. Landform designs and closure plans need to define tailings deposit performance criteria in terms of shear strength, density, hydraulic properties, and water quality. Tailings deposit engineers will need to deliver the required landform performance through tailings technology selection, tailings deposit design and tailings deposit landform construction. This paper provides dialog with respect to the required geotechnical properties and performance of tailings deposits and what these mean to tailings technology selection and design.

Oil sands reclamation

Oil sands mine reclamation is defined as "stabilization, contouring, maintenance, conditioning, reconstruction, and revegetation of the surface of the land to a state that permanently returns the plant [the disturbed site] to a land capability equivalent to its pre-disturbed state… so that the reclaimed soils and landforms are capable of supporting a self-sustaining, locally common boreal forest" (AENV 2007). At its heart, this is the goal of oil sands reclamation.

Approved closure plans for each oil sands operation show linked mosaics of upland, wetland, and lake ecosystems, the majority of which are underlain by various different tailings types. Reclaimed boreal forest landscapes require: mining landforms (eg individual overburden storage areas, tailings facilities, end-pit lakes (EPLs)) that are physically stable; sufficient water to support upland, wetland, and lake ecosystems; and surface water and groundwater water quality appropriate to the reclaimed land uses. Figure 1 presents examples of recent oil sands tailings reclamation projects that represent an area of 1450 hectares (14.5 km^2).

There are several geographic scales discussed in this paper: the landscape scale is approximately the same as that of a mining lease or mining operation, and is the integration of 10 to 20 landform-scale features (dumps, tailings facilities, end pit lakes (EPLs) and the adjacent lands and watersheds. Long-range mine planning and closure planning is done at the landscape scale. Detailed design for reclamation, watersheds, and tailings deposits is typically done at the landform scale.

A central element of landform design and closure planning is design for long-term settlement of tailings and its impact on flooding of upland areas, on water depth in reclaimed wetlands, and the subsequent impact on water quantity and quality.

Morgenstern (2012) describes key issues regarding the length of post-reclamation monitoring and maintenance of tailings areas. Landform and landscape designs typically are guided by a desire to limit the extent and timeframe for long-term post-reclamation maintenance to meet corporate, regulatory, and local community's expectations. There is a regulatory requirement that the reclaimed lands be certified and returned to the Crown, and a general expectation that this will occur within operational time frames. Reclamation certification is the declared goal for most operators and regulators.

Tailings technology

CTMC (2012) outlines the 50-year history of oil sands tailings research and development initiatives to improve the shear strength and density of oil sands fluid fine tailings (FFT). During this period, the oil sands operators have commercially implemented many tailings technologies – use of hydraulically placed sand for dyke construction, non-segregating tailings (NST), thickened tailings (TT), dried fluid fine tailings (dFFT), and centrifuge fluid fine tailings (cFFT). Several tailings capping technologies have also been employed at the landform scale, notably water-capped unamended fluid fine tailings (uFFT), hydraulically sand-capped NST, mechanically capped NST, and mechanically coke-capped FFT.

FFT are defined by COSIA (2014) as fines-dominated tailings with a solids content less than that corresponding to the liquid limit. Soft tailings are those that require specialized equipment and techniques for trafficking with mine equipment (Jakubick et al 2003). Soft tailings may be fluid or solid. NST is a type of soft tailings but not fine tailings (because it is mostly sand) whereas dFFT is a type of fine tailings but not soft tailings (because it is usually trafficable to dozers). Building upon a typical soil consistency classification (see Terzaghi and Peck 1967): firm tailings have a peak undrained (vane) shear strength between 25 and 50 kPa and stiff tailings have a shear strength of 50 to 100 kPa. "Firm to stiff" tailings in this paper have a peak undrained vane shear strength of more than 25 kPa.

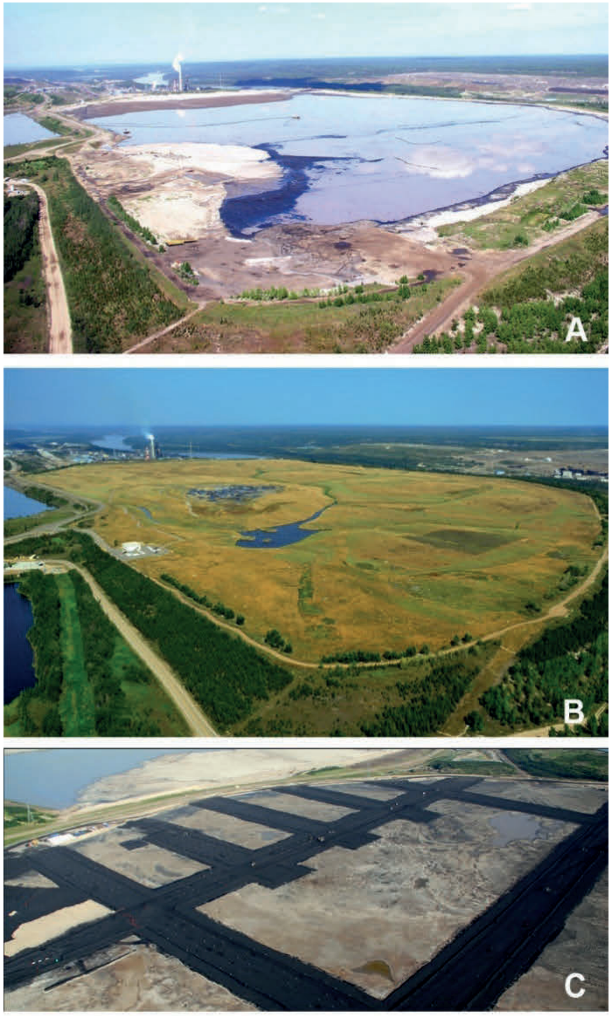

Figure 1. Recent oil sands tailings reclamation
A: Suncor Pond 1 during operations (www.suncor.com)
B: Suncor Pond 1 after reclamation (now Wapisiw Lookout)
C: Suncor Pond 5 FFT coke capping in progress
D: Syncrude West InPit water capped FFT (now Base Mine Lake)
E: Syncrude East InPit CT (now Sandhill Fen)

Fines content is defined the mass of fines (<44-micron diameter on the wet sieve) to the total mass of mineral solids. The solids content is the ratio of the mass of mineral solids to the mass of slurry (which includes water, bitumen, and mineral solids). If the tailings are saturated, the density can be calculated from the solids content if the specific gravity is known. Solids content is used in this paper as most of the tailings literature focusses on this measure. For geotechnical engineers focused on tailings deposit design and landform design, the bulk density and dry density of the tailings will be important measures.

Tailings areas and volumes today

Tailings form much of the oil sands mining landscapes. At the end of 2014, the total active footprint of oil sands (mining / tailings / plantsites) was 904 km^2 including 192 km^2 of tailings ponds (AENV 2016). About 87 km^2 of disturbed land has been reclaimed (see Figure 1), and 1 km^2 has received a reclamation certificate from Alberta Environment (AENV 2008).

Currently there are more than 30 tailings facilities in the oil sands region; 88 km^2 are covered by OSPW (AEP 2014), much of this area is underlain by FFT. AENV (2016) reports FFT inventories of 976 million cubic metres as of end of 2013. In response to the growing volumes and areas, the Tailings Management Framework (Alberta Government 2015) and Directive 085 (AER 2016) are crafted to limit, then reduce, the volume and extent of FFT.

Previous work

There are hundreds of papers and theses on oil sands tailings and perhaps as many more on related reclamation and environmental topics. Three technology reviews are highlighted – *Advances in Oil Sands Tailings Resear*ch (FTFC 1995), *Oil Sands Tailings Technology Deployment Roadmap* (CTMC 2012) and the OSRIN *Review of Reclamation Options for Oil Sands Tailings Substrates* (BGC 2010).

On a broader basis, the Royal Society of Canada's *Environmental and Health Impacts of Canada's Oil Sands Industry* report (RSC 2010) and the Council of Canadian Academies' *Technological Prospects for Reducing the Environmental Footprint of Canadian Oil Sands* (CCA 2015) are recommended. Devito, Mendoza, & Qualizza's (2012) *Conceptualizing water movement in the boreal plains: implication for watershed reconstruction* provides an excellent, up-to-date resource regarding landscape- and regional-scale hydrology for the Western boreal forest.

There have been several papers and reports linking tailings technology selection, tailings management, and reclamation goals (eg Sobkowicz and Morgenstern 2009; Hyndman and Sobkowicz 2010; Morgenstern 2012; McPhail 2006; Sobkowicz et al 2014).

As noted above, the Alberta Government (2015) released the *Tailings Management Framework for the Mineable Athabasca Oil Sands* (TMF) and the associated Directive 085 (AER 2016) to help "reclaim the areas where oil sands were developed to equivalent land capability and return them to the Crown after development." Regarding tailings technology selection, the TMF requires operators to consider the TMF outcomes, "including the promotion of a stable landscape that comprises a diverse, locally common and self-sustaining ecosystem after reclamation."

SOME NEEDS FOR BOREAL FOREST LANDSCAPES

The landscapes that are designed to be reclaimed to boreal forest need to provide, among other things, a sustainable water balance, acceptable water quality, and physical stability. It is recognized that creating self-sustain boreal forest requires the work of a multidisciplinary team (McKenna 2002). This paper focusses on the tailings and geotechnical components of constructing a deposit and surface for soil and vegetation placement.

Water balance

The oil sands region is characterized by a sub-arctic / boreal climate and thick deposits of porous glacial materials overlying bedrock (Devito et al 2012). Precipitation is variable, ranging from 242 to 646 mm/year at the Fort McMurray airport, with an average of 437 mm/year (CEMA 2012). Water yields (from surface water, interflow, and groundwater) to local rivers at the landscape-scale range from 102 to 158 mm/year, with an average of 137 mm/year (CEMA 2012, 2013). The potential evaporation (PE) of 598 mm/year exceeds precipitation (P) most years (Devito et al 2012; CEMA 2012).

Upland areas typically yield limited water, especially during the growing season, due to the efficiency of boreal forest vegetation in consuming available moisture by evapotranspiration (Devito et al 2012). Natural bogs and fens (terrestrial wetlands) are net sources of water because of extended frozen ground conditions and less efficient evapotranspiration, compared to either uplands or open water. Their actual evapotranspiration (AET) is much less than PE, and somewhat less than precipitation. Because open-water evaporation (which is close to PE) exceeds precipitation in most years, open water (beaver ponds and marshes, shallow-water wetlands, and lakes) is a net water sink in the landscape. Quantification of the water balance around reclaimed wetlands in the oil sands is the subject of ongoing instrumented-watershed research (eg Pollard et al 2012).

On average in the oil sands region, open-water bodies lose 161 mm/year to evaporation, but with variable climate, the net change can range from a loss of 356 mm in a drought year to a gain of 48 mm in a wet year. The combination of thick, porous deposits and variable climate results in large annual and decadal fluctuations in the amount of open water, particularly in areas of subdued relief (Devito et al 2012). Complicating matters is that the water balance varies seasonally, decadally, and multi-decadally as a function of the climate.

Wetlands and lakes (Figure 2) require sufficiently large contributing watershed areas to limit water level fluctuations during drought. As the area of open water in the reclaimed landscape increases, there is more evaporation and hence less flushing of wetlands and EPLs; salts can accumulate, affecting water quality. In addition, losses to

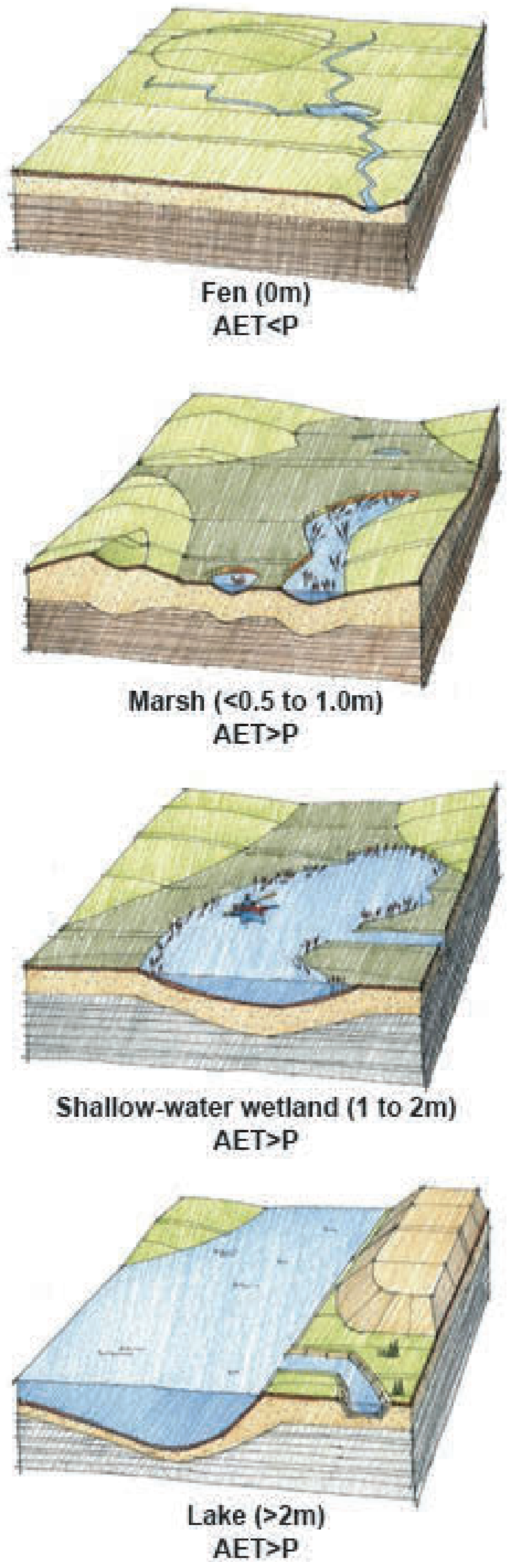

Figure 2. Four types of reclaimed wetlands, based on water depth (adapted from CEMA 2014)

evaporation reduce inflows and outflows for wetlands and EPLs, impacting their ecological functions. Numerical water-balance models are used for closure planning and watershed design (eg Golder 2003); from these calibrated models, a useful guideline is to design watersheds for wetlands and EPLs so that there is less than about 10% to 20% open water. As diagramed in Figure 3, water-capped tailings, such as may be part of EPLs, and soft tailings deposits that will eventually settle to form marshes, shallow-water wetlands, and lakes, all need to fit within the open-water limitation at the landscape scale (CEMA 2012, 2014).

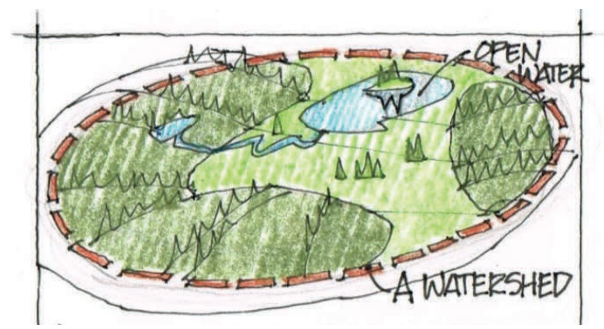

Figure 3. Reclaimed landscapes should be limited to less than about 10% to 20% of open water

Water quality

Boreal forest ecosystems require sufficiently fresh water to support plant growth for uplands and wetlands, and for aquatic life in lakes and streams (CEMA 2012). Landforms and landscapes are designed to meet target water quality in each wetland and EPL.

Tailings porewaters are comprised of OSPW. Undiluted OSPW in the root zone can negatively affect some terrestrial plants due to elevated concentrations of dissolved solids (salts) and some freshwater aquatic life due to the combination of inorganic and organic compounds (see NRC & CanmetEnergy 2010).

The reclaimed watersheds for each wetland and EPL are designed to provide sufficient water quality and quantity to allow the reclaimed ecosystems to perform as intended. Some reclaimed wetlands and EPLs will receive significant quantities of runoff from natural watersheds; others only have runoff and seepage from reclaimed areas. Tapping into natural runoff can allow larger open-water areas in the reclaimed landscape. Each watershed is unique. Each reclaimed watershed needs its own design, water balance, and water quality prediction.

Evaporation leads to reduced water quantity and quality in the reclaimed landscape. Closed basins with small contributing watersheds, such as a tailings deposit subject to large settlements, would lead to evapoconcentration and surface water that could be more concentrated than the tailings porewater. Keeping watersheds to less than 10% to 20% open water limits evapoconcentration and promotes flushing. Flushing also helps to reduce the impacts of salty seepage into wetlands and EPLs.

Reclaimed areas that are topographically low usually form wetlands. Some wetlands are designed and others form opportunistically (CEMA 2014). Differential post-reclamation settlement of the landscape causes wetlands to form in upland areas, and expands and deepens water in existing wetland areas. Wetland ecological function is mainly driven by water depth. Predicting post-reclamation water depth is further complicated by beaver activity – their dams can form ponds up to 3 m deep. Hundreds of beaver dams can be expected in each reclaimed landscape (Eaton et al 2013) further affecting the water balance.

Physical stability

Tailings deposits will generally require local topographic relief to support vegetation and ecosystem functions and to contain the lateral extents of wetlands (eg Pollard et al 2012). This topography may be built through excavation of deep channels (eg Russell et al 2010) or by constructing hummocks on the tailings beaches with sand or mine waste (McKenna 2002). These 3 to 6m high ridges, typically with slopes of 3H:1V to 8H:1V, must be supported by the underlying tailings. Figure 4 provides an example using a limit-equilibrium analysis that indicates shear strengths of about 25 kPa (firm tailings) are needed to support this relief. Overall conclusions remain similar whether the tailings shear strengths are specified using s_u/p' instead of a uniform undrained shear strength, or whether the tailings are somewhat thinner or thicker. However, the analysis is quite sensitive to the slope angle and hummock height. (Analysis using simple Taylor (1937) stability coefficients provide useful insights). Deformation analyses are also used in design when they can be calibrated to actual field conditions.

A major oil sands mine-reclamation objective is to be able to delicense oil sands tailings dams (OSTDC 2014). There can be little to no residual risk of a catastrophic failure after delicensing. The tailings and the landform must be designed to avoid ponding water within a critical distance of the dyke crest and to avoid having potentially mobile tailings near the dyke that could lead to a catastrophic outflow in case of dyke instability. Thus, a design criteria for tailings in this situation would be to have tailings near its terminal density at the time of delicensing to avoid excessive settlement and water ponding in uncontrolled areas. The landform needs to be designed to keep water out of the critical zone near the crest, and tailings need to have non-fluid strengths to avoid outflow (or the design needs to demonstrate the absence of a trigger of liquefaction or strain weakening). The location of ponded water on the tailings landform is typically controlled using local relief (eg Russell et al 2010).

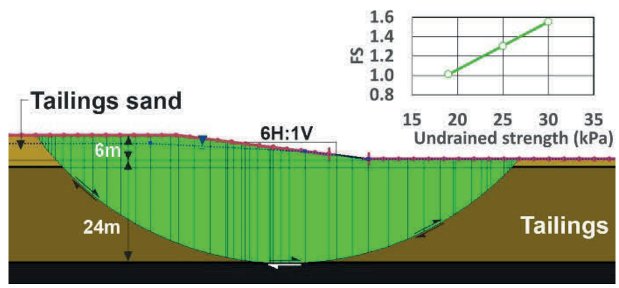

Figure 4. Limit-equilibrium slope stability analysis for hummocks on soft tailings

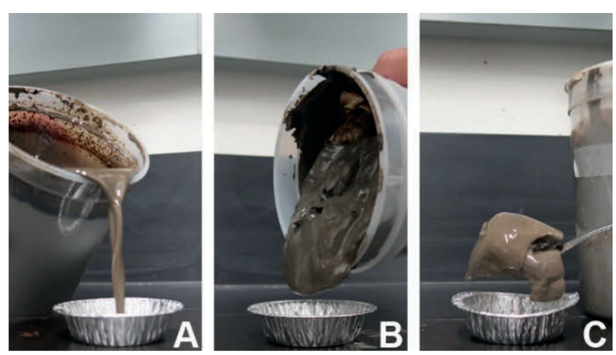

Figure 5. Three oil sands FFT in the lab.
A: Unamended FFT (uFFT)
B: Centrifuged FFT (cFFT)
C: Thickened tailings (TT) + fly ash

OIL SANDS TAILINGS PROPERTIES

Figure 5 shows three FFTs in the laboratory. Table 1 provides a summary of tailings types. Typical ranges of shear strengths and densities of commercial scale field deposits are indicated. For conventional tailings sand deposition, typically about 70% to 80% of the fines mined are captured in beaches and sand dykes, while the remainder segregate to form FFT (AMEC 2013). Tailings produced from FFT (uFFT, cFFT, TT, dFFT) are the focus of this paper.

Figure 6 shows the typical range of oil sands tailings shear strengths as a function of solids content. The graph is based on publicly available data, most of which is based on the laboratory vane shear strength. Suncor (2016) presents a similar plot of shear strength versus clay to water ratio for treated FFT that plots within the shear strength envelop shown in Figure 6 if typical FFT clay contents are assumed.

Peak undrained shear strengths and densities are highly correlated, but for any given density, there can be plus or minus one order of magnitude scatter to the shear strength data as shown in Figure 6. Low density tailings treated with additives, such as coagulants, flocculants, and cements, will have considerably higher shear strengths than untreated tailings. The relationship between the shear strength and density is largely explained by liquidity index. The relationship between density and shear strength for natural sensitive clays for a range of liquidity index values provided by Houston and Mitchell (1969) shows a similar pattern to published values for tailings and is plotted on Figure 6 (using a typical fine tailings liquid limit of 60% (based on geotechnical moisture content) and a plastic limit of 25).

The large scatter in Figure 6 and the general variability in tailings deposits indicates the need for site specific investigation and design (eg McKenna and Cullen 2008) for each tailings deposit including compilation of the history of deposition, LiDAR topographic surveys, deposit sampling, insitu cone penetration tests, laboratory tests, use of piezometers and wells. These programs are complicated by the need to characterize the deposit before, during, and after capping as the design and construction evolve together (eg Russell et al 2010). Understanding consolidation and the related settlements, water release, deformations, and changes in shear strength are fundamental to the design. The division between how much design is done up front versus field fitting to actual conditions during construction will differ with each deposit and each operator. The geotechnical work forms the fundamental basis for the rest of the landform design, which will be further affected by groundwater, surface water, soils, vegetation, and wildlife aspects of reclamation (CEMA 2005). The present challenge is conducting enough initial design work at the closure-planning level to be able to provide useful guidance to tailings technology selection and design of new tailings processes with long lead times, high capital and long service lives (CTMC 2012).

The large scatter in Figure 6 and the general variability in tailings deposits indicates the need for site specific investigation and design (eg McKenna and Cullen 2008) for each tailings deposit including compilation of the history of deposition, LiDAR topographic surveys, deposit sampling, insitu cone penetration tests, laboratory tests, use of piezometers and wells. These programs are complicated by the need to characterize the deposit before, during, and after capping as the design and construction evolve together (eg Russell et al 2010). Understanding consolidation and the related settlements, water release, deformations, and changes in shear strength are fundamental to the design. The division between how much design is done up front versus field fitting to actual conditions during construction will differ with each deposit and each operator. The geotechnical work forms the fundamental basis for the rest of the landform design, which will be further affected by groundwater, surface water, soils, vegetation, and wildlife aspects of reclamation (CEMA 2005). The present challenge is conducting enough initial design work at the closure-planning level to be able to provide useful guidance to tailings technology selection and design of new tailings processes with long lead times, high capital and long service lives (CTMC 2012).

The implication of sensitive behaviour is that once straining occurs and the tailings is sheared past its peak shear strength, the subsequent shear strength reduction may mean that deformations may accelerate, rather than stabilize after initial straining and redistribution of stress. The consideration of sensitivity for construction of caps on tailings surfaces is discussed below.

Table 1. Summary and typical properties of common oil sands tailings types

Name	Description	Typical properties
Unamended FFT (uFFT)	Settled fines segregated from whole tailings	30-40% solids content >80% fines content Fluid consistency.
Centrifuge FFT (cFFT)	Flocculated / coagulated FFT that has been centrifuged	45-60% solids >80% fines Fluid to very soft consistency.
Thickened Tailings (TT)	Flocculated (and may be also coagulated) FFT from a thickener or in-line treatment	35-50% solids 50-80% fines Fluid to very soft consistency.
Dried FFT (dFFT)	Flocculated FFT deposited in thin lifts for drying	60-85% solids >80% fines Very soft to firm consistency.
Non-Segregating Tailings (NST)	Mixture of cycloned sand, FFT, amended to form non-segregating slurry	75-84% solids 20% fines Very soft to soft.
Beach below FFT tailings (BB-FFT)	A mixture of sand tailings and FFT that forms in conventional tailings ponds	Highly variable <10% to 80% fines. Soft to firm consistency.
Froth treatment tailings (FTT)	Naphtha or paraffinic froth tailings	Highly variable. Fluid to firm consistency.
Tailings sand (TS)	Fine quartz sand that segregates during tailings deposition	>80% solids 5-10% fines. Forms beaches and caps.
Reference: CTMC (2012). See CCA (2015) for discussion of froth tailings		

Building on Terzaghi and Peck (1967), a simple soil classification based on consistency is plotted on Figure 6. In traditional civil engineering, very soft soils are avoided or removed from most projects. Most civil engineering projects require at least firm to stiff soils to provide adequate bearing capacity and limit settlement. Natural soft soils are managed with soil improvement (eg USDOT 2000), piling, bridging-over techniques (especially in case of roads and other linear infrastructure), or avoidance (Almeida & Marques 2013).

CAPPING OIL SANDS SOFT TAILINGS

Figure 8 plots the applicability of capping technology, based on shear strength and density. The zones are based on slope stability analysis and empirical evidence from laboratory and field studies. Details are discussed below. There are a number of caveats related to this figure:

- the zones for estimating applicability are presented for discussion and are necessarily judgement based as the published literature on capping of tailings is limited.
- the ranges of applicability of the techniques overlap but are shown as specific zones for discussion purposes. The actual boundary will vary with materials and techniques. Further analysis and field experience will allow refinement of the boundaries and methods.
- Site specific characterization and field trials are required before capping technology can be selected.

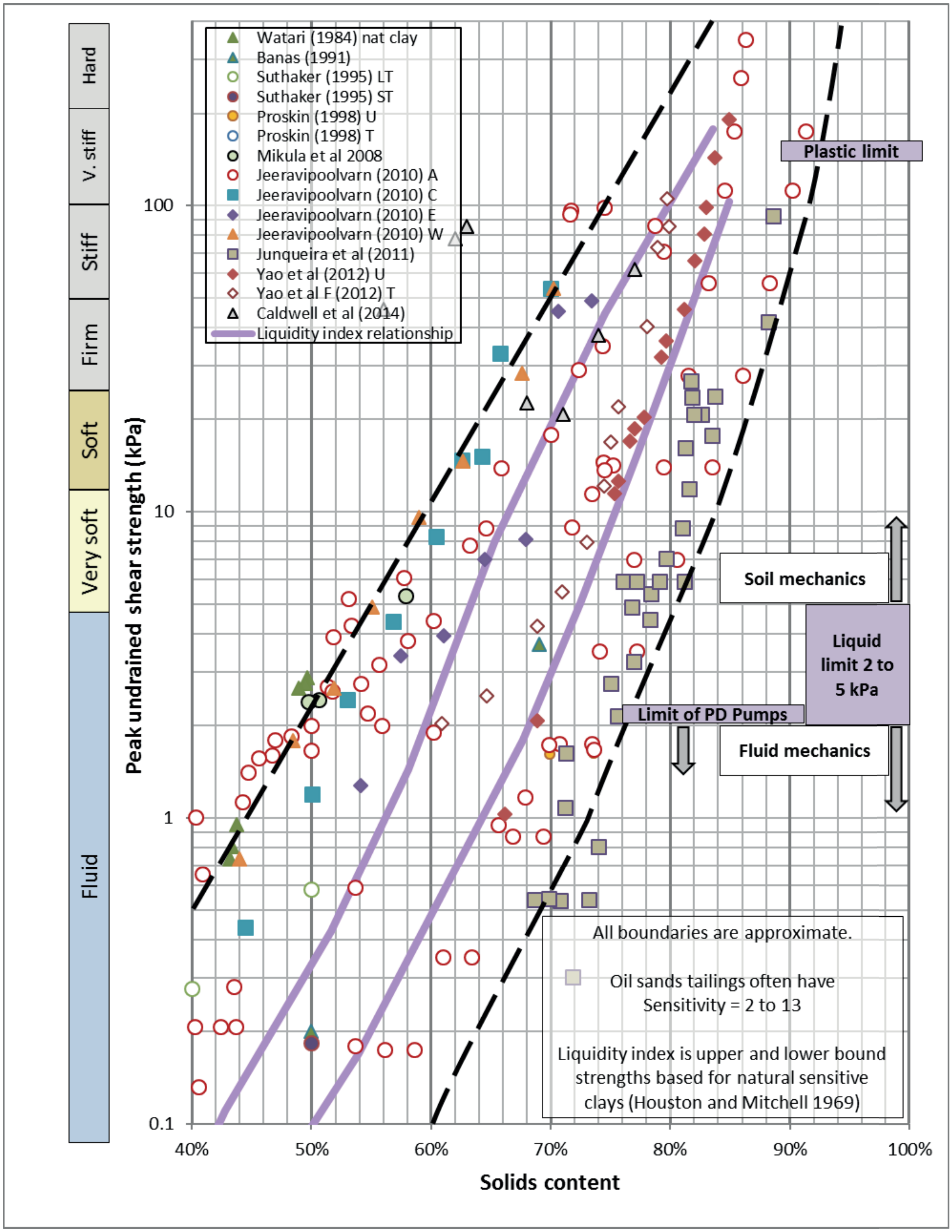

Figure 6. Shear strength and solids content of oil sands fine tailings (laboratory and field shear strength measurements, mostly by vane)

The capping methods shown in Figure 8 are useful at a planning level, but for tailings technology selection, tailings planning, geotechnical and landform design, there is a need to design against several failure modes. There are many ways a soft tailings cap may fail, particularly if the fine tailings show fluid-like properties:

- The cap fails to deposit onto the top of the tailings – it may:
    - report to the bottom of the deposit
    - partially displace tailings (creates a growth fault)
    - interlayer / interfinger with the FFT
    - incorporate fines into cap (erosion of mudline)
    - penetrate vertically into FFT.
- Cap is incapable of supporting placement equipment
    - equipment becomes mired due to penetration into underlying tailings
- FFT (or bitumen) blister up to surface
- Tailings cannot support leading edge of mechanically placed cap
- Tailings cannot support intended topography / local relief
- Capping triggers upstream liquefaction or lateral spreads (eg Varnes 1978)
- Cap itself is not trafficable
    - especially due to saturated tailings sand liquefaction
- Cap does not provide sufficient bearing capacity for post-mining land uses
- Excessive settlement causes flooding and unintended change in land use values
- Excessive settlement causes upset to water balance
    - salinized closed basins as an end-member.

In many cases, settlement considerations will govern design. As noted elsewhere in the paper, the high solids contents required to control settlement will, in many situations, provide adequate shear strengths for capping and construction of local relief.

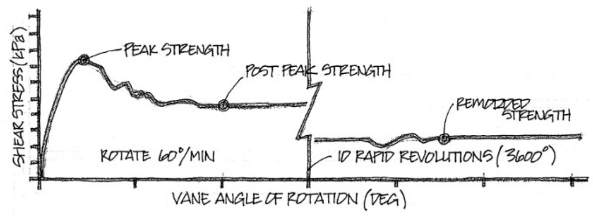

Figure 7. Illustrative representation of peak, post-peak, and remolded shear strength behaviour of oil sands fine tailings. Sensitivity is the ratio of peak to remolded shear strengths, often 2 to 13 for oil sands fine tailings

Floating water cap

The geotechnical requirement for tailings properties to support a floating cap are minimal. The lake and the water / tailings interface (mudline) must be designed to limit resuspension of low-density tailings into the water column.

Water-capped FFT has been piloted at several locations. Syncrude's Base Mine Lake (Syncrude 2015) is the first full-scale prototype of this technology (Figure 1D). The Oil Sands End Pit Lakes Guidance Document (CEMA 2012) provides additional detail for design, construction, and operation of EPLs using this technology.

Floating coke cap

A floating petroleum-coke cap is a design option available where the wet density of the coke is less than that of the underlying tailings. Coke is a byproduct of bitumen cracking, which is done at several oil sands operations. It is a low-density granular silt or sandy gravel comprised almost entirely of carbon.

Suncor has capped FFT using strong geofabric and mechanically placed coke at its Pond 5 (see Figure 1C and Abusaid et al 2011). Syncrude has a patent that includes placing coke over its cFFT (Lorentz et al 2012). For an EPL, a layer of coke deposited on the mudline may be used to separate tailings from the water cap (CEMA 2012).

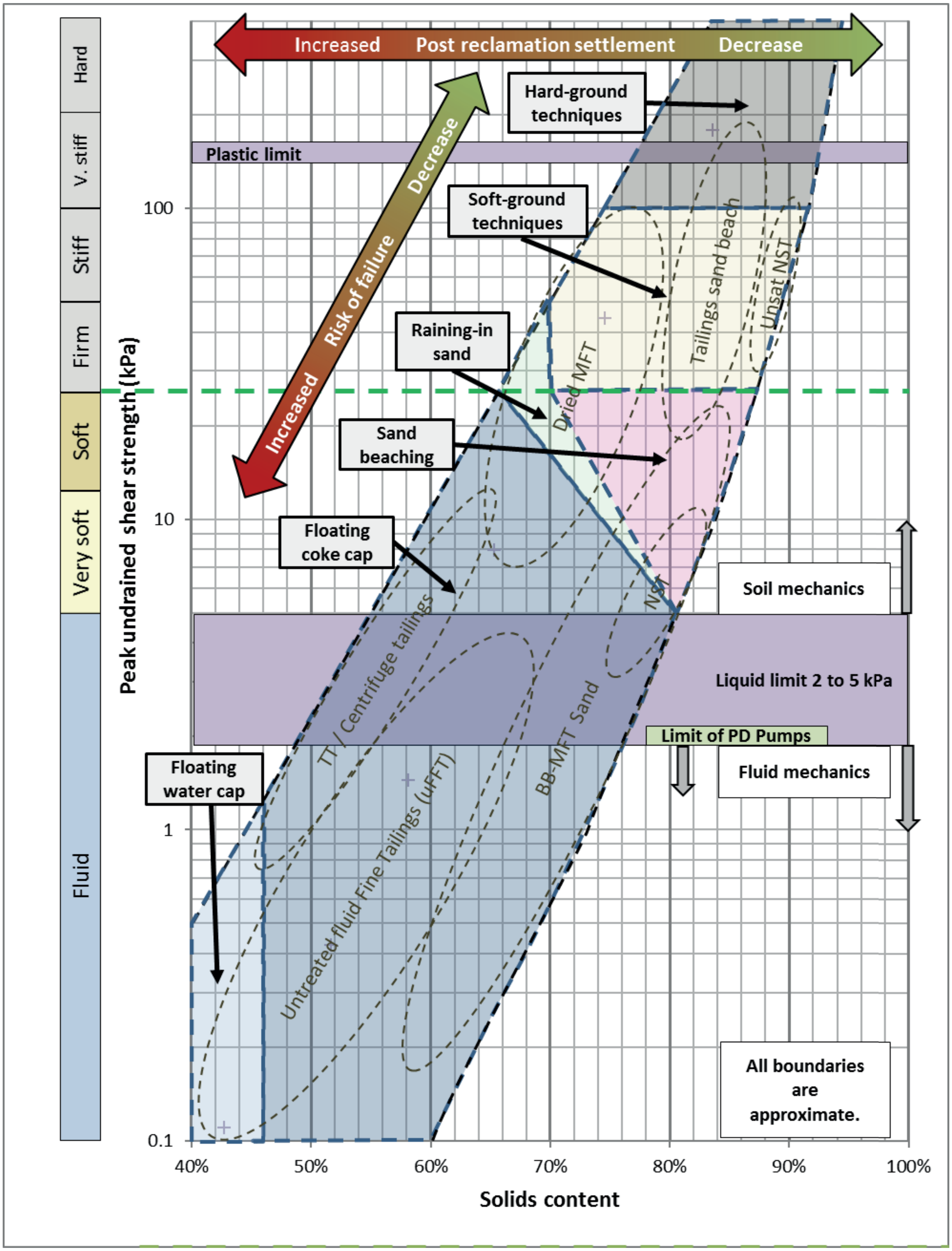

Figure 8. Applicability of capping technologies for approximate ranges of oil sands fine tailings shear strength and solids contents

Raining sand

Raining sand has not been attempted at commercial scale in oil sands but is a common technique to cap weak harbour and river sediments elsewhere. Raining sand involves gently depositing sands through a water column, to settle onto the material being capped, in even lifts that are typically just a few centimetres thick (eg Costello et al 2010). Raining sand generally relies on shear strength gains due to consolidation in the time between placement of each lifts. The very slow consolidation rates for oil sands tailings means there is no significant density or shear strength gain between lift placement. Therefore, this technology requires that the density of the underlying material is similar or greater than the cap (such that the rained in sand becomes a floating cap), or sufficient tailings shear strength is present to support the higher density sand layer. For a non-floating sand cap, a lower boundary tailings shear strength boundary of approximately 25 kPa has been selected (Figure 8) to limit the risk of widespread inversion (mixing of sand layers into the fine tailings). A separation layer (such as coke or geofabric) may be required at intermediate densities to limit penetration and mixing. Additional analysis and testing and a large-scale field trial would be needed to refine this estimated boundary of the minimum shear strength and density combination.

Sand beaching

Sand beaching (hydraulic placement) to form a cap on NST (Figure 1E) or firm to stiff tailings can be operationally complex, especially as the sand beach tends to form a shallower or steeper profile (slope angle) than that of the underlying tailings. The lower bound tailings properties for this technology shown in Figure 8 corresponds to where the density of the tailings is similar to that of the settled sand cap (80% solids), and at the correspondingly small undrained shear strength of 5 kPa. The energy of the rapidly flowing tailings is likely to cause some displacement and mixing, perhaps decreasing away from the discharge point. A point at 70% solids (with a corresponding peak shear strength of 25 kPa) is estimated as the other end of the lower bound curve where the somewhat lower density is perhaps offset by the higher shear strengths. The actual boundary will vary with materials and techniques and the mechanics are complex and difficult to observe. Some mixing of the materials should be accommodated in design. If the FFT solids content is too low, the tailings sand typically flows under the lower density tailings, with some mixing (eg Amec 2013). This submergence and mixing of sand slurry is a common technique used displacement method to push FFT to a dredge for removal.

Soft-ground techniques

Soft-ground techniques are the most common method of soft tailings capping for metal mines (typically over a few dozen hectares) and involve use of small trucks (5T to 40T) and small dozers (from a snow grooming vehicle to LGP Caterpillar D3s) (Jakubick et al 2003). Often geogrid and geofabric are employed (Figure 9).

The lower boundary for widespread use of this technology in Figure 8 is chosen as 25 kPa (with some consideration to sensitivity) and a density greater than 70% solids. The limitations are based on safety of the small dozers running on very thin caps and on the leading edge embankment stability. Larger shear strengths allow decreased risk, larger equipment, and greater efficiency and hence reduced costs.

Figure 9. An example of soft-ground capping technique at WISMUT uranium mine tailings, Germany

Safe placement of the cap is a critical design objective. To run equipment directly on tailings, it must be strong enough to support the bearing capacity of the track or wheel. This is akin to trafficability. More commonly, a granular layer is used for traffic, sometimes with geogrid reinforcement. In this case, the track or wheel load is “spread” and the underlying tailings need not be as strong. Several of the oil sand operators use trafficability testing procedures to prove up soft ground safely.

“Trafficable” is a colloquial term that implies being able to safely take mining equipment out onto the deposit to do what needs to be done, which is mostly related to capping during operations, and includes safety of people and equipment for post-mining land uses. The equipment size may range from a small dozer to a 100T haul truck. A surface is considered to be trafficable if equipment is unlikely to become mired and that any mired equipment can be retrieved safely without harming the operator or response crew.

Bearing pressures for mining equipment have considerable range (Caterpillar 2015):

- Small dozers: 30 to 60 kPa (actual bearing pressures vary considerable from machine to machine).
- Small haul trucks (<40 T): about 300 kPa.
- Large haul trucks (100 T): about 700 kPa.

Estimates of the ultimate bearing capacity (q_{ult}) of tailings can be made using the Terzaghi bearing capacity equation where

$$q_{ult} = s_i\, c_u N_c = (1\ to\ 1.3)\, c_u\, 5.14\ \approx 5 \text{ to } 7 \cdot c_u$$

$$q_{allowable} = \frac{q_{ult}}{FS}$$

Where:

- s_i is the shape factor, 1 for dozer tracks, 1.3 for haul truck tires
- c_u is the operational shear strength of the tailings
- N_c is the bearing capacity factor = 2 + π = 5.14 for undrained behaviour.

To account for progressive failure due to the sensitivity of the tailings, several options are available: a correction factor based on laboratory test results can be applied to the ultimate bearing capacity (Kalteziotis et al 1984); the operational shear strength can be determined using test fills or trafficability tests; or a high factor of safety (beyond the traditional FS≥3) can be employed.

Any surficial layer (the cap or a crust) must be sufficiently strong and thick to avoid traffic punching into the weaker layer below. Generalizing and using this allowable bearing capacity formulation and a FS=4, a peak undrained shear strength of the tailings of at least 30 to 50 kPa is needed for small dozers (Cat D5 and smaller), at least 100 to 200 kPa for small haul trucks (40T or smaller) and at least 300 to 400 kPa for large haul trucks (100T) operating directly on the tailings. (Truck traffic on tailings is in the realm of standard earthwork techniques discussed below). Each situation needs to be evaluated; formal test embankments or trafficability testing is typically used to confirm field conditions. Typically, equipment will be used on a cap rather than operating directly on tailings. Geogrid is often employed at the interface.

An alternative approach for embankment loading of soft tailings, is to use deformation analysis, calibrated to laboratory and field data (eg Abusaid et al 2011).

Standard earthworks techniques

Typical earth moving equipment can be employed when tailings consistency reach the “very stiff” classification (Figure 10) based on bearing capacity and slope stability calculations and field experience with non-tailings materials in the region.

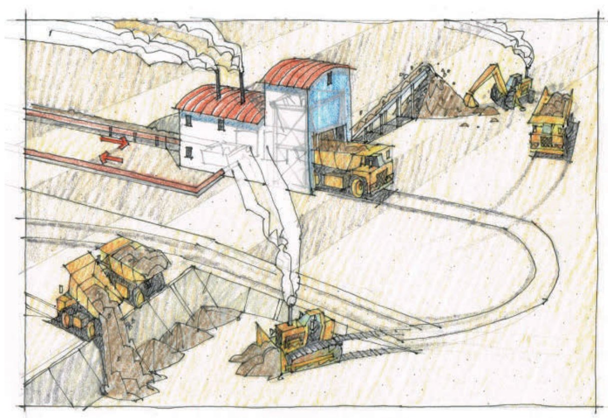

Figure 10. Firm to stiff tailings would allow standard earthworks construction techniques

With additional techniques, it may be practical to lower the shear strength criteria to 50kPa (“stiff”). The oil sands industry has abundant experience building dumps and dykes with various overburden fills (glacial materials and Clearwater Formation clayshales) and lean oil sands using large mining equipment. The industry has developed efficient and reliable techniques for managing the effects of climate and weather, especially methods of dump landform construction involving padding/plating over softer areas using 2 m to 5 m lifts. Some of the largest trucks need very stiff materials for good trafficability. Cameron et al (1995) provide a suite of five papers that describe oil sands earthworks using very large haul trucks. Tailings with solids contents above the liquid limit will have high shear strengths (Figure 8) but like the clayshales, will lose shear strength upon wetting. Placement with large equipment will require care.

SETTLEMENT OF OIL SANDS TAILINGS

Oil sands fine tailings settle due to both self-weight consolidation and consolidation due to the surcharge weight of the capping material (eg Pollock 1998). Practitioners continue to debate the details of the consolidation mechanics; for practical purposes, settlement is typically modelled as a large-strain consolidation phenomenon using effective stresses. Tailings deposit settlement occurs primarily through the upward vertical release of porewater as the tailings surface slowly decreases in elevation.

Each tailings type (see Table 2) typically has a different initial density, compressibility function, and hydraulic conductivity function. The rate of deposition, underdrainage, and the placement of a cap are inputs into the consolidation model. Given enough time, the tailings densify to form a normally consolidated deposit. At the base of the deposit, where effective stresses are high, the material will have a high solids content and cause the “pond bottom” to rise in elevation (COSIA 2012). At the active mudline (the top of the deposit), there is little effective stress, so the uncapped tailings remain weak, often fluid like, and typically governs the capping design.

Figure 11 presents modelled settlement graphs for oil sand tailings deposited at a constant rate into a 40 m deep cell over a period of eight years. Results are based on finite-strain consolidation theory and generic consolidation curves using publicly available data for compressibility and hydraulic conductivity relationships. FSConsol modelling software was used for the analysis. Single (upward) drainage was specified. No surcharge cap is modelled. The data for this analysis are adapted from Shaw et al (2010), Jeeravipoolvarn (2010), Pollock (1988). Pollock et al (2000), and Suncor (2016). Lacking publicly available consolidation data for cFFT, it was simply modelled using uFFT consolidometer properties with a discharge solids content of 50%. Actual cFFT is expected to have less settlement and shorter consolidation than shown in Figure 11, but the pattern of large settlement over long time frames is still anticipated. Table 2 provides the discharge solids contents and summarizes the results.

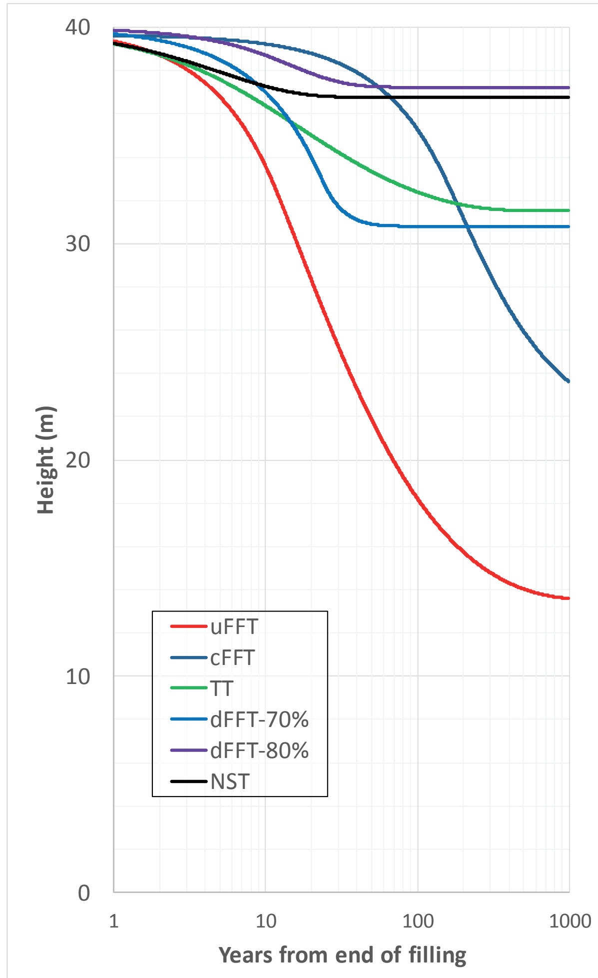

Figure 11. Tailings deposit height versus time for selected tailings types (see text for modelling info)

The model demonstrates that some tailings types show modest settlements completed over a few decades, while others have large settlements over periods of decades or centuries depending upon their compressibility and hydraulic conductivity. What is less clear from the table, is that different tailings types have much different storage efficiencies for fines – some (especially dFFT) allow storage of more tonnes of fines per cubic metre, some much less (such as NST which is mostly sand). Note that the finite-strain modelling is highly non-linear – interpolation and extrapolation of model results often lead to erroneous conclusions. Each case needs its own model run.

To keep long-term settlements to a minimum (less than 0.5 to 2m), placement of tailings close to or at the final expected solids content is required. Limiting settlements to less than 2m suggests initial solids contents of >70 to 75% are required for shallow deposits (10 to 15 m deep) and >80% solids for deep deposits (>20m). Solids contents in this range are in the realm of traditional civil engineering, with corresponding placed dry densities of over 1500 kg/m^3 and void ratios less than 0.8. This allows design to move to the range of properties encountered in traditional soil mechanics and allow designers to employ tools such Standard Proctor tests to control earthworks, and Terzaghi consolidation theory (using traditional c_c and c_v) to predict settlements (and strength gain). As indicated in Figure 8, this is also the realm of stiff soils and amenable to standard earthworks techniques as employed for oil sands dump construction. Cameron et al (1995) provide methods to estimate dump settlement and CEMA (2014) presents methods for design of overburden landforms to safely and productively accommodate this settlement.

ADDITIONAL MANAGEMENT TECHNIQUES

There are a number of management techniques (design, operation, construction etc) available to geotechnical tailings practitioners for working with weak tailings and potentially accommodating large settlement in the post closure landscape. Some of these techniques are particularly useful if considered in design prior to tailings deposition; use of these techniques will be important to many deposits. Designers will need to do considerable work before any of these techniques can be relied upon at oil sands scales – many are costly, require large volumes of material, and still require certain tailings shear strength and settlement properties. Experience has shown their application is almost always much more complex than originally envisioned and their utility, is usually less than first expected.

Table 2. Estimated average solids content and settlements for a theoretical 40m deep deposit based on finite strain consolidation analysis

Tailings type	% Solids at discharge, average at end of deposition	% Solids at end of consolidation average (range)	Total settlement, m
uFFT	29 32	70 (58-75)	28
cFFT	50 50	>76* >(52 to 76)*	>16*
TT	55 79	88 (85 to 92)	9
dFFT	70 72	82 (74 to 85)	10
	80 81	84 (80 to 86)	3
NST	60 80	83 (76 to 86)	4

* cFFT results presented at t=1000 years – the model was stopped prior to full consolidation.

dMFT is modelled here as vertically accreting tailings with no compaction (the same as the other cases). In reality, it would receive some level of compaction by placement equipment.

Utilizing crusts

A dried crust of fine tailings over much weaker material provides benefits for some activities but is of limited value for large-scale earthworks. The thickness of the crust is typically less than the width of the bearing surface of equipment or embankments because crusts are seldom thicker than 0.2 to 0.8 m. Thus, some of the bearing pressure of large equipment or embankments can apply large shear stress to the underlying weak material. A crust can be extremely beneficial to provide trafficability for foot traffic, errant wildlife, and light-weight amphibious vehicles (Argos). Water management on FFT or NST deposits to allow drying crusts to form, and to be sustained, is difficult operationally at oil sands scales. Saturation of the crust can cause considerable shear strength loss. Thus, the reliance on crusts must be evaluated on a case-specific basis and diligent observation and monitoring is required for use in construction.

Taking advantage of frost / frozen ground

Local experience on naturally soft ground and muskeg shows that a deep frost layer can provide much improved trafficability, provided underlying material does not deform appreciably. For FFT, ice road technology (USACE 2002) can be used to estimate the performance for equipment. Frost penetration is typically limited to a depth 0.3 to 1.0 m in saturated soft tailings under average winter conditions. Calculation and experience and testing indicate that while frost thickness can allow small dozers to operate, the risks of breakthrough are high. A common strategy is to conduct trafficability tests in the summer under unfrozen conditions, then conduct capping and reclamation operations over the same areas in the winter, taking advantage of the frost for additional shear strength and improved productivity while not relying on the freezing for trafficability. There is an opportunity to develop new techniques to allow better use of this frost cap through controlled experiments and incremental case histories.

Using staged-loading techniques

Many soft-ground projects elsewhere use staged loading – thin lifts are placed, the soil consolidates, densifies, and gain shear strength allowing an additional lift before the cycle repeats (eg Baecher & Ladd 1997). This type of approach is employed for dyke construction with tailings sand, but the very slow consolidation for fine tailings generally limits use of this approach for most operational or regulatory timeframes.

Adding fill in settled areas

As a subset of staged-loading, to counteract excessive settlement, it may be practical to periodically add additional capping material. Rates of a few metres every five to ten years are discussed by industry. This approach would be challenging to apply over large areas or longer time periods. If a reclamation cover is installed after the initial capping, then adding to the capping later will require rehandling and re-establishing the organic materials and replacing the vegetation used in reclamation. Future access to borrow materials is an additional consideration.

Using in-situ (post-depositional) remediation depositional treatments

Given the large volume of accumulated legacy tailings, there is strong interest in in-situ treatment of tailings, for example use of deep soil mixing (Bergado et al 1999; USDOT 2000). Such techniques are proven and effective but are costly to implement due to the cost of materials, low production rates, and specialized equipment (eg Wells 2014). Further research into less expensive ways to treat tailings in place to create the shear strengths and settlement performance targets would be worthwhile.

Wick drains and underdrains

Vertical wick drains at close spacing are being tested at Suncor Pond 5 (Abusaid et al 2011). Granular underdrains (and internal drains) have been tested at pilot scales. The head differential for drains in tailings needs to be carefully managed to avoid excessive consolidation (mud caking / blinding off) at the interface. Such drains do not change the final densities and shear strengths, but may be able to accelerate consolidation to time frames that facilitate post-depositional management. The low hydraulic conductivities of most tailings and lack of public information regarding large scale trials in oil sands makes this technology challenging to rely upon.

Advance construction of capping and landforms to accommodate future settlement

As discussed previously, after a tailings deposit is capped, there is generally a need to build some local relief for the upland areas to control the water table, prevent migration of ponded water towards a dyke crest (see next section), limit the extent of wetlands during settlement, provide bank storage for wetlands (Devito et al 2012), limit soil salinization, and generally build local relief / topographic diversity for ecological values.

Limit-equilibrium stability analyses (see Figure 4) indicate that even modest relief (4 to 6m) with modest slopes (6H:1V and flatter) will require shear strengths of at least 25 kPa and an appreciation for loss of shear strength of the tailings due to its sensitivity.

Overbuilding the cap in anticipation of future settlements may be practical in some locations, if the soft tailings deposit can support the additional fill and is stable with the dump slopes at the time of placement. Very shallow embankment slopes and periodic infilling may be needed.

Managed drainage outlets

In some cases, especially for dumps, if there is excessive differential settlement leading to ponded water, the drainage channel outlet can be lowered over time by subexcavating the outlet and rebuilding at a lower elevation. For large tailings facilities, managing the risk associated with rebuilding the large riprap-spillway outlets periodically may be costly, especially if cofferdams on soft tailings are needed to manage extreme events flows during construction. But if the outlet area is designed with this is mind, there may be some cost-effective options, particularly if settlements are largely complete during operations.

Two other design considerations

There is considerable experience in managing construction on natural sensitive clays (eg Quinn et al 2007; Aunaas et al 2016) that can be applied to capping fine tailings. The rapid loss of shear strength during loading can lead to large deformations. Selecting a representative design shear strength, a suitable factor of safety, creating safe working conditions for personnel and equipment, and monitoring performance are all critical. There is much to be learned from international experience with sensitive clays. Carefully controlled and monitored test fills are recommended; analysis of deformations under controlled loading can be used to refine design shear strengths or calibrate deformation models.

A major oil sands mine reclamation objective is to be able to delicense oil sands tailings dams (OSTDC 2014). There can be little to no residual risk of a catastrophic failure after delicensing. The tailings and the landform must be designed to avoid ponding water within a critical distance of the dyke crest and to avoid having potentially mobile tailings near the dyke that could lead to a catastrophic outflow in case of dyke instability. Thus, the design criteria for tailings in this situation would be to have a density near its terminal density at the time of delicensing (to avoid excessive settlement), the landform needs to be designed to keep water out of this critical zone near the crest, and tailings need to have non-fluid shear strengths to avoid outflow (or the design needs to demonstrate the absence of a trigger of liquefaction or strain weakening).

DISCUSSION

As discussed above and outlined in Table 2 and Figure 11, the initial solids content at deposition is an important factor for influencing the final density and post-operational settlement given the long time frames for settlements of fine tailings deposits. The correlation between tailings density and shear strength (Figure 8) suggests that high densities are required for fine tailings to limit settlement to manage the development of open-water features (and thus allow sustainable uplands) and will provide shear strengths that will facilitate capping. An added benefit of a higher density (higher initial solids contents) at deposition is the reduction of porewater within the deposit and thus a reduction in OPSW expressed as seepage and runoff. The use of water capping and EPLs can accommodate large settlements where the landscape water balance can be managed (CEMA 2012).

As noted above, working with sensitive clays is a geotechnical challenge. This paper includes some generalizations for sensitive clays to provide context to oil sands FFT behaviour from a geotechnical perspective. Design methods for sensitive clays commonly account for deformation and strain softening. So, while this paper is focused on peak shear strength, geotechnical characterization and detailed design will be required to assess FFT behaviour prior to construction.

Designing for zero settlement is not practical, as all earthwork fills (including dykes) are expected to undergo some settlements. For example, for the 60 m high Syncrude Highway 63 Berm, built using overburden and interburden compacted in lifts by 400T trucks, Cameron et al (1995) predict 1.1 m of settlement (much of the settlement is of loose foundation fills). There are methods to accommodate settlement if planned during initial design. Areas of wetlands and uplands may be designed to accommodate large settlement to evolve into reclamation lakes (Figure 2). Local relief around the wetland or lake can be designed to constrain enlargement of the open water. If consolidation time periods are within operational timeframes, there may be an opportunity to control water levels by adjusting the outlet invert elevations over time, especially if management methods are included in landform design. While limiting settlement to less than 0.5 to 2m is ideal to manage development of open water, landforms may be able to be designed to accommodate up to about 4m of settlement where certain circumstances require (CEMA 2014). Designers need to be careful to avoid creating new dams by impounding too much water.

New tailings technologies may provide the most suitable tailings deposits to support a terrestrial boreal reclaimed landscape. The oil sands industry and numerous third parties have examined relevant tailings technologies. Most are proven technologies at other mines and industries and are amenable to further evaluation. As noted in CTMC (2012), to be viable in the oil sands, such technologies would need to be able to process millions to tens of millions of tonnes of solids per year, be adaptable to the boreal climate, be robust, and result in acceptable water chemistry as well as meeting other regulatory approval conditions.

Tailings technologies that provide shear strengths and solids contents on the upper end of Figure 8 and show potential for facilitating capping and limiting settlement have been identified (see CTMC 2012; Wells 2014). They include:

- Thin-lift evaporative drying with landfarming
- Thermal drying
- Cement amended tailings
- Filtration – treated FFT (with or without sand addition) using pressure, vacuum, or filter press filtration hardware
- Co-mixing FFT and overburden
- NST variants: NST from FFT; NST from TT; high density NST (Super NST)

New tailings technologies at oil sands scale pose numerous challenges (CTMC 2012, CCA 2015) and long-development times. Large capital costs and increased energy costs (and related greenhouse gas generation) are significant challenges to new technologies. Conversely, the benefits of significantly reduced water import and treatment costs, reduced dam safety risks, and reduced liability are appealing. Suites of tailings technologies will need to be employed and will vary from site to site to meet the closure landscape design goals.

SUMMARY AND CONCLUSIONS

The goal of oil sands reclamation is to return capability equivalent to its pre-disturbed state, with reclaimed soils and landforms capable of supporting a self-sustaining, locally common boreal forest. Supporting objectives include a sustainable water balance, acceptable water quality, and physical stability, among others.

Because tailings will underlie the majority of the reclaimed oil sands mine landscape, they play a central role in creating the supporting landforms. FFT in particular are challenging to incorporate into the reclaimed landscape. The low FFT shear strengths and densities produce tailings deposits with poor trafficability and prone to geotechnical instability and large settlements. Tailings technology selection is central to creating tailings and tailings deposits that meet the needs of the reclaimed landscape. The tailings deposits need to be strong enough and dense enough to support capping, to allow local relief, and to meet design settlement criteria.

Northeastern Alberta has a precipitation deficit – potential evaporation is higher than annual precipitation. Open-water bodies (marshes, shallow-water wetlands, and lakes) are net sinks for water due to evaporation. To provide sufficient water quantity and quality at the landscape scale, every reclaimed watershed needs to have a positive water balance – water yields from the landscape need to exceed evaporation. Furthermore, there must be enough surface water moving across the landscape to flush the wetlands and end pit lakes to maintain acceptable water quality. Every watershed will be different, but as a rule of thumb, each watershed must have less than 10% to 20% open water, even after (especially after) it has fully settled over decades or hundreds of years. This means that 80 to 90% of the reclaimed landscape must be built, and remain, as terrestrial area (forest and fen ecosystems) to produce the water needed downstream.

The oil sands mining community has developed numerous tailings technologies and technologies for capping tailings deposits. The shear strengths and solids contents of tailings are highly correlated, but the relationship shows considerable scatter. The relationships between tailings shear strengths and solids contents are consistent with the shear strength versus moisture content relationships for natural sensitive clays, based on the liquidity index. FFT deposits are prone to tens of metres of post-reclamation settlement. These deposits are suitable for water capping and, in some cases, coke capping. Technologies such as NST and dFFT can be used to construct terrestrial landforms if the tailings production and deposition are well managed. Other technologies have the potential to be commercialized to amend FFT to allow creation of reclaimed boreal forest, such as thermal drying, cement amended tailings, filtration, commixing, and Super NST. Each technology comes with its own benefits and challenges.

Tailings deposits for terrestrial boreal forest need to be strong enough and dense enough to support capping and local relief needed for landform performance. Figure 8 presents the combinations of shear strength and solids content for various technologies. Densities of greater than 70% solids allow hydraulic capping with tailings sand (beaching) where shear strengths are more than 5 to 25 kPa. Soft-ground techniques are available for firm to stiff tailings (25 to 100 kPa). Standard construction (dump construction) techniques are available for tailings that are near their plastic limit such that the shear strength is greater than about 100 kPa (very stiff to hard).

Numerous methods have been proposed to allow capping of FFT and very soft tailings such as using evaporative crusts, seasonal frost, wick drains, overbuilding in anticipation of settlement, or managing the outlet invert elevation of wetlands over time. Undoubtedly, each of these methods will have a role to play in constructing tailings deposit caps. Conceptual designs have indicated that most of these methods have are expensive, and are more difficult to implement that anticipated. In many cases, they are not technically feasible for the situation. There is considerable room for innovation and optimization, but it seems unlikely these capping methods will produce terrestrial boreal forest landforms from soft tailings deposits in isolation. Tailings deposit design and construction that meets shear strength and density criteria for the overall closure landscape design will also be required.

To avoid creating large open-water bodies, allowable post-deposition settlement criteria will need to be specified for each tailings landform. Designed in advance, some low areas will be able to tolerate up to 2 to 4 m of settlement and satisfy the needs of the closure landscape design. More generally, settlements of these areas will need to be less than 0.5 m to 2 m. Options for managing this post-reclamation settlement are provided in the paper. Upland areas may be designed to allow up to 2 to 4 m of settlement. The potential of long-term maintenance (for decades or hundreds of years after mining operations cease) may allow more post-reclamation settlement to be accommodated in the reclamation design.

To meet settlement criteria, most tailings deposits will need to be close to their final (fully consolidated) solids contents when reclaimed. This requirement implies solids contents of at least 70% to 80% solids. More generally, firm to stiff tailings are needed to meet the shear strength and settlement criteria for successful reclamation at the landscape scale. Each landform will require its own design and its own specifications. The high sensitivity of the tailings (the ratio of peak to remolded undrained shear strength), means that geotechnical designs cannot simply rely on peak shear strength. Consideration of post-peak shear strengths, progressive failure, and managing deformations are all part of the required geotechnical design for these materials.

Building new boreal forest landscapes on oil sands tailings is a complex process involving many disciplines. The paper presents a high-level view of the key geotechnical requirements related to water balance, water quality, and physical stability at the landscape and landform scales. Selecting an appropriate suite of tailings technologies and tailings deposit designs for an oil sands mine requires reclamation design at the landscape and landform scales. To aid in the selection and performance criteria of tailings technology, the closure designers need to provide the design objectives and criteria for capping, stability and settlement and work with mine planners, process engineers and tailings engineers to design robust tailings systems to meet these criteria. The closure designs need to be robust enough to accommodate the realities of operations at the scale of oil sand operations.

Selecting technologies to produce tailings deposits that meet appropriate design specifications is an important component of achieving oil sands reclamation goals. Managing tailings deposition to ensure that the tailings deposit meets the design intent, ensuring the post-deposition specifications are met, monitoring shear strength and density gains over time, accommodating off-spec materials, designing capping and local topographic relief, and building uplands and wetlands are all critical elements to successful reclamation. Many of the techniques are already standard practice for dyke construction and reclamation with other materials – these skills and processes need to be fully applied to the fine tailings deposits to build successful landscapes, reduce costs, and manage long-term liability.

ACKNOWLEDGEMENTS

The authors wish to thank the following:

- To the IOSTC Organizers for accepting this paper and the opportunity to present its findings.
- As always, Derrill Shuttleworth of Gabriola Island, BC is thanked for the illustrations.
- Although any errors and omissions in the synthesis of this paper lie with the authors, this work could not have occurred without our oil sands colleagues sharing their insights and experience with soft tailings and landform design over the past 20 years. In particular, many of the concepts in this paper are based on ideas and work by Bill Shaw of WHS Engineering, John Sobkowicz of Thurber Engineering, Les Sawatsky of Teleo Engineering, and Richard Dawson of Norwest Corporation. Staff at the oil sands operations continue to make significant contributions in all areas of this work every day.
- BGC Engineering is thanked for supporting this research and preparation of the paper. Julian McGreevy is thanked for his geotechnical analyses, Carl Mendoza for sharing his work on boreal landscape hydrology, and BGC librarians Jana Purmalis, Krista Smith and Lynn Forrest for tracking down the references below.

REFERENCES

Abusaid A, Pollock G, Fear C, McRoberts E, & Wells S. 2011. An Update to the Construction of the Suncor Oil Sands Tailings Pond 5 Cover. Tailings and Mine Waste 2011. Nov 6-9. Vancouver.

AENV (Alberta Environment). 2007. Province of Alberta EPEA Approval 46586-00-00. November 9, 2007. Alberta Government. Edmonton. 67p.

AENV (Alberta Environment). 2008. Alberta issues first-ever oil sands land reclamation certificate: former oil sands site transformed into forested area. Alberta Government press release. March 19, 2008.

AENV (Alberta Environment). 2016. Alberta Environment and Parks Oil Sands Information Portal. Internet website: www.osip.alberta.ca. Accessed 2016-10-29.

AEP (Alberta Environment and Parks). 2014. Total Area of the Oil Sands Tailings Ponds over Time Dec 31, 1985 - Dec 31, 2013. http://osip.alberta.ca/library/Dataset/Details/542. Accessed 2016-10-29. Alberta Government. Edmonton.

AER (Alberta Energy Regulator). 2016. Directive 085. *Fluid tailings management for oil sands mining projects.* July 14, 2016. Alberta Energy Regulator. Calgary. 54p.

Alberta Government. 2015. *Lower Athabasca Region: Tailings Management Framework (TMF) for the Mineable Athabasca Oil Sands*. Alberta Government. Edmonton. 58p.

Almeida MSA & Marques MES. 2013. *Design and performance of embankments on very soft soils.* CRC Press. Leiden, The Netherlands. 197p.

AMEC. 2013. *Beach fines capture study*. Consultant's report to COSIA. Report CG25409. June 2013. AMEC Earth and Infrastructure. Calgary. 466p.

Aunaas K, Thakur V, Oset, F, Ottesen HB, Strand SA, Nyheim T, Havnen I, Lyche E, Viklund M, & Abokhalil M. 2016. An attempt towards harmonizing the Norwegian guidelines related to construction on sensitive clay. NGM 2016: 17th Nordic Geotechnical Meeting. May 25-28. 2016 Reykjavik. P1263-1272.

Baecher G & Ladd C.1997. Formal observational approach to staged loading. Transportation Research Record. Transportation Research Record: Journal of the Transportation Research Board. #1582: p49-52

Banas LC. 1991. Thixotropic behaviour of oil sands tailings sludge. MSc Thesis. Department of Civil Engineering. University of Alberta. Edmonton. 430p.

Beier N, Wilson W, Dunmola A, & Sego D. 2013. Impact of flocculation-based dewatering on the shear strength of oil sands fine tailings. Canadian Geotechnical Journal, 2013, Vol. 50, No. 9: pp. 1001-1007.

Bergado DT, Ruenkrairergsa T, Taesiriy YY & Balasubramaniam AS. 1999. Deep soil mixing used to reduce embankment settlement. Ground Improvement 3: p145-162.

BGC Engineering Inc. 2010. *Review of reclamation options for oil sands tailings substrates*. Consultant's report for OSRIN. Report No. TR-2. 59p.

Caldwell J, Revington A, McPhail G, & Charlebois L. 2014. Optimised seasonal deposition for successful management of treated mature fine tailings. 17th International Seminar on Paste and Thickened Tailings. Vancouver. Jun 8-12. Infomine Inc. Vancouver. p371–380.

Cameron R, Ashton C, Fong V & Strueby B. 1995. Syncrude's Highway Berm: Project overview and design philosophy." 48th Canadian Geotechnical Conference. Vancouver. Canadian Geotechnical Society. 2: p789-798.

Caterpillar. 2015. *Caterpillar Performance Handbook Edition 45*. Caterpillar. Peoria, IL. January 2015. 2264p.

CCA (Council of Canadian Academies). 2015. *Technological Prospects for Reducing the Environmental Footprint of Canadian Oil Sands. The Expert Panel on the Potential for New and Emerging Technologies to Reduce the Environmental Impacts of Oil Sands Development*. Council of Canadian Academies. Ottawa. 252p.

CEMA (Cumulative Environmental Management Association). 2005. *Landscape Design Checklist*, Revised RSDS Government Regulator Version. CEMA-RWG Landscape Design Subgroup. May 2005. CEMA. Fort McMurray. 8p.

CEMA (Cumulative Environmental Management Association). 2012. *Oil Sands End Pit Lakes Guidance Document.* CEMA. Fort McMurray. 434p.

CEMA (Cumulative Environmental Management Association). 2013. *Mineable Oil Sands Aquifer Management and Reclamation Concept Review*. North Athabasca Oil Sands Region. Consultant's report by BGC Engineering Inc to CEMA Water Working Group. Report 0731-020. December 20, 2103. 138p.

CEMA (Cumulative Environmental Management Association). 2014. *Guidelines for Wetland Establishment on Reclaimed Oil Sands Leases* (3rd Edition). CEMA. Fort McMurray. 494p.

CTMC (Consortium of Oil Sands Tailings Management Consultants). 2012. *Oil Sands Tailings Technology Deployment Roadmaps Project Report*. Consultant's Report to Alberta Innovates – Energy and Environment Solutions and the Oil Sands Tailings Consortium. Jun 29, 2012. Calgary. 4v

COSIA (Canada's Oil Sands Innovation Alliance). 2012. *Technical Guide. for Fluid Fine Tailings Management.* Report. August 30, 2012. COSIA. Calgary. 131p.

COSIA (Canada's Oil Sands Innovation Alliance). 2014. *Guidelines for Performance Management of Oil Sands Fluid Fine Tailings Deposits to Meet Closure Commitments*. COSIA. Calgary. Feb 2014. 31p.

Costello M, Hedblom E & Van Kesteren W. 2010 Capping soft tailings from a floating platform. International Oil Sands Tailings Conference. Edmonton. University of Alberta Geotechnical Center, University of Alberta, Edmonton. 7p

Devito K, Mendoza C, & Qualizza C. 2012. *Conceptualizing Water Movement in the Boreal Plains. Implications for Watershed Reconstruction*. Synthesis report prepared for the Canadian Oil Sands Network for Research and Development, Environmental and Reclamation Research Group. Edmonton. 164p.

Eaton B, Fisher JT, Muhly T & Chai S-L. 2013. *Potential impacts of beaver on oil sands reclamation success – an analysis of available literature*. report prepared by Alberta Innovates Technology Futures for the Oil Sands Research and Information Network (OSRIN). Alberta Innovates Technology Futures. Edmonton. 75p.

FTFC (Fine Tailings Fundamentals Consortium). 1995. *Advances in Oil Sands Tailings Research*. Alberta Department of Energy, Oil Sands, and Research Division. Alberta Government, Edmonton. 294p.

Golder (Golder Associates Ltd). 2003. *Calibration of the HSPF water quality model for the oil sands region in northeastern Alberta*. Report IP2-2501 (1000). Jan 2003. Golder Associates. Calgary. 189p.

Houston, W.N., and Mitchell, J.K. 1969. Property interrelationships in sensitive clays. Journal of the Soil Mechanics and Foundations Division, ASCE, 95(SM4): 1037–1062

Hyndman A & Sobkowicz JC. 2010. Oil sands tailings: reclamation goals and the state of technology. 63rd Canadian Geotechnical Conference, Sep 12-16. Calgary.

Jakubick AT, McKenna GT, & Robertson AM. 2003. Stabilisation of tailings deposits: international experience. May 25-28. Mining and the Environment. Conference. Sudbury.

Jeeravipoolvarn S. 2010. *Geotechnical behaviour of in-line thickened oil sands tailings*. PhD Thesis. Department of Civil and Environmental Engineering. University of Alberta. Edmonton. 432p.

Junqueira F, Sanin MV, Sedgwick A & Blum J. 2011. Assessment of water removal from oil sands tailings by evaporation and under-drainage and the impact on tailings consolidation. Tailings and Mine Waste 2011. Nov 6-9. Vancouver.

Kalteziotis NA, Menzies BK & Tarzi AI. 1984. A bearing capacity correction for strain-softening saturated clays. Ground Engineering. 7:30-31.

Lorentz J, Lahaie R, Mikula R, Donahue R, Reeb TL, Cameron R, & Mimura DW. 2012. Disposal of oil sand tailings centrifuge cake. Canadian patent CA 2825513 A1. Priority date October 26, 2012. Applicant: Syncrude Canada Ltd (in trust for the owners of the Syncrude Project).

McGreevy J, McKenna G, An R, & Scordo E. 2013. Regional mine closure plans – the next improvement in closure planning. Tailings and Mine Waste 2013 Conference. Banff. Nov 3-6. University of Alberta Geotechnical Centre, Edmonton.

McKenna GT. 2002. *Landscape engineering and sustainable mine reclamation*. PhD Thesis, Department of Civil and Environmental Engineering, University of Alberta, Edmonton. 660p.

McKenna G & Cullen V. 2008. Landscape design for soft tailings deposit. Tailings and Mine Waste 2008 Conference. Vail, CO.

McPhail, G, 2006. Implications of different tailings disposal options on future rehabilitation. Mine Tailings 2006. Feb 26-27. Brisbane. p1-15.

Mikula RJ, Munoz VA, & Omotoso O. 2008. Centrifuge Options for Production of 'Dry Stackable Tailings' in Surface Mined Oil Sands Tailings Management. Canadian International Petroleum Conference/SPE Gas Technology Symposium. Jun 17-19. Calgary.6p.

Morgenstern, NR. 2012. Oil sands mine closure - the end game. David C. Sego Symposium. Apr 26-27. Edmonton. University of Alberta Geotechnical Centre. Edmonton. p85-99.

NRC (Natural Resources Canada) & CanmetEnergy. 2010. *Oil sands water toxicity: a critical review*. Authors: Miskimmin B, Fedorak P, Lauman R, & Vinke K. Devon, Albert. Report 2010-089 (INT). 136p.

OSTDC (Oil Sands Tailings Dam Committee). 2014. *De-licensing of oil sands tailings dams*. Technical guidance document. Mar 2014. Oil Sands Research and Information Network (OSRIN). University of Alberta. Edmonton. 46p.

Pollard J, McKenna GT, Fair J, Daly C, Wytrykush C, & Clark J. 2012. Design aspects of two fen wetlands constructed for reclamation research in the Athabasca oil sands. Mine Closure 2012 Symposium. Brisbane. Australian Centre for Geomechanics p815-829.

Pollock GW, McRoberts EC, Livingstone G, McKenna GT, & Matthews JG. 2000. Consolidation behaviour and modelling of oil sands composite tailings in the Syncrude CT Prototype. International Conference on Tailings and Mine Waste v7:121-130.

Pollock GW. 1998. *Large strain consolidation of oil sands tailings sludge*. MSc Thesis. Department of Civil Engineering. University of Alberta. Edmonton. Fall 1988.

Proskin S. 1998. *A geotechnical investigation of freeze-thaw dewatering of oil sands fine tailings*. PhD Thesis. Department of Civil and Environmental Engineering. University of Alberta. Edmonton. 441p.

Quinn PE, Hutchinson DJ, & Rowe RK. 2007. Toward a risk management framework: sensitive clay landslide hazards affecting linear infrastructure in eastern Canada. 1st North American Landslide Conference, Vail, Colorado, 3–8 June. Association of Environmental and Engineering Geologists, Denver. p102-114.

Robertson PK, (Fear) Wride CE, List BR, Atukorala U, Biggar KW, Byrne PM, Campanella RG, Cathro DC, Chan DH, Czajewski K, Finn WDL, Gu WH, Hammamji Y, Hofmann BA, Howie JA, Hughes J, Imrie AS, Konrad J-M, Küpper A, Law T, Lord ERF, Monahan PA, Morgenstern NR, Phillips R, Piché R, Plewes HD, Scott D, Sego DC, Sobkowicz J, Stewart RA, Watts BD, Woeller DJ, Youd TL, Zavodni Z. 2000. The CANLEX project: summary and conclusions. Canadian Geotechnical Journal, 2000, 37(3): 563-591.

RSC (The Royal Society of Canada). 2010. *Environmental and health impacts of Canada's oil sands industry*. Report authors Gosselin P, Hrudey SE, Naeth AM, Plourde A, Therrien R, Van Der Kraak G, & Xu Z. The Royal Society of Canada. Ottawa. 414p.

Russell B, McKenna G, Leblanc M, Wells PS, & Anderson HB. 2010. Design and construction of the reclamation surface for the first oil sands tailings pond. Mine Closure 2010, Vina del Mar, Chile. Australia Centre for Geomechanics. Perth. 13p.

Sharma B & Bora P. 2003. Plastic limit, liquid limit and undrained shear strength of soil—reappraisal. ASC Journal of Geotechnical and Geoenvironmental Engineering. 129:8. p774-777.

Shaw B, Hyndman A, & Sobkowicz JC. 2010. Consolidation projections for thickened tailings. 2nd International Oil Sands Tailings Conference. Dec 5-8. Edmonton. University of Alberta Geotechnical Centre. Edmonton. p253-263.

Skempton AW & Northey RD. 1952. Sensitivity of clays. Geotechnique 3:1. p40-51.

Sobkowicz J, Hyndman A, Watts B, & Dawson R. 2014. Performance management of fluid fine tailings to meet closure commitments. 2014. Fourth International Oil Sands Tailings Conference. Lake Louise. Dec 7-10. University of Alberta geotechnical Centre. Edmonton. P 175-184.

Sobkowicz JC & Morgenstern NR. 2009. A geotechnical perspective on oil sands tailings. 13th Annual Conference on Tailings and Mine Waste. Nov 1-4. Banff.

Suncor (Suncor Energy Inc). 2016. *Suncor Base Plant Application for the Draft Tailings Directive*. Operator's report submitted to Alberta Energy Regulator. April 2016. 154p.

Suthaker NN. 1995. *Geotechnics of oil sand fine tailings*. PhD Thesis. Department of Civil Engineering, University of Alberta. Edmonton. 241p.

Syncrude. 2015. *Syncrude Sustainability Report 2015*. Syncrude Canada Ltd. Fort McMurray. 74p.

Taylor DW. 1937. 'Stability of earth slopes.' J. Boston Soc. Civil Eng., 24(3). Reprinted in*: Contributions to Soil Mechanics 1925 to 1940*, Boston Society of Civil Engineers, 337–386.

Terzaghi K & Peck. 1967. *Soil Mechanics in Engineering Practice.* 2nd edition. John Wiley. New York.

USACE (US Army Corps of Engineers). 2002. *Ice Engineering.* Department of the Army, Washington DC. Manual EM 1110-2-1612. October 30, 2002. 475p.

USDOT (US Department of Transportation). 2000. *An introduction to the deep soil mixing methods as used in geotechnical applications.* US Department of Transportation: Federal Highway Administration. McLean, VA. 146p.

Varnes DJ. 1978. *Slope movement types and processes*. Special Report 176: Landslides: Analysis and Control. Transportation and Road Research Board, National Academy of Science, Washington DC. p11-33.

Watari Y. 1984. Reclamation with clayey soil and method of earth spreading on the surface. Seminar on Soil Improvement and Construction Techniques in Soft-ground. Singapore. Japanese Society of Soil Mechanics and Foundation Engineering. p103-119.

Wells, PS. 2014. Changes in Tailings – Questions and a focus on solutions from the oil sands. PowerPoint Presentation. Paste 2014. 17th International Seminar on Paste and Thickened Tailings. June 8-12. Vancouver. Australian Centre for Geomechanics. Perth. http://www.paste2014.com/wp-content/uploads/2014/06/PatrickSeanWells_Paste2014_Presentation.pdf30p.

Wood RK. 2003. *Response of dense beach above water tailings to cyclic equipment loading at Syncrude's Southwest Sand Storage Facility*. MSc Thesis. University of Alberta. Department of Civil and Environmental Engineering, Edmonton. 223p.

Yao Y, Van Tol AF, Van Paassen LA. 2012. The effect of flocculant on the geotechnical properties of mature fine tailings: An experimental study. Third International Oil Sands Tailings Conference. Lake Louise. University of Alberta Geotechnical Centre. Edmonton. p391-398.

CAPPING AND CLOSING DEEP TAILINGS FINES DEPOSITS

Alexander Hyndman[1] and Richard Dawson[2]
[1]Magnus Limited
[2]Norwest Corporation

ABSTRACT

In-pit fines deposits are prevalent components within planned oil sands mine closure landscapes. Spatial efficiency and geotechnical integrity favour the use of completed mine pits for disposal of soft deposits having slow rates of consolidation.

An important consideration for these deposits is the method to be used to stabilize the upper zone of the deposit. Typically, the surface material in fines-dominated deposits and CT deposits will be fluid, in some cases due to segregation of fines during deposition. Without consolidation effected by self-weight (as occurs in the deeper parts of the deposit), the upper zone of sub-aqueous or saturated deposits will, in the absence of intervention, remain in a fluid state indefinitely.

Where the deposit is to be reclaimed to terrestrial upland, or a wetland, the surface zone will require some means to increase its density and strength to allow for placement of capping material and reclamation soils. In the case of a pit lake, the properties of the mudline surface must be such as to avoid upwelling of fines into the surface waters during thermal turnovers inherent in dimictic lake behaviour.

Several means of achieving these requirements will be addressed, including surface desiccation, sand raining, wick drains, modified surface composition and electro-kinetic treatment. Considerations respecting the different methods and the planned end-land surface will be discussed.

INTRODUCTION

Background

Extraction of bitumen from surface-mined oil sands deposits using the hot water process and its more recent variations has been practiced on a large commercial scale since the late 1960s. The tailings resulting from this process are a slurry, composed of about 50% water with the balance made up of the original oil-sand mineral and a small amount of unrecovered bitumen. The mineral content is predominantly silica sand with trace minerals and an average fines content (≤ 44μm) ranging from 10% to 30% (Figure 1) although seams within the deposits have even greater percentages. Clay content within the fines, as defined by the ≤ 2 μm fraction, is typically about 25% of total fines.

Tailings are typically deposited into cells and beaches to construct sand dykes which form the containment dams used to recover and recycle the process water (Figure 2).

The clay content of the oil sand, combined with the segregating behaviour of the tailings as the slurry is deposited to the cells and beaches, results in runoff water containing about half of the clay content. The percentage of clay captured in the sand depends on the slurry density and the discharge conditions.

Over a one-year period, the clay-dominated fines settle to a suspension of about 25%wt solids. Further densification is slow and mostly attributable to accumulation of silts and fine sand particles settling into the clay suspension as the

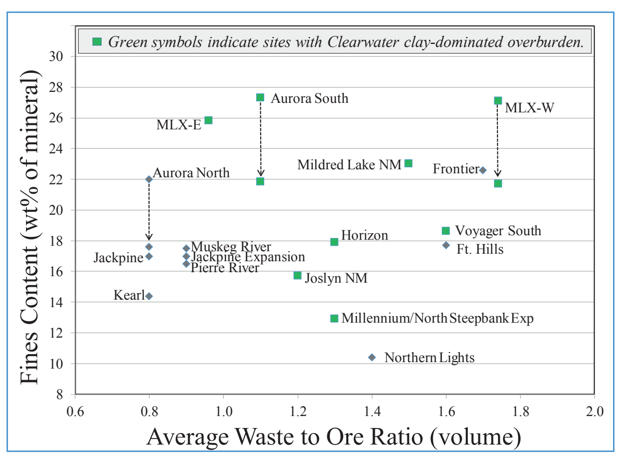

Figure 1. Surface Oil Sands Ore Body Properties (Fines content for Aurora N, Aurora S and MLX W are adjusted down to reflect full dispersion for fines analysis)

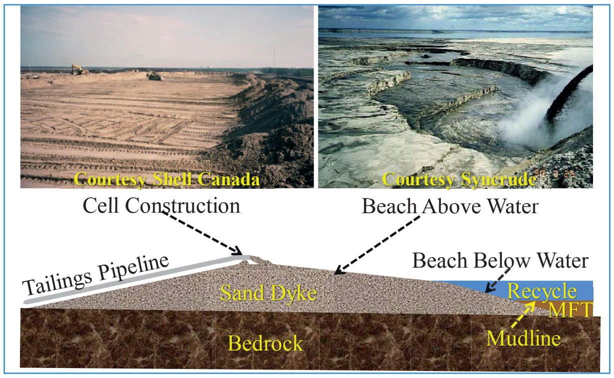

Figure 2. Tailings Dam Construction

fluid fines stratum in the recycle pond deepens. The upper zone of the deposit at the mudline is close to 100% clay while lower zones may have densities as great as 50% and, with the infiltration of fine silica sand and silt, clay contents of 20% or less.

Figure 3 shows a typical profile for total solids, fines and clay content for fluid solids in an active settling pond (Suncor South Tailings Pond). The volumetric impact of settling behaviour against pond depth is illustrated by the three charts - the top chart shows the concentration of total solids versus depth; the middle chart shows the clay as a percentage of the total mineral content; the bottom chart shows total solids, fines and clay concentrations per m^3 of FFT. In an active pond, once the settlement and infiltration attain a concentration of about 30%wt solids, the deposit has reached its minimum volume. Further infiltration of coarser particles settling into the clay suspension does not increase and may decrease clay concentration. This is an important consideration for site planning – in particular, for planning of fluid containment and disposal of FFT. Although high sand-content material near the pond bottom may attain strength through self-weight consolidation over a reasonable time frame, the containment volume will nevertheless have been used. Lenses of clay-rich material within the solid, sand-dominated pond bottom can result from beaching of sand over the MFT layer. Dredging and removal of MFT from an area of the pond may further complicate the picture.

Volume reduction of FFT requires some form of dewatering treatment through chemical, mechanical or evaporative methods or combinations thereof. The different methods for surface capping of these deposits in the context of

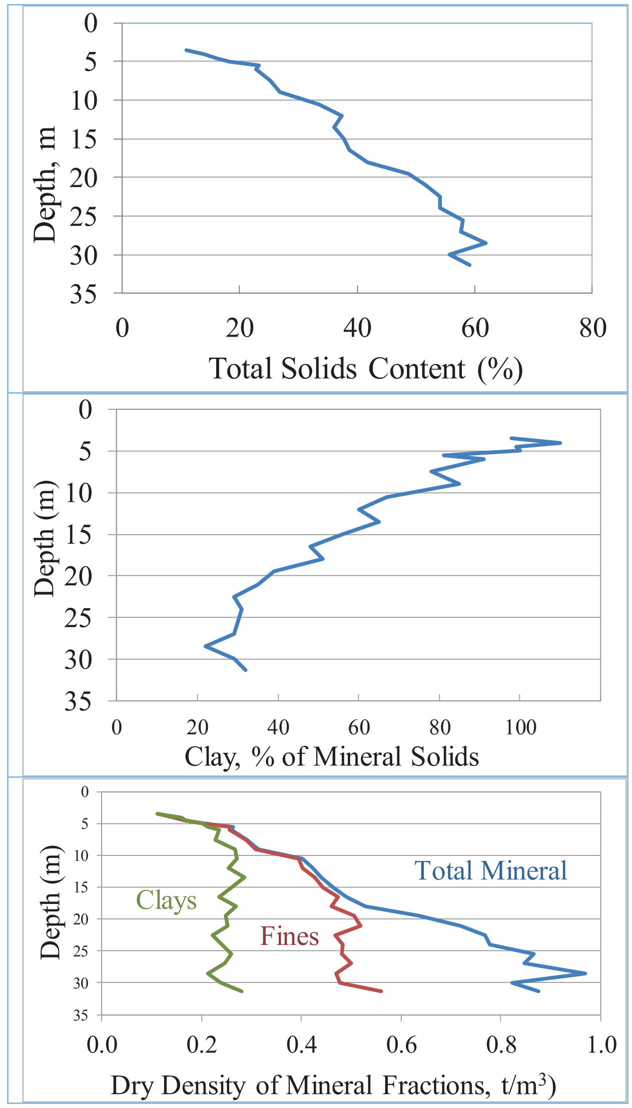

Figure 3. MFT Solids % and Clay Concentration (Clay Content by Methylene Blue)

their land-surface goals for closure is the subject of this paper.

Managing FFT deposits from planning through to capping and reclamation should be carried out consistent with management objectives for sustainable mine closure as specified in a series of FFT management guides published by COSIA:

1. To eliminate fluid containment dams in the closure landscape.
2. To establish a stable closure landscape, with sustainable and diverse ecosystems, within a reasonable time after cessation of mining.

3. To develop sustainable surface drainage including a functional lake system.
4. To facilitate progressive reclamation (i.e., the reclamation of mine areas, to the extent practical during mine life, to reduce post-closure liability).
5. To optimize full life-cycle costs and minimize life-cycle environmental impacts without compromising reclamation and closure objectives.
6. To understand technical uncertainties and appropriately manage their associated residual risks.[i]

DEPOSIT TYPES FOR DISPOSAL OF FFT

Clay-dominated fluid tailings material is referred to in the industry as fluid fine tailings (FFT) or after settlement, mature fine tailings (MFT). Over the past 50 years of oil sands mining, more than one billion m^3 of FFT have been accumulated in containment dams located on the six operating mine sites and two depleted mines under reclamation[1]. COSIA[ii] outlined four types of deposits used to sequester FFT in reclaimed mine sites: Thin-Layered Fines-Dominated Deposits; Deep Fines-Dominated (Cohesive) Deposits; Fines-Enriched Sand; and Water-Capped Deposits. Capping methods are concerned with the last three deposit types. Much of the FFT to be incorporated into the reclaimed mine closure landscapes will be deposited to deep deposits of treated FFT contained in pit to ensure long-term geotechnical stability. These fines-dominated (cohesive) deposits will have varying initial densities depending upon their method of treatment, the least dense being simple transfer of MFT at about 30%wt solids to the pit void. Dewatering of MFT through use of flocculation, either alone or in combination with centrifuging, leads to initial deposit densities in the range of 45%wt to 60%wt solids.

Two other methods of fines disposal include:

- Composite Tailings (CT - sometimes called consolidated tailings) are fines-enriched sand produced at a nominal ratio of 4:1 using gypsum as a coagulant to achieve non-segregating behavior. CT is designed to have a grain-to-grain sand skeletal structure with the fines contained along with water in the voids.
- Thickened Tailings are generally produced by flocculating fresh tailings fines withdrawn from the total tailings stream and processed through flotation to attain secondary recovery of bitumen in the extraction process. The fines are flocculated and settled within a large gravity thickener. MFT may be added to the thickener feed to attain additional fines capture. Thickened tailings generally have sand-to-fines ratios in the range of 0.5 to 1.5 depending upon feed composition and whether or not the feed stream has been cycloned for sand removal. In this range the sand particles occupy space within the deposit with deposit behavior akin to the high fines (cohesive) deposits.

This paper discusses the methods available for capping these types of deposits to achieve the intended end-surface terrain.

DEPOSIT CONSOLIDATION

Deep deposits of dewatered FFT require time to undergo self-weight consolidation. As settlement proceeds, the deposit surface subsides and the underlying deposit material increases in density and strength. The time to complete settlement is primarily governed by the deposit depth and its clay content. To illustrate the effects of clay content and deposit depth, two modelled cases are shown. Figure 4[iii] (first shown at Tailings and Mine Waste 2013) projects consolidation of thickened tailings having a relatively low clay content of 13%. The thickened tailings are deposited over 10 years to a depth of 25m. Once surcharged, and 12.5 years after fill completion, the deposit settles to within 1.5m of its ultimate elevation. Within 20 years, the entire deposit has a strength ≥30 kPa.

Settlement times are very sensitive to the deposit input parameters. A deeper deposit with much greater clay content and a rapid fill rate will undergo much longer-term settlement. Figure 5 shows model results for a 75m deposit with 50% clay content (saturated with no surcharge). After 100 years, surface subsidence of about 15m remains.

[1] The six operating mines: Syncrude North (Mildred Lake) Mine (1990); Suncor Steepbank and Millennium Mine (1998/2001); Syncrude Aurora North Mine (2000); Shell Muskeg River Mine (2003); Shell Jackpine Mine (2010); Canadian Natural Resources Horizon Mine (2009); Imperial Oil Kearl Mine (2013). The depleted mines: Suncor Tar Island (GCOS 1967); Syncrude Mildred Lake Base Mine (1978).

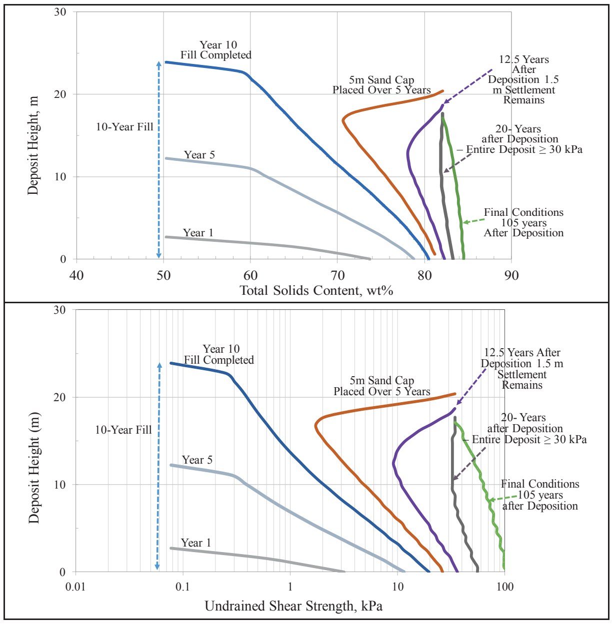

Figure 4. Deposit Settlement and Density Increase with Time (25m deposit 13% Clay, 0.8 SFR)[ii]

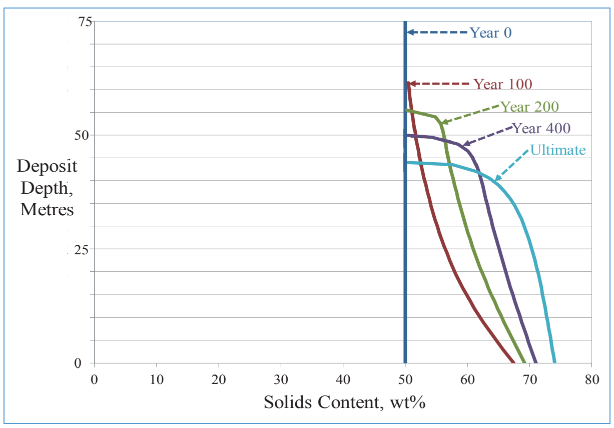

Figure 5. Deposit Settlement and Density Increase with Time (75m deposit – 50% Clay)[iv]

This prolonged settlement time is an important factor when considering the choice of surface topography and drainage design in the closure landscape.

ALTERNATIVES FOR DEPOSIT TYPES

End-surface Terrain Alternatives

Deep, in-pit, fines-dominated deposits are most suited to be reclaimed either as wetlands or lakes.

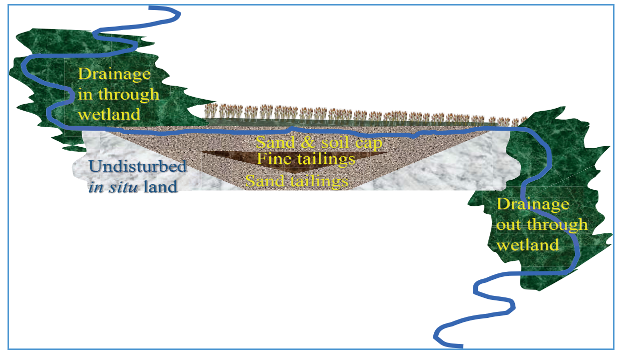

Figure 6. Wetland Over Treated FFT Deposit

Each deposit must contend with the density and strength profile at the time of capping and surface reclamation, while anticipating consolidation and settlement that will occur over time.

A **forested upland** surface must be designed so that uneven settlement does not cause the emergence of a water body within surrounding containment that would fall within the definition of a dam. While an elevated reclaimed surface can be profiled to accommodate deposit settlement, predicted from the measured geotechnical properties, a period of observation would be necessary to validate settlement predictions and, if necessary, amend surface drainage. For these reasons, wetlands or lakes are favoured for deposits with very long settlement times.

A **wetland surface** (Figure 6) could be designed so the emergence of any water bodies would be within an adequate amount of undisturbed surrounding terrain or a landform barrier of such composition and dimension so as to not constitute a dam.[v] Settlement over time would see the emergence of a lake feature - somewhat shallower and perhaps smaller than a pit lake established at closure.

Pit Lakes are design features of mine closure landscapes. A site may include only an end-pit lake (the final pit remaining at the cessation of mining) or in addition, a mid-pit lake formed over disposed tailings after which mining continues for many years on the site. Pit lake fill proposals have ranged from MFT capped with water, treated MFT capped with water to all water. At this point, the 800 ha Base Mine Lake (water-capped MFT) at Syncrude's Mildred Lake site is the only oil sands mine pit lake to have been put in place with conditional approvals. Figure 7 shows the lake two years prior to fill completion.

Figure 7. Base Mine Lake 2 years before final fill

In all situations, expression of process-affected pore water from a deposit under a lake or wetland and/or released from the surrounding drainage area will occur. The surrounding drainage area could include sizeable natural areas along with large elevated areas of tailings sand and overburden. A pit lake acts as a natural bioreactor to treat organic components in process water expressed from deposits draining through the lake. A period of observation and water management is needed prior to the lake discharge being integrated into the surrounding surface hydrology.

SURCHARGE AND CAPPING METHODS

Several methods for capping fine tailings deposits have been proposed to serve a number of functions which include:

- Placement of a surcharge load to assist consolidation
- Providing trafficable access to complete further reclamation activities
- Isolating or solidifying suspended fines to create a robust interface between the deposit and overlying water.

Geotechnical factors that must be considered in approaching cap placement include:

- Safety factors to be observed during the placement process and ongoing work and surface access.
- The timeline for ongoing consolidation of the deposit together with the associated strength profile and surface subsidence. These must be considered in the context of the surface landform and land-use intentions.

The attributes of the deposit and intended reclaimed surface along with cost, risk and the practicality of placement, will determine the choice of capping suited for each situation.

Table 1. Loads and Pressures[iii]

Equipment Type		Load, t	Bearing Pressure, kPa	Class
Foot Traffic		0-.1	30	Low
Pickup		0.7	190	Medium
Dozers	D3	7	45	Low
	D7	25	45	Medium
	D11	96	149	Medium
Loaded Haul Trucks	40 Ton	74	825	High
	100 Ton	161	620	High
	240 Ton	377	758	High

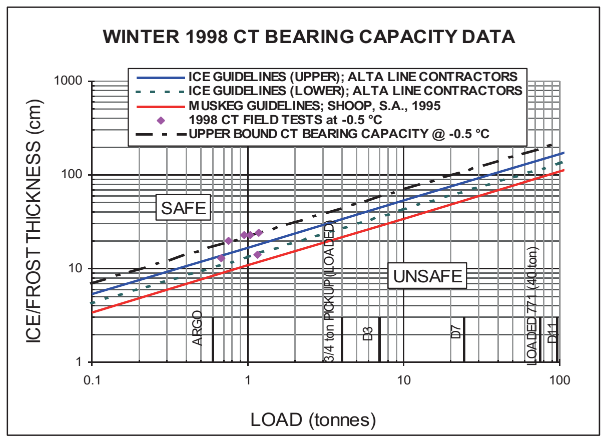

Figure 8. Ice Guidelines and Plate Bearing Tests[vi]

To form a terrestrial surface, placement of the initial cap provides access for equipment to commence the buildup of a deeper layer for further reclamation activities. Table 1 shows a range of equipment-type loads and their bearing pressures.

In winter, a frozen surface can be used to augment the bearing capacity of a crustal surface. An approach used to achieve safe cap placement over CT is an example of preparatory work conducted to achieve safe access. The relationship between the strength of frozen tailings and ice was developed. This allowed for guidelines developed for ice roads to be adjusted and used for safe access (Figure 8). One to two metres of frozen depth restricts the capping activity to use of only light equipment.

Standard Capping Methods

Generating a surface crust through desiccation makes use of atmospheric drying and freeze-thaw cycles to dewater a surface layer. Starting with a deposit that has been dewatered to ≥50%wt solids about a meter of crust can be developed over an 18-month cycle of drying and freeze thaw. The crust provides a base to assist with further capping activities. For a water-capped (pit lake) deposit, a single year of natural desiccation may provide a sufficiently robust crust for the water-mudline interface. The objective is to preclude fines from being carried up into the placed water cap during thermal turnovers which can occur each spring and fall in a dimictic lake.

To generate a deeper crust for surcharging the deposit, a rim-ditching method can be used. Water is drained from the deposit surface by constructing drainage ditches. Perimeter ditches can be readily excavated as the crust deepens. On a large deposit, access over the frozen surface in winter could be used to develop intermediate ditches. Rim ditching has been successfully used in the Florida phosphate industry[vii].

Sand spray or sand raining involves placement of a uniform layer of sand over a very weak deposit of clay-bearing fluid or soft soil to create a permeable surcharge layer. Sand slurry is discharged through an overlying layer of water from a barge. By slowly building up a layer of uniform thickness, a surcharge and trafficable surface can be created. The weaker, or more fluid the deposit, the greater is the challenge in preventing a failure where a portion of the sand layer sinks into the deposit (Figure 9). This method could be used where sand tailings are available and it is practical to distribute the sand through water overlying the deposit. Use of sand spray over untreated MFT would be outside of commercial precedent.

Mechanical placement of sand or overburden can be used where the deposit surface has sufficient crustal strength or surface freezing. Once grain-to-grain sand contact occurs in a CT deposit, it will rapidly attain bearing strength and may be suitable for mechanical (or hydraulic) placement (Figure 10). A fines-dominated, cohesive deposit that has previously undergone surface crust development is a suitable candidate for mechanical placement. Placement of geotextile over the deposit surface can be used to assist in load distribution.

Hydraulic sand deposition can be accomplished with discharge of a sand slurry either with or without use of a cyclone to dewater the slurry. Figure 10 shows a sequence of hydraulic capping followed by a mechanically placed lift over a prototype CT deposit.

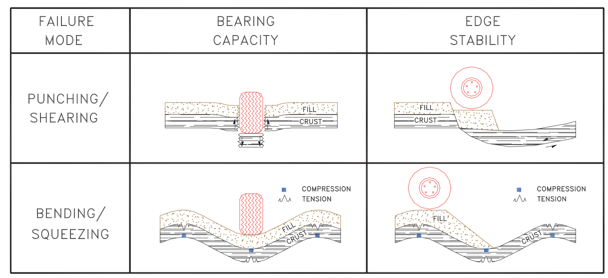

Figure 9. Failure Modes[iii]

Figure 10. Hydraulic and Mechanical Capping of a CT Deposit

Capping Methods Under Development

Sodium silicate can be used to generate a water-based low-density rigid deposit from FFT (or even water alone). The Dupont **Particlear®** silica microgel process[viii] has been tested and proposed as an alternative to drying operations. It can be dewatered by self-weight consolidation or drying to attain substantial strength (Figure 11). As a capping alternative, its low density and permeability that responds to surcharge loading make it a candidate to provide access over a weak deposit for subsequent placement of surcharge and reclamation materials with the thickness of the Particlear® layer engineered to provide access for bearing loads.

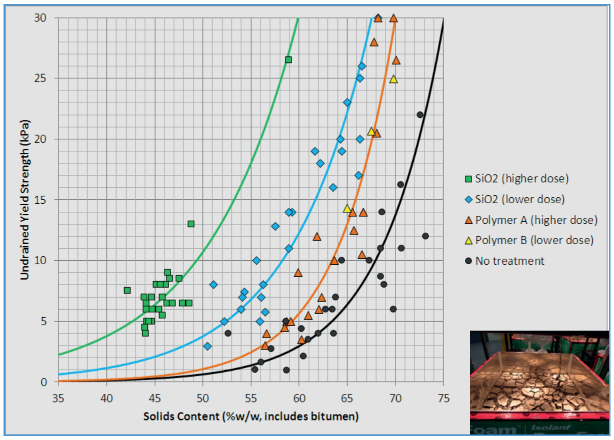

Figure 11. Particlear®-Treated Fines - Strength Increase with Dewatering[iv]

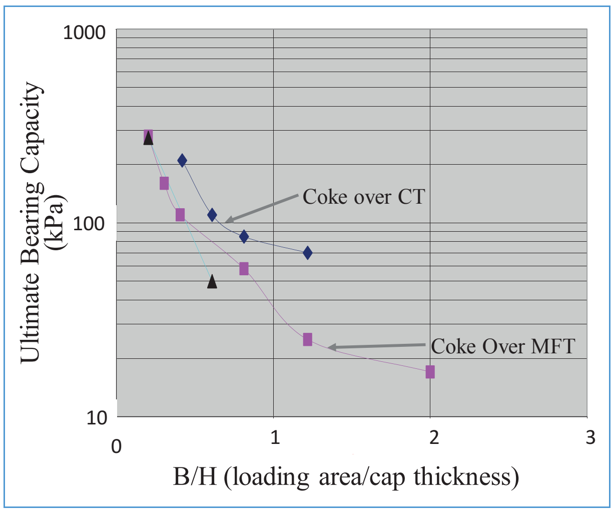

Figure 12. Coke Cap Bearing Capacity

Figure 13. Coke Cap Commences on Pond 5

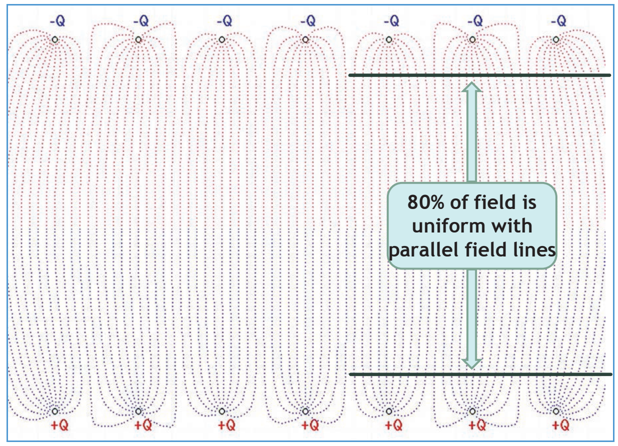

Figure 14. ElectroKinetic Field Pattern with 5m Horizontal Array Spacing (Courtesy EKS)

Coke Capping[ix] is an opportunity presented to oil sands projects with on-site upgrading operations generating coke. As a low-density aggregate, it can make a useful starting cover for weak soils (Figure 12). Crushed delayed coke or fluid coke have particle densities slightly above but bulk density less than water. Placed over a geotextile, it is even possible to construct a floating cap over a fluid deposit. This method was used to cap FFT for placement of wick drains into Suncor Pond 5.

Wick drains are a standard method of dewatering weak, wet soils. In the oil sands, they are being utilized to dewater a zone of fluid fines resulting from segregation during CT deposition. To provide access for wick drain insertion, a coke cap was placed, started by placing a floating road matrix (Figure 13) upon a geotextile which was spread over the deposit during the ice-covered winter period. High clay content and bitumen in the FFT, results in low permeability and slow drainage. The time from cap placement through the period of wick drainage to attain the conditions suited for a terrestrial cover, may exceed two decades.

Electro-kinetic dewatering of fluid tailings or of flocculant-treated fluid tailings have been proposed by EKS, Inc. The method generates an electric field through the deposit from an array of horizontal or vertical electrodes using a proprietary method of fluctuating voltage. In the context of weak deposit capping, it can be deployed from a surface water layer and generate a dense surface zone within a few years from about 5m of MFT in a single sequence of treatment. Figure 14 illustrates a horizontal electrode array deployed through 5m of FFT under 2m of surface water. The method can be considered as an alternative to placement of wick drains from a floating cap while completing dewatering within a few years rather than decades.

Natural formation of a detrital layer will appear over a deposit as plant life and micro-fauna invade a pit lake. For water-capped (untreated) MFT, this is anticipated to generate a mudline-water interface sufficient to avoid unacceptable turbidity occurrences during thermal turnovers common in regional lakes. The Syncrude Base Mine Lake demonstration should answer this question within a few years.

SUMMARY

With the ubiquitous use of deep, in-pit, clay-dominated, fine-tailings deposits in the oil sands, it will be necessary to develop and select capping methods most suited to the deposit characteristics and the chosen reclamation surface. Methods are available to cap a full spectrum of deposit conditions. The methods chosen will depend on factors existent at the time for capping, including:

- The geotechnical condition of the deposit at the time of capping
- The practicality for water removal and drainage from the deposit surface
- Cost and cost uncertainty associated with the method in the oil sands environment
- Expertise and experience with the method available to the operator
- The choice of reclamation surface – water, or wetland.

The attached Table 2 sets out characteristics and considerations for capping method(s) to complete reclamation with the desired surface for different end landforms.

Table 2. Deposit Closure and Capping Methods for Closure Landforms

	Pit Lake	Wetland
Atmospheric Drying & Freeze-Thaw for Surface Desiccation	Densifies low-density upper layer – isolates water from fines slurry.	Useful for both fines-dominant and CT deposits. Provides a trafficable base for adding a surcharge layer and reclamation soils.
	Water must be removed and stored or disposed to complete desiccation.	
Mechanical Placement of Sand or Overburden		Placement of sand, overburden and reclamation soil. Can be deployed over a surface crust or a frozen surface with or without geotextile.
Hydraulic Placement of Sand		Particularly suited to CT deposits.
Sand Spray	Could be used to densify upper zone of FFT or a treated FFT deposit.	
Coke Capping		Low-density aggregate for initial capping of very weak soils or fluid. Must be kept drained to provide trafficable surface.
Particlear®		Could be used to provide a trafficable surface for placement of surcharge and/or reclamation soils.
Wick Drains		Can be used to dewater after pre-capping with another method to provide access. Require close spacing and lengthy timeline.
ElectroKinetic Dewatering	Could be used to reduce volume and increase upper zone density of MFT deposit or treated deposit.	As an *in situ* treatment method, an alternative to wick drains that can be deployed from surface water with much-reduced treatment time.

REFERENCES

i *A Guide to Audit and Assess Oil Sands Fluid Fine Tailings Performance Management,* Canada's Oil Sands Innovation Alliance, August, 2014.

ii *Technical Guide for Fluid Fine Tailings Management*, COSIA, August 30, 2012.

iii *Oil Sand Tailings: Challenges to Managing Fluid Tailings*, Alexander Hyndman, Tailings and Mine Waste '13, November 3rd – 6th, 2013, Banff, Alberta, Canada.

iv The numerical analyses described in this paper were carried out using FSConsol based on the Finite Strain Consolidation Theory of Gibson, England & Hussey, Canadian Geotechnical Journal, 1967. The material parameters for the compressibility and permeability relationships were obtained from large strain consolidation tests derived from *Geotechnical Behaviour of In-Line Thickened Oil Sand Tailings*; Jeeravipoolvarn, S. 2010.. PhD thesis. Civil and Environmental Engineering. University of Alberta. Edmonton, Alberta. 410 p. For the treated MFT case, the tailings storage area is assumed to be 75 m deep. For simplicity, the storage area is filled instantaneously, with a slurry solids content of 50%.

v *De-Licensing of Oil Sands Tailings Dams - Technical Guidance Document;* Oil Sands Tailings Dam Committee; March 2014.

vi *Tailings Bearing Capacity of Composite for Reclamation*, Richard Dawson, Norwest Corporation, 2010.

vii *Rapid Clay Dewatering Phase II: Field-Scale Tests Final Report*; December 2001; W. David Carrier, III Principal Investigator Argila Enterprises, Inc. 76 Woodside Drive Lakeland, Florida 33813-3557

viii *Modification of fluid fine tailing's* (SIC) *rheological and stacking properties by in situ silica polymerization*, Fred Godbille, DuPont Research & Business Development, Canada and Bob Moffett, DuPont Chemicals and Fluoroproducts, USA; Paste 2014, June 8 - 12, 2014, Vancouver, Canada.

ix *Suncor Pond 5 Coke Cap*; Jack Caldwell, Patrick Sean Wells, Joseph Fournier; October 19, 2010; Tailings and Mine Waste, 2010 Vail, Co.

THE DBM APPROACH FOR SETTING ENGINEERING DESIGN CRITERIA FOR AN OIL SANDS MINE CLOSURE PLAN

Monica Ansah-Sam[1], Leah Hachey[1], Gord McKenna[2] and Brent Mooder[2]
[1]Shell Canada Ltd, Calgary, Canada
[2]BGC Engineering, Vancouver, Canada

ABSTRACT

A recent trend in the mining industry is to focus on closure landscape goals, design objectives and criteria supporting these goals. This avoids design omissions and extensive rework in the field. We propose an engineering approach to closure planning involving design basis memoranda (DBM). The proposed approach employs a hierarchical system of closure goals, objectives, and design criteria to support planned post-mining land uses. A closure goal is an overarching aim (e.g., to reestablish a locally common boreal forest on the reclaimed land). An objective is a design basis that supports the goals (e.g., the design manages the water table where commercial forest is required). Each design criterion is specific and measurable and supports a design objective. The DBM also specifies the design events, material parameters, and methods of analyses. Clearly stated goals, objectives, and criteria allow interested parties to review and contribute to the DBM before development of mine, tailings and reclamation plans. Clear design bases are especially critical to tailings technology selection. A DBM also allows construction and performance of the reclaimed landscapes to be easily compared to the design conditions. Examples from Shell Canada's 2016 DBM for its Muskeg River Mine are presented.

INTRODUCTION

A mine closure plan provides post-mining conditions for a planned or operating mine. This closure plan defines the final topography that will support watersheds, reclamation soil salvage and placement, revegetation, habitat development, etc., aligned with targeted end land uses. The closure plan should inform and guide mine planning as an integrated part of the whole operation. To be successful, the closure plan needs to evolve and adapt to changing conditions. Some examples of change could include new knowledge through advances in research and technology or feedback from continual stakeholder involvement.

Historically in the oil sands, mine closure plans have been developed to fulfil regulatory requirements rather than as an integral part of the

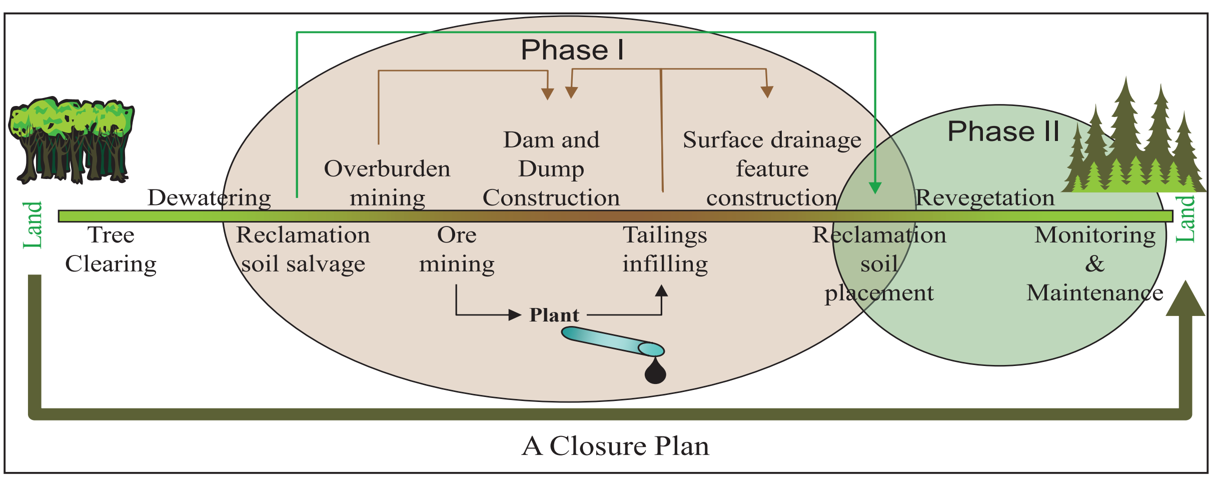

Figure 1. Schematic representation of the series of activities involved in successful closure planning (Hachey and Lanoue, 2011)

mine planning process. Within the past decade, improvements have been made to engineering rigour in providing a direct linkage between mine plans and the resultant post mining landscape. A closure landscape plan is a building block to the closure plan, which develops closure topography based on the underlying mine plan. The closure landscape plan is used to provide a realistic base or reclamation ready surface from which to develop plans for progressive reclamation, including placement of cover soil, revegetation, watercourse construction, and End Pit Lake (EPL) construction. Figure 1 provides a schematic of the activities included in the volumetric phase (referred to as phase 1) resulting in a closure landscape plan that can then undergo testing and modelling (referred to as phase 2). The life of mine closure plan encompasses both phase 1 and phase 2 planning and modelling activities.

In following this approach, at Shell's Muskeg River Mine (MRM), a life of mine closure plan is being developed and is intended to add value to the operation through:

- An integrated mine, tailings and closure plan that is volumetrically accurate. This alignment will minimize rehandle, rework, and allow Shell to meet its environmental and regulatory goals with respect to reclamation and closure;
- Identifying opportunities more easily for improved integration in the mining, tailings and closure plans and increasing transparency in reclamation plans;
- Identifying closure assumptions and risks in planning, schedule, and costs; and
- Fulfilling corporate social responsibility.

This paper describes how a closure landscape design basis contributes to developing an effective mine closure plan. Shell's MRM life of mine closure plan provides an example to illustrate the application of a design basis approach.

The design basis approach employs a hierarchical system of closure goals, objectives, and design criteria to support planned post-mining land uses. A closure goal is an overarching aim (e.g., to re-establish a locally common boreal forest on the reclaimed land). An objective is a design basis that supports the goals (e.g., the design manages the water table where commercial forest is required). Each design criterion is specific and measurable and supports a design objective. The design basis is documented in a design basis memorandum (DBM). The DBM also specifies the design events, material parameters, and methods of analyses. Clearly stated goals, objectives, and criteria allow interested parties to review and contribute to the DBM before development of mine, tailings and reclamation plans.

The MRM closure DBM was informed by land use expectations and closure goals developed through Shell's internal operations, regulatory requirements and the results from stakeholder engagements. The DBM was reviewed and accepted by Shell engineers, scientists and management at the start of the closure design process. The resulting closure plan was integrated with the mine plan and mine operations through the agreed-upon design criteria.

DESIGN BASIS APPROACH

The design basis approach is commonly applied to civil and structural engineering projects such as buildings and dams. Such projects feature well defined goals and objectives and readily defined and regulated design criteria (e.g., building codes). In contrast, the goals for a post-mining closure landscape are challenging to define and will evolve over the course of a long mine life (often greater than 20 years). Closure planning is inherently multi-disciplinary and includes geotechnical and mine engineering, hydrogeology, hydrology, geochemistry, soils, vegetation and wildlife specialists. Furthermore, the disciplines required for closure design interact in complex ways that make integrated planning critical for success. Closure plan development and implementation requires integration and collaboration by senior management, operations and the multi-disciplinary design team.

The first step in closure planning is to define possible end land uses which support the overarching goal. For the oil sands mines in north eastern Alberta, the primary goal is regulated to be a locally-common, self-sustaining boreal forest ecosystem. Typical end land uses for the region, can include commercial forestry, wildlife habitat and traditional use. In addition, as goals evolve other land uses may be agreed upon through partnership with local communities and regulators, such as commercial, industrial or recreational land uses.

Once end land uses are defined, the next step is to develop a clear closure design basis and objectives that support the goals and align with the targeted end land uses. The specific design bases link the design criteria to the targeted landform. The design criteria guide the closure landscape designs and provide a means to measure how closely the closure plan aligns with the closure goals. Design criteria need to be measurable and specific. The level of detail included in the design basis should be proportional to the level of design applied. During the detailed design phase, the expectation is that there would be more criteria and more detail than that provided during development of the conceptual level design.

Developing a DBM that aligns mine operational requirements with closure goals creates the conditions for agreement between the mine operator, regulators and other stakeholders. This leads to constructing a post-mining landscape that meets the expectations of local communities and regulators.

ADAPTIVE MANAGEMENT

Closure planning at Shell follows an adaptive management model (CEMA 2014) (see Figure 2), which includes an iterative approach to planning by applying learnings from experience and new information (see Figure 3). Where current experience or information is limited, models are relied on to predict future outcomes. When these outcomes are not fully aligned with the targeted end land use goals, they are addressed and incorporated into the next planning iteration or goals are adjusted accordingly. Other considerations that may introduce changes to the plan include changing stakeholder expectations and regulatory requirements that lead to changes in the closure goals.

Through iterations of mine and tailings plans, assumptions and gaps will continually be identified and addressed, which will drive progress towards a feasible and executable closure plan aligned with the underlying mine and tailings plans. The closure plan regulatory submissions represent the best integrated effort to date. However, further work will be required to test the sustainability of the current plan. For example, current plans that indicate a wetland in a specific location may require "testing" to confirm that the wetland is sustainable into the far future (post closure).

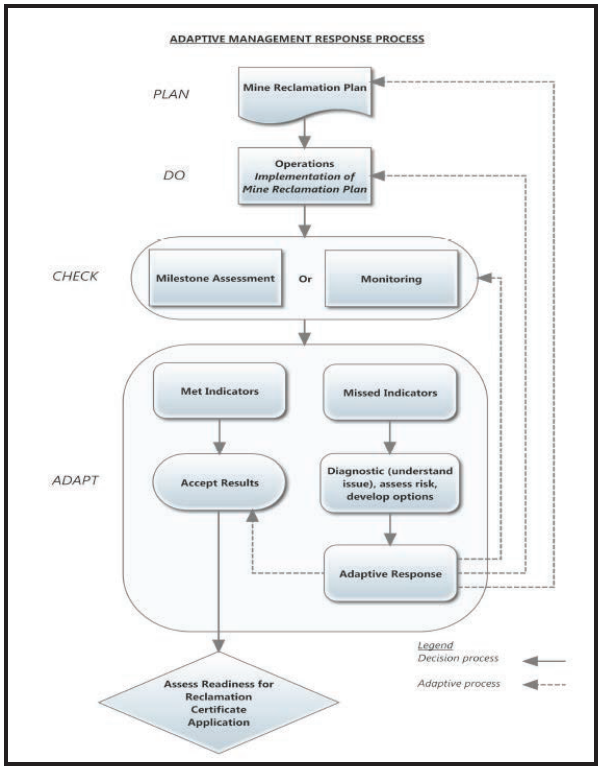

Figure 2. Adaptive Management Model (CEMA 2014)

HIGHLIGHTS OF THE MRM DESIGN BASIS

The DBM developed to support the MRM life of mine conceptual closure plan included 27 key design objectives with over 75 associated design criteria. These criteria were applied to the various landform designs, including mine waste dumps, tailings facilities (external and in pit), EPLs and the infrastructure and watercourses that connect these landforms. The design basis to support the closure plan is focused on the ground topography and long term stability of the landforms from the perspective of geotechnical, geomorphology, hydrogeology and hydrology, mine reclamation and biodiversity disciplines.

To illustrate the value of the DBM to closure planning, five of the design objectives are summarized below. Design criteria associated with each objective are described in the supporting text.

- **Accommodate beaver activity**. Beavers are a keystone species in the Oil Sands region. Beaver activity includes damming streams and rivers, enlarging wetlands, cutting down trees and burrowing into the banks of rivers and streams. Beavers will be active in the closure landscape and closure landform designs need to accommodate the impacts of beaver activity. To design for beaver activity, channels are designed to accommodate a 3m high beaver dam. Beaver dams are assumed to wash out in the 100 year return period flood events. Freeboard requirements for channels and outlets account for beaver activity planting prescriptions are adjusted near waterways to include species that beavers prefer.

- **Provide water table control in planned upland forest areas.** To allow for the establishment of upland forest vegetation, the rooting zone of the vegetation should be kept above the water table. In areas designed for 'uplands' (forest vegetation planting), the topography is adjusted to maintain a water table depth of 2m or greater.
- **Provide access for monitoring and maintenance**. The reclaimed landscape will be monitored for a post-construction period and elements of the reclaimed landscape may require maintenance. The closure plan should provide access consistent with the requirements of the monitoring and maintenance plan.
- **Avoid ponded water near slope crests**. Ponded water near slope crests can cause gullying and geotechnical instability on the landform. Prevention of water from ponding up to a 1:100 year flood event within the geotechnical buffer zone should be maintained. In addition, prevention of ponded water under flows up to the probable maximum flood within the geotechnical critical zone (these zones are delineated during design to manage risk of catastrophic slope failure) need to be adhered to.
- **Integrate designs across lease boundaries with natural areas and adjacent developments.** Other neighbouring developments that exist, are approved, or are planned within the Muskeg River watershed. The other operations may have an impact on MRM water balance, closure land use, and revegetation considerations. The following operations approved by Alberta regulators will be considered: Susan Lake Gravel Pit, Hammerstone Quarry, Muskeg Valley Quarry, Syncrude Aurora North and Aurora South, Jackpine Mine, Husky Sunrise Thermal Project and Imperial Oil Kearl Oil Sands Project. The design criteria are to maintain landform continuity across lease boundaries where reasonably practicable. This includes continuity of drainage system's elevations and flows across lease boundaries.

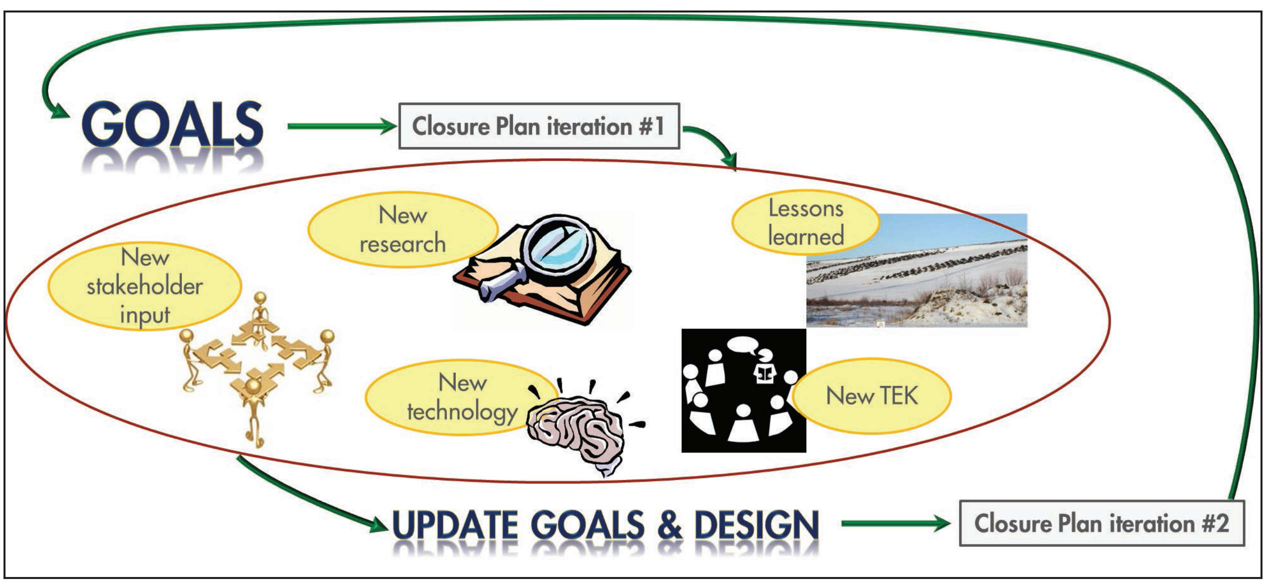

Figure 3. Iterative Approach

Figure 4 illustrates the closure landscape designed using the design objectives and associated design criteria defined in the MRM DBM. The design reflects the trade-offs inherent in the competing closure goals that form the foundation of the DBM.

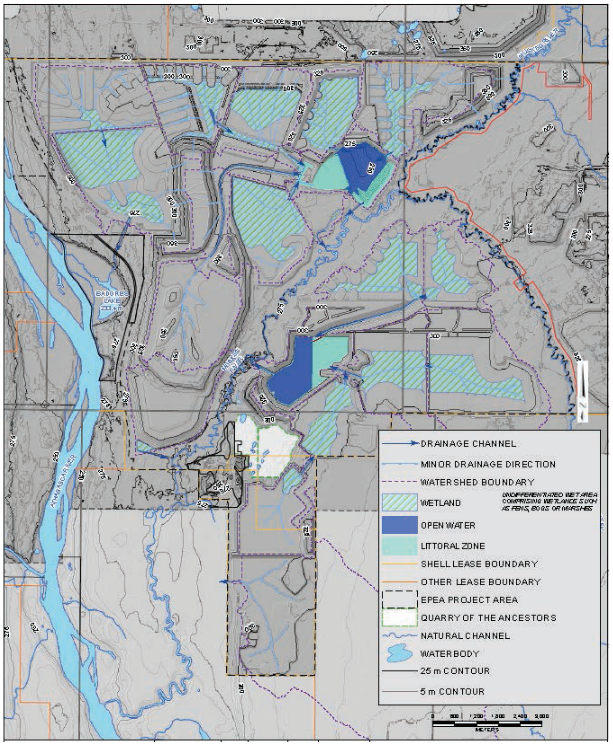

Figure 4. 2016 MRM Closure Landscape

For example, First Nations desire to have a landscape suitable for beaver activity must be incorporated in such a way that, it does not compromise geotechnical stability of landforms.

CONCLUSIONS

Application of the design basis approach to closure planning is challenging due to the inherently multi-disciplinary nature of closure planning. Clearly defined goals that are aligned with post-mining land uses form the foundation of an effective design basis. Developing concise, measurable design criteria from the design objectives requires weighing competing objectives and an appreciation of the various disciplines that influence closure landscape design.

The closure plan, and therefore the closure topographical surface, must be explicitly tied to the mine plan volumetrics, and vice-versa, to ensure that closure plan objectives can actually be achieved. The mine plan volumetrics are the pillars of the closure plan. So although there may be limitations to what can be achieved in reclamation, in the iterative approach previously presented, those limitations can be identified and improved in future versions of the mine and reclamation plan. This also provides further confidence that the closure surface can be constructed and thus, reclamation goals and objectives achieved. Post-mining land uses are based on appropriate stakeholder consultation during planning and execution of closure activities, constrained by the limitations imposed by mining operations.

The closure plans that are the outcome of using the design basis approach and meet well-defined design criteria inherently include more engineering rigour and are aligned with mine operations and post-mining expectations. In this way, a well-defined design basis developed in collaboration with the designers, mine operators, local communities, and regulators, provides a valuable linkage between mine development and operations and the post-mining landscape.

ACKNOWLEDGEMENTS

Sincere appreciation and thanks to Julian McGreevy of BGC, Dustin Theberge, Allison Norling and Scott Martens of Shell Canada who provided input into the closure landscape plan and associated design basis memorandum.

REFERENCES

CEMA. 2014. ”Guidelines for Wetland Establishment on Reclaim Oil Sands Leases”. Calgary, AB. Accessed at http://cemaonline.ca/index.php/administration/doc_download/285-guidelines-for-wetlands-establishment-on-reclaimed-oil-sands-leases-third-edition-2014.

Hachey, L.M. and Lanoue, A.V. (Sept. 2011) “Use of 3-dimensional topography as a tool for closure integration at Syncrude Canada Ltd.’s Mildred Lake and Aurora North leases” In paper presented at the Australian Centre for Geomechanics, Proceedings of the Sixth International Conference on Mine Closure, Volume 1. (P.403-412).

A REGIONAL VIEW OF SITE-SCALE RECLAMATION DECISIONS IN THE ATHABASCA OIL SANDS

Neeltje Slingerland and Nicholas Beier
University of Alberta, Edmonton, Canada

ABSTRACT

The post-mining landscape in the Athabasca oil sands has been widely debated by engineers, sociologists, ecologists, and economists alike. These articles and perspectives have hypothesized what may become of the region, but there has been limited graphic communication of the trajectory towards a post-mining Athabasca region, and thus our understanding of the regional end landscape is frequently thought of in silos.

This paper addresses the post-closure regional landscape graphically with special attention to the details presented in oil sands operators' latest combined Life of Mine (LOM) and Closure and Reclamation (C&R) submissions to the Alberta Energy Regulator. Specifically, we will be looking at proposed post-mining site topography, drainage plans, and substrates for each mining lease to identify site-scale effects. The cumulative effect of these plans at a regional scale will be assessed in order to reveal the connections between micro-scale decisions and regional-scale effects. Through the use of historical satellite imagery and mine plans for the region, a picture of the proposed future will emerge. By closely examining the cumulative effects of proposed closure plans and tailings properties across the Athabasca region, this project sheds new light on the role that scale plays in mining and the potential benefits attained through regional analysis.

INTRODUCTION

The Athabasca oil sands surface mining region has been noted globally for its large scale land disturbance. Mining is a temporary use of the land, and this global spotlight has increased the pressure on tailings and mine waste engineers, such that they must not only think of efficiency, but also now of closure and reclamation ramifications. As Dr. Morgenstern stated in his 2012 keynote presentation at IOSTC, "the reclaimed landscape is dominated by surface and subsurface water considerations, and given the current limited progress in dealing with these issues, it is my view that the updated End Game will … not be fit for purpose" (Morgenstern, 2012). Since 2012, new tailings technologies tested have been met with varying degrees of success.

The glossary of geology defines a landscape as a "distinct association of landforms, as operated on by geological processes (exo- or endogenic), that can be seen in a single view". A landform, as defined in the same glossary, is "any physical, recognizable form or feature on the earth's surface, having a characteristic shape, and produced by natural causes." (CEMA, 2006, p.2). While we may not be constructing landforms by this precise definition, anthropogenic waste-forms are certainly being constructed more rapidly than ever before in the Athabasca region, and creating a new, distinct landscape in doing so.

The overwhelming goal of the post-mining landscape is "to achieve maintenance-free, self-sustaining ecosystems with equivalent land capability to pre-development conditions, such that the developed and reclaimed lands can receive reclamation certification and be returned to the Crown" (Suncor, 2011). This all-encompassing end-goal is common to all mine operators in the region, but its ambiguous nature has left room for interpretation, and experts from various realms have honed in on what they see as the most important outcome post-mining. Engineers lean towards geotechnical stability as the foremost concern, hydrogeologists and geochemists focus on maintaining adequate groundwater quality and quantity, ecologists on diverse flora and fauna, while economists and sociologists are more likely to focus on the future economic productivity for the region/province/nation or long-term community sustainability, respectfully.

The focus of this work is to analyze the core of the reclaimed landscape – the proposed topography, resultant drainage regime, and construction materials (mine waste properties) – with respect to their impact on the region as a whole. For the purposes of this work, it is assumed that this new ground and foundation for surface works impact the region in terms of geotechnical stability, groundwater quality, and ecological diversity, which in turn affect the sustainability of a regions' community and economy.

Mine reclamation in the oil sands has greater complexity and more interconnections at play than in traditional mine reclamation projects: a broader scale and more challenging materials are just two examples of this. Spatial visualization of technical information can assist consultants, communities, and other stakeholders to understand and thus participate more productively in the planning and design of the future landscape (LaGro 2008). This work, particularly in the accompanying presentation, will visualize potential substrate challenges in the closure environment.

MATERIALS, TECHNIQUES, & RECLAMATION CHALLENGES

Mining Waste Products

Overburden is a variable-thickness layer of clay, silt, sand, and clay-shale overlying the oil sands ore body and lying below muskeg and soil salvage material harvested for reclamation (Figure 1). Once removed, this overburden is typically placed in an above grade (out-of-pit) Overburden Disposal Area (ODA), compacted, and landform graded to a pre-determined shape and elevation (Barber et al. 2015). When required, selected overburden is used for zoned fill on in-pit dams, and it is also occasionally used to backfill open pits (Kessler et al. 2010).

Overburden is not consistent in its composition – particularly with respect to mineralogy and water content (McRoberts, 2008). Some is considered to be lean oil sand (less than 7% bitumen), while in other areas no bitumen is contained. Some areas have water content such that "slop cells" are required to contain it.

All oil sands mines have overburden composed to some degree of the Clearwater formation: an interbedded marine-origin clay-shale, sandstone, and clay-silt unit (Chapman, 2008). Most mines, especially those on the east of the Athabasca River, also have sandy till outwash and the Grand Rapids formation (predominantly sandstone) overlying oil sands (Conly et al. 2002).

One challenge in reclaiming ODA's is that Clearwater formation overburden has been shown to be pyritic with acid generating potential (Wall, 2005) when exposed to oxygen. It is also saline-sodic to a degree which inhibits plant growth, required for erosion control and reclamation (Kessler et al. 2010). Compaction-induced low-permeability of underlying overburden, advective transport due to evaporation and evapo-transpiration, and strong diffusion gradients in salt content between overburden and surface reclamation soil are noted as mechanisms for upward mobility of saline water (Kessler et al. 2010).

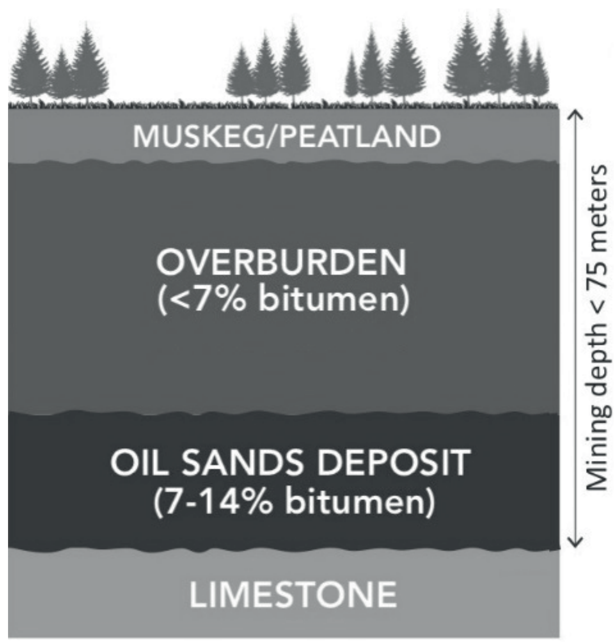

Figure 1. Schematic cross section of an oil sands deposit. Adapted from www.oilsandsmagazine.com

Adverse effects of Clearwater formation overburden on surface vegetation have been successfully avoided through the use of a thick 100 cm cover of glacial origin (Kessler et al. 2010). A groundwater flow system and oxidizing conditions exist within South Bison Hill; a landform constructed of Clearwater formation overburden removed and reclaimed on Syncrude's Mildred Lake Mine. However the presence of relatively low permeability materials surrounding reclaimed Clearwater ODA's have been credited for both lowering internal water tables, and directing the majority of groundwater flow around the structure (Chapman 2008). This is positive in terms of geotechnical stability of the structure and its geochemical impact on surrounding land.

Waste Products of Processing & Upgrading

Tailings ponds typically range from 40 to 100 meters in height and are constructed in the form of a ring dyke due to the low topographic relief provided by the natural landscape (McRoberts 2008). Ring dykes are initiated through construction of a started dyke made of overburden, then raised sequentially with compacted lifts of coarse sand tailings. Chimneys and other drainage devices as well as various monitoring instruments are also installed within the dykes for safety purposes.

Tailings are a by-product of the bitumen extraction process created by crushing ore until it is sufficiently fine to separate the bitumen from the sand using hot water and chemical processing aids. Bitumen is then recovered as froth, and the remaining solids, process water, and residual bitumen are deposited as a slurry in a tailings pond. Tailings are often treated to reduce their water content and volume, and process water is recycled as much as possible to reduce fresh water usage.

Fluid fine tailings (FFT) are a waste material composed of process water and suspended silts and clay solids. The settlement of this material is complicated by chemical interactions between the solids and small remaining bitumen fraction (Hyndman & Sobkowicz 2010). Tailings which remain unconsolidated in this way after 2 or more years are called mature fine tailings (MFT).

Slurried tailings - those that have not been dewatered – pose a challenge long term because they require a water cover. Delicensing of tailings dams requires, for geotechnical stability and liability reasons, the dam to no longer act as a dam (CDA, 2014). A water cover would therefore inhibit delicensing of above grade structures. Dewatered tailings – those that have had water removed or had sufficient solids added to attain a shear strength of 5 to 10 kPa – have more options for reclamation, and delicensing may be possible in the future. Given the properties of oil sands tailings, this is a challenge. For example, the water volume in MFT would need to be reduced by about 80%, and its total volume reduced to 70% of the original to reach a remoulded undrained shear strength of 5 to 10 kPa (Sobkowicz 2013).

In an effort to generate a more easily reclaimed tailings material several different treatment and management techniques have been employed which give the tailings different properties. Coarse sand tailings have had fine solids removed, and tend to be used in dyke construction. Mixed fine and coarse, or just fine tailings are preferably placed in-pit, but are often placed in external tailings ponds until space is available in-pit (Hyndman & Sobkowicz, 2010).

Some possible long-term behaviors of various oil sands waste products and post-reclamation substrate materials are listed below; however the list is not exhaustive as knowledge is still being acquired as technologies evolve and reclamation trials take place (BGC 2010).

Currently employed at commercial scale, hydraulic sand capping of fine tailings has been used where the underlying deposit is trafficable by small equipment (BGC 2010). A conservative design is necessary for such structures to guard against liquefaction failure of sand, as this remains a threat long after consolidation has occurred (BGC 2010). The sand cap must also be thick enough so that the salts from capped tailings process water can be flushed without negatively impacting the rooting zone of reclamation plant species. Salts can cause die-off of plant material, exposing the landform surface and increasing erosion potential.

The underlying tailings being capped in-pit or in above-ground tailings ponds are not always homogeneous: processing plants do not output consistent materials over time and often different methods of dewatering are attempted and deposited within the same structure (McRoberts 2008). For example, consolidated tailings (CT) may be placed next to mature fine tailings (MFT) and CST. Differential settlement occurs as stress is applied (for example, loading when placing a cover) across materials with variable water contents and permeabilities. This is a risk when a tailings pond has various tailings distributed unevenly within it, as occurs at virtually every containment pond where fine and coarse tailings are hydraulically deposited. This results in an alluvial fan-style distribution of coarse particles at the end of pipe, and fines furthest from the end of pipe.

Differential settlement is not a challenge when it occurs in small differences; however, in the case of larger differential settlements, large ponds can form in the lower elevations. Extensive ponding requires removal and thus ongoing maintenance at an addition cost to the owner, and also delays delicensing (BGC 2010). Modelling is required to determine expected total settlements for various tailings, and if large differential settlements are possible. This information will help to inform the best path toward reclamation for the landform in question.

In general, weak or liquefiable materials need to be constructed with sufficient factors of safety to guard against catastrophic failure due to loading, seismic action, or erosion, and consolidation after surface reclamation should be minimized. A summary of various specific tailings treatments and associated reclamation concerns can be found in Appendix 3 of BGC 2010.

Coke is a byproduct of the bitumen upgrading process, and is available at mine sites with upgraders. Coke is slightly less dense than fluid tailings, so when placed carefully overtop of tailings the coke naturally floats. This was most notably used on Suncor's Pond 5, where coke was placed over a frozen tailings surface in winter, and floated over the tailings after spring melt (Wells et al. 2011). Geogrid was used in this case for added reinforcement.

Water

Tailings dewatering is a major issue with respect to reclamation, but the process affected water (PAW) being removed from tailings on dewatering is also a concern. Sobkowicz (2013) estimates that this PAW could amount to 710 M m^3, which would need to be stored until it has been sufficiently treated to safely be released to the natural environment. This water is most likely to be leached gradually out of tailings landforms, requiring long-term monitoring and collection systems in place (Ferguson et al. 2009).

Each mine site has unique parameters and geology guiding the decision making process. Closure drainage and topography plans must take this into consideration at the site level while regional plans must consider the broader patterns and distribution of landforms, waterways, and their function with respect to one another.

LANDFORM DESIGN & CLOSURE WATER MANAGEMENT

Mine closure and reclamation (C&R) plans outline the post-mining reconstruction of soil profiles, topography, drainage systems and water bodies, vegetative communities, and habitat for a particular mining lease. Each mine C&R Plan consists of several different proposed landforms or features including backfilled pits, ODA's, solid tailings landforms (ETF's), lakes and ponds, and water conveyance features such as vegetated or armored outlet structures, channels, and creeks. Geotechnical stability is the foremost concern in landform design and is addressed first in the 'Landform Design' chapter within all C&R Plans.

Each of the presently operating mines expect to convert their ETF's into solid landforms and grade them with ridges and swales to facilitate a surface capable of draining excess precipitation via a breached area(s) along the ETF dyke. The particular method of achieving this end result varies from company to company and from landform to landform. The mine age, and correspondingly the extent of closure planning, at the time of the 2011/12 combined C&R submissions to the AER naturally varied dramatically. As a result the plans of older mines are generally more detailed and methods have been verified to a greater extent as compared to those of younger mines; however, this was not a steadfast rule.

Few C&R plans provided details with respect to the target slopes or range in slopes, slope lengths, etc. to be used in final landform construction, instead opting to provide qualitative characteristics they will aim to achieve. Some provided current tailings dam slopes but none for the target end landform. For those that did provide target slope angles, grading plans often illustrated slopes outside of these targets: plateaus were often excessively flat, while dykes and OBD's were excessively steep. Most provided general information on the type of covers that would be used for each type of landform.

With respect to ETF's, more than half of the mines indicated they would be installing a CST cap. CNRL proposed to cover and grade their relatively impermeable non-segregating tailings (NST) with a coarse, high permeability NST cap. CNRL pits in-filled with tailings will be given a thick layer of coarse sand tailings, while graded ridges and swales will transport excess precipitation and leached PAW from these structures to wetlands or pit lakes. Shell Canada's Muskeg River Mine and Jackpine Mine proposed to infill their tailings ponds with CST, then cap with undifferentiated overburden and 0.5 m of cover soil, or a combination of peat-mineral mix, surface soil, and coarse subsoil. Suncor's Base Mine and Fort Hills mines proposed both CST and low-sodic overburden depending on the location. All ETF's are proposed to be vegetated to some degree, and most propose armoring in areas with steep slopes.

Reclaimed in-pit and external ODA's are typically proposed to have steeper slopes than reclaimed ETF's. Two mines listed a target of 4H:1V to 10H:1V, while two had a target specified of less than 3H:1V, and the others did not specify. Overland flow and evolution towards directed vegetated swales are the typical drainage methods proposed for these landforms. Imperial Oil's C&R Plan for the Kearl mine site outlined their expectations for a high surface water yield due to steep slopes and relatively impermeable materials. This tended to be a guiding feature of most companies' topographic design and water management plans. Clearwater formation overburden tended to be prescribed thicker covers than did non-clearwater overburden materials due to their associated geochemistry issues and the desire to create a vegetated surface on closure which is not affected by saline or sodic pore water migration towards the root zone. Proposed covers consisted of clean overburden, CST, or cover soil. A summary of overburden capping materials and grading is provided in Table 1. Dykes are typically not contoured and all surfaces of overburden dumps are proposed to be vegetated.

There is limited commercial scale evidence on the degree of effectiveness of end pit lakes as a cover and water treatment system. As a result details on the mechanisms acting in reality are sparse in closure and reclamation plans; however, all mining leases propose at least one end-pit lake, and all include water treatment wetlands. The conceptual closure plans generally show a waterway linking landforms with positive topographic relief to a network of wetlands and lakes before exiting into the natural environment. They are anticipated to be supported by surface runoff after initial filling. Figure 2 shows an example of this drainage network concept provided by Shell Energy Canada in their 2012 combined Life of Mine and Closure & Reclamation Plan for Muskeg River Mine.

For all landforms, covers will need to be constructed to avoid seepage, create a surface suitable for vegetation growth, and in some cases to mitigate undesirable behavior of underlying substrates. Seepage collection at low elevations will be necessary, as will allowance for some surface alteration over time due to settlement. Landforms are considered to become more stable internally over time, but erosion and evolution of the landforms at the surface need to be considered through flexibility in the landform design.

Table 1. Surface design and capping criteria for overburden storage landforms. From 2011/2012 Closure and Reclamation Plans submitted to the Alberta Energy Regulator (AER)

Operator / Mine	Landform Surface Shape, Slope Angles, & Cap Material
CNRL Horizon	*Slope:* 4H-10H:1V (sides) *Shape:* Crowned from center or contoured with secondary drainage channels *Cap:* reclamation soil (a mixture of organic and mineral soils)
Imperial Oil Kearl	*Slope:* 4H-10H:1V (sides) *Shape:* Crowned from center or contoured with secondary drainage channels. *Cap:* Reclamation soil.
Shell Jackpine Mine	*Slope:* Less than 3H:1V *Shape:* Upland plateaus & swales *Cap:* Clearwater and lean oil sands capped with 1 m clean overburden plus 0.5 m cover soil. Undifferentiated overburden capped with 0.5 m cover soil.
Shell Muskeg River Mine	*Slope:* Less than 3H:1V *Shape:* Channelization of surfaces *Cap:* 0.5 m RM over undifferentiated overburden & 0.5 m minimum RM over lean oil sands.
Suncor Base Mine	*Shape:* Contoured for natural appearance, surface irregularities. *Cap:* tailings sand or suitable overburden, RM.
Suncor Fort Hills	*Shape:* Contoured for natural appearance, surface irregularities. *Cap:* Sodic overburden is capped with suitable overburden or CST
Syncrude Mildred Lake	*Shape:* Plateaus with horseshoes and swales. *Cap:* 1.2 m thick cap on Clearwater overburden, including soil cover.
Syncrude Aurora N.	*Shape:* Graded for natural appearance, topographic diversity.

Note: RM = reclamation material.

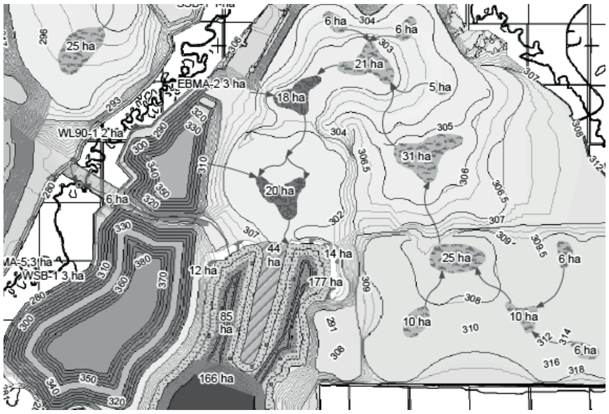

Figure 2. A portion of the proposed closure site topography and drainage network for Shell Canada's Albian Sands. Arrows show direction of drainage between wetlands and towards the end pit lake. Shell Energy Canada, 2012

REGIONAL ANALYSIS & THE ROLE OF SCALE

Ramifications and possible challenges with respect to the materials stored and those used as covers/ caps have been documented in operator's Closure and Reclamation plans, and can also be found in peer-reviewed literature. Liquefaction and process-affected groundwater mobilization are primary concerns where sand capping is implemented (Syncrude 2011). Where coke is used as a first capping layer, it has been noted that this material is also a natural resource that may be "mined" at a later date, disrupting the installed cover. Underlying fine tailings with mixed or variable tailings materials can lead to differential settlement and potential for ponding. Upward and lateral leaching of salts from saline-sodic overburden can affect water quality and the health of intolerant vegetation.

Wetlands planted with salt-tolerant vegetation are currently planned on all mine leases to capture process affected water and leached saline water from overburden. Here, the naphthenic acids will be allowed to degrade over time and the general water quality will be improved prior to entering the natural environment once again.

Each landform on each mine lease requires that countless design decisions be made. The consequences of these design decisions are multiplied when made on landforms hundreds of hectares in size, and over a cumulative area of 170 square kilometers. Minor water quality deviations from a single landform can be detrimental to surface and groundwater beyond the immediate environment, thus it is imperative that reclamation works of this regional magnitude perform optimally. Figure 3 shows the spatial extent of mine leases and their proposed regional topography in 2070, as indicated in the 2011 / 2012 Reclamation and Closure Plans submitted to the AER by mine operators.

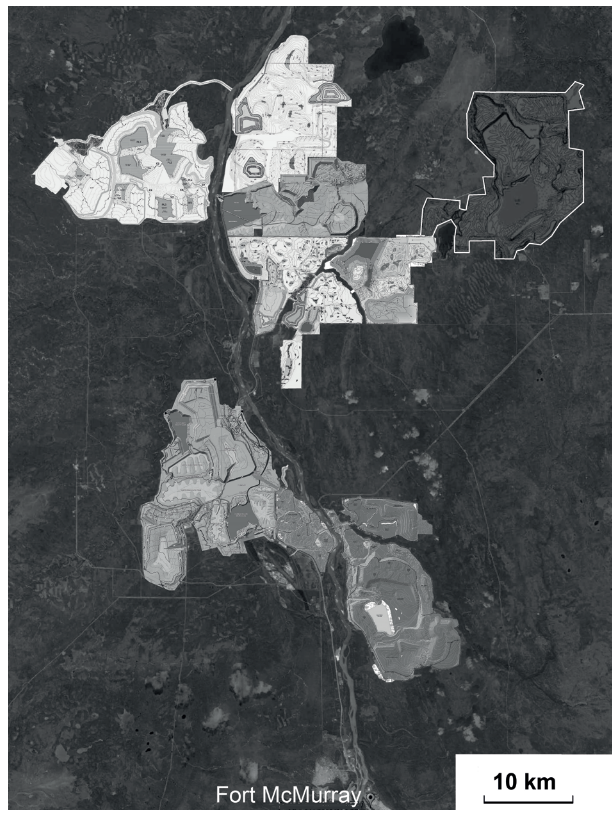

Figure 3. Regional compilation of proposed closure topography of all oil sands mining leases as submitted to the AER in 2011/2012. Approximate future date: 2070 A.D.

The fact that mine closure and reclamation plans are developed on a site-by site basis is in contrast to the scale of reclamation required. This sort of individual site-scale planning works well on small and medium scale mines which are isolated and located within the limits of one or two watersheds: Reconstruction of a functional landscape, surface water and groundwater regime is difficult, but manageable. As we can see in Figure 3, the scale of reclamation required in the Athabasca Oil Sands is much broader, lease limits directly abut one other, and rectilinear lease limits have no connection to the surficial environment. These limits make administrative sense, but the underlying purpose of reclamation is to create a natural analogue of local landforms, watersheds, and ecosites which are spatially non-linear (McGreevy et al., 2013).

Figure 4 shows a lease boundary between two adjacent mining sites owned and operated by separate parties. On the upper portion of Figure 4 (in grey) the mine operator has constructed an ETF with linear dykes delineating the perimeter. There is a roughly 200 m buffer between the dyke toe and the lease boundary. The mine site on the south (predominantly in white) has a similar 200 m buffer before their infilled pit edge is located. The northern mine has documented that "seepage from the tailings sand dykes… is expected to contain OSPW" (Oil Sands Process Water) and that seepage collection systems will be used to direct and capture this water (Syncrude Ltd., 2011). On the south side of the boundary a series of wetlands for water collection and treatment are located (Shell Energy Canada, 2012). A drainage divide has been constructed along the lease boundary, such that runoff from the north cannot enter the water treatment and collection system proposed on the south. An opportunity exists here to eliminate the relatively steep and linear edge of the former ETF (reclamation scheduled for 2051-2060) by elongating the slope through to the reclaimed wetland area in the south, scheduled for completion by 2025 (west) and in the years after 2055 (east). The resulting reduced slope gradient may be less susceptible to the erosion of this landforms' coarse sandy tailings. An additional benefit of collaboration and timeline coordination in this particular instance is a more naturalized aesthetic quality and likely less maintenance over the long term.

The approach taken by most oil sands mines is that knowledge will be gained over time, and as such, closure and reclamation plans will develop more detail as they near the end of their mine life or as structures approach their design life. Due to the early stage of many mines, relatively little detail is presented in closure plans, which tend to focus more on conveying an understanding of current best practices, rather than the precise methods with which those best practices will be applied to their site context. Topography and drainage plans are one component of the plan which are decisive, clearly communicating post-closure intentions. Slope gradient, length, aspect, elevation, ratio of upland to lowland, and spatial distribution are all readily observed or measured from a topographic map drawn with contours to scale.

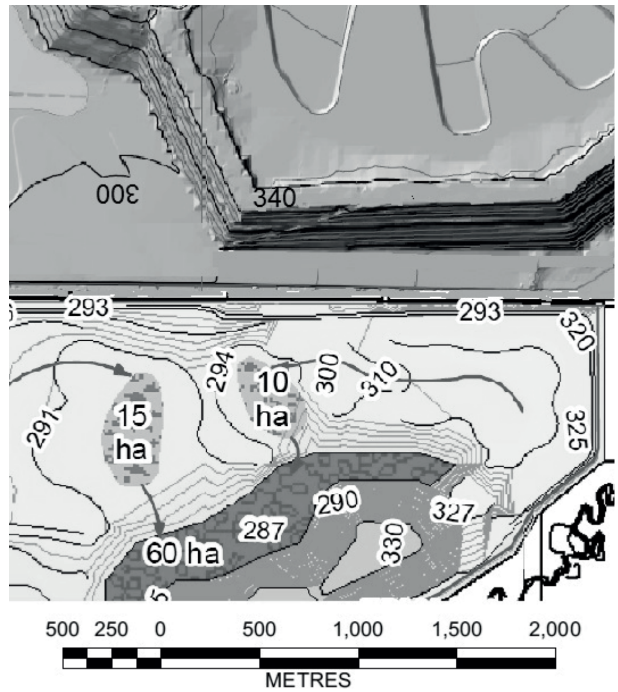

Figure 4. Example of a linear lease boundary (running horizontally at midpoint of figure) creating an opportunity for collaboration. Proposed closure topography of two adjacent mining leases with different operators.

Long-term erosion susceptibility of substrate material is a geotechnical and geochemistry concern as excessive erosion can expose tailings, and lead to loading of downstream wetlands and watercourses with excessive sediment. Across all mining leases, it has been noted that effort is made to re-grade the center of tailings and overburden landforms, while the grading of perimeter dykes are often not re-graded for closure: Slope gradients remain the same, and terraces initially required for maintenance are vegetated as is. For more than 30 years it has been widely documented that slopes created with an "s-curve" dominated by the concave portion are more mature and resistant to erosion than other types of slopes, including platform-bank (see Figure 5) or constant-slope hillsides (Toy & Hadley, 1987). The centers of these waste-landforms may cover more area than the side slopes on average, but in a region where negative effects are compounded simply due to the vast scale of work, there can be no margin of error.

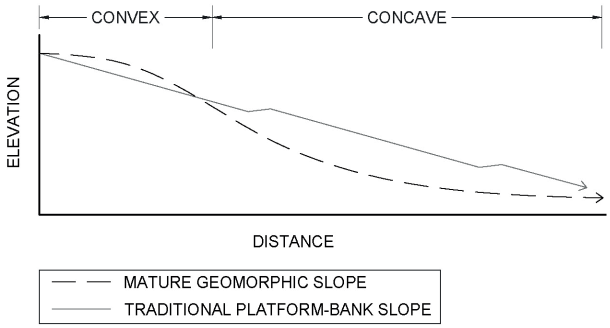

Figure 5. Mature slope with little erosion susceptibility compared to traditional platform-bank slope used on tailings dams.

Figure 6 shows the measured maximum length of slopes where water was allowed to flow over natural terrain in the AOS region. This figure illustrates that steep stretches occur over very short distances and most water is not directed via channels. Due to the more dramatic topography proposed for the closure landscape, channels have been proposed to guide water, but not where one would expect them according to Figure 6.

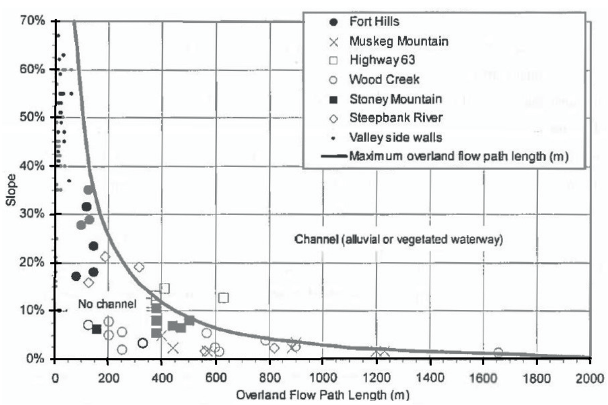

Figure 6. Recommended maximum overland flow length as measured in the Athabasca Oil Sands Region. From Golder (2004)

Figure 7 illustrates white highlighted areas where slopes may pose a risk due to long, uniform and steep slopes in excess of that found in the region on natural (more erosion resistant) terrain. Insufficient information was available on Kearl and Horizon mine sites to evaluate their proposed closure topography in this way, thus they have not been evaluated.

Where property limits allow, the highlighted slopes in figure 6 provide an opportunity for operators to re-assess their grading approach. Directing water via vegetated channels or through collaboration with adjacent lease owners and operators, slopes can be graded to a more mature profile such that they require less adjustment by nature post-closure.

Figure 7. Proposed topography for mine sites. Overland flow in excess of documented naturally occurring conditions have been highlighted in white for all mines except Horizon and Kearl.

CONCLUSIONS

Graphic imagery is an effective and efficient method of communicating both abstract and concrete ideas (Ackoff, 1989). Adapting reclamation best practices and guidelines to unique site conditions requires diverse information sources; the transfer of this information to a spatial context is an essential component of the planning and design process (LaGro 2008). This work has taken technical information on “waste-form” substrates, their documented reclamation challenges and/ or potential hazards, and applied it to the spatial distribution proposed by oil sands mine operators in their 2011 / 2012 combined.

Challenges encountered include surface settlement, leaching of saline groundwater from overburden and tailings substrates, and erodibility of coarse sand often used for capping landforms. The topographic design used to shape substrate materials can help or hinder reclamation. In particular grading of these waste-forms to mimic natural features, albeit with slopes adjusted for material type, can reduce the likelihood of erosion and potential exposure of tailings, loading of waterbodies, etc.

This work highlights the potential for topographic and drainage design to be completed from a regional perspective. The next combined life of mine and reclamation plan is due in 2021, leaving owners and operators 5 years to collaborate more on their boundaries with respect to site grading.

The leases shown in Figure 3 do not include Total SA's Joslyn North Mine, Suncor's Voyageur South Mine, Shell Canada's Jackpine Mine expansion or Pierre River Mine, Teck's Frontier Mine, or Syncrude's Aurora South which have either been placed on hold or are in early planning stages. With these additions to the landscape, an opportunity exists to begin planning from a more regional perspective before operations begin.

Multidisciplinary reclamation teams have been encouraged in recent years, as awareness of the complex inter-relationships at play in a closure environment have been recognized. However, reclamation requires extensive collaboration between mine operators as well. This is an enormous opportunity, given there is still time to do this effectively while reaping the diverse and plentiful benefits.

ACKNOWLEDGEMENTS

The authors would like to graciously thank the many stakeholders and consultants who have contributed to this paper and accompanying presentation through ideas and discussions. This work would not have been possible without the financial contributions of Golder Associates Ltd. and NSERC. The team from Golder Associates Ltd. in Edmonton, Alberta were generous with their time, insights, and resources, particularly Lisa Kempenaar.

REFERENCES

Ackoff, R.L. 1989. From Data to Wisdom. Journal of Applied Systems Analysis. 16:3-9.

Barber, L.A., Bockstette, J., Christensen, D.O., Tallon, L.K. and Landhäusser, S.M., 2015. Effect of soil cover system design on cover system performance and early tree establishment. 10th International Mine Closure Conference. Vancouver, Canada. June 1-3, 2015. Pp 1-9.

Canadian Dam Association (CDA). 2014. Technical Bulletin: Application of CDA Dam Safety Guidelines to Mining Dams. Canadian Dam Association. Pp 43.

Canadian Natural Resources Limited (CNRL). 2011. Canadian Natural Resources Limited Horizon Oil Sands 2011 Reclamation and Closure Plan. Submitted to Alberta Environment and Water.

Chapman, D.E. 2008. Hydrogeologic characterization of a newly constructed saline-sodic clay overburden hill. M.Sc. Thesis, University of Saskatchewan. Saskatoon, SK. Canada.

Conly, F.M., Crosely, R.W., and Headley, J.V. 2002. Characterizing sediment sources and natural hydrocarbon inputs in the lower Athabasca River, Canadian Journal of Environmental Engineering Science, 1: 187-199.

Ferguson, G.P., Rudolph, D.L., Barker, J.F. 2009. Hydrodynamics of a large oil sand tailings impoundment and related environmental implications. Canadian Geotechnical Journal. Vol. 46. Pp 1446-1460.

Golder (Golder Associates Ltd.). 2004. Vegetated waterway design guidelines. Submitted to Syncrude Canada Ltd.

Golder Associates Ltd. 2011. Imperial Oil Resources Ventures Limited 2011 Reclamation and Closure Plan. Submitted to Alberta Environment and Water, Alberta Sustainable Resources Development, and Energy Resources Conservation Board.

Hyndman, A. & Sobkowicz, J. 2010. Oil sands tailings: reclamation goals & the state of technology.

Kessler, S., Barbour, L., van Rees, K.C.J., Dobchuk, B.S. 2010. Salinization of soil over saline-sodic overburden from the oil sands in Alberta. Canadian Journal of Soil Science. Vol. 90: Pp 637-647.

LaGro, J.A. 2008. Site Analysis: A contextual approach to sustainable land planning and site design. John Wiley & Sons, Inc. Hoboken, New Jersey.

McGreevy, J., McKenna, G., An, R., Scordo, E. 2013. Regional mine closure plans – the next improvement in closure planning. Tailings & Mine Waste 2013. Banff, Alberta, Canada. November 3-6, 2013.

McRoberts, E. 2008. Considerations in oil sands tailings containment. In Proceedings of First International Oil Sands Tailings Conference, Edmonton, AB, 7-10 December 2008. Pp 13-22.

Morgenstern, N. 2012. Oil Sands Mine Closure – The End Game. Keynote presentation at the 2012 International Oil Sands Tailings Conference. Edmonton, Alberta. December 2-6, 2012.

Shell Energy Canada. 2011. Integrated Closure, Conservation and Reclamation Plan: Jackpine Mine – Phase 1. Submitted to Alberta Environment and Water, Alberta Sustainable Resources Development, and Energy Resources Conservation Board.

Shell Energy Canada. 2012. Muskeg River Mine Integrated Closure, Conservation & Reclamation Plan. Submitted to Alberta Environment & Sustainable Resource Development and Alberta Energy Resource Conservation Board.

Sobkowicz, J.C. 2013. Developments in treating and dewatering oil sands tailings. 16th International Seminar on Paste and Thickened Tailings. Belo Horizonte, Brazil. June 17-20. Pp 3-18

Suncor Energy Inc. 2011. Suncor Energy Inc. Oil Sands 2011 Reclamation and Closure Plan. Submitted to Alberta Environment and Water. December 2011.

Suncor Energy Operating Inc. 2012. Fort Hills Oil Sands Project 2011 Reclamation and Closure Plan. Submitted to Alberta Environment. January 2012.

Syncrude Canada Ltd. 2011. 2011 Mine Reclamation Plan and Life of Mine Closure Plan: Mildred Lake and Aurora North. Submitted to Alberta Environment and Water. December 2011.

Toy, T.J., Hadley, R.F. 1987. Geomorphology of Disturbed Lands. Academic Press: New York.

Wall, S.N. 2005. Characterizing geochemical reactions in an overburden waste pile: South Bison Hill, Syncrude, Canada. M.Sc. Thesis, University of Saskatchewan. Saskatoon, SK. Canada.

Wells, P.S., Caldwell, J., Fournier, J. 2011. Suncor Pond 5 Coke Cap – The story of its conception, testing, and advance to full-scale construction. In proceedings of Tailings and Mine Waste ’10. Vail, Colorado. October 17-20, 2010. Taylor & Francis Group, London.

http://www.oilsandsmagazine.com/oil-sands-surface-mining-open-pit-mining-techniques-overview/

VARIABILITY IN FLUID FINE TAILINGS

Heather Kaminsky[1] and Oladipo Omotoso[2]
[1]Northern Alberta Institute of Technology, Edmonton, Canada
[2]Suncor Energy Inc., Calgary, Canada

ABSTRACT

Although the oil sands literature is replete with basic fluid fine tails (FFT) properties such as bitumen, mineral, water, fines and clay contents, the concentrations are as variable as the number of reports. This paper attempts to consolidate the variability of these basic properties across two ponds and over a period of years. This should provide the research and innovation community with a better understanding of the range of properties so that new processes and chemistries account for the variations at an early stage of research and development. Treatment of fluid fine tailings is a major issue in oil sands operation. There are two main goals in the treatment - 1) minimize the volume of containment required for FFT by dewatering and 2) create geochemical and geotechnically stable deposits that are ready for reclamation. Current industry practice involves treating the fluid fine tailings in a number of different ways to meet these goals. In all cases the properties of FFT play a major role in determining how to operate the treatment process. One of the biggest challenges in treating fine fluid tailings is the variability in properties of the fluid fine tailings itself. This article describes the range of FFT density, solids, clay content by MBI, fines content, bitumen content, rheology, and water chemistry that have been measured in fluid fine tailings both from open source literature and from historical pond survey and test program data.

INTRODUCTION - FORMATION OF FFT

In the warm water extraction of bitumen from surface-mined oil sands, oil sands slurry is conditioned in pipelines to remove bitumen from sand grains. The conditioned slurry is then diluted in the primary separation vessel (PSV) to float bitumen in a froth. The bulk of the coarse and fine tailings are recovered in the middlings and underflow of the PSV. Residual minerals and water in the bitumen froth are removed in secondary extraction and constitute froth treatment tailings, which is a minor portion of the total fluid tailings. The bulk of the minerals in oil sands are coarse sands which are cycloned and used for building dykes for tailings containment. The fluid middling fraction, comprising mostly fine minerals (< 44 μm) goes to secondary and tertiary flotation circuits for further bitumen removal. The resulting waste stream containing over 70 % of the fines in the ore is impounded in containment facilities where the sand is generally captured in beaches and the fines segregates to form FFT.

The properties of FFT reflect to a large extent the mineralogy of the mined ore which is a combination of oil sands and clay shale lenses in the deposit, the ore connate and process effected water (PEW) chemistries, the bitumen chemistry and the bitumen separation process efficiency. These properties influence the behaviour of FFT from transport hydraulics to settling and consolidation, and biogenic activities in the tailings ponds. The rheological and geotechnical behaviours are largely determined by the water chemistry and mineralogy of the suspension while biogenic activities are controlled by the hydrocarbon water chemistries and mineralogy of the FFT.

DATA SOURCES

The bulk of the data in this paper is from pond surveys taken from multiple ponds over the period 1972-2015. This is a spinoff from the efforts initiated in block modeling (Wells & Guo, 2008).

VARIATION IN BITUMEN, SOLIDS AND WATER

Figure 1 shows the bitumen and mineral distribution in MFT for the survey of Suncor's active and inactive ponds from 1972-2015, for all samples. For the portion considered FFT (everything with a fines content >50%) the average bitumen content is 3±2% bitumen with a solids content of 38±14%. The average B/S ratio is 0.09±0.14. The uncertainty represents one standard deviation in the population. Table 1 shows the distributions in terms of percentile.

Table 1. 10th, 50th and 90th percentile of bitumen, mineral and B/S ratio for historical pond data (fines >50%)

	Bitumen	Mineral	B/S ratio
D10	0.9	20.7	0.03
D50	2.9	36.2	0.08
D90	5.5	58.3	0.15

This demonstrates the large variability that can exist within this material which is often reported to be relatively homogenous. The samples with very high bitumen contents (>~7%) represent areas where the bitumen has collected to form bitumen enriched mats/slugs. These areas are more or less randomly distributed within the ponds.

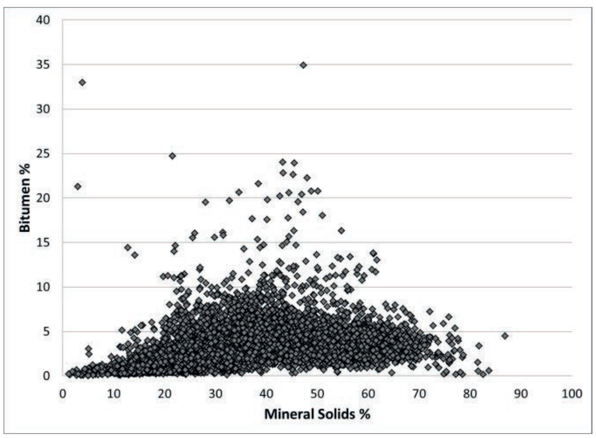

Figure 1. Distribution of bitumen and solids within the data set of FFT material sampled from ponds from 1972-2015. The material with solids >50% is usually from pond bottom/beach below water.

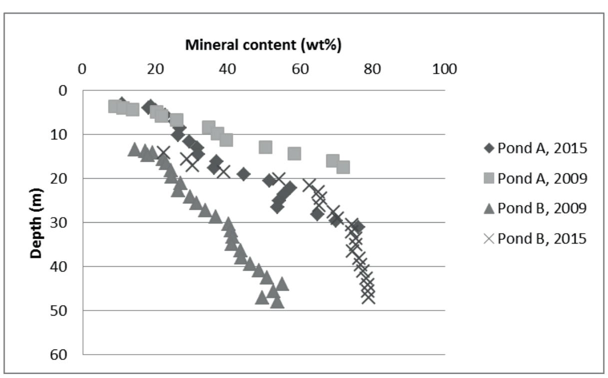

Figure 2. Examples of mineral content with depth profiles

Part of the reason for the range in solids content is that the tailings ponds are settling basins designed to allow material to gradually settle out and begin to consolidate. Therefore there is a consistent trend of increasing solids content with depth. The rapid solids content increase with depth ceases around a 70% solids content where the particles have come to very loose grain to grain contact. Further increases in solids contents are then controlled by consolidation. Figure 2 shows an example of the mineral content profiles for two different ponds at two different time points. Thus while one can generally suppose that the deeper in a pond one is the higher the solids content, it is not sufficient to know the depth a sample is collected in order to know the characteristics of the sample.

Figure 1 shows the distribution of bitumen with depth in two different ponds at two different times, while Figure 4 shows the bitumen/solids ratio of the same locations. As shown in the portion above pond bottom, the bitumen content is somewhat randomly distributed with a large variation in bitumen/solids ratio. Once consolidation occurs (Pond B) there is evidence that the bitumen content decreases which helps explain the almost triangular shape of the bitumen/solids scattergram in Figure 1. As a material with a given bitumen to solids ratio settles the bitumen content will increase as the solids content increases, however once consolidation has begun the bitumen is gradually displaced along with the water.

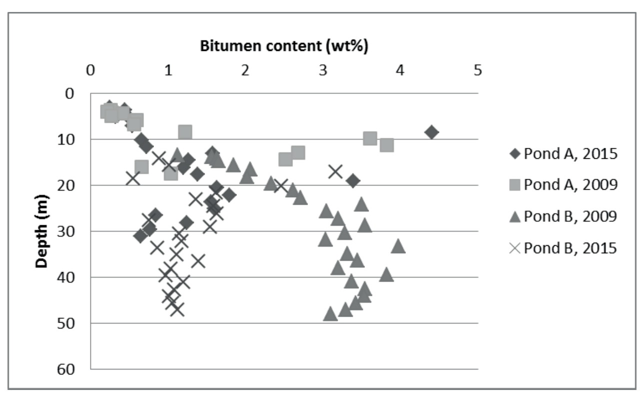

Figure 3. Distribution of bitumen with depth

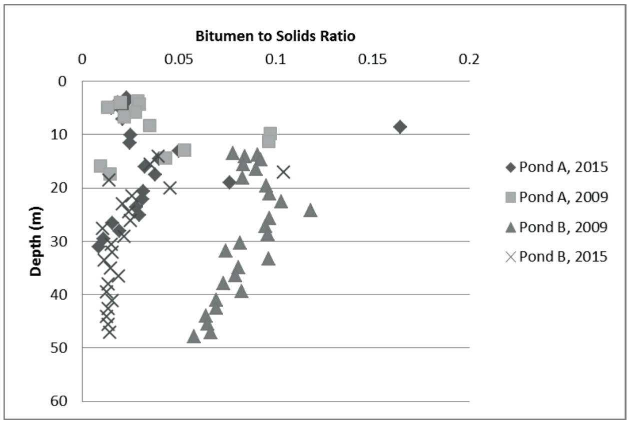

Figure 4. Bitumen/solids ratios with depth

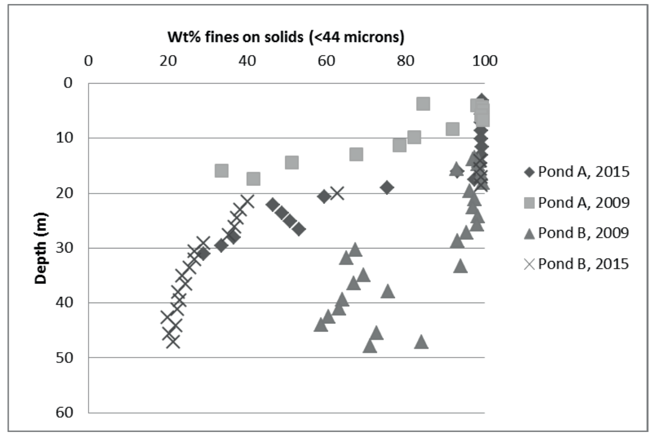

Figure 5. Examples of fines content with depth

VARIATION IN FINES AND CLAYS

MFT is a slow settling suspension with a dispersed water chemistry that favours particle segregation. Therefore, the particle size distribution will be dependent on the location in the pond. The average fines (< 44 μm) content (measured by wet sieving) of FFT measured in this data set is roughly 85% with a range between 50 and 100 % and the average clay content as measured by MBI is 51% with a range between 10 and 150%. It is important to remember that the "% clay" measured by MBI is really just an index of water active surface area and is an empirical correlation developed many years ago. For more information on this correlation please refer to "Demystifying the Methylene Blue Index" (Kaminsky, 2014).

Table 2. 10th, 50th and 90th percentile of clay on solids, CWR and CFR (fines >50%)

	Clay	CWR	CFR
D10	24	0.15	0.34
D50	48	0.29	0.55
D90	86	0.52	0.88

As shown in Figure 5 a substantial amount of FFT contains 100% fines with the fines content rapidly decreasing as sand settles to the bottom to form higher solids content material with grain to grain contact. As shown in Figure 6, there can be a very wide range of clay content by MBI within the 100% fines zone. This is particularly important as the % clay on solids significantly influences the rheological, consolidation and geotechnical properties of the tailings (Yong & Sethi, 1978) (Cerato, 2001), (Mikula & Omotoso, 2006), (Omotoso & Melanson, 2014) and (Wells & Kaminsky, 2015).

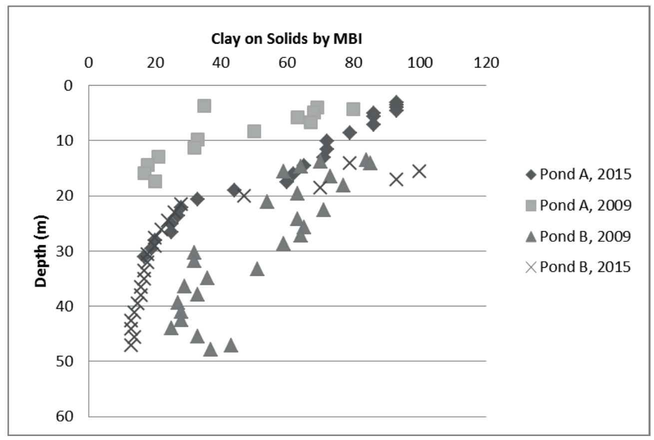

Figure 6: Examples of clay content with depth profiles

A slightly narrower variation of clay to water ratio with depth exists in different ponds as shown in Figure 7.

One common misperception is that the clay to fines ratio for oil sands is constant. While this is generally true for ores this is not at all true for FFT, as shown in Figure 8. This is because the settling rates of different size particles are different and so the highly surface active (and hence high MBI) fines will settle more slowly than the less active fines. This tends to create a density to % clay content relationship that is fairly similar between ponds and with time assuming that the water chemistry hasn't changed dramatically (Figure 9).

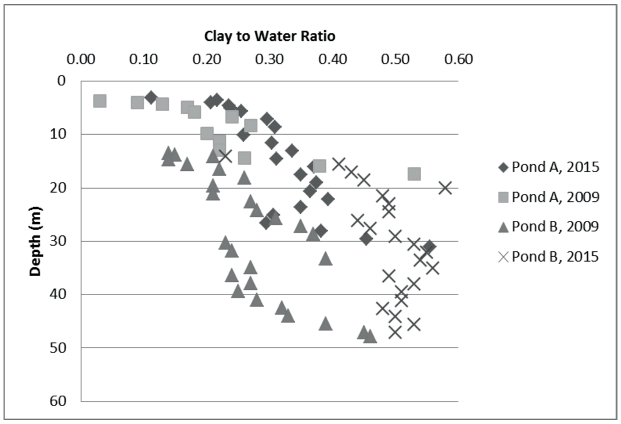

Figure 7. CWR with depth

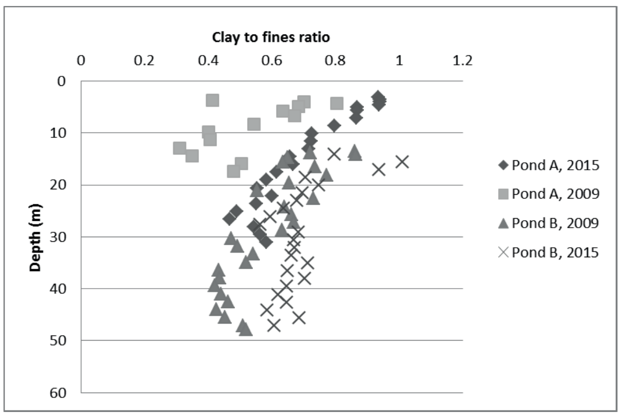

Figure 8. Examples of Clay to fines ratio with depth

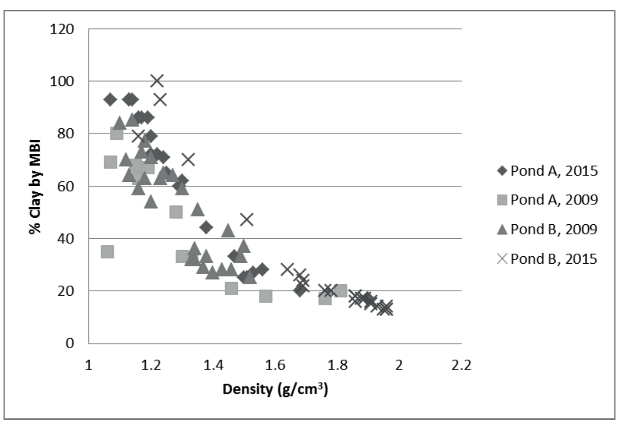

Figure 9. Relationship between density and % clay by MBI

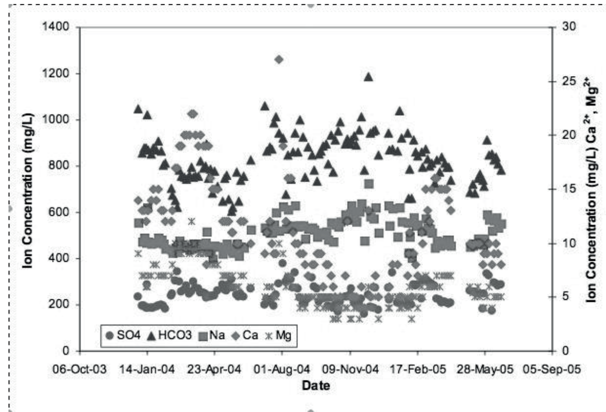

Figure 10. Trends in the major ion concentrations in a tailings pond release water

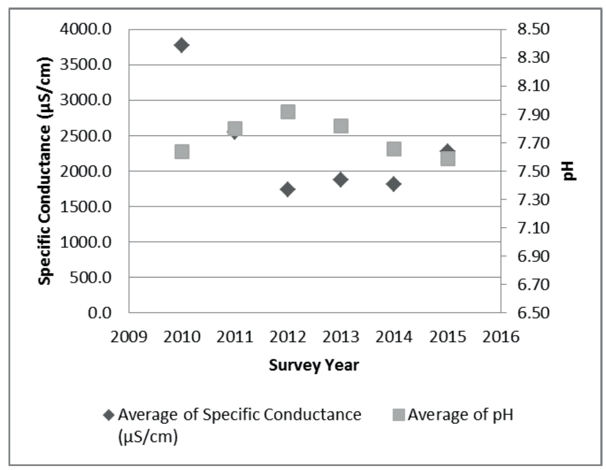

Figure 11. pH and Specific conductance for a pond with time

WATER CHEMISTRY

The process effected water (PEW) and the MFT pore water reflect the chemistry of the connate water in the mined ore. Of the major ions, Na and HCO_3 ions dominate the water chemistry, from the use of NaOH as processing aid prior to the implementation of hydrotransport for bitumen conditioning and liberation. The other major ions, Ca, Mg, K, Cl and SO_4 are largely from the ore connate water (FTFC (Fine Tailings Fundamentals Consortium), 1995). The concentration of the divalent ions Ca and Mg are impacted by the nature of clay minerals available for cation exchange as they have higher adsorption coefficients than Na. Calcium concentration is also affected by temperature changes as a result of decrease in calcium carbonate solubility as the temperature increases. Biogenic processes in the pond especially the activity of sulphate-reducing bacteria can reduce the concentration of sulphate in the pore water significantly. Figure 10 and Figure 11 show the trend in the major ions and pH in pond release water after co-mingling with consolidated tailings (CT) release water. CT release water has a high Ca and SO_4 concentration due to the use of gypsum in the process.

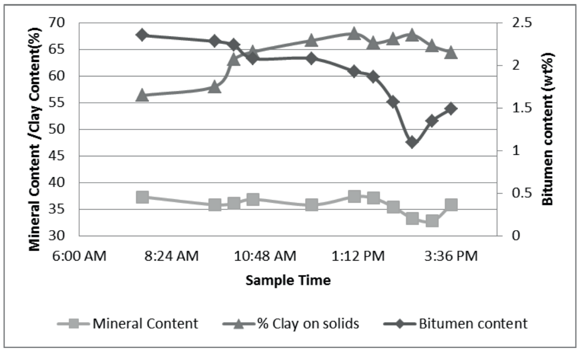

Figure 12. Bitumen and Mineral content as a function of time

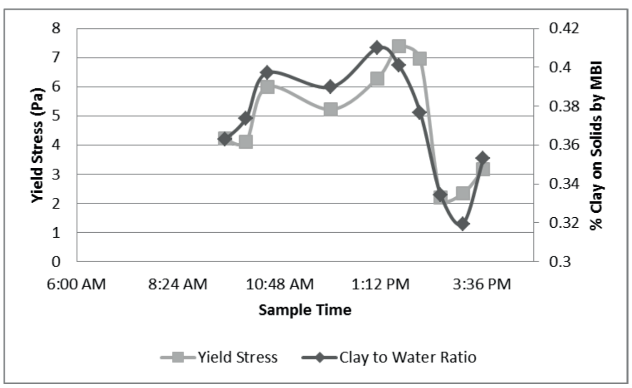

Figure 13. Yield stress and CWR as a function of time

VARIABILITY WITH TIME

The variability of FFT extends to the processing of FFT for the purposes of tailings treatment, Figure 12 shows the variation in bitumen, mineral and % clay by MBI as a function of time for samples taken from a single sampling point over the course of one day. The variations are relatively small when compared to the overall variability of the ponds and are attributable to the fact that the dredge supplying the FFT was kept at the same location and approximately same depth for the duration of testing. Although the variations were relatively small in the overall picture of things, the variation in yield stress was significant (ranging from 1-7pa). The changes in yield stress correlated exactly with the changes in clay to water ratio.

CONCLUSIONS

FFT is highly variable and simply knowing the pond source or even specific location within the pond can only provide a general estimate of properties (i.e. deeper usually means more solids and less clays). The profiles can change substantially year on year depending on the type of activity that the pond has seen in the interval. A knowledge of the ponds depositional and chemical history is quite helpful in predicting the evolution of the FFT but is no substitute for measurement when doing further research and development on a sample.

To that end there are four basic tests that should be done to characterize any fluid fine tailings used for research and development purposes, these are: Dean Stark to determine bitumen, mineral & water; Methylene Blue testing to determine clay index, particle size distribution measured by wet sieve (hydrometer and laser diffraction are often used to probe fractions smaller 44 μm); and water chemistry (major anions & cations). There are many other tests that would also be useful for getting a full picture of the behavior of the sample but these four provide the minimum level of knowledge. Bitumen, solids and water is of course necessary to calculate true void ratios. The value of clay index was referenced earlier in the paper. Water chemistry is important to long term reclamation goals as well as to get a better understanding of the behavior of the clay in the system (i.e. is it dispersive or coagulating). Particle size distribution is useful for understanding the packing potential of the solids as well as to effectively model slurry transport.

It is suggested that tailings treatment processes or strategies should be tested for robustness against the range of basic properties seen. Understanding the impact of the variability or better yet having a robust process significantly increases the probability of success of the process in operations.

REFERENCES

Cerato, A. (2001). *Influence of Specific Surface Area on Geotechnical Characteristics of Fine Grained Soils.* Msc Thesis in Civil & Environmental Engineering for University of Massachusetts.
FTFC (Fine Tailings Fundamentals Consortium). (1995). *Advances in Oil Sands Tailings Research (silver bullet).* Alberta Department of Energy, Oil Sands and Research Division.

Kaminsky, H. (2014). Demystifying the Methylene Blue Index. *International Oil Sands Tailings Conference.* Banff.

Mikula, R., & Omotoso, O. (2006). Role of Clays in Controlling Tailings Behaviour in Oil Sands Processing. *Clay Science Volume 12, Supplement 2*, 177-182.

Omotoso, O., & Melanson, A. (2014). Influence of Clay Mineralogy on the Behavior of Oil Sands Tailings. *PASTE* (pp. 31-42). Vancouver: InfoMine Inc.

Wells, P. S and Guo, C (2008): Application of block modeling to Suncor tailings characterization. 1st International Oil Sands Tailings Conference, December 7 – 9, 2008. Edmonton, Canada.

Wells, P., & Kaminsky, H. (2015). Slurry to Soil Clay Behaviour Model - Using Methylene Blue to Cross the Process/Geotechnical Engineering Divide. *Tailings & Mine Waste.* Vancouver.

Yong, R., & Sethi, A. (1978). Mineral Particle Interaction Control of Tar Sand Sludge Stability. *Journal of Canadian Petroelum Technology*, 76.

Session B-2

Chemical Interactions

POLYMER TREATMENT OF OIL SANDS TAILINGS: CONFOCAL MICROSCOPY AND RHEOLOGICAL STUDY OF THE CONSOLIDATION PROCESS

Aleksandra Govedarica and Milana Trifkovic
Department of Chemical and Petroleum Engineering
University of Calgary, Calgary, Canada

ABSTRACT

Efficient flocculation depends strongly on the interactions between dispersed minerals and added polymer while fast dewatering of the formed flocs depends on their structural evolution during the consolidation process. This work presents a novel method for studying the flocculation mechanism and consolidation (aging) process of the formed flocs by utilizing laser scanning confocal microscopy (LSCM) and rheology. This strategy allows us to gain better understanding of the relationship between microstructure and bulk material properties of the flocculated mineral suspensions. Kaolinite suspensions were flocculated using Flopam A338 polymer and the flocculated material was aged over the course of three days. Confocal 3D images showed initial formation of loosely connected flocs having large inter-floc channels which resulted in low shear strength and low critical work input needed to break the floc structure. Over the course of the aging period more compact and denser structures were formed. As expected, the most prominent consolidation was observed between the first and the second day during which large decrease of inter-floc channels and increased floc structure strength was measured. The presented method offers new possibilities for the in-depth correlation of micro scale characteristics to macro scale dewatering and consolidation properties of the flocculated tailings systems.

INTRODUCTION

Tailings are a waste product of bitumen extraction from oil sands whose efficient management has become a major challenge for oil industry from two aspects - environmental one due to its toxicity, and economical one due to the constant increase of the inventory of these waters. (Chalaturnyk et al. 2002) Tailings consist of stable mineral colloidal suspensions (Dusseault & Don Scott 1983; Don Scott et al. 1985; Kessick 1979) which show poor consolidation behavior and trap large amount of otherwise recyclable water. Considerable effort has been put into defining the most efficient treatment route (Wang et al. 2014) where flocculation using water soluble polymers has been identified as one of the most promising ones (Kitchener 1972; Wang et al. 2010; Lee et al. 2014). There are many factors affecting efficiency of polymer flocculation of mineral suspension such as mixing intensity during polymer addition (Sworska et al. 2000b; Demoz & Mikula 2012), salt addition and pH (Kotylar et al. 1996; Sworska et al. 2000a) as well as polymer dosage, type and charge density (Sworska et al. 2000a; Nasser & James 2006). These interplaying factors need to be optimized in order to achieve satisfactory flocculation results. Higher mixing power can result in good dispersion of the polymer but can also cause breakage of the formed flocs. Addition of salt or altering pH can help destabilize mineral suspension before the polymer addition while it can also reduce polymer efficiency due to changes in its conformation in the water. Increasing the flocculent dosage was found to increase the flocculation efficiency up to a certain value after which coating of clay particles with excess polymers provides steric hindrance for the flocculation. (Sworska et al. 2000a)

Characterizing microstructure and rheology of flocculated tailings samples is an essential step towards understanding of their settling behavior. Cryo-scanning electron microscopy (cryo-SEM) has been typically utilized for characterization of tailings systems microstructure before and after flocculation. (Zbik et al. 2008) Even though its resolution limit is suitable for the tailings systems, the technique is known to show microstructural artifacts as a consequence of the freezing process. LSCM has been identified as an alternative, non-invasive microstructure characterization technique, but since fluorescence is necessary to generate the contrast between different phases, a very few studies have utilized it thus far. Mikula & Munoz (2000) compared cryo-SEM and LSCM characterization techniques for the structural imaging of a real tailings sample exposed to different shearing patterns. LSCM showed more reliable results since freezing process is not required. In a recent study Wilkinson et al. (2016) showed how powerful LSCM can be for visualizing fine differences in bentonite flocs formed by using fluorescent cationic polymer with different ionic strength. The importance of flocculant architecture, charge and type for the flocculation performance and obtaining satisfactory rheological properties of flocculated sludge showing desired dewatering properties has been also identified previously. (Mpofu et al. 2003; McFarlane et al. 2005, Watson et al. 2011, Nasser & James 2007)

In this paper we present a novel strategy for studying the flocculation mechanism and consolidation process of the formed flocs using laser scanning confocal microscopy (LSCM) and rheology. The approach allows us to obtain the relationship between spatially resolved microstructure and shear rheology of the flocculated model tailings system. We observe that the microstructure and rheological properties of flocculated tailings samples undergo significant changes in a span of three days. In addition, we quantify the strength of the flocs and connect it to the underlying microstructural variables.

MATERIALS AND METHODS

Clay used for this study was Kaolinite (Sigma-Aldrich). Bitumen used for preparation of model MFT slurry was provided by Syncrude. Sodium bicarbonate (Sigma-Aldrich, ReagentPlus, ≥99.5%, crystalline) was used to adjust ionic strength of DI water (18 ΩM). Flopam A338, a high molecular weight anionic polyacrylamide, was provided by CANMET Energy. Nile blue fluorescent dye used for clay labeling for the purpose of LSCM imaging was purchased from Sigma Aldrich.

Fluorescent labeling of kaolinite

Natural kaolinite does not have any fluorescent characteristics. Thus, in order to visualize clay particles under the LSCM, kaolinite was fluorescently tagged with Nile blue dye. Nile blue is a suitable candidate for clay tagging due to the fact that its spectral excitation/emission does not overlap with bitumen autofluorescence (Shende et al. 2016; Bearsley et al. 2004; Mikula & Munoz 2000). Pre-weighted amount of kaolinite was mixed for at least 12 hours with DI water (18 ΩM) and Nile Blue (0.02 wt%). After mixing, clay was centrifuged at 4000 rpm for 15 min, supernatant was removed and solids were redispersed with fresh DI water. Centrifugation and washing was repeated several times until the supernatant contained no excess of nile blue dye. Clay was dried in vacuum oven at 30°C for 2 days and crushed with a metal spatula before using it for model tailings preparation. This procedure enabled clay tagging by physical adsorption of the dye on the surface of the particle. To ensure that nile blue does not desorb from the clay surface, small amount of tagged clay was left for days in fresh DI water and no leakage of the dye was observed via LSCM.

Zeta potential measurements

To test if the amount of fluorescent dye drastically changes the surface chemistry of kaolinite clay, zeta potential measurements were performed on Malvern Zetasizer Nano ZSP instrument. Reported values for zeta potential were the average of 3 x 100 runs.

Preparation of model tailings

For preparation of model tailings, bitumen was used as received, clay tagged as described above and 0.05 wt% sodium bicarbonate ($NaHCO_3$) solution in DI water was prepared and used as the water phase in order to mimic the ionic strength of tailings water. Model tailings were prepared to contain 5 wt% bitumen with 30 wt% clay and diluted to 10 wt% clay with the addition of the 0.05 wt% $NaHCO_3$ DI solution before flocculation.

Bitumen was preheated to 90°C in a glass jar after which it was mixed with two thirds of needed dry tagged clay using the overhead stirrer (equipped with A310 impeller with three blades). Mixing was performed until all bitumen was separated from the jar walls and thoroughly blended with added clay. In a separate glass jar the rest of the clay is mixed with prepared salt DI solution heated to 90°C. This clay-water mixture was then added to bitumen-clay mixture while mixing at 600 rpm and continuing heating for another 15 minutes until the mixture was homogenized.

Flocculation and aging

Polymer solution was prepared in the concentration of 0.1 wt% in 0.05 wt% $NaHCO_3$ DI solution and used for flocculation in the dosage of 100 ppm calculated per mass of solid clay in the sample.

Model tailings were placed in a 350 ml glass jar and mixed at 600 rpm with the overhead stirrer for 2 minutes to homogenize the sample. After this period, mixing speed was lowered to 150 rpm and polymer solution was added directly to the vortex with a syringe while maintaining the mixing for 15 seconds. Flocculated material was then placed in a glass aging funnel shown in Figure 1. This funnel consisted of two separation funnels fused together with a valve on each end. One end had the opening of 4 mm while the opposite one included an opening of 8 mm. Freshly flocculated sample was placed in the funnel on the side having 4 mm opening on the first day. After taking samples for imaging and rheological measurements, the content of the funnel was carefully inverted and placed on the side of the funnel with the bigger opening. Since inversion of the funnel content occurs shortly after the flocculation when the flocs are still loose and uniformly distributed throughout the funnel, smooth relocation of the material from one end of the funnel to the other is believed not to affect the aging process. The reason for having this kind of funnel was to allow sampling of the material from the bottom where the effect of aging was enhanced the most and to prevent flocs breakage while sampling allowing them to pass through the valve with bigger opening.

Figure 1. Aging funnel

Dynamic strain sweep testing

Rheological measurements were performed using Anton Paar MCR 302 WESP rheometer equipped with a custom made glass plate and 25 mm plate measuring system having a rough paper attached to it to eliminate slip effects. Glass portion of the plate was of microscopic quality and removable from the stage, which allowed flocculated sample to be taken from the aging funnel directly on the slide and to be directly imaged on the confocal microscope prior to the rheological test. Samples were probed using small angle oscillatory shear (SAOS) to obtain parameters of interest, namely, work needed to break the structure, yield stress, yield strain, and shear modulus. Critical work needed to completely break the structure was calculated using the following equation:

$$critical\ work = \int \sigma d\gamma = \frac{1}{2} G' \gamma_{critical}^2 \qquad (1)$$

Confocal imaging

Laser scanning confocal microscopy (LSCM) is a power imaging tool that allows one to acquire fluorescence images using a focus beam light. The main advantage of this technique compared to other microscopy techniques is that it features a pinhole set before the detectors which removes out-of-focus light and allows imaging not only in x-y but also in the z direction. Acquired images can be reconstructed into 3D models which give opportunity for more detailed quantification and study of the microstructure. Sample used with LSCM needs to be fluorescent, either showing natural autofluorescence or fluorescence coming from the fluorophores artificially attached to its surface. In LSCM fluorescence detection can be split into several detection windows which allows for simultaneous detection of different fluorescence regions. LSCM was performed using a Leica SP8 microscope equipped with Piezo Jena system which allowed faster image acquisition minimizing potential drying of the samples. 3D images presented in this work were reconstructed using LASX software.

Bitumen was reported to show autofluorescence (Shende et al. 2016; Bearsley et al. 2004; Mikula & Munoz 2000) which enabled its detection without any pretreatment in the range of 451-527 nm after excitation with 405 nm laser light. Nile blue adsorbed on clay allowed kaolinite detection in the range of 653-693 nm with excitation using 638 nm laser. Emission spectra of both bitumen and clay together with excitation lasers and detection ranges are shown in Figure 2. Even though some overlapping did exist between these two emission spectra, that did not interfere with the detection of specific bitumen and clay features in two different detection channels. Confocal 3D images were obtained using 10x and 63x magnification objectives and all images were taken in 1024 x 1024 resolution. To inspect the distribution of clay and bitumen in the flocculated tailings, a z-stack of flocculated sample was taken on the day of the flocculation with 63x magnification which was then post processed using Avizo software (FEI, v. 8.0.1). The images were reconstructed by performing thresholding which labeled zones of fluorescence and non fluorescence for each detection channel (clay and bitumen separately) giving binary images. Image noise of binary images was reduced using despeckle filter after which both bitumen and clay channel filtered images were surface rendered for 3D viewing.

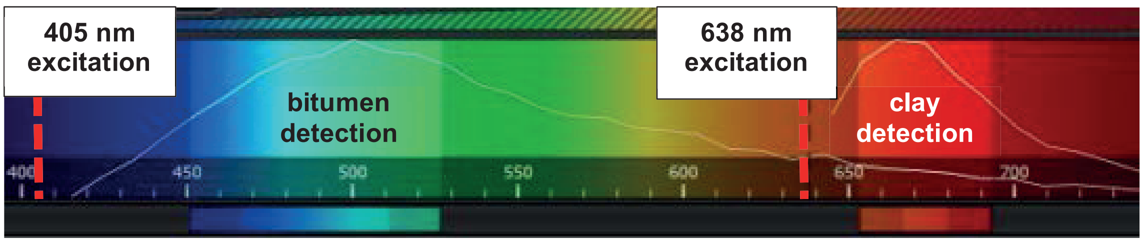

Figure 2. Emission spectra and detection ranges for bitumen (excitation with 405 nm; detection in the range of 451-527 nm) and clay (excitation with 638 nm; detection in the range of 653-693 nm)

RESULTS AND DISCUSSION

Zeta potential results shown in Figure 3. indicate that the amount of nile blue dye adsorbed on clay surface for the purpose of imaging does not change its surface chemistry since the mean zeta potential value out of 3 x 100 runs was -41 mV ± 13.3 mV for both fresh and tagged clay. This enabled imaging of clay using laser scanning confocal microscopy while ensuring that the observed flocs structures and behavior of the clay were not altered by introducing the dye molecules to the system. It should be noted that the applied technique for measuring zeta potential of platelet particles is not the most accurate since it is based on the Smoluchowsky equation, which is usually used for spherical particles of homogeneous charge (Chassagne et al. 2009). However, the fact that the relative change of surface potential between untagged and tagged clay is insignificant is a valid indicator that the clay surface chemistry was not altered by the dye addition.

Microstructure of generated flocs

The acquired 3D images using LSCM of the flocculated model tailings on the day of the flocculation (Figure 4a and 4b) showed loosely connected flocs with large inter-floc channels occupied by water phase. The second (Figure 4c an 4d) and third day (Figure 4e and 4f) flocs showed considerably less voids. The inter-floc channels were significantly smaller indicating that more enhanced compression of the flocs occurred on the days following the flocculation procedure.

Flocs aging process consisted of the compression of the pore space over time with the apparent increase of the flocculated regions. Figure 5. represents enlarged region of the flocculated sample on the first day of aging where bitumen and clay distribution in the sample indicated that bitumen always gets coated by clay particles and that the employed tailings preparation procedure did not leave any free bitumen globules throughout the sample.

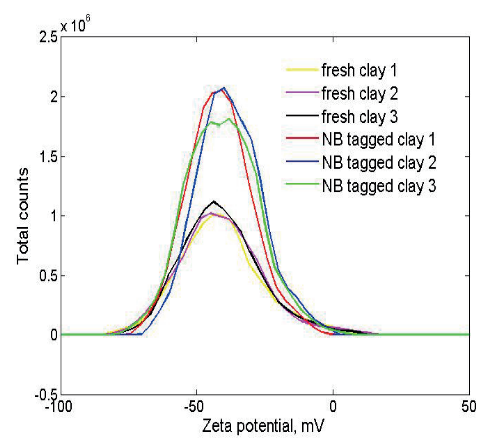

Figure 3. Zeta potential distribution of fresh and fluorescently tagged clay

Rheology of flocculated samples

Dynamic strain sweep tests were conducted to probe the differences in bulk properties of flocculated model tailings throughout the consolidation period. They showed reproducible results between 3 runs. Figure 6. shows that storage and loss moduli, G' and G'', increased considerably between first and second day of aging while the flocs did show further increase in strength until the third day, but not as drastic. Dynamic sweep results can be used to obtain yield stress, minimal stress needed for the complete breakage of the floc network and the corresponding work input needed to break the structure. Even though strength of the flocs showed major changes between first and second day of aging based on the values of two elastic moduli, critical strain showed the biggest increase between second and third day. Values for storage modulus and critical strain for each day of aging are displayed in Table 1. Strain sweep results can also be presented on the plot of shear stress as a function of shear strain displayed in Figure 7. Here, shear stress followed similar trend as storage modulus G' during aging period showing a drastic increase in the value between first two days upon flocculation. This is most clearly observed through the value of yield stress. Critical work needed to completely break the structure of the flocs over the course of aging had the same trend and its values are noted in Table 1. All presented rheological data agrees with the study of the microstructural evolution of the flocculated tailings. Larger storage modulus, critical strain, yield stress, and critical work were observed as the flocs were left to age which can clearly be related to the enhanced compression of the flocs giving denser and more compact structures. Breakage of the floc structure was observed in the confocal images taken before and immediately after rheological testing on the first day of aging as shown in Figure 8. It is obvious that larger flocs formed after flocculation got broken down into smaller regions during the rheological test while inter-floc channels reduced.

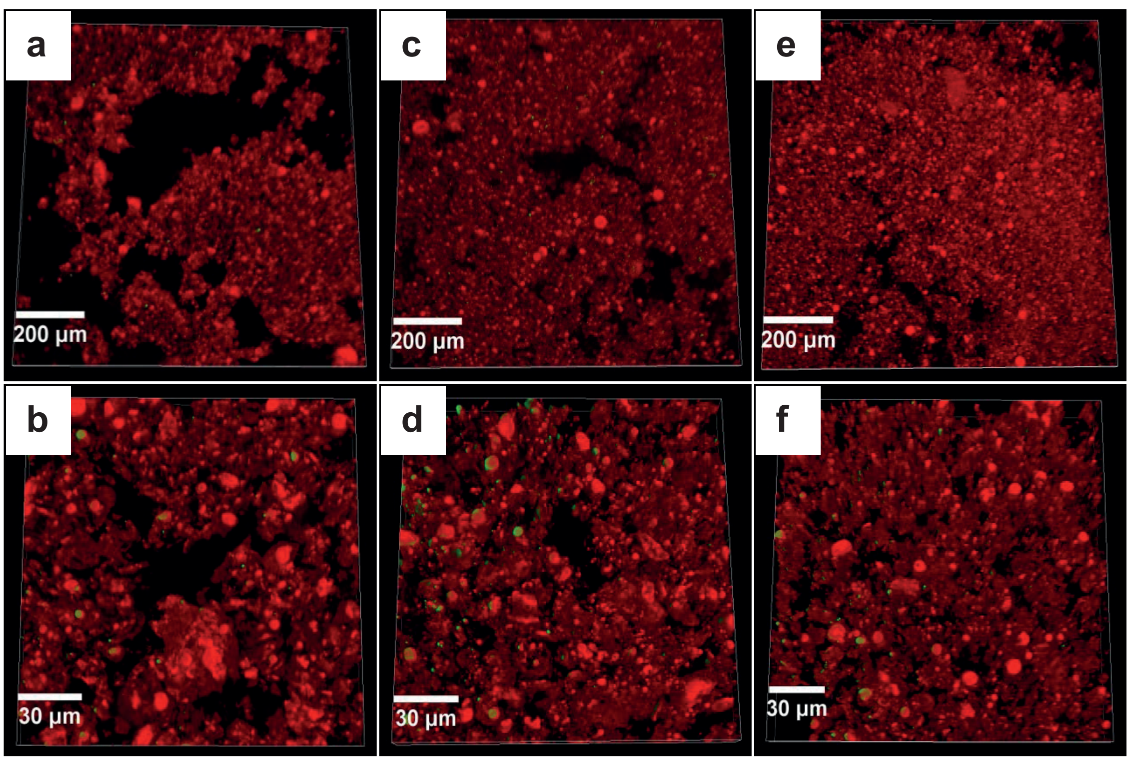

Figure 4. Flocs microsctructure evolution during aging for 3 days. Images were taken with 10x (top row) and 63x magnification objectives (bottom row). Red regions show tagged kaolinite, green regions represent bitumen while untagged water occupies black regions.

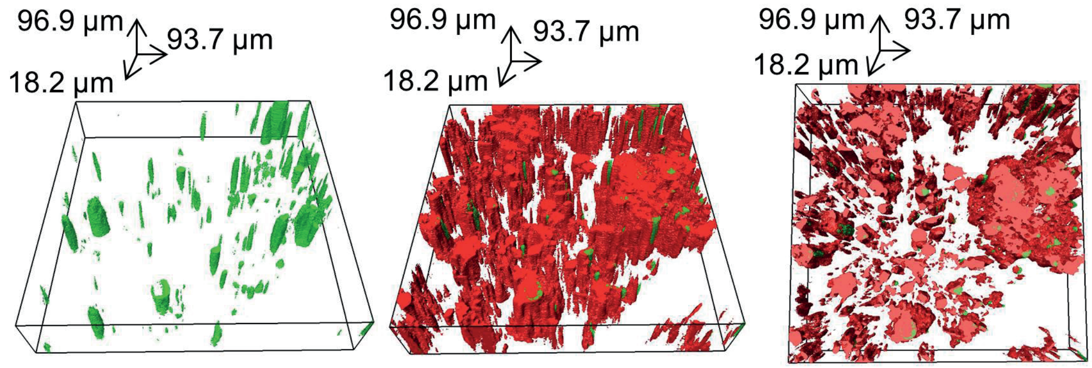

Figure 5. 3D reconstructed images of the flocculated model MFT taken on the first day right after flocculation. Bitumen in these images is labeled green, clay regions are labeled red, while transparent regions represent untagged water. Bitumen and clay are observed to always form structures together which implies that the bitumen is mainly adsorbed on the clay surface while no free bitumen globules were observed.

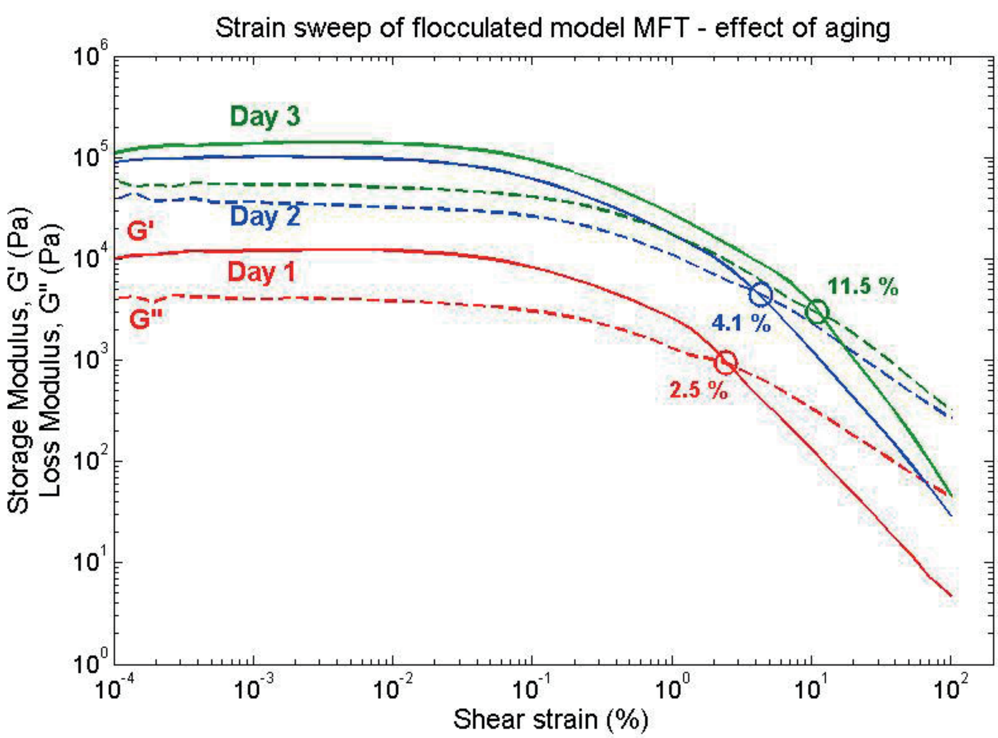

Figure 6. Dynamic strain sweep results of the flocculated model tailings aged for three days

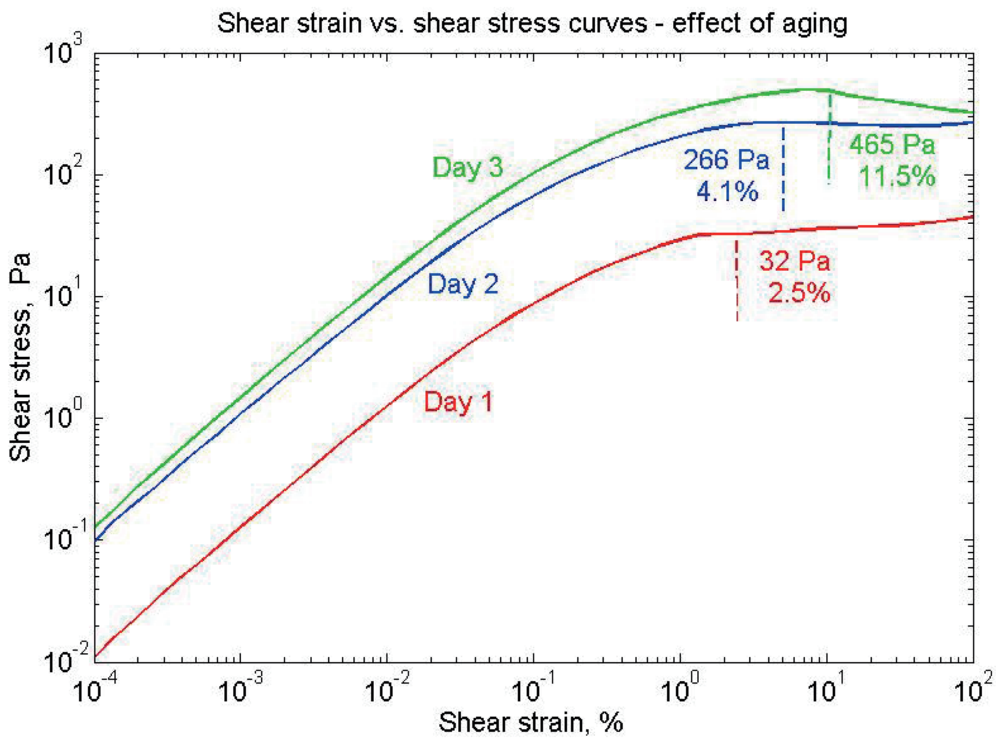

Figure 7. Shear stress vs. shear strain for flocculated aged model tailings. Noted values represent yield stress for determined critical shear strain above which the floc structure is completely broken.

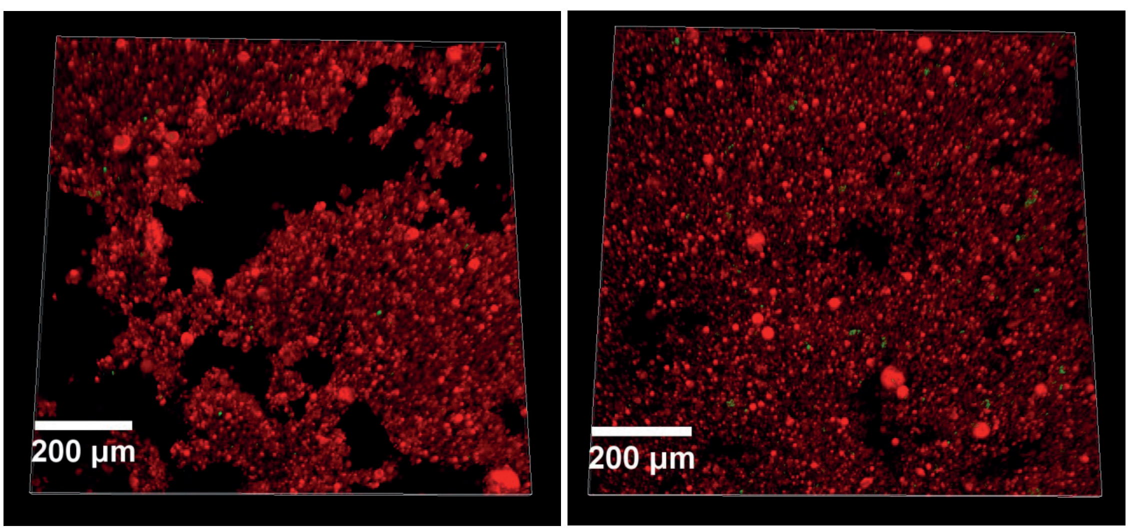

Figure 8. The difference in the microstructure of the flocculated model tailings on the first day before (left) and after performing dynamic shear strain testing (right). Images were taken with the 10x magnification.

Table 1. Rheology data (G' - storage modulus, γ_c - critical strain, σ_y - yield stress) and critical work (W) needed to completely break the floc structure calculated using Equation 1

	G', Pa	γ_c, %	W, Jm^{-3}	σ_y,Pa
Day 1	1.2 x 10^4	2.5	0.0038	32.5
Day 2	1.0 x 10^5	4.1	84.05	266.4
Day 3	1.4 x 10^5	11.5	925.75	465.3

CONCLUSIONS

Reaching a comprehensive relationship between microstructure of flocculated tailings and its bulk rheological properties is of great importance to the advancement and sustainable development of oil sands waste water management. After deposition of flocculated tailings, the aggregates create a loose matrix where flocs' shape and change impacts the pore microstructure and therefore macroscopic bulk properties, such as consolidation and rheology. Understanding the mechanism of flocculation and consolidation would allow for optimal design of the polymer flocculants tuned towards enhanced settling of tailings. In this work we have presented a novel approach that utilizes LSCM and rheological studies of flocculated tailings with the goal of obtaining a more direct and quantitative relationship between structural evolution of the flocs and the macroscale properties during consolidation process. Laser scanning confocal microscopy allowed for 3D images to be obtained which showed that at the beginning of the consolidation big inter-floc channels get reduced resulting in a more compacted and denser settlement bed. On another hand, rheological measurements of the same samples reinforced microscopy results where pore shrinking and bed compression resulted in an increase of storage and loss moduli and critical shear strain over the course of aging period giving stronger flocs which need more work input to be completely broken. This new strategy gives a wide range of possibilities for more systematic study of flocculation mechanism of oil sands tailings. Further quantification of obtained 3D images such as size distribution, connectivity of flocs over time, and floc fractal dimension analysis can be implemented using this technique which in combination with rheology can provide valuable scientific advancement regarding the dynamics of the flocculation and dewatering processes.

REFERENCES

Bearsley, S., Forbes, A. & Haverkamp, R.G., 2004. Direct observation of the asphaltene structure in paving-grade bitumen using confocal laser-scanning microscopy. *Journal of Microscopy*, 215(2), pp.149–155.

Chalaturnyk, R.J., Don Scott, J. & Özüm, B., 2002. Management of Oil Sands Tailings. *Petroleum Science and Technology*, 20(9–10), pp.1025–1046. Available at: http://www.tandfonline.com/doi/abs/10.1081/LFT-120003695.

Chassagne, C., Mietta, F. & Winterwerp, J.C., 2009. Electrokinetic study of kaolinite suspensions. *Journal of Colloid and Interface Science*, 336(1), pp.352–359. Available at: http://dx.doi.org/10.1016/j.jcis.2009.02.052.

Demoz, A. & Mikula, R.J., 2012. Role of Mixing Energy in the Flocculation of Mature Fine Tailings. *Journal of Environmental Engineering*, 138(1), pp.129–136.

Don Scott, J., Dusseault, M.B. & David Carrier, W., 1985. Behaviour of the clay/bitumen/water sludge system from oil sands extraction plants. *Applied Clay Science*, 1(1–2), pp.207–218.

Dusseault, M.B. & Don Scott, J., 1983. Tailings Pond Behavior and Characterization of Oil Sand Tailings Sludge. *Particulate Science and Technology*, 1(3), pp.295–309.

Kessick, M., 1979. Structure And Properties of Oil Sands Clay Tailings. *Journal of Canadian Petroleum Technology*, (2).

Kitchener, J. a., 1972. Principles of Action of Polymeric Flocculants. *British Polymer Journal*, 4(September 1971), pp.217–229. Available at: http://onlinelibrary.wiley.com/doi/10.1002/pi.4980040307/abstract.

Kotylar, L.S., Sparks, B.D. & Schutfe, R., 1996. Effect of Salt on the Floculation Behavior of Nano Particles in Oil Sands Fine Tailings. , 44(l), pp.121–131.

Lee, C.S., Robinson, J. & Chong, M.F., 2014. A review on application of flocculants in wastewater treatment. *Process Safety and Environmental Protection*, 92(6), pp.489–508. Available at: http://dx.doi.org/10.1016/j.psep.2014.04.010.

McFarlane, A.J., Addai-Mensah, J. & Bremmell, K., 2005. Rheology of flocculated kaolinite dispersions. *Kore-Australia Rheology Journal*, 17(4), pp.181–190.

Mikula, R.J. & Munoz, V. a., 2000. Characterization of emulsions and suspensions in the petroleum industry using cryo-SEM and CLSM. *Colloids and Surfaces A: Physicochemical and Engineering Aspects*, 174(1–2), pp.23–36.

Mpofu, P., Addai-Mensah, J. & Ralston, J., 2003. Investigation of the effect of polymer structure type on flocculation, rheology and dewatering behaviour of kaolinite dispersions. *International Journal of Mineral Processing*, 71(1–4), pp.247–268.

Nasser, M.S. & James, A.E., 2007. Effect of polyacrylamide polymers on floc size and rheological behaviour of kaolinite suspensions. *Colloids and Surfaces A: Physicochemical and Engineering Aspects*, 301(1–3), pp.311–322.

Nasser, M.S. & James, a. E., 2006. The effect of polyacrylamide charge density and molecular weight on the flocculation and sedimentation behaviour of kaolinite suspensions. *Separation and Purification Technology*, 52(2), pp.241–252.

Shende, S.S. et al., 2016. Total Internal Reflection Fluorescence Microscopy to Investigate the Distribution of Residual Bitumen in Oil Sands Tailings. *Energy and Fuels*, 30(7), pp.5537–5546.

Sworska, A., Laskowski, J.S. & Cymerman, G., 2000a. Flocculation of the Syncrude fine tailings Part I. Effect of pH, polymer dosage and Mg2+ and Ca2+ cations. *International Journal of Mineral Processing*, 60(2), pp.143–152.

Sworska, A., Laskowski, J.S. & Cymerman, G., 2000b. Flocculation of the Syncrude fine tailings Part II. Effect of hydrodynamic conditions. *International Journal of Mineral Processing*, 60(2), pp.153–161.

Wang, C. et al., 2014. Current state of fine mineral tailings treatment: A critical review on theory and practice. *Minerals Engineering*, 58, pp.113–131. Available at: http://dx.doi.org/10.1016/j.mineng.2014.01.018.

Wang, X.W. et al., 2010. Polymer aids for settling and filtration of oil sands tailings. *Canadian Journal of Chemical Engineering*, 88(3), pp.403–410.

Watson, P. et al., 2011. Breakage and Reformation of Flocs in Oil Sands Tailings Slurries. In *Proceedings Tailings and Mine Waste*.

Wilkinson, N. et al., 2016. Internal structure visualization of polymer - clay flocculants using fluorescence. *Colloids and Interface Science Communications*, 10–11, pp.1–5. Available at: http://dx.doi.org/10.1016/j.colcom.2016.03.002.

Zbik, M.S., Smart, R.S.C. & Morris, G.E., 2008. Kaolinite flocculation structure. *Journal of Colloid and Interface Science*, 328(1), pp.73–80. Available at: http://dx.doi.org/10.1016/j.jcis.2008.08.063.

ADSORPTION ISOTHERM AND KINETICS STUDY OF ACID-EXTRACTABLE ORGANICS REMOVAL FROM OIL SANDS PROCESS-AFFECTED WATER ON BIOCHAR AND ACTIVATED CARBON

Tazul I. Bhuiyan[1], Jin K. Tak[2], Don Harfield[2] and Josephine M. Hill[1]
[1]Chemical & Petroleum Engineering Department, University of Calgary, Calgary, Canada
[2] Processing Technologies, Alberta Innovates – Technology Futures, Vegreville, Canada

ABSTRACT

The acid-extractable organics (AEO) in oil sands process-affected water are mainly composed of naphthenic acids, which are toxic to aquatic organisms, and must be removed to allow reclamation of the land. Adsorption processes in batch (passive) or flow configurations, with various adsorbents, can be used to clean up the water. Biochar made from local biomass could be environmentally beneficial. Although significantly less expensive than activated carbon (AC), biochar is also much less effective. In this study, biochar and AC from locally available biomass were compared with three commercial AC samples (two coal based and one Malaysian wood based) for the adsorption of AEO from oil sands process-affected water. Adsorption isotherms were collected for Norit AC, and acidified hemp shives, with the former providing the basis to design a single-stage batch adsorption system. For the acidified hemp shives, precipitation occurred with the adsorption such that the isotherm could not be fit to a traditional model. Adsorption kinetics were measured for the Norit AC and for a wheat straw biochar. The data for both samples was best fit by a pseudo-second order model.

INTRODUCTION

Background

To extract resources with surface mining processes, 2.2 volumes of freshwater are required for each volume of bitumen produced. The used water, called oil sands process-affected water (OSPW), is placed in tailings ponds (COSIA, 2014) to allow the dissolved solids to settle. This water also contains salts, heavy metals, and dissolved organic compounds including organic acids, phenols, cresols, benzene, toluene and thiophenols (Allen, 2008). Some of the dissolved organic compounds present in OSPW have been identified as naphthenic acids (NA), which are a complex mixture of alkyl-substituted acyclic and cycloaliphatic carboxylic acids that are acutely toxic to aquatic organisms (Allen, 2008; Grewer et al., 2010). More specifically, NA concentrations above 5 mg/L cause liver and heart damage to mammals, decrease the survival rate of birds, and increase the deformity of fish eggs (Rogers et al., 2002; Gentes et al., 2006).

The decontamination of the tailings ponds has been studied with different technologies including activated carbon (AC) adsorption. On the lab scale, AC is effective in removing AEO from water but scaling up the process to the tailings ponds is not yet economically feasible (Quinlan and Tam, 2015). One alternative is the replacement of AC with a lower cost charred biomass (i.e., biochar). Inyang and Dickerson (2015) reported the cost of AC as \$1500/ton compared to \$245/ton for biochar. The physical and adsorption properties of these two types of materials are quite different, with AC generally having a much higher surface area, porosity, and capacity than biochar. The actual difference in the physical properties depends on the preparation method but the adsorption capacity is typically ~2 orders of magnitude lower for biochar (Veksha et al., 2016). The overall process cost has to consider the lower capacity of biochar but also available tax credits if locally sourced materials can be used.

The main objective of this study is to obtain adsorption isotherms and kinetics data required for process design. More specifically, the data from the isotherm studies was used to size a single-stage batch adsorption system. These studies also provided information on the adsorption process on the different adsorbents.

MATERIALS AND METHOD

Materials

Wheat straw (Alberta, Canada), hemp shives residue (Alberta, Canada) and aspen wood chips (Alberta-Pacific Forest Industries Inc., Alberta, Canada) were used for this study. The three commercial AC samples were ColorSorb G5 (Jacobi, Kalmar, Sweden), Norit, and Darco (Sigma Aldrich, Missouri, USA) carbon. The Norit and Darco carbon samples are coal based and steam activated, while ColorSorb G5 is also steam activated but wood based. OSPW was collected from an oil sands tailings pond (Pond 7, Suncor Energy Inc., Alberta, Canada) and transferred to the University of Calgary in April 2014. The OSPW sample was stored at 4 °C. The total organic content (TOC) of the water varied less than 10 % over the course of the experiments with the same batch of water.

Preparation of biochar and AC

Biochar from hemp shives and wheat straw were prepared in a rotary drum batch pyrolyzer. The samples were heated at 10 °C min^{-1} to 600 °C and held at this temperature for 0.5 h. No sweep gas was used. Acidification of the hemp shives was achieved with the impregnation of 13 % H_2SO_4, before drying at 105 ºC for 12 h. CO_2 activated aspen AC was prepared in a vertical down-flow packed bed reactor in which the biochar sample was heated at 10 ºC min^{-1} under N_2 flow to 800 ºC, then activated with CO_2 for 1 h.

Characterization of biochar and AC

The surface area and porosity were determined with N_2 adsorption at -196 ºC (Tristar 3000, Micromeritics, USA) using the Brunauer, Emmett and Teller (BET) equation in a relative pressure (P/P_o) range of 0.02 - 0.3. The total pore volume was determined at a relative pressure of ~0.97.

Adsorption studies

All adsorption studies were done in batch mode using glass vials shaken at 25 °C and 225 rpm in an incubating shaker (VWR symphony 5000I, Henry Troemner LLC, USA). To obtain the approximate adsorption capacities, 0.02 g or 0.4 g of sample and 20 mL of OSPW (at 25 °C) were added to the vials and then shaken for 24 h. For collection of the adsorption isotherms, 0.01-1.5 g of biochar or AC was mixed with 20 mL water. For the kinetics study, samples were taken after 30, 60, 120, 240, 480, 960, and 1320 min of shaking. A sample of the solution (~15 mL) was obtained with a syringe and filtered through a 0.45 µm polyethersulfone membrane filter (Sterile syringe filter, VWR International, USA). The solutions were analyzed by a total organic carbon (TOC) analyzer (TOC-VCPN, Shimadzu, Japan). Three replicates of each adsorption experiment were done, and the results are reported as averages ± standard deviation of the three measurements.

RESULTS AND DISCUSSION

Batch adsorption of AEO

Figure 1a compares the adsorption capacities of the samples at only a single set of conditions (0.02 g adsorbent in 20 mL OSPW) but illustrates the orders of magnitude difference in the adsorption capacities of the AC and biochar samples. The Norit AC sample had the highest AEO adsorption capacity (49 mg/g) followed by ColorSorb G5 AC (40 mg/g) and Darco AC (33 mg/g). The first two AC samples were in powdered form while the latter AC was in granular form, which may have led to diffusion limitations. The biochar from Aspen wood had essentially no capacity for AEO. After activation to AC, however, the capacity (41 mg/g) was between that of the Norit and Colorsorb AC samples. The biochar from hemp shives with and without acidification also had low capacity (1.5 mg/g and 1.2 mg/g, respectively), as did the wheat straw (2.1 mg/g).

If the amount of adsorbent is increased from 0.02 g to 0.4 g, more of the AEO is removed and the percent removals of each adsorbent in these conditions are shown in Figure 1b. Experiments with the addition of only acid (no biochar) to OSPW confirmed that precipitation occurred as the pH decreased. That is, the acid was released from the acidified hemp shives biochar, lowering the pH and resulting in precipitation of the AEO. With the larger amount of adsorbent, a larger pH decrease occurred and contact with the acidified hemp shives biochar resulted in a higher percentage removal of AEO (41 % versus 4 % without acidification).

Physical properties

The surface areas and pore volumes of the samples are listed in Table 1. The surface area and total pore volume of the commercial AC samples were 650-990 m^2/g and 0.61-0.78 cm^3/g, respectively. After acidification the surface area and total pore volume of hemp shives biochar were decreased from 56 m^2/g to 3 m^2/g and 0.04 cm^3/g to 0.01 cm^3/g, respectively. The increase in adsorption capacity was a result of the decrease in pH as discussed above. The surface area and total pore volume of CO_2 activated aspen AC were 1020 m^2/g and 0.56 cm^3/g, respectively, which were similar to the ColorSorb G5 AC, consistent with their similar adsorption capacities. The surface area and total pore volume for wheat straw biochar were 20 m^2/g and 0.02 cm^3/g, respectively.

Adsorption isotherms

The data shown in Figure 1 only represents two sets of conditions and so complete isotherms were collected for two of the samples - Norit AC and acidified hemp shives biochar. The experimental data was fit with the Langmuir, and Freundlich isotherm models and these fits are shown in Figure 2 with the model parameters in Table 2.

The Langmuir isotherm is as follows

$$q_e = \frac{a_0 b C_e}{1 + b C_e} \ldots\ldots..(1)$$

where q_e (mg/g) is the amount of AEO adsorbed on the solid surface at equilibrium, C_e (mg/L) is the equilibrium concentration of AEO, a_0 and b are constants. The Freundlich isotherm, with constants K_F and n, is as follows

$$q_e = K_F C_e^{\frac{1}{n}} \ldots\ldots\ldots(2)$$

The coefficient of determination (R^2) for the Langmuir and Freundlich model fits for Norit AC were above 0.98 (Table 2). The experimental data were best fit with the Langmuir isotherm, for which all error functions, including the residual root mean square error (RMSE) and the chi square (λ^2) error, were lower than for the Freundlich isotherm. The good fit to this isotherm is consistent with the pore space being completely filled upon monolayer adsorption. Under the experimental conditions, the maximum adsorption capacity was not reached as the curve is still increasing and has not reached a plateau. The limited solubility of AEO limits the equilibrium concentrations (Limousin, et al., 2007) that can be obtained.

The experimental data for the acidified hemp shives was not well fit by either the Langmuir or Freundlich models due to surface precipitation in addition to adsorption. A multilayer precipitation model was applied to the data (dashed line in Figure 2b). Even this model is not a good fit with the data.

Adsorption isotherms can be used to predict the design of single-stage batch adsorption systems by the following equation (Bulut et al., 2008)

$$V(C_0 - C_1) = M(q_1 - q_0) = Mq_1 \ldots\ldots..(3)$$

where C_1 is the effluent AEO concentration, C_0 is the initial AEO concentration, V is total volume of OSPW to be treated, M is the mass of adsorbent, and q_1 and q_0 are the amounts adsorbed at time, t, and initially. The latter, q_0, is assumed to be zero. As the system reaches equilibrium, $C_1 \to C_e$ and $q_1 \to q_e$ and

$$\frac{M}{V} = \frac{C_0 - C_e}{q_e} = \frac{C_0 - C_e}{\frac{a_0 b C_e}{1 + b C_e}} \ldots\ldots\ldots.(4)$$

If the volume of OSPW and target AEO removal amount are known, the amount of adsorbent required for the adsorption process can be calculated. For example, in Figure 3, 1000 L of OSPW containing 65 mg/L AEO is treated with a desired final concentration of 6.5 mg/L. The amount of Norit AC required for this single batch adsorption process using the parameters from Table 2 for the Langmuir isotherm is calculated as follows:

$$M = \frac{58.5\ \frac{mg}{L}}{\frac{187\frac{mg}{g}\times 0.02\frac{L}{mg}\times 6.5\frac{mg}{L}}{1 + 0.02\ \frac{L}{mg}\times 6.5\ \frac{mg}{L}}} \times 1000\ L = 2\ .72kg$$

More work is required to determine how to fit the isotherms when adsorption and precipitation are occurring simultaneously.

AEO adsorption kinetics study

The adsorption process can be a combination of the following consecutive steps (i) transport of adsorbate in the bulk of the solution (can be ignored if there is rapid mechanical mixing), (ii) diffusion of adsorbate across the liquid film surrounding the adsorbent particles (external mass transfer), (iii) diffusion of adsorbate in the liquid within the pores of the adsorbent particle and along the pore walls (intra-particle diffusion), and

(iv) adsorption and desorption of the adsorbate on/from the adsorbent surface. The overall adsorption rate can be controlled by any of the steps or by a combination of two or three steps (Plazinski et al., 2009). Mesoporous materials (2-50 nm pore size) reach equilibrium faster than microporous materials due to faster diffusion in the larger pores. To determine the rate-controlling steps for AEO adsorption on Norit AC, the rate of adsorption was measured and the data fit with several kinetics models. For comparison, kinetics data were also collected for wheat straw biochar, which had the highest adsorption capacity among all biochar samples tested. The kinetics models used were pseudo first-order (Eqn. 5), pseudo second-order (Eqn. 6) and intra-particle diffusion (Eqn. 7)

$$\ln(q_e - q_t) = \ln(q_e) - \frac{k_1 t}{2.303} \ldots\ldots(5)$$

$$\frac{t}{q_t} = \frac{1}{k_2 q_e^2} + \frac{1}{q_e} t \ldots\ldots(6)$$

$$q_t = k_{pi} t^{\frac{1}{2}} + c_i \ldots\ldots\ldots(7)$$

where q_t (mg/g) is the amount of AEO adsorbed at time t (min), k_1 (1/min) is the rate constant for pseudo-first order adsorption, k_2 is the pseudo-second order constant, k_{pi} (mg/g.min^{½}) is the intra-particle diffusion rate constant at stage i (two stages were observed as discussed later), and c_i is a constant applicable for stage *i.*

The AEO removal capacities at different contact times with Norit AC and wheat straw biochar are shown in Figures 4a and b, respectively. After 200 min both samples reached a plateau value, which was taken as the equilibrium value. Note the capacity for the Norit AC is lower than in Figure 1 because a different batch of OSPW with a lower AEO concentration was used for the experiments (see capacity versus concentration relationship in Figure 2a).

The pseudo-second order and intra-particle diffusion model fits are shown in Figures 4c and d, and 5a and b, respectively, with the corresponding kinetics parameters in Table 3. Based on the correlation coefficient (R^2), all models fit the data reasonably well. Considering the normalized standard deviation (Δq), the pseudo-second order fit was much better than the pseudo-first order fit.

The pseudo-second order model is based on the assumption that adsorption is the rate limiting step. The pseudo-second order rate constants (k_2) were the same for Norit AC and wheat straw biochar, consistent with the time required for equilibrium. In the pseudo-second order model, both chemisorption and physisorption can occur. At alkaline conditions, the AEO or naphthenic acids are essentially all deprotonated, forming naphthenates, which can chemisorb.

In the intra-particle diffusion model fits there are two regions with different slopes. Surface adsorption and intra-particle diffusion can both contribute to the adsorption process. The first region with the steeper slope is associated with the diffusion of AEO through the solution to the external surface of adsorbent - the boundary layer diffusion of AEO molecules is the rate-limiting step. The second region is associated with gradual adsorption, and the intra-particle diffusion becomes rate-limiting. The intra-particle diffusion constant k_{p1} is larger than k_{p2} for both samples, indicating a higher rate of surface adsorption initially, consistent with the higher number of vacant sites. Since the first linear region of the curves does not pass through the origin, there is some degree of boundary layer control.

Further analysis is required to determine which model and parameters should be used to design a column experiment. The pseudo-second order parameters have been used as follows (Reynold, 1982):

$$\frac{C_e}{C_o} = \frac{1}{1 + e^{\frac{k_2}{Q}(q_e M - C_0 V)}} \ldots\ldots\ldots\ldots(8)$$

$$\ln\left(\frac{C_0}{C_e} - 1\right) = \frac{k_2 q_e M}{Q} - \frac{k_2 q_e V}{Q} \ldots\ldots(9)$$

where C_e is the effluent AEO concentration, C_0 is the initial AEO concentration, V is total volume of OSPW need to be treated, M is the mass of adsorbent and Q is the volumetric flowrate of OSPW. If the volume and volumetric flowrate of OSPW, target AEO removal amount, and adsorption capacity are known, the amount of adsorbent required for the adsorption process can be calculated using rate constant value.

CONCLUSIONS

The equilibrium adsorption data for Norit AC were best fit with a Langmuir isotherm, while the data for acidified hemp shives was not fit with any models because both adsorption and precipitation occurred. The kinetics data for Norit AC and wheat straw biochar were both fit well by the pseudo-second order and intra-particle diffusion models.

ACKNOWLEDGEMENTS

We acknowledge funding from Alberta Innovates Bio Solutions and Suncor Energy, biomass from Alberta-Pacific Forest Inc., OSPW from Suncor Energy, and technical assistance with the TOC measurements from Farzin Malekani.

REFERENCES

Allen, E.W. 2008. Process water treatment in Canada's oil sands industry: I. Target pollutants and treatment objectives. Journal of Environmental Engineering and Science, 7(2), 123-138.

Bulut, E., Ozacar, M., Sengil, I.A. 2008. Adsorption of malachite green onto bentonite: Equilibrium and kinetics studies and process design, Microporous and Mesoporous Material 115, 234-246.

COSIA, 2014. Accessed on http://www.cosia.ca/initiatives/water/water-challenge-statements

Gentes, M. L., Waldner, C., Papp, Z., Smits, J. E. 2006. Effects of oil sands tailings compounds and harsh weather on mortality rates, growth and detoxification efforts in nestling tree swallows (Tachycineta bicolor). Environmental Pollution. 142:24-33.

Grewer, D.M., Young, R.F., Whittal, R.M., Fedorak, P.M. 2010. Naphthenic acids and other acid-extractables in water samples from Alberta: What is being measured? Science of the Total Environment, 408(23), 5997-6010.

Inyang, M., Dickenson, E. 2015. The potential role of biochar in the removal of organic and microbial contaminants from potable and reuse water: A review. Chemosphere, 134, 232-240.

Limousin, G., Gaudet, J.P., Charlet, L., Szenknect, S., Barthes, V., Krimisaa, M. 2007. Sorption isotherms: A review of physical bases, modeling and measurement. Applied Geochemistry, 22, 249-275.

Plazinski, W., Rudzinski, W., Plazinska, A. 2009. Theoretical models of sorption kinetics including a surface reaction mechanism: A review. Advances in Colloid and Interface Science, 152, 2-13.

Quinlan, P.J., Tam, K.C. 2015. Water treatment technologies for the remediation of naphthenic acids in oil sands process-affected water. Chemical Engineering Journal, 279, 696-714.

Reynold, T.D., 1982. Unit operation and process in environmental engineering. Wadsorth, CA.

Rogers, V.V., Wickstrom, M., Liber, K., and MacKinnon, M. D. 2002. Acute and subchronic mammalian toxicity of naphthenic acids from oil sands tailings. Toxicological Sciences, 66:347-355.

Veksha, A., Bhuiyan, T.I., Hill, J.M. 2016. Activation of aspen wood with carbon dioxide and phosphoric acid for removal of total organic carbon from oil sands produced water: increasing the yield with bio-oil Recycling. Materials, 9(1): 20-33.

Table 1. Physical property analysis of biochar and AC

Sample	Surface Area (m^2/g)	Total Pore Volume (cm^3/g)
Norit AC	950	0.78
ColorSorb G5 AC	990	0.61
Darco AC	650	0.69
Hemp shives biochar	56	0.04
Acidified hemp shives biochar	3	0.01
Wheat straw biochar	20	0.02
CO_2 activated Aspen AC	1020	0.56

Table 2. Isotherm parameters for adsorbent-OSPW system at 25 °C

Model parameters	Sample	
	Norit AC	**Acidified hemp shives biochar**
Langmuir		
a_0 (mg/g)	187	107
b (L/mg)	0.02	0.0003
R^2	0.99	0.72
RMSE	2.79	0.38
λ^2	1.29	0.48
Freundlich		
K_F [$(mg/g)/(mg/L)^{1/n}$]	4.99	0.02
n	1.31	0.81
R^2	0.98	0.74
RMSE	4.45	0.36
λ^2	3.57	0.42

Table 3. Model fits for AEO adsorption on Norit AC and wheat straw biochar at 25 °C

Model Parameters	Sample	
	Norit AC	**Wheat straw biochar**
Pseudo-first order		
$q_{e\ exp}$ (mg/g)	39.48	0.58
q_e (mg/g)	1.55	0.26
k_1 (1/min)	0.0128	0.0013
R_1^2	0.94	0.97
Δq(%)	39.23	22.76
Pseudo-second order		
q_e (mg/g)	39.53	0.60
k_1 (g/mg.min)	0.03	0.03
R_2^2	1.00	0.99
Δq(%)	0.05	1.13
Intra-particle diffusion model		
k_{p1} (mg/g.min$^{0.5}$)	0.20	0.03
C_1	36.35	0.15
R^2	0.97	0.98
k_{p2} (mg/g.min$^{0.5}$)	0.09	0.01
C_2	39.19	0.45
R^2	0.97	0.97

(a)

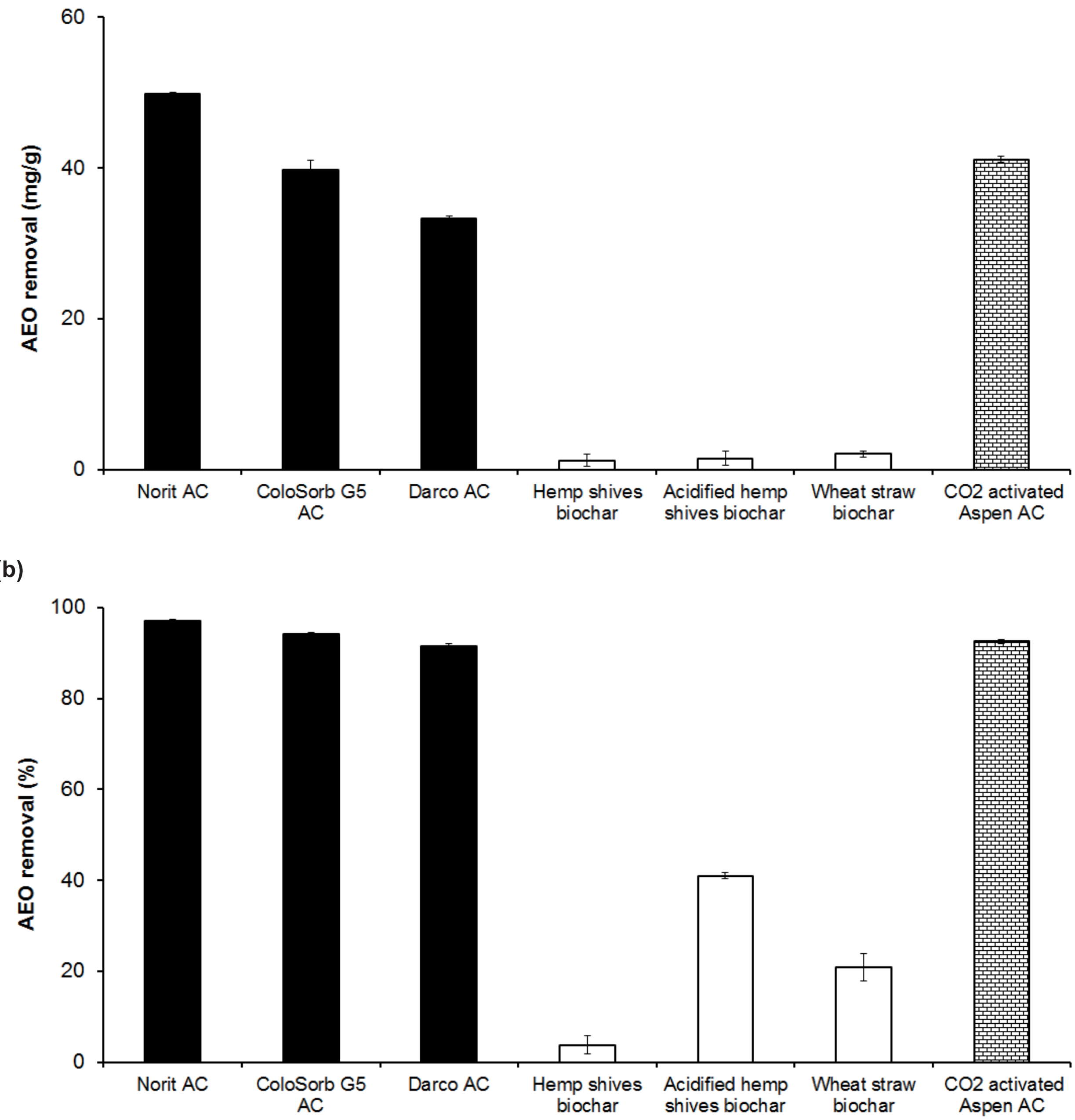

Figure 1. AEO removal in mg/g or in percentage for adsorption from OSPW by three commercial carbons (black bars), as prepared and acidified hemp shives biochar (white bars), wheat straw biochar, and CO_2 activated aspen AC (hatched bar) at 25°C with (a) 0.02 g adsorbent in 20 mL OSPW and (b) 0.4 g adsorbent in 20 mL OSPW

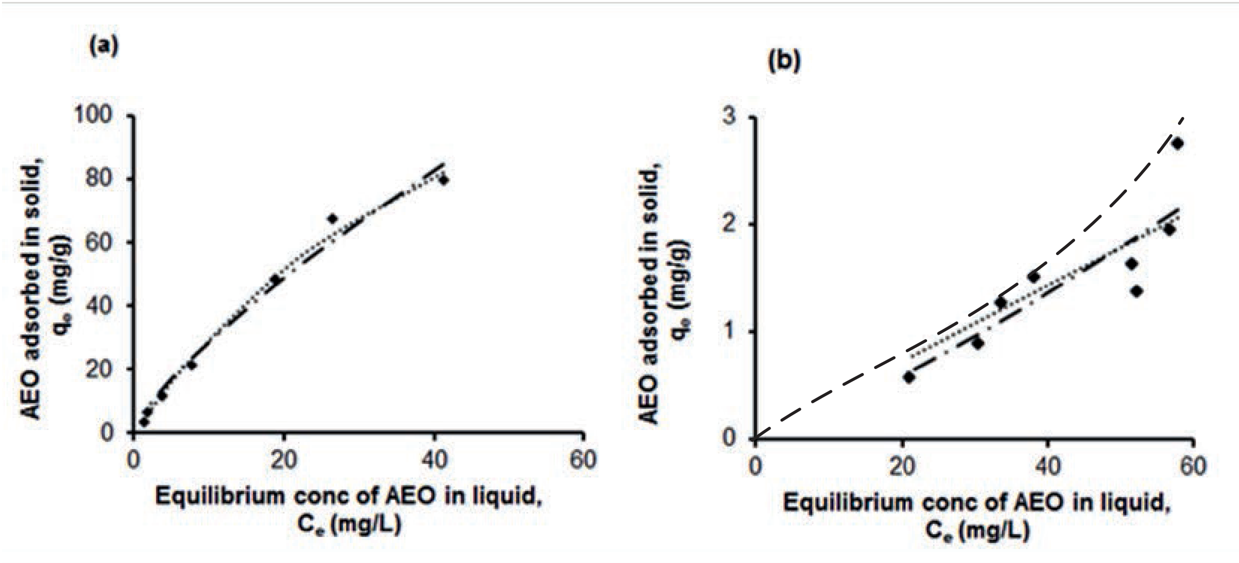

Figure 2. Adsorption isotherms (points) and model fits for the removal of AEO from OSPW by (a) Norit AC and (b) acidified hemp shives biochar at 25 °C. Isotherm models used are Langmuir (dotted line), Freundlich (dash-dot line) and multilayer precipitation (dashed line, only for hemp shives biochar).

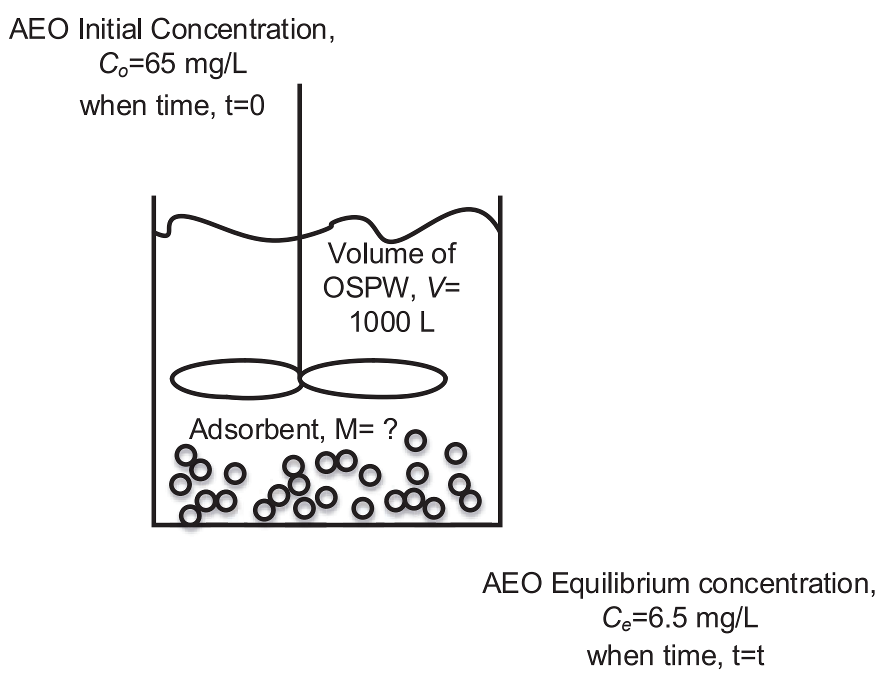

Figure 3. Schematic of a batch adsorption process for the removal of AEO from OSPW

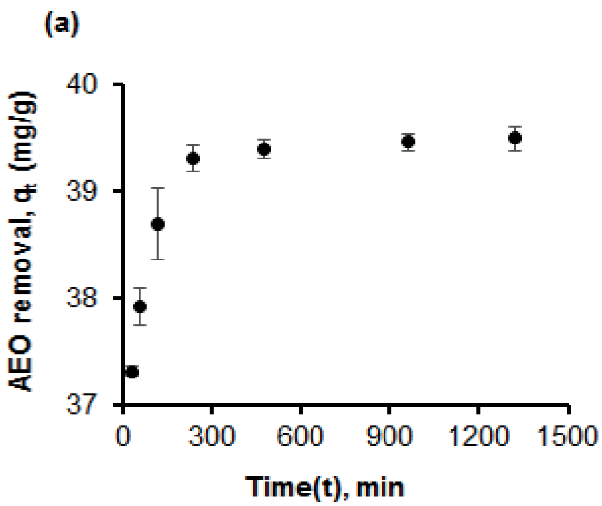

Figure 4. AEO removal at 25 °C as a function of time (a), (b), and model fits of this data to the pseudo-second order model (c), (d) for Norit AC (a, c) and wheat straw biochar (b, d)

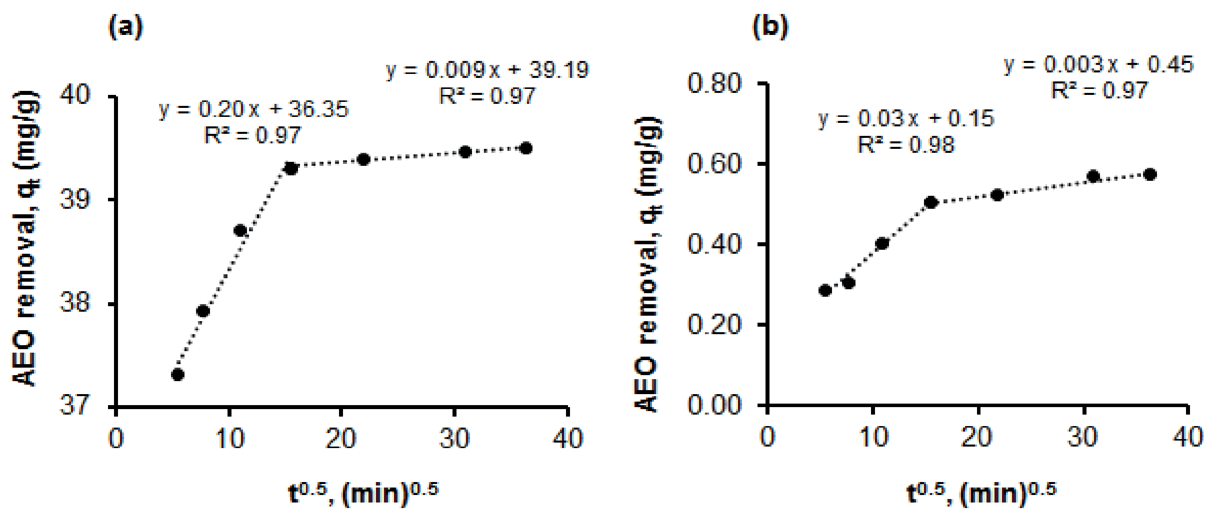

Figure 5. Intra-particle diffusion model for AEO adsorption by (a) Norit AC and (b) wheat straw biochar at 25°C

POLYMER-MFT INTERACTIONS: FROM SURFACE CHEMISTRY TO RHEOLOGY

Cliff T. Johnston[1], Mohammadhasan Sasar[1], Marika Santagata[1],
Antonio Bobet[1], Linna Duan[1] and Heather A. Kaminsky[2]
[1]Purdue University, West Lafayette, IN, USA
[2]Northern Alberta Institute of Technology, Edmonton, Canada

ABSTRACT

The presence of micron and nano-sized clay minerals that lead to slow consolidation rates of MFT, play a defining role in the management of mature fine tailings (MFT). At present, one of the most effective means of volume consolidation of MFTs is through the use of polymeric flocculants. The topic of this paper focuses on developing an improved understanding of both the rheology of MFT and of polymer-treated MFT (tMFT) and the surface chemistry that govern polymer-MFT interactions, bitumen release, net water release, and water chemistry of the release water. Rheological characterization of MFT and polymer-treated MFT show distinct differences in storage modulus and yield stress. The underlying surface chemistry of MFT and tMFT also show important differences. In comparison to untreated MFT, thermal analysis and spectroscopic analysis of treated MFT show that, for some MFTs, the polymer induces both bitumen release to the aqueous phase and bitumen redistribution on the MFT particles.

INTRODUCTION

Currently, the Clark Hot Water Extraction process used in the extraction of bitumen from Athabasca oil sands deposits lead to production of 1.5 barrels of slow settling mature fine tailings per barrel of extracted bitumen (Grant et al., 2013). As a result, close to one billion cubic meters of MFTs have accumulated in tailing ponds in Alberta, CA which makes the management of these tailings very challenging for the oil sands industry.

The presence of micron and nano-sized clay minerals and in particular the presence of clay minerals within the < 2 nm fraction and of ultrafine particles (< 300 nm) leads to slow consolidation rates of MFTs. As the result, they trap large quantities of process water that cannot be reused.

At present, one of the most effective means of volume consolidation of MFT is through the use of polymeric flocculants. High molecular weight polymeric flocculants have been used for many years to help remove slow settling particles in water treatment and other applications. However, in high concentration sludges such as MFTs (i.e. solid content of about 30%) successful flocculation depends strongly on polymer dosage and mixing energy. For example, one of the earlier works on the effects of dosing and mixing is documented by Gregory and Guibai (1991) on the treatment of kaolinite dispersions. Optimal flocculation is also dependent on the nature of the MFT and process water chemistry.

A better understanding of how high molecular weight polymeric flocculants interact with Mature Fine Tailings (MFT) will help with the design of more efficient polymers. It will also lead to more effective polymer dosing (i.e. using less polymer with efficient mixing), which will ultimately translate into cost savings.

Given that small changes in the particle-particle interaction manifest in the overall rheological behavior of the MFT, the topic of this paper is on the development of an improved understanding of both the rheology of untreated MFTs and of polymer-treated MFTs. Rheological characterization of treated and untreated MFTs may show distinct differences in e.g. storage modulus and yield stress, which coupled with surface chemistry characterization, may help provide a better understanding of the complex interaction that exists between the clay fraction, bitumen, polymer and water components of MFTs. Rheological studies may also help reveal differences in the particle-particle interaction across different types of MFTs.

RESEARCH APPROACH

Materials

In this paper, three distinct MFTs collected from various tailing ponds in Alberta, Canada have been studied. MFTs 1 and 2 are from ponds originated from primary and secondary extraction processes, respectively. MFT 3 is from a tailing pond where tailings from multiple different processes were discharged.

Unless otherwise stated, all MFTs were diluted to a reference CWR (Clay to Water Ratio by mass) of 30% prior to flocculation or testing. It should be noted that each MFT was diluted using the Process Effluent Water (P.E.W) relevant to the same pond where the MFT was obtained to make sure that the chemistry of the pore water was not affected. The relevant P.E.W was also used to make the 0.45% w/w polymer solution used in flocculation. The anionic polyacrylamide polymer used is the commercially available FLOPAM A3338 (average molecular weight of 18×10^{6} g/mol) by SNF (Riceboro, Georgia).

Table 1 summarizes some of the basic characteristics of the three MFTs. The solid content is reported as the ratio of weight after oven drying at 110°C for 24 hours and the total weight. Since oven drying does not result in evaporation of bitumen, the solid content in this document refers to the total solids (mineral and bituminous organics). The slurry method outlined by SGS Canada Inc. oil sands, was used to obtain repeatable methylene blue adsorption index (MBI) values. Also the Dean Stark method (COSIA, 2014) is used in this document to report the bitumen content as mass of the bitumen to total mass.

Optimum Polymer Dosage

Table 1 reports the amount of polymer used for the treatment of each of the MFTs. The optimal polymer dose was determined using a titration-like procedure. In this method, small quantities of polymer solution (2-5 ml) were added to a known mass of MFT (usually 300 gr) and the mixture was pulse-mixed for about 5 seconds at 320 rpm with a gang mixer. Injection of small quantities of polymer was done during pulse mixing until a clear change in the structure of the MFT similar to “cottage cheese structure” and water release were observed. The amount of polymer solution (in mL) required to reach this condition was recorded. The polymer dosages required to attain the cottage cheese structure were in general agreement with findings by Omotoso et al. (2011) for other types of MFTs. These researchers reported optimal dosages of 0.9 to 1.7 g of polymer per kg of solids and a consistent value of 1.850 g of polymer per kg of clay for different types of MFTs.

It is important to know the optimum polymer dosage for maximum de-watering of a given MFT. Using lower dosages will result in incomplete flocculation causing lower water release. With higher than optimum polymer dosages, on the other hand, excess free polymer will be present in the released water and cause low water release. Very high doses of Polymer can result in re-stabilization of the mix.

Table 1. Basic characteristics of the MFTs, as received (Total solid and clay contents)

ID #	Solid Content (%)	MBI	Organic content (%)	Clay to Water Ratio	Optimum Polymer Dose	
					g/kg of solids	g/kg of clay
1	33.5	11.2	2.4	40.00	1.048	1.305
2	35.7	8.4	6.4	35.00	0.782	1.261
3	34.9	11.0	-	43.00	1.189	1.522

Flocculation Monitoring

A schematic of the experimental setup used for optimum flocculation of the MFTs is shown in Figure 1. The flocculation vessel, with dimensions of a standard 600 ml glass beaker, houses the 300 g MFT sample.

A single flat blade, 75mm x 25mm x 1mm thick, is used for stirring the mix. The blade, which has a clearance of 7 mm with the base of the vessel, is driven by a motor via a 6 mm diameter spindle, centrally positioned in the vessel. The motor is equipped with a controller capable of keeping the rotational speed at a constant assigned RPM. Two tubes on each side of the vessel supply the polymer solution through an automatic syringe pump. The polymer is injected over a 3 second period between

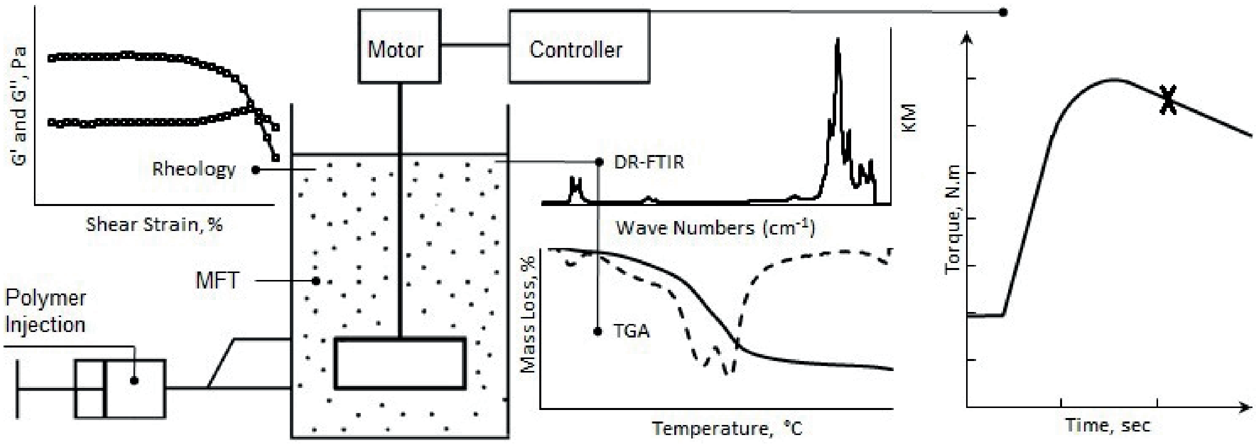

Figure 1. Schematic of the system for optimum flocculation of MFT

the blade and the vessel where the flow is most turbulent to ensure that it is distributed quickly and evenly into the MFT. The overhead stirrer is set to 320 rpm during polymer injection and mixing.

The controller to the overhead stirrer is connected to a digital multimeter that provides accurate measurements of the power going to the motor during mixing. The idea behind the setup is that changes in the viscosity of the MFT during polymer mixing cause the controller to adjust the power of the motor to keep the rotational speed constant. It is found that the power consumption of the motor is very sensitive to changes of the viscosity of the mixture and so the setup is effective in determining the optimum mixing time.

A recording of torque versus mixing time is shown in Figure 1. Time zero on this curve pertains to the moment when the polymer injection starts. The following four stages characterize the flocculation process:

1) The polymer is first brought into close contact with the MFT particles through mixing. During polymer injection and for a short time after that the no change in torque is observed. This suggests that the attachment of the polymer to the MFT has a reaction time of a few seconds.

2) Polymer is absorbed onto the clay surface and forms a network by bridging between particles. The sharp increase in the torque reading signals the rapid development of flocs.

3) As mixing continues the flocs begin breaking into smaller flocs and the water trapped between the particles begins to be release. This is manifested in the reduction of the torque and visible water release from the sample.

4) With further shearing, the flocs break down into smaller and smaller fragments and disperse again. This process appears irreversible and leads to very limited release of water from the MFT. When the sample reaches this stage of mixing it is said to be over sheared.

Avoiding over shearing is critical to maximizing water release in optimally dosed MFT samples. Therefore, in the tests presented in this paper, mixing at high rotational speed was stopped immediately after measuring the peak torque (X mark on curve in Figure 1). At this time the rotation speed is decreased to 100 rpm, and finally halted after observing evidence of water release.

Sample preparation

Water is released from the flocculated polymer-treated MFT (tMFT) over time. The majority of the water release occurs during the first 24 hours after flocculation but the process continues at a slower rate after that, with a continued increase of the clay-water ratio of the mixture. In this work, the change in the mechanical properties of the tMFT with clay water ratio was studied testing samples at different stages of the water release process. This required preparing samples that could drain freely with time. This was achieved placing the flocculated MFTs in aluminum cups with a perforated bottom that allowed free draining of water. The cups are designed to fit in the rheometer, allowing the rheological tests to be conducted without transferring the MFT samples. This minimizes sample disturbance, which can significantly affect the rheological measurements. The cups were kept in a sealed humid environment to prevent drying through evaporation up to the testing time.

Rheological measurements

Rheological tests were conducted using the Physica MCR 301 Rheometer, an air bearing, stress-controlled device manufactured by the Anton Paar Company. The standard 6 bladed vane geometry for this rheometer was used to conduct oscillatory and monotonic strain-rate controlled tests under temperature control. All rheological tests were conducted at 23±1°C on ~40 ml samples.

While rheological data have practical relevance to the design of pumping systems for the transport of MFT, and are directly relevant to the behavior of the polymer treated MFT following disposal, in this paper rheology is used as a means to gain insight into changes of the microstructure due to polymer treatment.

As discussed below, two different types of rheological tests, oscillatory and rotational tests, were conducted on both untreated and treated MFT to measure specific rheological properties.

Shear strain rate ramps were performed to measure the yield stress of the MFTs. In simple terms, yielding can be described as the point at which the material begins to flow. It is usually described by two parameters: a) the critical deformation after which the material starts to flow in the liquid regime ($\gamma_{critical}$) and b) the minimum stress (i.e. yield stress) required to reach this deformation (Coussot, 2005).

In shear strain ramps, increasing increments of shear rate are applied to the material and the yield stress is determined from the point where the material "apparently" begins to flow (Coussot, 2005).

It should be noted that clay dispersions are thixotropic materials with response markedly dependent on sample stress history. Because of this, the time between mixing and testing as well as small differences in the setup operations can have a very significant effect on the measured response. Therefore, rheological tests on clay dispersions typically involve a pre-shear stage and a subsequent rest period. The first stage is aimed at de-structuring the material in a consistent and reproducible manner, eliminating the effects of differences in the setup operations. The second stage is included to avoid testing the material immediately after the pre-shear stage, when rapid structure-buildup processes can cloud the interpretation of rheological data.

As a result of the above, the yield stress of the untreated MFTs was measured after pre-shearing of the sample at a shear rate of 600 s^{-1} for 5 minutes and a subsequent rest period of 15 minutes. The yield stress of the treated MFT (tMFT) samples was measured both in the intact state (no pre-shearing) and after significant remolding of the sample (i.e. pre-shearing at a shear rate of 600 s^{-1} for 30 minutes and allowing a subsequent rest period of 15 minutes).

In addition to the shear rate ramps, two types of oscillatory tests were conducted: time sweeps and amplitude sweeps.

The first involve the application of small strain oscillations $\gamma=\gamma_0 \sin[\omega t]$ with constant amplitude γ_0 and constant frequency ω, while measuring the resulting shear stress τ. This shear stress is, in general, shifted by a phase angle δ with respect to the strain wave. τ can also be expressed as the sum of an elastic (solid) component in phase with the applied strain, and an out-of-phase viscous component: $\tau = \gamma_0 \{G'\sin(\omega t) + G''\cos(\omega t)\}$, where G' and G'' are termed the storage (elastic) and loss (viscous) moduli, respectively.

If the applied shear strain is sufficiently small that the material remains in the linear visco-elastic regime, time sweeps can provide information on the small strain stiffness of the tested material in essentially a non-destructive way. These tests are also ideally suited to monitor changes in material response over time. In this testing program, oscillatory tests were used to monitor changes in the small strain storage modulus (referred to as G'_0) due to thixotropic behavior of the MFT slurry. A value of 0.1% for γ_0 was found to be appropriate for all the materials tested, and a constant frequency of 1 Hz was used for all the tests.

Amplitude sweep tests differ from time sweeps in that the applied oscillation increases, allowing the response of the material to be probed for a broad range of shear strains. In this testing program, amplitude sweeps were conducted varying γ_0 between 0.01% and 1000%, using a constant frequency of 1 Hz.

Diffuse reflectance FTIR (DR-FTIR) Analysis

Diffuse Reflectance Fourier Transform Infrared spectroscopy is a useful tool in obtaining information about the structure, bonding and reactivity of soil colloids. The details of DR-FTIR method is explained in detail by Johnston et al, 1996. In the current work, DR-FTIR was used to characterize MFTs because it detects the presence of clay minerals, bitumen and residual water and provides diagnostic information about the amount and type of bitumen present. Samples used for FTIR analysis were air dried for 24 hours prior to testing.

Thermal Analysis (TGA) of MFTs

In addition, thermal analysis methods were used to characterize the MFTs presented in this paper before and after polymer treatment. Gabbott (2008) provides a detailed explanation of the principles of Thermal Gravimetric Analysis. Samples used for TGA analysis were also air dried for 24 hours prior to testing. In this method the air dried material was subjected to a constant heating rate (here 20°C/min) and the mass of the sample is measured as a function of temperature. The main goal was to characterize the amount of bitumen and clay dehydroxylation for each of the MFTs.

RESULTS AND DISCUSSION

Rheology

Figure 2 summarizes the yield stresses values of the MFTs in the intact state as a function of clay-water ratio (CWR). The data are derived from measurements conducted on independent samples of the treated MFT (tMFT) over time as the water release process progressed. For all three tMFTs, the data show the expected trend of increasing yield stress with increasing CWR, with the yield stress increasing by over a ten fold, from values in the hundreds of Pascals to values in the kPa range, with the increase in CWR from 0.30 to 0.65.

Also included in Figure 2 are yield stress data for the untreated MFTs which for the CWR range considered fall in the 2-25 Pa range. Overall, these data are consistent with previously reported results for other MFTs (Omotoso et al., 2011). While also displaying a similar trend with CWR, at any CWR these data fall over one order of magnitude below the results for the tMFT. This difference reflects the effects of the addition of the polymer on the MFT structure, as well as contributions from the polymer itself.

Deviations between the three MFTs are observed when analyzing both the untreated and the treated data. Note, for example, the higher yield stress measured on tMFT-3 following treatment relative to the other two tMFTs. These deviations are a result of the different make-up of the MFTs, including the presence of organics, which impact both the response in the untreated state, as well as the level of effectiveness of the polymer treatment.

As discussed earlier, each of the data points shown in Figure 2 is derived from a shear rate ramp tests. Curves from three of these tests are reported in Figure 3. They pertain to untreated MFT-1, and treated tMFT-1 both in the intact state and following remolding, all tested at similar CWR values (40-42%).

Figure 3 shows the peak shear stress which is used as a measure of the yield stress (670 Pa and 34 Pa, for the two tests shown). Besides the previously discussed difference in the peak shear stress, the figure highlights how in the curve for the tMFT the peak shear stress occurs at much higher shear rate relative to the untreated MFT, reflecting a more “ductile” behavior following treatment. Both curves show a sharp decrease in the shear stress following peak. This behavior is a result of the de-structuring that occurs as the material flows. The reduction in shear stress as a result of this process is close to 80% for tMFT-1 versus less than 30% for untreated MFT-1, evidence of the greater sensitivity of the structure formed in the MFT following polymer treatment.

Figure 3 also shows the flow curve measured on the remolded tMFT-1. This curve falls in between the other two, with intermediate values of the yield stress and the corresponding shear rate. Relative to the intact tMFT-1 tested at the same CWR, the yield stress is reduced by over 75% following remolding. This is additional evidence of the sensitivity of the structure of the tMFT.

Complementary information on the effects of polymer treatment on structure and properties of the MFT can be gained examining the results of oscillatory measurements. Figure 4 summarizes values of the storage modulus obtained from strain oscillations with amplitude of 0.1% (i.e. small enough that the material remains in its linear viscoelastic range). As above, the data for the three MFTs both prior and after polymer treatment (intact results) are plotted as a function of CWR. Again, the data for the tMFT fall on a band above that for the untreated MFTs, with a power law describing the relationship between G'_0 and CWR for both types of materials. Unlike what was observed in Figure 2, the data for the three tMFTs fall on distinct parallel bands, with the data for tMFT-1 exceeding the values for tMFT-2 by almost a factor of 2. Recall from Figure 2 that the yield stress results for these two tMFTs fell on the same band, evidence of similar strength of the flocs formed as a result of treatment. The differences in G'_0 are thought to reflect variations in the microstructure at the clay particle level, which the small strain oscillation tests are designed to probe in what is essentially a non-destructive manner.

Additional insight into the effects of polymer treatment on the structure and properties of the tMFT can be gained examining the results of amplitude sweep tests, in which the amplitude of the applied oscillation is gradually increased while maintaining the frequency constant.

The results of three such tests on untreated MFT-1, and tMFT-1 both in the intact and the remolded state are shown in Figure 5. For each of the tests, the figure shows plots of storage modulus (G′) and loss modulus (G'') as a function of shear strain, γ. The G' and G" curves for untreated MFT-1 are typical of the response of concentrated clay dispersions: for small values of the shear strain G' and G" are constant and G'>> G", a reflection of the fact that the response is essentially elastic. For the test on the untreated MFT-1 shown in the figure the linear visco-elastic range extends to γ ~1-2%. Beyond this threshold, G' decreases rapidly, and eventually the G' curve intersects the G" curve. The shear strain corresponding to the point of intersection is referred to as the crossover strain and signals the transition to a region in which the viscous component dominates the response of the dispersion. This parameter can be related to interactions occurring at the particle-particle level (e.g. see Santagata et al. 2008).

Additional insight into the effects of polymer treatment on the structure and properties of the tMFT can be gained examining the results of amplitude sweep tests, in which the amplitude of the applied oscillation is gradually increased while maintaining the frequency constant.

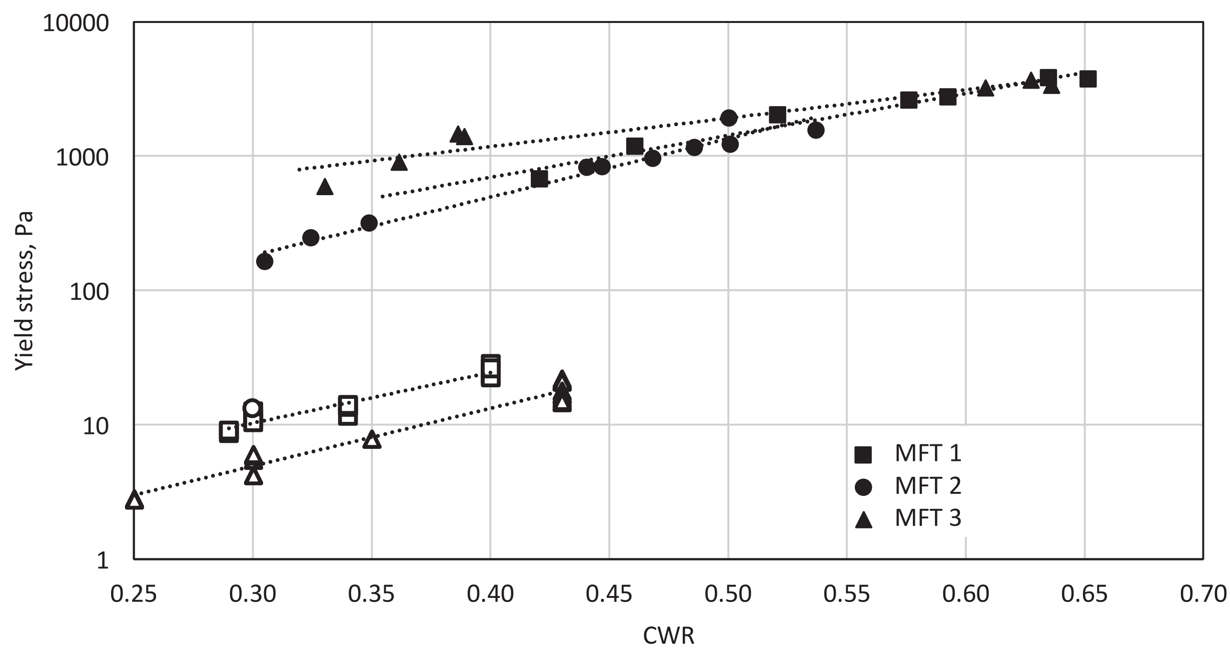

Figure 2. Yield stress of untreated and polymer treated MFTs as a function of CWR (Full markers are pertaining to the yield stress of intact tMFT samples and hollow markers are for untreated MFTs)

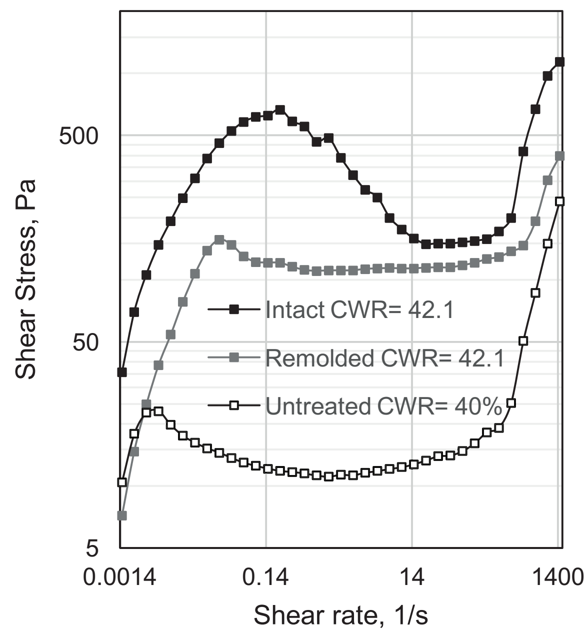

Figure 3. Comparison between the strain rate ramp tests between Untreated, Treated and remolded MFT 1 with similar CWR values

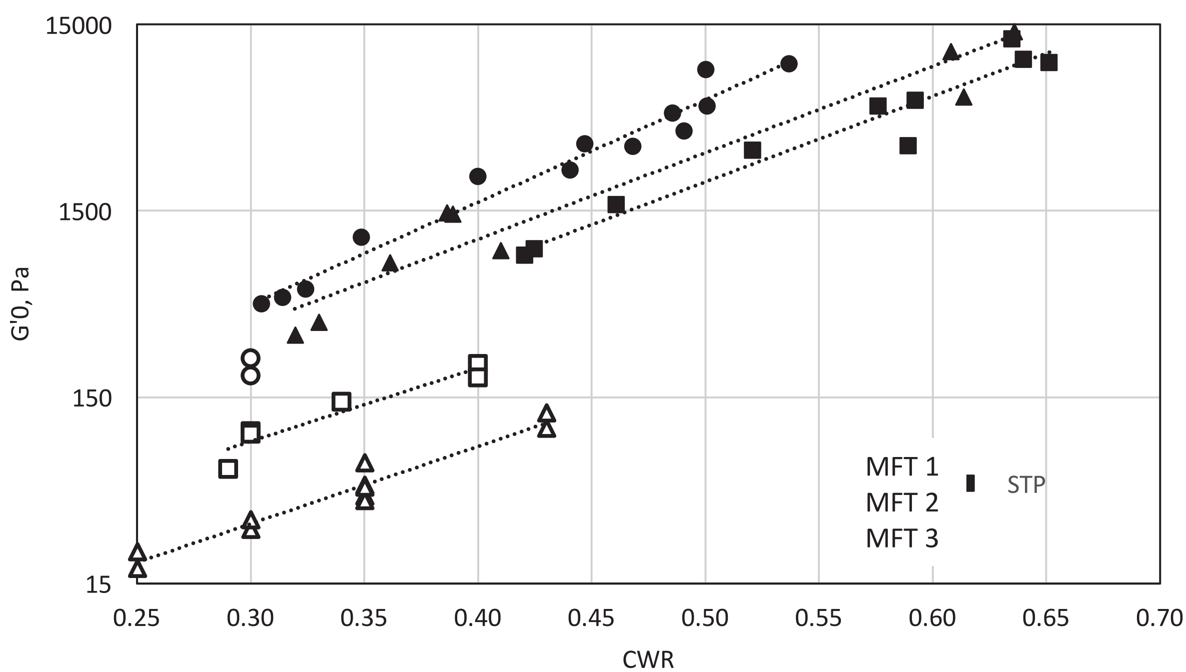

Figure 4. Initial shear stiffness untreated and polymer treated MFTs as a function of CWR (Full markers are pertaining to intact tMFTs and hollow markers show untreated MFTs)

The results of three such tests on untreated MFT-1, and tMFT-1 both in the intact and the remolded state are shown in Figure 5. For each of the tests, the figure shows plots of storage modulus (G′) and loss modulus (G'') as a function of shear strain, γ. The G' and G" curves for untreated MFT-1 are typical of the response of concentrated clay dispersions: for small values of the shear strain G' and G” are constant and G’>> G”, a reflection of the fact that the response is essentially elastic. For the test on the untreated MFT-1 shown in the figure the linear visco-elastic range extends to γ ~1-2%. Beyond this threshold, G’ decreases rapidly, and eventually the G’ curve intersects the G” curve. The shear strain corresponding to the point of intersection is referred to as the crossover strain and signals the transition to a region in which the viscous component dominates the response of the dispersion. This parameter can be related to interactions occurring at the particle-particle level (e.g. see Santagata et al. 2008).

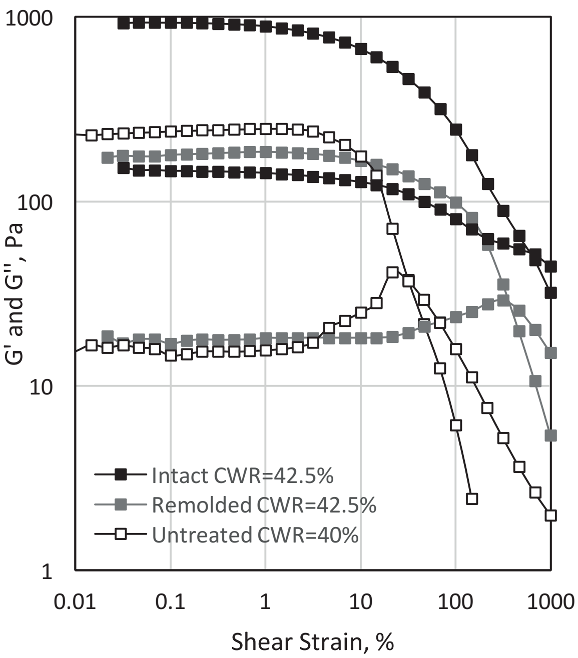

Figure 5. Amplitude test output for Untreated, Treated and remolded MFTs with similar CWR values

Comparison of the curves for untreated MFT-1 and intact tMFT-1 shown in Figure 5 reveals that, beyond the increase in stiffness discussed above, polymer treatment is associated with an increase in the crossover strain (from just over 30% to approximately 500%). This result, which is consistent with the increased ductility observed in the flow curves, indicates that polymer treatment is associated with a re-organization of the clay-water system at the particle-particle level.

Figure 5 also highlights the effect of remolding on the response. While the yield stress data for the remolded sample was observed earlier to fall between the data for the untreated MFT-1 and the intact tMFT-1, Figure 5 shows that as a result of remolding the measured storage modulus falls clearly below the curve for the untreated MFT-1. This result indicates a permanent damage to the microstructure due to the remolding process. The crossover strain of the remolded tMFT falls between the values measured on the other two materials.

To investigate the impact of the remolding process on the rheological response of the t-MFT issue further, data collected during the rest period following the pre-shear stage was examined further. As mentioned earlier, during this stage the response of the dispersions was continuously monitored conducting small strain (γ=0.1%) oscillation tests. The variation of G'_0 as a function of time derived from these tests reflects the structure-build-up processes that characterize thixotropic materials such as clay dispersions following a de-structuring stage.

Curves of G'_0 obtained from such monitoring stages are reported in Figure 6. The four curves shown pertain to untreated MFT-1 (CWR = 30% and 40%) and remolded tMFT-1 (CWR=42% and 52%). Note that the G'_0 values reported in Figure 4 pertain to the measurements conducted at the very end of the rest stage.

The figure highlights how for all materials G'_0 increases continuously at a rate that decreases with time. For a given material, the rate of increase in G'_0 depends on the CWR: the greater the CWR, the more rapid the rise in G'_0. This is to be expected as a higher clay concentration will promote interactions between the particles, and thus accelerate the structure-building processes. More interestingly, Figure 6 shows that for similar values of the CWR (40% and 42%), the restructuring process is much faster in the untreated MFT, relative to the remolded t-MFT. This indicates that the presence of the polymer modifies the thixotropic nature of the material. This may be in part responsible for the lower stiffness measured on the remolded tMFT-1 related to untreated MFT-1 (Figure 5).

As a side note, Figure 6 also highlights the importance of including a rest period following the pre-shear stage when testing thixotropic materials such as the clay dispersions examined in this work. This avoids conducting rheological measurements when the response of the specimen is in most rapid evolution.

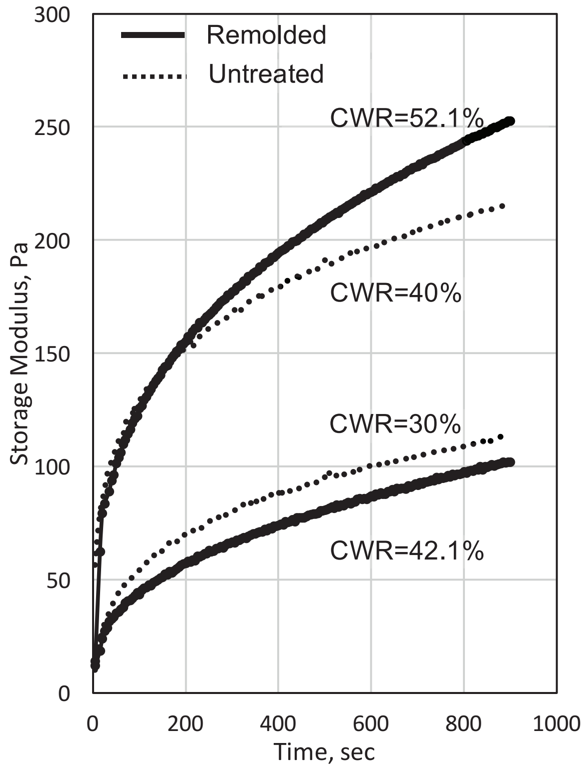

Figure 6. Structure rebuilding in the remolded tMFT compared to the untreated MFT in MFT-1

Chemical analyses

In addition to changes in rheology, MFT-polymer interactions were examined using FTIR spectroscopy, thermogravimetric analysis (TGA), and evolved gas analysis (EGA) (Figure 1). In other words, FTIR, TGA and EGA data were collected from the same materials used for the rheological testing (Figure 1). Optimally dosed/mixed MFT results in water release, as well as some bitumen release, which accompanies the build-up in strength of the material. FTIR spectra of MFT are characterized by spectral contributions from the clay mineral constituents, organic matter (including bitumen), carbonates, and H_2O. Replicated (4 or 5x) diffuse reflectance FTIR (DR-FTIR) spectra of untreated MFT and polymer-treated MFT samples were obtained for three different MFTs. Averaged DR-FTIR spectra from each treatment are plotted in the ν(CH) region and show that polymer treatment resulted in higher organic matter content for each of the three MFTs (Figure 7). Discriminant analysis statistical methods showed that for each MFT, the polymer treated MFT spectra were statistically different from the untreated spectra ($p < 0.05$). The

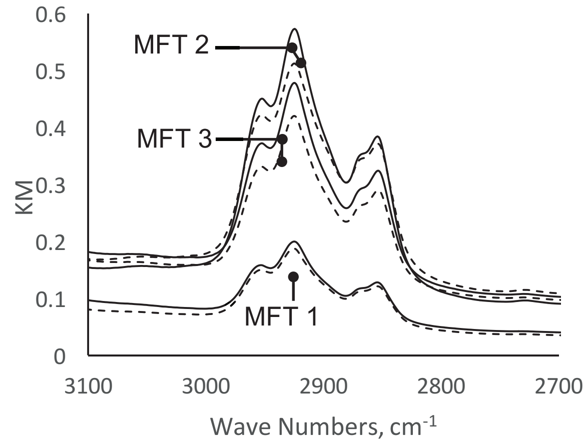

Figure 7. DR-FTIR spectra from each treatment are plotted in the ν(CH) region (Solid lines are for treated MFTs and dashed lines show the results for the untreated MFTs)

DR-FTIR results indicate that polymeric flocculation results in some redistribution of bitumen.

These samples were further interrogated with thermogravimetric analysis (TGA) and evolved gas analysis (EGA) methods. Replicated (4 or 5x) TGA thermograms were obtained for all untreated and polymer-treated MFT samples. Averaged TGA thermograms from each treatment are shown in Figure 8. In agreement with the DR-FTIR data (Figure 7), greater mass loss was observed for each of the polymer treated MFTs compared to untreated MFT. The polymer treated MFT samples had greater mass loss in the 200-550 °C region. Discriminant analysis statistical methods showed that for each MFT, the polymer treated MFT thermograms were statistically different from the thermograms from untreated MFT ($p < 0.05$). Consistent with the DR-FTIR results, the TGA data show that some redistribution of bitumen occurs during polymer treatment.

Together, the DR-FTIR and TGA results indicate that polymeric flocculation resulted in some redistribution of bitumen. For each of the three MFTs, the bitumen contribution increased as evidenced by increased intensity in the ν(CH) region and increased mass loss in the 200-550 °C region. One possible explanation is that the polymer functions as a ‘surface-active agent’ with some surfactant-like character which solubilizes bitumen droplets resulting in some bitumen redistribution on the inorganic MFT particles (e.g., clay minerals). These results suggest that the overall hydrophobic-hydrophilic nature of treated versus untreated MFT are different. The data suggest that polymer-induced redistribution of bitumen on the MFT clay particles results in a more hydrophobic material.

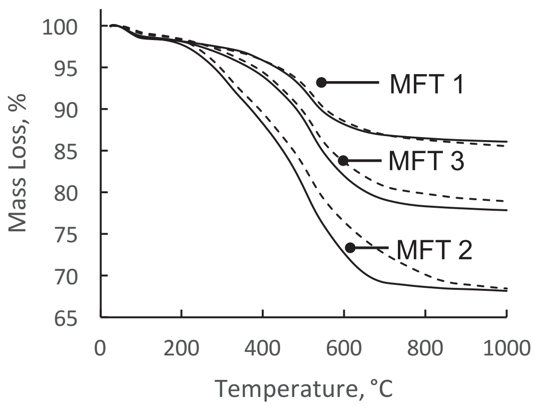

Figure 8. Averaged TG thermograms from each MFT (Solid lines are for treated MFTs and dashed lines show the results for the untreated MFTs)

CONCLUSION

Rheological and surface chemistry studies of untreated and polymer treated MFTs were used to probe the underlying characteristics of three distinct MFTs.

Rheological tests included shear rate ramps for measuring the material yield stress, as well as time sweeps and amplitude sweeps to examine the response of these materials as a function of time and shear strain level. Tests following polymer treatment were conducted both on the treated MFT in the intact state, as well as after significant remolding.

These tests not only provide a picture of the effects of polymer treatment on the rheological behavior of the MFTs, but also furnish insight into the microstructure produced by the addition of the polymer.

For both the untreated MFTs and the intact polymer treated MFTs, a power law is found to describe the relationship between both the yield stress and the small strain shear stiffness and the clay water ratio. At any given clay-water ratio, the yield stress and the small shear stiffness of the intact treated MFT exceed the values measured on the untreated material.

This improvement in mechanical properties appears to be associated with a reorganization of the clay-water system due to the particle bridging and networking action of the polymer. This is reflected, for example, in the tenfold increase of the crossover point measured in the amplitude sweep tests, evidence of a microstructure able to sustain much greater deformation prior to flowing. At the same time, the structure of the polymer treated MFTs appears to be very sensitive to disturbance. Significant degradation of the mechanical properties occurs as a result of remolding, and the shear stiffness of the remolded treated MFT is found to ultimately fall below the value measured on the untreated MFT with same CWR. This result is likely caused by the permanent destruction of some of the links between the particles by the polymer.

Polymer treatment is also found to reduce the thixotropy of the MFTs, and to ultimately limit the ability of the treated MFT to recover following a de-structuring process. This can be ascribed to the polymer interfering with the particle-to-particle interactions.

While the above observations are qualitatively applicable to all three MFTs examined in this work, testing of the three MFTs both prior and following polymer treatment revealed some variations in the response, which can be ascribed to differences in their chemical make-up.

In addition to rheology, MFT-polymer interactions were also examined using FTIR spectroscopy and thermal analysis. These tests are sensitive to short-range interactions (< 1 nm) of water and organic material on the MFT particles. Clear and consistent differences were observed among the treated and untreated MFTs in both the FTIR and TGA data. These data suggest that the polymer induces some bitumen redistribution on the MFT particles. This redistribution would presumably alter the hydrophobic/hydrophilic character of treated MFT particles, which would impact water release, as well as particle level interactions that are reflected in the rheological results.

REFERENCES

Gregory, J. and Guibai, L., 1991. Effects of dosing and mixing conditions on polymer flocculation of concentrated suspensions. Chemical Engineering Communications, 108(1), pp.3-21.

Omotoso, D., Revington, A., Wells, S., and Caldwell, J., 2011. A guide to MFT drying at Suncor, December 2010 Revision 1: May 19, 2011

Grant, J.; Angen, E.; Dyer, S., 2013. Forecasting the Impacts of Oilsands Expansion; Pembina Institute.

Coussot, P., 2005. Rheometry of pastes, suspensions, and granular materials: applications in industry and environment. John Wiley & Sons.

Johnston, C.T., Aochi, Y.O., Sparks, D.L., Page, A.L., Helmke, P.A., Loeppert, R.H., Soltanpour, P.N., Tabatabai, M.A. and Sumner, M.E., 1996. Fourier transform infrared and Raman spectroscopy. Methods of soil analysis. Part 3-chemical methods., pp.269-321.

Gabbott, P. ed., 2008. Principles and applications of thermal analysis. John Wiley & Sons

Santagata, M., Dalmazzo, D. and Santagata, E., 2008. Deformation behavior of clay-water suspensions from rheological tests. In 4th International Symposium on Deformation Characteristics of Geomaterials (IS-Atlanta). IOS Press, Netherlands (pp. 453-459).

APPLICATION OF NOVEL POLYMER COMBINED WITH INORGANIC COAGULATION FOR CONSOLIDATION OF OIL SANDS TAILINGS

Miguel Pelaez and Thomas Fenderson
Kemira Chemicals Inc, Atlanta, GA, USA

ABSTRACT

Effective actions are needed to reduce the environmental impact of oil-sands production in Alberta, Canada that is projected to more than double by 2030. It has been reported that tailings ponds treatment and greenhouse-gas emissions are two key areas where technical progress would make the greatest impact in oil sands processing. Recently, research has been focusing on schemes which utilize more than one technology and combining them into a solution package which is both technically and economically viable. These technologies include chemical processing, such as polymeric flocculation, which aids the consolidation of tailings by improving dewatering, and strength to accelerate land reclamation.

In this study, tailored polymeric flocculants with targeted properties were developed and applied to treat mature fine tailings (MFT) in conjunction with inorganic coagulants to enhance the flocculation process. High initial settling rate along with lower turbidity and solids content were obtained with the synthesized flocculants, in combination with the selected coagulant, compared to conventional flocculants. A synergistic effect was found in the dual coagulant-tailored flocculant treatment suggesting enhanced interaction and capture of the fines present in the tailings. This translates to higher potential dewatering and tailings' strength. Optimum coagulant concentration can minimize the novel flocculant dosage while maximizing efficiency of the process.

INTRODUCTION

Background

The hot water extraction process to obtain bitumen from oil sands in Alberta, Canada is very effective although it generates large volumes of tailings that are difficult to manage (Rao 1980; Botha et al. 2015). The major limitation for the treatment of the tailings is its unique composition which consists mainly of sand, clays, residual bitumen and small amounts of soluble organic compounds. In particular, the fine solid particles in the middle layer of the tailings pond, also known as mature fine tailings (MFT), can remain suspended for a long time. This translates in the incremental use of land to allocate the disposal of new tailings from the bitumen extraction process. This has become an environmental concern and significant efforts to implement a comprehensive strategy to treat and consolidate the MFT portion of the ponds have been tested and applied.

Several technologies aim to increase the solids settling rate and improve the quality of the recovered water to be reused in the bitumen extraction process. Consolidation and paste technology, CT and PT respectively, are among the several technologies tested for oil sands tailings (Vedoy et al. 2015). CT utilizes coarse sand and coagulant aids to form non-segregating mixture to be deposited in the pond. PT employs flocculation, which has been proven effective in accelerating solid-liquid separation processes, to rapidly thicken fresh fine tailings but have limited success when using MFT.

Polyacrylamide (PAM) is a polymer that is widely used as a flocculant in wastewater treatment. One of its main flocculation mechanism involves bridging of the fine solids with PAM molecules through hydrogen bonding (Cho et al. 2002). However, the high content of fine solids found in MFT limits the efficiency of flocculants based on PAM even at higher dosages. The flocs produced with PAM are not closely packed and require the additional treatment to increase the percent of solids [Ref]. Therefore, alternative polymeric flocculants to improve fine solids capture, enhance dewatering performance and improve strength are necessary to overcome the limitations of conventional polymer usage. Moreover, complimentary technologies such as coagulation could provide a synergistic effect and improve the overall efficiency of the treatment. Coagulation can facilitate agglomeration of charged particles and facilitate the flocculation process with the subsequent addition of a polymer. Lu et al. (2016) investigated a two-step flocculation process with oppositely charged polymer flocculants. The combination improved the clarity of the supernatant with high settling efficiency.

The main purpose of this study was to gain insight on the efficiency of novel polymers with unique functionalities in conjunction with an inorganic coagulant to enhance the flocculation process of MFT.

EXPERIMENTAL

Materials and Analysis

Table 1 provides the general characteristics of the two conventional and three novel polymers (Kemira Chemicals) tested in this study. Table 2 includes additional features of several commercially available aluminum-based coagulants that were used in conjunction with the selected polymer. Diluted solutions of MFT (10%) were prepared with produced water obtained from an oil sands producer in Alberta, Canada. The performance of the flocculants and coagulants was established based on key parameters such as settling rate, turbidity and solids content in the supernatant. A HACH DR/890 colorimeter was employed for turbidity analysis and solid contents was determined by gravimetric analysis after drying overnight the sample in an oven at 110°C. The stock solutions of flocculants were prepared as 0.4% wt in produced water.

Flocculation/coagulation procedure

The experimental tests were carried out using a high speed mixing head with a four-blade pitched impeller. The MFT was completely mixed, transferred, diluted with produced water and placed in a beaker. The beaker was positioned under the impeller and aligned for effective mixing. The MFT solution was mixed at 400 rpm for 1 min and then the selected flocculant was added and stirred for an additional minute. When the coagulant was added to the solution, an additional minute was timed between coagulant injection and flocculant addition. The polymeric flocculant and/or coagulant was added as a single injection at a predetermined dosage (500 ppm for the flocculant). Finally, each tailings solution was transferred to a graduated cylinder for visual inspection, initial settling rate calculation, turbidity and solid content (from supernatant) measurements. Turbidity and solid content measurements were performed after 24 hr.

RESULTS AND DISCUSSION

The performance of the polymeric flocculants to treat MFT in terms of settling rate and turbidity measurements can be seen in Figure 1. The data indicates that all novel polymers outperformed conventional 1. Novel 1 and 2 were successful in the flocculation of the MFT while obtaining the highest settling rate and the lowest turbidity in the supernatant. This translates to greater fines capture resulting in higher overflow clarity of the released water.

A slight decrease in the charge density at a medium molecular weight distribution, such as in Novel 1 and 2, delivers a better performance for enhanced flocculation. Nevertheless, there seems to be an optimum range between the anionic charge density and molecular weight that comes from the introduction of unique functionalities into the backbone of the novel polymer (see Table 1 for general characteristics) compared to conventional polymers. For instance, Novel 3 decreased significantly the turbidity compared to conventional 1 but similar settling rates were obtained. Polymer conventional 2 had a higher settling rate than Novel 3 which indicates that decreasing the anionic charge density is beneficial up to a point where potential stability effect arises between the fine particles and the flocculant. Nonetheless, similar turbidity values were obtained.

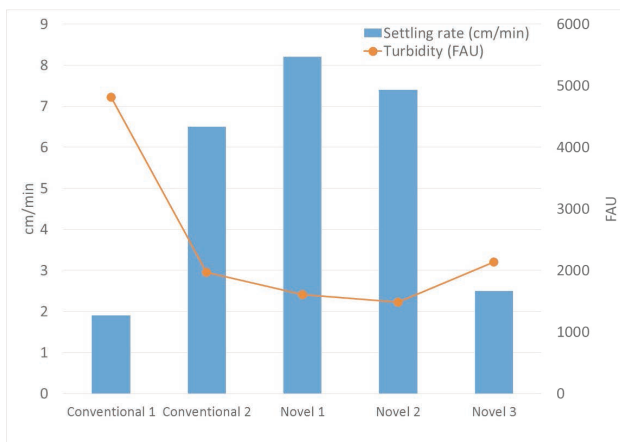

Figure 1. Performance difference between conventional and novel flocculants in the treatment of MFT (500 ppm dosage)

Table 1. General characteristics of polymers used as flocculants

Polymeric Flocculant	Anionic Charge Density	Relative molecular weight
Conventional 1	High	Low
Conventional 2	Medium	Medium
Novel 1	Medium	Medium
Novel 2	Medium/Low	Medium
Novel 3	Low	Medium

It is well documented that coagulation can decrease and neutralize the surface charge of suspended particles. In order to maximize the performance of flocculant Novel 1 and 2, which were the polymers with the highest settling rate and lowest turbidity during the treatment of MFT, an aluminum-based inorganic coagulant was tested in conjunction with the flocculants mentioned above.

Figure 2 shows a slight increase in the settling rate, as well as a decrease in the turbidity, when a low dosage of ALS was added (68 ppm) with the polymeric flocculant Novel 1. When the concentration of ALS was 85 ppm, the settling rate increased and the turbidity decreased furthermore at the same Novel 1 concentration. A synergistic effect that promotes the enhanced flocculation previously established with the innovative polymer can be determined.

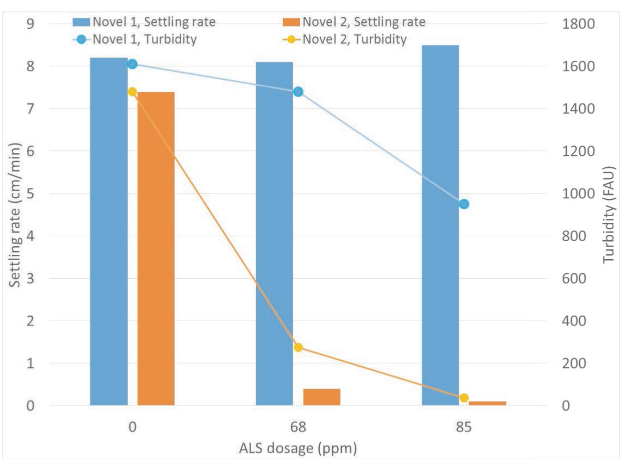

Figure 2. Synergistic effect of flocculant Novel 1 and 2 with aluminum sulfate (ALS) coagulant. Flocculant dosage: 500 ppm

For Novel 2, the addition of ALS decreased dramatically the settling rate at both dosages compared to the flocculant alone. However, the turbidity was lower when combining ALS and Novel 2. It is important to note that even though the clarity of the water was high, the volume of the supernatant for turbidity measurements was low which is in agreement with the minimal settling observed.

Results are consistent with the formation of aggregates by compressing the electrical double layer from fine suspended particles when the coagulant is added. The addition of the novel flocculant then bridge these coagulated aggregates more effectively creating strong flocs and improving consolidation of the tailings. Novel 1 has lower anionic charge compared to conventional samples indicating that the overall charge of each polymer synthesized, along with their specific modifications, can improve the treatment of MFT when an inorganic coagulant is introduced as an additive.

Table 2 lists a number of aluminum-based coagulants with some of their main properties. These characteristics, such as active content and basicity which is defined as molar ratio of hydroxide bound to metal ion (OH/Al), play a significant role in the coagulation process.

Table 2. General characteristics of aluminum-based coagulants employed

Coagulant	Type	Al content (%)	Basicity
ALS	Aluminum sulphate	4.3	n/a
PAX-XL60	PAC	7.5	Medium
PAX-18	PAC	9.0	Medium
PAX-XL6	PAC	5.4	Medium
PAX-XL3919J	PAC	9.9	High
PASS-10	Polyaluminum sulphate	5.3	Medium
PAX-XL19	PAC	12.5	High

PAC=Polyaluminum chloride

Each coagulant listed in Table 2 was tested in combination with flocculant Novel 1 for the treatment of MFT (see Figure 3). ALS revealed an enhanced performance when combined with Novel 1 compared to the other aluminum-based coagulants at a dosage of 85 ppm. Settling rates decreased and turbidity values were similar or slightly higher for all of polyaluminum chloride (PAC)-based coagulants as well as polyaluminum sulfate (PASS) compared to Novel 1 alone. This indicates that higher aluminum content and different basicity did not improve the consolidation of oil sands MFT when combined with the proposed novel flocculant.

In conventional coagulation, the fine particle removing effect is increased with the higher basicity of the coagulant. A similar effect was observed with the PAC coagulants since higher settling rates and lower turbidity were observed when the basicity increased from medium to high. However, these coagulants did not increase the overall performance of Novel 1 compared to ALS.
ALS has a low aluminum content and is not pre-hydrolyzed so the concept of basicity is not applied. In aqueous solution, it forms a number of dissolved monomeric aluminum species and aluminum hydroxide precipitates. Therefore, the resulting aluminum species can have different interactions with the organic and inorganic components in the MFT compared to other aluminum-based coagulants. Novel 1 contains a charge density and molecular weight that allows a high interaction with the colloidal particles formed with ALS.

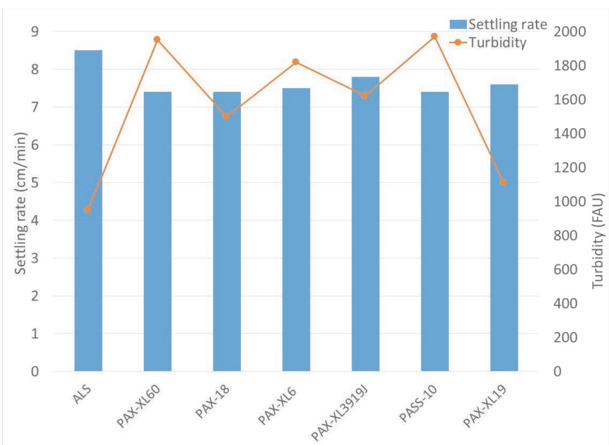

Figure 3. Effect of different aluminum-based coagulants (85 ppm dosage) with flocculant Novel 1 (500 ppm dosage)

The coagulant dosage was increased in order to determine the effect of higher aluminum concentration and establish optimum conditions for the enhanced flocculation process. From Figure 4 it can be seen that the settling rate decreased significantly when adding 125 ppm of ALS but the turbidity level was very low indicating excellent water clarity. Higher dosage of ALS provides more stability to the fine particles, limiting the settling rates. Most of the other aluminum-based coagulants have similar settling rates compared to the 85 ppm dosage. A slight impact on the turbidity was observed with lower values for these coagulants at the higher dosage of 125 ppm.

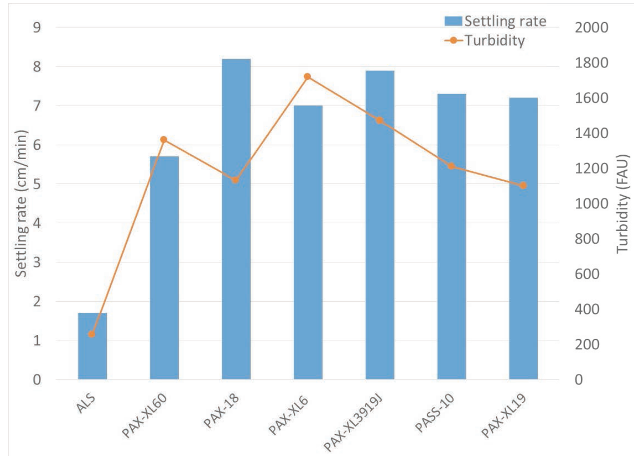

Figure 4. Effect of higher dosage (125 ppm) of aluminum-based coagulants with flocculant Novel 1 (500 ppm dosage)

It can be established that the enhancement of the novel polymer presented here is dependent of the type and concentration of the aluminum-based coagulant employed as a chemical aid. Optimum conditions of the inorganic coagulant can minimize the novel flocculant dosage while maximizing efficiency of the process.

CONCLUSIONS

The treatment of MFT from oil sands production with novel polymers can effectively enhance key performance parameters such as settling rate, and turbidity compared to conventional polymers. The unique functionalities incorporated to the novel flocculant offers the capability of enhancing the flocculation process by maintaining high settling rates and lowering the turbidity of the supernatant. The addition of aluminum-based coagulants was tested and a high synergistic behavior was found with aluminum sulfate compared to other coagulants. The aluminum species, as well as aluminum content and basicity, play a significant role in the ability to promote the enhanced flocculation with the proposed flocculants in this study. Optimum coagulant dosage is necessary in order to maximize the effect of the novel flocculant and maintain the performance requirements for oil sands tailings management. The application of these novel flocculants, in conjunction with an inorganic coagulant, can translate to higher potential dewatering and oil sands tailings' strength.

ACKNOWLEDGEMENTS

The authors would like to thank the management of Kemira for permission to publish this work.

REFERENCES

Botha, L. & Soares, J. B. P. 2015. The influence of tailings composition on flocculation. The Canadian Journal of Chemical Engineering, **93**: 1514-1523.

Rao, S.R., 1980. Flocculation and Dewatering of Alberta Oil Sands Tailings, Int. J. Miner. Process, **7**: 245-253.

Cho, M. S., Song, B. K., Yoon, K. J. 2002. Flocculation characteristics of copolymer of acrylamide with quaternary ammonium cationic monomer (running) flocculation by cationic polyacrylamide. J. Ind. Eng. Chem. **8**: 131-137.

Vedoy, D. R. L. & Soares, J. B. P. 2015. Water-soluble polymers for oil sands tailing treatment: A review. The Canadian Journal of Chemical Engineering, **93**: 888-904.

Lu, Q., Yan, B., Xie, L., Huang, J., Liu, Y., Zeng, H. 2016. A two-step flocculation process on oil sands tailings treatment using oppositely charged polymer flocculants. Sci. Total Environ. **565**: 369-375.

OPTIMIZATION OF NEW FLOCCULANT TECHNOLOGY FOR DEWATERING OIL SANDS MATURE FINE TAILINGS

Michael K. Poindexter, Paul A. Gillis, Jason S. Moore, Lizbeth Rostro, Wu Chen and Jason Tubbs
The Dow Chemical Company, Freeport, TX, USA

ABSTRACT

Tailings generated from oil sands mining operations, which are often stored in ponds, are highly resistant to dewatering. These legacy and somewhat concentrated tailings are frequently referred to as mature fine tailings (MFT). The resistance to dewatering hinders and delays efforts designed to restore the mined sites back to their original state. Over the last several decades, a variety of treatment approaches have shown that dewatering can be enhanced through the use of amendments. While dewatering is the key performance indicator for any treatment program, there are additional parameters (addressing operational efficiency and deposit properties) that also determine treatment program success.

These additional parameters include low treated MFT yield stress (to allow unencumbered transport to disposal areas), minimal power requirement (to effectively combine the amendment(s) with the process stream), and high quality release water. Furthermore, the amendment and its associated mixing systems should be capable of processing variable MFT feed streams (i.e. variations in total solids content, clay content, and solids particle size distribution). From an economic standpoint, dosage of the amendment should be minimized. The findings from a dosage minimization study will be presented. This effort also focused on understanding and optimizing several operational and performance parameters for a recently developed dewatering flocculant.

INTRODUCTION

During the early stages of oil sands mining operations, it was recognized that the produced tailings would not readily self-consolidate. The accumulation of tailings was termed the “pondwater problem” (Camp 1977) where the volume of watery mature fines tailings (MFT) produced exceeded the volume of mined material. The intricacies of handling and treating this by-product waste stream have been covered in several thorough reviews (Kasperski 1992, Mikula 1996, Botha 2015).

To date, operators continue to search for ways to improve their tailings treatment programs to maximize their investments (Nicolaisen 2015). A number of processes and their associated advantages have been proposed to dewater tailings (Sobkowicz 2009, BGC 2010, Read 2014); however, only a few have been fully commercialized. In most every case which has undergone significant scale up in the treatment of mature fine tailings (MFT), the addition of an amendment has been shown to enhance the dewatering performance (Oil Sands Tailings Technology Deployment Roadmaps 2012). This is probably not surprising since chemicals/additives are used in nearly every aspect of conventional crude oil and gas production (Kelland 2009). Thus, it is reasonable to assume that the same principle would apply to the dewatering of tailings streams.

Both the quality and quantity of the release water in the densification of tailings are important. The long-term management of water quality plays critical roles in: 1) the recycle water used for the bitumen extraction process; 2) the processing equipment where scale, corrosion and microbial activity are of concern; and 3) the remaining toxicity of the water which will ultimately be discharged back to the environment (Allen 2008). The water quality of proposed end pit lakes in closure plans has also received attention and is suspected to be dominated by the seepage and drainage from process-affected water (Holden 2014). In the recently released Directive 85, water management plans are to be aligned with the tailings management plans (Alberta Energy Regulator 2016). Thus, in the development of any tailings treatment process which uses an amendment, the additives should not exacerbate the release of unwanted species which might concentrate in the various water streams.

Amendment performance should be evaluated with criterion beyond the initial ability to densify treated tailings and prevent unwanted water quality issues.

The dewatering process must also continue to occur following transport of the treated material to the final rest area, i.e. the dedicated disposal area (DDA). Distances between MFT amendment treatment and the DDA are typically on the order of kilometers with transportation residence times in the range of minutes. The ability (or energy needed) to transport the flocculated clays from the point of treatment to the DDA is often gauged by yield stress measurements (Gillies 2012; Mizani 2014). High yield stress properties create concerns particularly if the transportation is halted due to operational activities followed by a resumption of flow. However, it is also believed that higher yield stress values can impart a degree of stability in the settling of sand from tailings streams during pipeline transport.

Identifying improved flocculants which possess multiple performance attributes remains an active area of research (Vedoy 2015). At Dow, high-throughput screening was used to identify promising classes of amendments (Mohler 2012). The most promising candidates were then scaled up using flow loops to further test their robustness with respect to dewatering performance as shear rates and dosages were varied (Gillis 2013). A new amendment, known as XUR, having high shear tolerance was identified. Following a geocolumn and casing evaluation of XUR (Poindexter 2015), this paper describes further efforts to better understand and optimize the performance of XUR with respect to dosage reduction. The yield stress of the XUR-treated tailings and the release water quality from these dewatered tailings will also be reported.

EXPERIMENTAL

MFT samples were received in totes and blended thoroughly (typically 1-2 days using an ITM 7000 Tote Mixer from Dynamix run at 175 rpm coupled with periodic scraping of the tote's corners using a paint mixer attached to a drill) before dividing into drums. During distribution of the tote into drums, large clumps of solids were removed using a ½" screen. Aside from mixing and the coarse filtration, the MFTs were used as received and not diluted prior to any experimental run. All MFT samples, as well as process water samples, were provided by Shell Canada.

Dewatering Experiments

MFT was mixed with XUR flocculant solution (0.4 wt% polymer in process water) using a proprietary, once-through dynamic mixer. Mixer speeds ranged from 100-900 rpm. Upon exiting the dynamic mixer, the treated MFT flowed though a 40' hose (1" inner diameter) and then poured into 5 gallon graduated pails. The samples were left undisturbed, and mudline measurements were taken visually to determine the solids content under the mudline over extended periods of time.

MFT Characterization

MBI (methylene blue index) values are reported in units of meq MB/100 grams of clay (Omotoso 2008). Solids weight percent values were determined using a Mettler Toledo HB43-S halogen moisture analyzer. Five different MFT samples were evaluated in this study, and a summary of their properties is provided in Table 1.

Table 1. Select Characteristics of MFT Samples

Sample	Wt%	MBI
MFT 1	41.6	8.7
MFT 2	29.3	9.0
MFT 3	32.0	8.2
MFT 4	35.6	7.6
MFT 5	38.6	6.8

Yield Stress Measurements

Yield stress values were determined using a Brookfield DVT-3 Rheometer with V-73 vane rotated at 0.2 rpm. Measurements were taken within a few minutes of collecting the treated MFT. If any release water was present at the time of the measurement, it was carefully removed using a pipette. In this way, it was possible to set the spindle depth uniformly across all samples (i.e. placement of the spindle notch at the mud-air interface).

Water Analyses

To obtain solids-free water from untreated MFT, raw MFT was centrifuged using an Eppendorf Centrifuge 5417R at 10,000 rpm for 10 minutes. The separated water was carefully withdrawn using a pipette, and the resulting water was analyzed for various elements using an ICP-EOS

(Horiba ULTIMA Expert). For all analyses presented in this paper, the following elements were <0.1 ppm: Ag, Be, Cd, Co, Cr, Cu, Mn, Mo, Ni, P, Pb, Sb, Ti, Tl, V and Zn. Carbonate and bicarbonate analyses were conducted under a nitrogen pad using a Metrohm 905 Autotitrator equipped with a pH electrode. Samples were diluted with carbonate free water and titrated to a pH <3 with 0.01N HCl. All samples were found to have two endpoints. Sulfate analyses were conducted using ion chromatography. Anion concentrations are reported in ppm (w/w). Total suspended solids (TSS) were determined using 1.5 µm filter paper. Total dissolved solids (TDS) were determined by drying until a constant weight was achieved.

RESULTS AND DISCUSSION

Dewatering Case Study 1 – Initial Dosage Reduction

Following the recently reported geocolumn study, which used 1,900 ppm of a newly developed flocculant (Poindexter 2015) and the follow-up casing study (conducted at 1,500 ppm), a series of studies ensued to further optimize the amendment formulation of XUR, its dosage and mixing requirements when combined with the MFT. Figure 1 summarizes the dewatering performance for one of the first studies where the amendment dosage was lowered substantially to 1,100 and then 500 ppm. **MFT1**, a relatively high solids, high clay sample, was used in this study (Table 1). After several hundred hours of monitoring, the solids content had reached 46-47 wt% for both dosages and at all levels of mixing. The dynamic mixer rotational speed (100-900 rpm) only showed an impact on the initial solids settling rate where the higher agitation levels slightly slow the dewatering rate. However, by 80-90 hours, all six dewatering curves were in strong agreement with each other. This type of similarity across several dosages and different mixing energies is reminiscent of a previous flow loop study (see Figures 6 and 7 of Gillis 2013).

Figure 1 illustrates another feature of treating MFT as it applies to the dewatering performance of XUR. When using a higher flocculant dosage, more water is combined with the MFT causing the initial solid content to be lower. This is shown by the lower starting level of solids for the 1,100 ppm runs versus the 500 ppm runs. Ultimately, this additional water had neither a positive nor negative effect on the solids content level achieved after several hundred hours of monitoring.

As will be seen in the next case study, Figure 1 also illustrates that dewatering often continues even after several hundred hours of settling. Thus, studies which are terminated prematurely can miss valuable information when efforts are intended to fully assess the attributes of different run conditions. The interaction of amendments with clays, mixing protocol and MFT characteristics should be examined over time frames which permit a full assessment of performance. Since solids settling and consolidation in the field will occur over years, it seems appropriate that laboratory studies should also be examined with long-term behavior in mind.

It is worth noting that in one of the conditions shown in Figure 1, the mudline is seen to reverse direction (see the 1,100 ppm run with a dynamic mixer setting of 100 rpm). This is most likely due to microbial growth and gas formation (Fedorak 2003).

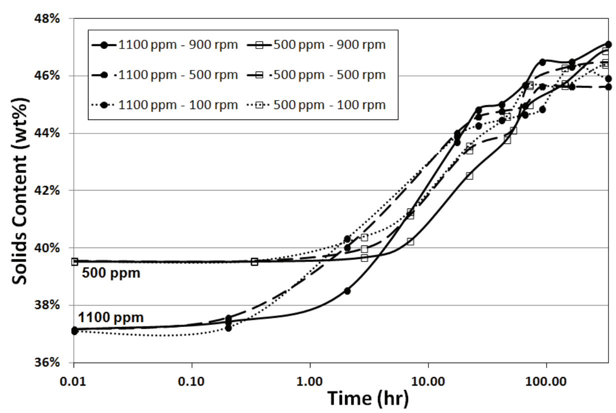

Figure 1. An early study where lower amendment dosages were found not to diminish the solids settling performance. Higher dynamic mixing (900 rpm) is represented by solid lines, while lower impeller speeds are denoted with ever more broken (i.e. dashed then dotted) lines.

Dewatering Case Study 2 – A Low Amendment Dosage and Robust Performance

The solids content and particularly the clay content, which is often defined by the MBI value, are known to play a role in the handling and dewatering performance of tailings. Between different ponds and even within the same pond, it is known that MFT dredged up for treatment will vary in its properties. To handle these variations, amendment treatment programs are expected to demonstrate robust performance across different MFT properties.

To demonstrate performance robustness, a single lower XUR dosage was tested against multiple MFTs. A dosage of 350 ppm was found to generate strong dewatering performance across four different MFTs. A summary of some of these findings is presented in Figure 2. In this study, the time to dewater was extended to 1,500 hours (~2 months). In three of the four cases, dewatering was still occurring; this further indicates that dewatering may not be fully characterized over shorter observation times. Only **MFT4** appears to show a mudline which has reached a solids content asymptote.

Like the previous study, the dynamic mixer was operated between 100 and 900 rpm, and like that study, the agitation speed was shown to not ultimately affect long-term settling performance. For the two higher solids content, lower clay MFTs (**MFT4** and **MFT5**), the settling curves for the different mixer speeds basically lay on top of each other. As mentioned, **MFT4** appears to have reached an asymptote, while **MFT5** exhibited a similar behavior followed by a further increase in solids settling. Well into the solids settling process, both dynamic mixer settings for **MFT5** (100 and 900 rpm) showed the same solids settling behavior.

For the two lower solids content, higher clay MFTs (**MFT2** and **MFT3**), initial dewatering rates vary with the rotational speed of the mixer. This suggests that clay content influences the initial solids settling rates, but this effect gradually diminished over time. In Dewatering Case Study 1, the higher clay content **MFT1** could also be exhibiting a similar influence in the early dewatering rates. However, it is important to realize that these differences are eventually erased over periods of prolonged settling. Particle surface studies, described elsewhere (Mohler 2014), are in progress to determine how amendment formulations interact with clay over the time frames which match the dewatering studies.

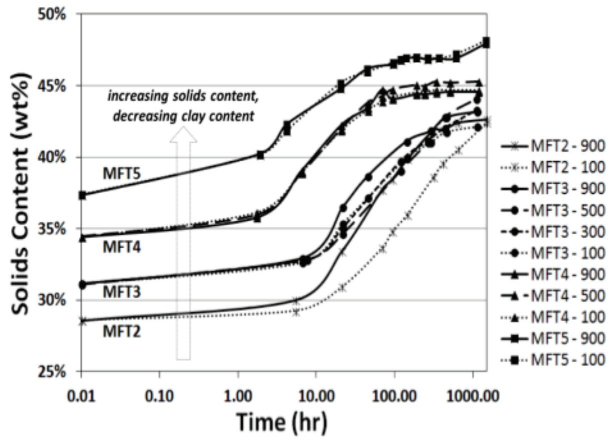

Figure 2. Comparison of XUR dewatering performance across four different MFTs and several different dynamic mixer settings where the last number in the legend signifies the rpm setting. All studies used 350 ppm of amendment. Higher dynamic mixing (900 rpm) is represented by solid lines, while lower mixing speeds are denoted with ever more broken (i.e. dashed or dotted) lines. MFT2 (ж), MFT3 (●), MFT4 (▲), MFT5 (■).

Yield Stress and Pipeline Transport

In the two case studies presented, yield stress values were taken for all treated MFT within minutes of their discharge into 5 gallon pails. When plotting the yield stress measurements against five experimental input parameters (namely, MFT solids weight percent, amendment dosage, clay content as determined by titration with methylene blue, the rotational speed of the dynamic mixer and the power input from the dynamic mixer), only the MFT solids weight percent showed a high statistically significant correlation. R-squared values (R^2), often called the coefficient of determination, are a statistical measure of the relationship between data and a regressed line (Alfassi 2005 and Harnett 1972). Table 2 lists these values for the five experimental input parameters. A plot of the yield stress by MFT solids weight percent is provided in Figure 3. This result agrees with related work where higher percent solids streams give higher yield stress values (McCaslin 2016). Additional studies are in progress to further define this relationship for XUR-treated MFT.

Table 2. R-squared Values for Five Input Parameters versus Initial Yield Stress Values

Input Parameter	R^2
MFT Solids, Wt%	0.85
ppm (dry flocculant versus dry clay)	0.50
MBI (meq MB/100 gm clay)	0.05
Mixer rotation, rpm	0.02
Power Input to Dynamic Mixer, kW	0

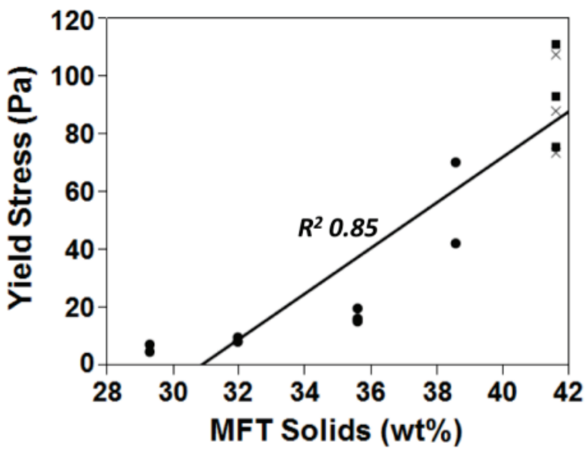

Figure 3. Plot of XUR-treated MFT yield stress by solids weight percent. XUR dosages: 350 ppm (●), 500 ppm (x), 1,100 ppm (■).

Release Water Quality

For three of the runs (each with a different MFT) using 350 ppm of XUR amendment, the release water was sampled after about 1,000 hours of settling and analyzed for various elements and common anions. These results were compared against water separated by high speed centrifugation from the three respective untreated MFTs (**MFT2**, **MFT4** and **MFT5**). As seen in Figure 4, very little change is noted between the three untreated MFTs and the release water from the treated samples. The only element which appears to show any pattern is calcium. In all three comparisons of untreated to treated, the untreated MFT calcium values are slightly higher than their respective treated sample release water values.

It should also be noted that the high clay content of **MFT2** shows higher levels of both aluminum and silicon than its release water as well as the other two MFTs. This indicates that the clay particles for this higher MBI tailings sample are somewhat resistant to separation even with the high speed centrifuge. However, treatment with XUR reduced the residual levels of aluminum and silicon indicating that these particles were removed.

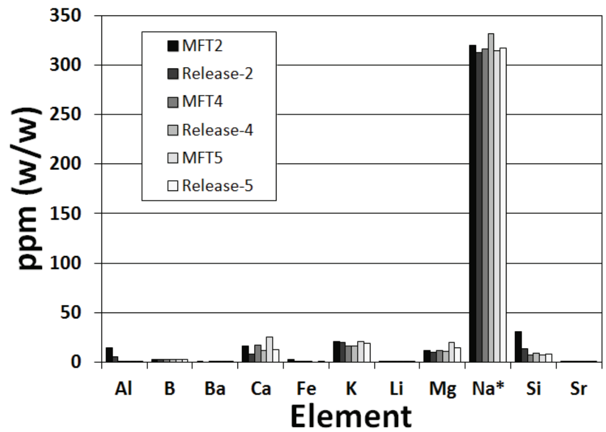

Figure 4. Element comparisons between untreated MFT water and their respective release water from treatments using 350 ppm of XUR. *Reported sodium results (*) are greater than the linear range of the method. Sodium levels indicate relative order of magnitude (~0.04-0.05%).

A portion of the water released from the three treatments involving XUR at 350 ppm was also analyzed for common anions. Carbonate and bicarbonate analyses were titrated using HCl, while sulfate was determined using ion chromatography. As before, these results were compared to their starting MFT samples (Figure 5). Treatment with XUR does not appear to alter the natural levels of these three anions.

An additional portion of the water released from the three treatments involving XUR at 350 ppm was also analyzed for total dissolved solids (TDS) and total suspended solids (TSS). In all three cases and for both parameters, the solids were found to be exceptionally low (Table 3). Collectively, these results suggest that the water quality should not be compromised when using lower dosages of XUR to dewater MFT.

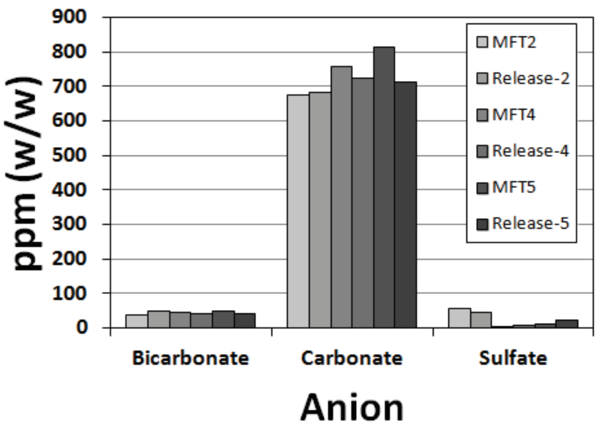

Figure 5. Comparison of common anions found in the untreated MFT water and their respective release water from XUR treatment at 350 ppm

Table 3. TSS and TDS of the Release Water from Three MFTs Treated with XUR (350 ppm)

MFT	TSS (mg/L)	TDS (wt%)
MFT2	0.7	0.2
MFT4	3.0	0.1
MFT5	1.1	0.1

CONCLUSIONS

Laboratory studies using a newly developed amendment, XUR, have shown that the material gives robust dewatering performance across a variety of MFTs when applied at a low dosage level of 350 ppm. For higher clay content samples, the level of mixing between XUR and MFT influenced the initial rate of dewatering. However, after several days of solids settling, the differences in dewatering performance due to mixing energy became insignificant. Additionally, continuous long-term solids settling (on the order of months) was demonstrated at the low XUR dosages. The initially treated material also exhibited a low stress across multiple treatment conditions which should aid pipeline transport. When compared to the water chemistry of several untreated MFTs, the release water quality from the XUR-treated tailings was almost identical. Furthermore, calcium, aluminum and silicon contents appear to have been slightly lowered with XUR treatment. XUR treatments should not alter the water quality from what is experienced in current operations.

ACKNOWLEDGEMENTS

The authors would like to thank 1) Albert Brennsteiner, Alice Hawkes, Isaac Negrete, and Lin Zhao for conducting the water analyses and 2) Shell Canada for supplying the MFT and process water.

REFERENCES

Alberta Energy Regulator Directive 85. 2016. Fluid Tailings Management for Oil Sands Mining Projects. Release date: July 14, 2016.

Alfassi, Z. B.; Boger, Z.; Ronen, Y. 2005. Statistical Treatment of Analytical Data; Blackwell Science: Oxford, U.K.; p 80.

Allen, E. W. 2008. Process Water Treatment in Canada's Oil Sands Industry: I. Target Pollutants and Treatment Objectives. Journal of Environmental Science, **7**, 123-138.

BGC Engineering Inc. 2010. Oil Sands Tailings Technology Review. Oil Sands Research and Information Network, University of Alberta, School of Energy and the Environment, Edmonton, Alberta. OSRIN Report No. TR-1.

Botha, L.; Soares, J. B. P. 2015. The Influence of Tailings Composition on Flocculation. Canadian Journal of Chemical Engineering, **93**, 1514-1523.

Camp, F. W. 1977. Processing Athabasca Tar Sands – Tailings Disposal, Canadian Journal of Chemical Engineering, **55**, 581-591.

Fedorak, P. M.; Coy, D. L.; Dudas, M. J.; Simpson, M. J.; Renneberg, A. J. MacKinnon, M. D. 2003. Microbially-mediated Fugitive Gas Production from Oil Sands Tailings and Increased Tailings Densification Rates. Journal of Environmental Engineering Science, **2**, 199-211.

Gilllies, R.; Spelay, R.; Sun, R.; Goldszal, A.; Li, C. 2012. Pipeline Transport of Thickened Oil Sands Tailings. 3rd International Oil Sands Tailings Conference; Edmonton, Alberta; December 2-5, pp 301-309.

Gillis, P. A.; Moore, J. S.; Poindexter, M. K.; Witham, C. A.; Chen, W.; Singh, H. Mohler, C. E.; Atias, J. 2013. The Effects of In-line Static Mixer Flow Loop Operational Parameters on Flocculant Performance in Mature Fine Tailing Samples.

Tailings and Mine Waste Conference; Banff, Alberta, November 3-6, pp 137-146.

Harnett, D. L. 1972. Introduction to Statistical Methods; Addison-Wesley: Reading, MA; pp 287-298.

Holden, A.; McKenna, G.; Fan, X.; Biggar, K. 2014. The Potential Impact of Different Types of Tailings on Water Quality and Quantity Reporting to Oil Sands End Pit Lakes: A Preliminary Modeling Exercise. 4th International Oil Sands Tailings Conference; Lake Louise, Alberta, pp 359-367.

Kasperski, K. L. 1992. A Review of Properties and Treatment of Oil Sands Tailings, AOSTRA Journal of Research, **8**, 11-53.

Kelland, M. A. 2009. Production Chemicals for the Oil and Gas Industry; CRC Press: Boca Raton, U.S.

McCaslin, M.L.; Johnson, J. 2016. Liquid-Solid Separation in Gold Processing. In Gold Ore Processing: Project Development and Operations; Adams, M. D. Ed.; Elsevier: Amsterdam, Netherlands; Chapter 18, p 284 (Figure 18-6).

Mikula, R. J., Kasperski, K. L., Burns, R. D., and MacKinnon, M. D. 1996. Nature and Fate of Oil Sands Fine Tailings, in Suspensions: Fundamentals and Applications in the Petroleum Industry, Advances in Chemistry, Schramm, L. (ed.), Washington, DC, pp 677-723.

Mizani, S.; Simms, P. 2014. Geometry of Polymer-Amended Fine Tailings Deposits: Yield Stress Measurement and Numerical Modeling. 4th International Oil Sands Tailings Conference; Lake Louise, Alberta; December 7-10, pp 81-90.

Mohler, C. E.; Poindexter, M. K.; Atias, J.; Chen, W.; Witham, C. A. 2012. Development of Flocculants for Oil Sands Tailings using High-Throughput Techniques. 3rd International Oil Sands Tailings Conference; Edmonton, Alberta; December 2-5, pp 113-120.

Mohler, C.; Poindexter, M.; Acevedo, C.; Sanders Jr., T.; Meyers, G.; Reinhardt, C.; Chen, W.; Singh, H.; Atias, J. 2014. Clay-Flocculant Interactions in Developing Next Generation Flocculants for Oil Sands Fluid Fine Tailings Management. 4th International Oil Sands Tailings Conference; Lake Louise, Alberta, pp 437-445.

Nicolaisen, J. 2015. Oil Sands Tailings Management Projects: Low Return, Business Critical. Proceedings of the Tailings and Mine Waste Conference; Vancouver, British Columbia; October 26-28, pp 521-528.

Oil Sands Tailings Technology Deployment Roadmaps 2012. Report to Alberta Innovates – Energy and Environment Solutions. Volume 1 Project Summary.

Omotoso, O.; Morin, M. 2008. Methylene Blue Procedure: Sludges and Slurries, CanmetENERGY – Devon, Natural Resources Canada.

Poindexter, M. K.; Gillis, P. A.; Moore, J. S.; Tubbs, J.; Mahood, R.; Freeman, G. 2015. Geotechnical Column Evaluation of New Flocculant Technology for Dewatering Oil Sands Mature Fine Tailings. Tailings and Mine Waste Conference; Vancouver, British Columbia, October 25-28, pp 490-499.

Read, P. 2014. Broad Suite of Practice and Technology Key to Success in Tailings Management. 4th International Oil Sands Tailings Conference; Lake Louise, Alberta; December 7-10, pp 9-15.

Sobkowicz, J. C.; Morgenstern, N.R. 2009. A Geotechnical Perspective on Oil Sands Tailings. 13th International Conference on Tailings and Mine Waste, Banff, Alberta, pp. xvii-xli.

Vedoy, D. R. L.; Soares, J. B. P. 2015. Water-Soluble Polymers for Oil Sands Tailing Treatment: A Review. Canadian Journal of Chemical Engineering, **93**, 888-904.

Session C-1

Tailings Properties and Measurements

ADVANCED ROBOTIC PAYLOADS FOR MEASURING PROPERTIES OF TAILINGS DEPOSITS

Nicolas A. Olmedo, G. Ward Wilson and Michael Lipsett
University of Alberta, Edmonton, Canada

ABSTRACT

There is an ongoing requirement to collect timely geotechnical measurements on engineered mine tailings deposits. Advanced robotic systems can be integrated into ground surveys to study dewatering performance of mine waste. This paper presents a description of advanced robotic systems designed for tailings monitoring. A robotic manipulator was developed to deploy different payloads in soft deposits. First, a surface sampler was used to collect undisturbed surface samples from soft soil deposits. The surface samples are required to calibrate moisture estimates obtained from hyper-spectral imaging cameras. Second, soil properties were estimated from terramechanics models using an instrumented wheel. This paper presents the design and development of these technologies.

INTRODUCTION

Robotic systems have been designed for environmental monitoring and mapping in difficult-to-access and hazardous locations, such as space exploration (Wettergreen, 2010 and Volpe, 2000) and river and rainforest monitoring (Freitas, 2011). Robotic systems have been used to collect measurements and samples on inaccessible terrains such as oil sands tailings deposits (Lipsett, 2014).

A prototype unmanned ground vehicle (UGV), RTC-I, was designed, developed, and field-tested to collect subsurface samples from tailings deposits that have developed crusts (Olmedo, 2016) As Figure 1 shows, the vehicle chassis was based on a Clearpath Robotics Husky A200 model wheeled robot vehicle, modified by our research group for soft ground conditions. The prototype carried two main subsystems: an auger mechanism to drill a hole through the tailings crust, and an industry- standard material sampler deployed on a linear extension mechanism to collect a core at a depth of up to 2 m. The system was not designed to collect surface samples, although it did carry video cameras that allowed qualitative assessment of the crust. The prototype was successfully tele-operated at an operating oil sands facility to demonstrate the feasibility of using robotic systems as part of environmental monitoring campaigns in difficult terrain. The vehicle was also capable of autonomous operation, although it lacked control schemes to deal with situations such as getting stuck. The system carried a tether so that it could be retrieved if it sank (and fortunately it was not needed.)

Samples collected by the robotic system were analyzed to determine the mineral, water, and bitumen content of the tailings, as well as the particle size distribution of the material. An MBI analysis was also conducted to analyze the clay activity of the samples collected.

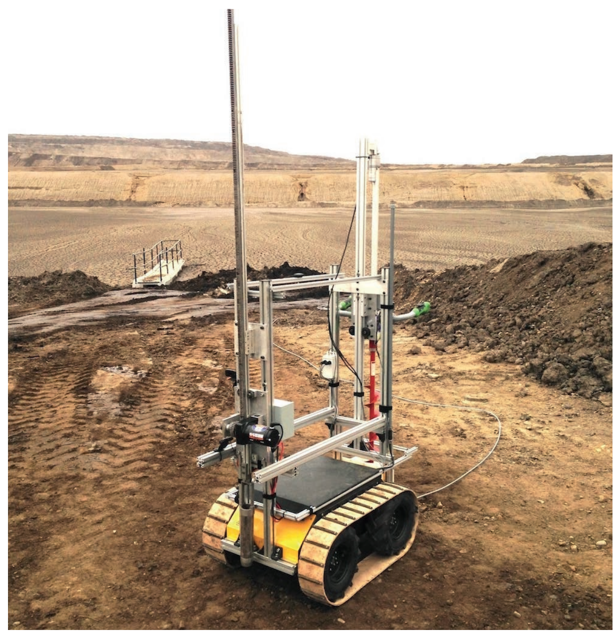

Figure 1. RTC-I field tests on an oil sands tailings deposit (Olmedo, 2016)

RTC-I was designed to conduct terramechanics experiments based on the wheel-soil interactions. One wheel of the mobile platform was instrumented to measure the torque, angular velocity, linear velocity, and sinkage experienced while traversing deformable terrain. Key soil parameters can be estimated using these measurements and linearized terramechanics models.

Figure 2 shows the unit driving on a tailings dyke with no tracks. Experiments were conducted on dyke dry sand to estimate the cohesion stress and internal friction angle of the material. The favorable results demonstrated the feasibility of using wheel-soil interaction to estimate soil parameters for environmental monitoring (Olmedo, 2016).

A key limitation of the terramechanics package developed for RTC-I was the coupling of the terramechanics sensor (the instrumented wheel) to the locomotion of the system. In order to estimate soil parameters, the instrumented wheel is required to slip on the material at different slip ratios:

$$s = 1 - v/(r\,\omega),$$

where ω is the angular velocity of the wheel, v is the linear velocity, and r is the wheel radius.

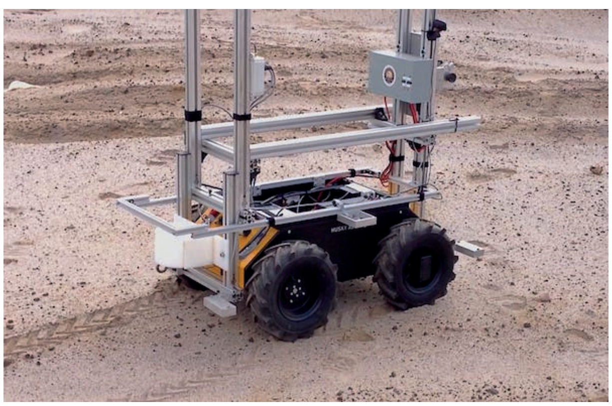

Figure 2. RTC-I conducting terramechanics experiments on dry sand. The front left wheel was instrumented to measure the linear and angular velocities, sinkage and torque (Olmedo, 2016).

In some soils, increasing the angular velocity of the wheel increases the linear velocity of the robot without changing the slip ratio. To control the slip ratio, the linear velocity and angular velocity must be independently controlled, which was not possible in RTC-I.

The limitations of RTC-I, and the need of timely characterization of tailings deposits, motivated the development of additional robotic payloads to collect surface samples and to conduct advanced terramechanics studies. New terramechanics payloads are required to be able to control the slip ratio of the instrumented wheel.

A robotic platform can also be used to collect data needed for other activities related to characterization of tailings. Straightforward geometric mapping can be done more simply using an unmanned aerial vehicle (UAV) carrying a laser-based light-detection and ranging (LIDAR) payload.

But a drone can only make remote-sensing surface measurements, while models of post-depositional performance require in-situ measurements of density, dewatering performance, and soil strength. For example, undisturbed surface samples are required to calibrate algorithms to estimate key soil characteristics from hyper-spectral images. A robot that can travel on a fresh tailings deposit can map the geometry of the deposit and track changes over time, as well as collect samples for analysis at the surface and below.

The remainder of this paper presents the developments of a robotic manipulator for soft soil surface sampling and soil characterization.

DEVELOPMENT OF A ROBOTIC MANIPULATOR FOR SOIL CHARACTERIZATION AND SAMPLING

A new robotic manipulator for soil characterization and sampling was then designed and prototyped at the University of Alberta, built on the same vehicle platform. Figure 3 shows how it was designed to deploy a surface sample collection mechanism and an instrumented wheel for terramechanics experiments. The following subsections describe the manipulator and instrumentation development.

Robotic Manipulator

A serial robotic manipulator with three degrees of freedom was developed to allow dynamic interactions of instruments with soil. The mechanism comprises three revolute joints actuated by linear actuators, with a carrying capacity of 50 kg, through its workspace, and vertical and horizontal end-effector velocities of at least 1 cm/s. The new design was motivated by a lack of commercial manipulators that could meet the design requirements.

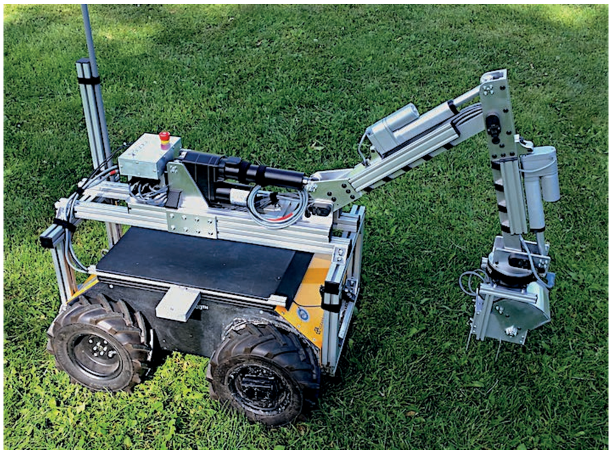

Figure 3. Robotic manipulator prototype mounted on a Husky A200 platform

A review of commercially available manipulators found that small, lightweight (less than 30 kg) manipulators have very limited lifting capacities. For example, the Universal Robot Series have a maximum lifting capacity of 10 kg (Universal Robots, 2016). These manipulators do not require high lifting capacities because they are typically used for pick and place operations of small components. Factory robots in industrial assembly operations have very high lifting capacities, but are not suitable for deployment from a mobile robot, due to their high mass, size, and power requirements.

Commercially available manipulators use DC motors to rotate each joint directly. This design has the advantage that very fast joint speeds can be achieved, especially if the manipulator is light, which are essential for high agility maneuvers for which the manipulator has to follow a trajectory quickly. Gearboxes are typically used to increase the torque available in each joint (while reducing the speed achievable); but gearboxes typically increase the overall mass and inertia of each link.

A main disadvantage of using a motor directly connected to each joint is that the motors must be always powered to hold a joint position. In many cases, the weight of the manipulator may be sufficient to rotate the joints if they are left unpowered. This impacts the overall energy requirements of the system, because it would consume energy even if it the manipulator is not being used. During instrument deployment operations, the manipulator was left in a resting configuration for most of the time, and was only actuated when collecting a sample or conducting an experiment. It is necessary for the robot arm to hold any position when unpowered.

Linear actuators were used instead of motors to manipulate each degree of freedom and to keep the joints locked when unpowered. The linear actuators comprise small DC motors, gearboxes, and linear-drive nut-screw mechanisms to convert rotational motion to linear displacement. Using this mechanism, the joints of the manipulator do not move unless the motors inside the linear actuators are energized.

The linear actuators used were instrumented with linear potentiometers. These sensors have an analog output proportional to the linear position of the actuator. The angular position of each joint can be determined using these sensors and the geometry of the system, without the need of additional external encoders in each joint.

ROBOTIC MANIPULATOR PROTOTYPES

Two robotic manipulator prototypes were built: first a proof of concept prototype for laboratory testing shown in Figure 4, and then a field deployable prototype shown in Figure 5.

The proof of concept prototype was developed to test the linear actuators and control systems, while keeping the material and manufacturing costs of the structure of the robotic arm at a minimum. A lightweight shell was built to support the components tested. All the structural pieces were manufactured with a water jet cutter from 1/8 inch aluminum sheets, and assembled with standard attachment blocks.

The linear actuators were tested in simple lift-and-place operations. From the laboratory experiments, it was determined that the linear position sensors in the actuators were not adequate to estimate the joint positions accurately. Two main problems were found. First, the analog output signal of the sensors was affected by electrical noise generated from the actuator DC motors. Hardware and software filters were used to manage the noise to an acceptable level, but a small delay in the signal was introduced. Second, the linear position sensors did not measure the backlash of the joints. This is a problem because a small backlash in the angular position of the joint can cause a linear displacement of the end effector on the order of several centimeters. In some tasks this can cause the arm to hit other parts of the robot or its surroundings.

Following the initial laboratory experimentation with the proof of concept prototype, a field deployable manipulator was developed. The design of this manipulator focused on the robustness required for field applications. The same linear actuators from the proof of concept prototype were used, and each joint was instrumented with an optical encoder to address the limitations of the linear potentiometers. The optical encoders measured the position of each joint shaft with a resolution of 0.09 degrees.

The geometry of the manipulator was designed in parallel to the selection of the linear actuators used. Several design constraints were imposed: i) the manipulator needs to work on top of a Husky A200 mobile platform (as pictured in Figure 5), ii) the arm needs to be able to apply a vertical force (up or down) of 500 N and a horizontal force of 100 N, in any position of the workspace, iii) the arm needs to be able to move an end effector at 1 cm/s in the vertical and horizontal directions.

A computer program was developed to aid in the design process. The performance of the robotic manipulator was analyzed in terms of the forces and velocities of the end-effector. The program was used to compute the inverse and forward kinematics of the manipulator to find these forces and speeds as functions of the torques and angular speed applied to each joint, and the geometry of the links. The main design variables were the length of each link and the attachment points of the linear actuators. Several design iterations were required to find a configuration that met all the design constraints.

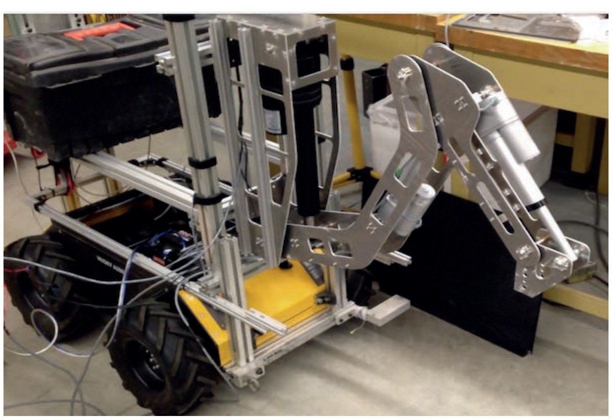

Figure 4. Robotic manipulator Mark 1 for laboratory testing

Figure 5. Field deployable prototype with sample collection mechanism

Electronics, control systems, and sensors

Three HB25 motor drivers were used to control the linear actuators (Parallax, 2016). These controllers modulate the input signal to the motors at a frequency of 9.2 kHz. The pulse width of the signal to the motor is proportional to the input command to the driver. A 12 VDC lead-acid battery was used to power the system.

An Atmel SAM3X8E ARM Cortex-M3 CPU microcontroller was used to sample the optical encoders and to interface with the motor controllers. The micro-controller communicated with an on board computer to publish sensor data and to receive motor commands. A Mini-ITX Linux computer was used to interface with the user and to compute control commands to send to the motor controllers. The control software was developed using the Robot Operating System (ROS) (Quigley, 2009). Software routines for independent joint control and trajectory following were packaged in modules to be integrated to high level control software used to conduct tasks, such as deploying a sample collection mechanism.

A Robotiq FT 150 force-torque sensor was installed in the interface between the robotic manipulator and the end-effector (Robotiq, 2016) (Figure 6). This sensor measures the forces and moments in 3 axes, providing the necessary information to determine the tool-environment interactions. This information can be used to determine the reaction forces on the soil of a terramechanics package, or the contact forces of a sampling mechanism with the surface of the material. The measured loads can be used to prevent overloading the arm or the end-effectors and prevent damage.

SURFACE SAMPLING MECHANISM

Undisturbed surface samples are required to calibrate non-contact methods for soil characterization. Hyperspectral images can be used to estimate soil moisture content, bitumen content, and clay abundance and cation exchange capacity in tailings deposits (Entezari et al 2016). It is necessary to collect samples to fine-tune the data processing algorithms to estimate soil properties. Robotic systems can collect these surface samples in terrains that are not accessible to workers.

A mechanism to collect undisturbed surface samples was designed and prototyped. The mechanism consists of a scoop-type material sampler as presented in Figure 6. The mechanism is positioned close to the surface of the material to be sampled with a robotic manipulator. An indentation plate is used to maintain the mechanism stable and to provide a containment surface for the scoop. Once the indentation plate is placed in the material, the scoop is closed slowly to capture the material without disturbing its surface. A sequence of images illustrating this process is presented in Figure 7.

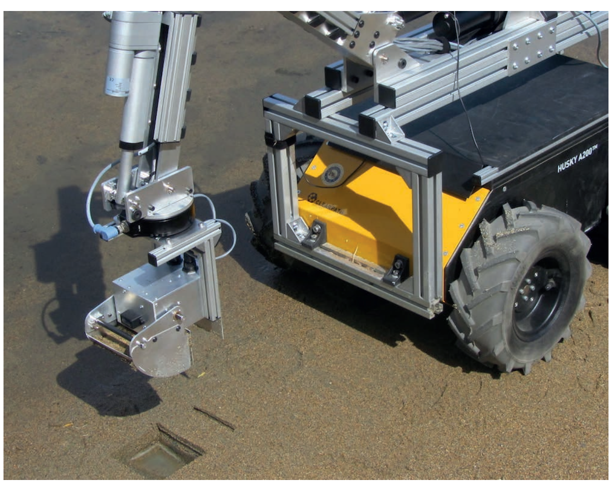

Figure 6. Surface sampler mechanism deployed from the robotic manipulator

Figure 7. Surface sample mechanism collecting a material sample. The container is closed against an indentation plate to capture an undisturbed surface sample.

The surface sample mechanism was designed to be a modular subsystem comprised of mechanical components to capture the sample, various sensors, and a control system. The scoop is actuated by a DC motor and gearbox. The motor has a built-in shaft encoder that was used to measure the position of the scoop and to control the speed of sampling. The current drawn by the motor is used to estimate the torque applied to the scoop. The torque required to close the mechanism can be an indicator of the strength of the material being sampled. The torque estimate can also be used to prevent overloading the mechanism.

In many cases the mobile platform carrying the mechanism can experience a few centimeters of sinkage as it moves over soft material. In that case, measuring the joint positions of the robotic manipulator is not sufficient to determine the distance between the end-effector and the ground. An infrared distance sensor was added to the surface sampler to position the mechanism close to the deposit safely.

TERRAMECHANICS SENSOR

A new terramechanics sensor was developed to address the limitations of RTC-I. The terramechanics sensor was decoupled from the locomotion of the vehicle to allow the slip ratio to be controlled. The terramechanics payload comprises an instrumented wheel deployed by the robotic manipulator and a collection of sensors to measure the state and loads on the wheel. This sensor system is shown in Figure 8.

The wheel was 3D printed with ABS plastic. The dimensions were chosen to be similar to those used in planetary rovers to allow for comparative assessment (Ding, 2013).

A geared DC motor provides torque to rotate the wheel; and an optical encoder on the shaft of the motor measures the angular speed of the wheel. The motor can be controlled in open-loop or closed-loop speed control. The slip ratio of the wheel can be controlled by setting the linear velocity of the mobile platform while controlling the angular velocity of the terramechanics wheel.

A wireless torque sensor was developed to measure the reaction torque on the wheel as it slips on deformable terrain. Strain gauges are used to estimate the torque applied to the wheel from amplified strain measurements. The transducer is built using a Wheatstone bridge in shear configuration. The analog signal is sampled by a low-power micro-controller and transmitted to a base station on the mobile platform using 2.4GHz transceivers. The wireless torque sensor can receive commands from the base station to start the data acquisition as well as to modify the amplification gains of the strain measurements.

The frame of the terramechanics wheel was instrumented with two distance sensors to estimate its sinkage.

Front and back distance sensors estimate the leading and exit contact angles of the wheel, respectively. These are necessary to determine the contact area of the wheel in order to determine the expected normal and shear stresses.

INITIAL PROTOTYPE LABORATORY TESTING

The robotic manipulator, surface sampler, and terramechanics package were tested in laboratory experiments. The surface sampler was tested on dry sand, saturated sand, and Mature Fine Tailings (MFT) with moisture contents of 68%. The sampler was successful in collecting undisturbed samples in the materials selected, as shown in Figure 9. For capturing samples in materials with higher shear strength, the mechanism can be modified to have a higher gear ratio gearbox.

Figure 10 shows an experimental configuration of the terramechanics wheel. Initial experiments show favorable results; but a laboratory based parametric investigation is still in progress.

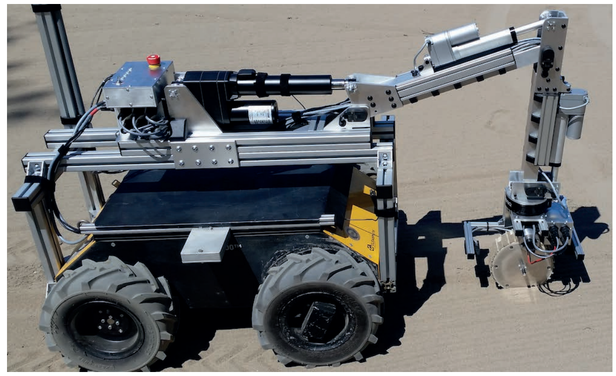

Figure 8. Robotic arm with terramechanics sensor

Figure 9. Surface sampler collecting an undisturbed sample on MFT

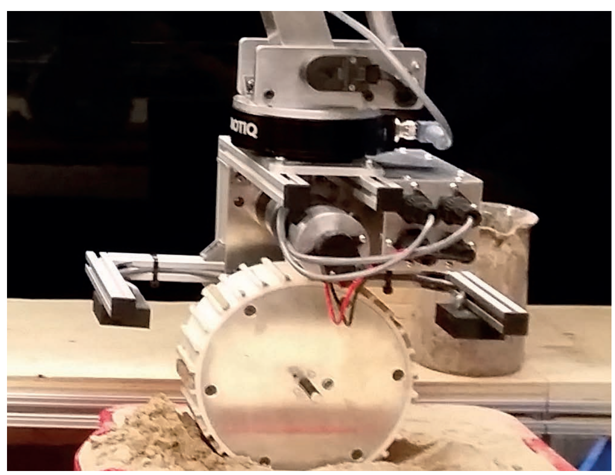

Figure 10. Initial laboratory experiments with instrumented wheel

The measurements collected were used to estimates soil properties as outlined by Iagnemma *et al*, 2004. The controllability of the slip ratio allows for more operating points to be tested, increasing the accuracy of the parameter estimation algorithms.

CONCLUSIONS AND FUTURE WORK

The design and development of a robotic manipulator capable of deploying a surface sample mechanism and a terramechanics sensor was presented. This paper describes the design of each subsystem and discussed the sensors used to collect the measurements required for control of the systems and to estimate soil properties.

Near-term future work will focus on: i) developing soil strength estimation algorithms based on the tool-soil interaction of the surface sampler mechanism; ii) improving soil parameter estimation algorithms based on non-linear wheel-soil interactions; and iii) developing more versatile sampling and soil measurement payloads for other robotic delivery systems and for automating measurements.

Long-term future work will aim to deploy these new robotic payloads on real tailings deposits. Further technological developments will be addressed to increase the sampling capabilities of the robot, such that more than one sample can be obtained per trip. In other work, alternative locomotion methods are being trialed to allow for navigation on saturated soils and other types of challenging materials.

ACKNOWLEDGEMENTS

Financial support is gratefully acknowledged from the Natural Sciences and Engineering Research Council of Canada (NSERC), COSIA, and the University of Alberta. The authors wish to thank the Mechanical Engineering Machine Shop staff for their technical support.

REFERENCES

L. Ding, Z. Deng, H. Gao, J. Guo, D. Zhang, and K. D. Iagnemma, “Experimental study and analysis of the wheels’ steering mechanics for planetary exploration wheeled mobile robots moving on deformable terrain,” The International Journal of Robotics Research, vol. 32, pp. 712–743, June 2013.

I Entezari, B Rivard, M.G. Lipsett, G.W. Wilson. “Prediction of Water Content and Normalized Evaporation from Oil Sands Soft Tailings Surface Using Hyperspectral Observations,” Can Geotechnical J. (CGI-2015-0105.R1 accepted).

I Entezari, B Rivard, M.G. Lipsett. “Estimation of Methylene Blue Index in oil sands tailings using hyperspectral data,” Can J Chem Eng (CJCE-16-0092.R1 accepted)

G. Freitas, F. Lizarralde, L. Hsu, V. Paranhos, N. R. S. dos Reis, and M. Bergerman, “Design, modeling, and control of a wheel-legged locomotion system for the environmental hybrid robot,” in Proceedings of the IASTED International Conference, no. CMU-RI-TR-, November 2011.

K. Iagnemma, S. Kang, H. Shibly, and S. Dubowsky, “Online Terrain Parameter Estimation for Wheeled Mobile Robots With Application to Planetary Rovers,” IEEE Transactions on Robotics, vol. 20, pp. 921–927, Oct. 2004.

M. G. Lipsett, N. Olmedo, B. Rivard, and W. Wilson, “Robotic Systems for Measuring Properties of Tailings Deposits and Collecting Samples,” in Proceedings of the Fourth International Oil Sands Tailings Conference, (Lake Louise, AB), Dec. 2014.

N. A. Olmedo and M. G. Lipsett, “Design and field experimentation of a robotic system for tailings characterization,” J. Unmanned Vehicle Systems., Mar. 2016.

Parralax, “HB-25 Motor Controller”, parallax.com/product/2914. Accessed August 2016.

Robotiq, “Force Torque Sensor”, robotiq.com/products/robotics-force-torque-sensor/. Accessed August 2016.

M. Quigley, K. Conley, B. P. Gerkey, J. Faust, T. Foote, J. Leibs, R. Wheeler, and A. Y. Ng, “Ros: an open-source robot operating system,” in ICRA Workshop on Open Source Software, 2009.

Universal-Robots A/S, “Collaborative Robots from Universal Robots”, www.universal-robots.com/products. Accessed August 2016.

R. Volpe, E. Baumgartner, P. Scheaker, and S. Hayati, “Technology development and testing for enhanced Mars Rover Sample Return operations,” vol. 7, pp. 247–257 vol.7, 2000.

D. Wettergreen, S. J. Moreland, K. Skonieczny, D. Jonak, D. Kohanbash, and J. Teza, “Design and field experimentation of a prototype lunar prospector,” International Journal of Robotics Research, vol. 29, pp. 1550 – 1564, October 2010.

HYPERSPECTRAL SENSING IN SUPPORT OF OIL SANDS TAILINGS OPERATION AND MANAGEMENT

Iman Entezari, Benoit Rivard, Michael G. Lipsett and G. Ward Wilson
University of Alberta, Edmonton, Canada

ABSTRACT

This study provides an overview of our research on the applications of hyperspectral sensing for the characterization of oil sands tailings. We have developed quantitative estimates of characteristics of tailings using shortwave and longwave infrared hyperspectral observations. Focus was given to the estimation of water content and the normalized evaporation, clay swelling potential indicated by the Methylene Blue Index (MBI), and mineral content, in particular clay and quartz content. Our research contributions have established the foundation for developing rapid predictions (in real-time) of important tailings characteristics based on hyperspectral measurements.

INTRODUCTION

The bitumen production from oil sands surface-mining operations produces large volumes of mineral wastes, or tailings. Characterization of oil sands tailings is of importance to monitor their state for trafficability and reclamation, to assess the tailings dewatering and consolidation performance, and to develop more effective measures for tailings management.

Considerable work has been done characterizing oil sands ore and tailings (e.g. Bayliss and Levinson 1976; Bichard 1987; Omotoso et al. 2006; Mercier et al. 2008; Kaminsky 2008; Hooshiar Fard 2011; Osacky et al. 2013a, 2013b). However, most of the laboratory methods used to measure tailings properties are time consuming, costly, and limited to a small number of samples or locations. Therefore, introducing reliable and accurate methods, which are also fast and cost effective, capable of monitoring and measuring the characteristics of tailings at a large scale is potentially of great benefit for tailings management.

Hyperspectral sensing (so-called reflectance spectroscopy) is an emerging technology used for the characterization of materials, such as the identification and quantification of minerals. Hyperspectral sensors collect the natural radiation reflected from or emitted by materials for an extended portion of the electromagnetic spectrum. These sensors divide the electromagnetic spectrum into hundreds of narrow continuous wavelength intervals (spectral bands), and measure the radiation in these bands. The spectral response from each material is wavelength dependent, and largely controlled by the chemical composition and crystal structure of the minerals and other materials within. An array of sensors allows for spectral images to be created by cameras.

This paper presents the summary of our investigation on the application of hyperspectral sensing for the characterization of oil sands soft tailings (Entezari 2016, Entezari et al. 2016a, and Entezari et al. 2016b). Shortwave infrared (SWIR, 1.0-2.5 μm) and longwave infrared (LWIR, 7.5-11.5 μm) hyperspectral observations were used for the quantitative estimation of characteristics of tailings surfaces. Among the different tailings characteristics, we focused on the estimation of some crucial and trackable properties including water content and the normalized evaporation (Entezari et al. 2016a), the swelling potential (Entezari et al. 2016b), and mineral content - particularly clay mineral species and their abundances. Here we present the key findings of our investigations.

EXPERIMENTAL PROCEDURE

The experimental procedure including sample description and spectral measurements for each test are presented in this section.

Estimation of Water Content and Evaporation

Sample suite

Four tailings samples were provided by a major oil sands operator in northern Alberta. Each sample was stirred to create a homogenous mixture before conducting the experiments. The Methylene Blue Index (MBI) and bitumen content of each sample were estimated using standard analytical methods, as listed in Table 1.

Evaporation tests and spectral measurements

The evaporation tests were conducted using the experimental setup developed by Wilson et al. (1997). Using an Analytical Spectral Device (ASD) portable spectrometer, spectral time-series data in the SWIR were collected for tailings samples at variable moisture conditions to determine the spectral metrics of greatest sensitivity and to derive predictive models (see Entezari et al. (2016a) for further details on the experimental procedure, such as lighting source and calibration). Tailings samples with known varying degree of swelling potential (determined with MBI) and residual bitumen were tested to assess the robustness of spectral estimators against the tailings composition. Spectral features such as absolute reflectance, absorption depth, and normalized soil moisture index (NSMI) (Haubrock et al. 2008) were derived and tested from the spectral time series for water content and evaporation estimation.

Estimation of MBI

Sample suite

Thirteen tailings samples were provided by an oil sands operating company. All tailings samples contained residual bitumen, which was removed from the solids at a commercial laboratory using Dean-Stark soxhlet extraction to extract the water and oil from the solids. Table 2 lists the MBI and bitumen content of each tailings sample. Prior to the acquisition of spectral measurements, each sample was stirred to create a homogenous mixture and then allowed to air-dry to remove the effect of water from the spectrum, as water significantly reduces the reflectance by absorbing light.

Table 1. Tailings samples examined for the estimation of water content and normalized evaporation

Sample No.	MBI (meq/100g)	Bitumen (wt%)
MFT1	2.3	3.5
MFT2	2.3	4.0
MFT3	3.5	4.3
MFT4	3.4	3.3

Spectral measurements

Short-wave infrared spectral imagery of the samples was collected with a Specim SisuROCK imaging system. From these data, an average spectrum was calculated for each sample. Long-wave infrared reflectance spectra were collected using a Bomem MB102 Fourier transform InfraRed (FTIR) spectrometer. Five spots were measured on each sample and the resulting spectra were averaged to produce a spectrum per sample.

Development of spectral predictive models

In the SWIR, attention was given to the ratio of the reflectance at two spectral bands (that is, two different wavelengths) as a measure of the slope of the spectrum, which is affected by the mineral makeup of the sample. We explored all band ratios from the available band set and selected the ratio yielding the highest linear correlation with MBI for the sample suite. In the LWIR, the strength of the reflectance peaks at 9.67 and 11 μm, attributed to clay minerals, were used for model development.

Estimation of Clays and Quartz

Sample suite and spectral measurements

Three sample suites were used in this section: 1) a suite of four bitumen-removed oil sand ore samples (bulk samples) and their different size fractions (<2 μm, 0.2-2 μm, and <0.2 μm) with quantitative mineralogy that was obtained in a prior study from quantitative x-ray diffraction (QXRD) (Table 3), 2) a suite of oil sands ore samples (Table 4), and 3) a suite of oil sands tailings samples (Table 4). The first suite was used to define spectral metrics with the strongest correlation to mineral content (clays and quartz). The other two suites were used for investigating the applicability of the spectral metrics for the mineral characterization of ore and tailings. Each sample of the first suite was crushed and mixed using a mortar and pestle to achieve a relatively uniform particle size for spectral measurements. The seven ore samples were crushed and mixed using a rotary breaker to have a homogenous mixture and allowed to air-dry to remove the impact of water on the spectrum. The seven tailings samples were initially saturated with water. Each sample was stirred to create a homogenous mixture and remove any effects of segregation after long-term storage. They were then allowed to air-dry and were crushed using a mortar and pestle to minimize the potential impact of segregation on the spectral measurements. Spectral data were collected in the SWIR and LWIR using the same instruments described earlier in the text.

Table 2. MBI and bitumen content measured for the tailings samples

Sample	1	2	3	4	5	6	7	8	9	10	11	12	13
MBI (meq/100g)	2.3	2.3	3.1	3.4	3.5	3.4	0.7	2.7	3.4	5.2	5.2	5.9	10.5
Bitumen (wt%)	3.5	4.0	4.8	4.2	5.5	6.7	0.7	4.2	4.4	4.6	3.4	3.7	0.4

Table 3. Summary of the mineral composition (wt%) of the oil sands samples determined by QXRD

Sample	**Size** (µm)	**Quartz**	**Kaolinite**	**2:1 clays**[2]	**Total clays**[3]
MC1[1]	Bulk	72.1	8.9	7.5	16.6
	<2	N/A	N/A	N/A	N/A
	0.2-2	16.4	38.4	33.7	73.3
	<0.2	15.9	21.5	40.8	63.4
EC1[1]	Bulk	52.3	14.4	25.3	41.0
	<2	4.2	28.9	58.9	92.4
	0.2-2	6.9	37.0	52.6	91.9
	<0.2	1.2	21.4	64.8	95.1
MC2	Bulk	51.7	11.7	17.8	29.5
	<2	6.6	36.7	52.4	89.1
	0.2-2	N/A	N/A	N/A	N/A
	<0.2	0.0	11.3	82.6	93.9
EC2	Bulk	62.9	12.2	20.2	32.4
	<2	12.4	28.7	55.9	84.6
	0.2-2	N/A	N/A	N/A	N/A
	<0.2	0.0	14.9	82.7	97.6

[1]The mineralogical and chemical composition of the samples MC1 and EC1 have been thoroughly investigated in Osacky et al. (2013a, 2013b).
[2]Total of illite and illite-smectite.
[3]Total of kaolinite, 2:1 clays, and chlorite.

Spectral analysis

Reflectance spectra were analyzed with the objective of identifying spectral metrics correlated with the content in clays (total 2:1 clays, kaolinite, and total clays) and quartz obtained from QXRD data. Band ratios (i.e. reflectance ratio) were calculated to capture the variation in overall shape and slope amongst spectra as it relates to sample mineralogy. Ratios of all possible band combinations were calculated for the available SWIR and LWIR bands, respectively. Linear regression analysis was then performed between these band ratios and QXRD data to define the band ratios of highest correlation with quartz and clay mineral content. The bulk and fine fraction samples were analyzed together in the regression analysis because they were considered to represent quartz-rich and clay-rich samples, respectively. Using these samples as a single population expanded the range in clay content, for comparison with that observed for both the oil sands ore and tailings (as quartz-rich and clay-rich materials).

RESULTS

Estimation of Water Content and Evaporation

The SWIR measurements were found to be of value for the estimation of water content and normalized evaporation of the soft tailings. Among the spectral metrics tested, the best estimate of moisture content of soft tailings was achieved using NSMI (Figure 1a). For samples tested, the reflectance at 1920 nm was found to be the best spectral estimator of normalized evaporation with the NSMI index also being of value (Figure 1b). In both instances, the NSMI index shows the most potential for estimations in a field setting, as it is less sensitive to the effects of the intervening atmospheric column between the spectral camera and the target. However, NSMI appears to be sensitive to the sample composition including the bitumen concentration when the evaporation rate is very low.

Table 4. Characteristics of the ore and tailings samples examined

Ore	Fines (wt%)	Bitumen (wt%)	Tailings	Fines (wt%)	MBI (meq/100g)
O1	13.83	14.15	**T1**	93.85	10.5
O2	40.06	7.40	**T2**	76.91	5.9
O3	40.75	9.75	**T3**	81.74	5.2
O4	24.98	7.80	**T4**	75.94	5.2
O5	27.30	12.02	**T5**	70.87	3.4
O6	46.24	6.97	**T6**	54.61	2.7
O7	31.00	8.23	**T7**	17.80	0.7

Estimation of MBI

Results of laboratory experiments demonstrated that remote sensing methods are generally successful to estimate the swelling potential of oil sands tailings indicated by MBI. In the SWIR, a band ratio of reflectance at 2.111 to 1.992 µm was highly correlated with MBI values for air-dried tailings (Figure 2a). Towards the estimation of MBI in outdoor settings, where the intervening atmosphere can impact the spectral measurements, a band ratio of reflectance at 1.773 µm to 1.307 µm provided an estimation of MBI of tailings (Figure 2b). A water sensitivity analysis (Entezari et al. 2016b) showed that the SWIR model based on these bands is robust against variations in the tailings moisture content for values less than 20 wt%. At moisture levels above 20 wt%, the MBI value was overestimated. Of relevance to the estimation of MBI in a field setting, a first step would involve imaging the tailing surfaces to delineate areas with less than 20 wt% moisture using the spectral models developed for moisture content estimation. In a second step, the MBI predictive models could be applied to areas with moisture less than 20 wt%. The best MBI predictions were obtained in the LWIR using reflectance peaks at 9.67 µm and 11 µm attributed to total clays and kaolinite, respectively (Figure 2c and 2d). For the sample suite examined, a mostly constant relative abundance of kaolinite to total clays was observed (using spectral analysis, Entezari et al. 2016b) which explains why both of these clay features were successful for MBI estimation.

Estimation of Clays and Quartz

Band ratio analysis was found to be an effective spectral analysis method for estimation of clay and quartz content in oil sand solids. Spectral metrics derived from the LWIR data performed considerably better for the estimation of clay and quartz content. The existence of characteristic quartz and clay features in the LWIR explains the better performance of the LWIR spectral metrics. The best estimation of total 2:1 clay and kaolinite content was achieved using a ratio of bands at 9.428 to 9.276 µm and 9.858 to 9.873 µm, respectively (Figures 3a and 3b). A ratio of reflectance at 8.377 to 9.638 µm was found to be the best spectral estimator of quartz and total clays (Figures 3c and 3d).

For quartz, although the bulk and fine fraction samples formed two separate populations in Figure 3c, the regression appears to fit both populations well and shows a slight deviation from the regression lines fitted to each population. For total clays, the data form two populations and the regression line appears to fit better for the bulk samples compared to the fine fraction samples (Figure 3d). Figure 4 displays the estimated contents of kaolinite and total 2:1 clays for the ore and tailings samples obtained using the LWIR spectral metrics. Also shown are the estimated values for the bulk and fine fractions. For the ore samples, kaolinite and total 2:1 clays are positively correlated. The tailings samples are generally

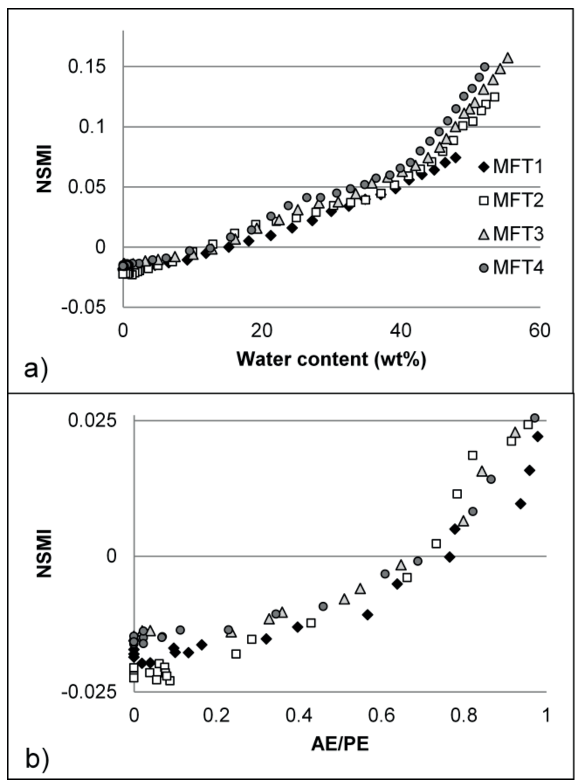

Figure 1. Relationship between NSMI and (a) water content, (b) AE/PE for the tailings examined

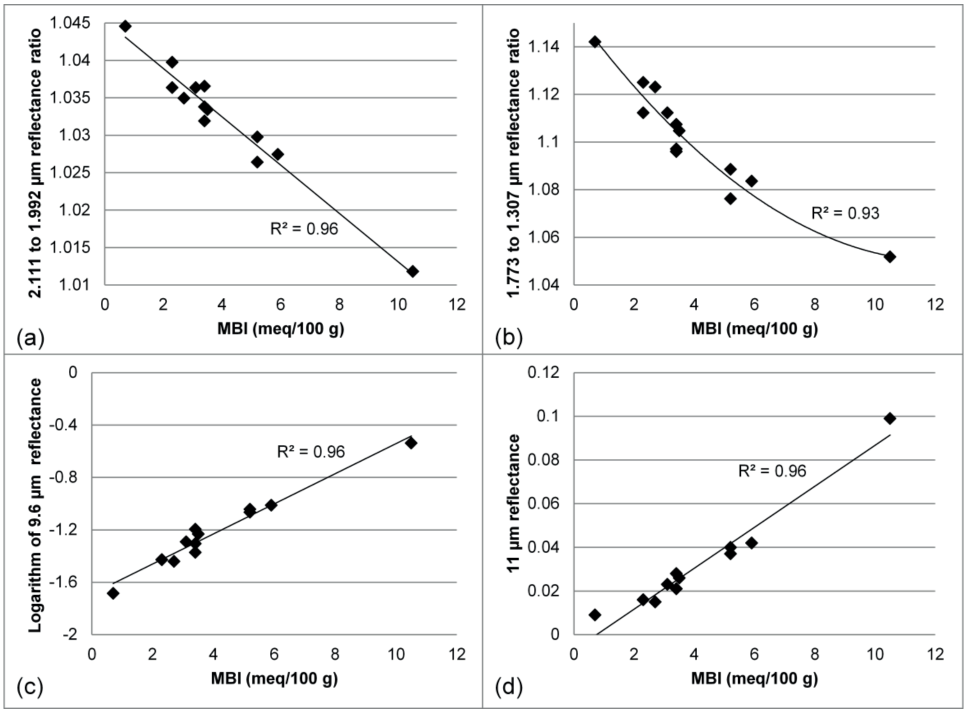

Figure 2. Relationship between MBI and: (a) the 2.111 to 1.992 µm reflectance ratio, (b) the 1.773 to 1.307 µm reflectance ratio, (c) the logarithm of 9.6 µm reflectance, and (d) the 11 µm reflectance

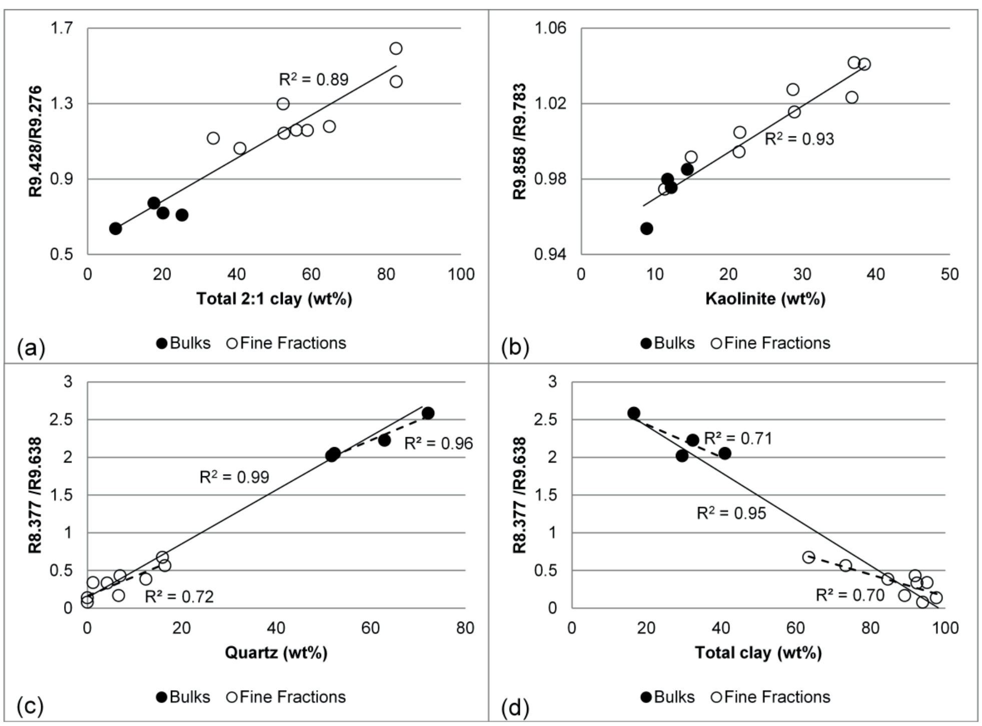

Figure 3. Strongest correlations observed between: (a) total 2:1 clays and the 9.428 to 9.276 µm reflectance ratio, (b) kaolinite and the 9.858 to 9.783 µm reflectance ratio, (c) quartz and the 8.377 to 9.638 µm reflectance ratio, and (d) total clay and the 8.377 to 9.638 µm reflectance ratio

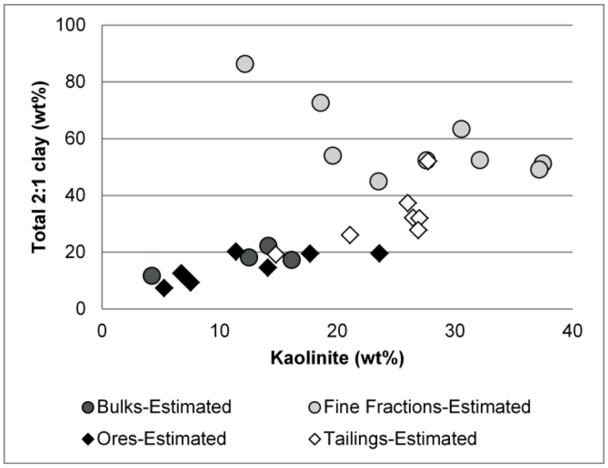

Figure 4. Relationship between kaolinite and total 2:1 clay estimated from the LWIR models for the bulk and fine fraction samples as well as ore and tailings samples

aligned with the pattern of the ore samples though they show a higher kaolinite and total 2:1 clay content, owing to their clay-rich nature. The spectral metrics of this study can potentially be used to detect anomalous samples in terms of their ratio of kaolinite to total 2:1 clays.

CONCLUSIONS

The main objective of this research was to evaluate the potential of hyperspectral remote sensing for the characterization of oil sands tailings. The focus was to develop spectral models to estimate key and trackable properties of tailings. The results of this research lay the foundation for future work to establish a fast, accurate, and reliable in-situ method for determining the moisture content and evaporation, MBI, and mineralogy of oil sands tailings based on hyperspectral sensing. Remote estimation of moisture content and evaporation could help to assess the drying process and to determine when the deposit has stopped drying at the surface, as part of a decision determining when the next lift should be deposited. Quick prediction of MBI provides insights into the settling and consolidation of tailings and the geotechnical stability of a final tailings deposit for reclamation purposes. In addition, estimation of MBI can improve the controllability of the flocculation dosage in the polymer-based technologies developed to treat tailings inventories. The real-time detection and quantification of clay minerals and quartz can provide useful insights into bitumen recovery and tailings consolidation and could enhance bitumen production processes and tailings operation.

ACKNOWLEDGEMENTS

The authors would like to acknowledge the Institute for Oil Sands Innovation (IOSI) at the University of Alberta, the Natural Sciences and Engineering Resarch Council (NSERC) Industrial Research Chair in Oil Sands Geotechnique at the University of Alberta, and Shell Canada for their support of this research.

REFERENCES

Bayliss, P., and Levinson, A.A., 1976. Mineralogical review of the Alberta oil sand deposits (Lower Cretaceous, Mannville Group). Bulletin of Canadian Petroleum Geology 24(2): 211–224.

Bichard, J.A., 1987. Oil sands composition and behaviour research. Edmonton: Alberta Oil Sands Technology and Research Authority.

Entezari, I., 2016. Applications of remote hyperspectral sensing in the characterization of Alberta's oil sands tailings. PhD Thesis. Department of Earth and Atmospheric Sciences, University of Alberta.

Entezari, I., Rivard, B., Lipsett, M.G., and Wilson, G.W., 2016a. Prediction of water content and normalized evaporation from oil sands soft tailings surface using hyperspectral observations. Canadian Geotechnical Journal. 53(10): 1742-1750.

Entezari, I., Rivard, B., and Lipsett, M.G., 2016b. Estimation of Methylene Blue Index in Oil Sands Tailings Using Hyperspectral Data. Canadian Journal of Chemical Engineering. In press.

Haubrock, S.N., Chabrillat, S., Lemmintz, C., and Kaufmann, H. 2008. Surface soil moisture quantification models from reflectance data under field condition. International Journal of Remote Sensing. 29(1): 3-39.

Hooshiar Fard, M.A., 2011. Characterization of clay minerals in the Athabasca oil sands in water extraction and nonaqueous solvent extraction processes. Ph.D. Thesis, Department of Chemical and Materials Engineering, University of Alberta, Canada.

Kaminsky, H., 2008. Characterization of an athabasca oil sands ore and process streams. PhD Thesis, Department of Chemical and Materials Engineering, University of Alberta.

Mercier, P.H.J., Le page, Y., Tu, Y., and Kotlyar, L.S., 2008. Powder X-ray diffraction determination of phyllosilicate mass and area versus particle thickness distributions for clays from the Athabasca oil sands. Petroleum Science and Technology 26(3): 307–321.

Omotoso, O., Mikula, R., Urquhart, S., Sulimma, H., and Stephens, P., 2006. Characterization of clays from poorly processing oil sands using synchrotron techniques. Clay Science 12(2): 88–93.

.

Osacky, M., Geramian, M., Dyar, M.D., Sklute, E.C., Valter, M., Ivey, D.G., Liu, Q., Etsell, T.H., 2013a. Characterisation of petrologic end members of oil sands from the Athabasca region, Alberta, Canada. The Canadian Journal of Chemical Engineering 91: 1402–1415.

Osacky, M., Geramian, M., Ivey, D.G., Liu, Q., Etsell, T.H., 2013b. Mineralogical and chemical composition of petrologic end members of Alberta oil sands. Fuel 113: 148–157.

Wilson, G.W., Fredlund, D.G., and Barbour, S.L. 1997. The effect of soil suction on evaporative fluxes from soil surface. Canadian Geotechnical Journal. 34: 145-155.

THE EFFECTS OF FLOCCULATION ON THE METHYLENE BLUE INDEX

Yunhui Li, Ron Currie, Heather Kaminsky, Andrea Sedgwick and Taimur Qureshi
NAIT Applied Research Centre for Oil Sands Sustainability, Edmonton, Canada

ABSTRACT

Clay minerals have a large effect on the bitumen extraction efficiency and tailings consolidation strategies for Alberta oil sands. The methylene blue (MB) titration of clays is the principle tool used to assess clay activity in various oil sands sources. In oil sands tailings treatment, flocculant addition has been widely used to consolidate solids due to enhanced water release. Measurement of clay activity in tailings streams is critical to develop appropriate flocculant treatment procedures. Measurement of clay activity in a mature fine tailings (MFT) slurry before and after flocculant treatment can reveal if all the clays are captured by the consolidation procedure. This paper is an initial study to explore the effects of flocculants on clay activity by measuring the methylene blue index (MBI) in the slurry before and after the treatment with a flocculant. Following drying of the MFT slurry and flocculated MFT slurry, it is also desirable for the MBI values to be the same as the slurry states. The paper discusses the development of a standard operating procedure to measure MBI on MFT with and without flocculant addition in both the slurry and dried forms. The paper focuses on the effects of dispersion energies required to disperse the clays within these samples.

INTRODUCTION

Background

The methylene blue index (MBI) is used to assess the activity of clays in various oil sands sources. The goal of this study is to assess the ability of MBI to reliably determine clay activity following various treatments involved in the reclamation of tailings. One of the methods to treat tailings is the addition of flocculant to effect water release and improve consolidation. It is desirable to understand how the treatment methods impact the activity or deportment of the clays. In order to assess this, it is important to understand whether or not a treatment method (such as flocculation or Dean and Stark analysis) has a fundamental impact on MBI, the method used to measure clay activity.

This work shows the effects on clay activity (MBI values) of MFT treatment with certain flocculants: after removing bitumen, drying at 60°C and drying at room temperature. The purpose was to determine whether changes in the MBI value were due to difficulties in dispersing the samples or if they represented a fundamental change in activity.

Dispersion is the most critical step in the MBI test method (Kaminsky, 2014). Ultrasound is a key tool to effect dispersion of aggregated materials. Dispersion energy can be used to determine the amount of effort that has gone into the dispersion process. Dispersion energy can be calculated using the following equation:

$$Energy\,(\frac{Joule}{mL}) = \frac{Power\,\left(\frac{Joule}{s}\right) * Time(s)}{Volume\,(mL\ or\ cm^3)}$$

where Power is the output of the sonotrode (Watts or Joule/s), Time is the sonication time in seconds, and Volume is the volume of the suspension of aggregated materials (cm^3).

Breakage and alteration of the structure of the aggregate building blocks is undesirable. Thus Kaiser and Berhe (2014) caution that too high an energy should be avoided to cause physical damage and even chemical modification of certain aggregates. The review article published by Kaiser and Berhe (2014) suggests the choice of energy needed to disperse aggregates is related to the type of material. Materials with a high clay content require more energy to disperse. In demonstrating how robust clay particles are, it was shown that energies in excess of 12,000 Joule cm^{-3} were needed to achieve breakage of kaolinite particles. Schrumpf (2013) illustrated the difference in dispersion energies needed for different sample types; 900 Joule/mL was needed to cause disaggregation of soil samples containing clay content between 0 and 70% but only 100 Joule/mL was required to disperse aggregates from samples with high sand content in the range of 60 to 90%. For MFTs with low sand and a high clay content, it is evident from the above that high levels of ultrasonic energy can be used for disaggregation without affecting the inherent structure of the clays.

There are two common ultrasound devices; probe and bath sonicators. The probe sonicator is usually a stronger source of ultrasound but it is important to position the probe at an appropriate depth in the suspension and to observe the tip for progressive erosion. Erosion of the tip ultimately reduces the power transmitted to the sample. The probe can only be used for one sample at a time which may be viewed as an issue when a large number of samples are being analyzed. The bath sonicator allows more than one sample to be dispersed at a time but the energy imparted to the sample is usually less. This study is mainly performed with probe sonicator in order to provide effective dispersion of clays.

EXPERIMENTAL

Materials

MFT and process effected water (PEW) tested were from an oil sands tailings pond. The bentonite sample was from Alfa Aesar. Kaolinite (high-defect) was from Warren County, Georgia, USA and was sourced from the Clay Minerals Society source clay repository (KGa-2).

Equipment and procedures

The study was performed at Centre for Oil Sands Sustainability (COSS) at Northern Alberta Institute of Technology (NAIT), Edmonton, Alberta.

Sonication equipment. A QSONICA sonicator model Q700 including a standard ½" diameter probe was used for all the sonication tests. The amplitude was set at 90% for all the sonication dispersion times.

Dean and Stark. Dean and Stark (D&S) extraction was used to treat MFT and flocculated MFT in this study. COSS extracted the samples in the range of 21 to 24 hours to ensure complete removal of bitumen from the solids. The solids after D&S were dried at 100°C and filter through a sieve (#10, 2 mm).

Methods

Subsampling. The slurry subsampling procedures in this study involved mixing of the 0.2 clay to water ratio (CWR) MFT tote for 5 minutes using a Hammer Drill. MFT was transferred from the bottom spout of the tote into a 2 L beaker to be used as stock slurry. Subsampling from the stock slurry for MBI titrations was accomplished using a Gang mixer at 300 rpm for 5 minutes. Subsampling was recovered during the final stages of mixing using a wide-mouth plastic pipette to achieve the requisite mass (~5 g) for the MBI titration.

Flocculation. Two anionic HPAM flocculants used in this study are referred as Polymer-A and Polymer-B. The MFT was diluted to a 0.20 CWR using PEW to aid in identifying the dosage needed to achieve an optimal flocculation of the MFT. Suncor's pulsed mixing technique (0-320 rpm) was used to form flocculated MFT. Concerns related to subsampling discrepancies due to flocs and water layers separating were overcome by homogenization of the flocculant treated MFT through 15 minutes over-shearing at full speed of 320 rpm. Then the homogeneous flocculated subsamples were recovered during 50 rpm mixing using a wide-mouth plastic pipette to achieve the requisite mass (~5 g) for the MBI titration.

Slurry titration. From previous applications of the MB titration at COSS, the MB titration procedures on slurry and solid samples were developed (Curries et al., 2014). A ~5 g subsample (untreated and flocculant treated MFT) of MFT slurry was diluted with deionized water to a 50 mL volume and mixed at 500 rpm for 5 minutes using a magnetic stirrer. 1 M sodium bicarbonate was then added to achieve a 0.015 M bicarbonate concentration. The pH was adjusted to 9.6 using 10 wt% NaOH while stirring, and then the sample was probe sonicated with the dispersion times ranging from 0.5 to 60 minutes using a 90% amplitude. The pH was then adjusted to 3.0 while stirring using a 10% H_2SO_4 solution. The solution was titrated by adding 1.0 mL of 0.006 N methylene blue (MB) with a pipette until a 15 µL aliquot shows a halo at 20 seconds. Reduce the MB volume to 0.5 mL and continue the titration until a permanent halo remains at 60 seconds for the aliquot taken. This was considered the endpoint of the titration. The actual quantity of subsamples ensured that a minimum of 10 mL of 0.006 N MB is required to complete the titration.

Solids titration. Subsamples of flocculant-treated MFT were dried at 60°C in an oven or room temperature in a fume hood. This approach ensured the mass of solids was similar to that of the slurry titration procedure. The dried samples were dispersed in 0.015 M bicarbonate buffer and adjusted to pH 9.6 using 10 wt% NaOH. The dispersion procedures were conducted using the sonication probe in the same manner as the slurry subsamples.

Control chart samples. Bentonite (Alfa Aesar) and kaolinite (high-defect, Warren County, Georgia, USA) were used as check standards for control charting. The samples were dried at 100°C overnight. Both bentonite and kaolinite samples were wetted by isopropyl alcohol (IPA) before titrating as solids titration to enhance dispersion. Dispersion was accomplished using the sonication probe in the same manner but at a constant 15 minutes dispersion time.

RESULTS AND DISCUSSION

MFT and PEW from an oil sands tailings pond were characterized. Table 1 shows the D&S results for bitumen, solids, and water (BSW) for the MFT (0.36 clay to water ratio (CWR)) and the diluted MFT (0.20 CWR) with PEW used in this study. The D&S extraction was performed by COSS in the range of 21 to 24 hours to ensure complete removal of bitumen from the solids. The % of fines with less than 44 micron for the D&S cleaned solids was 96.8%.

Table 1. %Fines and D&S data for bitumen, solids and water

Sample	Bitumen (wt%)	Solids (wt%)	Water (wt%)	Fines% (<44 µm)
0.36 CWR	2.8	29.9	63.6	96.8
0.20 CWR	1.9	24.2	73.7	

The MB solution, used as titrant, was prepared fresh each day and took considerable time to prepare due to its low solubility. It should be noted that the MB solution concentration should be consistent from the day to day preparation. The MB solution concentration at 0.006 N is also critical to generate reliable MBI data. A study involving the use of check standards of purchased representative clay types was used to calculate a corrected MB solution concentration based on experimental MBI values for the check standard. The corrected concentration of the MB solutions was calculated using the following equations:

$$\mathit{Calculated\ Ratio\ using\ fresh\ MB\ solution} = \frac{\mathit{Experimental\ MBI\ (check\ standard)}}{\mathit{Prepared\ MB\ solution\ concentration}}$$

$$\mathit{MB\ solution\ concentration\ (corrected)} = \frac{\mathit{Average\ MBI\ of\ batch\ check\ standard}}{\mathit{Calculated\ Ratio}}$$

The calculated ratio was also plotted on a control chart. If the MBI value for the check standard was reliable then an outlier associated with this ratio could be attributed to an error in the prepared MB solution concentration.

Bentonite and kaolinite clays are available from a variety of suppliers. Both bentonite and kaolinite were dried at 100°C before use in order to ensure the mass used for the titration did not include water. Another aid to disperse the solid clay samples is to add a few drops of isopropyl alcohol (IPA). This wets the clay and reduces the hydrophobicity of the sample when placed in the buffer. All the MBI data in this paper have had MB solution correction using bentonite or kaolinite as check standard.

Effects of different flocculants

The MFT was diluted to a 0.20 CWR solution to aid in identifying the dosage needed to achieve an optimal flocculation of the MFT. Two flocculants – Polymer-A and Polymer-B were used to treat diluted MFT (0.2 CWR) in this study. Concerns related to subsampling discrepancies due to floc and water layers separating were overcome by homogenization of the flocculant treated MFT through overshearing. Although the flocs would be lost by homogenization, the subsampling consistency was improved. The flocculant dosage levels for both polymers were: under dose, optimal dose, and over dose.

Table 2. Comparison of slurry forms of treated MFT with Polymer-A and untreated MFT. %RSD is referred as Relative Standard Deviation.

Sample	Average MBI values	%RSD
MFT Slurry	14.5	2.55%
Flocculated MFT Slurry (Optimal dosage)	13.6	0.81%
Flocculated MFT Slurry (Under dosage)	14.6	1.01%
Flocculated MFT Slurry (Over dosage)	13.6	0.47%

Table 2 contains data comparing the results for the slurries of treated MFT using Polymer-A at various dosage levels with untreated MFT. It is apparent that when the MFT slurry is treated with Polymer-A at optimal or over dosage levels the MBI values are reduced compared to MFT slurry without treatment. ANOVA provides a *P* value of 1.42E-06 showing statistical differences in the data exists due to dosage levels using Polymer-A. Table 3 reveals the source of the statistical differences. The Tukey group means for the ANOVA data confirm that the A grouping of MFT slurry and Polymer-A at an under dosage level are statistically different from the B grouping of optimal and over dosage levels of Polymer-A. This suggests that the Polymer-A at high dosage levels is in some manner interfering with the ability of MB to fully cation exchange when this flocculant type interacts with MFT clays.

Table 4 compares the untreated and treated slurry MFT samples with variable dose levels of Polymer-B. Contrary to the data with Polymer-A, there is very little difference in the mean MBI values for any of these samples. This is supported by ANOVA data, where the P value is 0.053 thus showing no statistical differences in untreated and treated samples of MFT at any dosage levels. This data suggests that Polymer-B is not inhibiting the cation exchange of MB with the clays.

Table 3. Grouping information using Tukey's method for treated (Polymer-A) and untreated slurry forms of MFT. Different letters indicate significant difference between groups (Tukey's test, P < 0.05).

Sample	N	Mean	Grouping
MFT slurry	7	14.5	A
Flocculated MFT slurry (under dosage)	5	14.6	A
Flocculated MFT slurry (optimal dosage)	4	13.6	B
Flocculated MFT slurry (over dosage)	5	13.6	B

Table 4. Comparison of slurry forms of treated MFT with Polymer-B and untreated MFT. %RSD is referred as Relative Standard Deviation.

Sample	Average MBI values	%RSD
MFT Slurry	14.5	2.55%
Flocculated MFT Slurry (Optimal dosage)	14.5	1.38%
Flocculated MFT Slurry (Under dosage)	14.1	0.55%
Flocculated MFT Slurry (Over dosage)	14.2	1.99%

Thus all polymer additives are not behaving in the same manner regarding the clay interactions leading to flocculation of the MFT. It should be noted that Polymer A typically produces a flocculated product with a higher yield stress than Polymer B. There is no apparent evidence that Polymer-A and Polymer-B themselves are interacting with MB since the MBI values are not statistically elevated compared to the slurry sample themselves.

Since treatment with Polymer-A lowers the MBI values compared to MFT slurry, further study on the effects of Polymer-A on MBI values were performed. Four different sample treatments on Polymer-A treated MFT slurry plus MFT slurry without any treatment were performed: Polymer-A treated MFT slurry, dried (60°C) Polymer-A flocculated MFT, dried (room temperature) Polymer-A flocculated MFT, D&S on the Polymer-A flocculated MFT.

Effects of dispersion time on flocculated MFT slurry

The optimal dosage level of Polymer-A was used throughout the following study. Figure 1 compares MBI values for slurry MFT and Polymer-A flocculated MFT slurry at an optimal dosage with probe sonication time. The plot reveals it is much easier to disperse MFT slurry than the flocculated MFT samples, using probe sonication. The individual datum points are corrected with check standard samples and error bars representing the 95% confidence interval.

The difference between the maximum and minimum MBI values for the MFT slurry samples is 0.4 meq MB/100 g solids. The change in MBI values with increased probe sonication times is relatively small since the clays in MFT are less aggregated in the slurry.

The data, however, suggests that in order to achieve the highest level of dispersion, energies of about 1500 Joule/mL are required. This may suggest that although most of the aggregated clays are dispersed in as little as 5 minutes, the complete dispersion of the aggregated clays requires additional energy. The additional energy may be sufficient to alter some of the organics associated with the clays which may be impeding complete dispersion (Robertson, et al., 1984; Di Stefano et al., 2010).

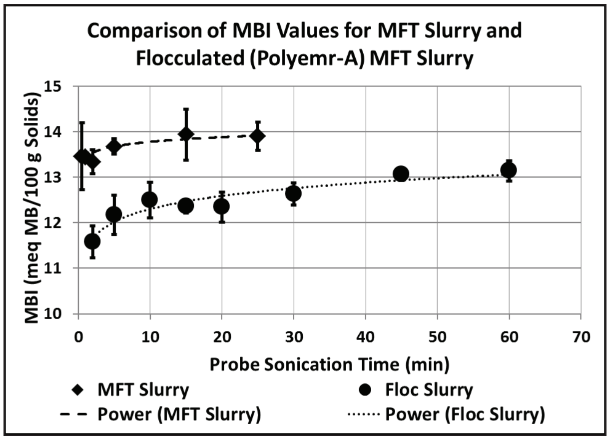

Figure 1. Comparison of MBI values for MFT slurry and Polymer-A flocculated MFT slurry with probe sonication time

The MBI values for the Polymer-A flocculated MFT slurry at an optimal dosage level are shown to increase with increased sonication time (Figure 1). The MBI values are much lower at shorter dispersion times than the MFT slurry. This suggests that the interaction of Polymer-A with the clays interferes with dispersion of the clay aggregates or alternatively prevents MB interaction with cation exchange sites. These issues can only be partially remediated with much higher dispersion energies.

Table 5. Grouping information for Polymer-A flocculated MFT slurry MBI using the Fisher LSD method. Means that do not share a letter are significantly different.

Sonication time (min)	Sonication Energy (Joule/mL)	N	MBI Mean	Grouping		
2	200	3	11.6			C
5	500	3	12.2		B	C
10	1000	3	12.5	A	B	
15	1500	3	12.4		B	
20	2000	3	12.3		B	
30	3000	3	12.6	A	B	
45	4500	3	13.1	A		
60	6000	3	13.1	A		

Table 5 reveals the grouping of the MBI means for the Polymer-A flocculated MFT slurry based on the Fisher Least Significance Difference (LSD) method following ANOVA. The grouping of the MBI means is at a 95% confidence level and the mean MBI values that do not share a letter are significantly different. The C grouping has the smallest MBI values and the A grouping the largest. Unlike the MFT slurry, dispersion times over 30 minutes are needed before the MBI values begin to show similar MBI values. The data suggests increasing dispersion energy will not elevate MBI values to that found for MFT slurry samples when using the Polymer-A as flocculant.

With the MFT slurry samples, dispersion of the clay aggregates becomes similar with only about 1500 Joule/mL, whereas the flocculated MFT slurry samples require at least 3000 Joule/mL to generate reasonable consistent MBI data, although never as high as the MFT slurry. The maximum dispersion energy imparted to the sample, assuming 100% efficiency based on the readout for the probe sonicator, was approximately 6000 Joule/mL at 60 minutes of probe sonication time.

The MBI values of flocculated MFT increased by 1.5 meq MB/100 g solids from the minimum values using probe sonication. This too shows the importance of increasing the sonication time to obtain more consistent MBI values for the MFT flocculated slurry samples.

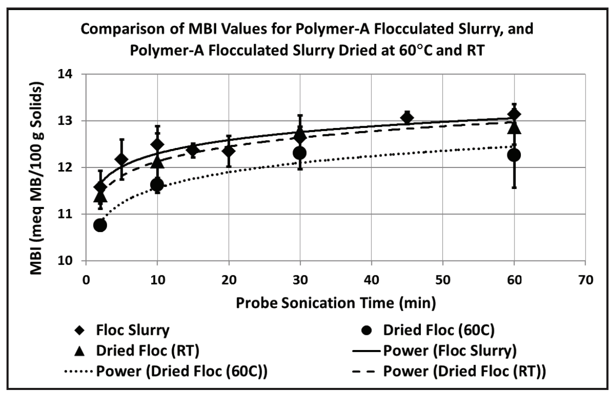

Figure 2. Comparison of MBI values for Polymer-A flocculated slurry, and dried flocs at room temperature and 60°C with probe sonication time.

Effects of dispersion time on dried flocculated MFT slurry

A common theme for the most detrimental variable affecting MFT is high temperature drying of the MFT. This applies to flocculated MFT slurry being dried at 60°C. Room temperature drying of flocculated MFT was also studied alongside for comparison. Figure 2 compares the effect of drying the flocculated MFT slurry at two different temperatures: 60°C and room temperature (RT). Samples dried at 60°C are much more difficult to disperse. Increasing probe sonication time could not reach the MBI values of flocculated slurry. Drying of the flocculated MFT at room temperature is shown in Figure 2 to rapidly disaggregate indicating that under these drying conditions, the clay aggregates are not so tightly associated. This suggests that when the water removal is at a slower rate, the aggregates are not so tightly bound.

Table 6. Grouping information for dried flocs at 60°C treated with Polymer-A using the Fisher LSD method. Mean that do not share a letter are significantly different.

Sonication time (min)	Sonication Energy (Joule/mL)	N	MBI Mean	Grouping	
2	200	3	10.8		b
10	1000	3	11.6	a	b
30	3000	3	12.3	a	
60	6000	3	12.3	a	

Table 7. Grouping information for dried flocs at room temperature treated with Polymer-A using the Fisher LSD method. Mean that do not share a letter are significantly different.

Sonication time (min)	Sonication Energy (Joule/mL)	N	MBI Mean	Grouping	
2	200	3	11.4		b
10	1000	3	12.1	a	b
30	3000	3	12.8	a	
60	6000	3	12.9	a	

Tables 6 and 7 compare the MBI grouping information for the 60°C dried and RT dried flocculated MFT by Polymer-A with different sonication times, respectively. The Fisher LSD analysis means that 30 minutes dispersion time with probe sonicator, that is 3000 Joule/mL of energy, are required to obtain consistent MBI values for dried MFT flocculated slurry samples. The difference between the minimum and maximum MBI values are 1.5 meq MB/100 g solids (~9 wt% clay) for both dried MFT flocculated slurry samples at 60°C and room temperature.

The MBI values of dried flocculated MFT indicate that the more rapid the release of water from the MFT, the more severe the aggregation of the clay and consequently the more energy that is required to disperse. A plateau in MBI values begins at about 3000 Joule/mL for both dried flocculated MFT at 60°C and room temperature. However, room temperature drying shows relatively high MBI values with as little as 1000 Joule/mL suggesting a reduction in the strength of the clay aggregates. The 60°C dried flocculated MFT has very low MBI values even when 6000 Joule/mL is applied.

Kaiser and Berhe (2014) have indicated in their review paper that energies as high as 12000 Joule/mL have not affected the basic building blocks of the clays. Perhaps energies near these values may be needed to fully effect dispersion of MFT following some of these sample treatments. Both flocculation and organics in MFT are believed to contribute to the lower MBI values of flocculated MFT compared with the MFT slurry. Therefore, organics removal was further investigated to confirm that organics interfere with MBI values when flocculated MFT was dried.

Effects of dispersion time on D&S extracted flocculated MFT slurry

Figure 3 presents the MBI data for MFT slurry and flocculated MFT slurry that have undergone D&S extraction. D&S is a process in which toluene soluble organics, principally bitumen, and water is removed from samples. The extracted solids were dried at 100°C to remove solvent. In contrast to the flocculated MFT dried at RT and 60°C, the recovered solids using D&S are free of bitumen. Although the temperature of drying used is much higher than that used at RT and 60°C, its affects are not as severe on the ability to disperse the clays as when bitumen is present. D&S MFT solids are able to generate comparable MBI values with MFT slurry by 20 minutes of probe sonication (~2000 Joule/mL).

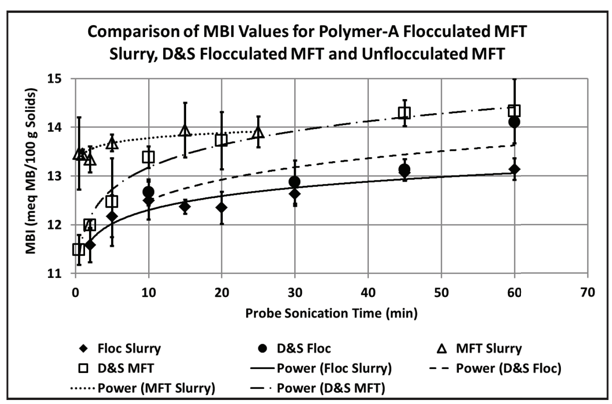

Figure 3. Comparison of MBI values for Polymer-A flocculated slurry, D&S treated Polymer-A flocculated MFT slurry, MFT slurry, and D&S MFT with probe sonication time

Table 8. Grouping information for D&S Polymer-A treated flocculated using the Fisher LSD method. Mean that do not share a letter are significantly different.

Sonication time (min)	Sonication Energy (Joule/mL)	N	MBI Mean	Grouping	
10	1000	3	12.7		b
30	3000	3	12.9		b
45	4500	3	13.1		b
60	6000	3	14.1	a	

Figure 3 also shows by 10 minutes of probe sonication (~1000 Joule/mL) the D&S treated flocs are dispersed; generating MBI values comparable to that of MFT flocculated slurry samples, and even higher MBI values with long sonication time. By 60 minutes of probe sonication (~6000 Joule/mL) the MBI value of D&S treated flocs is comparable to that of MFT slurry (Table 8). Both D&S MFT and D&S flocculated MFT dispersions confirm that organics interfere with MBI when flocculated MFT slurry samples are dried.

Although most of the organics have been removed, toluene insoluble organics will remain associated with the clay after D&S. A humic acid determination used to reflect the presence of toluene insoluble organics suggests a concentration of about 0.04% of the MFT consists of these organics. Hydrogen peroxide addition has been used to remove organics (Adeyinka el al., 2009) and improve dispersion (Robertson, et al., 1984; Di Stefano et al., 2010). Since hydrogen peroxide is generated during sonication (Ince et al., 2001) it is possible that the amount of peroxide generated is sufficient to disperse these low levels of remaining organics and allow dispersion of the MFT solids resulting in values comparable to MFT slurry at 60 minutes. Kaiser and Berhe (2014) also suggested very high energies can affect the organics in soil. With the majority of the organics removed by D&S this level of dispersion can be achieved earlier than the dried flocculated MFT where bitumen is present.

CONCLUSIONS

- The MBI data acquired for flocculated MFT slurry indicates flocculant addition has the potential to effect differences in MBI values between MFT slurry and the flocculant treated MFT slurry samples, especially at higher dosage.
- There are differences in the functionality of the polymers that can affect MB interaction with clays.
- There is no apparent evidence that the polymers themselves are interacting with MB since the MBI values are not statistically elevated compared to the slurry sample themselves.
- Treatments which form strong clay aggregates (drying, high temperature drying or flocculation) make the clay more difficult to disperse and hence lead to a lower MBI.
- The presence of organics in the aggregated structure further impedes dispersion.
- Removing the toluene soluble organics and most of the flocculant with D&S treatment mitigates the impact of the flocculant on the MBI of the material.

REFERENCES

Adeyinka, O. B., Samiei, S., Xu, Z., and Masliyah, J.H. 2009. Effect of particle size on the rheology of Athabasca clay suspensions. The Canadian Journal of Chemical Engineering, 87, 3, 422-34.

Currie, R., Bansal, S., Khan, I., Mian, H. 2014. An investigation of the methylene blue titration method for clay activity of oil sands samples. Oil Sands Research and Information Network.

Di Stefano, C., V. Ferro and S. Mirabile, 2010. Comparison between grain-size analyses using laser diffraction and sedimentation methods. Biosystems Engineering 106: 205-215.

Ince, N. H., Tezcanli, G., Belen, R. K., Apikyan, I. G., 2001. Ultrasound as a catalyzer of aqueous reaction systems: the state of the art and environmental applications. Applied Catalysis B: Environmental 29, 167-176.

Kaiser, M. and Berhe, A. A. 2014. How does sonication affect the mineral and organic constituents of soil aggregates? – A review. Journal of Plant Nutrition and Soil Science 177: 479-495.

Kaminsky, H., 2014. Demystifying the methylene blue index. International Oil Sands Tailings Conference, Banff, Alberta, Canada.

Robertson, J., C.J. Thomas, B. Caddy and A.J.M. Lewis, 1984. Particle size analysis of soils – a comparison of dry and wet sieving techniques. Forensic Science International 24: 209-217.

Schrumpf, M., Kaiser, K., Guggenberger, G., Persson, T., Kögel-Knabner, L., Schulze, E.-D. 2013. Storage and stability of organic carbon in soils as related to depth, occlusion within aggregates, and attachment to minerals. Biogeosciences 10: 1675-1691.

Session C-2

Chemical Interactions (2)

CHEMICAL AMENDMENT OF FLUID FINE TAILINGS AND RELATED LABORATORY PERFORMANCE TESTS

Randy Mikula[1] and Gavin Freeman[2]
[1]Kalium Research
[2]Shell Canada Limited

ABSTRACT

The three generally important regimes of oil sands fluid fine tailings behavior are the initial settling or dewatering rate, followed by hindered settling or settlement, and finally the longer term consolidation of the tailings deposit The goals for chemical amendment of fluid fine tailings are to improve performance in all of these regimes. Initial dewatering might be more important than long term consolidation rates, or vice versa, dependent upon the tailings management objectives.

Quantifying and predicting behavior in the initial dewatering stages is relatively straightforward, while the effect of chemical amendments on the hindered settling tailings properties are often inferred from a variety of what are best described as index tests. Finally, the consolidation regime is often well described by geotechnical or soil science test protocols.

The scientific interest in oil sand tailings fundamentals arises from the fact that tailings mineral suspensions are too concentrated for the application of colloid theory and too disperse to rigorously apply soil science principles. These fundamental limitations have not prevented the sometimes inappropriate expansion of the range of applicability for a variety of characterization and test protocols that are common to both disciplines. With tailings at either very low or very high solids contents, colloid science or soil science (respectively) are reasonably applicable. The critical hindered settling regime is where fluid fine tailings transition from a fluid to a solid and there is a need for more rigorous mass balance and sample characterization protocols.

This paper includes a discussion of common tests for initial dewatering, solids settlement, and consolidation. The intent of this discussion is to provide clarity on which performance metrics are viewed as important and how chemicals are currently being screened for oil sands applications, including what criteria might be important for chemical performance in a commercial application.

INTRODUCTION

Background

Conventionally, there are two tailings streams of note in the oil sands industry; sand tailings and fluid fine tailings. The sand tailings are the coarser of the two streams, with a mineral particle size greater than 44 microns. The fluid fine tailings are characterized by a mineral particle size of less than 44 microns, approximately 50% of which are clays less than 2 micron in size (FTFC 1995). The sand tailings rapidly dewater and gain enough strength to be used in construction of above ground or out of pit containment for the fluid fine tailings. The fluid fine tailings settle in months to years to approximately 30 to 35% mineral solids by weight, at which time they are characterized as being a weakly flocculated electrostatically stabilized suspension, and commonly called mature fine tailings (MFT).

The water associated with the fluid fine tailings defines both the strength of the tailings suspensions and the volume of tailings that has to be managed. In the oil sands industry, mature fine tailings is accumulating in various containment areas at a rate of approximately 1.5 barrels per barrel of bitumen production. With the current zero discharge policy for process affected water, an objective of tailings management is to minimize the amount of water accumulating on site. With any reduction of water content in the tailings there is an increase in the strength of the resulting dewatered tailings. The greater the strength development in the tailings, the more options that are available in terms of mine planning and tailings management. For example, a tailings treatment technology that results in production of a dry stackable tailings that does not require containment will provide more options than a tailings treatment that requires in pit containment.

Composite or non-segregating tailings, thin lift drying, or centrifugation are just a few of the commercial technologies used to dewater and reduce the stored volume of mature fine tailings. These processes provide a material with which to create a more readily reclaimable landscape, along with water suitable for reuse in the extraction process.

Variations in extraction tailings properties, treatment, and deposition options results in a wide variety of fluid fine tailings or even sand tailings properties. As a result, in any chemical screening program it is important to characterize the sand to fines and clay content of the tailings test sample (COSIA 2014, Mikula 2015).

The clay to water ratio has been used for several decades to quantify tailings properties when there is separation of the minerals based on size and where the simpler F/F+W characterization is not adequate. The clay to water ratio was used as a link to geotechnical conventions, although Clay/Clay+Water would be a more intuitive characterization metric. In tailings treatment processes that separate large volumes of water, the suitability of the water for reuse and any mineral in the water should be characterized and quantified to completely understand the effectiveness of the treatment.

In the decades of data collection with fine tailings deposits it is clear that there are limits to the dewatering that can occur in the absence of some chemical or physical intervention, even after very long time periods. Because of the electrostatically stabilized nature of the mature fine tailings, at least one estimate of the elapsed time to achieve a trafficable deposit is “never” (FTFC 1995). The past two decades have focused on methods to significantly extend the limit of natural dewatering. The development of the composite, consolidated, or non-segregating tailings process has provided data on the effects of inorganic salts and even polymers on strength development and dewatering of fluid fine tailings (MacKinnon 1999). Research into the paste thickening process provided extensive data about polymer interactions with the clay minerals in MFT.

Since the research programs developed around CT/NST and paste thickening, several further advances in tailings management have been developed, including atmospheric fines drying, rim ditching of deep deposits, and centrifugation. All of these technologies require additives to achieve the desired results, and any alternative additives need to be carefully screened (Mikula 1999, Omotoso 1999).

A new tailings regulatory environment, coupled with more expensive and complicated tailings management systems means that additive screening and performance evaluations should be scrutinized very carefully. Inexpensive but consistent additive performance evaluation tests are critical as a first step before committing to large or commercial scale testing.

DISCUSSION

Many public discussions about MFT accumulation in tailings ponds have referred to the slow settling rate of the oil sands tailings suspensions. In fact, the accumulation of fluid fine tailings and in particular MFT is really due to the very slow hindered settling and consolidation rates. The slow settling explanation for the tailings management challenge in the popular press was a matter of expediency in terms of explaining a complex tailings scenario to the public. Unfortunately this misunderstanding about what performance parameters are important has manifested itself in the research community with a number of publications that propose additives and complex processes that in the end only get to the relatively easily achievable MFT state in terms of fines/fines+water contents.

Tailings management is essentially water management and that ultimately relates to accumulating volumes. With the recent regulatory emphasis changing from a deposit strength criteria performance basis (Directive 74, ERCB 2009) to a fluid fine tailings volume performance basis (Directive 85, AER 2016), there is also a potential for misplaced research effort.

It is well established that the settled volume of a dispersed mineral suspension is smaller than for a flocculated suspension (Van Olphen 1968, Lambe 1958). In other words, there is a trade-off between settling rate and settled volume. The current trend to use high molecular weight polymer additions to achieve improvements in hindered settling regime water release needs to be balanced against any limitations that this might cause in the final consolidation behavior. Currently, it is clear that some chemical intervention is necessary to overcome the electrostatic stabilization of the MFT suspension. It is then assumed that any coincident detrimental impact on final consolidation would be acceptable. This trade off in fact might not be acceptable as it depends upon the mine plan and the tailings management objectives at a particular site.

Scale up testing in tailings deposit performance is essential, due to challenges in interpreting the dewatering results from small sample sizes. The most prevalent problem is where sample representativeness might be an issue. Another is that increasing the sample size also demands an increase in scale of the tailings treatment. The sensitivity of polymer performance to the mixing regime means that process scale up questions can be answered at the same time as deposit performance scale up. With the complexity associated with modern oil sands mine plans and tailings management objectives, sometimes even large scale testing has to be limited to a particular tailings source. As a result, even large scale test programs may not meet the criteria of testing on a representative sample.

Initial Settling

Understanding the fundamental behavior of the clay minerals in the mature fine tailings has always been an industry priority, but ultimately it is how these fundamentals affect the dewatering properties of the tailings suspension that are important. Figure 1 shows a tailings pond profile with a steadily increasing fines/fines+water ratio, coupled with the associated clay to water ratio (Mikula 2015). Although the fines data appears to indicate some densification of the deposit is occurring with depth, there is clearly no increase in the clay to water ratio. The misinterpretation that is possible when only looking at fines content emphasizes the need for complete characterization and mass balance data for solids, fines, and clays in any chemical or process screening protocol.

The Fine Tailings Fundamentals Consortium (FTFC 1995) was established in 1989 in order to systematically characterize the properties of mature fine tailings. At the time, the only commercial operations were the Suncor and Syncrude surface mined oil sands operations, and fluid fine tailings were reasonably similar from site to site. The book which summarized highlights of the six year research program discusses only some of the characterization tests that were done to understand the effects of water chemistry on the oil sands fine tailings minerals. A more complete appreciation of the characterization test work can be found in the associated yearly research report summaries. Most if not all of these test methods were modified or adopted directly from colloid science, or other industries that typically deal with clay suspensions.

Figure 2 shows the relationship between zeta potential and pH for a typical mature fine tailings. The vertical axis on the right shows the ESA or electrosonic amplitude, which is a novel way to measure the charge repulsion of particles in slurries. The vertical axis on the left shows G' which is the elastic modulus of the suspension; related to the yield point of the slurry. It can be seen that the maximum electrostatic repulsion between the mineral particles is in the pH range of oil sands tailings (between pH 8 and 9). This corresponds to the minimum yield point for the same slurry.

Figure 3 shows settling rates for a variety of inorganic chemical additives, in line with the Schulze-Hardy rule and DLVO theory that states that minerals in suspension will settle at a rate determined by the water chemistry and in particular by the charge of the cations in solution to the sixth power (Schulze 1882, Hardy 1900). Although fluid fine tailings suspensions at 5% solids are outside of the infinitely dilute range of DLVO theory applicability, many colloid science test protocols were successfully adapted to help understand MFT behaviour. These two examples show that the MFT mineral suspension is amenable to some extension of fundamental colloid science testing and evaluation protocols.

Thickeners in the mineral industry commonly use high molecular weight organic polymers and for oil sands applications, high molecular weight polyacrylamides with medium charge densities have proven to be very effective (Xu 1999). This early work demonstrated that some of the most effective polymers were high molecular weight, medium charge density polyacrylamides. Although other chemistries were effective, these particular commodity chemicals were readily available. The research work with thickeners in the laboratory and in field pilots demonstrated that the rapidly settling flocculated mineral suspensions did not achieve the same clay to water ratio as a slower settling MFT suspension. This observation is consistent with the early clay studies that demonstrated the trade-off between rapid settling and final settled volume (Mikula 2015).

The weakly flocculated and electrostatically stabilized mineral suspension known as mature fine tailings can be described as a card house structure of the clays. This visualization, although simplistic, provides a view of a matrix with pore spaces containing a large fraction of the water. At the same time, the card house provides some strength preventing collapse of the structure and preventing any increase beyond 30 to 35% solids. Collapsing this structure would release a lot of interstitial water, and allow for a higher solids content settled suspension. The role of the chemical additives is to disrupt this card house structure in favour of a more compact, denser arrangement of the clays.

The application of colloid science theory to oil sands mineral suspensions has been very successful in helping to understand the initial settling regime and the effect of various process changes.. As a result, the effect of pH, temperature, water chemistry, and the role of flocculants in determining settling behavior is well understood from both an empirical and theoretical basis. This is in spite of the fact that fluid fine tailings are strictly speaking not an infinitely dilute, non-interacting suspension of mineral particles.

Hindered Settling

Changing or increasing the rate of dewatering after or beyond MFT formation offers the most promise to decrease the volume of stored tailings. The space occupied by one dry tonne of tailings at 55% solids is less than half the volume of the same dry tonne at 30% solids, with the added benefit of providing an equal volume of water suitable for the extraction process. There is therefore a benefit to moving beyond the electrostatically stabilized MFT structure and improve dewatering in the hindered settling regime.

Several technologies have been commercialized or tested at commercial scales that disrupt the electrostatically stabilized mature fine tailings to produce a fluid fine tailings with an increased F/F+W and clay to water ratio. These include atmospheric drying (thin lift) processes, rim ditching, and centrifugation. All of these start with an MFT like material in terms of solids content and improve the hindered settling regime performance by disrupting the card house structure of the clays.

Coagulants, polymers, or combinations, are added which serve to increase the water release and therefore the solids content and the F/F+W. Polymer and coagulant additions are generally added as solutions or slurries and when evaluating additive performance, it is important to account for this added water. The concept of net water release is an important one since it clearly presents dewatering results in a format which discounts the added water from the process aids. Of course any mass balance data including a discussion of the clay to water ratio before and after the process would do the same, but more rigorously.

For both the coagulant addition and the polymer addition, there is a trade off with improved short term water release against the possibility of inhibited long term consolidation. In the case of the polymer addition, the presence of the high molecular weight, medium charge density polymers disrupt the card house of clays to produce a more compact clay and mineral matrix. At some point in the densification of the mineral suspension, the presence of the polymer will not help card house collapse but inhibit further close approach of the minerals. As the solids content increases (void ratio decreases) the presence of the polymer will then potentially limit further dewatering.

In processes that improve the dewatering in the hindered settling regime, the release water from these processes is seldom solids free. It is therefore essential that mass balances be completed that quantify the solids content and size distribution in the separated water, whether it is runoff from a thin lift drying process, a rim ditch deposit, or the centrate in a centrifuge process.

In order to rapidly evaluate the dewatering effectiveness of any chemical additive or mixing protocol, two tests are commonly used. These are the specific resistance to filtration (SRF) and the capillary suction time (CST). Both tests are empirical in nature and are used to evaluate the potential for dewatering mineral slurries using commercial filtration equipment (Smollen 1986, Kan 1978). The specific resistance to filtration test has been developed to the point that results can be used to establish whether or not a particular sludge or mineral slurry will be amenable to commercial scale filtration processes. The ability to use the SRF data to predict filtration equipment capacity and performance is of course dependent upon adherence to a particular experimental protocol. The same is true of the capillary suction time.

For oil sands applications, both of these tests have been modified to provide more applicability to MFT suspensions. The SRF specifies a certain suspension volume loaded into an apparatus of a particular size, with a specified filter media at the bottom and a specified pressure applied. All of these specifications have been modified at various times in order to better evaluate chemical additives (Xu 1993). These changes were necessary in order to extend the range of applicability of the test to very low permeability MFT suspensions.
More recently, the capillary suction time test has been modified by a variety of researchers (to improve applicability to MFT suspensions), often without specification as to the changes. While this might be suitable for additive or process comparisons within a particular test program, it makes inter-laboratory comparisons almost impossible.

The capillary suction time is a measure of the time it takes for water to wet a particular filter paper over a distance of 1cm. The CST will depend upon the weave of the filter paper (tighter weaves will pull water from the sample more slowly), the thickness of the filter paper (thicker paper will require more water to wet a given distance of the paper), the volume of the sample (more sample will have more water available to we the paper), the dimensions of the sample holder, the density of the sample (with higher sample solids, less water is available to wet the filter paper), and the way the sample is introduced into the apparatus (spooned or syringed). It is a common mistake to assume that low capillary suction times imply better dewatering when the sample solids contents are different. A chemical additive that does not release much water is assumed to have a better hydraulic conductivity when it is really performing better in the CST because there is more water in the sample being tested.

Often CST or other index test data is quoted without specifying the wide variety of experimental variables that can affect the results and allow for comparison of performance from laboratory to laboratory (Scholz 2006). Any additive performance claims also have to be associated with a confirmation of MFT properties in terms of fines content and where appropriate with clay content. Performance data has been presented at various conferences for all of the enhanced dewatering processes mentioned earlier.

Previous work has emphasized that mixing is a critical part of the process optimization and the chemical effectiveness in improving dewatering (Demoz 2012). As a minimum, comparisons of performance for alternative additives should refer to the published baseline performance, properly accounting for optimum mixing. It is also critical that the additive/MFT mixing process can be scaled up and not simply a function of the small scale of the laboratory test. The apparent effectiveness of any additive is often overestimated because of the small scale of the screening test with which it was evaluated. The large surface area to volume ratio for samples tested on the beaker scale can impact water release rates, especially if drainage paths are established at the hydrophilic container surfaces. Verifying results at larger laboratory pilot scale in order to understand potential scale up issues is an important step before investing in the more expensive and time consuming larger scale field tests.

There is another aspect of chemical additive performance that is often overlooked, and that is the consistency in the properties of the additive itself. High molecular weight polymers, with specific charge densities have manufacturing variabilities that can sometimes affect test results because both molecular weight and charge density are not perfectly controlled in the polymer manufacturing process.

The hindered settling regime as we have defined it here is squarely between colloid science and soil science in terms of both a theoretical foundation and the applicability of laboratory test procedures. As a result, there is a reliance on index tests and empirical performance comparisons when screening additives. The reliance on index tests that are sometimes out of their range of applicability in turn requires careful experimentation, mass balance, and thorough sample and additive characterization.

CONSOLIDATION

The geotechnical community and soil scientists use a variety of empirical tests such as Atterburg limits to quantify the properties of dewatered tailings (Gan 2011). The determination of liquid limits and plastic limits have subsets that account for clay content and the effects of water chemistry. In addition, a suite of other tests commonly used include pore pressure dissipation and determining hydraulic conductivity as a function of solids content or void ratio. The window of applicability of the suite of soil science tests, just like the applicability of colloid science conventions, has always been pushed to its limits in oil sands tailings (Carrier 1984).

The transition from hindered settling to consolidation is sometimes defined by pore pressure dissipation in the deposit. In other words, particle to particle contact has been achieved. With enough water removal, particle to particle contact means that the mineral suspension is supported from the bottom up. This is process is monitored in large settling columns which measure the pore pressure in the mineral matrix. In a hindered settling regime, a pressure sensor in the fluid tailings will measure a pressure related to the density of the fluid. As the minerals in the suspension settle and contact each other, this pore pressure dissipates to the point where the pressure sensor is only measuring the hydrostatic pressure proportional to the depth at which the sensor is placed in the column. The rate at which this occurs is the rate of pore pressure dissipation.

Although conceptually simple, these column tests with pore pressure measurements are subject to a lot of uncertainty due to the bitumen in the fluid fine tailings and the clay content, both of which can foul sensors. In addition, the weakly flocculated nature of the mature fine tailings, even without additives can result in bridging. Bridging can occur in surprisingly large diameter settling tests, leading to unrealistically rapid pore pressure dissipation. Reported results should specify whether bitumen is considered to be part of the voids, or part of the solids, or neither. Most results do not specify this potentially important distinction. Careful interpretation of pore pressure results, coupled with duplicate measurements, and multiple analytical tools (compare solids content with depth to pore pressure for example) will help in removing the uncertainty associated with these column tests.

On top of various experimental challenges, some long term MFT settling experiments noted a phenomena known as syneresis where the sample collapses inward on itself and away from the settling vessel wall (Melton 1977 and Brinker 1990). When this occurs, a pressure sensor mounted near the settling column wall will show rapid pore pressure dissipation that is not necessarily due to particle to particle contact in the suspension. This phenomena can be very prevalent with polymer flocculant process aids as shown in Figure 4. In this example, the tailings sample had pulled away from the wall of the settling container so much that it could easily be removed as an intact cylinder. Clearly any pore pressure sensor at the wall of the vessel would indicate that the pore pressure had dissipated and grain to grain mineral contact was achieved. This mistaken interpretation of the point of pore pressure dissipation would not necessarily be the case in a large deposit.

Once pore pressure is dissipated, consolidation can occur via rearrangement of the mineral particles, coupled with further water release. This process is typically very slow. In order to collect data in a reasonable time on the consolidation properties, soil scientists and geotechnical engineers rely on the large strain consolidation test (Scott 1985 and Suthaker 1994 and 1996).

The large strain consolidation test is where a tailings sample is subjected to a stress which will cause the mineral particles in the suspension to rearrange, consolidating and releasing water. When the tailings material is first put under some strain, there will be an elapsed time before the consolidation is complete. It is sometimes a subjective decision as to when the particles have rearranged and consolidation is complete at that stress point. At the smaller void ratio (when consolidation at a particular stress has completed), the hydraulic conductivity can be measured and a larger load applied to repeat the cycle. This process is continued until data is collected over a void ratio or stress regime of interest. This experiment is time consuming and can be subject to some errors, especially with the electrostatically stabilized mineral suspensions that are MFT. In fact, the test is often started with tailings suspensions well beyond the range of the large strain consolidation test applicability (Ding 2010).

The long time involved in collecting data relating the void ratio (e) to hydraulic conductivity (k) data or void ratio to effective stress (p) data means that tests are seldom performed in duplicate. This data is typically plotted as e-log(k) or e-log(p) graphs with some important experimental data often not included. The rate at which the slurry samples are loaded and the time at which consolidation has equilibrated for a given load can affect the results. When large strain consolidation data is obtained, it is often useful to check for over-consolidation behavior and to report the rate at which equilibration is occurring at each loading point. This helps to compare data from laboratory to laboratory when sample volumes and initial starting conditions are variable. The expense and time associated with the large strain consolidation tests demands that chemical additives be appropriately screened and evaluated before pilot work or large strain consolidation tests are contemplated.

Testing of hindered settling and consolidation demands scale up at some point in order to avoid the multiple pitfalls of smaller scale tests. As test deposits move from laboratory scale pilots at 1 to 10 m^3 to large columns (35 to 50 m^3) and field deposits (100 to 100,000 m^3) there is a need to address the process scale up as well since large scale test columns or deposits will not be filled with material from laboratory scale processes. The transition from lab to pilot testing requires a rigorous additive screening protocol, with complete mass balance around solids, fines, and clays.

SUMMARY

Chemical amendment performance criteria of importance will be dependent upon the mine planning or tailings management objectives. For instance, the performance criteria for an additive will be different for a commercial filtration process compared to a thin lift atmospheric drying process. These chemical performance criteria expected in terms of dewatering would be even more different for an end pit lake deposit compared to an out of pit deposit. Even for similar tailings management objectives, unreported variations in sample composition and lab testing procedures can make comparisons very difficult.

Scale up is critical in the ultimate selection of an additive, and that means scale up in both the size of the deposit being tested and the process by which the deposit would be created. Often, but not always, scale up of the process is required in order to create the scaled up test deposit.

Geotechnical or soil science testing protocols are becoming more important as tailings technologies are producing dewatered deposits closer to what will be ultimately reclaimed. Test details in terms of sample loading rates, evaluation of over-consolidation effects, and hydraulic conductivity test procedures, should all be part of the reporting process, not simply graphs of e-log(k) and e-log(p). A better appreciation of the uncertainty in these test protocols is also required.

The economics of oil sands tailings management has changed considerably in the past decade or more, increasing research interest from industry, academia, and vendors. Although one could argue that the fundamental chemistry and physics that control the behaviour of tailings mineral slurries is well established, there are a multitude of sometimes competing fundamental factors that have to be taken into account. That complexity will always demand an empirical approach to process and chemical performance evaluation, and some compromises and modifications to sample characterization procedures. Moving forward, comparison of chemical and process performance across laboratories will be improved with more information about sample characterization, and test protocols.

REFERENCES

AER (Alberta Energy Regulator), 2016, Fluid Tailings Management for Oil Sands Mining Projects, Directive 85, July, 2016.

Brinker, C.J., and Scherer, G.W., 1990, *Sol-Gel Science—The Physics and Chemistry of Sol-Gel Processing*; Academic Press, Inc.: San Diego, CA, USA.

Carrier, W.D. and Beckman, J.F. 1984, Correlations between index tests and the properties of remoulded clays, Geotechnique, 34, no. 2, 211–228.

COSIA (Canada's Oil Sands Innovation Alliance). 2014. Oil Sands Tailings Measurement Protocol. Report to COSIA by Thurber Engineering Ltd. and Barr Engineering.

Demoz, A. and Mikula, R.J., 2012, Role of Mixing Energy in the Flocculation of Mature Fine Tailings, *J Environmental Eng* ISSN 0733-9372, January 2012

Ding, Y., Wang, B.W., and McLeod, H., 2010, Characterizing Tailings to Better Predict Consolidation Behaviour During Deposition, Canadian Dam Association Annual Conference, Niagara Falls, Oct 2-7.

ERCB (Energy Resources Conservation Board). 2009. Directive 074: Tailings performance criteria and requirements for oil sands mining schemes.

FTFC (Fine Tailings Fundamentals Consortium), 1995, Advances in oil sands tailings research, Vol 2 -12 and Vol 3-52.

Gan, J., Ebrahimi-Birang, N. and Haug, M. 2011, Consolidation and Hydraulic Conductivity Testing of Slurries, in Proceedings Tailings and Mine Waste.

Hardy WB., 1900, A Preliminary Investigation of the Conditions which determine the Stability of irreversible Hydrosols, Proc. Roy. Soc. Lon. 1900;66:110–125.

Karr, P.R., and Keinath, T.M., 1978. Limitations of the specific resistance and CST tests for sludge dewatering. Filtr. Sep., 21:2, pp 100-102.

Lambe, T.W., 1958, The Structure of Compacted Clay, Journal of the Soil Mechanics and Foundations Division, Paper 1654, May.

MacKinnon, M. "The CT Process at Syncrude - Some Short and Long Term Effects on Water Quality", Oil Sands Process Water Workshop, Fort McMurray, July 7 and 8, 1999.

Melton, I.E., and Rand, B., 1977, Particle Interactions in Aqueous Kaolinite Suspensions, Journal of Colloid and Interface Science, Vol. 60, No. 2, June 15.

Mikula, R. J. and Zrobok, R. 1999. Oil Sands Tailings Reclamation Via Manipulation of Clay Behaviour: The role of Rheology. Rheology in the Minerals Industry Conference, Hawaii, March 1999.

Mikula, R.J., 2015, Surface Mined Oil Sands Tailings: Fundamentals and Applications, COSIA short course, Banff, March 2015.

Omotoso, O. E. and Mikula, R.J. 1999, Alternative consolidated tailings chemicals, CWRC 99-23 (CF), CANMET, Natural Resources Canada.

Scholz, M., 2006. "Revised capillary suction time (CST) test to reduce consumable costs and improve dewaterability interpretation." *J. Chem. Technol. Biotechnol,* 81, 336-344.

Schulze H. J., 1882, Arsenic Sulphide in Aqueous Solution, Prakt. Chem. 1882;25:431–452.

Scott, J.D., Dusseault, M.B. and Carrier, W.D., 1985. Large-Scale Self-Weight Consolidation Testing. In R.N. Yong and F.C. Townsend, ed. Consolidation of Soils: Testing and Evaluation, ASTM Special Technical Publication 982. , Ft. Lauderdale, Fla., 24 Jan. 1985, pp. 500-515.

Smollen, M., 1986. Dewaterability of Municipal Sludges 1: A comparative study of specific resistance to filtration and capillary suction time as dewaterability parameters, Water SA 12:3, pp 127-133.

Suthaker, N.N and Scott, J.D., 1994. Large Strain Consolidation of Oilsands Fine Tails in a Wet Landscape, Proceedings of the 47th Canadian Geotechnical Conference of the Canadian Geotechnical Society, Halifax.

Suthaker, N.N. and Scott, J.D., 1996. Measurement of Hydraulic Conductivity in Oil Sand Tailings Slurries, Canadian Geotechnical Journal, 33: 642-653.

Van Olphen, H., 1963, Introduction to Clay Colloid Chemistry, Interscience, New York.

Xu, Y. and Mikula, R.J., 1993, The Filterability and Surface Tension of Mature Fine Tailings: The Effect of pH and Calcium Ions, CANMET DEVON Division Report 93-37

Xu, Y. and Mikula, R.J., 1999, Flocculation of Shell Noncaustic Oil Sand Tailings: Selection of Flocculants. CANMET DEVON Division Report 99-05.

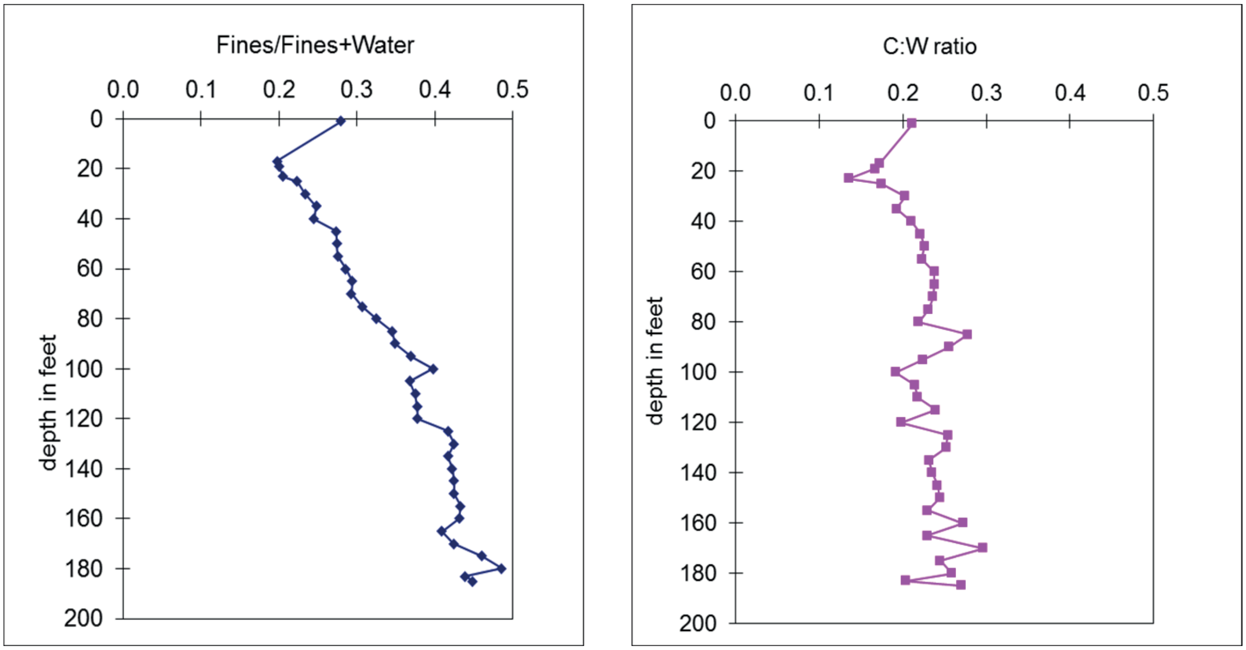

Figure 1. Fines and clay profiles with depth in a tailings pond (Mikula 2015)

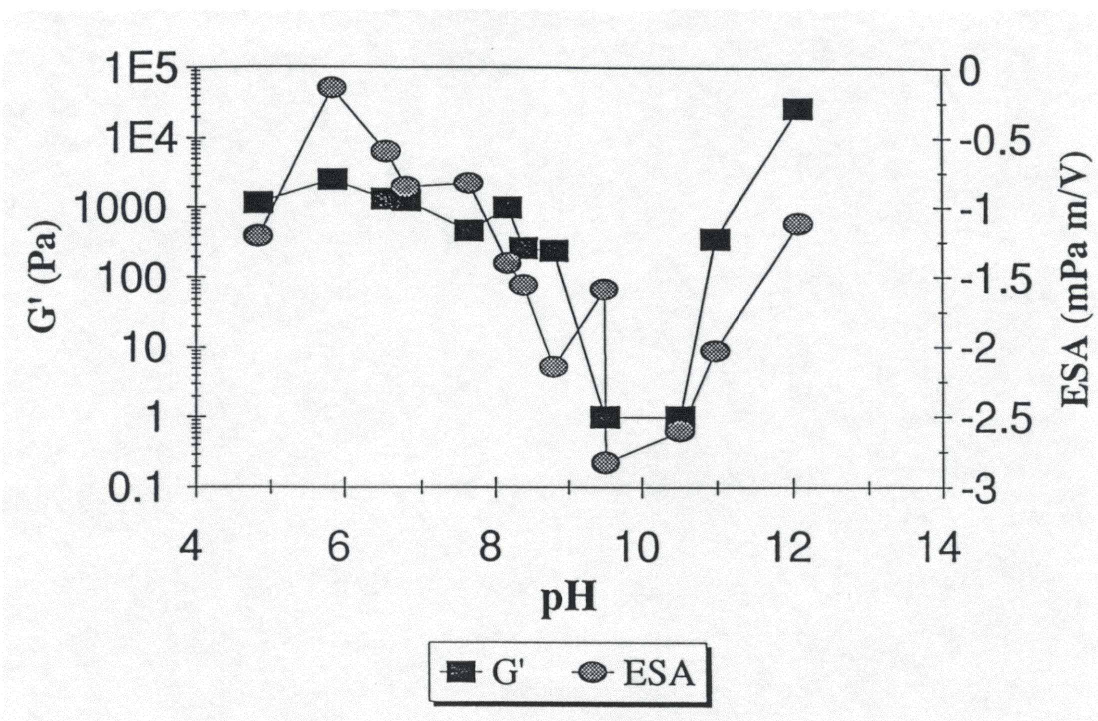

Figure 2. The pH dependence of zeta potential and yield point for a mature fine tailings slurry (FTFC 1995)

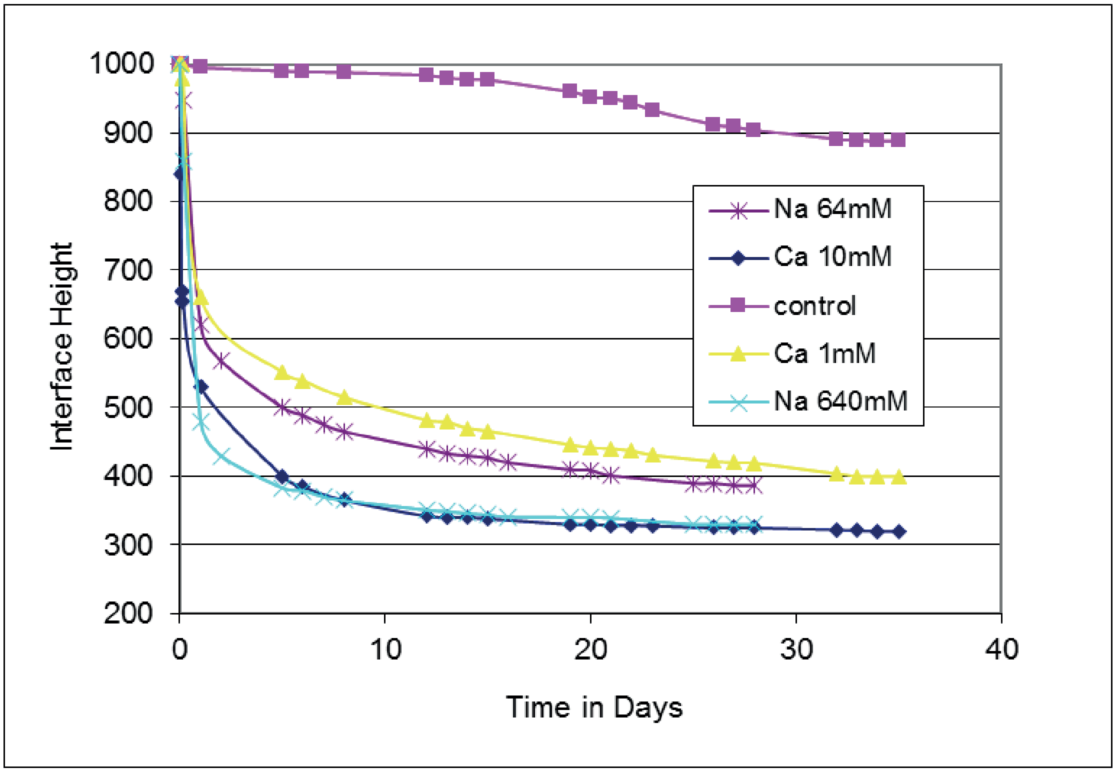

Figure 3. Settling rates of some fine tailings slurries illustrating the Schulze-Hardy relationship

Figure 4. Photograph of two tailings samples which have undergone syneresis and pulled away from the walls of the settling vessel. The water from the vessel wall is clearly seen in the upper photo.

A COMPREHENSIVE CONTROL SCHEME FOR DYNAMIC INLINE FLOCCULATION OF OIL SANDS TAILINGS

Scott E. Webster[1], Wayne A. Brown[1], Babak Derakhshandeh[1], Neville Dubash[1], Clara Gomez[1], Christian N. Veenstra[1] and Abu Junaid[2]
[1]Coanda Research and Development Corporation, Burnaby, Canada
[2]Shell Canada Limited, Calgary, Canada

ABSTRACT

Inline flocculation is a promising technique for the dewatering and remediation of oil sands tailings. In recent years the industry has undertaken a number of exploratory programs aimed at defining the process operating windows that will produce flocculated materials with the desired properties. The major challenges related to the process include determining flocculant dosing sensitivities, mixer operating windows, influence of pipeline shear, and development of effective instrumentation technique and process control relationships. To be applicable in a field setting, the inline flocculation process must be controllable such that process disturbances can be addressed, ensuring consistent production of acceptable material. This paper presents lab-scale evaluation of a comprehensive control scheme developed by Shell for dynamic inline flocculation. A feed forward scheme is implemented to control the mixing intensity and flocculant dosage based on the properties of the fluid fine tailings and polymer. Inline image analysis and particle size measurements performed on the flocculated product are used to add a feedback trim to the scheme, accounting for the errors in the model or unmeasured disturbances. Results from the laboratory-scale tests are presented to demonstrate the efficacy of this control strategy.

INTRODUCTION

The oil sands extraction process produces significant quantities of fluid fine tailings (FFT). Producers are required to determine effective strategies to manage the volume of these tailings throughout the life of their mines. Fine clay particles can remain in suspension over long time periods and therefore intervention is required to extract water from the tailings and allow accelerated consolidation of the solids.

Inline flocculation (ILF) is one potential tailings treatment strategy currently being evaluated by Shell. In ILF a polymer flocculant is added to the tailings stream to help bind clay particles together into larger flocs, which settle more rapidly. Dynamic inline flocculation refers to the use of a moving mixing element to blend the polymer with the tailings, ensuring effective contact between the clays and the flocculant. Two challenges involved in the implementation of an ILF scheme are maintaining an optimal flocculant dosage and an optimal level of mixing, regardless of process disturbances, such as changes in input properties or flow rates.

The required amount of additive depends on the solids content of the tailings stream as well as the clay content of the solids. Both insufficient and excessive polymer dosages result in inferior treatment performance. Also, excessive dosing results in unnecessary costs as flocculants are expensive chemicals. Similarly, the amount of mixing must be maintained at an optimal level to ensure that the additive is blended effectively, while avoiding excessive shear which can be undesirable for the deposition strategy. The required mixing intensity varies with flow rate as well as the solids and clay content of tailings.

Unfortunately these challenges can be difficult to overcome using standard instrumentation and control techniques. Determination of the tailings clay content can be particularly challenging, and while the use of a dynamic mixer allows easy variation of the amount of mixing, finding the optimum level is non-trivial. Other elements of the ILF process also require attention, such as selection of the mixer design, and the polymer and tailings delivery systems. This paper presents a comprehensive control system developed by Shell to optimize the commercial implementation of the ILF process.

FLOCCULATION APPARATUS

In this study a laboratory apparatus operating around the 10 m^3/h scale was used. However the control strategies that have been developed should also be applicable at much larger scales. In the current laboratory setup, FFT was fed into a 5" pipeline equipped with an inline mixer. Polymer was injected just upstream of two hydrofoil impellers as shown in Figure 1. Samples were collected at the discharge from the pipeline several meters downstream of the mixer. Various sensors were placed upstream and downstream of the mixer, as described in the following section.

Figure 1. Photograph of an inline mixer with a polymer injector directly upstream of dual hydrofoil impellers

CONTROL SYSTEM

Two standard control architectures are feedforward and feedback control. In feedforward control, input disturbances are measured and a model is used to determine the required control action to compensate (see Figure 2 (a)). Feedback control does not require a model, and instead measures an output parameter and adjusts the controlled variable based on the deviation from the desired setpoint (Figure 2 (b)). An advantage of feedforward systems is that they can compensate for upstream disturbances before they have a chance to impact performance. However they require an accurate process model to respond appropriately and therefore it is inevitable that there will be some discrepancy between the desired and actual results due to deficiencies in the model. Feedback systems can achieve a target setpoint regardless of unexpected behaviors, provided an appropriately accurate measurement of the performance metric can be made.

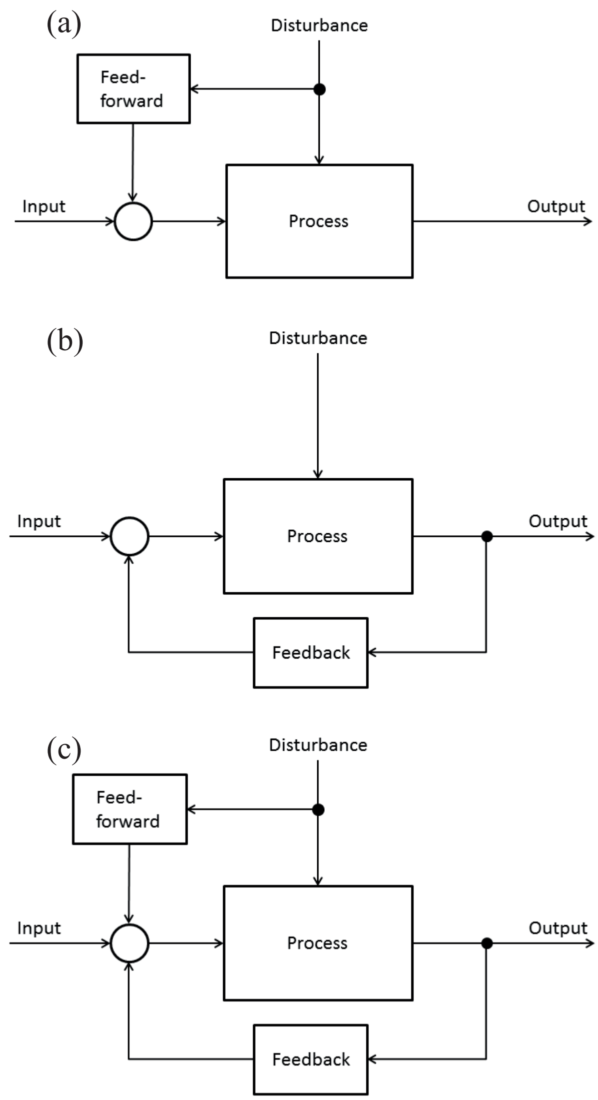

Figure 2. Block diagrams for (a) feedforward, (b) feedback, and (c) feedforward with feedback trim control systems

Feedforward and feedback control can also be combined, where the feedback signal is used to "trim" the control action after the feedforward adjustments are made (Figure 2 (c)). This combined scheme has been selected for the Shell

ILF process to control the impeller speed of the dynamic mixer. A feedforward-only system is used to control the polymer dosage on a tailings stream standardized to a desired density.

POLYMER DELIVERY

Flocculant dosages are typically quoted in terms of grams of polymer per tonne of solids in the tailings, where the optimal solids based dosage depends on the clay content of those solids. The required polymer flow rate therefore depends on the flow rate of the tailings stream as well as its properties and the properties of the polymer solution (1):

$$Q_{poly} = f(Q_{FFT}, \rho_{FFT}, \beta, \phi_{poly}) \qquad (1)$$

where Q_{poly} and Q_{FFT} are the flow rates of polymer and FFT respectively, ρ_{FFT} is the FFT density, ϕ_{poly} is the solid polymer fraction, and β is the polymer dosage. With a known FFT flow rate, the FFT density, polymer concentration and desired dosage need to be determined to control for the appropriate amount of polymer delivery.

FFT Density

The density of the tailings was measured using an Endress and Hauser Gammapilot nuclear densitometer with a Cs-137 source. The source container was placed on one side of the FFT feed pipe and the detector on the other, allowing the absorption of the gamma rays to be used to measure the density of the material in the pipe. A first principles estimation of the calibration coefficient, combined with a pure-water calibration under-reported the density by 1-2.5%. An in-situ calibration with FFT across the range of expected densities was performed to further improve the accuracy.

Polymer Concentration

As the polymer concentration can vary with some preparation techniques, we infer the value through a measure of the solution viscosity. An Anton Paar L-Vis 510 inline viscometer was calibrated for this purpose. Figure 3 shows a photograph of the viscometer. Internally the viscometer consists of a partially open tube containing a rotating cylindrical shaft, which is inserted into the polymer pipeline. The inner bob rotates and draws fluid into the gap. The outer cylinder is split and a sensor measures a deflection caused by the fluid flowing in the gap that depends on the viscosity. Polymer solutions with varying concentration and temperature were measured and a calibration was developed to yield the concentration as a function of measured viscosity and temperature.

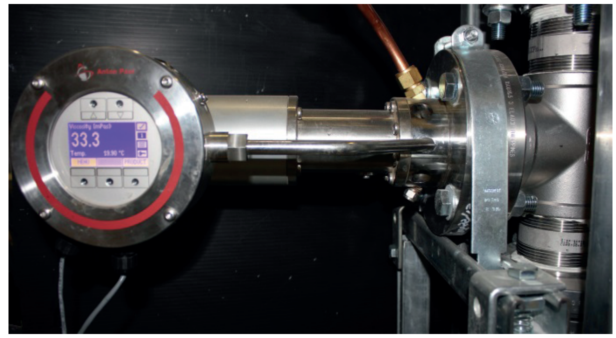

Figure 3. Anton Paar L-Vis 510 inline viscometer

Desired Optimal Polymer Dosage

The desired polymer dosage is directly correlated to the feed FFT. A Bruker Matrix-F near-infrared (NIR) spectrometer was used to measure the clay content of the FFT. NIR reflection spectra were obtained for a series of calibration samples with varying clay content, prepared by blending several master sources in varying ratios. Example spectra are shown in Figure 4. A chemometric analysis using the partial least squares approach was performed to develop a calibration relating the spectra to the clay content of the tailings, as represented by the methylene blue index (MBI). The NIR region between 4200 and 7500 cm^{-1} (1.3 to 2.4 μm) was used for the calibration. This analysis allowed an effective calibration to be found despite the fact that the clay peaks are relatively weak and obscured by strong water interactions. Figure 5 shows example validation results for the calibration performed with two data-preprocessing techniques. The validation procedure steps through each sample spectra and removes it from the calibration set before calculating the estimated value based on the data from the rest of the samples. Good agreement is achieved, demonstrating that the NIR system is capable of measuring the MBI of the samples.

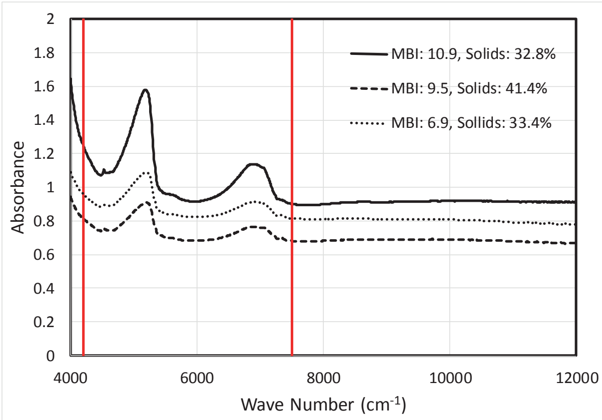

Figure 4. Example NIR reflectance spectra for three FFT samples. The region between the red lines was used for the calibration analysis.

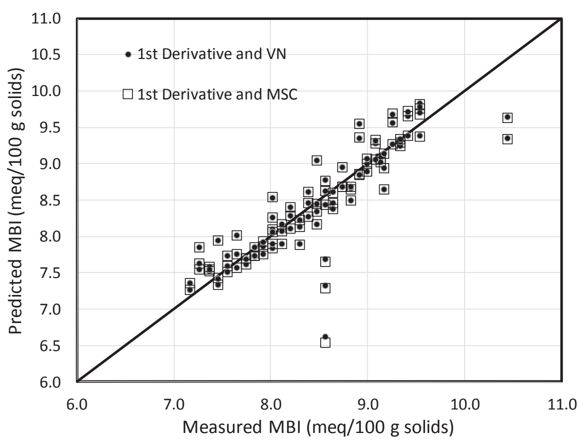

Figure 5. Example validation results for the NIR calibration for data pre-processing methods two methods: 1st deverivative with vector normalization (VN) and 1st derivative with multiplicative scatter correction (MSC)

A pipe spool was fabricated with a sapphire window to allow optical access to the FFT flowing in the feed pipeline. A Bruker emission head was used to illuminate the window and collect the reflectance spectra as shown in Figure 6. The Bruker software was set to automatically perform an analysis once every 20 seconds and the resulting MBI value was transmitted to the control system using an analog output card.

Figure 6. Custom pipe spool with NIR sensor head attached

To determine the optimal dosage a series of approximately 150 laboratory flocculation experiments were conducted using several FFT feeds with different MBI and density. The dosage and mixer speed were varied and an optimal value for dosage was selected for each feed material based on an analysis of dewatering and rheology metrics. An optimal mixing intensity was also selected, as described in the following section. Once the optimal values were determined, the optimal dosage was fitted as a function of density and MBI:

$$\beta = f(\rho, \mathrm{MBI}) \qquad (2)$$

With this we now have all of the data required to calculate Q_{poly} using equation (1) and can program the control system to implement feedforward control.

MIXER SPEED

The feedforward aspect of the mixer speed control was developed similarly to the system described above for polymer delivery. The desired mixer speed was calculated using the following functional relationship (3):

$$N = f(K, Q_{FFT}, Q_{poly}, D) \qquad (3)$$

where N is the impeller speed, D is the impeller diameter and K is proportional to the amount of mixing required and is a function of density and

MBI. This dependence was established by prior work (Gomez 2016). In the current work we added an additional functional dependence (4) for K:

$$K = f(\rho, \mathrm{MBI}) \qquad (4)$$

Again the data on the optimal levels of mixing for each feed were fitted to establish this relationship.

Feedback Trim

Equation (4) enables feedforward control of the mixer speed, however the optimal mixer speed is difficult to predict accurately. Therefore a feedback trim element is desirable to bring the level of mixing to an optimal level based on the measured flocculation results. Two instruments were investigated to provide online measurements of the properties of the flocculated tailings stream: the Particle Vision and Measurement (PVM) system and the Focused Beam Reflectance Measurement (FBRM) system, both from Mettler-Toledo.

The PVM is essentially an in situ microscope, capturing close-up images of the tailings flowing in the pipe. A sapphire window located at the end of a shaft that protrudes into the pipe allows the recording of images of the process material. Illumination is provided by six pulsed lasers behind the window. We operated the camera at a framerate of 5 Hz, the maximum rate which provided consistent timing. The 1360×1024 pixel greyscale images correspond to a ~ 1075×825 μm area, for a nominal resolution of ~ 0.8 μm/pixel. Figure 7 shows a photograph of the PVM head. Figure 8 shows sample images of untreated and flocculated FFT, with much more structure apparent in the flocculated example.

The FBRM system also uses a cylindrical probe that is inserted into the process pipeline. A miniature air motor sweeps a focused laser spot around a circular pattern through the sapphire window and measures reflectivity as a function of time. By analyzing changes in this reflectivity signal the FBRM deduces a "chord-length distribution" for particles in the process fluid, returning one distribution every 2 seconds. The chord length distributions are very similar to particle size distributions, in that they give a particle count as a function of "length" but the chord length corresponds to the distance traversed across the particle by the laser, which is not

Figure 7. PVM V819 instrument head

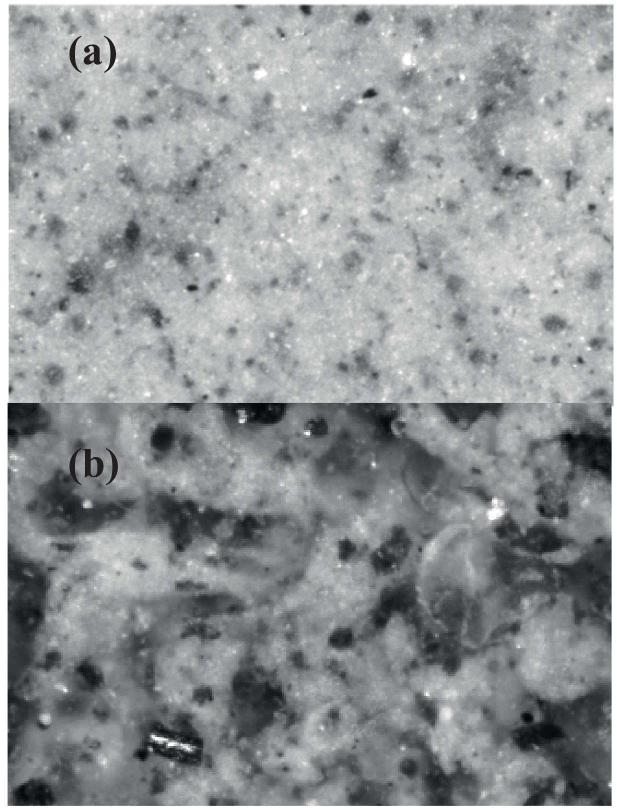

Figure 8. Example PVM images of (a) untreated and (b) flocculated FFT.

necessarily the true size of the particle. Figure 9 shows an example chord length distribution from flocculated FFT.

To control the mixer, the ideal feedback measurement would give a signal that is monotonic with mixer speed, and has a well-defined optimal value to use for the controller setpoint. There are many ways to process the data from the PVM and FBRM instruments. Unfortunately it appears that most simple metrics can suffer from a lack of a universal optimal setpoint across multiple types of feed and can also exhibit non-monotonic behaviour. For example, one image metric is the coefficient of variation (CoV): the standard deviation of the image

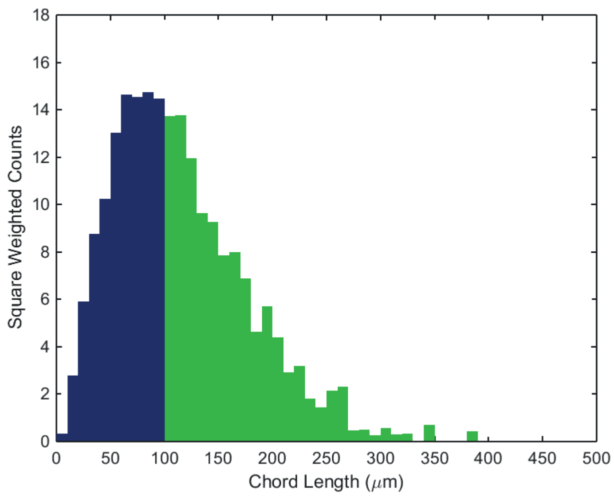

Figure 9. Example FBRM chord length distribution. The number of counts above a threshold of 100 μm (green area) has been identified as being correlated with the flocculation quality of the material.

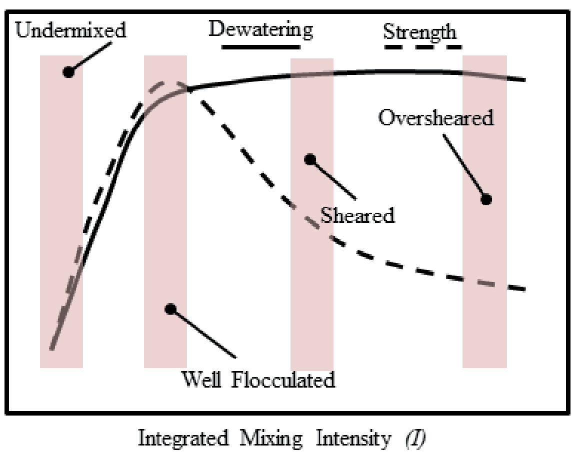

Figure 10. The relationship between the integrated mixing intensity and the mixing state. Dewatering (solid line) increases with mixing intensity before levelling off at high levels of mixing. Material strength (dashed line) increases to a maximum and then declines for excessive mixing. Four generic mixing states have been identified: undermixed, well flocculated, sheared, and oversheared.

brightness divided by the mean brightness. The CoV can be observed to increase during the flocculation process. However, for certain tailings feeds a value of around 0.2 might be optimal, while for another feed type a value of 0.3 would be superior. Additionally, the CoV has been observed to saturate at high levels of mixing.

Similarly for the FBRM, one possibility is to monitor the number of counts for chord lengths above some threshold size, possibly corresponding to the presence of flocs. However, the desirable absolute value of these counts similarly seems to depend on the feed material. This FBRM metric exhibits a peak at a certain degree of mixing and for increased mixing intensity the number of counts can decrease. While this can make sense intuitively as flocs may break down and become smaller at high mixer speeds, the position of this peak does not appear to be universal and implementing a peak finding algorithm in the control system would be more complicated than a traditional simple feedback controller.

We have chosen to explore the concept of evaluating the “mixing state” of the material in order to address these difficulties. Figure 10 shows a schematic diagram illustrating the relationship between the integrated mixing intensity or “amount of mixing” and the dewatering and strength properties of the flocculated material. Four mixing states have been identified. At low levels of mixing the flocculant is not distributed properly resulting in poor dewatering and strength for the treated material (state 1, undermixed). Increased mixing improves both dewatering and strength with the region of the peak in material strength denoted as state 2, well-flocculated. With further mixing the dewatering remains high and possibly increases slightly, while strength declines (state 3: sheared). With excessive mixing the strength continues to decrease while dewatering remains similar or declines slightly (state 4, oversheared).

While the actual dewatering and strength properties that are achieved can vary significantly for different tailings materials, the trends in mixing state are consistent for varied levels of mixing intensity. If we can use the feedback instruments to estimate a mixing state for the material then we can select a desired setpoint value for our controller. The mixing state should be monotonic with mixer speed. The optimal setpoint can be selected based on operator requirements, perhaps at a value of 2 for well flocculated, or 3 if more shear is desirable. Fractional values such as 2.5 are also possible.

The algorithms used to estimate the mixing state based on the instrument outputs are the subject of previous work (Veenstra et al. 2016). An “eigenface” analysis technique (Turk and Pentland 1991) was used to process the PVM images and a maximum likelihood classifier was used to match the results with one of the mixing states. Additional information from the FBRM and even the instruments can also be incorporated into the classification routine to improve results.

The estimate of the mixing state from the feedback system can now be used to trim the feedforward output. A simple feedback controller uses the estimated mixing state for the measured variable and compares that to the mixing state setpoint. The resulting control action is summed with the feedforward signal and sent to the mixer speed controller. The result is a system that uses the instrument feedback to reach the desired setpoint, but responds quickly the feed disturbances in flow rate, clay content, or density without having to wait for the material to go off-specification. Additionally, keeping the speed close to optimal with the feedforward system should make it easier for the feedback system to perform correctly by avoiding wildly varying conditions.

LABORATORY TEST RESULTS

We present results from preliminary laboratory testing. The feedforward system was implemented along with feed standardization. The feedback system was not used to actively adjust the mixing speed, but data was recorded and post-processed to provide information about how the system would have responded.

Two experiments are described here. For the first test, the system was started with one batch of FFT and the control system was enabled. After the system was stable, data was recorded for approximately 100 s and then the FFT feed source was manually changed to a different tank containing a second batch of FFT with higher density and clay content. Figure 11 shows data recorded during the experiment. The top pane shows the standardized FFT flow rate, which was held constant during the experiment. The measured MBI value jumped up shortly after the feed tank was switched. This resulted in immediate increases in the mixer speed, *N*, and polymer flow rate, though the later had a slower control loop response. The density of the FFT feed also increased at the tank switchover, resulting in an increase in the feed standardization dilution water, which eventually brought the density back down to the target of 1190 kg/m^3. The feed standardization implementation used here had a slow response time. The polymer flow rate and impeller speed declined slightly from their peak as the density dropped to its final value.

Samples were collected during the steady state periods just before the tank change and at the end of the test. The capillary suction time (CST) dewatering metric rose slightly from 8 s to 36 s and the peak yield fell from 99 Pa to 39 Pa. Results from a permeability index test remained constant. The results for the second set of samples from the high MBI material were not as good as those for the initial samples, however the feedforward system had not been tuned for the materials used in the experiment, and additionally it was not necessarily expected to achieve the same absolute results for the different feed types. The goal was to achieve the best possible results for the given feed and to at least maintain acceptable performance.

The bottom pane of Figure 11 shows the estimated mixing state from the feedback system. The results changed in character after the switch in feed tank, delayed by the time it took for the material to make it through the mixer to the discharge instruments. The estimated mixing state value became more variable and dropped slightly. The variability can be handled by a smoothing algorithm. In this case it appears that if the target mixing state were the initial value of “3” then feedback trim would have slightly increased in mixer speed after the feed change.

The results of a second control test are shown in Figure 12. Again the experiment was started with one type of FFT and allowed to reach a steady state. This time, before switching to a different FFT tank, the feedforward control system was disabled at the 125 s point and the feed tank was switched (the feed standardization system was manually adjusted to maintain a constant density). This time there was no immediate response in polymer flow rate or mixer speed when the MBI increased. The sample CST worsened from 8 s to 20 s and the peak yield dropped from 96 Pa to 38 Pa. The permeability index test result dropped dramatically. Feedforward control was re-enabled at the 300 s point, causing an immediate increase in polymer

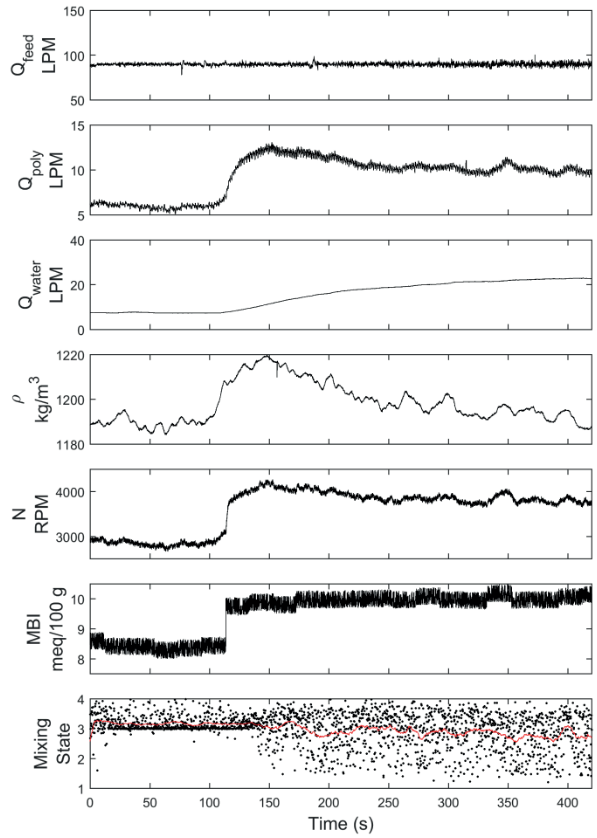

Figure 11. Results from the first feedforward control test. The FFT feed tank was switched at around the 100 s point. From top to bottom the charts show Q_{feed} (standardized), Q_{poly}, ρ_{FFT}, N (mixer speed), MBI, and the estimated mixing state from the feedback system (not used for control). The red line in the bottom mixing state plot is a moving average.

flow rate and mixer speed. The final sample had a slightly lower CST of 14 s, a much higher peak yield of 125 Pa, but the permeability value did not recover to the previous value, likely due to the higher MBI of the material.

The estimated mixing state results started at slightly above 3, perhaps indicating that the material was being mixed somewhat excessively. After the tank was switched with control disabled the mixing state dropped significantly, as expected because the higher MBI material should require more mixing. When control was re-enabled the estimated mixing state returned close to the previous value, indicating that the feedforward system had acted appropriately. In this case it appears that the feedback system would not have been required to trim to final mixer speed.

CONCLUSION

This paper presents a scheme that provides feasible solutions to many of the control issues that can affect commercial success of the inline flocculation process, including adjusting polymer dosage and mixing intensity based on FFT feed properties, compensating for polymer concentration fluctuations, and providing an online estimate of flocculation quality.

Future trials are planned at the pilot scale to further evaluate and adjust the scheme, including implementation of the real-time feedback trim component.

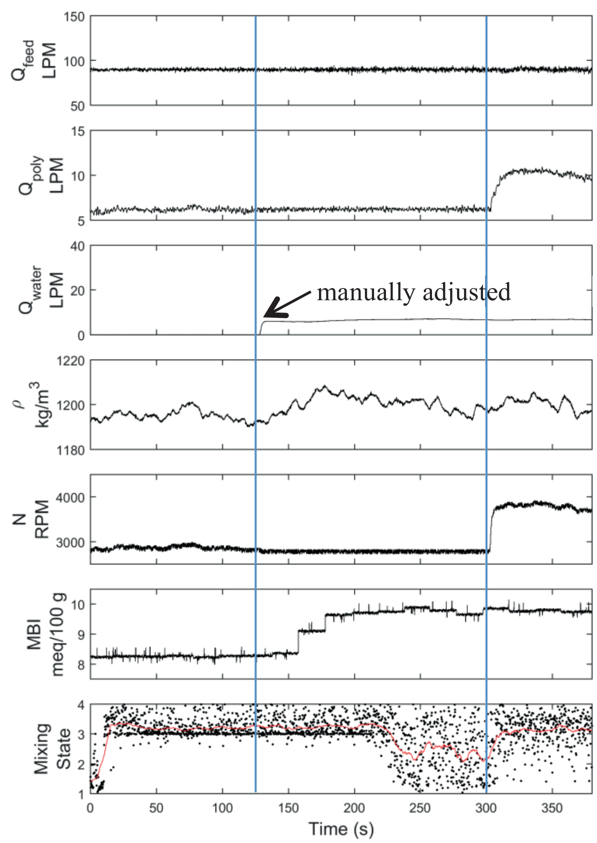

Figure 12. Results from the second feedforward experiment with the same charts as shown in Figure 11. Control was disabled at the 125 s and the FFT feed tank was switched. After a second steady state was reached, control was re-enabled at the 300 s point.

REFERENCES

C. Gomez, *Mixing XXV*, Quebec City, QC, 2016.

M. Turk & A. Pentland, “Eigenfaces for Recognition,” *Journal of Cognitive Neuroscience*, vol. 3, no. 1, pp. 71-86, 1991.

C.N. Veenstra et al, “Image recognition for flocculation quality estimation,” *Tailings and Mine Waste ‘16*, Keystone, CO, 2016.

THICKENING AND REFLOCCULATION PILOT PLANT

David Rennard[1], Atoosa Zahabi[2], Jason McMullan[1], Givemore Sakuhuni[2], Yijun Liu[1], Scott Hickman[1], Payman Esmaeili[2], Paul Cavanagh[2], Phil Lenart[1], Justin Loman[2], Ernesto Dela Rosa[2], Trevor Huculak[2], Rosario Jara[1], Kyle Baier[1], Jorge Medrano[1], Ashar Mirza[3], Aref Najafi[3] and John Clark[4]

[1]ExxonMobil

[2]Imperial Oil Resources

[3]CNRL

[4]Paterson & Cooke

ABSTRACT

Imperial Oil, CNRL, and Teck Resources recently completed an on-site pilot project of a tailings treatment technology that was subsequently deployed at Kearl. The technology involves thickening a whole flotation tailings stream (SFR ~ 2), shearing the underflow while transporting it, and reconstituting the flocs by the addition of a second polymer prior to deposition. The pilot evaluated the technology's operability, robustness, and sensitivity to variations in feed. Tests were conducted in thickener operation, second stage mixing of the thickener underflow (>45% solids + flocculant), deposition and winter deposition, and system-wide interactions, such as the impact of first stage flocculation on second stage mixing and final dewatering. Key performance indicators were developed to predict product quality from rapid screening tests, supporting real-time controls. The results indicate that thickener operation is best tuned by rapid sample analysis of the thickener feed after flocculation by settlement in a graduated cylinder, a parameter that responds quickly to changes in feed and can be leveraged for the live tuning of flocculation dosage. Dilution can be a control parameter to ease the stress of controlling bed height. On the mixing side, the competition between mixing and shear can be tuned with fines content and depends strongly on both mixing energy and time. Furthermore, visual observation of dynamic deposition can inform process controls.

INTRODUCTION

Regulation requires Kearl to process tailings in order to maintain no more than a few year's inventory of untreated FFT. In addition, Kearl stores process water and fluid tailings in the same holding cell, the West External Tailings Area (W-ETA). While dykes are planned to grow over time, the volumes that can be stored in the W-ETA are essentially limited, and an increase in fluid tailings consumes precious volume required for process water availability to operate Kearl. Poor settling rates, fines treatment, or fines capture by tailings treatment and deposition in the E-ETA can result in an excess of fines in the W-ETA. These excess fines can occupy too much volume, resulting in a lack of available process water, which can shutdown Kearl operations.

For these reasons, Kearl has invested in a tailings treatment package comprising thickeners, transport toward a disposal area, and second stage flocculation en route to reconstitute flocs.

Kearl's tailings treatment process requires the successful operation of a flowsheet that involves several new elements relative to other commercially practiced processes. These innovations include:

- Kearl is installing the first thickener package in the oil sands that will not use cyclones to condition the feed. This results in a higher sands content in the thickener feed, as well as potentially greater variability in the feed characteristics, especially PSD. To date, most industry experience in thickening applies to a feed with a sand to fines ratio (SFR) between 0.5 and 1.3, whereas Kearl's flotation tailings have a typical SFR in the range of 0.8-3.5.
- Kearl's process will be the first application of a second stage flocculation of thickened tailings. The industry has generated some know-how in flocculating Fluid Fine Tailings (FFT) with a solids content of 30 wt% in water. Kearl's process will re-flocculate thickened tailings (to reconstitute flocs that have been sheared due to transport) at a solids content of 45-52 wt%. This involves contacting a non-Newtonian slurry with a viscous polymer solution in a static injector environment with sufficient energy to achieve distribution and contact but not so much energy that the resultant flocs are destroyed by shear forces within the mixer or subsequent transport system.

- Kearl's second stage mixer will be located far upstream of the transport system. Most tailings treatment processes with a flocculation step perform the flocculation within 100 m of deposition. Kearl will inject the second stage flocculant 1.5 km away from deposition.

Lab tests were conducted on individual units within this system, such as flocculation studies in settling columns, dynamic thickening studies, and batch tests on mixing parameters for the second stage flocculation. However, lab scale is insufficient to explore the operability and interdependency between units within the full flowsheet. To develop controls, identify Key Performance Indicators (KPIs), and ascertain the potential response points to varying feed as it propagated through the system required a pilot of the full flowsheet.

The purpose of this pilot was to look at three main areas of an integrated tailings process operation, motivated by the upcoming commercial startup of the Kearl Fine Tailings Treatment (KFTT) process (second half of 2016).

1. First, this pilot examined the interdependences of the different process equipment steps of KFTT, including the thickener plant, the transport pipeline, the secondary chemical injection, and the deposition of material. This includes changes in the feed stream (i.e. SFR, SC, Fines addition, etc.) and how such changes impact each additional unit through the process. Key questions included: are changes flagged upstream and is response possible downstream? Do changes get buffered by units within the system? Are product KPIs capable of being measured sufficiently quickly to provide meaningful operational guidance in real time? Measurements of KPI's for each variable are critical to knowing if the process remains stable and on-spec for each change in feed condition.

2. Second, the pilot provided an opportunity to investigate mixing of the dense thickened tailings slurry with flocculant. A variety of mixing setups were explored, including low flow static and dynamic mixers. A scaled-down version of the commercial Venturri mixer was also successfully tested.

3. Finally, the pilot interrogated the performance of the final product, including the deposition of different feed material compositions. This was done through observing the dynamic flow properties of the treated material, as well was the geotechnical information measured in flumes and boxes. The ability to place a relatively large volume of freshly produced tailings product enabled the pilot to examine a variety of deposition conditions, including flumes, winter deposition - accomplished via placement of a freeze box deposition of the material outside in the Fort McMurray winter, and subaqueous discharge of tailings.

SETUP

Figure 12 depicts the most used pilot flowsheet. A dual feed system enabled feed variation tests by adjusting the feed ratio derived from two separate feed storage tanks. MFT was introduced to the system inline. The resulting slurry mixed with dilution water from the thickener overflow to form a 10 wt% solids mixture. Flocculant, a commercially available anionic polyacrylamide (PAM), was introduced to the slurry, which then passed through several inline static mixers before being introduced to the a 50 cm diameter thickener at a flux rate matching the Kearl design.

Flocs settled in the thickener vessel to form a bed, which was raked to facilitate water release. Overflow from the thickener drained to a storage tote where it was pumped into other parts of the system. The overflow was monitored periodically to ensure low (<0.5 wt%) solids content, but a result of the operational effort which is detailed below quickly identified that this was not the key parameter for monitoring fines capture in the first stage flocculation. The thickener underflow recycled through a shear loop over a set of static mixers and was replaced to the cone of the thickener. Dilution water from the overflow was introduced upstream of the static mixers to control underflow density. This sheared underflow, controlled to around 45 wt% solids, was pumped out of the shear loop at a rate of 3 L/min.

The underflow was subjected to a second stage flocculant, another anionic PAM, introduced via T-injector. The flocculated slurry was mixed using either several static mixers, a dynamic continuously stirred mixer, or a combination of the two. The fully treated slurry was typically deposited into subaerial flumes for flow observation or consolidation quantification. Some slurry was used to charge boxes for winter deposition simulation, and some slurry was deposited subaqueously.

The system employed 1-1.5" hoses with quick-connect seals which enabled rapid reconfiguration, extremely well suited to a mini-pilot of this nature. A rupture disk on the line between the thickener underflow pump and the second stage flocculation ensured safe operation despite occasional plugs in the static mixers due to debris.

The system was controlled at 4 main points:

- The feed to the thickener was sampled from a drain valve. This provided flocculated thickener feed, which was identified as the most important control point for the thickener operation. Samples were collected in a 2 liter graduated cylinder, allowed to stand for 1 minute, and the resultant separation was observed. Water was decanted off and evaluated for solids content by clarity wedge. Settled material was analyzed for floc structure and settled volume.
- Samples of underflow were taken periodically for density by mud balance with regular verification by moisture analyzer.
- From the hose leading into the deposition cells (flumes), samples were obtained to evaluate the performance of the second stage flocculation dosage and mixing setups. These samples were examined for density (mud balance), solids content (moisture analyzers), rheology (Brookfield vane rheometer), immediate water release by Capillary Suction Timer (CST), fines capture by "drop test," a floc settling test detailed below, and 24 hour and 7 day drainage tests.
- Pressure was monitored in the shear loop and immediately upstream of the second stage flocculation.

In addition to these key control points, the flumes themselves were used to evaluate product quality, both by visual inspection of the flocs, their flow patterns, and their water release over time. FBRM and PVM probes were applied downstream of the second stage chemical injection point, and, as mentioned above, overflow water was periodically sampled for solids content. The feed tanks were also continuously monitored for solids content, and periodically monitored for PSD: a simple SFR sieve cut was performed at least 2-3 times per tank during operation, and samples were obtained for later full PSD analysis. Feed rates were calculated to achieve the desired ratios and solids contents, and were validated periodically during experimentation. All equipment was calibrated at the start of experimentation and periodically throughout.

In addition to this configuration, a number of tests were performed to evaluate high rate flow and a scaled-down chemical injector. To achieve this, thickened material was stockpiled by operating the system up until the shear loop at or near the commercial flux rate. Stockpiled material was then stored in one of the feed tanks, from where it was pumped at 250-300 L/min through a 3" line, receiving secondary flocculation and being deposited at 20% of the anticipated commercial flow velocity. This configuration further introduced a flow meter. Most of the mixing discussion is focused on this configuration.

Feed for the system comprised Kearl process water, Kearl flotation tailings (i.e., underflow from the flotation cells), beach sand, and FFT. Syncrude FFT was also used for several early runs, but was replaced with Kearl FFT once that material became available, though very little difference between the two was observed in any of the KPIs.

The pilot was operated in the first quarter of 2016 at CNRL's Applied Process Innovation Centre onsite at the CNRL Horizon Mine near Fort McMurray as part of a COSIA Joint Interest Project between Imperial, CNRL, and Teck Resources.

RESULTS AND DISCUSSION

System Operations and Feed Variability

The thickener operated as anticipated based on lab tests with a smaller thickener unit at the same, constant flux rate. Flocculation dosage at this scale was consistent with dosing behavior from smaller scales, and showed strong dependence on the fines content (see Figure 1). Thickener underflow showed a negative linear relationship to fines content (Figure 2). Increases in bed height had much lower impact on settled bed underflow density than anticipated (Figure 3). This, in combination with increased ease of operation, enabled the bed height to be an uncontrolled parameter, maintained above a minimum threshold while density was controlled by the addition of dilution water into the shear line. This introduced a new degree of freedom, decoupling performance metrics (overflow water and underflow density).

Feed was varied in several dimensions, including increase/decrease to Sand to Fines Ratio (SFR), introduction/removal of FFT addition to the FT, high sand excursion to simulate process upset conditions. These tests revealed some buffering capability within the system. The thickener underflow behaves like a plug flow reactor, while the overflow behaves like a CSTR. At this scale, bed residence times and overflow turnover times were on the order of 20 minutes. Feed transients confirmed the trend as anticipated by volumetrics and flow (see Figure 4), and also revealed potential opportunities to mitigate feed variation within the system. In particular, a deeper bed lessens the immediacy of a feed change, and for small variations, can partially obfuscate the effect.

The delay in response to feed variability created by the thickener bed allows for adjustments to be anticipated in the second stage flocculation. However, the delay also means that overflow water is not the best metric for catching feed variation early. Rather, samples of the flocculated feed show within 1 minute the change, and provide an opportunity for response. Decanting water from a feed sample after 1 minute of settling time allows for a quantification of fines capture, a proxy of water clarity, which is relevant to the discrete incoming sample rather than the average of water qualities from a 20 minute period. An example of how feed and underflow vary as a result of a process change are depicted in Figure 4.

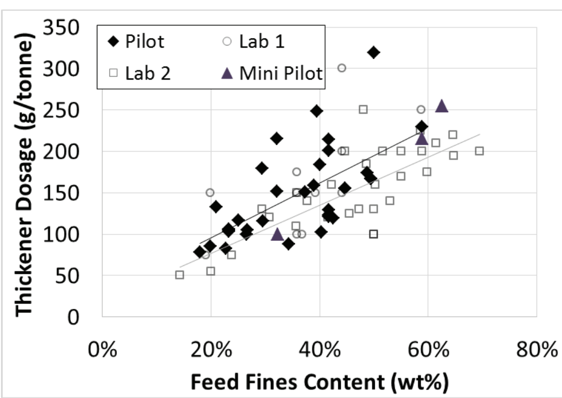

Figure 1. First stage flocculant dosage is proportional to fines content at constant solids content and flux. The gray line is a linear data fit to the lab data; the black line is a linear data fit to the pilot data.

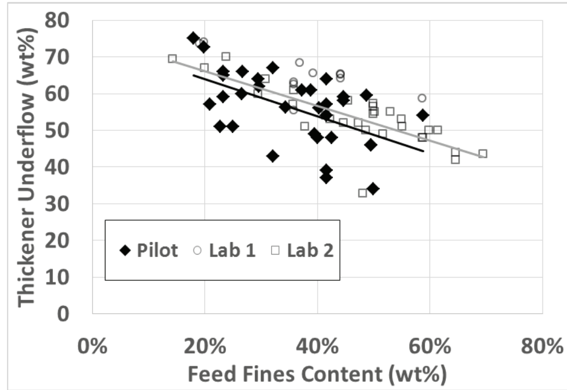

Figure 2. Thickener underflow decreases in density with increasing fines content (constant solids content and flux). The gray line is a linear fit to the lab data; the black line is a linear fit to the pilot data.

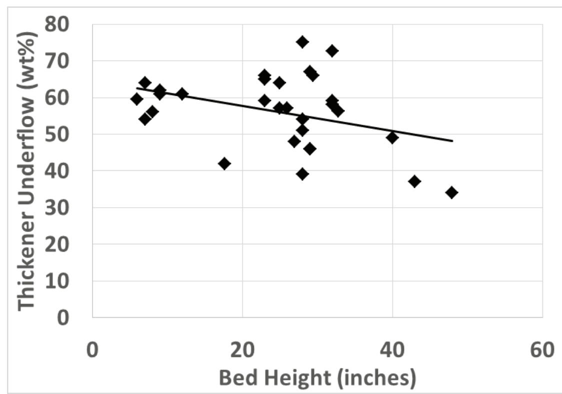

Figure 3. Bed height has a weakly decreasing trend with underflow density in the depths explored; this is due to bed height increases as an attempt to mitigate low underflow densities that were less effective than desired.

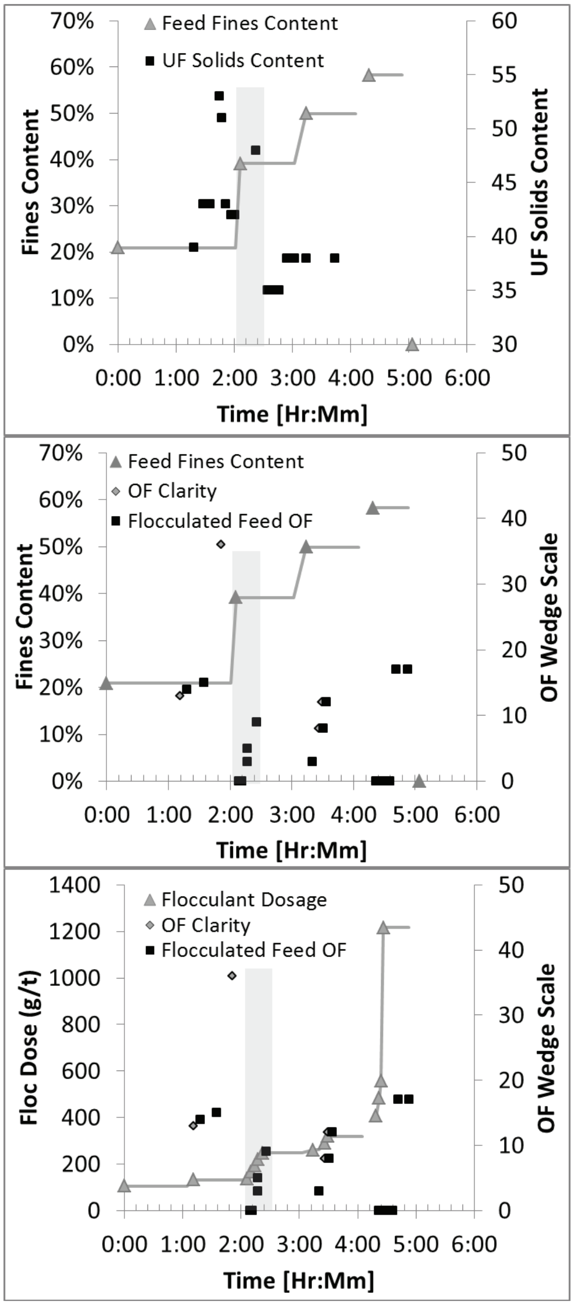

Figure 4. Feed variability is observable in the grayed section, the beginning of which marks the introduction of FFT into the feed. Underflow takes a bed residence time, here about 30 minutes (width of the gray section) to respond (top panel), while feed samples respond within a minute (middle panel) and can be used to adjust flocculant dosage immediately (bottom panel).

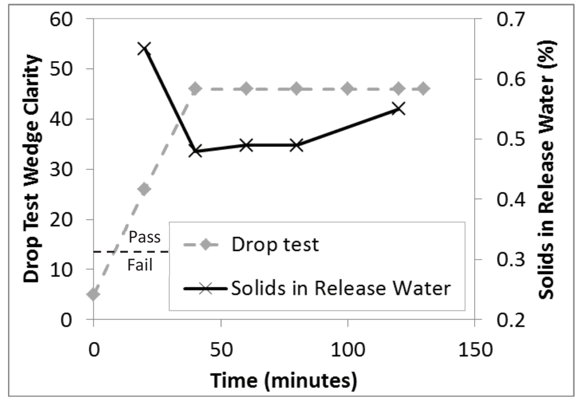

Figure 5. Water runoff from a flume test suggest a correlation to the drop test results. Note: 46 is the maximum for this clarity wedge.

Second stage flocculation, which is new to the industry, required a set of robust KPIs to enable independent operators to identify proper mixing and flocculation. Rheology and dewater rate are the typical KPIs examined for these applications, but they do not provide insight into fines capture or segregation. Without a measure of fines capture, it is difficult to ascertain if the material is properly flocculated or if the sample is representative. For example, dewater rates can be very high for a segregating slurry – after fines run off, residual sand may test well. The new drop test attempts to close this gap. A sample of flocculated slurry is dropped into a column of water. After 3 minutes, the water is decanted into a wedge for a clarity assessment. Empirically, a >12 exhibited favorable characteristics and was deemed a pass. The test provides insight into the fines capture, ie., floc stability, of the material. Fines that do not settle in a commercially reasonable timeframe will not be captured in the DDA. Figure 5 depicts water runoff quality from a flume in conjunction with drop test data, showing a correlation between fines capture within the flume and drop test results.

For this pilot, Capillary Suction Timer and Drop Tests were combined to identify when a material was suitable for placement. Material with a CST of < 60 seconds and a drop test wedge reading > 12 appeared to have both water release and fines capture. These materials also showed good floc structure and dewatering characteristics.

Mixing

A set of mixing tests were conducted at commercially-representative flow velocities (1 m/s pilot; 5 m/s field) to validate the injector design and ascertain how the system handles mixing and shear energies. The setup differed from Figure 12 in that the first half of the flowsheet fed into a tank at pump 10. Then the stockpiled material was pumped semi-batch through a flocculant injector to the deposition cells. The key parameters for some of these tests are summarized in Table 1.

Table 1. Average values for a 250 L/min reflocculation configuration

Parameter	Value
Pipe size (inch)	3
Velocity (m/s)	0.92
SFR	2.2
Solids wt%	45
Shear Stress at Wall (Pa)	60-70
Avg Dissipation Energy (W/m^3)	3000-3600
Max Dissipation Energy (W/m^3)	6500-7500
Length (m)	26-41
Time in nozzle (sec)	0.4
dP/dL Front (kPa/m)	1.94
dP/dL Back (kPa/m)	3.54
Effective Viscosity Front (cP)	385.7
Effective Viscosity Back (cP)	702.3
Effective Viscosity Injector (cP)	29.5
Re Injector	9289
Re 3" Post Injector (pre-floc)	3096
Re 3" Flocculated Material	144.5

It is noteworthy that yield stress increases along the length of pipe following the injector, providing a first indication that flocculation continues to occur downstream of the injector. This observation is corroborated by the KPIs measured for such tests: drop test values and CST, as shown in Figures 6 and 7, respectively.

In addition to the time-latency effect observed in mixing, the test revealed a sensitivity to shear/transport effects for underflocculated material that is not as apparent for well-flocculated slurry. Figures 8 and 9 depict the drop test and CST results for two exemplary cases. The steady deterioration of the underflocculated case is apparent on both KPIs.

Mixing energy also appears to have a maximum efficiency. Underperformance on the low energy side may be derived from insufficient contact of viscous polymer with dense non-Newtonian slurry, while excess mixing may translate to overshear and degradation of the resultant flocs. Interestingly, this peak may depend on the fines content at a constant solids rate: more fines appears to shift the optimal energy to a higher range, while fewer fines (and more coarse) requires a lower energy, depicted in Figure 10.

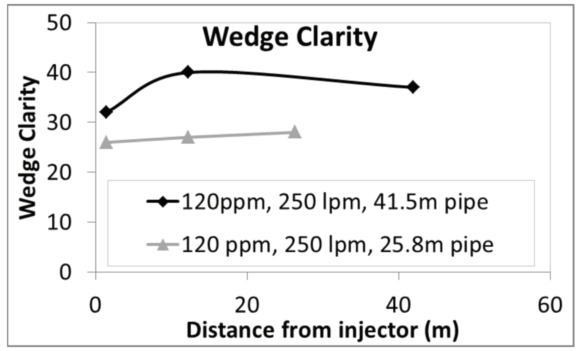

Figure 6. Wedge clarity from the drop test shows an increase in performance (improved clarity) in the first 10 m post injection in the 41 m long experiment

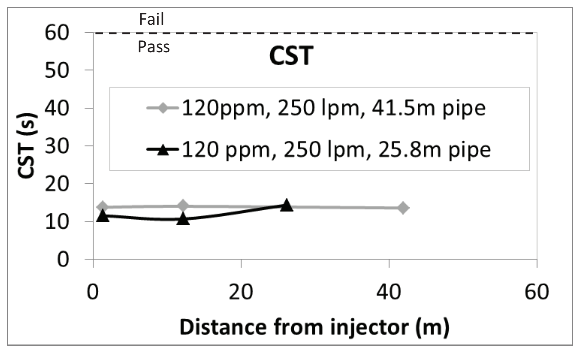

Figure 7. CST results are unchanged from one sample point to the next

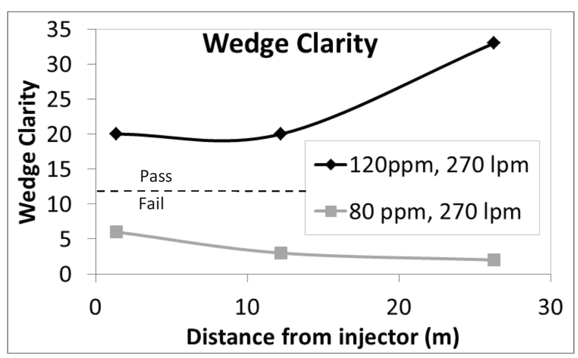

Figure 8. Sufficiently dosed material improves in fines capture with some flow. Insufficiently dosed material fails the KPI and gets worse with flow.

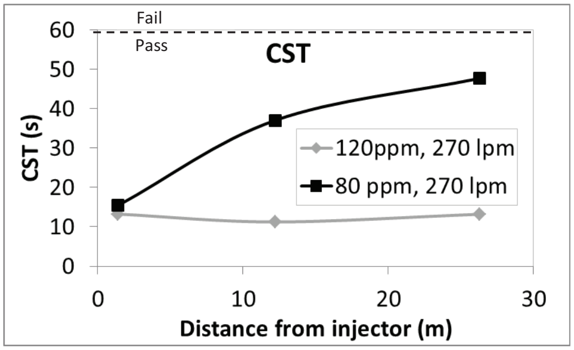

Figure 9. Sufficiently dosed material passes the KPI and is largely unaffected by transport (shear) at this scale. Insufficiently dosed material also passes the KPI, but gets progressively worse as it flows, trending toward a failure for the KPI.

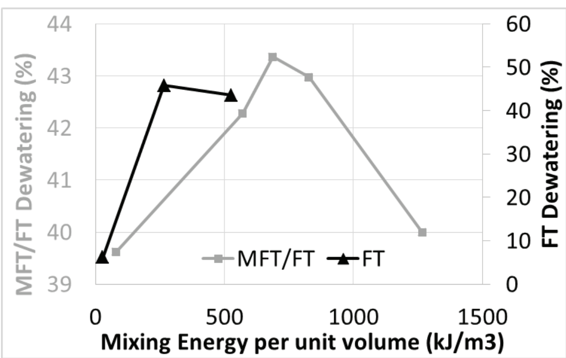

Figure 10. 24 hour dewatering vs mixing energy for two materials – FT with and without FFT addition. The introduction of FFT shifts the optimal mixing zone to a higher regime.

Deposition

A variety of depositional tests were performed, leveraging the large quantity of material produced from the feed variability and mixing studies. These deposits were placed in subaerial and subaqueous flumes as well as boxes which were placed outdoors in the Fort McMurray February to examine freeze-conditions. Data from the subaerial flumes is depicted in Table 2. Segregation is indicated and should be anticipated for these types of deposits. Dewatering is consistent with deposit SFR, so segregation or high fines conditions result in lower solids contents after 7 days.

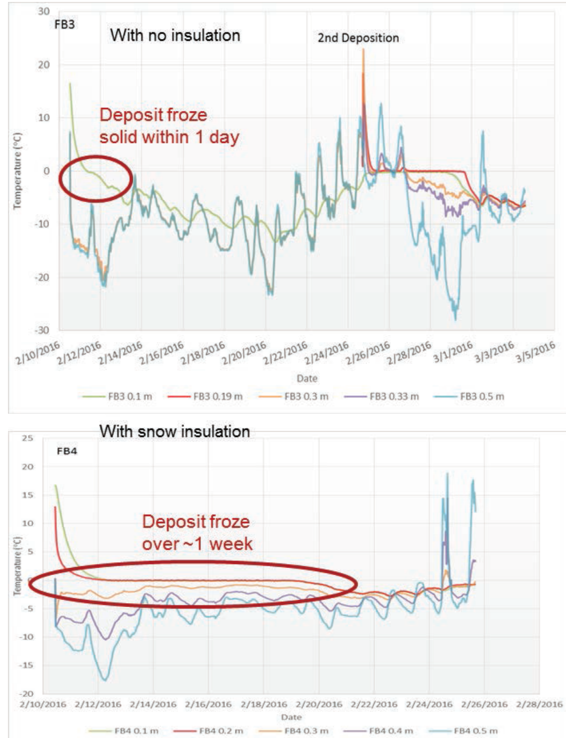

Figure 11. Circled are the freeze times for the uncovered (top panel) and snow-covered (bottom panel) thickened tailings deposits. The presence of snow cover delayed frost penetration by a week.

A subaqueous test run is also depicted in Table 2. This run was less rigorously studied than the subaerial flume studies, and was conducted as a proof of concept only. Initial data from the test indicated an increase in subaqueous slope vs subaerial slopes of the same material (consistent with usual pond dynamics), as well as a continued consolidation comparable with the subaerial flume. More study is warranted on this type of subaqueous deposition of TT.

Figure 11 depicts a comparative study of frost penetration with and without snow cover for a depth of FFT placed into a box insulated on all sides. Thermistors, placed within the deposit, reveal the onset of freeze conditions. The open box froze through to the bottom thermistor within a day, while a 3-5 inch snow cover delayed freeze penetration to about a week.

CONCLUSIONS

The Kearl Tailings Treatment flowsheet was successfully demonstrated in fully continuous operation in pilot mode. The system enabled evaluations of feed variation, thickener operation, second stage flocculation, and deposition, and provided insights into critical parameters required for smooth operation. Key learnings include:

- Sampling of the thickener flocculated feed is the first signal to reveal ineffective/insufficient flocculation
  - Dosage correction based on a thickener flocculated feed sample is the best route to avoid upset conditions and allows the thickener to maintain steady operation throughout the runs. Underdosage was readily apparent in samples that did not settle within 1 minute. Overdosage can be dialed back by reducing the dose, waiting a minute, taking another feed sample, and repeating until signs of underdosage appeared
  - Much more rapid than waiting for the bulk thickener O/F (2-3 minutes vs 45-90 minutes at pilot scale) or the bulk thickener underflow (2-3 minutes vs 20-45 minutes)
  - With one operator observing the feed and another making changes to the feed system (flocculant dosage, dilution, etc.), feed/dosage relationships could be optimized within 5 minutes after a feed change using just a graduated cylinder, a stopwatch, and a clarity wedge.
- Dilution introduced to the shear loop rendered the thickener underflow density independent of the bed height, and provides smooth flow conditions to the second stage flocculation treatment.
  - Independence in these systems creates an extra degree of freedom. This allows bed height to increase, enabling buffering of feed variation, reducing the effect it has on the underflow rate or density.
  - Dilution of the underflow after the underflow pump creates a dependence between density and flowrate that can be avoided by introducing the dilution in the shear loop.
  - Bed height is challenging to measure both in a pilot and in the field, but maintaining a bed height range that is well in excess of a minimum threshold is much simpler.
  - Underflow density shows surprising lack of correlation to bed height in the bed heights tested, so adjusting the bed height to affect density can sometimes be ineffectual, introduces a time-lag for the change, and interdependency in the system.
- Flocculation of a high density slurry with a viscous polymer requires an assessment of fines capture or segregation.
  - In the absence of an indication of fines capture or segregation, dewatering rates can be high as a result of experimental error due to water separating preferentially from a coarse fraction, the fines fraction being underrepresented.
  - The newly introduced “Drop Test” resolved this challenge by providing a simple, operator-independent test to quantify fines capture in the slurry.
- Mixing appears to have a time latency or kinetic effect. The first stage of mixing occurs within the injector, during which time the flocculant is substantially contacted with the slurry. After the injector, the material continues to “react” as measured by several different KPIs (pressure drop, CST, drop test).
- Exceeding the minimum dose appears to have greater process tolerance for poor mixing/shear conditions than underdosing in the second stage flocculation. This is a double edged sword, because the tendency will be to operate towards an overdosed condition to ensure process KPIs are met, though this can have deleterious effects on deposit performance.
- Material properties define an optimal mixing window. This window appears to be more tolerant of mixing energy for higher fines- (and flocculant-) containing materials and less tolerant of mixing energy for lower fines-containing materials.
- Segregation within the deposit is a likely outcome resulting from the solids content and SFR conditions of the Kearl KFTT. The degree of segregation will need to be quantified to ensure consolidation is properly managed.
- Subaqueous discharge of reflocculated TT showed considerable promise and warrants further study.
- Deposition in winter conditions highlighted a significant risk for freezing effects emerging in the layered deposition scheme.

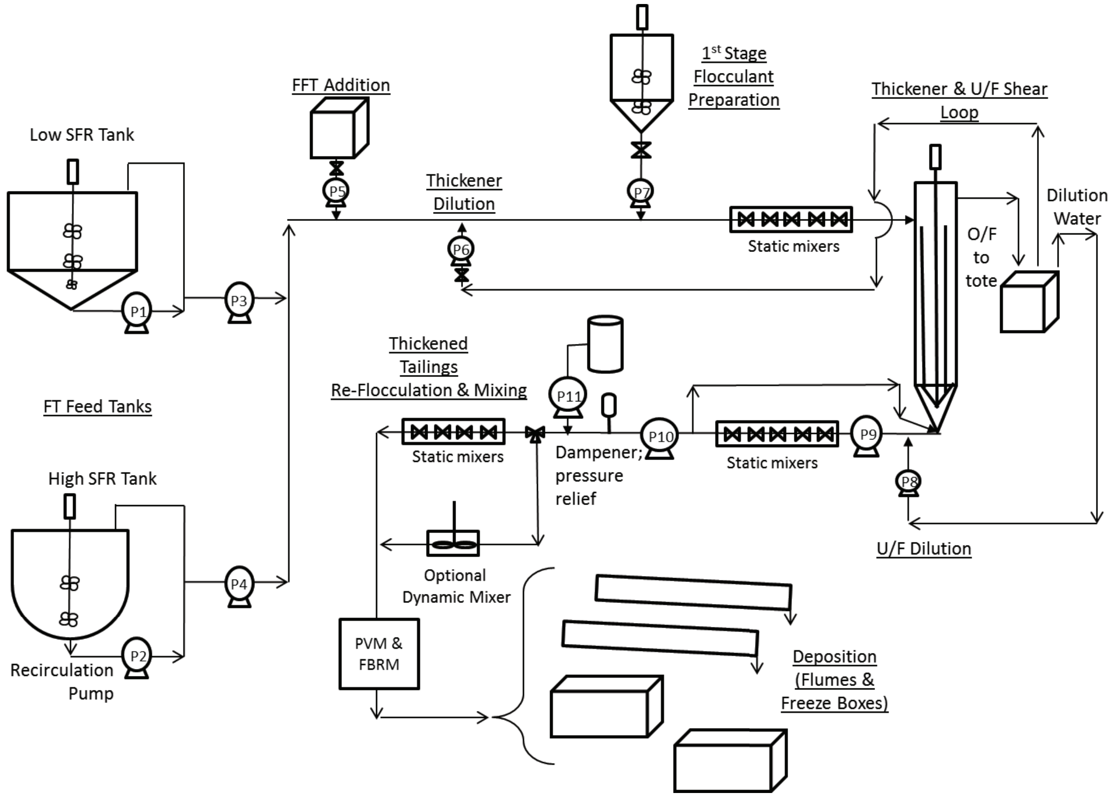

Figure 12. Process flow diagram for the Kearl Tailings Treatment Pilot operated at CNRL's Horizon Mine Site

Table 2. Flume data from 4 continuous flow tests and 2 fast flow tests. Segregation manifests in the differences in fines content from head to toe of the flumes. The third row, indicated with an (*), identifies the conditions of a subaqueous flume trial conducted opportunistically with residual material from the 70:30 test in the immediately preceding row. This test should have had lower SFR, but the opportunistic nature of the test did not allow for confirmation by feed sample.

Feed	Feed SFR	Feed SC (Avg wt%)	Slope (%) - after deposition	Slope (%) - 7 day	Run-off water SC	1 hour Deposit SC, (wt%)		7 day Deposit SC (wt%),		(%) Mass Balance-Fines Capture	SFR,	
						Head	Toe	Head	Toe		Head	Toe
100% FT	High (2.8-4.4)	50.1	13.4	9.6	0.41	65	50	72	60	99	4.56	2.10
70:30 FT:MFT	High (1.43-1.6)	41.6	6.5	5.6	0.38	63	47	67	54	99	2.2	1.3
70:30 FT:MFT	*	41.6	16	12	N/A			58	68		0.81	0.75
100% FT	Low (1.69-2.11)	49.51	13.8	11.4	0.22	63	55	71	70	99	2.4	1.8
70:30 FT:MFT	Low (1.02-1.37)	41.49	5.9	5	0.62	53	39	62	51	99	1.2	0.8
70:30 FT:MFT	Off-spec (0.4-1.3)	25-43	2.16	1.7	0.4	42	35	39	42	99	0.8	0.6
HFR-24	3.1	57.4		N/A	N/A	59	58	N/A		N/A	3.8	3.2
HFR-23	2.3	N/A	6			60	62				3	3.2

Session D

Tailings Dewatering

TUBIFEX: A BIOLOGICAL METHOD FOR ENHANCING DEWATERING OF OIL SANDS TAILINGS. LATEST RESULTS AND NEXT STEPS

Miguel de Lucas Pardo[1], Xiaojuan Yang[2,3], Maria Ibanez[4], Luca Sittoni[1],
Lijun Deng[3] and A. Ulrich[3]
[1] Deltares, the Netherlands
[2] Sichuan University, China
[3] University of Alberta, Canada
[4] Delft Technical University, The Netherlands

ABSTRACT

Facilitating the dewatering and consolidation processes of fine oil sands tailings is a major challenge to researchers and practitioners of Canada. Deltares and the University of Alberta (UoA) are investigating the use of *Tubifex,* an earth worm endemic in Canada, as an innovative (bio)technology to enhance oil sands tailings dewatering, through a laboratory test program. This paper first presents a more in-depth analysis of the results shown on previous presentations and scientific papers (Yang et. al, 2016) over the first round of measurements back in 2015. Further, it follows-up with the latest promising results of the 2016 research program. The analysis of the 2015 data shows an increase in the permeability of the tailings caused by the movement of worms. The 2016 tests showed that: (a) the mud-water interface of *Tubifex*-treated oil sands tailings settled faster than non-treated tailings; (b) solids contents of *Tubifex*-treated tailings went up to 48 wt%[1] (solids percentage by weight) from initial 30 wt%, i.e. 10% more than the non-treated tailings, and had not yet reached equilibrium; (c) undrained shear strength of tailings amended with *Tubifex* is higher than non-treated tailings.

INTRODUCTION

In 2015 Deltares and UoA started a research project on the use of *Tubifex* for enhancing dewatering of oil sand tailings. This technology consists of adding *Tubifex* worms, endemic in Canada, to the tailings, upon which the worms will move up and down creating tunnels, which favor dewatering. Some of these *Tubifex* worms are visible in Figure 1. This work is inspired by the findings reported in de Lucas (2014), where *Tubifex* abundant beds were found to have higher characteristic permeability than defaunated beds. With the support of UoA and the contribution of UoA staff, a first set of laboratory experiments took place in the Sediment Lab of Deltares in 2015. The results of this first laboratory campaign are presented in Yang et al. (2016). Essentially, the 2015 experiments consisted of a set of settling columns experiments, where low concentration tailings mixtures of 20 g/l, 40 g/l and 60 g/l (thus in the 5 wt% to 10 wt% range) were let settle and consolidate with and without *Tubifex* treatment. The tailings settling interface was monitored in time, from which the solids content could be calculated. The *Tubifex* treated mixtures achieved 20% relative higher final solids content and survival rates of 20% to 40% (Yang et al., 2016). Further analysis to the settling interface data of 2015 is presented in this paper.

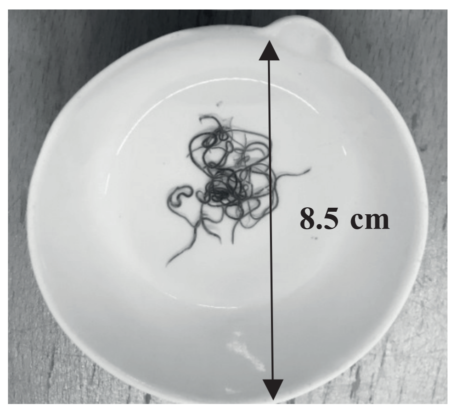

Figure 1. *Tubifex* worms

Later in 2016, again in collaboration with UoA staff, a new and more extensive laboratory campaign took place in the Sediment Lab of Deltares. The current paper reads mainly over the findings of this 2016 campaign. The objective of the 2016 campaign was to investigate the effect of *Tubifex* in dewatering tailings of higher initial concentration, thus in agreement with the concentrations in practice. The initial tailings concentrations were of about 350 g/l (one order of magnitude larger than

[1] wt% = percentage of solids by weight

in 2015), which corresponds to 30 wt%. Tailings were left to consolidate for 3 months, and the effect of applying several densities of *Tubifex* was addressed. The survival rate of *Tubifex* under several temperatures and other conditions were studied as well. Pore water pressure and sediment density were monitored in a selection of the columns during the dewatering process. This data is however still under analysis, and thus it is not included in this paper.

Further to the results presented in this paper, new laboratory investigations are planned for 2017 and 2018. This new phase will be a collaborative effort between Deltares, UoA, the Institute for Oil Sands Innovation (IOSI) and the Dutch Government sponsored program Topconsortium voor Kennis en Innovatie (TKI) Deltatechnologie, which promotes private – public research and development of socially impacting innovative technologies. This upcoming phase of the research will take place at UoA and Deltares, and its objectives will be to: 1) quantifying the dewatering properties and strength produced by different Tubifex densities, on different tailings types (i.e. fluid fine tailings and thickened tailings) and temperatures (i.e. 2 and 20 °C).; 2)to test several strategies to enhance *Tubifex* reproduction, to investigate and optimize survival and reproduction potential of Tubifex in an oil sands environment so to assure not only sustainability, but the optimization of this technology ; and 3) scale up to larger columns towards a future pilot scale trial.

METHODOLOGY

Quantification of Sedimentation and Consolidation Parameters

In the 2015 phase of the project, the first sediment settling and dewatering experiments were performed in settling columns, aiming at characterizing the evolution of the wt% of the bed (as reported in Yang et al., 2015), but also at determining the tailings sedimentation and consolidation parameters, as a continuous process. With these parameters the (hindered) settling (i.e. sedimentation) and initial consolidation behaviour of sediments is defined. These experiments are based on the work of Dankers and Winterwerp (2007), Merckelbach and Kranenburg (2004), and Merckelbach (2000), where sedimentation and consolidation parameters and equations are derived under the assumption of self-similarity of the bed. Essentially the experiments follow the sedimentation and consolidation process of a highly concentrated suspended sediment concentration. The sedimentation-consolidation curves are obtained by following the sedimentation interface (separating muddy from clear water), from which the following parameters can be derived:

- Sedimentation velocity w_s and gelling concentration c_{gel} (Dankers and Winterwerp 2007).
- Permeability K_k and fractal dimension n_f (Merckeclbach and Kranenburg, 2004; Merckelbach 2000).
- Effective stress coefficient K_p, only when final bed level height is achieved (Merckeclbach and Kranenburg, 2004; Merckelbach 2000).
- Consolidation coefficient, c_v, derived from a.o. K_k, n_f and K_p, which gives an indication of the consolidation behaviour of the soil.

This set of parameters are in particular applicable to sediment transport, sedimentation and consolidation models that describe infilling and the transition from a fluid to a “solid” (soft mud) state as a continuous system, such as the one described in Winterwerp (2001). Given all these parameters, the permeability of the bed k, the effective stress σ_{kk}, and the consolidation parameter Γ_c can be defined as a function of the volume concentration of mud and the volume concentration of sand (ϕ_s^m and ϕ_s^{sa}) as follows:

$$\sigma_{kk} = K_p \left(\frac{\phi_s^m}{1-\phi_s^{sa}}\right)^{\frac{2}{3-n_f}} \quad (1)$$

$$k = K_k \left(\frac{\phi_s^m}{1-\phi_s^{sa}}\right)^{-\frac{2}{3-n_f}} \quad (2)$$

$$\Gamma_c = \frac{2}{3-n_f}\frac{K_k K_p}{g\rho_w} \quad (3)$$

Note that Γ_c is equal to the consolidation coefficient c_v used in traditional soil mechanics under the assumption of self-similarity of the bed (Winterwerp and van Kesteren, 2004).

The settling column is a cylindrical column with a height of 0.55 m and a diameter of 11 cm. Process water and mature fine tailings (MFT) samples were used for these specific tests. Each sample utilizes three columns. The tests are done at three sediment concentrations, 20 g/l, 40 g/l and 60 g/l.

At the beginning of the experiment, the sediment-water mixture is gently stirred (to prevent breaking of the flocs) to get a uniform distribution over the settling column. Over time, the sediments settle in the column and an interface between the water-sediment mixture and the clear water above becomes visible. In the meantime the suspended sediment accumulates at the bottom of the column. A camera is used to take pictures of the column(s) at an increasing time interval, to be able to determine the position of the interface over time with the help of a FORTRAN code.

The consolidation of the sediment in the column goes through three distinct phases, with different process dominating the rate at which the sediment-water interface decreases in height:

1. Hindered settling phase (i.e. sedimentation)
2. Phase I consolidation process
3. Phase II consolidation process

Hindered settling phase

In hindered settling or sedimentation phase, three layers can be distinguished in the column: at the bottom, there is a layer of settled sediment in which the particles do not sink. Overlaying this, there is a layer of suspended sediment in which the particles have a downward movement relative to the water. Finally, there is layer of clear water on top of this layer. The sedimentation process is referred to as 'hindered settling or sedimentation' because neighbouring particles influence the settling of an individual particle within a suspension. The larger the mud concentration in suspension, the smaller the sedimentation velocity will be. The end of hindered sedimentation phase is characterized by the gelling concentration cgel at which a space filling network develops, meaning that all particles are in contact with each other leaving no possibility for further sedimentation. At this point, effective stresses start to build up. Consolidation starts immediately after thee gelling concentration is achieved. The effective sedimentation velocity w_{eff} is calculated based on the rate of sinking of the water / settling particles interface during the hindered sedimentation regime. Once the effective sedimentation velocity w_{eff} is determined, the sedimentation velocity of individual particle aggregates $w_{s,0}$ and the gelling concentration c_{gel} can be calculated. This is different from the dilute particle settling sedimentation as determined with the sedimentation balance. Dankers and Winterwerp (2007) established the mathematical relations to be used in this estimation. Both gelling concentration and sedimentation velocity of individual flocs are important parameters in the understanding (and modelling) of mud behaviour in nature.

It is important that the experiment starts at a concentration below the gelling concentration. Otherwise the Phase I consolidation process starts immediately without hindered settling phase. In this case the consolidation rate becomes dependent on the initial solids concentration. In order to ensure the occurrence of a hindered settling phase, preliminary experiments in beakers are performed to estimate the order-of-magnitude of the gelling concentration.

Phase I consolidation process

After the sedimentation phase, only two layers are left in the column: a layer of consolidating sediment, and a layer of clear water on top of it. Consolidation of the sediment then proceeds in two distinct phases. During Phase I of the consolidation process, consolidation is governed by the permeability of the soil: water leaving the sediment is the prime factor responsible for consolidation. The process can best be characterized by geometric parameters that characterize the possibility for water to leave the sediment column: the fractal dimension and the permeability parameter have been shown to provide a sufficient characterization (Merckelbach, 2000). These parameters are a property of the studied sediment (e.g. a sediment with for example a large permeability parameter is a sediment whose intrinsic capability for dewatering is large), and are estimated from the rate of sinking of the sediment-water interface. The procedure is to plot the mud-water interface versus time on double logarithmic scales. For these curves, the fractal dimension n_f and the permeability parameter K_k can be obtained by fitting (Merckelbach and Kranenburg, 2004; Winterwerp and van Kesteren, 2004).

Phase II consolidation process

After completion of Phase I, the final phase of consolidation (Phase II of the consolidation process) starts, where deformations are relatively small and interactions between particles (effective stresses) dominate the consolidation process. From this phase, the effective stress parameter K_p is obtained by using the final settlement heigth (Merckelbach & Kranenburg, 2004). The transition between Phase I and Phase II is observed as a change in slope of the double logarithmic plot of sinking of the interface versus time. The effective stress parameter is estimated from the slope observed after this transition.

RESULTS

Sedimentation and Consolidation Analysis to the 2015 Data

From studying the sedimentation phase, a gelling concentration of 165 g/l was found consistently for the two studied set of columns in 2015. *Tubifex* were added upon formation of the bed, and thus their addition did not affect the concentration at which the bed starts to exist. Note that the result of solving Dankers and Winterwerp equation (2007) is a pair of a gelling concentration and a sedimentation velocity of the individual particles (without hindered sedimentation effects). In this case, a sedimentation velocity of the individual particles $w_{s,0}$ of 0.05 mm/s was found.

The study of the so-called consolidation phase I, were permeability governs the dewatering process, resulted in the set of parameters reported in Table 1. Note that columns C4, C5 and C6 are just triplicates of the exact same characteristics. The *Tubifex* treated samples exhibit a permeability parameter K_k approximately one order of magnitude larger than the non-treated samples. In theory this means that the *Tubifex*-containing sediments are intrinsically more capable of dewatering. The fractal dimension of the *Tubifex*-treated samples is slightly smaller than the one of the non-treated samples. A smaller fractal dimension means a more open and complex floc structure, though the differences in this case are too small to draw any conclusion. The permeability parameters K_k and the fractal dimensions n_f reported in Table 1 are introduced into Eq. (2) to compute the permeability of the bed. This was done for all void ratios observed during the settling tests. The results are plotted in Figure 2. The square markers and solid lines stand for *Tubifex* treated beds, whereas the triangles and dotted lines represent non-treated beds. The color of the line and marker is a proxy of the initial sediment concentration, with light grey being 20 g/l, grey 40 g/l, and black 60 g/l. In fact, the permeability of a *Tubifex* treated bed is a factor 2 to 3 larger than non-treated beds. Furthermore the shape of the permeability to void ratio curve for *Tubifex* treated samples, exhibiting a decrease in slope towards small void ratios, suggests a better dewatering behavior under further compaction.

The effective stress parameter can be obtained by computing the equilibrium height of the sediment bed (Merckeclbach and Kranenburg, 2004; Merckelbach 2000). The results from these computations can be seen in Table 2. The differences in effective stress parameters are small, in contrast with what reported with respect to the effect of sediment in natural systems (de Lucas Pardo, 2014). By introducing the effective stress parameters reported in Table 2 into Eq. (1), the effective stress can be plotted as a function of the void ratio. This relationship is shown in Figure 2. Color and lines are the same as in Figure 1. For small void ratios, *Tubifex*-treated tailings exhibit smaller void ratios than non-treated tailings, given the same effective stress.

Table 1. Results from studying consolidation Phase I in the 2015 experiments

Column number	Concentration (g/L)	*Tubifex* - treated	K_k (m/s)	n_f
C1	20	No	$6.86\ 10^{-14}$	2.68
C2	40	No	$2.96\ 10^{-14}$	2.70
C3	60	No	$2.42\ 10^{-14}$	2.70
C4	40	yes	$2.51\ 10^{-13}$	2.65
C5	40	yes	$2.94\ 10^{-13}$	2.65
C6	40	yes	$5.33\ 10^{-13}$	2.64

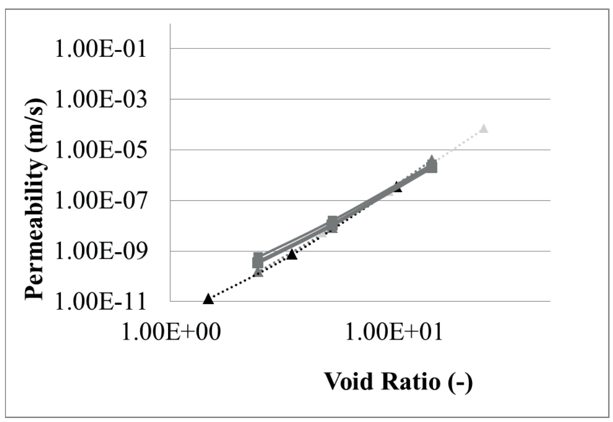

Figure 2. Calculated permeability as a function of the void ratio for all studied sediment samples. Square markers and solid lines are for *Tubifex*-treated beds, triangles and dotted lines are non-treated beds. Light grey: 20 g/l; grey: 40 g/l; black: 60 g/l.

Table 2. Calculated effective stress parameter K_p

Column number	Concentration (g/L)	*Tubifex* - treated	K_p (Pa)
C1	20	no	$5.42\ 10^5$
C2	40	no	$3.42\ 10^6$
C3	60	no	$8.53\ 10^6$
C4	40	yes	$3.76\ 10^5$
C5	40	yes	$1.84\ 10^5$
C6	40	yes	$2.46\ 10^5$

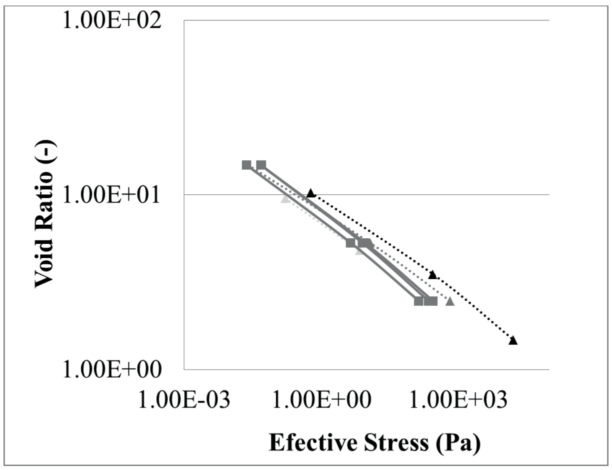

Figure 3. Calculated effective stress as a function of the void ratio for all studied sediment samples. Square markers and solid lines are for *Tubifex*-treated beds, triangles and dotted lines are non-treated beds. Light grey: 20 g/l; grey: 40 g/l; black: 60 g/l.

Finally, Table 3 shows the consolidation parameters c_v obtained for all sediment samples. The effect of *Tubifex* on c_v is within the margins of the intrinsic variability of this parameter (exhibited by the variation between 20, 40 and 60 g/l; this is a property of the material, and thus should be the same for all tests containing the same sediment type).

Laboratory Campaign 2016

In 2016 a total of 11 settling columns were used to further study the effect of *Tubifex* in dewatering MFT, with higher initial solids content. The dimensions of the columns were the same as those used in the 2015 phase: 0.55 m height and 0.11 m diameter. Table 4 shows an overview of the initial and final *Tubifex* densities in each of the 11 settling columns studied in 2016. All columns were filled with a 30 cm height sediment mixture of 30 wt%. Note that a 30 wt% is equivalent to a bulknde sity of 1190 kg/m3 and thus to a void ratio of about 0.11, thus beyond the void ratios studied for the 2015 tests. In columns C11, C12 and C13, *Tubifex* were added at the beginning of the test, and then again one and two months after the beginning of the test. Every addition represented a *Tubifex* density of 1400 individuals/m^2, arriving to a final amount of 4200 individuals/m^2. For all other columns containing *Tubifex*, there was only one addition at the beginning of the test. *Tubifex* were not added in two of the columns, C41 and C43.

Table 3. Overview of obtained consolidation parameters

Sample	Concentration (g/l)	c_v (m^2/s)
non-treated	20	$2.33\ 10^{-11}$
non-treated	40	$6.78\ 10^{-11}$
non-treated	60	$1.38\ 10^{-10}$
Tubifex	40	$5.42\ 10^{-11}$
Tubifex	40	$3.10\ 10^{-11}$
Tubifex	40	$7.32\ 10^{-11}$

Table 4. Overview of initial and final *Tubifex* densities over the tests in the 2016 phase

Column	Initial solids content (%)	*Tubifex* initially (individuals/m^2)	*Tubifex* final (individuals/m^2)
C11	30	1400	4200
C12	30	1400	4200
C13	30	1400	4200
C21	30	2000	2000
C22	30	2000	2000
C23	30	2000	2000
C31	30	1400	1400
C32	30	1400	1400
C33	30	1400	1400
C41	30	0	0
C43	30	0	0

Just as in 2015, the sediment-water interface was monitored for all the columns presented in Table 4 to determine the evolution of wt% over time. Direct sampling to obtain the solids content via drying in the oven was performed at the end of the test as well. In addition to the study of the sediment-water interface, strength measurements were performed at the end of the experiments, to characterize the effect on tailings strength of *Tubifex* treatment.

These were performed with a Haake rotoviscometer rv100 vane.

Figure 4 shows the solids content as a function of time for all the columns in the 2016 Phase. Dotted lines represent sediment beds that were not treated with *Tubifex*, whereas the solid lines represented *Tubifex*-treated samples. In the *Tubifex*-treated samples, the thicker the plotted line, the higher the density of *Tubifex* added to the bed. The three different thicknesses represent *Tubifex* densities of 4200, 2000 and 1400 individuals/m^2. Non-treated beds showed the slowest increasing solid content rates, reaching no more than 43% solids contents after 3 months, which is approximately a 19 cm thick bed, thus decreasing 30% approx. in height. High densities of *Tubifex* resulted in the highest solid contents after 2 months, reaching 48%, which is approximately a 16 cm thick bed, thus decreasing 45% approx. in height. In general, the higher the *Tubifex* density, the higher the observed solids content after 2 months. *Tubifex* were observed to distribute themselves evenly throughout the whole bed thickness. Note that our tailings had a solids content of 48% after 3 years of consolidation of a 40 to 50 cm thick layer in a barrel. Thus we have so far achieved the same consolidation state in one eight of the time. The slope of the plotted lines suggests on-going dewatering, so that solids content larger than 48% can be expected after more consolidation time. Unfortunately test planning and lab logistic forced to stop the experiment at this point.

Figure 5 shows the solids content as measured in the bed at the end of the experiments. Two samples were taken from the final bed, 5 cm and 15 cm above the bottom of the cylinder (10 cm and 1 to 2 cm below the water-bed interface). Color coding and line thickness is the same as Figure 4. The overall trend confirms the higher the *Tubifex* density to have the higher measured solids content. However there are some exceptions to this trend, like the very low solids content displayed by one of the 1400 individuals/m^2 samples.

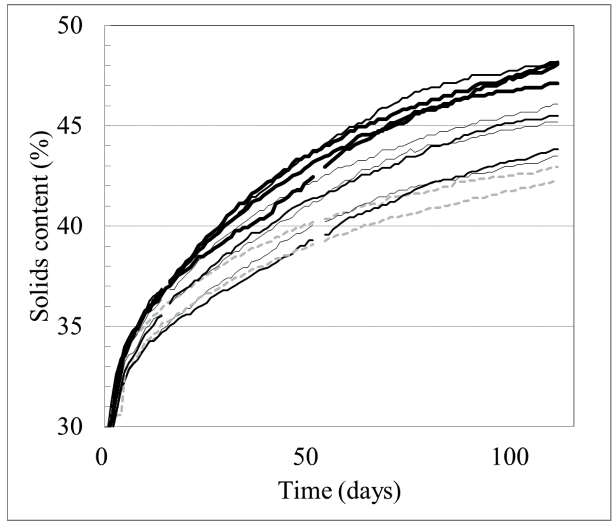

Figure 4. Solids content of the sediment beds as a function of time for several *Tubifex* treatments. Dotted lines represent sediment beds not treated with *Tubifex*, the solid lines are *Tubifex*-treated samples. In the *Tubifex*-treated samples, the thicker the plotted line, the higher the density of *Tubifex*. The three different thicknesses represent *Tubifex* densities of 4200, 2000 and 1400 individuals/m^2.

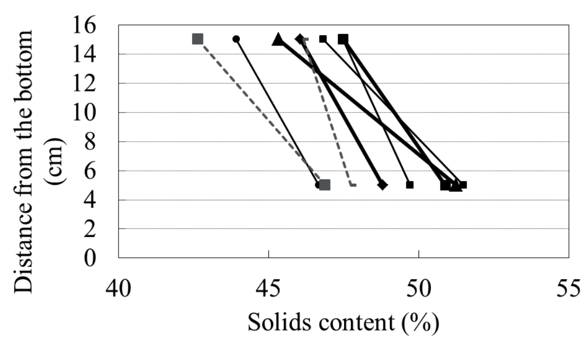

Figure 5. Final solids content measured at the end of the tests at two depths within the final bed, for several *Tubifex* treatments. Dotted lines represent sediment beds not treated with *Tubifex*, the solid lines are *Tubifex*-treated samples. In the *Tubifex*-treated samples, the thicker the plotted line, the higher the density of *Tubifex*. The three different thicknesses represent *Tubifex* densities of 4200, 2000 and 1400 individuals/m^2.

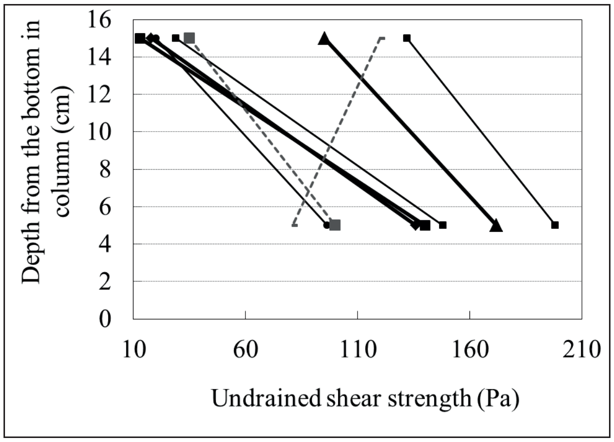

Figure 6. Undrained shear strength measured at the end of the tests at two depths within the final bed, for several *Tubifex* treatments. Dotted lines represent sediment beds not treated with *Tubifex*, the solid lines are *Tubifex*-treated samples. In the *Tubifex*-treated samples, the thicker the plotted line, the higher the density of *Tubifex*. The three different thicknesses represent *Tubifex* densities of 4200, 2000 and 1400 individuals/m^2.

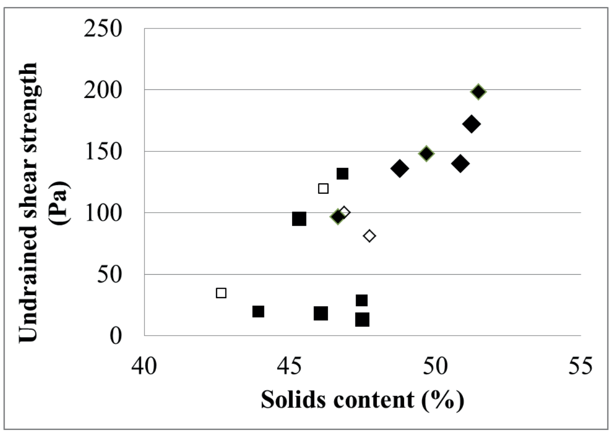

Figure 7. Relation between measured solids content and measured undrained shear strength at two depths within the final bed. Diamonds stand for points close to the bottom of the column (e.g. deep in the bed), whereas squares represent measurements close to the water-bed interface. The size of the marker is an indication of the *Tubifex* density, with empty markers representing non-treated beds.

Figure 6 shows the undrained shear strength measured at the end of the test at two depths within the final bed, the same depth as for solids content. Color and line coding are the same as Figure 4. This time, there is not a clear relation between *Tubifex* density and measured strength, at least not as clear as in previous cases. *Tubifex* treated samples develop however a larger undrained shear strength deep in the bed, varying between 100 and 200 Pa. Non-treated tailings stayed in the 100 Pa range. Note that the at the beginning of the test, when the solids content was 30%, the tailings showed an average undrained shear strength of 60 Pa. Figure 7 shows the relation between the measured solids content and the measured undrained shear strength at two depths within the final beds. Diamonds stand for points close to the bottom of the column (e.g. deep in the bed), whereas squares represent measurements close to the water-bed interface. The size of the marker is an indication of the *Tubifex* density, with empty markers representing non-treated beds. For the deeper measurements (diamonds), the undrained shear strength seems to follow the solid contents, whereas there is larger scatter in the relation between strength and solids for measurements close to the surface. Small increases in the solids content result in substantial increases of the undrained shear strength.

CONCLUSIONS

The analysis of the 2015 data and the application of the equations of Merckelbach and Kranenburg to quantify sedimentation and consolidation properties confirmed that:

- The addition of *Tubifex* affected the permeability to void ratio relation of the bed in a beneficial way for dewatering and consolidation.
- The effective stress to void ratio relation was also modified upon the presence of *Tubifex*, resulted in smaller void ratios given a constant effective stress.

Furthermore, the 2016 laboratory campaign revealed the following important consequences of the addition of *Tubifex* to the bed:

- *Tubifex* treated beds can increase their solids content from 30% to 48% within 3 months, in contrast to a maximum of 43% in the absence of Tubifex. Note that 48% is reached naturally in 2 years for a

comparable (but thicker) thickness of tailings;
- The higher the *Tubifex* density, the faster the increase in solids content;
- The strength of a 15 cm deep *Tubifex*-treated beds is approximately a factor two larger than the strength of non-treated beds.

Quantification of the sedimentation and consolidation parameters for the 2016 campaign is on-going.

Overall all the results suggest that *Tubifex* is a beneficial treatment to increase dewatering speed of tailings, showing promising results with respect to the constitutive soil relations and the solids contents and strength. The 2016 laboratory campaign provided a first quantification of the effect of *Tubifex*, continuing the promising but more qualitative results reported by Yang et. al (2016). However the process of studying the effect of *Tubifex* in dewatering tailings is on-going s, and further quantification of the effect of *Tubifex* and a quest for the optimization of the impact of *Tubifex* in the bed will follow-up in the 2017 and 2018 phase of the project. This phase is expected to inform on applicability to larger scales, and large production volumes, to further assess applicability of this technology to oil sands operations.

REFERENCES

Dankers, P. J. T., & Winterwerp, J. C. (2007). Hindered settling of mud flocs: theory and validation. Continental shelf research, 27(14), 1893-1907.

De Lucas Pardo, M. A. (2014). *Effect of biota on fine sediment transport processes: A study of Lake Markermeer* (Doctoral dissertation, TU Delft, Delft University of Technology).

Merckelbach, L. M. (2000). *Consolidation and strength evolution of soft mud layers*. TU Delft, Delft University of Technology.

Merckelbach, L. M., & Kranenburg, C. (2004). Equations for effective stress and permeability of soft mud–sand mixtures. *Géotechnique*, *54*(4), 235-243.

Winterwerp, J. C. (2001). Stratification effects by cohesive and noncohesive sediment. *Journal of Geophysical Research: Oceans*, *106*(C10), 22559-22574.

Winterwerp, J. C., & Van Kesteren, W. G. (2004). *Introduction to the physics of cohesive sediment dynamics in the marine environment* (Vol. 56). Elsevier.

Yang, X., Pardo, M. D. L., Ibanez, M., Deng, L., Sittoni, L., Ulrich, A., & Chen, Q. (2016). Addition of Tubifex accelerates dewatering of oil sands tailings. *Canadian Journal of Civil Engineering*, (ja).

UTILIZATION OF PLANTS TO DEWATER AND STABILIZE MATURE FINE TAILINGS

Kera Yucel[1], Amanda Schoonmaker[1], Dani Degenhardt[2], Jasmeen Kaur[3] and Bhupesh Khadka[1]
[1]Boreal Research Institute, Northern Alberta Institute of Technology, Peace River, Canada
[2]Alberta Innovates Technology Futures, Edmonton, Canada
[3]Center for Oil Sands Sustainability, Northern Alberta Institute of Technology, Edmonton, Canada

INTRODUCTION

Tailings are a waste by-product of synthetic crude oil production. They consist of connate (liquids originating from pore space in sedimentary rocks), processed water, sand, silt, clay, residual bitumen and diluent, and inorganic and organic by-products (Lo et al., 2006, Allen, 2008). Tailings may also include organic phenols, naphthenic acids (NA), polycyclic aromatic hydrocarbons (PAH's), naphtha, as well as heavy metals, salts and alkaline substances (Quagraine et al., 2005). There are approximately 830 million m^3 of tailings material in the Lower Athabasca Region of Alberta, covering an area of 176 km^2 (Grant et al., 2013).

Sufficiently consolidating (or de-watering) tailings to allow human and vehicular trafficability is the greatest geo-technical challenges for tailings ponds. As the mature fine tailings (MFT) surface dries, it creates a hydrophobic layer that reduces further subsurface evaporation. This is a primary limitation with many of the de-watering techniques currently employed in the oil sands or under development. In nature, plant roots are designed and are highly effective at the extraction of soil pore water. In principle, plant roots can penetrate the hydrophobic surface and pull moisture from the subsurface of a tailings deposit and transpire to the atmosphere. The use of plants to de-water tailings has shown early promise where a number of plant species have demonstrated survival and persistence on mine tailings both in a greenhouse environment (Silva 1999) and in the field on tailings sands (Woosaree and Hiltz, 2011). However, knowledge gaps still exist with respect to broader use of species native to northern Alberta (Silva, 1999), establishment methods, potential toxicological or nutritional constraints to growing plants on tailings and how to combine plants with natural freeze-thaw cycle (BCG Engineering, 2010) and other dewatering processes employed by the industry such as atmospheric fine drying (AFD) or centrifugation.

The goal of this project was to evaluate the establishment potential and de-watering capacity of native and non-native plant species in MFT after undergoing other dewatering processes. Three trials were conducted to address the following objectives:

1. Evaluate direct seeding in field conditions of a targeted group of plant species (both annual and perennial) previously shown to have reasonable establishment (or significant potential) and growth on oil sands tailings materials. (Trial 1)
2. Test laboratory germination and early growth potential of a broader range of non-native and native plant species on oil sands tailings. (Trial 2)
3. In two contrasting processed tailings: (a) Evaluate two types of inorganic nitrogen-addition on growth and production of plant species grown on oil sands MFT. (b) Determine daily water-use of plants. (Trial 3)

MATERIALS AND METHODS

Trial 1: plot-scale field trial

In June 2015, eight plots (20 x 20 m) each of barley (*Hordeum vulgare* L.), fall rye (*Secale cereal*), slender wheatgrass (*Agropyron trachycaulus*), slough grass (*Beckmannia syzigachne)* and tufted hairgrass (*Deschampsia cespitosa*) were seeded (each species at a rate of 200 seeds m^{-2}) within a 300 x 100 m area within a single AFD pond. In June 2015, a low concentration starter fertilizer blend (Table 1) was applied concurrently with seeding. Urea (46-0-0) was subsequently applied in early August 2015 at a rate of 150 kg ha^{-1} to increase the overall availability of nitrogen. Plant density (to estimate % emergence based on known seeding rates) were assessed in August of 2015 and 2016 by measurement of three 0.5 x 0.5 meter quadrats along a transect within each plot.

Trial 2: greenhouse germination and early establishment

Germination tests were conducted with six agricultural (barley, fall rye, canola (*Brassica napus* L.), flax (*Linum usitatissimum*), sweet clover (*Melilotus officinalis* L.), and alfalfa (*Medicago sativa))*, five perennial native grasses (slough grass, slender wheatgrass, tufted hairgrass, northern wheatgrass (*Agropyron dasystachyum*), and fringed brome (*Bromus ciliatus*)) and four perennial native woody species (Bebb's willow (*Salix bebbiana)*, balsam poplar (*Populus balsamifera*), aspen (*Populus tremuloides*), and green alder (*Alnus viridis*)). Bench top germination and early growth tests were initially performed in shallow trays (5 cm depth), however, the shallow depth resulted in difficulty keeping moisture consistent throughout the study. In addition, application of fertilizer at the onset of the study resulted in algae growth that inhibited plant establishment of species with small-sized seeds. Therefore, this study was subsequently repeated utilizing styrofoam or plastic cups with greater depth (>9 cm) and lesser surface area. Cups were watered to field capacity daily and fertilizer (Table 1) was added only after initial plant germination when individual germinants were > 2 mm in height. Four replicates of each species on two tailings types AFD and centrifuge processed tailings and one control substrate (1:1 sand:peat mixture) were evaluated. Native grasses and native woody plants were grown for 36 days and agricultural plants for 24 days as the agricultural species tended to out-grow their containers beyond the 24 day period.

Germination rates were recorded every second day during the establishment phase (first two weeks). Ongoing survival (or mortality) was tracked throughout the study period. At the end of the trial, shoot dry mass was determined for all surviving plants in each substrate treatment. Comparing shoot dry mass of plants between treatments provided a preliminary indication of growth limitations in plants in response to the tailings chemistry.

Trial 3: greenhouse evaluation of N application, water-use and comparative growth

In order to evaluate the effects of tailings material on seasonal plant establishment, we used one native shrub, pussy willow (*Salix discolor*), and two grass species, fall rye (*Secale cereal*) and slender wheatgrass (*Elymus trachycaulus*). These species had all shown positive performance either in the field study or early establishment trial #2. On November 9, 2015, twenty graminoid seeds were sown into 5 liter-buckets filled with one of two tailings types (AFD and centrifuge processed tailings) or a control treatment in pure silica sand. Germinants were thinned to three individuals per bucket within 3 weeks of establishment. Willow seedlings (dormant 6 month old nursery stock produced spring-summer 2015) were planted into the buckets on December 14, 2015. Two types of N fertilizer (Urea or SuperU, 46-0-0) were also evaluated: SuperU is urea polymer-coated with inhibitors that prevent denitrification thus reducing the loss of N through volatilization, it is however considerably more expensive than conventional urea. Eight replicates of each treatment combination (3 substrates X 2 N addition types X 3 species) as well as a secondary control group (3 substrates, no N addition and no plants) were included in this study for a total of 120 buckets (each bucket contained ~ 5 L of substrate by volume). Plants were initially fertilized with a starter blend (Table 1) and 1.4 grams of N (150 kg ha^{-1}) once the seeds had germinated. A second application of N and one application of monopotassium phosphate (1.02 g per bucket) was added on January 28, 2016 and February 23, 2016, respectively. Plants were watered as needed to ensure moisture was not limiting growth.

Graminoids were destructively harvested at the end of March 2015 and willow at the beginning of May 2015 (as these plants were started later than the graminoids). All aboveground biomass was clipped and three core samples (2 cm diameter X depth of substrate) were taken from each bucket to determine total root biomass (or density). Substrate cores were washed to separate roots and all roots were composited for a single sample per bucket. Above and belowground biomass was oven dried at 70˚C and weighed.

Plant water-use was tracked by weighing buckets daily as well as post-watering until the final week prior to destructive harvesting. This time period represented the maximal growth (and therefore potential water-use); in addition, the water-use scaling per unit dry mass required destructive harvest of the plants. Water-use per unit shoot (leaf + stem) dry mass (mL g^{-1}), per unit leaf dry mass (mL g^{-1}) were calculated for willow and water-use per unit shoot dry mass (mL g^{-1}) was calculated for slender wheat grass and fall rye since these plants have no effective stem or woody material (100% leaves). There was substantial variability in plant size between replicate buckets, as the smallest plants (< 0.5 g in shoot dry mass for willows, < 5.0 g in shoot dry mass for fall rye or slender wheatgrass) transpired very little and the bench scale sensitivity was to four significant digits (necessary given the large mass of tailings), we were not able to adequately quantify water-use on these plants and did not include those samples into data analysis on water-use. These individuals, however, are represented in all other data presentations on growth.

Data analysis

Data was analyzed using R statistical software (R Core Team, 2015). Average germination (G) of each plant species was compared across the substrate treatments (AFD, centrifuge and control) using one-way ANOVA. When significant ($p \leq 0.05$), differences in the average germination percentage among the treatments were compared with a post-hoc Tukey test. A Weibull function was fitted to the cumulative germination percentage for each of the species using the “drc” package in R (Ritz and Streibig, 2005). The “Rmisc” package (Hope 2013) was used to calculate mean and standard errors of germination percentage, and the “ggplot2” package (Wickham 2009) was used to plot mean germination percentages per treatment. Data on physiological parameters were analyzed using a two factor (Soil type x Fertilizer type) randomized complete-block design with the ‘nlme’ package (Pinheiro et al., 2015). Post-hoc comparisons were performed using Tukey contrasts with the lsmeans (Lenth, 2016).

RESULTS AND DISCUSSION

Trial 1: plot-scale field trial

Of the five grass species sown, only 3 species (barley, fall rye and slender wheatgrass) emerged into viable plants. Observed emergence for barley was over 20% in the first year; this species is an annual and did not persist beyond 2015. Emergence of fall rye increased from 2015 (at a mean of 5.7%) to 2016 (at a mean of 23.5%, Table 2). For slender wheatgrass, emergence was similar between years at 3.1 to 4.7% (Table 2). The increase in emergence observed for fall rye is likely attributable to continual germination through the fall period in 2015 as the vegetation assessment was conducted in the middle of August 2015. With the second urea application in August, healthy and vigorous growth of established grasses was observed in September of the same year.

Trial 2: greenhouse germination and early establishment

Agronomic species and native grasses sown in the peat-sand mixture germinated earlier relative to plants in tailings (Figure 1-2). For most of the agronomic and native grass species, plants in control group had significantly higher overall germination rates compared with those in the AFD and centrifuge processed tailings (Tukey, $p < 0.05$, Table 3), with the exception of sweet clover. The earlier germination rate and overall better germination observed in the peat-sand mixture for these species was likely driven by differing osmotic gradients (it was easier for seeds to imbibe water) in the peat-sand substrate compared with tailings. The rate of water uptake in seeds is a key factor driving germination; it is quite plausible that some of seeds were never able to imbibe sufficient moisture from the tailings surface (which dries very quickly). In this case, the microsite condition, whether the seed landed in a slight depression or in a convex position may have been a driving factor for the germination differences. Interestingly, germination rates and overall germination was similar for woody species grown in control substrate and tailings substrate (Figure 3, Table 3). All of the woody species tested had substantially smaller seeds and greater surface area relative to the agronomic species and grasses. For example, fall rye seed weighs in at ~ 25 mg seed^{-1}, slender wheatgrass at 2 mg seed^{-1} while the woody species range from 0.1 – 0.3 mg seed^{-1}. This would have allowed the woody species to imbibe water easily and the water requirement for a small seed would have been much less, allowing for similar initial germination.

Of the germinated seeds, mortality rates of these plants varied substantially by species (Table 3). In general, the native grasses showed very low mortality with comparable rates of mortality between tailings and peat-sand substrates (Table 3). The agronomic species were more variable (Table 3) with no consistent pattern of higher or lower mortality with substrate type. Silva (1999) recognized long ago that native species may be positively suited due to their greater tolerance for adverse conditions. It is known that tailings have some residual toxicity (higher heavy metals concentrations, presence of polycyclic aromatic hydrocarbons) which may affect the early establishment of the plant growth. In addition, young plants are known to be more sensitive to the stress factors such as salinity (Vicente et al., 2004), which is present in tailings. All woody species showed the highest mortality than agronomic and native grass species, which was typically higher on average, in tailings relative to the peat-sand substrate (Table 3). The notable exception was green alder, which showed no difference between substrate types (Table 3) and balsam poplar mortality rates were higher in AFD compared with either centrifuge tailings or peat-sand (Table 3). The higher overall mortality rates seen in the woody species may also be attributable to their small seed size which do not have the carbon reserves with which to develop an extensive root system, therefore, other environmental conditions or initial physiological stresses affect these species more than the larger-seed species (such as the agricultural species or the native grasses tested) which have the carbon reserves to develop a more extensive plant prior to becoming photosynthetically active.

Aside from mortality, overall aboveground shoot mass is another comparative indicator of plant development. On average, all agronomic and native grasses had lower per plant aboveground biomass compared with tailings (Table 4) and centrifuge tailings generally resulted in larger plants (= greater aboveground dry mass) compared with AFD tailings (Table 4). Despite this, two agronomic species (barley and fall rye) and the native slender wheatgrass showed impressive growth on tailings substrates (Table 4). Slender wheatgrass per plant biomass was only significantly different between the peat-sand and AFD substrate (Tukey, $p = 0.0482$). Barley and fall rye were identified as good candidates for tailings sand reclamation in an earlier field study (Woosaree et. al., 2011).

Trial 3: greenhouse evaluation of N application, water-use and comparative growth

The comparative use of two different types of nitrogen (urea or SuperU) did not significantly impact growth or water-use of any of the three species evaluated. The results for this section will therefore focus on impact of substrate (tailings types vs. control (sand) substrate).

Tailings type had a significantly negative effect on shoot dry mass of willow plants (Figure 4a, $F = 4.03$, $p = 0.0304$) compared to sand substrate where shoot dry mass was significantly reduced in centrifuge processed tailings and marginally lower in AFD processed tailings compared with the plants in the control (Tukey, $p < 0.05$). However water use per unit shoot dry mass (mL g^{-1}) or on a per plant basis in willow did not differ among the substrate types. Shoot dry mass production in slender wheat grass plants was significantly reduced in AFD processes tailings (Figure 5c, $F = 10.17$, $p = 0.0003$) but plants in centrifuge tailings showed similar shoot dry mass as sand. Interestingly, water use per unit shoot dry mass (mL g^{-1}) was significantly higher for both tailings substrates compared with the sand (Figure 5c, F=6.21, p=0.0044). There was no significant difference in shoot dry mass (Figure 4b, $F = 0.47$, $p = 0.6283$) or per plant water use (F=2.80, p=0.0824) (Figure 5b,e) for fall rye among the substrates. However, the AFD processed tailings showed significantly lower water-use per unit shoot mass compared with sand (F=3.68, p=0.0418).

Root dry mass was significantly lower in both the AFD and centrifuge processed tailings compared with the control treatments for willow (Figure 4d, $F = 8.57$, $p = 0.0015$), fall rye (Figure 4e, $F = 7.14$, $p = 0.0023$) and slender wheatgrass (Figure 4f, $F = 26.86$, $p < 0.0001$). The effective texture of the tailings substrate is much different from the coarse sand substrate. Although not quantified in this study, it is likely that bulk density was much higher in both tailings substrates compared to the sand.

For the willow and slender wheatgrass, the fact that water-use was comparable (or better) in tailings relative to the sand was an interesting finding and suggests, based on this preliminary study, the plant species tested were not experiencing severe physiological limitations by growing in tailings. Even the fall rye was only significantly lower in AFD treated tailings, plants grown in centrifuge tailings showed comparable water-use to the sand substrate. The aboveground growth results also support this, where fall rye showed no aboveground growth difference in tailings compared with sand. Slender wheatgrass grew similarly aboveground in centrifuge tailings and sand though aboveground growth was significantly less in AFD processed tailings (Figure 4).

Of the three species evaluated, slender wheatgrass showed the most remarkable per plant daily water use. Over 70 mL per plant per day on AFD tailings and over 100 mL per plant per day on centrifuge tailings (Figure 5f). Scaling these values up if 10,000 plants were established per hectare, daily water use (transpiration) could be as much as 1000 L per day. This would be in addition to evaporative surface water loss.

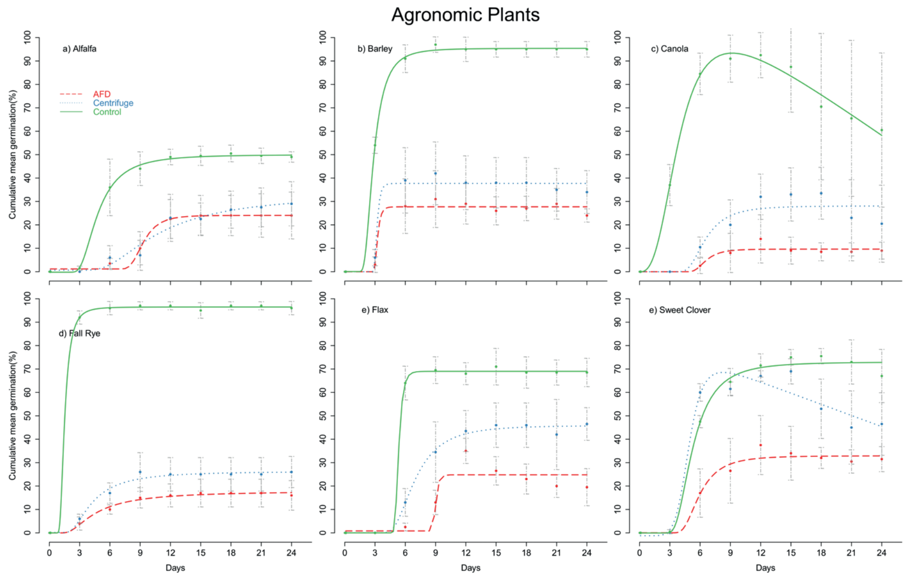

Figure 1. **Trial 2 cumulative mean germination percentages of agronomic plants, alfalfa (a), barley (b), canola (c), fall rye (d), flax (e), and sweet clover (e), during a 24 day period in three different substrate types (AFD processed tailings [red], centrifuge processed tailings [blue] and control [green]) under greenhouse conditions. Error bars represent the means ± SE (n=4).**

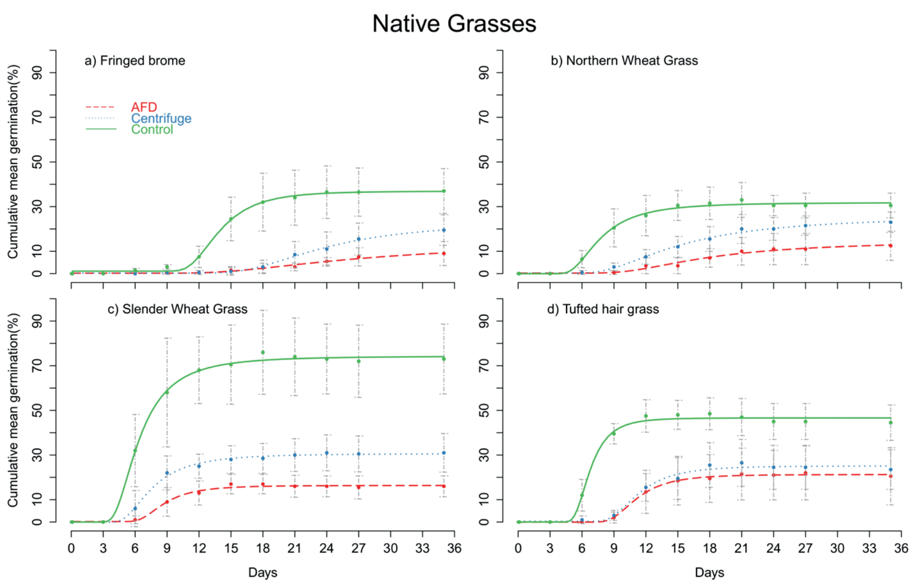

Figure 2. **Trial 2 cumulative mean germination percentages of native grass species, fringed brome (a), northern wheatgrass (b), slender wheatgrass (c), and tufted hair grass (d) during a 36 day period in three different substrate types (AFD processed tailings [red], centrifuge processed tailings [blue] and control [green]) under greenhouse conditions. Error bars represent the means ± SE (n=4).**

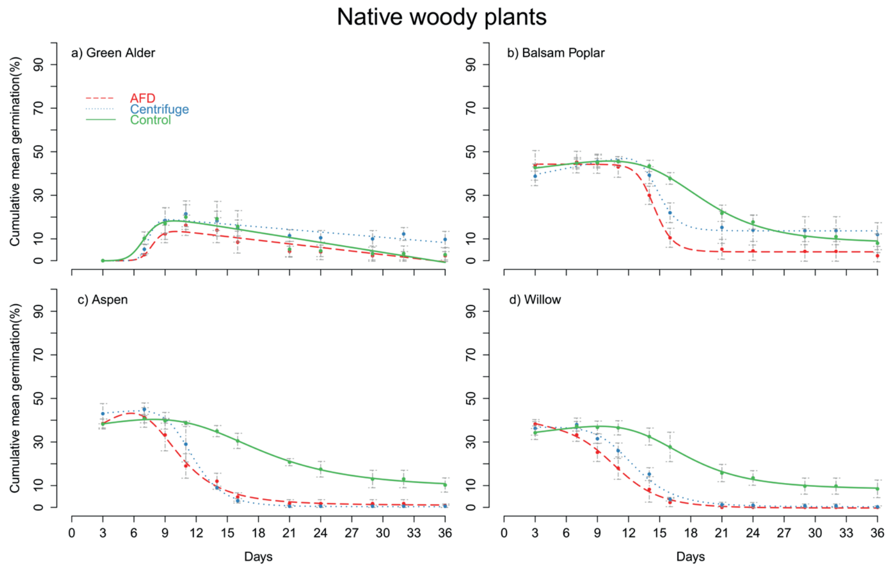

Figure 3. **Trial 2 cumulative mean germination percentages of native woody species, green alder (a), balsam poplar (b), aspen (c), and willow (d) during a 36 day period in three different substrate types (AFD processed tailings, centrifuge processed tailings [blue] and control [green]) under greenhouse conditions. Error bars represent the means ± SE (n=4).**

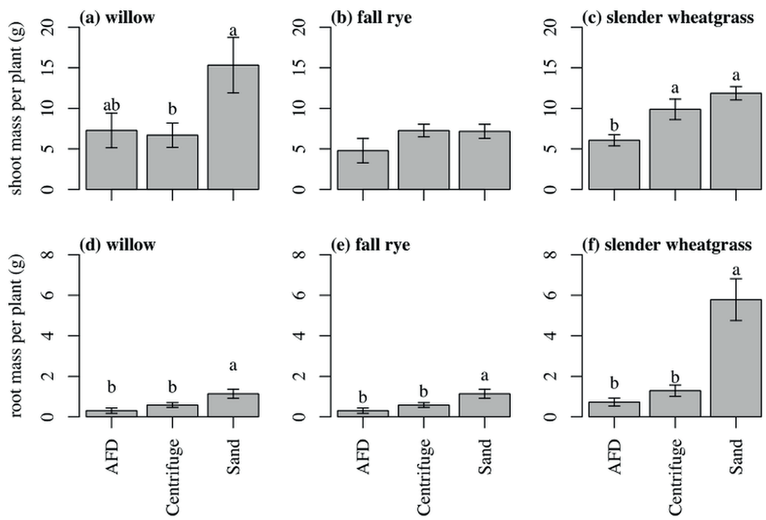

Figure 4. Trial 3 (a-c) shoot dry mass and (d-f) root dry mass for (a,d) willow, (b,e) fall rye and (c,f) slender wheatgrass plants grown in three different substrate types (atmospheric fine drying (AFD) processed tailings, centrifuge processed tailings and sand). Error bars represent the means ± SE (n=9-16) and different letters indicate significant statistical differences with-ANOVA-Tukey's ($p < 0.05$).

Table 1. Composition of starter nutrient blend utilized in field trial #1 and greenhouse trial #2

Element	kg/ha
Nitrogen	29.3
Phosphoic acid (P2O5)	58.5
Potash (K20)	13.5
Sulfur (S)	2.6
Magnesium (Mg)	1.4
Calcium (Ca)	1.8
Iron (Fe)	2.3
Zinc (Zn)	0.5
Organic matter	33.8

Table 2. Trial 1 mean percentage emergent and established (± standard deviation of the mean) plants seeded on an experimental AFD tailings pond in June 2015

Species	2015 (year 1) % emergent and established plants	2016 (year 2) % emergent and established plants
Fall rye	5.7 ± 5.2	23.5 ± 17.0
Slender wheatgrass	4.7 ± 7.2	3.1 ± 2.8
Barley	20.3 ± 13.8	-

Table 3. Trial 2 mean germination, mortality and survival (± SE) of agronomic (alfalfa, barley, canola, flax and sweet clover), native grasses (fringed brome, north wheatgrass, slender wheatgrass, and tufted hair grass) and native woody plants (aspen, balsam poplar, green alder, and Bebb's willow) at the end of early establishment trial in atmospheric fine drying (AFD), centrifuge and 1:1 peat:sand substrate

Substrate type	Agronomic species			Native grass species		
		Germination (%)	Mortality (%)		Germination (%)	Mortality (%)
AFD	Alfalfa	25.5 ± 5.6	1.5 ± 1	Fringed brome	9.0 ± 3.1	0.0 ± 0.0
Centrifuge	Alfalfa	32.0 ± 5.9	3.0 ± 1.9	Fringed brome	20.5 ± 4.3	2.0 ± 3.2
Peat-sand	Alfalfa	53.0 ± 1.7	4.0 ± 0.8	Fringed brome	38.0 ± 6.3	1.2 ± 1.8
AFD	Barley	34.0 ± 7.4	10.0 ± 7.6	Northern Wheatgrass	13.0 ± 4.1	0.5 ± 0.5
Centrifuge	Barley	48.0 ± 9.9	14.0 ± 6.2	Northern Wheatgrass	24.0 ± 3.2	1.0 ± 1
Peat-sand	Barley	98.0 ± 2	3.0 ± 1.9	Northern Wheatgrass	34.0 ± 5	3.5 ± 2.1
AFD	Canola	17.5 ± 4.9	8.5 ± 3.9	Slender Wheatgrass	18.0 ± 2.2	2.0 ± 0.8
Centrifuge	Canola	34.5 ± 6.4	14.0 ± 3.2	Slender Wheatgrass	31.5 ± 5	0.5 ± 0.5
Peat-sand	Canola	93.0 ± 5.7	32.5 ± 15.4	Slender Wheatgrass	79.0 ± 9.5	6.0 ± 2.2
AFD	Fall Rye	17.0 ± 3.4	1.0 ± 1	Tufted Hair Grass	22.5 ± 7.3	2.0 ± 1.2
Centrifuge	Fall Rye	35.0 ± 6	9.0 ± 5.3	Tufted Hair Grass	27.5 ± 5.9	4.0 ± 1.8
Peat-sand	Fall Rye	99.0 ± 1	3.0 ± 1	Tufted Hair Grass	49.0 ± 4	4.5 ± 1.7
AFD	Flax	37.0 ± 3.3	17.5 ± 4.8			
Centrifuge	Flax	52.0 ± 3.9	5.5 ± 3.6			
Peat-sand	Flax	75.0 ± 4.7	6.5 ± 2.9			
AFD	Sweet clover	42.5 ± 3.8	11.0 ± 4.4			
Centrifuge	Sweet clover	73.0 ± 3.3	26.5 ± 8.6			
Peat-sand	Sweet clover	77.0 ± 2.6	10.0 ± 4.2			
	Woody species					
AFD	Aspen	83.5 ± 4.4	82.0 ± 3.6	Bebb's Willow	76.5 ± 2.4	76.5 ± 2.4
Centrifuge	Aspen	90.0 ± 3.4	89.0 ± 3.8	Bebb's Willow	76.0 ± 3.5	75.5 ± 3.9
Peat-sand	Aspen	82.5 ± 1.7	62.0 ± 2.4	Bebb's Willow	76.0 ± 2.7	59.0 ± 5.6
AFD	Balsam poplar	92.0 ± 6.1	87.5 ± 6.4	Green Alder	32.5 ± 5.4	28.0 ± 5.4
Centrifuge	Balsam poplar	93.5 ± 2.4	69.5 ± 8.2	Green Alder	48.0 ± 7.4	28.5 ± 8.1
Peat-sand	Balsam poplar	91.5 ± 2.5	75.5 ± 7.4	Green Alder	43.0 ± 7.2	37.5 ± 7

Table 4. Trial 2 mean aboveground dry mass (± SE) of agronomic (alfalfa, barley, canola, flax and sweetclover), native grasses (fringed brome, north wheatgrass, slender wheatgrass, and tufted hair grass), native woody plants (aspen, balsam poplar, green alder, and Bebb's willow) at the end of early establishment trial in atmospheric fine drying (AFD), centrifuge and 1:1 peat:sand substrate

Substrate type	Shoot dry mass per plant (mg)					
	Agronomic species		Agronomic species / Native grass species		Woody species	
AFD	Alfalfa	52.1 ± 20.3	Sweet clover	71.8 ± 12.8	Aspen	7.1 ± 3.4
Centrifuge	Alfalfa	123.7 ± 73.4	Sweet clover	283.0 ± 50.4	Aspen	6.5 ± 1.4
Peat-sand	Alfalfa	365.8 ± 21.6	Sweet clover	480.0 ± 39.7	Aspen	357.1 ± 58.6
AFD	Barley	755.9 ± 66.2	Fringed brome	14.6 ± 2.9	Balsam poplar	25.6 ± 12.5
Centrifuge	Barley	898.4 ± 62.8	Fringed brome	27.9 ± 4.1	Balsam poplar	255.5 ± 207.0
Peat-sand	Barley	2396.1 ± 165.7	Fringed brome	747.3 ± 128	Balsam poplar	143.3 ± 44.5
AFD	Canola	15.8 ± 3.3	Northern Wheatgrass	29.8 ± 8.3	Bebb's Willow	0 ± 0
Centrifuge	Canola	131.1 ± 55.1	Northern Wheatgrass	70.3 ± 17.3	Bebb's Willow	1.2 ± 0
Peat-sand	Canola	513.6 ± 133.2	Northern Wheatgrass	842.9 ± 52.6	Bebb's Willow	162.8 ± 74.3
AFD	Fall Rye	549.1 ± 66.5	Slender Wheatgrass	858.2 ± 131.4	Green Alder	1.5 ± 0.6
Centrifuge	Fall Rye	750.8 ± 76.1	Slender Wheatgrass	1580.5 ± 187.5	Green Alder	6.2 ± 1.1
Peat-sand	Fall Rye	2161.1 ± 138	Slender Wheatgrass	2693.9 ± 243.9	Green Alder	23.6 ± 14.3
AFD	Flax	366.0 ± 90.4	Tufted Hair Grass	13.7 ± 5.2		
Centrifuge	Flax	650.6 ± 87.9	Tufted Hair Grass	10.9 ± 1.9		
Peat-sand	Flax	1160.6 ± 75	Tufted Hair Grass	1020.8 ± 65.9		

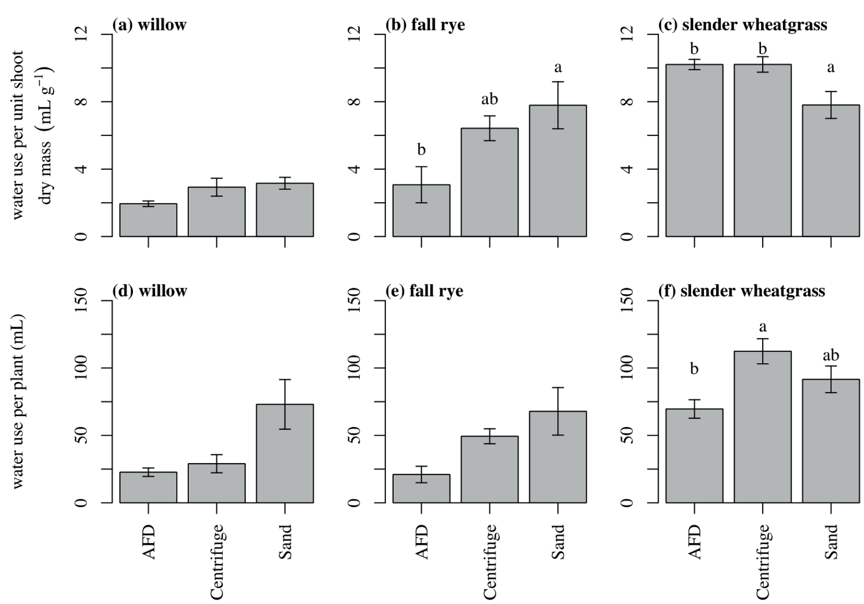

Figure 5. Trial 3 (a-c) daily water-use per unit leaf mass and (d-f) daily water use per plant for (a,d) willow, (b,e) fall rye and (c,f) slender wheatgrass plants grown in three different substrate types (atmospheric fine drying (AFD) processed tailings, centrifuge processed tailings and sand). Error bars represent the means ± SE (n=9-16) and different letters indicate significant statistical differences with-ANOVA-Tukey's ($p < 0.05$).

ACKNOWLEDGEMENTS

We would like to acknowledge the support of Shell Canada and the many helpful and insightful discussions provided by their staff throughout this trial.

REFERENCES

Allen, E.W., 2008. Process water treatment in Canada's oil sands industry: I. Target pollutants and treatment objectives. *Journal of Environmental Engineering and Science*, *7*(2), pp.123-138.

BCG Engineering Inc., 2010. Oil sands tailings technology review. Oil Sands Research and Information Network, University of Alberta, School of Energy and the Environment, Edmonton, Alberta. OSRIN Report No. TR-1. 136pp.

Fellet, G., Marchiol, L., Delle Vedove, G. and Peressotti, A., 2011. Application of biochar on mine tailings: effects and perspectives for land reclamation. *Chemosphere*, *83*(9), pp.1262-1267.

Grant, J., Angen, E., Dyer, S., 2013. Forecasting the impacts of oilsands expansion. Pembina Institute. Retried online October 5, 2016 at https://www.pembina.org/reports/oilsands-metrics.pdf

Hope, R.M., 2013. Rmisc: Ryan miscellaneous. R package version 1.5.

Hothorn, T., Bretz, F. and Westfall, P., 2008. Simultaneous inference in general parametric models. *Biometrical journal*, *50*(3), pp.346-363.

Lo, C.C., Brownlee, B.G. and Bunce, N.J., 2006. Mass spectrometric and toxicological assays of Athabasca oil sands naphthenic acids. *Water research*, *40*(4), pp.655-664.

Pinheiro, J., Bates, D., DebRoy, S. and Sarkar, D., 2014. R Core Team (2014) nlme: linear and nonlinear mixed effects models.

Quagraine, E.K., Peterson, H.G. and Headley, J.V., 2005. In situ bioremediation of naphthenic acids contaminated tailing pond waters in the Athabasca oil sands region—demonstrated field studies and plausible options: a review. *Journal of Environmental Science and Health*, *40*(3), pp.685-722.

Renault, S., Qualizza, C. and MacKinnon, M., 2004. Suitability of altai wildrye (*Elymus angustus*) and slender wheatgrass (*Agropyron trachycaulum*) for initial reclamation of saline composite tailings of oil sands. *Environmental Pollution*, *128* (3), pp.339-349.

Ritz, C. and Streibig, J.C., 2005. Bioassay analysis using R. *Journal of statistical software*, *12*(5), pp.1-22.

Rowland, S.M., Prescott, C.E., Grayston, S.J., Quideau, S.A. and Bradfield, G.E., 2009. Recreating a functioning forest soil in reclaimed oil sands in northern Alberta: an approach for measuring success in ecological restoration. *Journal of environmental quality*, *38* (4), pp.1580-1590.

Silva, M.J., 1999. *Plant dewatering and strengthening of mine waste tailings* (Doctoral dissertation, University of Alberta).

Team, R.C., 2014. R: A language and environment for statistical computing. R Foundation for Statistical Computing, Vienna, Austria. 2013.

Vicente, O., Boscaiu, M., Naranjo, M.Á., Estrelles, E., Bellés, J.M. and Soriano, P., 2004. Responses to salt stress in the halophyte *Plantago crassifolia* (Plantaginaceae). *Journal of Arid Environments*, *58* (4), pp.463-481.

Wickham, H., 2009. *ggplot2: elegant graphics for data analysis*. Springer Science & Business Media.

Woosaree, J., Hiltz, M. and Innovates, A., 2011. Cover Crop Program for Tailings Sand Stabilization.

DEWATERABILITY OF TAILINGS FROM A HYBRID BITUMEN EXTRACTION PROCESS

Feng Lin[1], Yuming Xu[1], Tadeusz Dabros[1] and Richard Nelson[2]
[1]Natural Resources Canada, CanmetENERGY-Devon, Canada
[2]Alberta Innovates, Edmonton, Canada

ABSTRACT

This communication reports on an experimental investigation of the dewaterability of tailings from an alternative extraction technology ─ aqueous/non-aqueous hybrid bitumen extraction (HBE) process. A laboratory centrifuge−based technique was used to characterize the settling and consolidation behaviors of suspended solids generated from the standard aqueous process and the hybrid process. The instantaneous sediment height at a given centrifugal acceleration and equilibrium consolidation height were measured as functions of time and acceleration, respectively. By fitting the measurements to an analytical consolidation model, compressive yield stress – an important suspension property in compression – was obtained as a function of solids weight fraction. It was shown that solids in the tailings from the hybrid process had higher settling rates than those from the standard aqueous process and that less time was required for sedimentation to reach equilibrium at a given g-force. Interestingly, for each sedimentation curve, the settling velocity of the sediment interface increased initially with time, a significant departure from classic Kynch theory, which predicts a constant initial setting rate. The data also suggest that the suspensions from the HBE are more compressible, as indicated by higher final compressed solids weight fraction for a given yield stress.

INTRODUCTION

Accumulation of tailings stored in ponds is a huge liability for the oil sands industry and a serious risk to the environment. Meeting the minimum target specified by the Alberta Energy Regulator (AER) for consolidated oil sand tailings is still very challenging for the oil sand companies under the current technology development paths. Currently, the two most common technologies used in commercial-scale operations to treat oil sand tailings are consolidated tailings (CT) and paste technology (PT). The use of inorganic salts, e.g. gypsum, in the CT process appears to be effective and affordable, but raises a concern that multi-valent cations, e.g. calcium, in recycled water can significantly depress bitumen recovery in the extraction process. The use of polymeric flocculants ─ mainly polyacrylamide (PAM) ─ in PT rapidly thickens fresh fine tailings; however, the sediments formed retain a high degree of fluidity such that trapped water in the flocs cannot be easily drained or removed. Therefore, in addition to developing a new generation of chemicals to achieve more effective densification, it seems prudent to proactively reduce or ultimately end tailings accumulation in ponds by changing the process of bitumen extraction.

Recently, an aqueous-nonaqueous hybrid bitumen extraction (HBE) process was reported to show promise as an alternative to the currently used commercial Clark hot water extraction (CHWE). In HBE, a fraction of solvent already applied in froth treatment was distributed upstream to soak the mined ore prior to slurry conditioning, and then the water-based process was applied as usual, but at ambient operating conditions and without caustic addition (Harjai et al. 2012, Lin et al. 2016). It was demonstrated that HBE is a robust process for obtaining high bitumen recovery, regardless of ore grade**.** The use of HBE instead of CHWE would eliminate the need to heat water and maintain high-temperature flotation facilities, which could significantly reduce energy consumption and greenhouse gas emissions per barrel of bitumen produced. Importantly, HBE is easily integrated into the facilities currently used for the commercial CHWE process.

Since no caustic is required for the HBE process, it is hypothesized that HBE would potentially ease the challenges of managing oil sand tailings by keeping away from the negative impacts of caustic on the formation of stable dispersions of clays, as in the commercial aqueous extraction process. Our objective in this communication was to prove this hypothesis. To this end we compared the settling and consolidation behaviors of fine tailings generated during regular aqueous extraction with those of tailings generated by the hybrid process.

MATERIALS AND METHODS

Materials

Three Athabasca oil sand ores were used: OS1, OS2, and OS3. Based on their relative extraction performance, OS1, OS2, and OS3 were classified as poor-, medium-, and good-processing ores, respectively. In the preparation of tailings samples, simulated process water (SPW) was used, which contained 25 mM NaCl (>99% purity), 15 mM $NaHCO_3$ (99.9% purity), 2 mM Na_2SO_4 (99% purity), and 0.5 mM $CaCl_2$ (anhydrous, 4-20 mesh) in deionized water. The pH was 8.1±0.1. In a few experiments a dilute solution of sodium hydroxide (Fisher Scientific) was added to the SPW to adjust its pH to 9.0. Organic solvents including *n*-pentane (C5), *n*-hexane (C6), *n*-heptane (C7), and toluene purchased from Fisher Scientific (ACS grade) were used as received.

Tailings sample preparation

Tailings samples from HBE for the dewatering analysis were generated by bench-scale bitumen extraction tests using a 1.2-L batch extraction unit (BEU). The HBE test protocol was modified version of what was reported previously (Harjai et al. 2012, Lin et al. 2016). In the first step, a desired amount of a solvent was mixed uniformly into the oil sand ore by the tumbling action of a roller. Depending on the ore processability, the quantity of solvent added was 1 wt% to 3 wt% based on the mass of the ore sample, corresponding to about 10 wt% to 30 wt% of bitumen in the ore, in order to achieve the optimal bitumen recovery and quality.

After 30-min tumbling, the soaked oil sand ore (approximately 500 g) was quickly transferred to the BEU where SPW (about 200 g) was added to make a slurry at the desired flotation temperature. The temperature was kept constant by a water jacket connected to a temperature-controlled bath. After the slurry had been conditioned for 20 min, a second amount of SPW (about 850 g) and air were introduced simultaneously. The froth was collected after 15 min of flotation. After froth collection, the remaining suspension, which included most of the solids and water and trace amounts of bitumen and solvent, was ejected from the bottom of the BEU as the extracted oil sand tailings. Samples were taken to study their dewatering behaviors. All the hybrid BEU tests were conducted at 20^{o}C without caustic addition. The HBE tailings samples are marked as 10% to 30% solvent (scaled by bitumen mass), 20^{o}C, pH 8.1 in the figures that follow. For comparison, tailings from the standard water-based process at 50^{o}C with and without caustic addition were also generated and are denoted as 0% solvent, 50^{o}C, pH 9.0, or pH 8.1, respectively. According to Dean-Stark analysis of the collected bitumen froth, the tailings composition from standard aqueous extraction and HBE were similar for each ore: about 28.0% solids and 71.5% to 71.8% water as well as trace amounts of unrecovered bitumen (~0.2% to 0.5%).

Characterization of tailings dewatering

A laboratory-scale centrifuge technique (LUMiFuge stability analyzer) was used to characterize the sedimentation-consolidation behaviors of the suspended solid particles in the tailings. In this technique, parallel near infrared (NIR) light illuminates the entire sample cell and transmission profiles (i.e. transmitted light intensities at different radial positions) can be documented in such a way that changes in the height of the solids/water interface (i.e. sediment height) are tracked in situ. In this study, tailings samples were placed into cylindrical, transparent, flat-bottomed glass tubes for centrifugal settling and consolidation. The initial heights of the tailings suspensions were set to similar values. Settling experiment was carried out at a given centrifuge speed (i.e. a given g-force), while consolidation experiment conducted at various centrifuge speeds generating different dynamic g-forces, respectively. All the tailings dewaterability tests were conducted using the identical procedure at room temperature. The instantaneous sediment height was measured as a function of time, from which the settling rate of suspended particles was derived.

As illustrated in Figure 1, the equilibrium sediment height (H_{eq}) against acceleration (g) profile was obtained using a multi-speed centrifuge method. By fitting the data to an analytical consolidation model, compressive yield stress $P_y(\phi)$, an important material property of suspension in compression, was obtained as a function of solids weight fraction (ϕ). The details of this consolidation theory and the governing equations have been described elsewhere (Buscall and White 1987, Green et al. 1997).

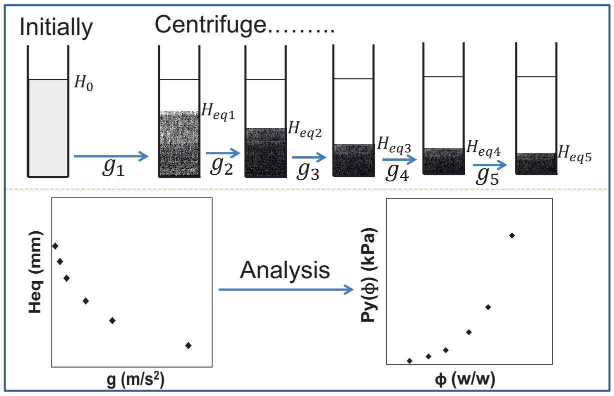

Figure 1. Schematic of multi-speed centrifuge technique to obtain compressive yield stress

RESULTS AND DISCUSSION

The effect of solvent dosage and type on the *sedimentation* speed of tailings samples generated from hybrid and normal aqueous processes at a fixed acceleration is described first, followed by a discussion on *consolidation* phenomena of these systems.

Sedimentation

Typical quantitative descriptions of instantaneous sediment height as a function of sedimentation time for the tailings samples are shown in Figure 2. Here, the centrifuge speed was fixed at 500 rpm, corresponding to 355 m/s^2 of acceleration in this system. Under this enhanced acceleration, the sedimentation tests ran much faster than when performed in a test tube at 1 g. For a given tailings sample, sedimentation ranking was completed in hours instead of weeks or months. While the initial heights of tailings samples were similar, the changes of sediment height are normalized by the initial height of each sample. As can be seen in Figure 2, and especially in the magnified view, at a given condition (i.e. the same curve symbols) the initial movement of the sediment interface was not linear. Instead, the movement of the sediment/water interface was initially slow, then increased, and finally plateaued at zero when the interface reached its equilibrium value. The nonlinear initial settling velocity observed for all the tailings samples in this study was in contrast with what the well-known Kynch theory of sedimentation predicts, that is a constant initial settling rate (Kynch 1952, Concha and Bustos 1991). The settling rate was found to be higher for tailings from ambient HBE than for those from the higher-temperature standard aqueous process, thus reducing the time required for sedimentation to reach equilibrium for a given ore.

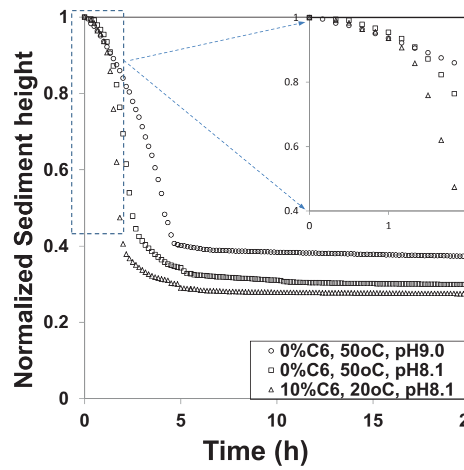

Figure 2. Normalized sediment height as function of sedimentation time at a given centrifuge speed (i.e. acceleration) for ore OS3

For more precise comparison, the normalized average settling speed (R_{ave}) is defined in Figure 3 by the following equation:

$$R_{ave} = \frac{\left(\frac{H_i - H_{eq}}{H_i}\right)}{t_{eq}} = (1 - NH_{eq})/t_{eq}$$

Here, H_i and H_{eq} are the initial and equilibrium sediment heights, respectively. NH_{eq} and t_{eq} are normalized equilibrium sediment heights and the minimum time required for the settling to reach equilibrium at a fixed acceleration, respectively.

Figure 4 summarizes the average settling rates of tailings from the HBE process for the three grades of ore at identical settling conditions but with different ratios of solvent to ore; behaviour of aqueous tailings are shown for comparison. Regardless of ore characteristics, it is obvious that, for the same ore, the settling rate of solids in tailings suspension from the HBE process was far more rapid than that from the caustic aqueous process. The particles took less time to attain the zero-velocity state (i.e. equilibrium sediment height) for the HBE tailings of the same ore at a given g-force. The significant improvement in settling rate for the hybrid tailings could be attributable to the impacts of not only being a non-caustic process, but also due to the lower process temperature. Although ore-dependent, the sedimentation velocity for non-caustic extraction with warm water approximately intermediate between those for non-caustic/ambient HBE and the caustic/warm water process.

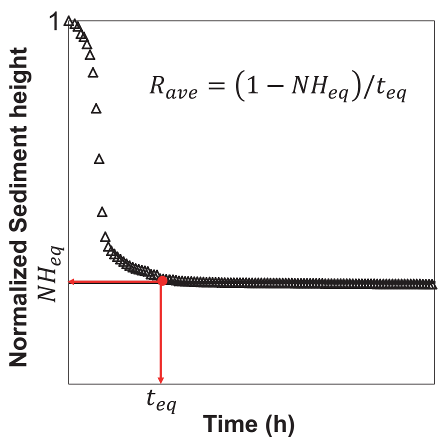

Figure 3. Illustration of calculating average settling rate (R_{ave})

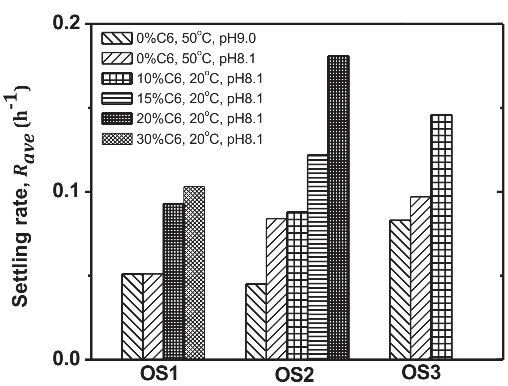

Figure 4. Effect of solvent dosage (scaled by bitumen mass) for each ore (OS1, OS2, OS3) on settling rate at a given acceleration. Tailings generated by the warm-water process with caustic addition were used as a reference.

In addition to improving the settling rate, HBE also led to enhanced tailings densification for a given acceleration. Figure 5 shows that HBE produced a lower equilibrium sediment height than the caustic aqueous process for the same ore.

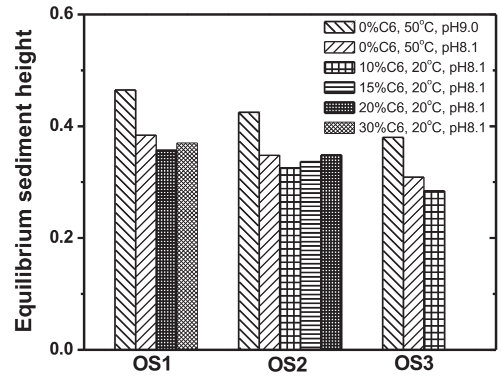

Figure 5. Effect of solvent dosage (scaled by bitumen mass) for each ore (OS1, OS2, OS3) on equilibrium sediment height at a given acceleration

To evaluate the role of solvent type in improving average settling rate, the sedimentation tests at fixed centrifugal acceleration were examined using OS1. Figure 6 shows that at a given solvent dosage for soaking the ore, different solvents, including C5 to C7 and toluene, gave very similar solids sedimentation rates and equilibrium sediment heights in the HBE tailings suspensions.

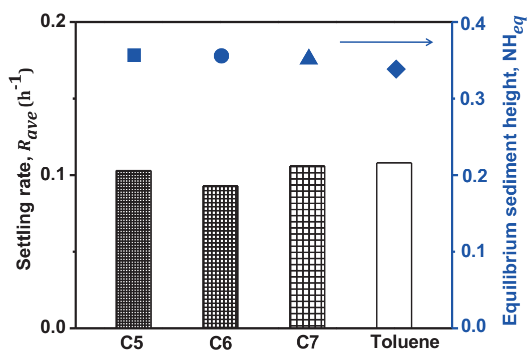

Figure 6. Settling rates (columns) and equilibrium sediment heights (blue symbols) for HBE tailings using different solvents. Solvent dosage to OS1 was 20% of the bitumen mass.

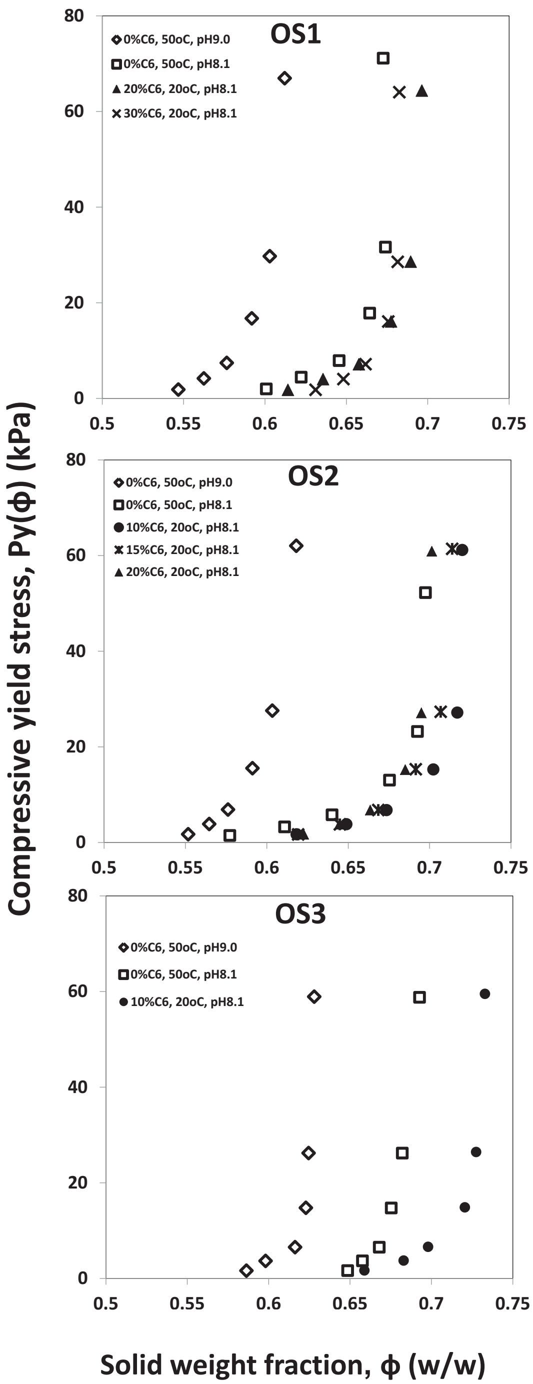

Figure 7. Effect of solvent dosage (scaled by bitumen mass) for each ore (OS1, OS2, OS3) on compressive yield stress of the tailings in the ambient HBE process as a function of solids weight fraction. Tailings generated by the warm-water process with caustic addition are used as a reference sample.

Consolidation

Benefits of non-caustic and ambient HBE processes. The data in Figure 7 suggest that, regardless of the ore source, suspensions from HBE without caustic addition appeared to be more compressible, as indicated by higher final compressed solids weight (or volume) fraction at a given yield stress than those from the caustic process. For instance, about 60 kPa of compression stress was sufficient to compress the OS2 tailings from the hybrid process from the initial value of about 0.28 to the final 0.71 of solids weight fraction (w/w), in contrast to the final 0.61 w/w for the tailings from the warm-water-based method with caustic addition. The origins of such consolidation enhancement for the hybrid process appear to be ore-dependent: For ores OS1 and OS2, caustic addition was the main factor as indicated by the nearly overlapping consolidation curves among the tailings from the warm-water process without caustic and the HBE process. However, temperature also played a significant role for ore OS3.

It is interesting to note that at identical conditions (e.g. same solvent dosage and yield stress), the ranking of ore on the basis of tailings consolidation ability was OS3 (a high-processing ore) > OS2 > OS1 (a low-processing ore). As shown by the same symbol points (from top to bottom) in Figure 7, for example, the curves of OS1 to OS3 tailings compared to the standard water-based process were shifted to higher solids weight fraction at a given yield stress.

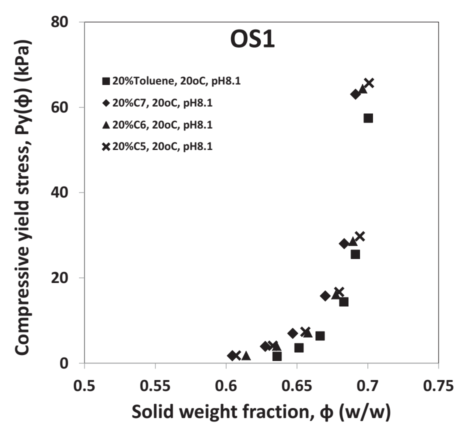

Figure 8. Compressive yield stress of the tailings as a function of solids weight fraction for HBE tailings using different solvents. Solvent dosage to OS1 was 20% of the bitumen mass.

Effect of solvent dosage. Results presented in Figure 8 indicate a negligible effect of solvent type on the consolidation behavior of OS1 tailings when the same amount of solvent was added in the lab-scale hybrid bitumen flotation tests.

CONCLUSIONS

Single and multi-speed centrifuge techniques were developed to study the dewatering of solid particles in tailings samples. The extraction tailings from three ores of different processabilities were used to examine the benefits of a novel hybrid bitumen extraction (HBE) process, not only on sedimentation but also on consolidation of the tailings. Soaking of these three ores with 10-30% solvent on bitumen, using pentane, hexane, heptane, or toluene, in the ambient HBE process significantly enhanced both sedimentation rate and the final compressed solid weight fraction at a given yield stress as compared to the commercial aqueous/caustic extraction process.

ACKNOWLEDGEMENTS

This work was financially supported by the Government of Canada's interdepartmental Program of Energy Research and Development (PERD) and Alberta Innovates (AI). The authors thank Mr. Nathanael King for his support in generating about half of the tailings samples by batch extractions.

REFERENCES

Buscall, R.; White, L. R. 1987. The consolidation of concentrated suspensions. Part 1: The theory of sedimentation. Journal of Chemical Society Faraday Transaction, 1: 873-891.

Concha, F.; Bustos, M. C. 1991. Settling velocities of particulate systems, 6. Kynch sedimentation processes: Batch settling. *International Journal of Mineral Processing*, 32: 193-212.

Green, M. D.; Eberl, M.; Landman, K. A. 1996. Compressive yield stress of flocculated suspensions: Determination via experiment. AICHE Journal, 42: 2308-2318.

Harjai, S. K.; Flury, C.; Masliyah, J.; Drelich, J. and Xu, Z. 2012. Robust aqueous−nonaqueous hybrid process for bitumen extraction from mineable Athabasca oil sands. *Energy Fuels*, 26: 2920-2927.

Kynch, G. J. 1952. A theory of sedimentation. *Transactions of the Faraday Society*, 48: 166-176.

Lin, F.; He, L.; Hou, J.; Masliyah, J. and Xu, Z. 2016. Role of ethyl cellulose in bitumen extraction from oil sands ores using an aqueous−nonaqueous hybrid process. *Energy Fuels,* 30: 121-129.

IMPROVING SCROLL DECANTER CENTRIFUGE EFFICIENCY BY PREFLOCCULATION OF FEED

Alebachew Demoz
Natural Resources Canada, CanmetENERGY, Devon, Canada

ABSTRACT

Industrial separation of fluid fine tailings (FFT) by scroll decanter centrifuge (SDC) produces a paste containing 52–56% solids (w/w). However, in order to clarify the centrate for materials such as FFT, which contain particles 2 μm in size and smaller, the use of flocculant is required. Accordingly, the mechanism in the centrifuge is flocculation followed by sedimentation under the influence of the applied G-force. In this work we test the effect of preconditioning the feed so that flocculation occurs before it enters the centrifuge.

Preconditioning in this work consisted of injecting flocculant solutions at the inlets of 1-inch KMS™ and Koflo™ inline static mixers. Centrifuge performance was evaluated with and without preflocculation using 23% (w/w) solids FFT feed in which 90% of particles were smaller than 9 μm. Operating conditions included steady flow rate, flocculant dosage 1100 ppm (solids basis), 14.5 rpm scroll differential speed, and varying G-force up to 1500G. The minimum G-forces to achieve the industry acceptable separation benchmarks of centrate solids < 1% (w/w) and fines capture rate >97% were 750G without and 400G with preflocculation. Power consumption of the centrifuge, as expected, was directly proportional to the G-force, and savings in power due to preflocculation amounted to 47%. The power expenditure for the preflocculation process was < 2% that of the centrifuge. Preflocculation also increased SDC capacity by up to 50% volumetric flow rate.

Operating at low G-force reduces wear and downtime of the high-capital-cost SDC as well as noise exposure for the operators.

INTRODUCTION

Background

All of the current commercial restoration technologies for managing the oil sands mature fine tailings (MFT), also known as fluid fine tailings (FFT), start with flocculation of the suspended fine solids to form larger and denser aggregates to make them amenable to subsequent dewatering processes. After flocculation, the following methods are in use or are favored by the industry for final tailings disposal: thin-lift drying, rim ditch dewatering, water capped MFT lakes, and scroll decanter centrifugation (1). Thin-lift drying relies in part on evaporation for consolidation in addition to the release of overflow water at the instant of discharge. Rim-ditch dewatering capitalizes on the self-weight compression of deep pit deposits and continuous drainage of the release water and any runoff through channels dug on the surface of the deposit. A water capped FFT lake is a concept in which fresh and process water of at least five meters in depth caps deposits of either untreated or treated FFT. The concept applies provided there is no mixing between the cap water and the underlying tailings deposit. Over time, the submerged FFT is expected to release water to form a denser, more stable sediment. During the intermediate period and in its final form, the water capped lake is projected to develop a biologically active, self-sustaining ecosystem. Syncrude Canada has been running a near commercial scale water capped MFT pilot test lake (1).

The scroll decanter centrifuge, SDC, separates the fine solids by the principle of sedimentation, exploiting differences in the specific gravities of the solids and water. The primary separation mechanism by SDC is similar to that of the settling tanks but the sedimentation rate is enhanced by spinning the bowl to increase the centrifugal acceleration up to several thousand times that of the gravitational acceleration. At high bowl rotation speeds, the larger and denser particles migrate outwards from the centre axis and onto the bowl wall, while the liquid occupies the inner volume near the centre axis of the centrifuge. Accumulation of the denser flocculated material at the bowl wall creates a mass of solids having reduced water content, referred to as cake, and a watery inner core called centrate. The cake is scraped to one end of the centrifuge bowl by a concentric screw-scroll, while the centrate makes its exit over a weir. Of the industrial dewatering technologies in use, SDC produces the most highly dewatered fine tailings waste at the moment of separation. The cake solids content from commercial separation of oil sand FFT ranges from 52% to 56% (w/w). In this context, the SDC provides a head start towards creating stackable fine waste solids over the other oil sand tailings management methods.

The horizontal SDC is widely used in the chemical and processing industries to separate materials based on specific gravity, spg, differences (2-5). It is particularly easy to maintain, can be operated automatically, and needs no consumable replacement parts such as filter cloths. The steady scrolling out of the solids from the centrifuge bowl enables continuous processing of suspensions over a wide range of flow rates. As a result, the SDC frequently finds application in minerals solids speciation and waste water sludge treatment, and also broadly in the food, medicine, and chemical industries. Other solid-liquid separation technologies, including belt-filter press centrifuges and traditional filtration have inadequate capacities to handle the vast inventory of FFT and are constrained because of the low permeability and blockage of the filter medium (fouling) by the fine solids.

The SDC can clarify feeds containing particles having settling rates from 1.5 to $15*10^{-4}$ cm/s at moderate bowl rotation speeds. However, particles around 2 μm in size and smaller cannot be collected without the addition of flocculating agents (6). As a significant fraction of the solids in the oil sand tailings containment ponds is less than 2 μm in size, the use of flocculants is absolutely necessary. Field observations and studies confirm that there are combinations of mixing time and mixing intensity, corresponding to the disposal method, that yield optimally flocculated FFT (7-8).

The options for introducing flocculant solution to the SDC are: 1- at the centrifuge feed inlet, 2- at the feed acceleration zone, 3- in the bowl area identified as the pool, or 4- into the line transporting the FFT. The literature does not recommend any particular addition method as there are some instances where injecting the flocculant solution into the machine is claimed to improve performance, while some operators have reported improved performance when the flocculant is injected into the feed pipe of the centrifuge (9). The present work tries to address the systematic effect of the flocculation step on FFT separation by SDC, considering the location of the chemical addition as a possible factor. In parallel, the study examines the effect of feed preconditioning and, more precisely, pre-flocculation, on the power consumption by the SDC. Reducing the power consumption and increasing the feed throughput of the SDC provide strong incentives to examine feed preconditioning effects that could lead to reduced environmental impact, lower power and maintenance costs, as well as longer allowable shift hours for operators because of reduced machine noise.

MATERIALS AND METHODS

Materials

Referring to Table 1, the particle size distribution (PSD) of the solids in the FFT obtained from one northern Alberta oil sand producer for this work is similar to that of another batch sample reported earlier (7). Sedigraph measurements show that 60% and 98% (w/w) of the solids were smaller than 2 μm and 44 μm, respectively. Methylene blue titration of the solids after Dean-Stark extraction gave 12.73 meq per 100 g solids, indicating that the MFT solids were very high in clay content, as this translates to 91% clay content using conventional comparisons (10-11).

Table 1. Basic properties of the FFT suspension

Solids (wt%)	Dean-Stark analysis			Sieve PSD	
Total solids wt%	Bitumen (wt%)	Water (wt%)	Mineral (wt%)	- 45 μm (wt%)	sand-to-fines ratio
37.23	2.72	61.29	35.86	98.83	0.04
Methylene blue titration of Dean-Stark minerals					
MBI (meq/100 g solids)	MB # (mL MB/100 g solids)			Clay (wt%)	
12.73	2121.21			91.19	
Sedigraph PSD after Dean-Stark extraction of MFT (wt%)					
-45 μm	-22 μm			-2 μm	
98.3	96.8			59.7	

A high-molecular-weight, partially charged anionic polyacrylamide commercial macromolecule was used as flocculant. The flocculant solution concentration was 0.2% (w/w). The flocculant dosage (dry FFT solids basis) was 1100 ppm. Gypsum was added to the feed while in the retaining tank at 1.0 kg per ton of FFT solids. Municipal water from the North Saskatchewan River was used to prepare feed and flocculant solutions. The ion concentrations of the water were inconsequential to the separation process.

Methods

Process units, flow rate and pressure drop measurements, pump controls, and data acquisition have already been described (7). Figure 1 is a schematic of the separation process setup. A GEA SDC (model CD205, Westfalia Separation GmbH, Oelde, Germany) was used. The bowl drive uses a 7.5-kW electric motor coupled by belts. A 1.5-kW electric motor drives the scroll via a gearbox. These WEG™ electric motors are located on the cone side of the centrifuge [Figure 2]. The bowl speed of the centrifuge can reach 5500 rpm while the differential scroll speed, $\Delta\omega$, spanned the range 14.5 rpm < $\Delta\omega$ < 27 rpm. Each motor had its own variable frequency drive (model ACS800, ABB™, New Berlin, WI, USA). The diameters of the SDC bowl and cone are 200 and 120 mm, respectively, where the beach angle is 10°. The tests were conducted at a neutral pool level using a weir plate 120 mm in height. The weighted sound level of the operating centrifuge was measured by a noise meter (model NM103, NoiseMeters Ltd, Berkeley, MI, USA).

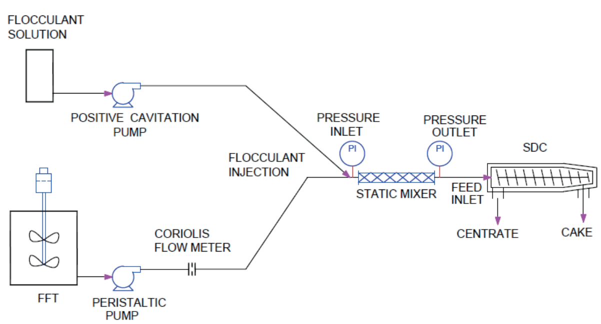

Figure 1. Schematic of the SDC separation process

Combinations of Chemineer-Kenics KMS™ and Koflo 275™ commercial stainless steel static mixers were utilized to mix the FFT and flocculant to examine the preconditioning effect on FFT separation by SDC (7). The inline static mixers and the rest of the pipeline were all 1-inch in diameter. For preflocculation, the flocculant solution was injected at the centre line of the 1-inch diameter pipe, as close to the static mixer inlet as possible to ensure rapid mixing and limit the flocculation to the action within the static mixers.

SDC separation performance is based on the centrate clarity, mainly solids concentration in centrate, and the rate of fines capture. Fines capture rate is the recovery of the total fines in the feed as a mass of solids in the cake:

$$Fines\ capture\ rate(\%) = \frac{x_C}{x_f} * \frac{(x_f - x_{Ce})}{(x_C - x_{Ce})} * 100 \quad \text{(eq.1)}$$

where, x_f, x_C, and x_{Ce} are the solid fractions in the three streams of material: feed, cake, and centrate, respectively. The solids concentration was determined gravimetrically using a Smart Machine model 907990 microwave (CEM corp. Matthews, NC, USA). The total solids content of the wet cake was also determined gravimetrically by drying the sample in an aluminum dish at 100°C overnight. The fines capture rates reported are the means of triplicate centrate samples and the average of duplicate cake samples.

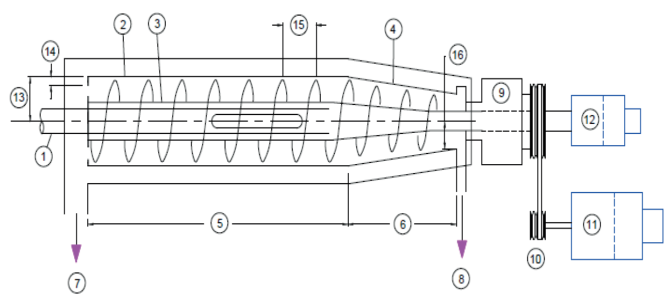

Figure 2. Schematic showing the principal parts of the SDC: 1-feed inlet, 2-bowl, 3-scroll, 4-cone, 5-pool zone, 6-beach, 7-centrate, 8-cake, 9-gear box, 10-belt, 11-bowl motor, 12-scroll motor, 13-bowl radius, 14-pool depth, 15-pitch length, 16-cone radius

RESULTS AND DISCUSSION

The SDC removes water mechanically using the centrifugal field effect produced by the bowl rotation. There are inevitable power losses by different components of the system that may be viewed as waste. Only part of the supplied power is used for the actual solid-liquid separation. SDC operation was therefore explored to identify ways to reduce the power consumption associated with ancillary processes while retaining comparable throughput and benchmark separation efficiencies. The machine variables, which refer to the centrifuge motors, bowl diameter, length, beach angle, etc., are decided upon acquisition of the equipment and are likely selected from what manufacturers supply (12). Plant engineers have to decide the operating conditions to get the best separation performance for the particular materials to be processed.

The SDC cannot clarify feeds such as MFT that contain particles around 2 μm in size without the addition of flocculating agents. The initial process in the bowl is therefore flocculation followed by sedimentation under the influence of the applied G-force. This consideration forms the basis for supplanting flocculation in the SDC by flocculation outside the centrifuge, a process referred to as feed preflocculation. The core objectives of this work are to examine preflocculation effects on power consumption and separation efficiency of the SDC while, at the same time, clarifying ambiguities concerning flocculant injection locations.

The main power-consuming processes within the SDC can be broken down into acceleration of the rotating assembly, feed acceleration, cake transport, windage, and power transmission losses by friction (2,3,6,13-14). The analysis (breakdown) of power consumption is usually established through tests done at different rotation speeds utilizing a specific centrifuge. At the same time, power losses in the various parts of the centrifuge have well-known general correlations with bowl rotation speed and are discussed below to substantiate the test results and show how operating the SDC at lower G-force reduces the environmental impact and operating cost of the separation process.

Feed acceleration: The feed stream is accelerated within the hub of the scroll as it arrives at the centrifuge pool. Without this acceleration, turbulence would be created that could re-suspend settled solids and reduce centrate clarity. The total power required to bring the feed material up to the bowl speed is given by (2-3,13-14):

$$P_{FA} = Q\rho_f x_f \omega^2 \left[r_C^2 + r_L^2\left(1 - \frac{1}{x_f}\right)\right] \quad \text{(eq.2)}$$

where P_{FA} is the feed acceleration power (w), Q is the feed volumetric flow rate ($m^3 \cdot s^{-1}$), ρ_f is the feed density ($kg \cdot m^{-3}$), x_f, is the solids mass fraction in the feed, ω is the bowl angular speed ($rad \cdot s^{-1}$), and r_C and r_L are the cake and centrate overflow radii (m), respectively. Upon entry into the pool, half of the P_{FA} is carried as tangential kinetic energy by the feed and the rest is dissipated as turbulence (13,14). For a given feed material and centrifuge, the power required to accelerate the feed is therefore directly proportional to the G-force, G, which is usually referenced relative to the gravitational acceleration constant, g ($9.81\ m \cdot s^{-2}$).

Acceleration of the rotating assembly: Power is consumed to accelerate and keep the bowl, scroll, gearbox and end hubs of the centrifuge at operational rotational speeds. The rotational inertia of the bowl, scroll, gearbox and end hubs can be computed using their masses and radii. The power supplied, P_{RA}, to reach the operational rotational speed is:

$$P_{RA} = \alpha\, \omega \sum I_i \quad \text{(eq. 3)}$$

where α is the radial acceleration in $rad \cdot s^{-1}$ and I_i, represents the moment of inertia ($kg \cdot m^2$) of the rotating centrifuge components. The acceleration power dependence on rotation speed can more explicitly be expressed by expanding α with the average angular speed change:

$$P_{RA} = \frac{\omega^2}{t} \sum I_i \quad \text{(eq. 4)}$$

where t (s) is the time for the centrifuge to reach the operating rotational speed. As in the feed acceleration, the power needed is directly proportional to the square of the angular rotation speed. P_{RA} is required only during the startup period while the P_{FA} has to be supplied for the entire separation process. The mass of the CD205 GEA centrifuge decanter rotating assembly is given to be 230 kg while the greatest mass of FFT feed retained in the centrifuge can approach only about 20 kg. The scroll mass is greater than the centrifuge cylinder mass but its inertia is limited because its body is compact and close to the axis of rotation. A significant part of the power goes to maintaining the angular speed of the rotating assembly because of relatively very large moment of inertia and the higher impact of the power loss factors associated with it. The power consumption rates of the bowl motor with and without feed at different rotation speeds were found to be similar, as shown in Figure 4 indicating that feed acceleration and cake transport consume relatively little power.

Cake transport: The scroll conveyor transports the solid particles packed against the centrifuge bowl wall. The scroll conveys the solids by overcoming the friction between the solids and the machine components and the effect of the high centripetal acceleration. The power consumed is a function of the coefficient of friction between the settled solids and the machine components (13). The settled solids follow a complex path as they are conveyed to the cone (or beach). To expedite axial transport of the cake, the coefficient of friction of the cake with the bowl has to be greater than that with the scroll (13). The power to the screw conveyer, P_T, of the centrifuge is given by the product of the scroll differential speed, $\Delta\omega$, and the scroll conveyer torque, τ (N·m).

$$P_T = \tau * \Delta\omega \qquad \text{(eq. 5)}$$

This power is used to convey the cake against Coulomb frictional force. An alternate expression in terms of the cake solids mass and centripetal acceleration is (3):

$$P_T = M_c \omega^2 \, r \, C_f v \qquad \text{(eq. 6)}$$

where M_c is the mass of the cake, C_f is the coefficient of friction, and v is the cake axial velocity along the centrifuge. C_f is regularly assumed not to depend on velocity (15). The cake conveyance velocity is a function of $\Delta\omega$, the scroll pitch, (which is the distance between adjacent scroll blades), and is influenced by the scroll blade angle as well as the solids friction with the bowl wall versus that with the scroll face (16). Equation 6 shows that the conveyance power at constant $\Delta\omega$ increases in proportion to the centrifuge G-force.

Windage: The force exerted on a rotating body by the viscous effects of the surrounding atmosphere is defined as windage. Windage exerts drag on the rotating body and additional power is taken up to overcome it. Windage is a function of the fluid properties, geometry, and speed of rotation as given below (6):

$$P_W = k_S \, \mu_A^{0.2} \, \rho_A^{0.8} \, \omega^3 \, D^{4.5} \qquad \text{(eq. 7)}$$

where P_W is the windage power (w), μ_A and ρ_A are the viscosity (Pa·s) and density (kg·m^{-3}) of the surrounding atmosphere, respectively; D is the rotating body outer diameter (m); and k_S is a shape constant. The power loss due to windage varies only with speed for a given geometry. Equation 7 shows that the power consumed due to windage is proportional to the cube of the angular speed, and lowering the centrifuge speed therefore reduces the windage power loss.

Friction power loss: There is some loss of power when power is transmitted from one unit to another. The electric motors are coupled to the moving centrifuge components by belts, gearboxes, seals, and bearings. The relative motion of these parts inevitably gives rise to friction that reduces the transmitted power. In most cases, the frictional power loss, P_F, is a fixed percentage of the transmitted power, independent of the load (13). Therefore, the power loss cost becomes more significant as the rotation speed of the centrifuge increases. Although friction losses are unavoidable, they can be reduced by operating the centrifuge at lower speed.

The power as expressed by eq. 4, 7 and P_F is required even without any throughput to the centrifuge, and can be referred to as idling power. From the discussion above, reducing the centrifuge G-force reduces idling power consumption. Figure 3 is a chart of bowl power at varying rotation speeds and constant FFT feed rate and constant $\Delta\omega$ of 14.5 rpm. The power initially shows fluctuations as the centrifuge responds to the changing rotation speed, and later becomes steady. The mean bowl motor power of Figure 3a is analyzed to determine the relationship with G-force.

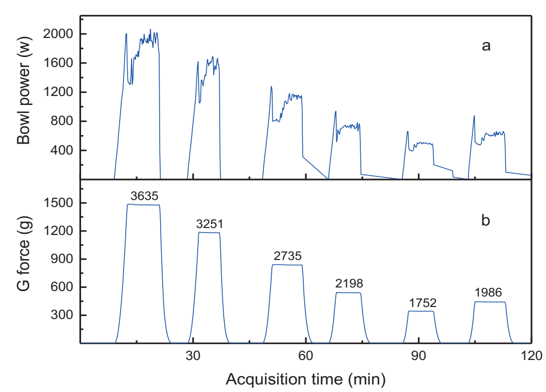

Figure 3. Bowl motor power (a) at varying bowl rotation speeds indicated on the plateau of curves (b) for a feed flow rate of 18.32 L/min, spg of slurry 1.17, $\Delta\omega$ = 14.5 rpm

The results in Figure 4 are in agreement with the discussion above in which the amounts of power consumed by the various processes are either directly or predominantly related to the square of the centrifuge rotation speed. The bowl power comparison between that in idle mode and while separating FFT indicates that a substantial amount of the power goes to maintaining the SDC rotation speed.

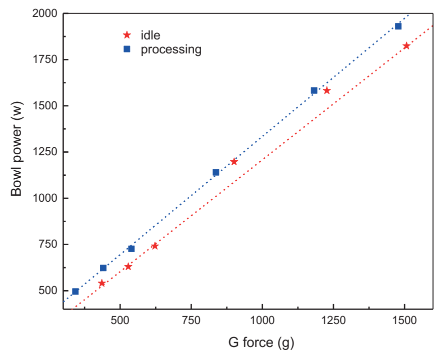

Figure 4. Bowl motor power in idle mode and during processing as in Figure 3. The lines are best least-squares fits of data.

Flocculant brings the fines together, creating aggregated solids structures of higher fractal dimensions that settle out relatively easily (17-18). When the polymer flocculant solution is injected to the centrifuge directly, flocculation occurs during acceleration of the solids in the pool. Consequently, the residence time of the flocs is shorter than if the feed were flocculated before entering the pool. The preconditioning step consisted of injecting flocculant solution at inlets of 1-inch KMS™ and Koflo™ inline static mixers (7). In the inline static mixers the fine solids particles are aggregated to form larger flocs in advance of entering the centrifuge. Conducting the preflocculation to the correct degree outside the centrifuge improves the separation efficiency as it: 1- increases floc residence time; 2- introduces faster-settling flocs, and 3- reduces the solids content in the pool for less-hindered settling.

Inline static mixers were selected for the preconditioning because they offer superior control of the flocculation time and applied hydrodynamics compared to flocculation in stirred vessels. Similar performance improvements could be achieved if the preconditioning were done using other equipment, as the performance gain is related to feeding the centrifuge with optimally flocculated material.

Giving primary consideration to the separation, Figure 5 shows that for separation without preconditioning, the centrate solids concentration became greater than the industry benchmarks of 1% (w/w) and fines capture rate below 97% at G-force of around 750G. By contrast, when the feed was preflocculated using inline static mixers, on spec separation was achieved starting from a little below 400G. Since the bowl power consumption, as discussed above, is directly proportional to the G-force, the preflocculation enabled on-spec separation at 47% lower power consumption than that required without preflocculation. The power consumption of the scroll motor depends on the specific design of the SDC, as it can for instance lead or trail the bowl speed. Depending on the gearbox type, the scroll drive can be regenerative (i.e. use the mechanical energy of the scroll to generate electric power to the source) or non-regenerative (i.e. lower the kinetic energy of the scroll by braking). Scroll power consumption is therefore not included in the discussion because it is specific to the machine used while the power reduction at lower G-force is applicable to any SDC design.

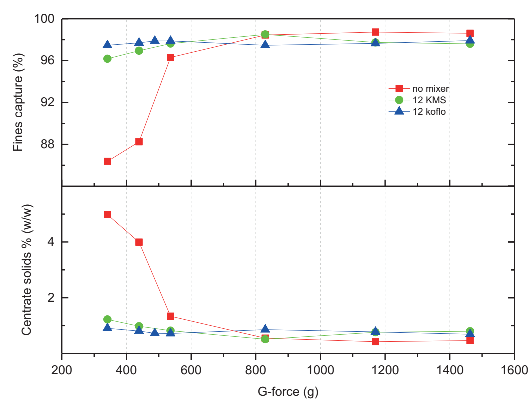

Figure 5. Effect of preflocculation on FFT separation performance. FFT density of 1.16 g/ml, at 18.2 L/min feed flow rate, was preflocculated using 12-element of KMS and Koflo inline static mixers.

Preflocculation enabled the centrifuge to be operated at lower G-force while retaining the same separation efficiency, at the cost of marginal losses in cake dryness. The cake solids contents at

1463G, 536G, and 438G, respectively, were 54%, 51%, and 49% (w/w) for comparison. The other cost of the preconditioning step is power consumption by the static mixers, which was calculated from the pressure losses across the mixers. For comparison, the average mixing power dissipation of the 12-element static mixers presented in Figure 5 was only 8 watts. The reduction in power consumption by the centrifuge is many times greater than the preconditioning power consumption, indicating that the benefit of preflocculation is not limited to energy conservation only. Larger flocs are easier to separate by centrifugation as indicated by equation 9. The impelling force, F_I, acting on a spherical particle in a centrifugal field is given by

$$F_I = \frac{\pi}{6} d_S^3 (\rho_S - \rho_W)\omega^2 r \qquad \text{(eq. 9)}$$

where d_S is the particle diameter, ρ_S and ρ_W are the densities of the solids and water respectively, and r is the distance of the particle from the centrifuge axis of rotation. The relation between the centrifugal force acting on a particle and its diameter is to the third power. Thus, even a small increase in particle size results in a large increase in the force acting upon it. This increases the terminal settling velocity of the particles as expressed by Stokes law or other settling velocity expressions that correct for solids shape effects and hindered settling in concentrated suspensions (13,19).

Flocs comprised of fine particles are sensitive to shear. The energy input of the inline static mixing is related to the mixer geometry as shown in Figure 6. *ΔP* across the static mixers increases linearly with the number of mixing elements, much like the length effect in regular pipe flow. The slopes of log *ΔP* vs. log *Q* were 1.6 and 1.8 for the KMS and Koflo static mixers, respectively, indicating that the preconditioning conditions are such that the flow is turbulent and the mixing corresponds to orthokinetic flocculation (7).

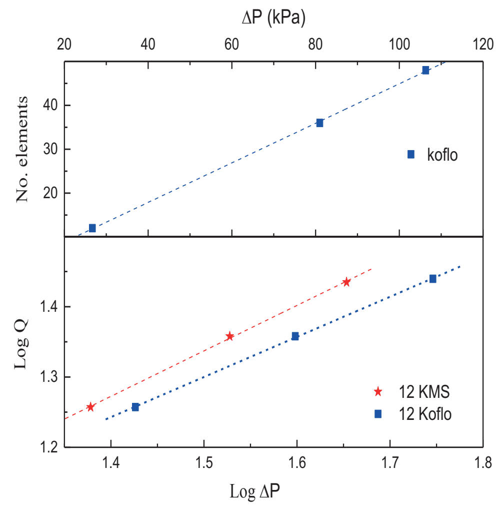

Figure 6. Hydrodynamics of 23% (w/w) solids FFT during flocculation using inline static mixers

Just as considerable mechanical shear is needed to mix the feed and create large flocs, shear can also rupture the flocs when the hydrodynamic stress exceeds the floc strength. Steady shear and dynamic oscillation rheological measurements, as well as stereo microscopic images reveal that the mixing intensity and duration are determinant of the flocs and network structure of the flocculated FFT (7). Structural changes caused by excessive mixing lead to poor dewatering rates in systems that rely on overflow or drainage water release. Similarly, preconditioning can form material that separates either well or poorly in the SDC, as shown in Figure 7 below.

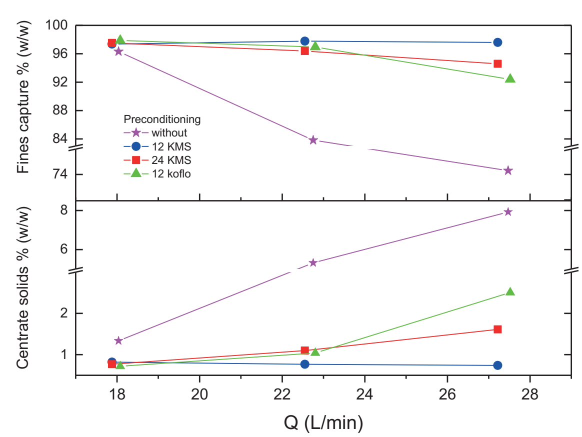

Figure 7. Volume flux and preflocculation effect on centrifuge separation performance

Increasing the feed volume flux reduces the residence time of the feed in the centrifuge. The low separation efficiencies of FFT preconditioned using 12-element Koflo and 24-element KMS static mixers cannot be attributed solely to shorter or longer flocculation times since preconditioning of the feed by the 12-element KMS mixer gave satisfactory separation over the whole flow rate range. The friction factor for Koflo static mixers has been measured to be higher than that for KMS static mixers (7). Koflo elements impart more mixing energy than an equivalent number of KMS elements. The separation deteriorated not owing to the number of static elements used, but to the mixing energy imparted. At high mixing energy the shear present induces orthokinetic breakup of flocs. The preconditioning input energy effect is analogous to the optimal mixing energy corresponding to the most rapid dewatering of flocculated MFT. Centrifuge separation performance improves and then deteriorates with increased mixing intensity or duration, which indicates that, for a set of operating and feed conditions, there is a range of orthokinetic flocculation conditions that form optimally separating tailings. The centrifuge separation efficiency observed with increasing numbers of mixing elements further supports the optimal preconditioning mixing condition as presented in Figure 8.

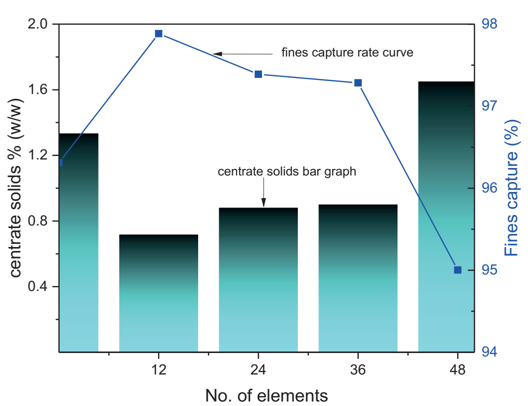

Figure 8. Effect on centrifuge separation of increasing number of Koflo static mixer elements for 1.17 spg FFT at flow rate of 18.1 L/min and 356G. The highest standard deviation of the centrate solids was 0.02%.

These results demonstrate that preconditioning not only allows separation at lower G-force, but also increases the capacity of the centrifuge. In the particular case of the 12-element KMS mixer presented in Figure 7, for instance, this capacity increase amounted to 50%. The increase in throughput capacity also suggests that upset separation conditions are less probable when the SDC is coupled to a preconditioning operation.

The SDC creates noise, as any rotating equipment does. Noise is a definite health and safety hazard whose effects are usually long-term or permanent. Workplace sound exposure in North America is regulated by the Canadian Centre for Occupational Health and Safety and the federal Occupational Safety and Health Act (OSHA) in the USA (20-21). It is possible to control noise at three different stages, namely, reducing sound production, interrupting the path of the sound, and using hearing protective devices. The two principal noise sources of the centrifuge are the bowl and the AC electric motors. The sound level in decibels for the test machine was found to be linearly related to the rotation speed as given in Figure 9. Since horizontal SDCs are geometrically similar in design and utilize the same kinds of machinery parts, the noise emission correlations with rotation speed for all similar units are likely to be similar to that shown in Figure 9. The noise level of a larger centrifuge namely, Alfa Laval, Lynx 40™, confirms this linear correlation of sound level and rotation speed (see Figure 9). In fact, even rotating machines dissimilar to the SDC, such as warp knitting looms, diesel engines, and gasoline engines also display the linear noise level trend with rotation speed (22). The difference in sound levels at the minimum G-forces for effective separation with and without preconditioning in this study was 2.5 dB(A). This is a significant noise reduction since, by the regulations, a 3-dB(A) increase halves the permissible exposure time. Noise reduction at the source is the first choice to improve noise pollution and carrying out the separation at lower speed achieves this goal.

The high centrifugal force necessary for separation coupled with the trailing scroll rotation in a body containing solids that are abrasive is a formula for high material wear. Excessive wear can lead to inefficient centrifuge operation and frequent costly repairs. Leung states that the wear is proportional to the product of the G-force and $\Delta\omega$ (3). Operating the centrifuge at reduced rotation speed without loss of separation performance is a protective strategy that reduces wear and increases component service life of the high-capital-cost SDC.

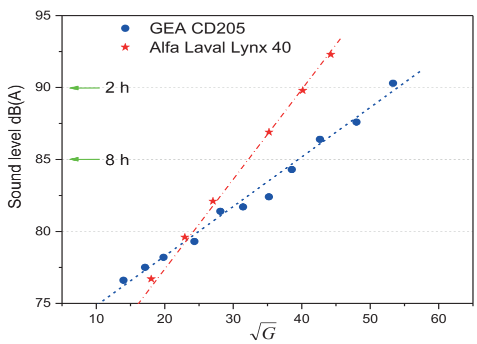

Figure 9. Sound level dependence of two different SDCs on operating G-force. The dashed lines are linear regression fits.

CONCLUSIONS

The separation of FFT by SDC starts with flocculation followed by sedimentation under the influence of the applied G-force. These processing steps are implemented by: a) preceding the solid-liquid separation in the SDC with an external flocculation step to improve the centrifugation performance, and b) employing low-cost and low-power equipment, such as inline static mixers, to improve flocculation and reduce power consumption by the centrifuge. The findings of this study are:

1. Power consumption in any SDC is directly proportional to the operating G-force.
2. Most of the power is consumed to maintain the rotation speed of the SDC machine. This unavoidable power loss is greater for higher rotation speeds of the centrifuge.
3. Industrial SDC FFT separation is conducted at 800G and above. In this study too, FFT separation falls below the acceptable benchmarks at G-force < 750G. Preflocculation enabled lowering of the G-force needed for acceptable separation to 400G. The coupling of the SDC separation with a preflocculation step resulted in a 47% reduction in power consumption.
4. Preflocculation of the FFT prior to feeding the centrifuge increases the throughput capacity of the SDC. Increases in the volume flow rate of up to 50% were demonstrated in this work.
5. The systematic effect of increasing the orthokinetic flocculation energy on SDC separation efficiency ranges from poor separation to good separation and back to poor separation of the feed. Therefore, within the available range of mixing energy inputs for preflocculation, an energy input can be found that corresponds to optimal separation performance.
6. High rotation speed intensifies the sound level and wear of SDC components. The sound level of any SDC can be expected to be directly proportional to the rotation speed as empirically shown in this work. Reducing the operating speed lowers ambient noise levels.

Higher costs and increased environmental awareness have increased the need for technologies and methods that reduce energy consumption. Preflocculation of the feed is shown to reduce the operating G-force of the SDC without adversely affecting the fines capture rate. Operating the SDC at lower speed also reduces wear and downtime of the machine, as well as noise pollution.

ACKNOWLEDGEMENTS

The author is thankful for support and funding for this project provided by the federal ecoENERGY Innovation Initiative (ecoEII) program. Pilot plant tests were conducted with help from Craig McMullen of CanmetENERGY-Devon. Shawn Stevenson, Tuan V. Tchen, Alvis Kawan and Nirpal Dhillon, all students from the University of Alberta faculty of Engineering, also helped in the pilot plant tests as part of their co-op training programs.

REFERENCES

1. Oils sands tailings technology review, BGC Engineering Inc., July 2010. (cited July 2016): Available from www.infomine.com/library/publications/docs/BGCEngineering2010.pdf

2. Records, A., Sutherland, K., Decanter Centrifuge Handbook. 1st edition. Elsevier, New York, USA, 2001.

3. Leung, W.W.F., Industrial Centrifugation Technology. McGraw-Hill, New York,1998.

4. Axelsson, H., Madsen, B., Centrifuges, Sedimenting. in Ullmann's Encyclopedia of industrial chemistry Chap. 5, 494-519.

5. Svarovsky, L. (Editor): Solid-liquid separation 4th ed. Butterworth-Heinemann, Boston, USA, 2001

6. Letki, A, Corner-Walker, "centrifugal separation" in A.Kirk-Othmer Encyclopedia of chemical technology, John Wiley & Sons Inc.
vol. 5, pp 505-551,

7. Demoz A, Scaling inline static mixers for flocculation of oil sand mature fine tailings. *A. Inst. Chem. Eng*. 2015; 61:4402-4411.

8. Demoz A, Mikula RJ, Role of mixing energy in the flocculation of mature fine tailings. *J Environ Eng ASCE.* 2012; 138:129-136.

9. Schwoyer, W.L. and Luttinger, L.B. "Dewatering of water-plant sludges," *JAWWA, 65:6, 1973*

10. Well, PS., Kaminsky, HAW., "Slurry to soil clay behaviour model-using methylene blue to cross the process/geotechnical engineering divide", Proc. Tailings and mine waste 2015, Vancouver, October 26-28, 2015.

11. Currie, R., Bansal, S., Khan, I., Mian, H., "An investigation of the methylene blue titration method for clay activity of oil sands samples". Dec. 2014. (cited July 2016): Available from https://era.library.ualberta.ca/downloads/08612p70g

12. Sanin, F.D., Clarkson, W.W., Vesilind, P.A., "Sludge engineering: the treatment and disposal of wastewater sludges". DEStech Publications, Inc. Lancaster, USA, 2010.

13. Bell, G.R.A., "Analysis and development of a decanter centrifuge", Ph.D. thesis, the University of Canterbury, New Zealand. 2013.

14. Bell, G.R.A., Symons, D.D., Pears, J.R., "Mathematical model for solids transport power in a decanter centrifuge", Chem.Eng.Sci. 107 (2014) 114-122

15. Halliday, D., Resnick, R., Walker, J., Chapter 6, in "Fundamentals of physics", 2001, John Wiley & Sons Inc., Toronto, Canada.

16. Lindner, J., Nirschl, H., "A hybrid method for combining high-gradient magnetic separation and centrifugation for a continuous process", 2014, 131, 27-34.

17. Thomas, D.N, Judd, SJ, Fawcett, N, Wat. Res 33(1999)1579-1999

18. Heath AR, Bahri PA, Fawell PD, Farrow BJ. Polymer flocculation of calcite: experimental results from turbulent pipe flow. *AIChE J* 2006; 52:1284-1293

19. Heiskanen, K., Particle Classification, Chapman & Hall, London 1993.

20. Noise control in industry (cited July 2016): Available from http://ccohs.ca/products/publications/noisecontrol_toc.html

21. Occupational noise exposure (cited July 2016): Available from https://www.osha.gov/SLTC/noisehearingconservation/

22. Gerges, N.Y., Sehrndt, A., Parthey, W., "Noise sources" chap. 5, in "Occupational exposure to noise; evaluation, prevention and control", WHO, Geneva, 25–27 September 1995. (cited October 2016): Available from www.who.int/occupational_health/publications/noise.pdf

THE MFT CENTRIFUGING EXPERIENCE

Neil McMinn, Bryne Gramlich and Graham Stephens
Newalta Corporation, Calgary, Canada

ABSTRACT

Newalta has designed, built and operated a number of centrifugation plants in the Fort McMurray oil sands region that process Mature Fine Tailings (MFT) or Fluid Fine Tailings (FFT). Newalta's experience began by working with a major oil sands mining operation and CanmetENERGY (Natural Resources Canada) in 2010 on the design and optimization of a pilot project at their primary tailings pond, which delivered results to support the commercialization of centrifugation technology. An additional pilot project initialized in 2013 with Shell Canada Limited (Shell) further supported effective commercialization of the technology.

Newalta has worked effectively with the relevant stakeholders to advance the technology to the commercial applications being utilized today. Newalta has been involved in the design, procurement, fabrication, construction, commissioning and operation of five MFT centrifugation facilities. The past six years have provided extensive operating experience in overcoming the associated technical challenges. These experiences have firmly established MFT centrifugation as a commercially viable option for state-of-the-art fines capture in oil sands tailings environments.

INTRODUCTION

Background

Newalta is a publicly traded company head-quartered in Calgary, Alberta. Newalta provides recovery and reclamation services to the exploration and production energy sector across North America through a fixed facility network that is complemented by specialized facilities at customer sites.

More than 10 years ago, Newalta started an initiative to incorporate the technologies used throughout its fixed facility network to create mobile or portable solutions deployed on customer sites. The market has engaged Newalta to create a number of long-term onsite solutions that are Design, Build and Operate (DBO) projects. To date, Newalta has delivered 10 locations that incorporate DBO solutions for a number of oil and gas, oil sands and mining customers where initiatives range from pilot operations to full-scale commercial projects.

Newalta's model is unique in that it is not tied to any one technology and that it works to supply the most value-added solution to meet customer requirements. Newalta utilizes a team of internal engineering resources and external consulting engineers in the design and detail phases of these projects. The customer and the customer's engineers are actively engaged in each project to ensure that the design meets or exceeds expectations and customer-specific standards.

Wherever possible, Newalta uses off-site fabrication to shop-build and pre-commission process modules which enables quick installation at the site. Commissioning is performed in coordination with Newalta's Operations group, ensuring continuity between the installation and production phases. Typical DBO projects are installed and operating in less than a year on a customer's site.

THE MFT CENTRIFUGE PROCESS

A centrifuge process for fluid tailings had been under active development since 2005. Bench trials began in 2005, and CanmetENERGY further developed the process with bench scale tests that led to a successful field demonstration using small pilot centrifuges in the fall of 2008.

With the 2008 regulatory enactment of *Directive 074: Tailings Performance Criteria & Requirements for Oil Sands Mining Schemes*, oil sands mining operators were required to commit to the reduction of fine fluid tailings and reduce any current inventories. Fluid fines were to be captured in Dedicated Disposal Areas (DDA), which must form a trafficable deposit with undrained shear strength of 5 kPa within one year of deposition. Directive 074 created an immediate need for oil sands operators holding legacy tailings to produce non-fluid trafficable deposits within a short period of time.

Directive 074 has since been replaced by the *Tailings Management Framework* and *Directive 085: Fluid Tailings Management for Oil Sands Mining Projects*.

Newalta's involvement enabled process demonstration on an expanded scale using larger commercial-sized centrifuges. Newalta has extensive experience operating centrifuge systems that process slop oil and drilling muds throughout North America, and currently operate a fleet of approximately 200 centrifuges. Newalta also has experience operating these large commercial-sized centrifuges in other industrial industries including mining, municipal and pulp and paper.

Newalta was engaged in 2010 for the design and optimization of a pilot project at the primary tailings pond of a major oilsands mining operation. Again in 2011, Newalta became involved with designing an even larger pilot that utilizes full-scale commercial centrifuges. Both of these projects were integral to delivering the results that support the commercialization of the technology.

Centrifuge Process Overview

Tailings centrifugation broadly comprises:

1. Dredging,
2. Pre-Screening
3. Coagulant & Polymer Injection
4. Centrifuging
5. Centrate Pumping
6. Solids Transport to Deposition

The MFT is generally dredged from a tailings pond and is initially screened for the removal of any tramp materials. The screened slurry is then typically sent to a small surge storage pond. The MFT can then be pumped from the surge pond to a centrifuge process feed tank, where a coagulant may be added to assist in achieving process output specifications. An anionic polymer is injected into the MFT stream flocculation of the fine particles just prior to centrifugation. Figure 1 is a simplified process flow diagram of this process.

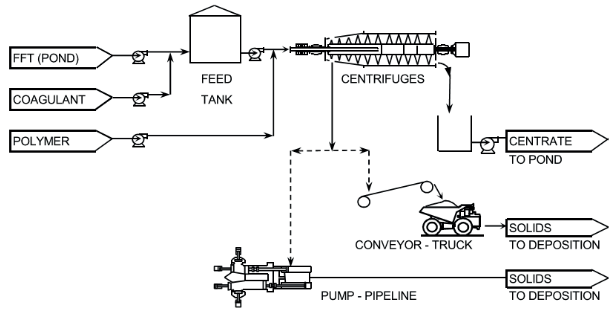

Figure 1. Simplified Process Flow Diagram

Each decanter centrifuge train has dedicated handling systems for feed, polymer, water addition, solids and centrate (effluent). Solids can either be conveyed and trucked or pumped and pipelined to deposition areas.

Each centrifuge system incorporates a state-of- the-art fully automated process control system. Components of each centrifuge process train are predominantly fully winterized in skids and designed to be easily relocated. Ancillary facilities for each system include polymer make-down, coagulant preparation, process water filtration systems and lab and office facilities.

General MFT Centrifuging Comments

The MFT has proven challenging to centrifuge, particularly at high throughputs with large-scale commercial centrifuges. Prevalent observations of Newalta's experience include:

- Centrifuge feed of about 30% solids appears to work best;
- Polymer is essential to the process, but the position and method of polymer injection is less sensitive than other MFT processes;
- Even though polymer consumption rates are moderate, the polymer remains the largest single operating cost;
- A high g-force is neither critical nor desirable;
- Performance is sensitive to differential speeds;
- Coagulant addition can be advantageous, particularly if high solids densities are desired;
- Commercially solids can be produced over a wide range (45 - 55% solids);
- Centrate (effluents) can be produced over a range of 0.5 - 2% solids with 95% or more fines capture rates; and,
- Maintenance costs have been much lower than initially estimated.

Advantages

Utilizing centrifugation in tailings management provides several distinct advantages, including but not limited to:

1. *Year Round Operation*
   Newalta has successfully optimized centrifugation plant operations in MFT to achieve results year round through winter seasons since 2012.
2. *Timely Results*
   Utilizing centrifugation has delivered a trafficable deposit in the desired timeframe.
3. *Dryness*
   Newalta's process improvement and operations can achieve MFT solids dryness to 55% by weight or more, ensuring that targets are met through solids deposition.
4. *Parallel Train Design*
   By utilizing parallel centrifuge trains, Newalta can handle variable feed rates and achieve high plant availability.
5. *Chemical Optimization*
   Newalta has extensive experience in finding ways to reduce costly polymer consumption while maintaining effective results. Newalta has successfully conducted various different MFT trials related to chemical mixing and chemical injection.
6. *Modular*
   Newalta's processes can be sized to the required throughput that meets target results when considering legacy ponds or inline production.

MFT Centrifuging Overview

Newalta's experience in tailings fines capture utilizing centrifugation includes:

1. Dredging
2. Pre-screening
3. Chemical / Poly Hydration
4. Process Automation
5. Equipment Operation / Optimization
6. Equipment Maintenance
7. Onsite Lab Analysis

TAILINGS CENTRIFUGE PROJECTS

Newalta has been involved in the design, procurement, fabrication, construction, commissioning and operation of five oil sands tailings centrifugation facilities. The past six years have provided comprehensive operating experience in overcoming the associated technical challenges.

Newalta has delivered three DBO projects for the management of MFT at a major oil sands mining operation.

Centrifuge Processing Trial (2010)

Newalta conducted a centrifuge processing trial at the primary tailings pond at a major oil sands mining operation. Newalta provided design, equipment and labour supply for this trial.

Centrifuge Pilot Facility (2011)

Newalta conducted another centrifugation processing trial at the same location and provided design, equipment, operating labour and infrastructure to support the trial. The primary reason for this trial was to test increased centrifuge capacity and substantiate the infrastructure required to support increased volumes.

Commercial Demonstration Plant (2012)

Newalta's first commercial scale project was capable of processing over 35,000 m^3/day of pond MFT, equivalent to over 12,500 bone dry tonnes (bdt) per day. This plant was initially comprised of eight full scale centrifuges complete with feed and solids handling systems. These systems are operated as eight independent process trains each with dedicated electrical distribution skids with 5kV voltage supply.

Figure 2. 8-Train Centrifuge Plant (2012)

The plant feed is pumped a distance of approximately one kilometre from a pre-screening plant near the pond's edge, which removes pond tramp material and debris. Water for polymer make-down is pumped from a remote supply pump barge over 4.5 km away and directed to the polymer make-down system, which includes a silo for bulk supply of polymer connected to a large-scale polymer hydration system. Additionally, Newalta employed a coagulant slurry induction system.

The plant is equipped with an extensive Process Control Network capable of state-of-the-art automation from a central control trailer, or independently at each process train. The plant has been designed and constructed to sit on compacted gravel without piling or foundations which allows for ready relocation, in whole or in part depending on the requirements. Other infrastructure associated with the plant includes a utility water supply skid, a 5kV switching & electrical distribution, and several supporting Operations Trailers.

Addition of a Ninth Train (2013)

Newalta increased the processing capacity of the facility in 2013 with the addition of a ninth centrifuge train. With this expansion, the plant was capable of processing over 40,000 m^3/day of pond dredged MFT, equivalent to over 14,000 bdt per day.

Figure 3. 9-Train Centrifuge Plant (2013)

Full-Scale Commercial FFT Centrifuge Plant

The operational success from Newalta's MFT centrifugation trials propelled the oil sands operator to develop a full-scale commercial initiative of the process. Newalta was awarded the contract in 2014 to provide labour support for the commissioning of the newly constructed full-scale centrifugation plant. The contract was expanded in 2015 to provide operational support on an ongoing basis.

SHELL CANADA

Utilizing extensive research and development work made available through Canada's Oil Sands Innovation Alliance (COSIA), Shell began developing a tailings centrifugation technology in 2012 to meet the MFT dewatering requirements of its Jackpine Mine (JPM) operations. Shell partnered with Newalta to install a commercial centrifugation facility consisting of two trains in 2013, augmented with two additional trains in 2014. While the other centrifugation plants transport the MFT to the disposal area utilizing conveyors and trucks, Shell developed a pipeline system to transport the material. The design requirements of a centrifuge product pump and related pipeline system for high density centrifuged MFT products presented new challenges.

Units 1&2 Jackpine Mine

Newalta was awarded the contract in 2013 to supply two full-scale centrifuge trains including infrastructure for fines capture at Shell's JPM operations. Again Newalta provided design, build and operations support.

This project resulted from Shell's collaboration through the COSIA forum and evaluating the experience with Newalta and the delivery of previous MFT centrifuge projects. Newalta provided a proposal to construct a pilot plant to test specific technologies related to MFT. The process has a design capacity of approximately 8,500m^3/day.

Figure 4. Units 1&2 Jackpine Mine

Units 3&4 Jackpine Mine

Newalta was awarded the contract in 2014 to supply an additional two centrifuge trains to support the operational needs for fines capture at JPM.

Figure 5. Units 3&4 Jackpine Mine

OPPORTUNITIES

These projects have firmly established MFT centrifugation as a commercially viable option for state-of-the art fines capture in oil sands tailings environments.

With existing installations, there are several opportunities for improvements including:

- Throughput;
- Optimization of chemical dosage;
- Type of polymer utilized; and,
- Lower operating and maintenance costs.

When examining application to future installations, there are several supplementary improvements being evaluated, such as eliminating trucking/piping to disposal areas and reducing the footprint of the centrifuge facilities in tailings areas.

SUMMARY

Newalta has successfully implemented DBO projects to customers across multiple industries. Operational expertise is a fundamental aspect of Newalta's offering, and our operator training is exceptional and comprehensive, as verified by our onsite performance. Safety standards are strictly adhered to, and Newalta has consistently either met or exceeded our customers' requirements onsite.

Newalta is technology neutral which can deliver a differential advantage in project execution by combining technologies to meet specific output requirements of the customer. Newalta provides internal and external functional resources, and engages the customer's in-house engineering teams and functional resources to ensure that a customer's specific design standards are met. Newalta has a proven track record of delivering the construction and commissioning of projects in short timelines without compromising quality or design.

Operationally, Newalta designs in redundancy and uses the process train strategy to ensure certainty with regards to continuity in process outputs. We provide reporting to customer process control systems, as well as quarterly operational reporting.

Newalta's commercial flexibility for contract architecture and pricing structure can provide cost certainty to oil sands mine operators while satisfying our customer's contract strategies.

REFERENCES

BGC Engineering Inc., 2010. Oil Sands Technology Review. Oil Sands Research and Information Network, University of Alberta, School of Energy and the Environment, Edmonton, Alberta. OSRIN Report No. TR-1. 136 pp.

Lahaie, R., 2008. New Tailings Concepts, Proceedings of the International Oil Sands Tailings Conference, Edmonton, December 9, 2008.

Mikula, R.J., Munoz, V.A., Omotoso, O., 2009. Centrifugation Options for Production of a Dry Stackable Tailings – Mined Oil Sands Tailings Management. Journal of Canadian Petroleum Technology, vol 48, Issue 09, September 2009. 5 pp.

Read, P. 2014. Broad Suite of Practice and Technology Key to Success in Tailings Management. Fourth International Oil Sands Tailings Conference, OSTC 2014, p 9-15.

GEOTECHNICAL PERFORMANCE AND WATER BALANCE OF CENTRIFUGED FFT DURING A ONE-YEAR FIELD TRIAL AT SHELL ALBIAN SANDS OPERATIONS

Reza M. Nik[1], Jack T.C. Seto[2] and Jason Song[3]
[1]Shell Canada Energy, Calgary, Canada
[2]BGC Engineering Inc., Edmonton, Canada
[3]O'Kane Consultants Inc., Calgary, Canada

ABSTRACT

Centrifugation of Fluid Fine Tailings (FFT) provides one option for fine tailings management in the oil sands. During the centrifugation process, FFT is first diluted and treated with a flocculant and then processed through decanter centrifuges. The resultant higher-density product, known as "cake", is transported to a dedicated disposal area through a pipeline with a positive displacement pump.

To provide input data and insight for the implementation of commercial-scale centrifuge-dewatered FFT, Shell Canada Ltd. conducted a field trial during 2014-15. Four test cells were constructed and instrumented: two earthen cells (one open-ended and the other closed-ended) to investigate the depositional behavior and geotechnical performance of cake deposits exposed to the environment over a one-year period, and two lined environmental cells to provide a better understanding of the dewatering mechanisms. Centrifuge cake was deposited into the test cells at an initial solids content of approximately 48 percent, and an initial thickness of 1.0 m to 2.2 m. The deposits were monitored for a period of one year, from August 2014 to September 2015. The monitoring phase included sampling for geotechnical characterization, in-situ strength measurements, and periodic sampling of water and cake for chemical analysis.

Analysis of the data indicated the thinner cake deposits that froze to their full depth showed a significant increase in the solids content compared to the thicker deposits that did not fully freeze. Also, evaporation was found the most significant contributor to water removal in the deposits over the one year monitoring period, emphasizing the important role of surface water management.

INTRODUCTION

Background

In June 2014, Shell Canada Ltd. (Shell) commenced a field trial for producing and storing centrifuge-dewatered Fluid Fine Tailings (FFT). The intent of the trial was to provide input data and insight for the improvement of commercial-scale centrifuge-dewatered FFT (also known as "cake"). BGC Engineering Inc. (BGC) and O`Kane Consultants Inc. (OKC) were commissioned by Shell to provide technical support, direction, and execution for designing, instrumenting, monitoring, sampling, and testing of pilot-scale deposits of centrifuge-dewatered FFT.

Construction of the test cells commenced in late-June 2014. The test cells were filled with cake between August 31 and September 9, 2014. The test deposits were periodically sampled, tested, and monitored over a one-year period (until September 9, 2015). This paper provides a summary of the performance of these test deposits over the one-year monitoring period, including the climatic conditions under which the deposits were exposed, the transient changes in geotechnical properties such as solids content (density) and shear strength, and an assessment of the water balance of these deposits.

Test Cells Design

Four test cells were constructed on top of mechanically placed mine waste at the northwest corner of the external dedicated disposal area at Shell's Jack Pine Mine (JPM). These included:

- An Open-Ended Cell: 80 m long, 15 m wide, up to 1.5 m deep, open at one end,
- A Closed-Ended Cell: 50 m long, 30 m wide, 2.4 m deep,
- A 1 m Environmental Cell (1 m Cell): 12.2 m long, 2.4 m wide, 1 m deep, and

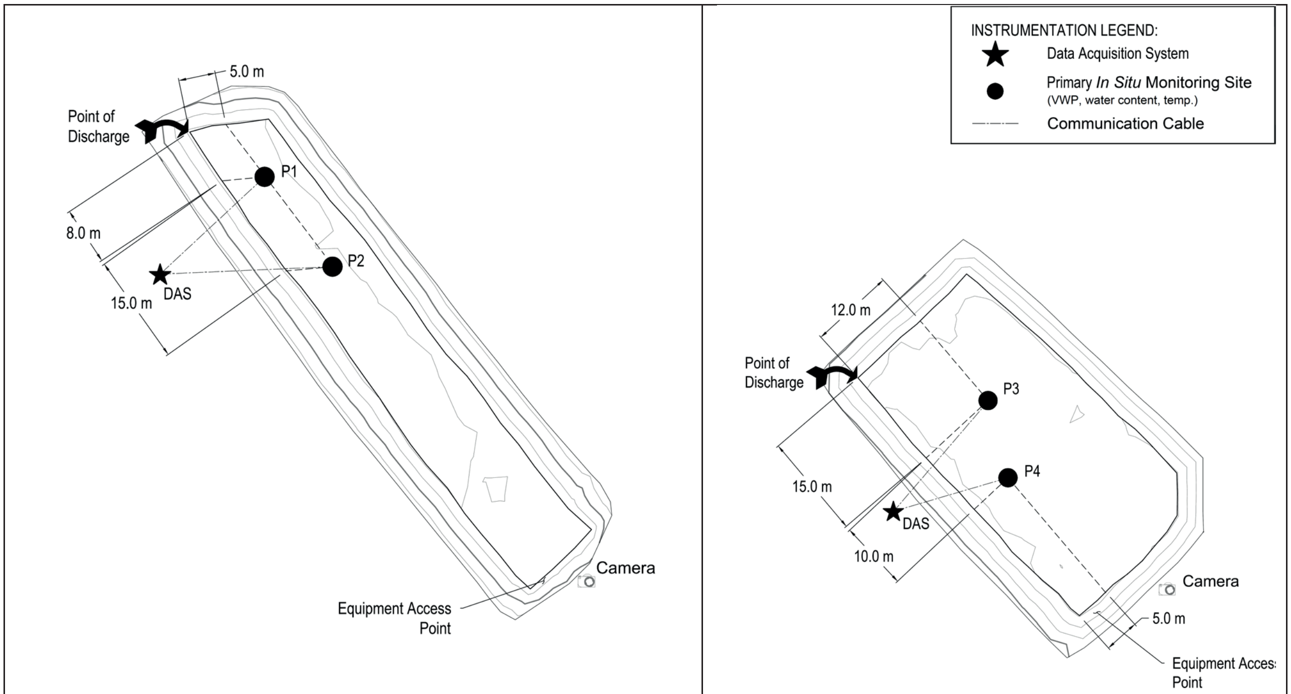

Open-Ended Test Cell (80m x 15m) | Closed-Ended Test Cell (50m x 30m)

Figure 1. Design of the Open-Ended and Close-Ended Test Cells and Instrumentation Posts

Open-Ended Test Cell | Closed-Ended Test Cell

Figure 2. View of the Open-Ended and Close-Ended Test Cells (September 2014)

- A 2 m Environmental Cell (2 m Cell): 12.2 m long, 2.4 m wide, 2.15 m deep.

Figure 1 shows the layout of the Open-Ended and Closed-Ended Cells. Figure 2 presents photographs of the deposits. These cells were unlined, such that moisture losses from the cake deposits through the floors and walls of the test cells were not controlled nor directly measured.

The 1 m and 2 m Environmental Cells were so named because they were designed specifically to be able to capture and measure all sources of water infiltrating, being removed from, or changing within the deposit, due to physical processes such as precipitation, evaporation, freeze-thaw, and consolidation, so that a complete water balance of the deposits could be undertaken.

Instrumentation

A meteorological station was installed at the test site and connected to a data acquisition system (DAS) to provide climatic data for interpreting transient changes of water balance for the test deposits, particularly for the fully lined Environmental Cells. Parameters measured included air temperature, relative humidity, net radiation, wind speed and direction, and rainfall.

The test deposits were instrumented with automated sensors connected to DASs to provide continuous measurements of parameters used to measure or interpret transient physical changes within the deposits. Because the cake material was expected to be initially soft and untrafficable by foot for many weeks following cell filling, all instrument sensors were fastened to wooden power poles (instrumentation posts) within the cake deposits and were installed at prescribed heights above the cell base prior to pumping or dumping cake into the test cells. The locations of the instrumentation posts in the Open- and Closed-Ended Cells are shown in Figure 1. Table 1 lists the instruments employed during the field trial program.

Aluminum survey rods were also fastened to each instrumentation post for the Open- and Closed-Ended Cells to provide a visual reference for estimating transient settlement of the deposit surface at the post locations.

Finally, cameras were installed at fixed locations around the deposits and programmed to record photographs at prescribed time intervals to provide a visual record (photo log) of transient changes to the deposit surfaces during and after deposition.

Cells Filling and Sampling

Centrifuge cake was pumped into the Open and Closed-Ended Cells using positive displacement pumps that transported the cake through a 300 mm diameter, approximately 800 m long pipeline. The two smaller Environmental Cells were filled with tailings by an excavator that collected cake within its bucket from the pipe discharge into the dedicated disposal area, and then transported and placed in the Environmental Cells. Table 2 presents the initial cake deposit thickness and volume in each of the tests cell, along with a summary of their design specifications.

TEST DEPOSIT MONITORING

Weather

During the one-year monitoring period, mean monthly air temperatures ranged from -17°C in February to +18°C in July, averaging +2.0°C over the year. Mean monthly temperatures were below freezing from November through March.

During the one-year monitoring period, total rainfall was 233 mm, with 93 mm (40%) falling during the month of July.

Compared to average climatic conditions for the Fort McMurray area for the period of 1908 to 2015, temperatures were warmer than average, through both the summer and winter. In addition, the area received less total annual rainfall (by 28%) than average.

Frost Penetration

In situ temperatures within the deposits were measured with thermistor strings and thermistors built into the piezometers. According to the thermistor measurements, freezing of the test deposits commenced in early-November 2014 and reached its maximum depth (0.73 m to 0.87 m) by late-February 2015. All test deposits began to thaw by mid-April 2015. The frozen layers fully thawed by early- to mid-June 2015.

Test Deposit Thickness

The test deposit thickness was measured monthly by measuring the deposit surface relative to survey rods fastened to the instrumentation posts. In the Environmental Cells, settlement was also monitored continuously by a sonic ranger.

Table 3 summarizes the measured deposit thicknesses immediately after tailings pour (initial thickness) and one year after (final thickness).

Table 1. Instruments employed in the test cells

Sensor Location	Sensor	Parameter Measured	Purpose
Within Deposit	Total earth pressure cell	Total stress exerted by deposit on its base	Used in conjunction with pore-water pressure measurements to measure effective stress, consolidation
	Vibrating wire piezometer	Pore-water pressure	Characterize saturated hydraulic gradient; used in conjunction with total earth pressure cell for transient effective stress
	Sensors embedded into a single thermistor string	*In situ* temperature	Measure extent (depth) of freezing, characterize surface energy balance of deposit surface
	Heat dissipation matric potential sensor	*In situ* matric suction and temperature	Characterize unsaturated hydraulic conductivity of cake, measure the potential for water flow in unsaturated cake
	Infrared radiometer	Surface temperature	Characterize surface energy balance of deposit surface
	Time Domain Reflectometry (TDR) soil probe	*In situ* volumetric water content and electrical conductivity	Measure transient changes in deposit water (solids) content
Above Deposit	Sonic ranger	Deposit settlement or snow thickness	Measure distance to the deposit surface (i.e., settlement) and transient changes in snow thickness in the winter
	Net radiometer	Net radiation and albedo at deposit surface	Used to characterize surface energy balance of deposit surface
Cell Drainage	Tipping bucket flow gauge	Under-drainage flows	Measure the transient rate of water flow through the base of the deposit

Table 2. Test cell design specifications and initial thickness and volume of the cake deposits

Cell Name	Nominal Plan Dimensions (Length x Width)	Initial Deposit Thickness (m)	Approximate Initial Deposit Volume (m^3)	Under-drainage control?	Design Purpose
Open-Ended	80 m x 15 m	Varies from approximately 1.6 m to 0.3 m	1,000	No	Characterize depositional nature of cake deposits. Provide deposit with varied initial deposit thickness that sheds surface waters.
Closed-Ended	30 m x 50 m	2.4 m	3,000	No	Characterize geotechnical properties of thick cake deposit that only partly freezes during the winter and does not shed surface water by gravity.
1 m Environmental Cell	12.2 m x 2.4 m	1.0 m	30	Yes, fully-lined	Quantify water removal from deposit that may freeze completely during the winter.
2 m Environmental Cell	12.2 m x 2.4 m	2.15 m	60	Yes, fully-lined	Quantify water removal from cake deposit that only partly freezes during the winter.

Table 3. Initial and Final Deposit Thickness

Cell Name	Post Location	Cake Deposit Thickness (m)		Vertical Strain (%)
		Initial	Final	
Open-Ended Cell	P1	1.5*	0.79	37*
	P2	1.29	0.69	47
Closed-Ended Cell	P3	2.50	1.88	25
	P4	2.27	1.66	27
2 m Cell		2.15	1.34	38
1 m Cell		0.95	0.53	44

*The deposit thickness decreased rapidly from 1.5 m to 1.25 m after pouring due to the open design of the cell.

Figure 3 presents the deposit thicknesses histories measured from sonic rangers and manual measurements for the 1 m and 2 m Environmental Cells. The shaded area highlights the months when snowpack and/or pooled water were on the deposit surface and for which sonic ranger measurements should be disregarded. The sonic ranger measurements showed good agreement with the manual measurements when the surface was unobstructed.

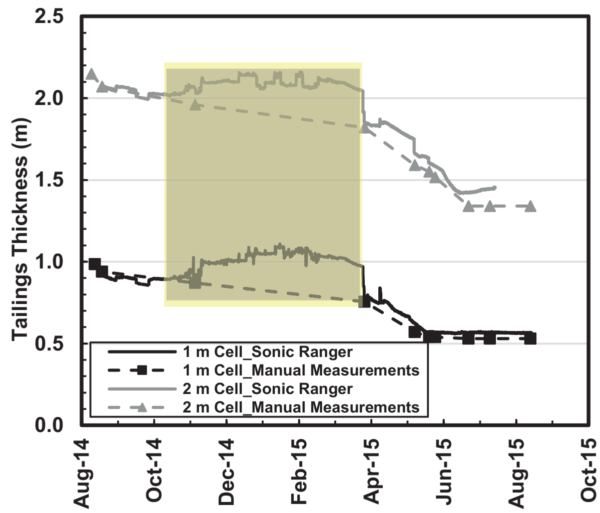

Figure 3. Deposit thickness histories, 1 m and 2 m Environmental cells

GEOTECHNICAL SAMPLING AND TESTING

During cell-filling, a number of samples of centrifuge cake were collected at the centrifuge plant for the purpose of characterizing the geotechnical properties of the produced cake. Following this, in situ sampling and testing of the test deposits were carried out for the purpose of characterizing the changes in geotechnical properties in the test deposits over the one-year monitoring period, as follows:

- Coring of frozen crust (for November-December 2014 and February 2015 sampling programs) using a Cold Regions Research Engineering Laboratory (CRREL) core barrel attached to a two-man portable auger (Figure 4a).
- Coring of unfrozen cake (for November-December 2014 and August 2015 sampling programs) using a piston tube sampler.
- Vane shear testing (VST) of unfrozen cake (for November-December 2014 and August 2015 testing programs) using a rectangular vane with height/diameter dimensions of 150 mm/75 mm.
- Ball penetrometer testing (BPT) of unfrozen cake (for November-December 2014 and August 2015 testing programs) using a ball with 100 cm^2 tip base surface area.

Geotechnical Laboratory Test Results

Table 4 presents the geotechnical solids content and associated peak and remolded yield stress of the cake collected at the centrifuge plant during cell-filling. The initial solids content was approximately 48 percent, with an initial undrained shear strength of less than 1 kPa.

The centrifuge cake had approximately 90% fines (smaller than 44 μm particle diameter), with a liquid limit of approximately 70% and a plastic limit of approximately 22%.

Geotechnical laboratory tests were also conducted on frozen and frozen-thawed cake for determination of compressibility, saturated hydraulic conductivity, thaw strain, and soil water characteristic curve, but the results are not presented herein. In summary, never-frozen cake has a compression index of approximately 0.6 and the hydraulic conductivity ranged from 10^{-11} to 10^{-6} m/s, indicative of a slowly-consolidating and low-permeability material. Thaw strain values ranged from 12% to 37%, meaning that a frozen sample could settle up to 37% upon thawing, without any applied load.

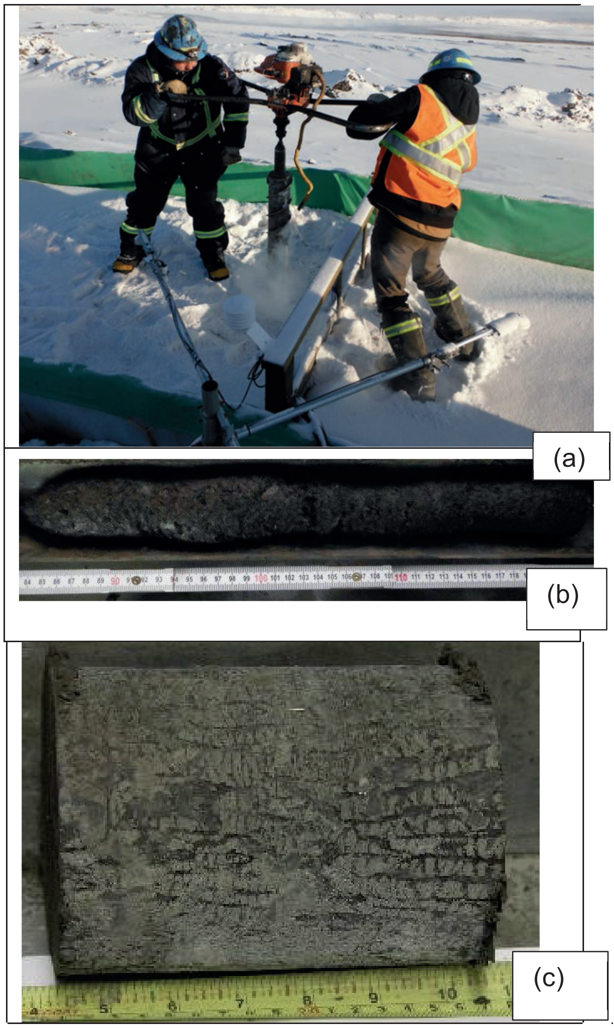

Figure 4. (a) Coring of frozen crust; (b) Typical *in situ* cored sample of unfrozen cake; (c) Typical trimmed sample of frozen cake (dark lines represent ice lenses)

In Situ Sampling and Testing Results

Figure 5 presents the measured solids content and undrained shear strength (peak, S_u, and remolded, S_r) profiles for one example test hole within the Closed-Ended Cell from the November-December 2014, February 2015, and August 2015 sampling and testing programs. The mean cell-filling solids contents and undrained shear strength, as presented in Table 5, are shown for reference.

All solids content profiles from November 2014 showed decreasing solids content in the upper portion (frozen crust) relative to the cell-filling solids content. Immediately below the frozen crust

Table 4. Solids Content and Yield Stress of Cake Samples Collected During Cell Filling

Property	Cell (number of tests)			
	Open-Ended	Closed-Ended	1 m Enviro.	2 m Enviro.
Solids Content of Cake at Plant (%)	48 (36)	48 (45)	48 (12)	48 16)
Peak Yield Stress of Cake at Plant (Pa)	860 (4)	780 (8)	700 (12)	740 (16)
Remolded Yield Stress of Cake at Plant (Pa)	660 (4)	600 (8)	560 (12)	560 (16)

(approximately 30 to 40 cm thickness), the solids content is generally higher than the cell-filling solids content. This clearly shows the effect of freezing-induced suctions that draw water from the unfrozen cake below to the freezing front, causing consolidation of the unfrozen cake. This effect is further evident in the February 2015 solids content profiles, which showed a lower solids content near the deposit surface than at depth, and generally showed a lower solids content within the upper layer compared with that measured in November 2014 and during cell-filling, due to water being drawn from the unfrozen cake to the frost front.

The solids content profiles also show increased solids content at the base of the deposits, which is a result of consolidation through the cell bottom (under-drainage). The shapes of the BPT undrained shear strength profiles are similar to the solids content profiles, as expected.

On average, the undrained shear strength of the cake increased from under 1 kPa at cell-filling, to between 1 and 2 kPa, with slightly higher values (up to 4 kPa) obtained in areas with thin deposits (less than 0.5 m thickness) of the Open-Ended Cell. The comparatively high densification in the thinner deposit areas is due to the combined effects of freeze-thaw dewatering and consolidation. In August 2015, the thicker Closed-Ended and 2 m Environmental cells showed a noticeably higher solids content within the upper 0.5 to 0.6 m depth compared to the cake below. This difference is attributed to the fact that the upper layer densified with freezing and thawing but the lower layer did not freeze and experienced less dewatering because

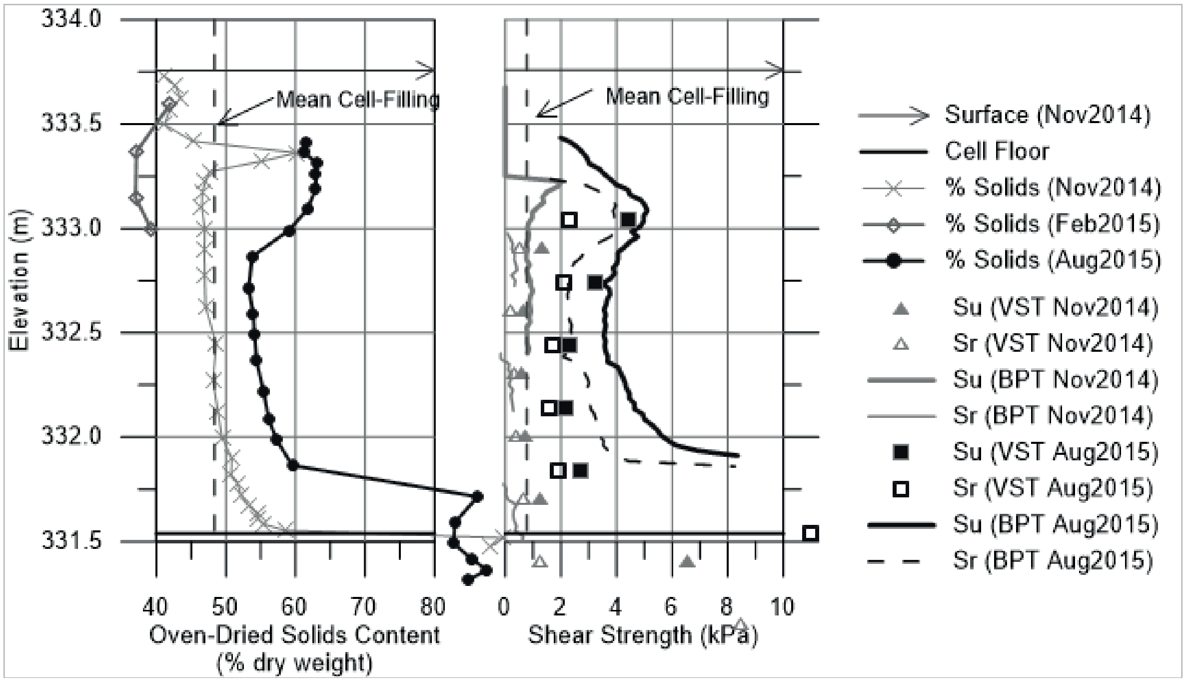

Figure 5. November 2014 to August 2015 solids content and shear strength profiles, Close-Ended Cell test hole CE-2

Table 5. Initial and final average solids content and undrained shear strength

Cell	Average Initial Solids Content (%)	Average Initial Yield Stress (kPa)	Average Final Solids Content (%)	Average Final Undrained Shear Strength (kPa)
Open-Ended Cell	48	0.9	64-67	7
Closed-Ended Cell	48	0.8	56-57	3-4
1 m Enviro Cell	47.5	0.3	73	14
2 m Enviro Cell	47.6	0.2	64	8

self-weight consolidation on its own was a less effective dewatering mechanism. Table 5 compares the approximate average initial and final solids content and undrained shear strength of the cake in the different test cells.

WATER BALANCE EVALUATION

The water balance was computed to evaluate the flow of water into and out of the test deposits during the one-year monitoring period. The water balance evaluation was conducted for the two Environmental Cells and the Closed-Ended Cell.

The following equation was used to evaluate the water balance:

$$\Delta S = P - AE - RO - UD \qquad (1)$$

where *ΔS* = water storage change within the deposit; *RO* = surface runoff (water removed via pumping); and *UD* = under-drainage, which is assumed to equal net recharge to the groundwater.

Precipitation (*P*) is the sum of the measured rainfall (obtained from the site meteorological station) and snow-water equivalent (obtained from a March 2015 snow survey). Actual evaporation (*AE*) was calculated from measured data (meteorological measurements and tailings measurements). Runoff (*RO*) was determined from pumping records. Under-drainage was measured from a tipping flow meter or estimated from other water balance components (i.e. by re-arranging the water balance equation). Water storage change can be calculated from the following equation:

$$\Delta S = S' - TPW \qquad (2)$$

where *S'* = stored water in the deposit, available from TDR measurements; and *TPW* = tailings product water.

Depending on the availability of water balance components, the water balance evaluation calculates water storage from other components and then compares water storage change obtained from TDR measurements for the Environmental Cells or calculates *UD* in the Closed-Ended Cell. The robustness of the water balance depends on the accuracy and reliability of each water balance component representing test-wide conditions.

Snow Survey

A snow survey was conducted for all test deposits in March 2015. Based on the snow survey, a snow water equivalent value of 90 mm was applied to the two Environmental Cells and 76 mm to the Closed-Ended Cell and added to the precipitation totals.

Actual Evaporation

Before evaluation of water balance for the Environmental Cells, Actual Evaporation (*AE*) was first evaluated through the following steps:

1) Daily potential evaporation (*PE*) over the monitoring period was calculated using the Penman (1948) method. The measured net radiation from the two cells was used in the PE calculation, along with other data measured from the site weather station.

2) Daily AE/PE ratio was estimated to equal 1 before June 4, 2015 because it was visually apparent that the deposit was saturated. After June 4, 2015, AE/PE ratio was calculated from the following equation (Fredlund et al., 2011):

$$\frac{AE}{PE} = e^{\frac{-\emptyset g m_W}{\alpha(1-RH)\gamma_W R(T_S+273.15)}} \qquad (3)$$

where Φ = total suction (i.e. Matric suction plus osmotic suction, kPa); g = gravity acceleration (m/s^2); m_w = molecular weight of water, 0.018 kg/mol; α = reduction factor, 0.7; RH = relative humidity of air; γ_w = unit weight of water, 9.81 kN/m^3; R = universal gas constant, 8.314 J/mol/K; and T_s = deposit surface temperature (˚C).

3) Total suction at the deposit surface was calculated as:

$$\emptyset = \varphi \times 10^{-\delta} \qquad (4)$$

where, φ = matric suction (kPa) at the deposit surface, obtained from extrapolation of the measured matric suction at 0.09 m and 0.19 m below the tailings deposit surface in the Environmental Cells; and δ = empirical adjustment factor to consider osmotic impact, between -0.5 and -2.0 for tailings according to Innocent-Bernard (2013). It was found that δ = -0.7 provided reasonable AE values for the 2 m Environmental Cell.

4) Calculated AE from daily PE and the daily AE/PE ratio. The calculated PE was 812 mm from September 6, 2014 to September 9, 2015 for the 2 m Environmental cell, and AE was 779 mm over the same period. As a result, the overall AE/PE ratio for the 2 m Environmental cell was computed to be 0.96. From June 4 to September 9, 2015, PE was 426 mm and AE was 393 mm, resulting in AE/PE of 0.92.

Water Balance in 2m Environmental Cell

The water balance for the 2 m Environmental cell is presented in Figure 6-a. Positive water volume indicates water flow into the deposit, while negative water volume indicates water flow out of the deposit. Over the one year monitoring period, cumulatively 9.1 m^3 of surface ponded water was manually removed from the 2 m Environmental Cell.

Figure 6-a shows that the calculated water storage change matched very well with water storage change obtained from TDR measurements. During the winter months, the water storage change from the TDR measurements was smaller than the calculated water storage change. This may be attributed to low measured volumetric water contents due to freezing effects. Spring melt was captured in the calculated water storage change but not in the water storage change from the TDR. Figure 6-a also shows that AE was the most important contributor in dewatering the cake deposit, followed by runoff, while under-drainage

was the least important contributor to water removal in the 2 m Environmental Cell.

The calculated water storage change was further used to calculate the remaining volume of water within the deposit and the average solids content with time, as shown in Figure 6-b for the 2 m Environmental Cell. Over the one-year monitoring period, water remaining in the 2 m Environmental Cell deposit decreased from approximately 47 m^3 to 25 m^3 (Figure 6b), and the average solids content increased from approximately 46% to 62%. The calculated solids content on August 10, 2015 was approximately 61%, compared with the average solids content of approximately 63% obtained from in situ sampling on that day.

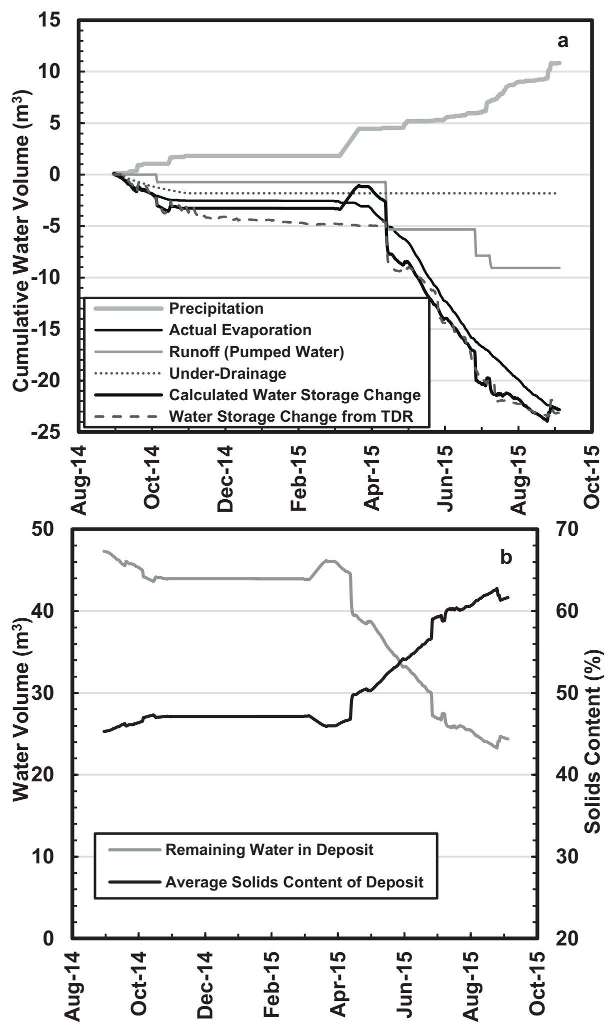

Figure 6. (a) Water balance and (b) Water remaining and average solids content with time, 2 m Environmental cell

SUMMARY

In August and September 2014, four test cells located at the northwest corner of the external dedicated disposal area at Shell's Jack Pine Mine were filled with centrifuge cake with an initial average solids content of approximately 48 percent, an initial undrained shear strength of less than 1 kPa, and initial deposit thicknesses ranging from 1.0 m to 2.2 m.

After one year of exposure to the environment, the average solids content / undrained shear strength increased to approximately 55 percent / 3-4 kPa in the Closed Ended Cell and up to approximately 72 percent / 16 kPa in the 1 m Environmental Cell. The cake deposits experienced 22% to 47% of vertical strain compared with the initial deposit thickness, with higher strains (and densification) recorded in the thinner deposits (initially 1 m or less) compared to the thicker deposits (initially up to 2.2 m).

Freeze-thaw contributed significantly to the densification and dewatering of the exposed test deposits. The thinner cake deposits that froze to their full depth experienced greater overall strain compared to thicker deposits that did not freeze completely. Freeze-thaw contributed to more water that could be removed through drainage (e.g., runoff), evaporation, or consolidation compared to never-frozen cake.

During the winter of 2014/15, frost penetrated the deposits to a maximum depth of 0.8 m to 0.9 m. In the case that use of thin lifts is considered in the tailings management plan, lift thicknesses no more than 1.0 m are recommended to allow for freeze-thaw over the full lift thickness and maximize densification of the cake deposits over a one-year period.

Water balance evaluation of the Environmental Cells and Closed-Ended Cell indicated that evaporation was the dominant contributor to water removal in these deposits. Under-drainage did not appear to be an important contributor to water removal, likely because of the low permeability and slowly-consolidating nature of FFT. Surface water (e.g. runoff) management may play an important role for evaporation to efficiently dry the deposit.

The deposit average solids content determined from the water balance evaluation matched well with solids content measurements from field sampling.

These small instrumented test deposits provided considerable insight into how climatic factors influenced transient dewatering and changes in geotechnical properties of centrifuge-dewatered FFT deposits.

REFERENCES

Fredlund, M.D., Zhang, J.M., Tran, D., Fredlund, D.G., 2011. Coupling heat and moisture flow for the computation of actual evaporation. Paper presented in 2011 Pan-Am CGS Geotechnical Conference. October 2-6, 2011, Toronto, Ontario.

Innocent-Bernard, T., 2013. Evaporation, cracking, and salinity in a thickened oil sands tailings. M.Sc Thesis. Department of Civil and Environmental Engineering, Carleton University, Ottawa, Canada.

Penman, H.L., 1948. Natural evapotranspiration from open water, bare soil and grass. Proceedings of the Royal Society of London, Series A, 193:120-145.

Session E

Tailings Properties and Measurements (2)

THE GEOTECHNICAL VANE SHEAR STRENGTH OF SOFT TAILINGS COMPARED TO SOFT FOODS

Gord McKenna[1], Vanessa Mann[1], Bereket Fisseha[2], Nicholas Beier[2], and Nicolas Olmedo[2]
[1]BGC Engineering Inc, Vancouver, Canada
[2]University of Alberta, Edmonton, Canada

ABSTRACT

Soft tailings strengths and consistency are often compared to that of common foods to simply communicate geotechnical properties of these unusual mine wastes. For oil sands tailings, informal comparisons to fluid and semi-solid foods such as chocolate milk, yogurt, porridge, cottage cheese, or peanut butter are common.

To provide a framework for such comparisons, a literature review of the shear strength of soft foods was compiled and laboratory testing of approximately 75 samples of tailings, soft foods, and other common household products was performed according to ASTM laboratory geotechnical vane and geotechnical moisture content procedures.

Tests were conducted with a University of Alberta custom-built, computerized vane device on foods in their original containers. For each test, the torque applied and the angular rotation of the vane were measured with time. Software provides a real-time output of vane strength versus rotation angle and vane strength versus time, allowing close monitoring as each test progressed. Peak, post-peak and remolded shear strengths were determined from the data output. Visual observations were also recorded and subsamples were oven dried for geotechnical moisture content.

Peak vane strengths for tailings ranged from 0.007 kPa (for untreated fluid fine tailings) to approximately 1.2 kPa (for flocculated fine tailings). Results for the foods compared favourably to published values for yield stress. Peak vane strengths ranged from about 0.005 kPa for chocolate milk and apple sauce, 0.08 to 2.5 kPa for jams, jellies, and condiments, and 1 to 12 kPa for butter, peanut butter, and other spreads. Sensitivities typically range from 4 to 8, but are much higher for some samples.

INTRODUCTION

Oil sands mining and extraction in the Athabasca Oil Sands of northeastern Alberta, Canada, produces large volumes of soft tailings. CCA (2015) highlights the challenges of reclaiming these soft tailings deposits to boreal forest landscapes as required by regulatory approvals. Soft tailings are a special geotechnical material defined as those that are so weak that they cannot be trafficked with typical earthmoving equipment (Jakubick and McKenna 2001). Research and development into managing these tailings from the standpoints of volume management and containment, reprocessing, capping, and ultimately reclaiming for future land uses, have been going on since oil sands mining began in the late 1960s (FTFC 1995).

The strength of these soft tailings is much lower than most geotechnical engineers are accustomed to. While there are some parallels with off-shore muds and harbor muds, soft tailings are typically one to three orders of magnitude lower strength that those expected by foundation, highway, and dam engineers. Given that the tailings strengths are outside of those normally encountered by professionals or laypeople, in discussion (and in some papers), people describe the consistency (strength, sensitivity, and density) of soft tailings using informal comparisons to foods such as chocolate milk, yogurt, porridge, cottage cheese, or peanut butter.

To provide a better basis for such geotechnical; comparisons, a literature review of the shear strength of soft foods was compiled and laboratory testing of approximately 75 samples of tailings, soft foods, and other common household products was performed according to ASTM geotechnical laboratory vane and geotechnical moisture content procedures.

As noted below, Sun and Gunasekaran (2009) describe the numerous methods for measuring the rheology of soft foods. They recommend that the type of testing be selected for the intended use of the data. Since the use here is geotechnical comparison to tailings and soils, the geotechnical laboratory vane test for measuring the vane strength of saturated fine-grained soils (ASTM D4648) was chosen. The test method is similar to the vane rheometer for measuring yield stress in food processing (eg De Vito et al 2014; Cunningham (undated)).

The results also provide an opportunity to reflect on 50 years of oil sands research and development and commercialization of soft tailings production and reprocessing. Few technologies to date have provided strengths that would make fine tailings easy to reclaim to upland or wetland boreal forest land uses (eg CTMC 2012). There is an opportunity to move beyond fluid-like strengths and into the soil mechanics realm (tailings with firm to stiff consistencies) to reliably and economically build the required reclaimed oil sands landscapes in the western boreal forest.

LITERATURE REVIEW

Food process engineering

Rheology for food processing is a mature science and the subject of numerous undergraduate text books in food process engineering (eg Heldman and Sing 1981; Fellows 2009). The yield strength (and post-peak behavior) is important to the selection, design, and monitoring of food processing systems (eg Cunningham (undated)).

Yield strength is a fluid mechanics analog to the geotechnical vane peak strength. Sun and Gunasekaran (2009) provide an excellent summary of the state of practice. The food industry uses yield-stress concepts to design foods to drain from containers, design thicknesses of coating layers, estimate settling of particles in fluids, and process design calculations. Pourability, spreadability, spoonability, and product stability are also a function of the yield stress (De Vito et al 2014).

A wide variety of methods are used to measure yield stress in foods, with different techniques providing different results. The testing technique is typically chosen to match the questions of interest to the food designer. Typical methods include extrapolation of rheometer data to zero shear rate, stress relaxation test, creep/recovery response, shear stress ramp test, cone penetrometer, dynamic oscillatory testing, static stability on an inclined plate, squeezing flow, plate method and slotted-plate device, slump test, tube viscometer and magnetic resonance imaging, and the vane test (Sun and Gunasekaran 2009).

Yield stress for common products

Table 1 provides a listing of yield stresses for common processed foods and household products from the literature. Strengths range from 0.015 to 72 kPa with many below 0.3 kPa and most below 2 kPa.

Tailings strengths

The shear strength of oil sands soft tailings has been of interest for many years (eg FTFC 1995; ERCB 2009; Kaminsky 2014) and the subject of dozens of theses and papers (CTMC 2012). Jeeravipoolvarn (2010) correlates the peak undrained strength of oil sands fine tailings against the fines-bitumen void ratio from which the following relationship is provided:

- 40% solids – 0.05 to 0.2 kPa
- 60% solids – 0.1 to 3 kPa
- 70% solids – 0.2 to 5 kPa
- 80% solids – 5 to 50 kPa

There is about an order of magnitude of scatter to the dataset, even when normalized.

Tailings strengths are mostly a function of the geotechnical moisture content. Low strengths are good for processing and pumping but difficult to cap or reclaim terrestrially. Firm or stiff strengths are good for capping and reclamation but such tailings are not pumpable – they will require conveyors or trucks/dozers to haul and place as is done for overburden and interburden dumps and dykes.

The laboratory remolded shear strength (Terzaghi et al 1996) is only occasionally reported for oil sands tailings, perhaps as it is can be below the detection limit of the equipment employed. Given the large deformations of oil sands fine tailings under load, the remolded shear strength is an important design consideration in choosing a design shear strength – a value typically between the peak and remolded values. Beier et al (2013) provide data on shear strengths of flocculated oil sands tailings.

In addition to the peak strength, the density, remolded shear strength, and hydraulic conductivity are all important to oil sands tailings – for tailings planning, settlement and water release rate, ability to stabilize / cap / make trafficable to mining

Table 1. Published yield stresses for foods

Item	Yield stress (kPa)
Ketchup [C]	0.015
Tomato sauce [B]	0.015
Salad dressing [C]	0.03
Yogurt [B]	0.08
Mayonnaise [C]	0.10
Skin cream [C]	0.11
Toothpaste [B]	0.11
Hair gel [C]	0.14
Sour cream, (non fat/ regular) [S]	0.25 / 0.66
Yogurt, fat free [S]	0.30
Jelly, grape [S]	0.30
Chocolate spread [D]	0.36 to 0.72
Jam, raspberry (seeds / seedless) [D]	0.59 / 0.97
Peanut butter [B]	1.2
Margarine spread (20°C / 4°C) [S]	1.2 / 4.5
Peanut butter (reg, reduced fat) [S]	1.6 / 2.6
Peanut butter, creamy [D]	1.8
Hazelnut spread [F]	2 to 5
Cream cheese [S]	2.5
Process cheese spread [S]	4.2
Stick of butter [F]	14 to 24
Mozzarella cheese [F]	28 to 34
Sharp cheddar cheese [F]	57 to 72
B: Boger et al (2015) C: Cunningham (undated) D: De Vito et al (2014) F: Fiegel and Derbidge (2015) S: Sun and Gunasekaran (2009) Various measurement techniques have been employed for these tests. Yield stresses have been converted to kPa, a common unit for geotechnical soil strength. 1 kPa=1000 Pa.	

equipment, and ability to create topography for surface water drainage in the reclaimed landscape (McKenna et al 2016). The present paper focusses on undrained shear strength, particularly that measured by the geotechnical vane.

Additional background

There is often a distinction made between fluid

Table 2. Consistency of fine grained soils

Estimated consistency	Estimated shear strength (kPa)
Very soft extruded between fingers when squeezed	<12
Soft molded by light finger pressure; easily penetrated several inches by thumb	12 to 25
Firm / Medium molded by strong finger pressure; penetrated several inches by the thumb with moderate effort	25 to 50
Stiff readily indented by thumb but penetrated only with great effort	50 to 100
Very stiff readily indented by thumbnail	100 to 200
Hard indented with difficulty by thumbnail	>200
Adapted from NAVFAC (1986)	

tailings (which are best described using fluid mechanics) and those to which soil mechanics might be applied in the oil sands; the division between the two is a subject of considerable debate (eg Azam et al 2007; Sharma and Bora 2003) and is complicated by the fact that shearing of the tailings often takes them from a plastic solid, though the liquid limit, to a fluid. The liquid limit is a geotechnical test (ASTM D4318) that corresponds to an undrained shear strength of about 0.5 to 4 kPa (Kayabali and Tufenkci 2010). In practice, accurate bearing capacity and slope stability designs for oil sands need to consider the effects of tailings sensitivity (the ratio of the undisturbed to remolded shear strength (Skempton and Northey 1952)). Reliable use of soil mechanics for these sensitive tailings for bearing capacity and slope stability calculations likely requires design shear strengths greater than 5 kPa, and perhaps remolded strengths greater than 5 kPa (McKenna et al 2016).

Food strengths (and fine tailings strengths) are very much less than most soils. Table 2 provides a common classification for soil consistency that shows that most soils are one to three orders of magnitude stronger than processed foods. Normal earthmoving equipment generally requires firm to stiff soils to traffic (eg CTMC 2012). Very soft soils are often removed from civil projects footprints.

METHODS

Selection of foods and household products

Foods and household products were selected to provide a broad range of strengths and consistencies with an attempt to cover a range of common foods and condiments (see Figures 1 and 2). Foods were purchased from an Edmonton grocery store and tested within a few days.

Figure 1. Foods, condiments, and household products purchased for vane tests

Vane test

Laboratory methods followed ASTM D4648 (Standard test method for laboratory miniature vane test for saturated fine-grained soils). Following food industry norms, where practical, food was tested in the product container. To minimize edge effects, the vane was inserted to middle of the sample, with an insertion depth of at least two vane heights and keeping the vane at least one diameter away from the edges of the container. In some cases, these constraints could not be met and a notation was made. Foods were tested at either room temperature (20°C) or fridge temperature (4°C). The temperature of each sample was measured with a digital thermometer.

The test employed a high-resolution vane shear device designed at the University of Alberta to conduct field vane tests on a soft ground rover (Olmedo and Lipsett 2016). The design consists of a DC motor, a gearbox, three angular position sensors, and a torsional spring (Figure 3). A DC motor was selected to provide continuous rotation of the vane while permitting precise speed control. A reconfigurable gearbox was designed to allow the rotational speed of the vane to meet ASTM lab or field criteria.

The sample shear stress is calculated using the torque transmitted through the vane (see Figure 3). High-resolution torque estimates are obtained from accurate angular displacement measurements across the calibrated torsional spring with a torsional constant of 0.00649 N·m / degree, and a maximum torque of 1.00 N·m. Two optical encoders with a resolution of 0.009 degrees were used to measure the spring's rotation. Using a 25 mm diameter vane, the capacity of this system is 0.005 to 30 kPa.

Geotechnical vanes usually have a height to diameter ratio of 2. Most of the measurements were made with a vane 12.7 mm diameter and 25.4 mm high; a few tests utilized 22 and 34 mm diameter vanes. The rod diameter was 4.8 mm. The vane was rotated at 60 degrees per minute (as per ASTM D4648). Note that the field vane is conducted with a much slower rotation (ASTM D2573). The angular displacement of the vane was recorded along with the torque and plotted on a computer in real time.

After the "peak strength" is reached, the torque drops, then starts to level. This point was recorded as the "post-peak strength" following oil sands convention. The vane was then rotated rapidly through 3600 degrees, then the test restarted at 60 degrees per minute again to determine the "remolded shear strength." See Figure 3.

Geotechnical moisture content

Subsamples (Figure 2) were dried for geotechnical moisture content (ASTM D2216) at 110°C. The moisture contents reported are the ratio of the mass of water (the difference in weight before and after drying) to mass of solids. Typical subsamples weighed about 40 g. Larger samples would have provided better accuracy for the very high moisture content samples. Some samples may have lost some non-water components.

Figure 2. Geotechnical moisture test (samples ready for the oven)

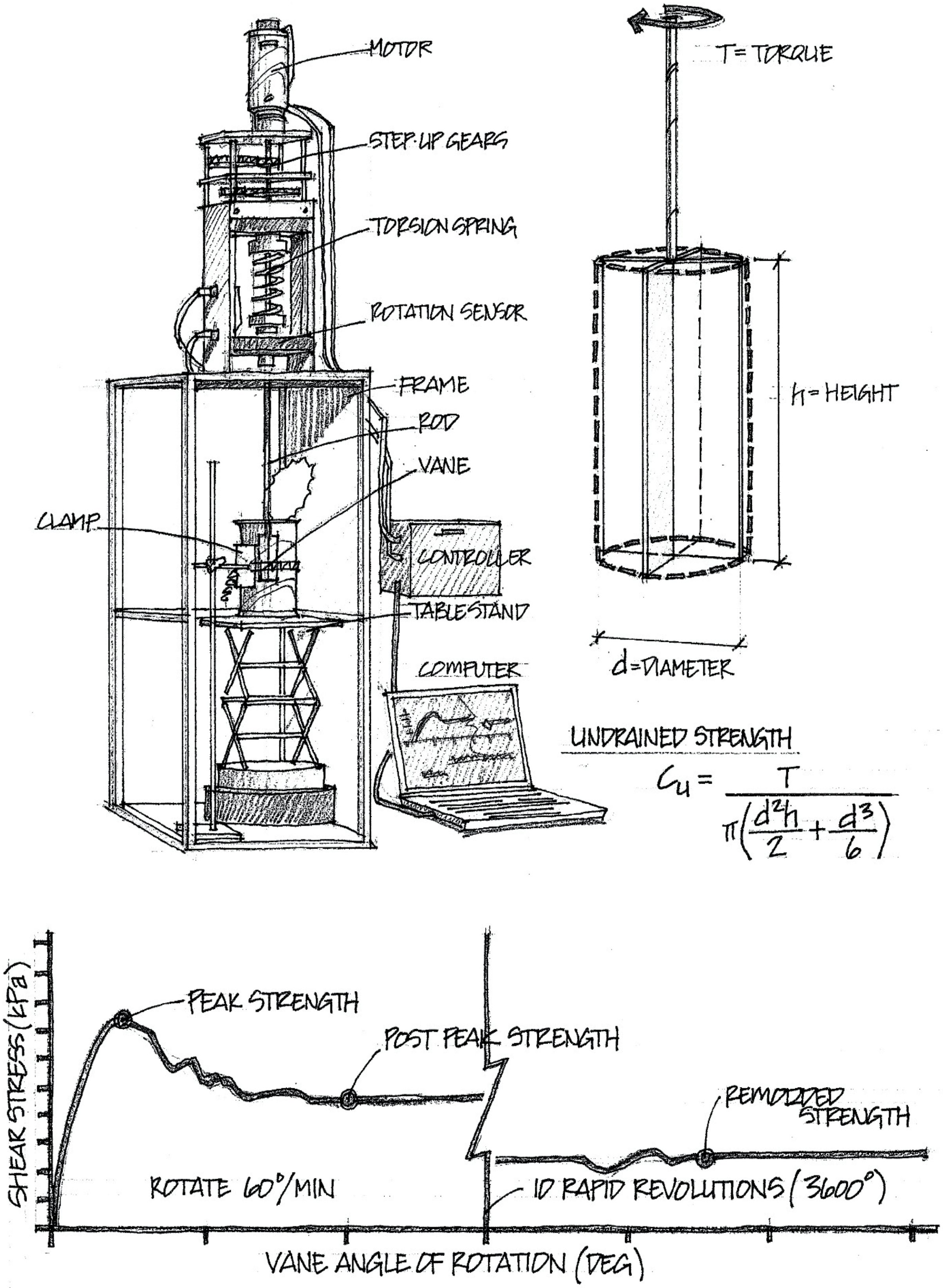

Figure 3. UofA vane device, calculation details, and typical output

Figure 4. Spoon test: A: condensed milk (0.07 kPa fail); B: ketchup (0.22 kPa pass vertical); C: peanut butter (1.8 kPa pass horizontal)

Other tests

Spoon test: A common descriptor for tailings and other slurry consistency is whether a spoon will stand in it (see Figure 4). A steel teaspoon (154 mm long, 53 mm wide, 17.5 g mass) was inserted vertically into the sample and observed. If there was no movement, the sample was tipped until the spoon tilted. Results were recorded as “Fail” if the spoon did not stand vertically and “Pass Vertical” if it did. If the spoon remained in place relative to the sample surface as the sample was tilted through 90° from vertical to horizontal, the test was recorded as “Pass Horizontal.” The tests were conducted on partially remolded samples – with disturbance from the vane, or decanting into a beaker to allow the spoon to fit. There may have been some edge effects from some of the narrower containers.

Fist test: a few samples were tested for fist penetrating (Figure 5). The fist employed had a bearing area of about 60 mm x 90 mm with approximately 20 kg (0.2 kN) to create a bearing pressure of about 35 kPa (similar to the bearing pressure of a small tracked dozer).

Pour test: the sample was also quickly tipped to pour out (or not) and also photographed to provide an additional qualitative description (see Figure 6).

Figure 5. Demonstration fist test. Cool whip (0.39kPa)

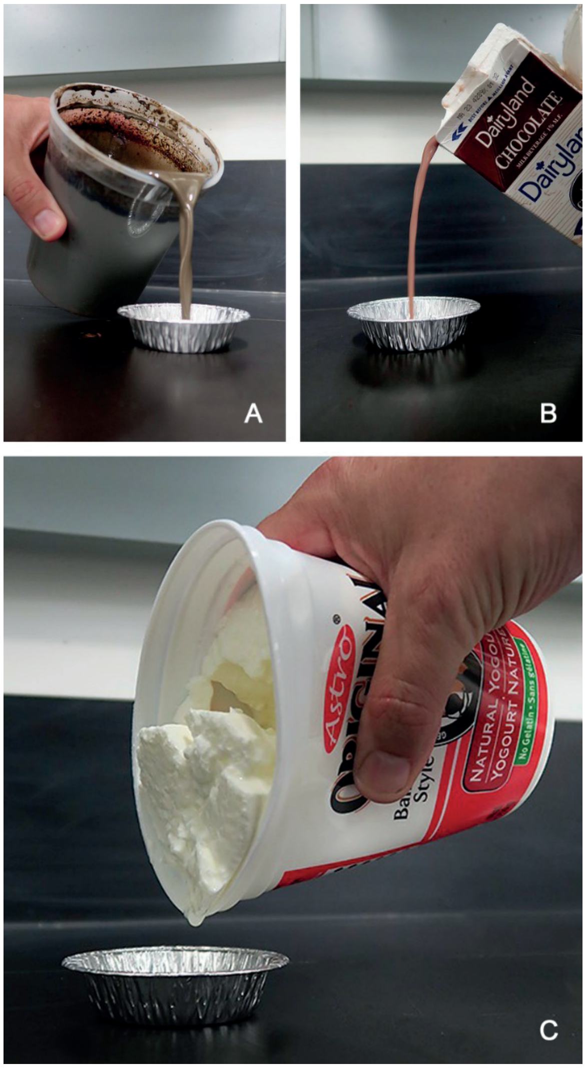

Figure 6. Demonstration pour test. A: fluid fine tailings (0.07 kPa); B: chocolate milk (0.05 kPa); C: yogurt (0.4 kPa)

RESULTS

About 75 tests were completed, about half of which are presented in this paper. Figure 7 provides a bar chart of the peak vane shear strengths in ascending order. Each test has been classified as either food, household product, or tailings.

Figure 8 shows the shear stress versus vane rotation for ten replicate samples of Greek yogurt. The variation between tests is due to a combination of experimental error and mostly differences between different samples of the same product.

Peak vane strengths

Most of the foods (in particular sauces and spreads) had peak vane strengths less than 1 kPa and were very similar to that of the fine tailings samples tested. A few foods had slightly higher strengths, the highest being a yellow banana at 12 kPa. Two waxes had peak strengths in the 40 to 50 kPa range. Results are similar to literature yield strengths in Table 1.

Post-peak vane strength

The post-peak strength is not a standard strength to report and is likely test dependent. It is often 20 to 40% of the peak strength and typically occurs at 2 to 4x the peak angular displacement. This measure did not correlate well with the peak or remolded strengths and is likely not that useful other than to indicate how quickly the strength falls from its peak.

Remolded vane strength

For many samples, the remolded strength was below detection limits. Using the larger vane would have allowed more remolded strengths to be measured.

For samples with measurable values, remolded strengths are generally less than 0.3 kPa.

Sensitivity

The sensitivity of a soil is the ratio of the peak to the remolded strength (Skempton and Northey 1952), and here defined as the ratio of the peak to remolded vane strength (see Terzaghi et al 1996). Sensitive clays have a sensitivity of 4 to 8. Quick clays have sensitivities greater than 16.

The large number of remolded strengths in this test that were below detection limits generalization about sensitivities of the materials tested. Using geotechnical terminology, most of the foods tested were “sensitive” – they had a sensitivity between 4 and 8. A few materials had sensitivities greater than 16 (peanut butter, banana, refrigerated butter and margarine, car wax and candle wax).

The remolded strength of most tailings tested was below detection limits. Two treated tailings with higher strengths had sensitivities of about 5. Beier et al (2013) indicate sensitivities from vane tests for oil sands fine tailings range from 2 to 13.

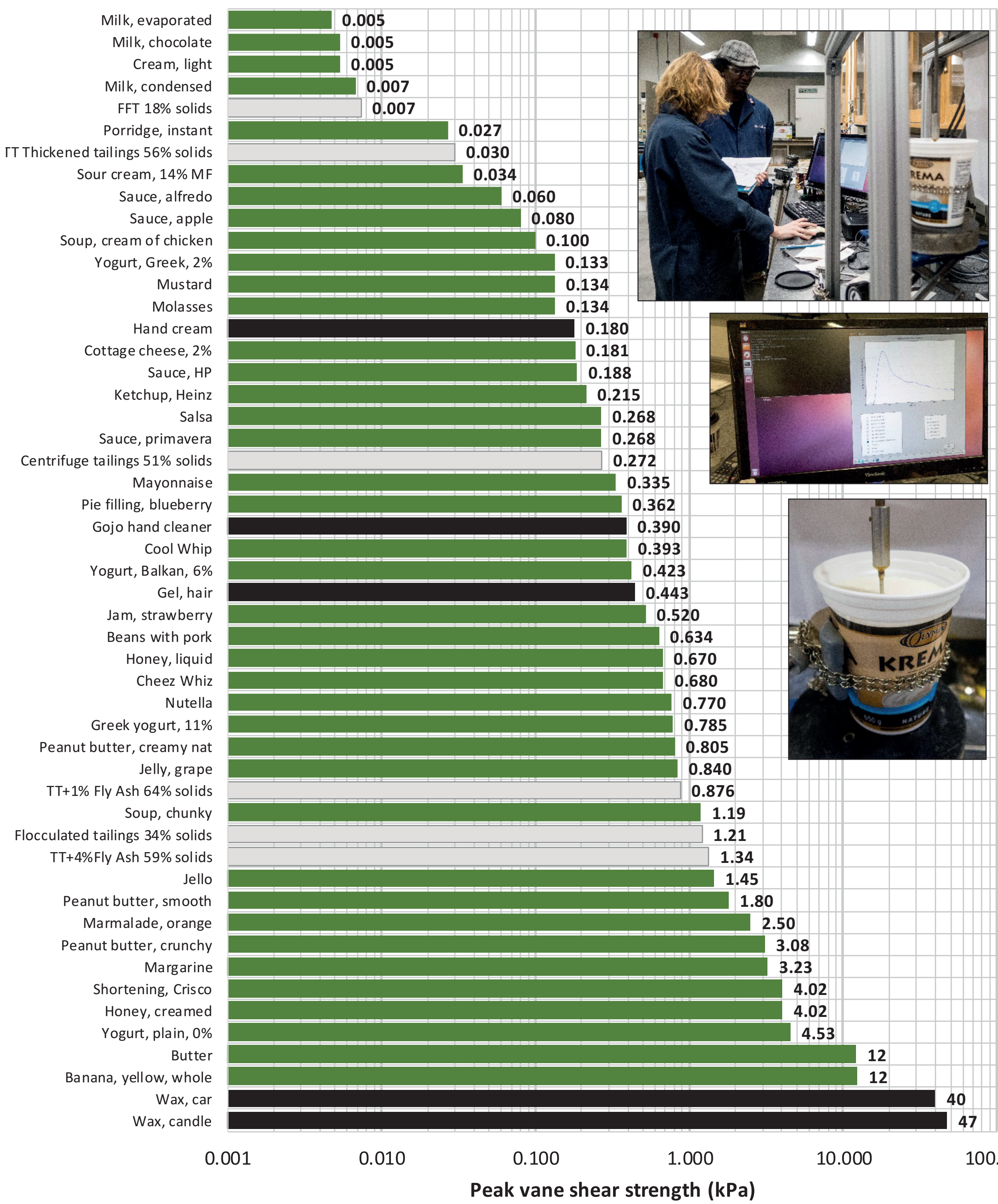

Figure 7. Geotechnical vane strength of soft tailings compared to soft foods and household products

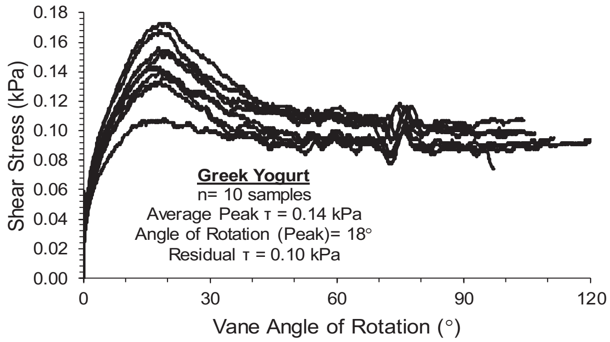

Figure 8. Test results for 10 different samples of Greek yogurt (2%, no fat) to demonstrate repeatability.

Geotechnical moisture test

Many of the oil/fat based foods (eg peanut butter, Nutella, margarine) had low geotechnical moisture contents (<20%). Like oil sands tailings, the large amount of oil in many samples complicates the fluid content. In the case of peanut butter (as for oil sands fine tailings), the Dean Stark Extraction for oil and water content is preferred (eg Pepper and Freeman 1953).

Results are not reported here other than to indicate a very wide range of geotechnical moisture contents with many falling between 100 and 1000 % (mass of water over mass of solids). There was little correlation between strengths and geotechnical moisture contents for foods.

Spoon and pour tests

Spoons stood vertically where the peak vane strengths were more than about 0.2 kPa. Spoons remained in position horizontally where the samples had strengths more than 0.4 to 0.8 kPa. Samples would pour from the jar if they were less than about 0.3 kPa peak strength. But there was considerable overlap in the data, perhaps due to disturbance of the samples during vane tests. Testing of undisturbed samples may have yielded more consistent results. Shear thinning / remolding of the samples (as would occur in a pipeline) would have also produced much different results.

DISCUSSION

Strength testing for food is a common technique and commercial vane rheometers are easy to buy and use. Such an approach is common place for quality control for food processing.

Comparisons of tailings consistency to that of food is common and this paper provides an expanded database to allow direct comparison. The values from the present study are consistent with those in the literature. Soft tailings fit well within the foods tested. Both soft tailings and many foods fit within the “sensitive” category and experience large strength reductions when strained.

The spoon test is not a formal measure but is descriptive and simple to conduct in the field. The pour test and the fist test are just for demonstration but are part of a broader message regarding fluid tailings.

SUMMARY AND CONCLUSIONS

A wide variety of common processed foods and household products were tested following geotechnical ASTM vane test procedures to determine peak and remolded strengths. The peak vane strengths of the foods and tailings generally lie within 0.005 and 1 kPa with remolded strengths typically 4 to 8 times less than peak. The reported strengths are similar to those in the literature.

Indeed, fluid fine tailings (FFT) has a consistency like chocolate milk. Thickened tailings can be compared to sour cream and various sauces. Centrifuge tailings are similar to mayonnaise and ketchup. Thickened tailings with fly ash or flocculated tailings are similar in consistency to grape jelly, peanut butter, or jello.

Such foods are designed to be easy to manufacture, easy to get out of the bottle or container, to spread on food, to consume and digest. Some foods that are a bit stronger require remolding to be enjoyed.

As indicated in OSTC (2012) and McKenna et al (2016), the focus on creating fluid tailings that can somehow be capped and become uplands and wetlands in a reclaimed oil sands mining landscape has perhaps been misguided. Fluids and fluid mechanics are poor substitutes for soils and soil mechanics for building tailings deposits, landforms, and landscapes that provide bearing capacity, slope stability, and acceptable consolidation settlements. There is an opportunity, and a need, to move to tailings technologies that produce strengths more like the medium and stiff soils as classified by our forbearers to make tailings capping and reclamation reliable, safe, and economical.

ACKNOWLEDGEMENTS

The authors wish to thank:

- The University of Alberta for providing use of the geotechnical lab
- BGC Engineering for its support of this effort
- Derrill Shuttleworth for the illustration
- Brent Mooder of BGC for his review of the draft.

REFERENCES

ASTM. 2010a. ASTM D2216-10. Standard Test Methods for Laboratory Determination of Water (Moisture) Content of Soil and Rock by Mass, ASTM International. West Conshohocken, PA.

ASTM. 2010b. ASTM D4318-10e1, Standard Test Methods for Liquid Limit, Plastic Limit, and Plasticity Index of Soils. ASTM International. West Conshohocken, PA.

ASTM. 2015. "ASTM D2573/D2573M-15 Standard Test Method for Field Vane Shear Test in Saturated Fine-Grained Soils." ASTM International. West Conshohocken, PA.

ASTM. 2016. D4648/D4648M - 16 Standard Test Method for Laboratory Miniature Vane Shear Test for Saturated Fine-Grained Soils." ASTM International. West Conshohocken, PA.

Azam S, Scott JD, & Jeeravipoolvarn S. 2007. When does a slurry become a soil? Geotechnical News. Volume 25, Number 3, September. p44-46.

Beier N, Wilson W, Dunmola A, & Sego D. 2013. Impact of flocculation-based dewatering on the shear strength of oil sands fine tailings. Canadian Geotechnical Journal, 2013, Vol. 50, No. 9: pp. 1001-1007. http://www.nrcresearchpress.com /doi/pdf/10.1139/cgj-2012-0262

Boger D, Scales P, & Sofra F. 2015. Chapter 3: Rheological Concepts. In Paste and Thickened Tailings - A Guide. Australian Centre for Geomechanics. Perth. p25-37

CCA (Council of Canadian Academies). 2015. Technological Prospects for Reducing the Environmental Footprint of Canadian Oil Sands. The Expert Panel on the Potential for New and Emerging Technologies to Reduce the Environmental Impacts of Oil Sands Development. Council of Canadian Academies. Ottawa. 252p.

CTMC (Consortium of Oil Sands Tailings Management Consultants). 2012. Oil Sands Tailings Technology Deployment Roadmaps Project Report. Consultant's Report to Alberta Innovates – Energy and Environment Solutions and the Oil Sands Tailings Consortium. June 29, 2012. Calgary. 4v

Cunningham N. Undated. What is Yield Stress and Why does it Matter?. Vendor website: Brookfield Engineering. https://www.pcimag.com/ext/ resources/WhitePapers/YieldStressWhitePaper.pdf Downloaded 2016-10-08.

De Vito F, Meyer F, & Soergel F. 2014. Yield stress of jam, chocolate spread and peanut butter measured with Thermo Scientific HAAKE Viscotester iQ and vane rotors. Vendor website. Application notes V-272. 4p. https://tools. thermofisher.com/content/sfs/brochures/V-272-e-Yield-stress-of-jam.pdf. Downloaded 2016-10-08.

ERCB (Energy Resources Conservation Board). 2009. Directive 074: Tailings Performance Criteria and Requirements for Oil Sands Mining Schemes. February 3, 2009 Alberta Government. Calgary. 14p. (Suspended March 13, 2015).

Fellows, PJ. 2009. Food processing technology: principles and practice. Third edition. CRC Press. Boca Raton. 913p.

Fiegel GL & Derbidge N. 2015. Introducing soil property evaluation in geotechnical engineering – some food for thought. 122nd ASEE Conference and Exposition. June 14-17. American Society for Engineering Education. Seattle. Paper ID 12085. 19p. https://www.asee.org/public/conferences /56/papers/12085/download

FTFC (Fine Tailings Fundamentals Consortium). 1995. Advances in Oil Sands Tailings Research. Alberta Department of Energy, Oil Sands, and Research Division. Alberta Government, Edmonton. 294p.

Heldman DR & Singh RP. 1981. Food Process Engineering. Second edition. The AVI Publishing Company Inc. Westport, CN. 415p.

Jakubick AT & McKenna GT. 2001. Stabilization of soft tailings. practice and experience. Eighth International Conference on Radioactive Waste Management and Environmental Management (ICEM'01). Brugge Belgium. American Society of Mechanical Engineers.

Jeeravipoolvarn S. 2010. Geotechnical behaviour of in-line thickened oil sands tailings. PhD Thesis. Department of Civil and Environmental Engineering. University of Alberta. Edmonton. 432p.

Kaminsky, H. 2014. Measuring strength in oil sands tailings deposits. IOSTC 2014, vol. December 7-10. Lake Louise. University of Alberta Geotechnical Centre, Edmonton.

Kayabali K & Tufenkci OO. 2010. Shear strength of remolded soils as consistency limits. Canadian Geotechnical Journal. Volume 47. P259-266. http://www.nrcresearchpress.com/doi/pdf/10.1139/T09-095

McKenna G, Mooder B, Jamieson A, & Burton B. 2016. Closing the gap: designing oil sands tailings and tailings deposits to become boreal forests. International Oil Sands Tailings Conference. Lake Louise. University of Alberta Geotechnical Group. Edmonton.

NAVFAC (Naval Facilities Engineering Command). 1986. Soil Mechanics Design Manual 7.01. September 1, 1986. 389p. Naval Facilities Engineering Command. NAVFAC DM7.01. US Navy, Alexandria, Virginia.

Olmedo NA & Lipsett MG. 2016. Design and field experimentation of a robotic system for tailings characterization. Journal of Unmanned Vehicle Systems. 4:3 169-192. http://www.nrcresearchpress.com/doi/pdf/10.1139/juvs-2015-0034

OSTC 2012. Technical guide for fluid fine tailings management. Consultant's report prepared for COSIA. Canadian Oil Sands Innovation Alliance. Calgary. 131p.

Pepper MB & Freeman AF. 1953. Determination of moisture in peanut butter. Journal of the American Oil Chemists Society. 30: 335-337.

Sharma, B & Bora, P. (2003). "Plastic Limit, Liquid Limit and Undrained Shear Strength of Soil—Reappraisal." J. Geotech. Geoenviron. Eng., 10.1061/(ASCE)1090-0241(2003)129:8. 774-777.

Skempton AW & Northey RD. 1952. "Sensitivity of Clays," Geotechnique 3:1. p40-51.

Sun A & Gunasekaran S. 2009. Yield stress in foods: measurements and applications. International Journal of Food Properties, 12: 70-101.

Terzaghi K, Peck RB, & Mesri G. 1996. Soil mechanics in engineering practice. Third Edition. John Wiley & Sons Inc., New York. 565p.

PERMEABILITY OF OIL SAND TAILINGS – A COMPARISON OF DIRECT CONSTANT HEAD MEASUREMENTS WITH BACK CALCULATED HYDRAULIC CONDUCTIVITY MEASUREMENTS FROM LARGE STRAIN CONSOLIDATION TEST

Moir D. Haug[1], Julian Gan[1], Mohammad Al-Mamun[1] and Heather Kaminsky[2]
[1]SNC-Lavalin Inc., Center for Advanced Materials Testing and Research, Saskatoon, Canada
[2]Northern Alberta Institute of Technology, Edmonton, Canada

ABSTRACT

A series of constant head hydraulic conductivity tests were conducted on consolidated Mature Fine Tailings (MFT) samples. The tailings had a sand-to-fine ratio (SFR) of 0.18. The test samples were consolidated from 0 kPa to 500 kPa, in 150 mm diameter large-strain consolidation test apparatus. The direct hydraulic conductivity measurements were conducted by measuring the rate of tailings water flow through the MFT at different stages of consolidation. Constant head low gradient flow was maintained during the entire consolidation process. This was designed to eliminate changes in stress state caused by the initiation of flow through the sample. The direct measured hydraulic conductivity of the consolidated MFT from the constant head test ranged from approximately 1×10^{-8} m/s to 1×10^{-9} m/s. The consolidation test results were used to compute the coefficients of consolidation (c_v) and coefficients of compressibility (a_v). The hydraulic conductivity at the various consolidated states were calculated using these coefficients based on Terzaghi's theory of consolidation. The resulting hydraulic conductivity values ranged from approximately 1×10^{-9} m/s to 1×10^{-11} m/s. This paper presents an examination of the potential reason for the nearly two orders of magnitude difference in hydraulic conductivity.

INTRODUCTION

This paper presents the results of a series of low gradient direct "constant head" hydraulic conductivity tests carried out during large-strain consolidation of Mature Fine Tailings (MFT), and compares and contrasts these results with indirect back-calculated hydraulic conductivity test results.

Oil sands MFT is pumped to tailings facilities and deposited as a low solids content slurry, where it is left to settle and consolidate. The hydraulic conductivity of these tailings, along with compressibility is required to provide a reasonable estimate of the time required for their consolidation. Measurements of the hydraulic conductivity of oil-sands tailings present a number of challenges due to the presence of bitumen (plus other chemicals, were added) and their highly compressible nature (Suthaker and Scott, 1996). Large-strain consolidation testing used to assess settlement provides an opportunity to obtain large numbers of indirect back-calculated measurements of hydraulic conductivity, based on Terzaghi's (1925) theory of consolidation. These test are generally consider less reliable than direct measurements, however, accurate direct measurements using traditional k-test apparatus also present a number of challenges. In order to address these challenges, direct measurements of hydraulic conductivity were obtained using specially designed large-strain consolidation/permeability test apparatus. This test apparatus measures the hydraulic conductivity of the tailings at the end of selected stages of consolidation, under continuous flow and "constant head" low hydraulic gradient conditions. The properties of the MFT tested in this program are shown in Table 1.

Table 1. Properties of tested MFT

Property	Value
Mineral content (Mass solids) %	43.0
Mass water (%)	52.0
Mass bitumen (%)	4.5
MBI (meq/100g)	7.6
Bulk density (Mg/m^3)	1.35
Solids specific Gravity	2.12
SFR	0.18
Liquid Limit (%)	47.7
Plastic Limit (%)	17.7

The MFT tested in this program had a sand-to-fines ratio of 0.18. The direct measured hydraulic conductivity ranged from approximately 1×10^{-8} m/s to 1×10^{-9} m/s, with a near linear relationship between log hydraulic conductivity and void ratio. In comparison, the indirect measurements of hydraulic conductivity ranged from approximately 1×10^{-9} to 1×10^{-11} m/s, or 1 to 2 orders of magnitude lower. The largest difference generally occurring for the lower void ratios.

BACKGROUND

SNC-Lavalin's Advanced Materials Testing and Research facility operates 12 large-scale consolidation testing apparatuses (Figure 1). This equipment was specially designed for use on soft tailings to measure consolidation and hydraulic conductivity during consolidation testing. The equipment consists of a mechanical loading system and consolidation cell. The unique feature of this apparatus is its ability to apply low loads, which are required to accurately characterize soft tailings. These units are capable of accurately applying loads from as low as 0.2 kPa and as high as 500 kPa. The mechanical loading system is composed of a counterweight device, direct loading yoke and a mechanical arm to provide leverage for high loads. The stainless steel loading cap is of significant dimension and weight. It is balanced by an adjustable counterweight system to enable the application of small loads necessary for testing slurry materials.

Figure 1. Twelve Large-strain consolidation test apparatus

The stainless steel consolidation cells are 150 mm in diameter and 165 mm high (Figure 2). These cells are designed for two-way drainage through the top and bottom. Drainage through the bottom can be closed off for one-way drainage through the top only. Ports for manometers are distributed over the height of the cell for monitoring pore water pressures during consolidation and heads during hydraulic conductivity measurements. The lower porous stone is sealed into the base of the cell to allow for hydraulic conductivity measurement of the consolidated slurry during or at any selected stages in a consolidation test. A Marriott bottle is used to provide a constant head during consolidation; and, to provide continuous flow of permeant during consolidation and for hydraulic conductivity measurement. Maintaining a constant head ensures that there is no disturbance to the equilibrium of the system at any time, whether during consolidation or hydraulic conductivity testing.

Figure 2. Large-strain consolidation cell and constant head hydraulic conductivity test apparatus

A schematic illustration of the method used to control and maintain a low gradient across the test specimen is shown in Figure 3. The slurried sample is situated inside a two-component/ring cell between two porous stones. The cell is tightly sealed to the base by tightening wing-nuts on bolts extending up the sides of the cell from the base. This process compresses O-rings between the two components of the cell and the base. The test specimen is consolidated in this configuration under increasing applied loads. A constant inflow head is maintained at the top of the cell, and fed by the Marriott bottle. The outflow is collected in a sealed bottle to prevent evaporation and to enable visual inspection of the outflow fluid. The sealed outflow bottle is weighed periodically and that value is used to calculate the flow passing through the sample.

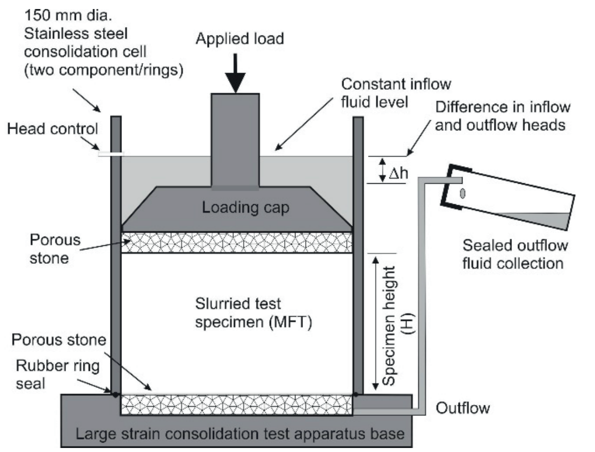

Figure 3. Schematic of large-strain consolidation test cell

MFT does not have significant rebound after loading to 500 kPa. Thus, it is possible to transfer the consolidation cell and measuring devices to one of four high load consolidation apparatus, where the load can be increased to approximately 5000 kPa (Figure 4). While this level of stress may not occur in the field, the procedure is useful for establishing a more precise virgin compression curve. The typical length of time for conducting a single full-test on clay rich MFT type material can take up to six months.

Figure 4. High pressure loading test apparatus

LABORATORY TEST PROGRAM

The large-strain consolidation test was initiated by placing slurried MFT into the consolidation cell at a gravimetric water content of 114.1% and solids content (including bitumen) of 46.7%. MFT was placed up to the top of the lower portion of the cell and covered with a porous stone. The upper portion of the cell was attached and tightly clamped before the loading cap was gently lowered into place.

A constant head across the sample was established to provide a low gradient during consolidation testing and assist in ensuring saturated conditions throughout the test specimen. Since the head difference remained “fixed” during the entire test, small changes in hydraulic gradient were considered acceptable, as the height of the MFT in the consolidation cell decreased with time. The fluid used during the test came from the source of the MFT to ensure that there were minimal if any chemical impacts on the test results.

Consolidation testing was initiated with a load of approximately 0.2 kPa. The time-deflection was monitored until primary consolidation was completed. The load was then doubled and the process continued, doubling the loads at each stage.

Direct measurements of hydraulic conductivity were taken at completion of 5 stages of consolidation. These were at effective stress levels of 1.1 kPa, 2.2 kPa, 8.6 kPa, 34.4 kPa and 140.4 kPa. At those levels, the consolidation process continued while measurements of the flow passing through the MFT were made. Since flow through the sample was maintained at all times, even during consolidation, there was no need to wait for the flow rate to come to equilibrium. As a result, k-test took less than one day to complete.

Indirect back-calculated hydraulic conductivities were calculated for each of the effective stress and corresponding void ratios, and coefficients of consolidation and compressibility.

TEST RESULTS

Direct k-test measurements

A summary of the test results for the direct measurements of hydraulic conductivity is shown in Table 2. This table shows the levels of effective stress at the end of the selected stages of consolidation, the hydraulic gradient across the MFT test specimen at that stage, the measure flow rate during the k-test and the measured hydraulic conductivity. It also shows the void ratio for each k-test.

Table 2. Test results for direct k measurements

Effective stress, kPa	Hydraulic gradient	Flow q, cc/min	Direct K, m/s	Void ratio, e
1.1	0.172	0.0044	2.343E-08	1.865
2.2	0.267	0.0052	1.778E-08	1.760
8.6	0.311	0.0021	6.180E-09	1.375
34.4	0.384	0.0019	4.517E-09	0.918
140.4	0.468	0.0011	2.147E-09	0.575

Two of the k-tests results are presented to provide for more detailed interpretation. Figure 5 shows a plot of deflection versus time for the application of 1.1 kPa of stress. In this plot the three stages of consolidation are represented. Initial compression took place due to the application of the load, that stage was followed by primary consolidation as the excess pore fluid was released. Finally, the test specimen entered the secondary consolidation stage where the individual particles undergo deformation. At this stage (approximately two weeks of testing) the void ratio had decreased to 1.87, and the test specimen was considered ready for direct k-test measurement.

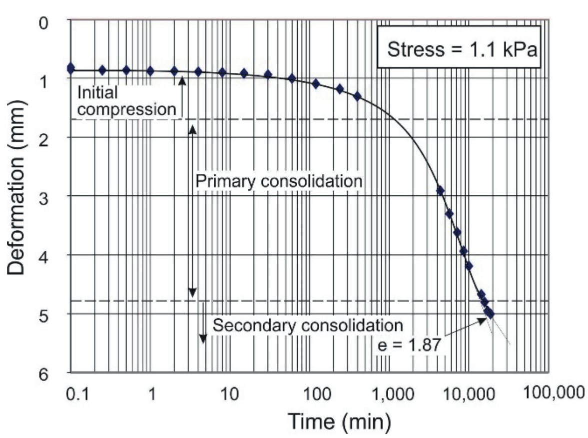

Figure 5. Time deflection plot for 1.1 kPa load

Figure 6 shows the corresponding time-deflection plot for the application of 34.4 kPa of stress. The void ratio at the end of this test (approximately two weeks) had decreased to 0.92. This plot also shows that the test specimen was undergoing

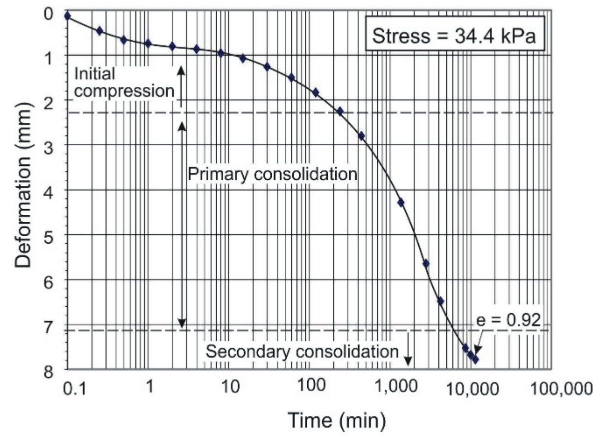

Figure 6. Time deflection plot for 34.4 kPa load

secondary consolidation before start of the direct k-test.

The cumulative direct hydraulic conductivity out flow versus time for the 1.1 kPa load test is shown in Figure 7. The average rate of flow for this one-day plus long test was approximately 0.0044 ml/min. This figure also shows that there is little appreciable change in the rate of flow with time.

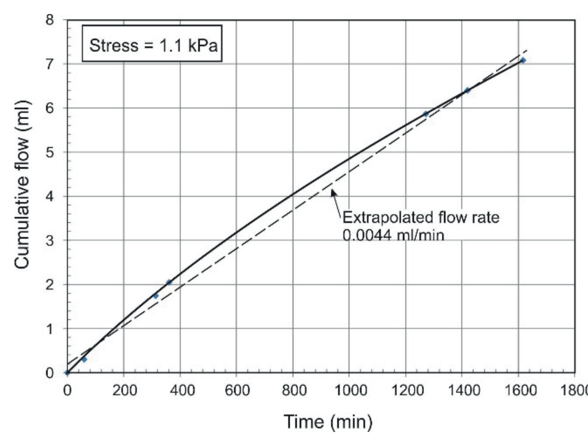

Figure 7. Cumulative flow versus time for direct k-test conducted following 1.1 kPa of loading

Figure 8 shows a similar plot of cumulative out flow during time for the hydraulic conductivity test conducted following 34.4 kPa of consolidation. Both figures were plotted to the same scale. The decreased rate of flow from 0.0044 to 0.0019 ml per min between these two plots is readily apparent. This figure also shows that there is no appreciable change in the rate of flow with time.

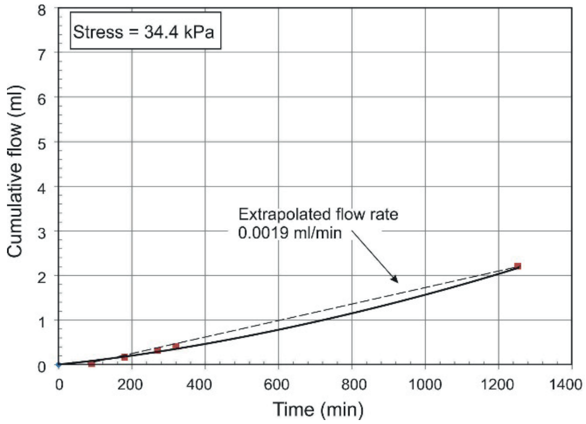

Figure 8. Cumulative flow versus time for direct k-test conducted following 34.4 kPa of loading

A plot of hydraulic conductivity versus void ratio for the five tests conducted during the large strain consolidation test is shown in figure 9. This figure also shows the hydraulic gradients for each test. The hydraulic conductivities ranged from a high of 2.3 x 10^{-8} m/s at a void ratio of 1.87 (solids content = 58.5%), to a low of 2.1 x 10^{-9} m/s at a void ratio of 0.58 (solids content = 81.9%). The void ratio versus hydraulic conductivity for this MFT and under these low hydraulic gradients is essentially linear.

Observation of the outflow fluid during consolidation and hydraulic conductivity showed that it was clear. No sign of bitumen was observed during these tests.

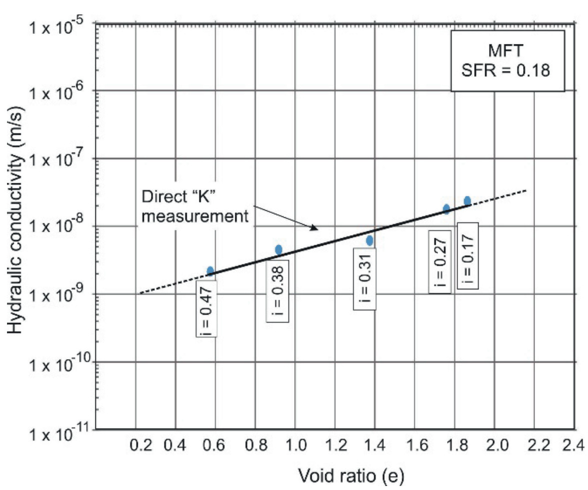

Figure 9. Plot of 0.18 SFR MFT direct hydraulic conductivity test results versus void ratio

Back calculated k-test results

A summary of the indirect k-test results for the five effective stress loads is shown in Table 3. This table shows the effective stress, void ratio, coefficient of consolidation, coefficient of compression and calculated hydraulic conductivity.

Table 3. Indirect hydraulic conductivity test results

Effective Stress, kPa	Total Void Ratio, *e*	Coeff. of volume compresss (a_v), m^2/N	Coeff. Consol. (c_v), cm^2/s	Back-calculated Hydraulic conductivity (*k*), m/s
0.6	1.97			
1.1	1.86	2.20E-04	2.06E-05	1.50E-09
2.2	1.76	9.09E-05	2.35E-05	7.33E-10
4.3	1.58	8.57E-05	1.82E-05	
8.6	1.37	4.88E-05	1.56E-05	2.90E-10
17.2	1.13	2.79E-05	3.41E-05	
34.4	0.92	1.22E-05	5.53E-05	3.11E-10
69.9	0.75	4.79E-06	4.89E-05	
140.4	0.58	2.41E-06	4.77E-05	6.44E-11

A plot of indirect back calculated hydraulic conductivity versus void ratio is shown in figure 10. This figure also shows the effective stress level to which the MFT was consolidated. The indirect hydraulic conductivities ranged from a high of 1.5x10^{-9} m/s to a low of 6.44x10^{-11} m/s. This plot shows an increasingly "downward" trend as the void ratio's decrease. This trend is approximated with a slight curve, however, it is also possible to interpret the results as linear.

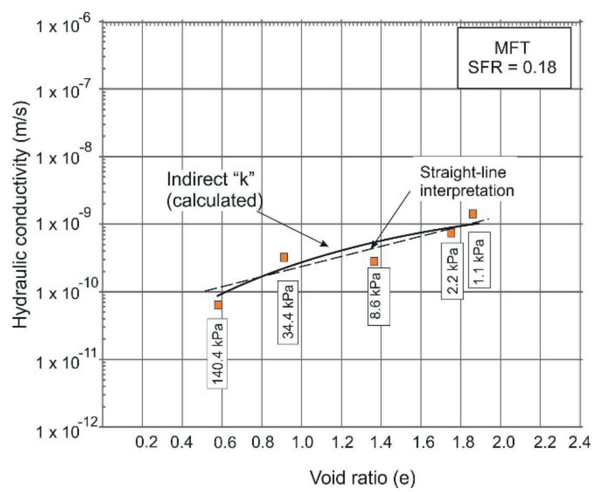

Figure 10. Plot of 0.18 SFR MFT indirect hydraulic conductivity test results versus void ratio

ANALYSIS OF TEST RESULTS

A comparison of the direct hydraulic conductivity measurements with calculated indirect measurements is shown in Figure 11. The indirect hydraulic conductivity values are 1 to 1 ½ orders of magnitude lower than the direct "true" hydraulic conductivity values. Using a slightly curved interpretation of the indirect results suggests a divergence at lower void ratio, however, the slope of the straight line interpretation of the calculated values closely matches that of the direct k measurements.

Indirect hydraulic conductivity calculations are generally known to provide lower values than direct measurements. Matyas (1967) found that the ratio of direct to indirect values ranged from 1.8 to 1, to 2.8 to 1, with comparisons being increasingly poor for higher effective stresses.

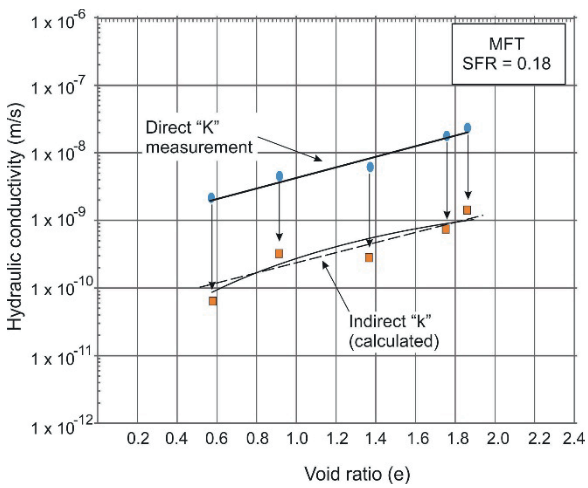

Figure 11. Indirect hydraulic conductivity versus void ratio comparison

Figure 12 shows a comparison of direct and calculated hydraulic conductivity test results from the 0.18 SFR program with Shell and Syncrude's 0.75 SFR Pastes (Masala, and Matthews, 2010). The range (band) of anticipated hydraulic conductivity values for the 0.75 SFR tailings reflects the challenges in obtaining accurate measurements. And while this "band" does encompass most of the 0.18 SFR MFT measured in this test program, it also show a significant reduction in hydraulic conductivity with decreased void ratio. This pattern was not reflected in the direct k-test measurements from the test program carried out on the 0.18 SFR tailings.

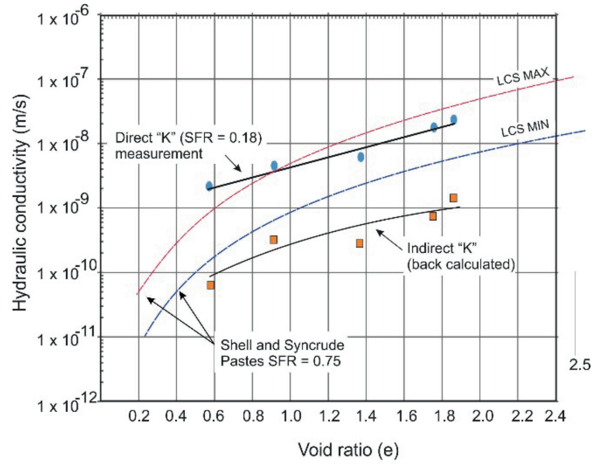

Figure 12. Comparison of direct hydraulic conductivity with Shell and Syncrude 0.75 SFR Pastes

A comparison with other early research on oil sand hydraulic conductivity with these direct and indirect test results is shown in Figure 13. The test results reported by AGRA (1997), Suthaker (1995), and Pollock (1998) were based of back analysis of large strain consolidation tests. This large group of tests results fall along the results for the indirect k-tests measurements obtained during this test program. All of these hydraulic conductivity test values are lower than those obtained from the direct k-tests.

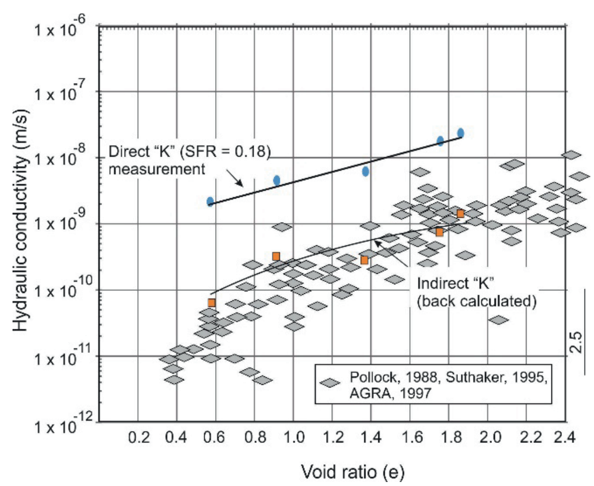

Figure 13. Comparison of industry reported hydraulic conductivity values with test program results

SUMMARY AND CONCLUSION

These result suggest that "true" relationship between void ratio and log hydraulic conductivity for this 0.18 SFR MFT is "linear". The results also found that the direct hydraulic conductivity measurements were 1 to1 ½ orders of magnitude higher than for those calculated based on consolidation theory, with slightly increasing discrepancy occurring at lower void ratios.

The maximum hydraulic gradient during the constant head hydraulic conductivity tests was 0.47. The straight line relationship between log hydraulic conductivity and void ratio, plus the lack of bitumen in the outflow suggest that it may be possible to permit a slightly higher hydraulic gradient than the (0.2) limit suggested by Bromwell, 1983. This increased hydraulic gradient level of acceptability (i.e. up to 0.47) for direct k-testing, may not be appropriate for void ratios in excess of 0.58.

There is a large volume of indirect test data which suggests that the hydraulic conductivity of oil sands tailings is lower than that reported in this test program for direct k-tests. This early data also suggests that the hydraulic conductivity of oil sands tailings decreases sharply at lower void ratios. The MFT tested in this program had a SFR of 0.18 which may be lower than most of the earlier tests on oil sands, however, that difference in SFR is unlikely to account the range of disagreement between the results.

There are a number difficulties in obtaining "true" hydraulic conductivities from the back analysis of consolidation test data. Tavenas et. al (1983) conducted an in-depth study on indirect back-calculated hydraulic conductivities. The conclusions of these authors included the following statement:

"The indirect methods of evaluating *k* or e *vs. k* relationships from consolidation test of all kinds should be disqualified due to the important error produced by the abusive assumptions in the methods of interpreting the test results on the basis of Terzaghi's consolidation theory".

Direct measurements of the hydraulic conductivity of oil sands tailings have challenges, however, most if not all of the traditional sources of error in hydraulic conductivity testing have been eliminated with this test apparatus. These include application of seepage stress at the start of testing, side wall leakage, inability to obtain sufficient flow through the sample, lack of precision in measurement of flow, etc. SNC-Lavalin is currently carrying out a tailings testing program to collect more direct measured k values and will further investigate the relationship between compressibility and hydraulic conductivity, and contributing factors. These factors include MFT fines content, chemical addition and thixotrophy.

The use of indirect back-calculated hydraulic conductivity values to predict settlement of tailings facilities is inherently problematic, since they significantly underestimate flow. It is difficult to imagine a situation where the "conditions" represented by back-calculations of hydraulic conductivity would exist in the field.

REFERENCES

AGRA, 1977. Large Strain Consolidation Analysis of Composite Tailings Oedometer Tests. Report to Syncrude Canada Ltd., AGRA Earth & Environmental Limited, Edmonton, Alberta, 14p.

Bromwell, (1983) Bromwell Engineering Inc. Geotechnical investigation of Mildred Lak oil sand tailings sludge deposal, Report prepared for Syncrude.

Masala Srboljub, Matthews, Jonathan. 2010. Predicting Development of Undrained Shear Strength in soft Oil Sands Tailings. International Oil Sands Tailings conference, University of Alberta, Dec 2-5.

Matyas E.L. (1967) Air and Water Permeability of Compacted Soils. Permeability and Capillarity of Soils, ASTM STP 417, AM. Soc. Testing Mats., pp. 160-175.

Pollock, G.W. (1988) Large Strain Consolidation of Oil Sand Tailings Sludge, M.Sc. Thesis, University of Alberta, Edmonton, Canada

Suthaker, Nagula, N. (1995) Geotechnics of Oil Sand Fine Tailings, Ph.D. Thesis University of Alberta, Edmonton, Canada

Suthaker, Nagula N. and Scott, Don J. (1996) Measurement of hydraulic conductivity in oil sand tailings slurries. Canadian Geotechnical Journal. Vol. 33: pp 642-653.

Terzaghi's (1925) Erdbaumechanik, Franz Deuticke, Vienna.

Tavenas, F. Jean, P, Leblond, P, and Leroueil, S (1983) Canadian Geotechnical Journal, Vol. 20., pp. 645-660.

Session F

Tailings Management (2)

SUNCOR'S TAILINGS POND FACILITY SAFETY MANAGEMENT DURING THE FORT MCMURRAY WILDFIRE OF MAY 2016

Tanys MacGowan, Norm Eenkooren and Shawn Slattery
Suncor Energy Inc., Calgary, Canada

ABSTRACT

On 03 May 2016, Suncor's Base Operations site was largely evacuated in response to an evacuation order for the town of Fort McMurray. This order resulted from the threat of a rapidly advancing wildfire encroaching upon the southwest edge of the town. The evacuation of most of site staff put Suncor's dam structures in a sudden and unexpected care and maintenance environment. This was further complicated, when the wildfire changed direction to the north on 16 May 2016 and put Suncor's Base Operations site at risk. The entire site was then shut-down and fully evacuated.

During this event, Suncor Geotechnical and Operations groups had to respond quickly with a geotechnical risk evaluation and with appropriate response actions to safely manage the many large tailings dams on site with minimal or no staff present. Normal geotechnical management of structures was impacted in the areas of dam performance monitoring (instrument readings and visual inspection), surface pond water elevations, and manual seepage control systems.

This paper will discuss Suncor's initial response efforts, remote site management activities, recovery actions and learnings from this unprecedented wildfire event.

INTRODUCTION

Horse River Wildfire

On 01 May 2016, a small forest fire started south west of Fort McMurray. The fire had grown and threatened Fort McMurray forcing the unprecedented mandatory evacuation of the entire city of approximately 80 000 people, on 03 May 2016. By 04 May 2016 the size of the Horse River Wildfire was estimated to be 7 686 hectares or 18 993 acres (Alberta Agriculture and Forestry, May 03, 2016). On 15 June 2016, the Horse River Wildfire was considered to be 'being held' at 589 617 hectares or 1 456 975 acres (Alberta Agriculture and Forestry, June 15, 2016), approximately the same size as Prince Edward Island, with the perimeter of the fire estimated at 1006 km (Government of Alberta) as shown on Figure 1.

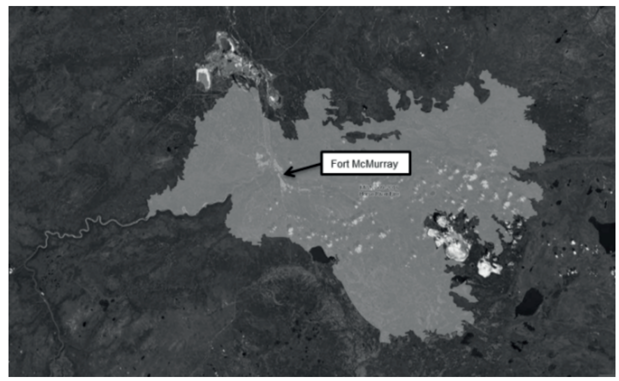

Figure 1. Estimated Impact Area of the Horse River Wildfire

Although the number of firefighters and equipment varied throughout the fire, Alberta Agriculture and Forestry indicated that 2161 firefighters, 80 helicopters and 228 pieces of heavy equipment were deployed and fighting the wildfire (Alberta Agriculture and Forestry, June 04, 2016). It was reported that the fire was moving at a rate of 30 m to 40 m per minute and that the size of the wildfire had created its own weather pattern (CBC news), figure 2. On 04 July 2016, the wildfire was considered to be 'under control' (Alberta Agriculture and Forestry, July 4, 2016).

In Fort McMurray, 2 400 homes and buildings were destroyed. Two neighbourhoods suffered 70% and 90% loss of houses. The Insurance Bureau of Canada estimated that the fire would cost \$3.58 billion (Global News) and be the costliest disaster in Canadian history. The lost production of oilsands is estimated at 30 million barrels of oil and will cost industry upwards of \$1.4 billion (Global News). The Horse River wildfire is considered to be the largest wildfire in Alberta's History.

Figure 2. Showing fire plume above the top of clouds

Impact to Suncor

On 03 May 2016, the town of Fort McMurray was evacuated as a result of the rapidly advancing Horse River wildfire. The evacuation impacted all of Suncor's Oilsands Base Mine (OSB) operations. Some of the operations staff remained at site to manage the operation in safe mode, no bitumen production. During this time, operations staff were monitoring the tailings facility with the assistance of the Calgary based Geotechnical group. Operations not only monitored the water levels but also completed visual monitoring on the dam structures in the absence of Suncor's regular field monitors.

While the site was functionally in safe mode, some water transfer systems needed to be maintained. This required Geotechnical, Process Engineering and Operations staff working together to anticipate changes to the pond elevations and ensure the appropriate freeboard levels were maintained..

It was during this time that the Geotechnical group assessed individual dam structures for risk as discussed below.

While the Geotechnical group was focussed on the safety of the tailings dam structures, Suncor was focussed on other areas where the wildfire may impact the site by creating fire breaks. Some of the fire breaks extended onto the downstream slopes of tailings dams.

This paper strictly deals with the response to the tailings facilities on site and does not address the many other aspects of Suncor's response to the Horse River wildfire evacuation of personnel and the risk to the operation.

Timeline of Events

On 10 May 2016, personnel in the Geotechnical Engineering group returned to site to visually assess the pond levels and the dam structures and determine if any damage had occurred in the absence period when no visual and instrument monitoring had taken place. Instruments that were deemed as critical were promptly read. On 12 May 2016, members of Field Services returned to assist in the monitoring of the tailings dams.

On 16 May 2016, the Horse River wildfire changed directions and put Suncor's OSB at risk. Emergency Response personnel were the only Suncor staff allowed to remain on site. All other personnel were evacuated from the site. This included personnel that were visually monitoring and managing all the tailings ponds and seepage systems.

On 21 May 2016, critical staff once again returned to manage important infrastructure, including tailings facilities and seepage collection systems. Geotechnical staff returned on 23 May 2016 with Field Services staff returning on 31 May 2016.

A timeline of events of the fire as it related to OSB is presented in Figure 3.

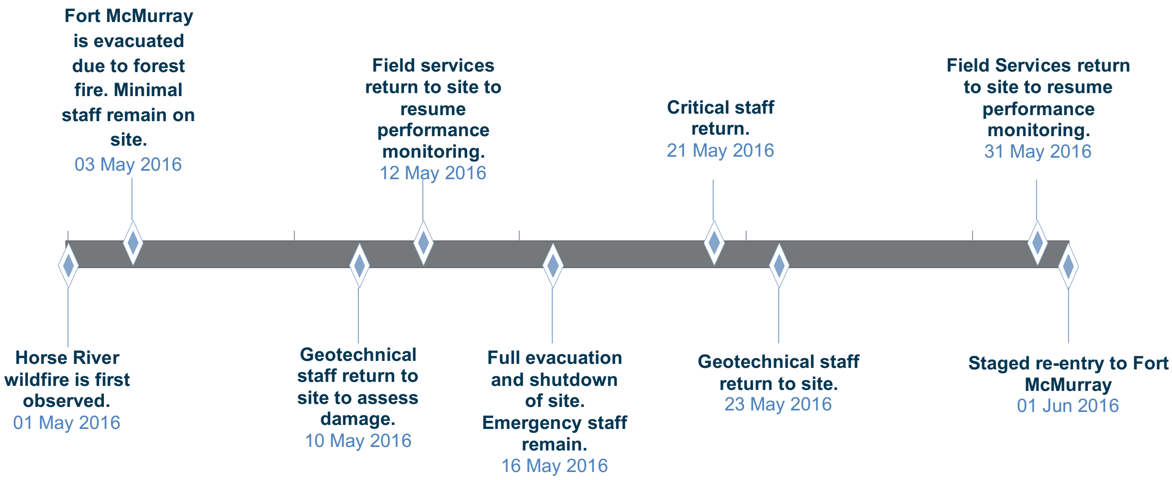

Figure 3. Timeline of events

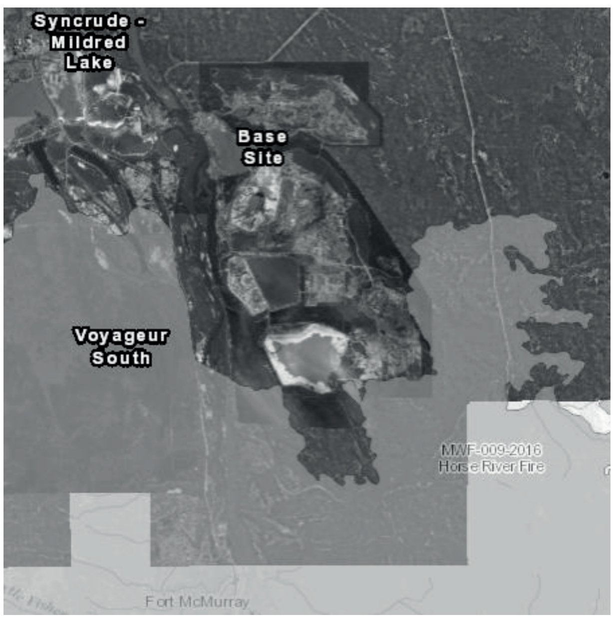

Figure 4. Proximity of Horse River wildfire (grey area) in relation to Suncor Facilities

The proximity of the Horse River wildfire in relation to Suncor OSB is illustrated on Figure 4.

Figures 5 and 6 show the fire at the south of Suncor's site and the proximity of the fire to one of the tailings structures.

Figure 5. Horse River wildfire approaches Suncor's southern extents

GEOTECHNICAL RISK ASSESSMENT

Immediately after Fort McMurray was evacuated resulting in a reduced workforce at site, key personnel in the geotechnical group initiated a risk assessment of Suncor's tailings pond facilities under the lens of the evacuation with the consideration of what risks could exist should the site have to be fully evacuated.

Generally, the performance management of tailings facilities relies heavily on instrumentation readings, visual monitoring, surface water level measurements and seepage control systems which are all people dependant. With the loss of personnel on site, fundamental information was not available to manage these high risk facilities. The risk assessment yielded the highest risks and alternative options available for management.

Initial actions of the risk assessment were twofold. The first was to establish regular and consistent communication with operations staff and management. The second was to assess the potential risk to all of Suncor's dam structures and then communicate the risks to operations and management.

Figure 6. Burned area on south side (dark area on left) against pond perimeter road

Communications

Initial communications to operations and management were focused on maintaining visual observations on the freeboard limits. This communication involved a list of all structures, and their pertinent information:

- pond name,
- last known pond surface water elevation,
- operating levels (minimum, maximum),
- crest elevation,
- flows (in/out),
- estimated pond surface water elevation,
- residual storage volume as a function of pond elevation.

It was quickly realized that estimating the residual storage volume would afford a better assessment of risk as it provided an opportunity to determine time to a freeboard issue based on flows from process engineering. This was communicated daily.

A field check on the pond surface elevation was implemented the day after the 03 May 2016 evacuation. Operations personnel placed stakes in the ground with a mark at existing pond surface water level to show relative changes to the water level. While rudimentary, it was effective in ensuring Suncor did not violate freeboard.

Daily phone calls between Operations, Process Engineering and Geotechnical Engineering provided the feedback on what actions could be taken and if any issues were noted. The communication proved effective as the second portion of the risk assessment could be shared once completed.

Risk Assessment

The risk assessment was conducted using a structured approach for assessing each of the eleven tailings facilities at Suncor OSB. The assessment expanded on the already compiled information from the daily communication. The additional information covered included:

- current status (active or closure),
- risks to the structure,
- stability,
- ancillary structures (seepage management),
- consequence of a complete shutdown,
- action plan,
- key personnel.

Part of the assessment was to project how long before the risk event might occur. This provided a targeted approach to the risks associated with Suncor's many tailings facilities.

The current status of the pond was an important component of this strategy since maintaining adequate storage capacity for a major storm event is managed differently for ponds in a closure phase than those in the an operations phase. In both phases, the changing inflow and outflow fluid streams must be understood and managed.

The assessment identified that the two main issues of concern due to reduced staffing were one, freeboard exceedances and potential overtopping, although the risk to exceedances and overtopping of the structure was very low, and two, overtopping seepage collection systems. Through the risk assessment, it was determined that at no time were the tailings facilities at risk of failure but the seepage collection ponds were a potential for release to the environment. With the active management of the water levels reported in daily communications, freeboard requirements were effectively managed.

Many of the sites seepage collection systems are passive and are not able to be shut down in the event of an evacuation. This seepage from the passive drains in the dam was still reporting to seepage collections ponds, which were a risk of a release to the environment. The return seepage systems were both automated and manual. While personnel were on site, overtopping of the seepage collection ponds was not a concern. In the event personnel left the site, both manual and automated systems were at risk, although for different reasons. The manual systems were at risk as the passive systems would continue to have water report to the collection system. The automated systems were at risk if the fire caused a power outage.

The assessment of the consequences of a complete shutdown of the seepage collection pumping systems was completed and the estimated time for overtopping of the seepage collection ponds varied from 2 to 60 days. The short term risk was the time to a release of water to the environment. As the timeframe estimated for release for some systems was so short, action plans were developed with operations to mitigate those risks. The action plans were then implemented by operations.

The key personnel were identified in a contact list such that in the event of a change in status of any tailings facility, management and site operations knew who to call. The central role for this communication was the Geotechnical Engineer of Record for that structure.

FULL EVACUATION

All of the earlier work identifying potential issues allowed operations personnel time to prepare the site in the event of a full evacuation, which indeed occurred on 16 May 2016 in the late afternoon and evening. Figure 7 shows the conditions on site that preceded the evacuation order.

Figure 7. Smoke filling the parking lot outside of Tailings offices

Most of the preparation work related to the tailings ponds was focused on the seepage collection systems. Systems identified as having low storage capacity were pumped down to change the time for overtopping from 2 to 8 days to greater than 7 to 14 days. Any seepage system that could be shut down with no anticipated impact was shut down.

One tailings facility's surface water pond level was pumped down to increase the capacity to carry the seepage water that was routinely being pumped up to it.

Unforeseen Issues

Through all the planning and assessment of what could happen in the event of a full evacuation, a few minor misses still occurred but which did not result in any incident.

A sticking floating valve that was easily managed while personnel were on site became a potential release to the environment during the evacuation.

A siphon, originally broken (i.e. stopped), re-established itself and started flowing water into an adjacent pond. This could have resulted in a freeboard exceedance.

One of the passive seepage systems was not accounted for in the overall flow volumes. This water was still flowing into a pond and could have resulted in a freeboard exceedance.

On one seepage collection pond, a pumping return system was thought to be automated but was not. This did not cause an issue as the collection pond was pumped down and had available capacity.

FIRE BREAKS

During the initial evacuation, 03 to 10 May 2016, where personnel remained on site, Suncor developed a plan to construct fire breaks to help defend the site from the wildfire. Some of the firebreaks extended onto the downstream surface of tailings dams.

The fire break removed some of the vegetation on some dam structures thereby re-introducing erosion issues on the structure. Although no instruments were destroyed, some minor damage was sustained to buried passive drains. Damaged drains were within the dam footprint and continued to report to the existing seepage collection system.

The areas of disturbed soil have been repaired by Suncor to reduce the erosion potential on the downstream side of the dam.

These unforeseen issues informed Suncor of areas to improve and are addressed in the Conclusions.

RECOVERY PERIOD

The dam performance monitoring recovery period occurred in two stages. These stages were when geotechnical engineering personnel returned to site temporarily after the first evacuation and then again when they returned to site after the full site evacuation.

During the first return period, approximately 6 days, the geotechnical team conducted visual inspections of all tailings structures on a priority basis. The only issue identified was a drainage pipe exposed during the fire break construction. The inspection included the burned area adjacent to the south side of Suncor's Base Mine Operations.

Instruments

As a result of the fire, 238 dam instrumentation readings were unable to be completed. These were the instruments that were required to be read more frequently than once a month. Instruments that were required to be read less frequently than once a month, e.g. quarterly, were rescheduled and collected. These delayed readings increased the burden of monitoring in the recovery period as monitors had to complete these 368 dam safety readings in addition to their regular work.

With the proximity of the fire to the south extent of Suncor's Base Mine Operations, the serviceability of some instruments in the area was in question. To deal with this risk, Suncor placed a drill rig on standby for emergency replacement drilling. None of the instruments were damaged by the fire and this plan did not have to be activated.

SUMMARY AND CONCLUSIONS

This unprecedented event of evacuating the town of Fort McMurray's approximately 80,000 people provided Suncor with the opportunity to test the preparedness of the systems to manage during extreme events. While there were no incidents out of the management of the tailings structures with both minimal or no personnel, there were learnings to be taken from this event.

In the initial uncertainty of who needs to evacuate and who needs to remain behind, some critical staff were evacuated. Critical staff, or roles, should be determined ahead of an event such that the correct people remain on site. These people should be informed of their status and where to meet in the event.

One of the risks to the site was freeboard exceedances. An automated system may be a solution to remove this concern.

Instruments were not read during most of the evacuation, and only instruments that were deemed critical were read during the first return to site. Automating high density areas of instruments, high risk areas and sentry instruments for each structure may be an improved approach to providing 'eyes' on high risk structures at all times.

A detailed understanding of in/out flows for all structures would allow for informed decisions on shut downs, and ensures that all systems are shutdown. Updating the Operations, Maintenance and Surveillance (OMS) manuals with this information would provide all operations personnel (and all personnel that deal with the tailings facility) access to this data.

Understanding of the power supply networks for all seepage collection systems helps to understand the risk to seepage systems. The risks to the structures changed when it was understood that some of the systems were automated and others were manual. In addition, it is important to understand what may happen to the power system if one part of it is tripped. In some instances, the one area tripping the line will take other pumping systems out of operation as well.

Conducting a critical loss scenario for each tailings facility for both dam safety and environmental release may provide management with a better understanding of the risks should a situation like this ever occur again.

It turned out that the biggest concern during the evacuations is generally the smallest concern during normal operations. A few of the seepage collection ponds had the least amount of flexibility/capacity in the event of zero active management. Again, at no time were the tailings facilities at risk of failure but the seepage collection ponds were a potential for release to the environment. The success of managing these ponds to achieve zero release to the environment can be directly attributed to the active risk assessment conducted to identify the risk and the communication with operations who pumped the systems down prior to the full evacuation.

ACKNOWLEDGEMENTS

The authors would like to thank Ken Willis, P.Eng, Process Engineering Manager and Johann Mueller, Field Services Manager, who help geotechnical engineering actively manage the structures. All of Suncor operations and geotechnical staff who all worked tirelessly through this time (while their families were evacuated) and helped to successfully manage these structures through this unprecedented event. Additional thanks to Chris Levesque who provided the photos.

REFERENCES

Alberta Agriculture and Forestry, (May 03, 2016). *Fort McMurray Wildfire Update – May 4, 2016*. Available at: http://srd.web.alberta.ca/fort-mcmurray-area-update/fort-mcmurray-wildfire-hazard-very-high (Accessed 04 October 2016)

Alberta Agriculture and Forestry, (June 04, 2016). *Please do your part in preventing a wildfire and respect the Fire Ban and restriction*. Available at: http://srd.web.alberta.ca/fort-mcmurray-area-update/please-do-your-part-and-respect-the-fire-ban-and-off-highway-vehicle-restriction (Accessed 04 October 2016)

Alberta Agriculture and Forestry, (June 13, 2016). *Horse Rive Wildfire is Now Being Held / Fort McMurray Forest Area.* Available at: http://srd.web.alberta.ca/fort-mcmurray-area-update/horse-river-wildfire-is-now-being-held-fort-mcmurray-forest-area (Accessed 04 October 2016).

Alberta Agriculture and Forestry, (July 04, 2016). *Horse Rive Wildfire declared UNDER CONTROL this morning*. Available at: http://srd.web.alberta.ca/fort-mcmurray-area-update/strong-winds-create-unsafe-conditions-stay-safe-by-avoiding-burned-areas-fort-mcmurray-forest-area-0-0-0-0-0-0-0-0 (Accessed 04 October 2016).

CBC News. (Jul 05, 2016). *Fort McMurray wildfire now considered under control.* Available at: http://www.cbc.ca/news/canada/edmonton/fort-mcmurray-wildfire-now-considered-under-control-1.3664947 (Accessed 03 October 2016).

Global News. July 7, 2016. *Fort McMurray wildfire: $3.6B in damage, says Insurance Bureau of Canada.* Available at http://globalnews.ca/news/2808805/fort-mcmurray-wildfire-cost-of-damage-from-alberta-disaster-to-be-released/ (Accessed 03 October 2016).

Government of Alberta (2016). *Wildfire Update 38: June 9 at 3:30 pm.* Available at: http://www.alberta.ca/release.cfm?xID=41701E7E CBE35-AD48-5793-1642C499FF0DE4CF (Accessed 03 October 2016).

COST EFFECTIVE AND RESPONSIBLE TAILINGS MANAGEMENT

Jeremy Boswell
Thurber Engineering Ltd., Calgary, Canada

ABSTRACT

The Oils Sands industry is currently facing a prolonged period of low oil prices which has provoked a careful re-examination of every cost associated with bitumen production. Tailings management is no exception. What could we be doing as an Oil Sands tailings industry to reduce the cost of tailings management?

Other mining sectors worldwide have faced longer and deeper recessions and commodity price challenges in the past. Indeed, copper, coal, and many other mining commodities have been depressed for as long as a decade. The gold industry has weathered many slumps since the heady days of the 1970's. What lessons might we draw from their experiences?

At the same time, tailings dam safety is under greater scrutiny than ever, following two of the largest tailings breaches in living memory, in Canada and Brazil in the past two years. Much of the debate over the past two years in tailings has been about catastrophic failures and how to avoid them. Reckless cost cutting is clearly not the way to go. However, can costs be cut responsibly without escalating the risk of tailings failure?

In these tough economic times, operators, designers and regulators are under considerable pressure to limit the costs of tailings management. This paper identifies aspects of tailings management typically responsible for high cost and advances methods for the responsible reduction in cost, while giving due regard to dam safety.

INTRODUCTION

In a tough climate of low commodity prices, when faced with the challenge to cut costs, the first thought that springs to mind is: "How do I cut costs without introducing excessive risk?" Indeed, the long history of tailings failures is replete with examples of operations where costs were cut to the bone, with disastrous consequences. Although the price of gold is currently over $1400 per ounce, at the time of the Merriespruit gold mine tailings failure, the gold price had been severely depressed for a considerable period, at times to below $300 per ounce. It therefore becomes quickly apparent that in order for tailings costs to be reduced responsibly, a careful understanding of the risks involved, and how reducing expenditure might escalate the risk, needs to be developed.

In response to the Mount Polley and Samarco tailings failures over the past two years, renewed emphasis has been placed on dam safety, with increasing demands and costs across a broad front, for dam owners regarding dam safety classification, design, responsibilities, surveillance, review, reporting, and a whole host of new areas such as detailed consideration of credible failure modes. Increased demands for dam safety are however, unlikely to lead to a reduction in costs, especially in the short term. There is a recent spate of new downstream and centerline designs, where previously tailings dams constructed in an upstream mode were commonplace. The associated escalation in unit costs of tailings disposal is enormous, even prohibitive.

It may be noted that demands for cost reduction very seldom do anything to consider dam safety. Neither are the increased demands for dam safety measures ever weighed against what they might cost.

LOOKING FOR ANSWERS

Blight (2010) records that for two examples of catastrophic failure involving loss of life, which led to a subsequent judicial inquest, the root cause of both was: "poor management, resulting from ignorance of the principles of soil mechanics, poor training of staff, negligence..."

The underlying message from the above statement is the critical reliance placed on tailings operators, and the imperative to focus on avoiding these critical weaknesses if future failures are to be avoided.

Wagener et al (1997) draw attention to a number of specific management failures that led to the deaths of 17 people in the second of these examples.

In dissecting this failure further, Caldwell & Charlebois (2010) note that "the mining company *had cut to the bone to reduce costs* and as a result the dam was neglected, competent people were not involved, and the contractor's staff were overly confident" (italicization by this author).

Upstream construction demands technical and management quality. Strachan & Caldwell (2010) note among the conclusions from the tailings failures reported by USCOLD, UNEP and ICOLD that the majority of incidents were associated with tailings facilities constructed using the upstream method. The upstream method places greater reliance on the quality of engineering, operating and management expertise.

Boswell and Sobkowicz (2011) link quality and risk in tailings management to a concept of duty of care, and provide pointers to the responsible reduction of tailings costs. Some material from that paper is included below.

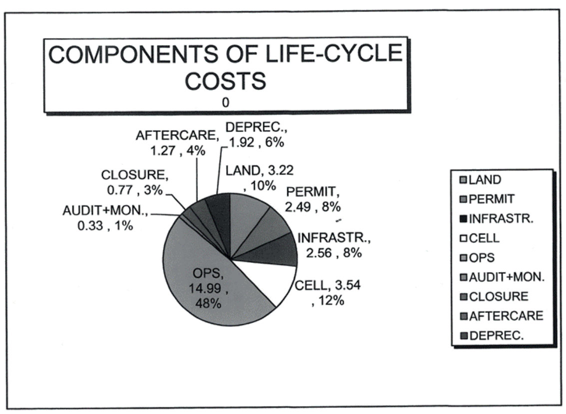

Figure 1. Components of Cost in the Life Cycle Costing of Waste Management Facilities (Boswell 1997)

In the life cycle costing model shown in Figure 1, Boswell (1997) shows the significant contribution that operational costs make to the overall cost of a waste management facility. Even seemingly small daily operational costs when accumulated over 30 to 50 years amount to a huge cost. In facing high costs, and the need to reduce them, the operational items in a life cycle are usually most vulnerable. In a high risk tailings management environment, those cost cutting decisions could prove to be disastrous.

The wise operator may find the following pointers useful regarding tailings costs:

a. Know how much your facility costs. Keep tabs on individual costs. Track changes and trends in costs.
b. Know which items are risky. Track changes in risk profile for key components of the facility.
c. Know which operational actions are essential. Prioritize. Revisit the list on a quarterly basis.
d. Accept that certain items may be satisfactorily postponed, and that timing of expenditure can be varied (in other words, every tailings facility has a cash flow that can be pro-actively managed).

Resource boom and bust market cycles lead to skills shortages and cost cutting. The upstream method and tailings operations in general, are also particularly vulnerable to commodity price variation (shortage of skills in boom times and cost cutting in bad times). Davies and Martin (2009) make the qualified observation that an increase in tailings failures and incidents appears to occur in a two year window after a boom in commodity cycles.

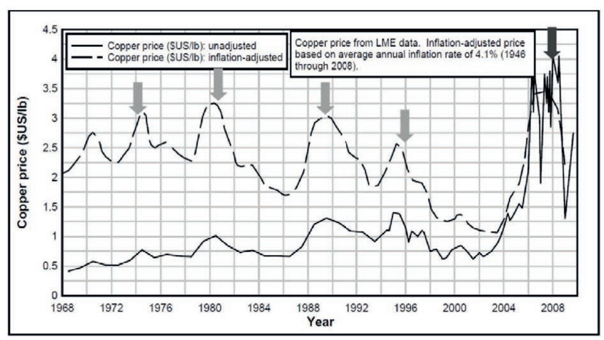

Figure 2. Copper Price Inflation Adjusted – 1968 – 2009 (Ref. Davies & Martin, 2009), showing link between commodity price and tailings incidents

Figure 2, drawn from their paper shows the high points in the copper price life cycle, when adjusted for inflation. They appeared not to link failures to periods of low commodity prices. Could it be that tailings management receives more attention in bad times than in good times? The authors did not find a link, but those of us who have seen a few failures are of the view that there is a clear link – perhaps more so for some mineral sectors rather than for others, and possibly for smaller (junior) mining companies.

Van Zyl (2009) and Devenny and Nelson (2009) make the valid observation that economic analysis should be based on appropriate methods (such as life cycle costing) in order to not yield skewed results (for example, from a net present worth approach, which virtually ignores long term liabilities and costs).

Lack of engineering and management quality can lead to failures. Standard practice in oil sands tailings engineering is to use the "observational approach" to manage structure performance risks while allowing design optimization. This approach has both technical and management components. These are discussed at length in Morgenstern (2010), who provided a "score card" for practice in the oil sands industry. Inadequate attention to the requirements of this design philosophy can lead to failures, which Morgenstern argues to date have been avoided in the oil sands industry by high technical and management quality.

In MAC (2011), the Mining Association of Canada provide a fundamentally sound approach to balancing risk and cost, and include some useful checklists when evaluating, assessing or inspecting tailings facilities.

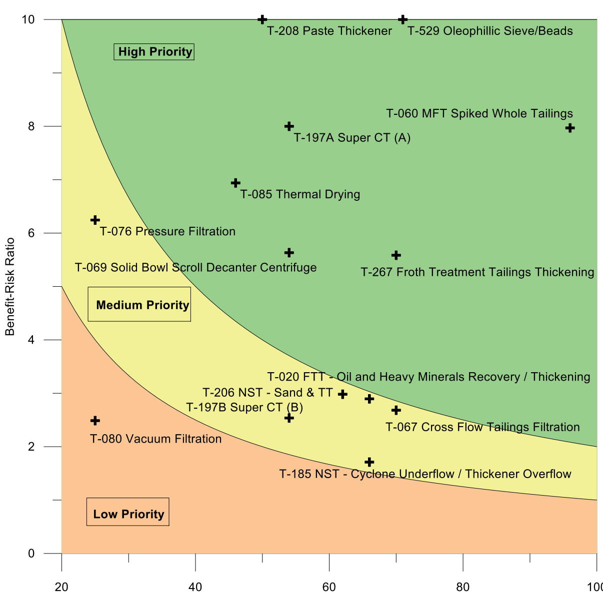

Figure 3. Cost-Risk-Benefit Approach to Oil Sands Tailings Processing Technology Prioritization (Ref Boswell et al 2012)

Boswell, Sobkowicz and Davachi (2012) used a cost-risk-benefit approach to evaluate and screen tailings technologies for the Alberta oil sands, as a means to earmark promising technologies for future development. Figure 3 provides an example output from one of the cost-risk-benefit analyses.

WHERE TO CUT WITHOUT REGRET

In preparing this paper, the author posed two questions to about 40 of his peers – consultants and operators located both within the Oil Sands, as well as those spread across the international mining community:

1. In your view, what are the top three areas in which money is wasted in tailings management?

2. Which ill-advised cost cutting measures employed in the past, upon reflection, have done the most damage in substantially escalating tailings risks?

The responses below made for some fascinating reading.

PRIMARY AREAS WHERE MONEY IS WASTED

These are some of the more obvious and common areas in which money is wasted in tailings management, and where responsible cost cutting and rethinking the approach will add much value:

1. Rework

- Overuse of mechanical equipment in tailings deposition, and double handling and rework.
- Poor planning – ill-conceived planning based on limited or incomplete information and aggressive assumptions, resulting in rework.
- Lack of communication. Changing the plan without communicating the change to others, or delay in communicating the change.
- Unclear direction and/or lack of supervision due to inexperience or changing goals.
- Non-compliance to OMS and lack of routine TSF performance monitoring,

leading to emergency raises, rushed designs etc., which are not efficient.
- Reinventing the wheel - researching the same technology because literature was not read or absorbed at the time. Failing to learn from past mistakes in implementing new technology (variability and scale are important).

2. Planning only for the short term

- Planning facilities that are too small, which need frequent replacement and yield very high unit costs of disposal, and which develop excessive rates of rise which later require intervention and remediation.
- Building Ex-pit tailings ponds too small (which then trigger the urgent need for space in-pit earlier than planned, thereby requiring many in-pit ponds as you chase mining too closely because of immediate tailings space requirements).
- Pursuing short term solutions that do not address the true problems (i.e. fixing a containment issue in one pond by transferring to another pond that has a bit more space temporarily).

3. Poor water management

- Carrying too much fluid inventory (have to build and manage additional ponds and dams).
- For fine tailings – not effectively removing water (transportation and storage of large volumes of water on or within solid landforms).
- Poor water management at both process plant and tailings dam – leading to dilute tailings, excess water pumped around, excess energy consumption, loss of storage capacity.
- Inefficient water pumping and conveyance systems.

4. Mistakes in the application of technology

- Subaqueous deposition of tailings (BBW) instead of subaerial deposition (BAW), and failure to leverage environmental benefits from the forces of nature (solar and wind desiccation, capillary suction, gravity).
- Polymer or chemical overuse due to feed variation.
- Lack of proper instrumentation and or inability to measure key process parameters (such as PSD, clay content, bitumen content and rheology) to be able manage them properly.
- Inefficiencies and delays in the development of new technology. Millions of dollars can go into a tailings technology prior to determining if it works. After putting that much money into the technology, it is hard to tell management that there is a better solution (in the years that the first technology is being proven). Therefore, newer, better technologies are not being looked at in a timely manner.
- Inefficient operations that unnecessarily waste sand production, or other scarce construction resources.
- Changing to a new bright and shiny technology because it looks cheaper or more promising without understanding the fundamentals or drawbacks of the technology, and mitigating them accordingly.
- Non-involvement of subject matter experts in technology application.

5. Not considering closure

- Design scope and operations only catering for the problem at hand. Scope should be expanded so that closure goals are borne in mind at all stages of design and operation. If closure is not considered throughout life of mine, the cost of closure activities at the end of mining when there is no longer a revenue stream or a ready source of materials etc., becomes excessive.
- Lack of planning for eventual closure that substantially increases closure costs. Decisions made during operations can have a large effect (positive or negative) impact on closure costs.

ILL ADVISED COST CUTTING MEASURES WHICH HAVE ESCALATED RISK

Hindsight is a wonderful gift. Perhaps the reader will be able to draw benefit from the list below, without having to fall into the same traps into which others have fallen. This list was also largely provided by a group peers of the author, in reply to the questions posed earlier:

1. Departure from the design

- Steepening of dyke side slopes; omission of berms and step backs and cutting back on sustaining capex.
- Employing tailing deposition or construction practices that save a small amount of money in the short-term, but negatively impact the technical performance of the tailing dam (drainage for example) in the long-term.
- Poor beaching efforts leading to liquefaction risks (dam safety issues).
- Deferring tailings plans (creating dykes) because it doesn't fit with operation's immediate mandate (often bitumen production). This also includes continually adding height to tailings dams because they need the space immediately.

2. Storage of water

- Storing water in tailings impoundments, sometimes associated with reduced size of recycle water dam or foregoing a recycle water dam altogether.
- Allowing freeboard to be used up; relaxing contingency requirements.
- Operating a hydraulic fill structure without pumped delivery of tailings.
- Accepting less freeboard to get through the short term lack of storage space to avoid having to raise the dyke.
- While I am not sure this is a "cost cutting measure" it is key to this discussion. Rather than pushing hard at the Alberta/Canada governments for water release, companies have focused on other things. The amount of water retained behind these large dykes is a concern. They should have made plans to allow water release years ago. That would have enabled better tailings management at less risk.

3. Cutting on geotechnical investigation and instrumentation

- Deferring critical risk mitigation measures. For example deferring geotechnical instrumentation installations to points in time that are technically unacceptable.
- Reducing the site investigation and laboratory testing programs at the start of the project.
- Cost cutting on geotechnical foundation investigations (dam safety issues).
- Ignoring recommendations from senior technical staff on the importance of conducting a particular study to get necessary design information and instead making designers use "best guess" from sparse available information.

4. Going cheap

- Making operational decisions to save money in the short-term that preclude or limit the possibility of future expansions in the long-term.
- Steepening the dyke slopes and/or constructing narrower/smaller dykes to reduce the construction costs.
- Short term cost savings strategies without the long term end in mind. (Resulting in difficult and costly closure of tailings facilities).
- Rapid fire changing consultants on a lowest bid process for small scopes of work – leading to lack of continuity, loss of awareness of the big picture, deviation from original design intent.
- Consultants being used on basis of cost / convenience and not competency. (Cheapest consultant approach). This is aggravated by the use of mine procurement offices who may have limited resources to assess technical competency of the consultants.
- Using lowest cost consultant.
- Not listening to consultant's advice.
- Doing designs in-house. Bringing design work in-house without appropriate expertise, seniority and oversight.
- Choosing a technology solution which appears the least expensive in the short term but has a low reliability/probability of meeting tailing planning targets.
- Cost cutting without due regard for risk.

5. Training cuts

- Giving control of tailings facilities to mine staff with other portfolios (i.e. process plant engineers) who lack the qualifications/ experience/ time to administer them properly rather than having a dedicated staff person in control.

- Not training tailings people in tailings at all levels. There should have been a tailings technology program implemented years ago. Also educating upper management about tailings (formally) and ensuring that tailings personnel are trained before entering the job. This is a big concern – companies have managed to get by – sometimes by training themselves (but that typically is for on-line technology personnel in the field).

HOW TO APPROACH RESPONSIBLE COST CUTTING

How is the demand for cost reduction reconciled with the demands for dam safety? How might this be achieved?

The Mining Association of Canada, MAC (2011) sets forth a practical and useful approach for a joint consideration of both cost and risk. A key first action recommended by MAC is to define responsibility. This is typically allocated to the chief executive and senior vice presidents (depending on the size of the mine), with a comprehensive reporting system. A small effective team of key personnel may then be established which includes the CEO, metallurgical (process) manager, tailings, geotechnical, planning, accounting and environmental leaders. The choice of team members should be based on having the right number of people, streamlined and efficient, and justified based on the types of risk. It goes without saying that a team whose mandate is to improve efficiency should be as efficient as possible and not just be a talk shop.

The use of reliability concepts coupled with the observational approach is useful, identifying and assessing credible failure modes, and making provision for monitoring, record-keeping, reporting and reviewing. Monitoring and surveillance actions and the implementation of the observational method should directly target failure modes. Techniques for cost cutting should be weighed very carefully, balancing the requirements of budget and cash flow against the integrated needs of personnel, mechanical plant, materials, systems, and senior review. Division of all cost elements into three categories is always useful: essential, nice-to-have, and luxuries.

A process should be established whereby the deferral of decisions is justified, and consideration is given to the ongoing needs of training, continuity and standards. Anyone with tailings accountability needs to consider the effect of decisions (especially financial) which are made by other people in the organization. After the recent tailings failures of the past two years, the Canadian Dam Association and the Mining Association of Canada have published a number of important new guidelines and updates in recent months (available on their respective websites www.cda.ca and www.mining.ca) which place renewed demands on tailings management. The definition of Engineer of Record (EoR) has been revised to be much more specific, with delineation of a list of accountabilities and responsibilities. Any cost cutting process needs to consider whether the demands of these new guidelines are able to be met. The planning and deployment of in-house and external resources needs to be prudently balanced. Some areas may in fact need to have additional costs allocated in order to reduce risk to appropriate levels.

DANGERS AND PITFALLS

Sometimes the process is not just about cost cutting. Careful thought needs to be given to other areas, and how the components of a tailings management strategy are integrated with one another. What other less obvious aspects, indeed dangers and pitfalls, need to be borne in mind when contemplating a cost cutting exercise?

Pitfall 1: Looking short term only

An ill-considered cost cutting exercise may introduce new risk. In not looking far enough ahead, the escalation of risk is ignored. In the financial planning realm, a net present value (NPV) approach instead of life cycle costing approach will yield altogether different results, since an NPV approach places heavy emphasis on costs and actions in the short term, and is unable to analyse the impact of a cost cut which escalates risk.

Planning and engineering design should begin with the end in mind, especially in regard to reclamation and closure of tailings facilities. Robustness, resilience and flexibility are hallmarks of a good tailings design.

Pitfall 2: Not identifying dangers and risks

Tracking changes in tailings risks can be very challenging, for the following reasons:

- Many tailings risks are only apparent after detailed investigation, monitoring or analysis, such as liquefaction, introduction of a weak layer, or a rise in phreatic surface. For this reason, the development of monitoring triggers associated with key credible failure modes is essential to sound dam safety management.
- Some risks are more significant when combined with others. Without sufficient experience it is difficult to conceive a chain of events (for example a rain-on-snow flood event, or changes to the OMS system as a result of change of consultant or contractor).
- Some risks arise from unusual and unexpected quarters: a change in the law; a change in adjacent land use; environmental and community opposition; a change in particle size distribution caused by a change in ore or process; codisposal of other waste or wastewater on a tailings dam; accidents; loss of key staff; delays; litigation.

Pitfall 3. Using expensive resources

Selection of inappropriate resources can be very expensive:

- Not planning in advance, and being painted into a corner - “A stitch in time saves nine”. Cutting on scheduled maintenance, or sustaining capex, occasioning high cost emergency interventions later.
- Using untrained or inexperienced human resources.
- Using mechanical plant to do what nature could do for nothing (gravity, solar radiation, wind).
- Using up contingency (freeboard; space for buttress construction).

CONCLUSION

Cost cutting in tailings should not be attempted willy-nilly, nor without careful consideration of the risks involved.

This paper has presented an approach to cost cutting which is responsible, and which gives due consideration of the risks inherent in tailings management, particularly those regarding dam safety.

The ultimate goal of any profitable mining operation should be to safely operate to closure a tailings facility which is lowest in life cycle cost.

ACKNOWLEDGEMENTS

The support offered by my colleagues at Thurber Engineering, particularly from Dr. John Sobkowicz, is gratefully acknowledged.

During the preparation of this paper useful further contributions regarding cost cutting and risk were made by a number of my peers and associates, sometimes on an anonymous or confidential basis. For that reason I have not named each of them in this paper in order to thank them. You know who you are. (Besides, it’s much more fun trying to work out which comment applies to which structure, and in which country). Nevertheless, my grateful appreciation is extended to my peers in this most rewarding industry to which I belong.

REFERENCES

Boswell, J.E.S., Sobkowicz, J.C. and Davachi, M. 2012. Oil Sands Tailings Technology Development Roadmap. Project Report Vol 5. Component 4 Results. Report to Alberta Innovates – Energy and Environment Solutions, June 26, 2012. Page 58.

Boswell, J.E.S. and Sobkowicz, J.C., 2011. Duty of Care Applied to Tailings Operations. Plenary Paper: Tailings and Mine Waste 2011, Vancouver, November 2011.

Boswell, J.E.S., 1997. The Life Cycle Costing of Landfills. Presented at a seminar of the Landfill Special Interest Group in Cape Town. Institute of Waste Management of Southern Africa.

Blight, G.E., 2010. Geotechnical Engineering for Mine Waste Storage Facilities. Leiden: Balkema, 322-338; 453-479.

Blight, G.E, and Fourie, A.B., 2005. Catastrophe revisited – disastrous flow failures of mine and municipal solid waste. Geotechnical and Geological Engineering, 23: 219–248.

Caldwell, J. and Charlebois, L., 2010. Tailings impoundment failures, black swans, incident avoidance and checklists. Tailings and Mine Waste ’10, Vail, Colorado, USA, 33-39

Davies, M. and Martin, T., 2009. Mining Market Cycles and Tailings Dam Incidents. Tailings and Mine Waste 2009, Banff, AB, Canada, 3-14.

Mining Association of Canada (MAC), 2011. Developing an Operation, Maintenance and Surveillance Manual for Tailings and Water Management Facilities. Ottawa, Ontario, p 5-2 to 5-8.

Morgenstern, N.R., 2010. Improving the Safety of Mine Waste Impoundments. Tailings and Mine Waste ’10, Vale, CO, USA. 3-10.

Strachan, C. and Caldwell, J., 2010. New directions in tailings management. Tailings and Mine Waste ’10, Vail, Colorado, USA, 41-48.

Some useful websites

www.cda.ca. Dam Safety Guidelines

http://www.acr-alberta.com/AboutACR/Committees/DamIntegrity/tabid/333/Default.aspx The Alberta Dam Integrity Advisory Committee, established after the Mount Polley tailings failure. This link will take you to a short summary of the committee’s mandate.

www.mining.ca. General guidance regarding tailings management.

http://aep.alberta.ca/. Responsible for updating the AB Dam Safety Regulations. Update due to be issued in 2017.

https://www.aer.ca/. Enforcement of Dam Safety in the Oil Sands, and all regulatory compliance for Oil Sands mining.

CONTINUOUS SATELLITE SURVEYING FOR OIL SANDS TAILINGS MANAGEMENT

Gerry Mitchell, Jim Turner, Adrien Ghariani and Adrian Mitchell
PhotoSat, Vancouver, Canada

ABSTRACT

PhotoSat has been continuously surveying oil sands tailings at a major mine in the Ft. McMurray region every two weeks since January 2013.

Satellite surveying is the best tool for mine tailings beaches. Tailings beaches are usually too soft and wet to walk or drive on safely, prohibiting GPS surveying. They are also too flat to be effectively surveyed by ground-based laser scanning. Airborne LiDAR and drone photogrammetry require mobilization, complex logistics, and often experience long processing delays.

To survey the tailings sites, PhotoSat uses high resolution stereo photographs from the WorldView satellites, which scan of hundreds of square kilometers in a few minutes. The WorldView images provide a near-instantaneous snap shot of the entire mine site. Mine pit, waste dump, stockpile and tailings are measured simultaneously, for easy and accurate reconciliation of volumes. While satellite surveying was initially developed for tailings application, it has now spread and is used throughout mine sites for many purposes.

Achieving better than 15cm vertical accuracy was PhotoSat's initial challenge. The accuracy level was established through numerous accuracy studies, including tens of thousands of ground survey points and direct comparisons to highly accurate LiDAR surveys.

PhotoSat provides topographic survey data to clients in a range of formats, so that it can be quickly imported and immediately used. Waterbody size and location, beach length and other measurements can be done quickly, and with confidence.

Satellite surveying does not require a site visit, eliminating both the safety and security concerns that come with having external staff onsite, as well as any associated standby costs.

While shorter timelines can be met for exceptional circumstances, mine site surveys are generally processed and delivered within five days of the satellite pass.

INTRODUCTION

PhotoSat has conducted a number of monitoring projects for operators in the Fort McMurray oil sands region. The concept was initially put forward in 2012 by the survey group at one major mine, which had been challenged to do monthly topo surveys of their tailings reduction optimization (TRO) cells.

The survey group tested a number of survey technologies to determine the best tool for their needs. The four tools identified that could meet the vertical resolution required included ground GPS (Trimble GPS), ground spatial scanners (Trimble VX), areal LiDAR, and PhotoSat's satellite surveying.

The conclusion of the various technology options evaluated was that PhotoSat provided the best survey product for their needs. Since this time, PhotoSat's survey scope has increased to include the entire mine site on a bi-monthly basis.

SURVEY TECHNOLOGY COMPARISON

At the oil sands mine, the ground survey tools had significant limitations to meeting the challenge of generating topographic surveys of the TRO cells. Because of ground conditions, less than twenty percent of the TRO cells were accessible to be surveyed with the GPS, even when mounted on bulldozers. The Trimble VX spatial scanner was used to survey non-compacted tailings beaches. The VX has a range of 250m and a collection speed of five points per minute, requiring multiple set-ups and long collection time. Additionally, while the VX was good for surveying pit walls and vertical surfaces, it was not good with flat horizontal surfaces (such as tailings beaches) and resulted in a high density of data points near the scanner but increasingly sparse data away from the scanner.

LiDAR met the oil sands mine monthly survey requirements, but there were some associated problems with large point clouds and processing delays. Large point clouds can be troublesome and time consuming to import. PhotoSat survey data files are delivered with a thinned version, which uses a proprietary thinning algorithm, and so do not have the large point cloud problems associated with LiDAR.

PhotoSat's survey processing algorithms were adapted from oil and gas seismic processing algorithms customized to run on massively parallel multicore Graphic Processing Units (GPUs), enabling survey data to be reliably delivered within five days of the satellite image acquisition. In cases where timing of is paramount, delivery of a preliminary version of can be as early as two days from acquisition, with final QA/QC versions to follow a within three days.

Because it met all the needs of the of the survey group, with none of the issues faced by LiDAR, PhotoSat surveying was chosen for a continuous monitoring pilot project.

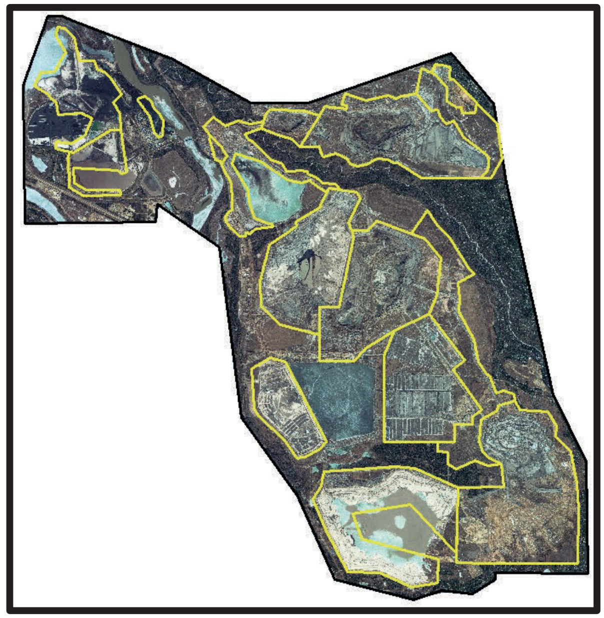

Figure 1. WorldView stereo satellite photo of an oil sands mines showing outlines of the areas of continuous satellite elevation surveying

ACCURACY OF PHOTOSAT SURVEYS

Oil Sands Survey Accuracy

In PhotoSat's original oil sands tailings monitoring proposal, stereo satellite survey grids were specified to be accurate to better than 50cm in elevation. However, based on previous experience with accuracy claims by LiDAR and photogrammetry contractors, the survey team's expectations were that the PhotoSat satellite survey would actually be accurate to about 1m in elevation.

Subsequent evaluation of the survey by the client determined that the first PhotoSat survey accuracy was approximately 20cm in elevation by comparing the data with hundreds of GPS survey points. Continuous processing improvements by PhotoSat have since improved the elevation surveying accuracy to between 10cm and 15cm.

Since the beginning of 2015, PhotoSat surveys of the oil sands mine have all been accurate to better than 15cm in elevation in areas of the mine site with slopes of less than 20% grade. In areas with steeper slopes, the accuracy is usually better than 30cm.

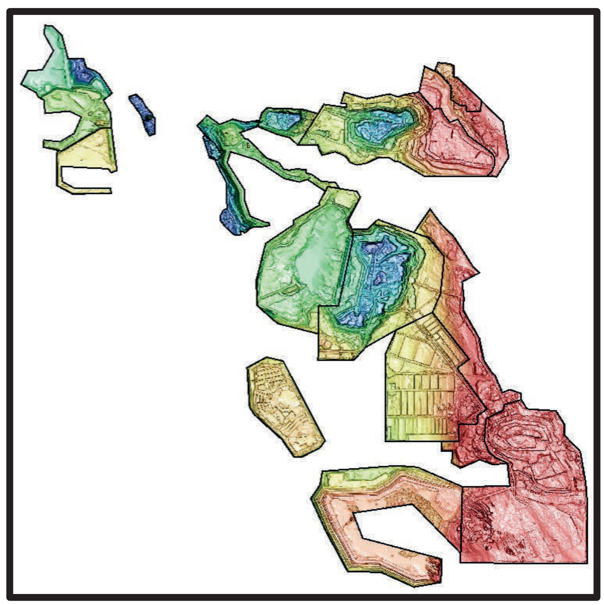

Figure 2. Image of the 1.25m satellite survey grids for the mine

Accuracy Measurements

PhotoSat measures the accuracy of every mine survey grid using a distribution of "as built" survey points. These survey points are from areas that have not changed between the date of the "as built" survey and the date of the satellite photo. Accuracy check points for the mine are shown in Figure 3.

The differences between the satellite survey and the check points are plotted on North–South and East–West scatter plots, as well as in a histogram, to confirm that the tilts and offsets of the satellite survey data have been properly adjusted. The Root Mean Square (RMSE) accuracy and elevation difference including 90% of the check points (LE90) are also measured in this process.

For the data shown in Figures 4, 5 and 6, assuming that the “As-Built” surveying is perfectly accurate, the PhotoSat survey is calculated to match the “As-Built” survey data with RMSE of 12.5cm and LE90 of 21cm. These plots are used to confirm the absence of tilts and offsets in the satellite survey.

Results of 15cm RMSE were repeated in two follow-up accuracy studies conducted in 2014 and 2015. The 2014 study compared PhotoSat surveying using WorldView-2 to a sample set of 731 established survey check-points from a gravity survey in Eritrea. The 2015 study compared PhotoSat surveying with a high-resolution LiDAR survey over an 88km^2 area covering part of the Garlock Fault in California.

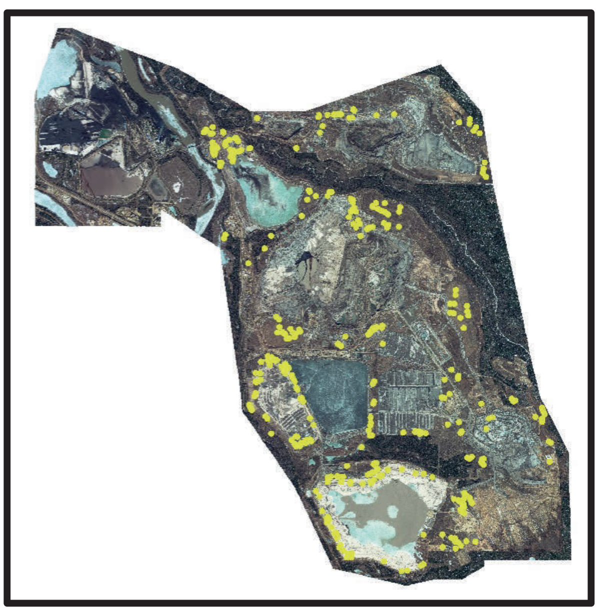

Figure 3. PhotoSat survey accuracy check points from “as built” survey grid

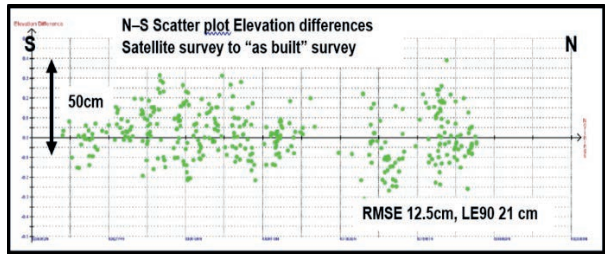

Figure 4. North-South scatter plot of the elevation differences between the PhotoSat survey and 359 survey check points

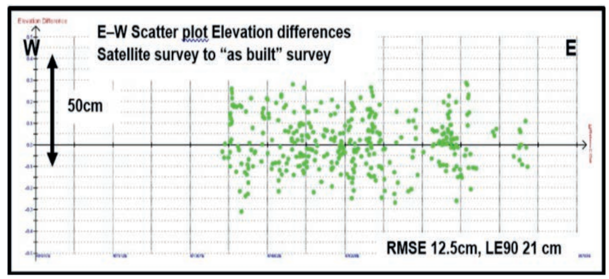

Figure 5. East-West scatter plot of the elevation differences between the PhotoSat survey and 359 survey check points

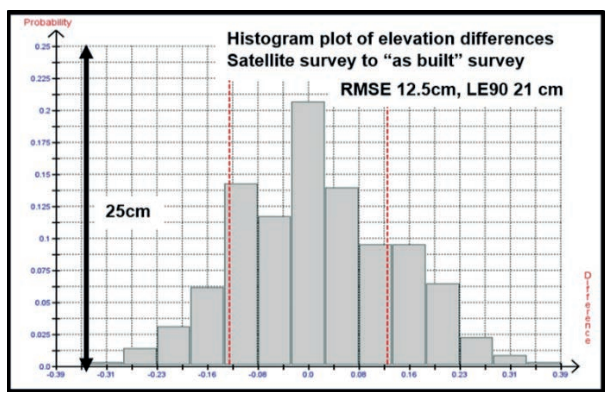

Figure 6. Histogram of the elevation differences between the PhotoSat survey and 359 survey check points

EVOLUTION OF PHOTOSAT SURVEYS

Thinning

Originally, the survey grids that PhotoSat delivered were very large and contained a massive number of data points in xyz format. Each data point contained Easting, Northing and elevation values, and was equidistant from its neighbours in the East-West and North-South directions.

After learning that importing these grids into data systems was a significant bottleneck, PhotoSat tested several commercially available grid thinning programs to help deliver a more compact product that could be more easily used. Simply described, grid thinning is the process of removing points from a large dataset to reduce its size. Since the resulting dataset has fewer points, grid thinning can result in a loss of fidelity and has the potential to reduce grid resolution and accuracy.

The commercially available programs were tested by first thinning the original survey grids and then producing Triangular Interpolated Network (TIN) surfaces and new grids from the thinned points. The TINs and new grids were then compared with the original survey grids. PhotoSat found elevation differences of over a meter in every test and concluded that the existing commercially available software would not be adequate for its customers' requirements. Subsequently, PhotoSat developed its own proprietary grid thinning process for producing accurately thinned grids to help overcome the data import bottleneck.

Since grid thinning is a computationally intensive process, PhotoSat developed its system to run on modern GPUs, which perform numerical calculations more than 100 times faster than conventional Central Processing Units (CPUs).

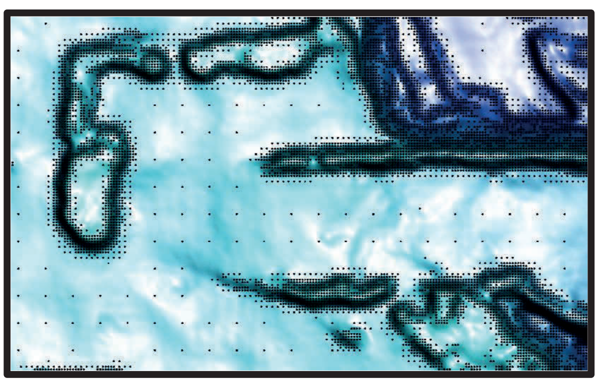

Figure 7. Thinned grid points generated by PhotoSat's system over an image of the survey grid

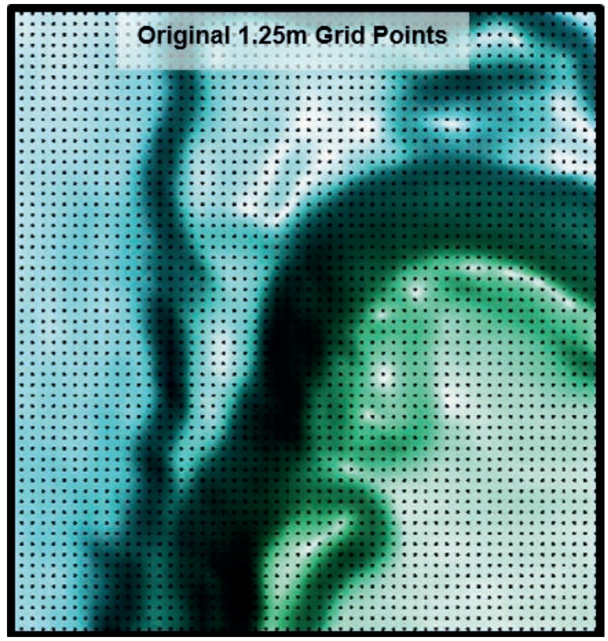

Figure 8. 1.25m grid points

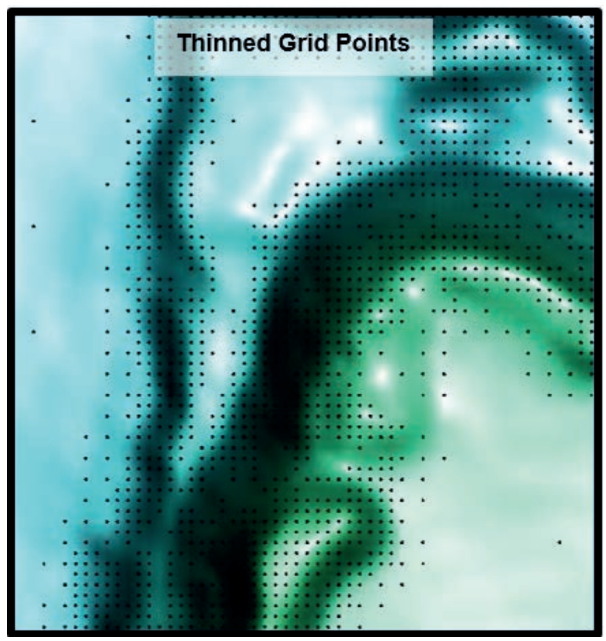

Figure 9. Thinned Grid points for the same area as Figure 8

Figure 7 shows the points in a typical thinned grid generated by PhotoSat's system. Points are removed if they are less than 10m from the nearest adjacent point and can be interpolated to within 10cm in elevation by the surrounding points. No points are removed near changes of slope, preserving most of the detail in the original survey grid.

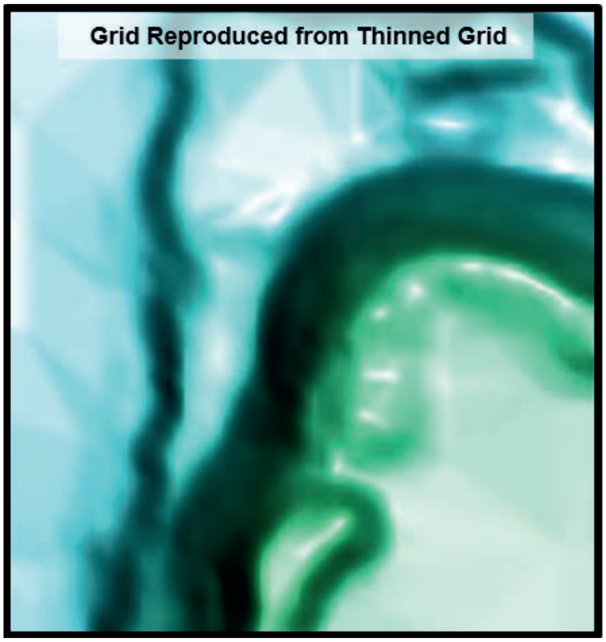

Figure 10. Grid reproduced by linear interpolation of the Thinned Grid points

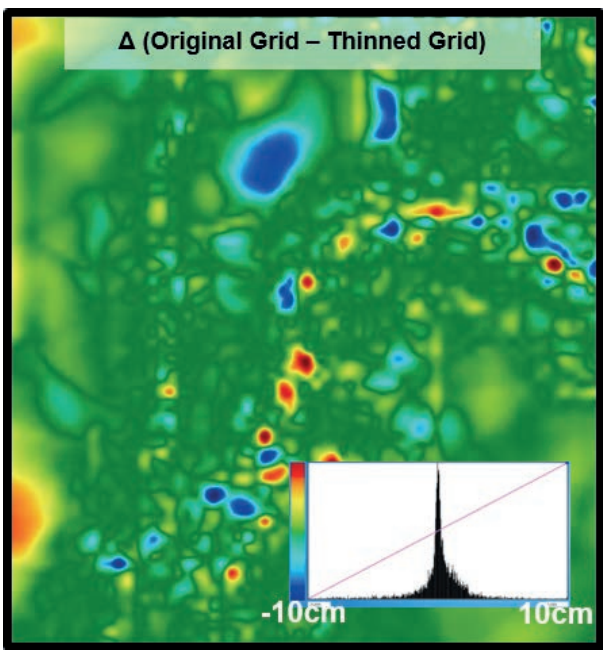

Figure 11. Image and histogram showing the elevation difference between Figure 10 and the Original Grid from Figure 8

For a typical survey grid of the oil sands mine, the PhotoSat thinned grid has only 10% of the points of the original 1.25m grid. When re-gridded and compared with the original grids, the elevation differences were found to be less than 10cm.

This process is shown in Figures 8-11, where 90% of the re-gridded points (LE90) are within 3.5cm of the elevations of the original points – a very small accuracy trade-off for a ten times improvement in data handling time.

Toes & Crests

The lower and upper edges of each open pit mine bench wall are respectively called the toes and crests of the mine pit benches.

Conventional survey of mine pit toes and crests has been used by mining engineers for mine pit volume control since the first open pit mines, and the convention of surveying the crests and toes of all sloping surfaces has since extended to cover entire mine sites. Mining engineering software systems use surveyed toes and crests for a variety of applications.

In mid-2014, PhotoSat was asked to investigate the possibility of producing toes and crests for the at the oil sands mine with each update of the satellite survey. As had been done with the grid thinning, PhotoSat tested a variety of existing processes and algorithms for producing toes and crests from the survey grids and precision ortho-photos.

None of the existing processes produced toes and crests of comparable quality to those produced by conventional surveying, and PhotoSat once again successfully developed its own process using GPUs, allowing for toes and crests to be included alongside the regularly updated survey data delivery (Figures 12 & 13).

Waterbodies

Because water management is an important aspect of modern oil sands mining, PhotoSat maps all of the waterbodies on the oil sands mine site with each survey update (Figures 14 & 15).

The majority of the waterbodies are due to accumulations of surface or ground water in topographic lows. As snow and ice melt during spring, there are thousands of these water bodies on the mine site. Mapping of waterbodies enables the survey team to replace the waterbody elevations with the bare ground elevations from the most recent surveying prior to the water accumulation.

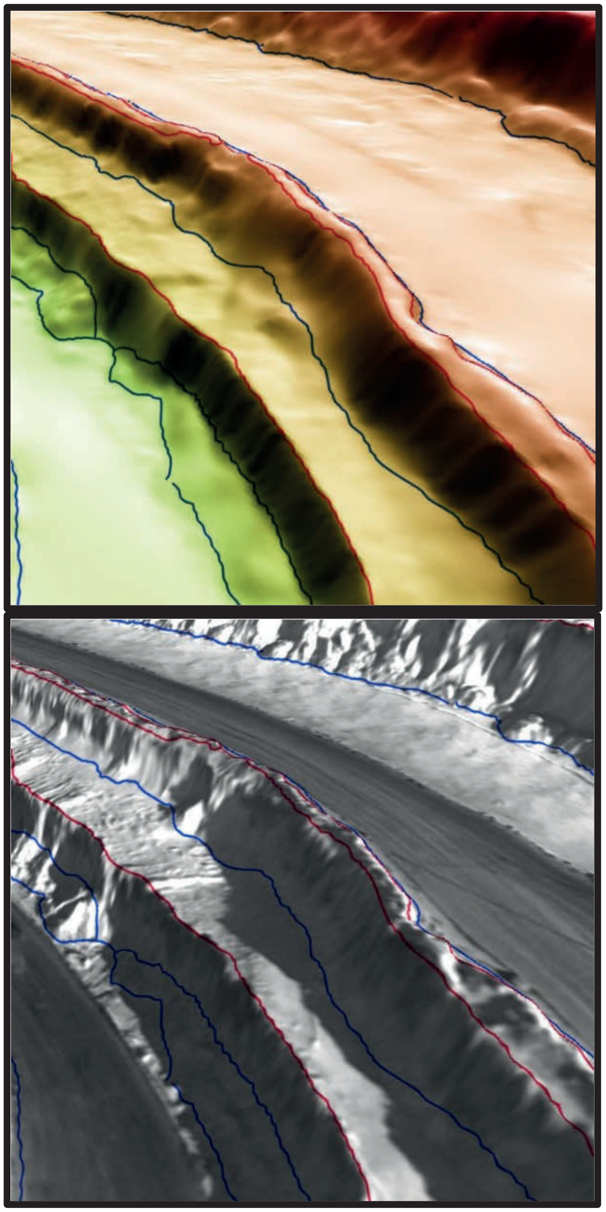

Figure 12. **Toes and crests from the satellite surveying shown draped over 3D images of the survey grid above and the satellite photo below**

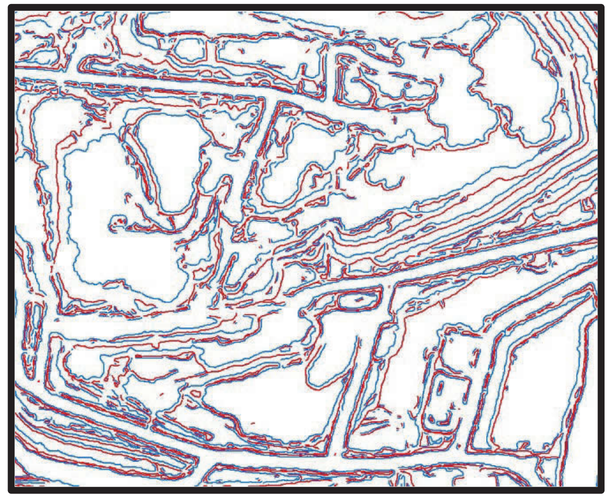

Figure 13. **Toes and crests from a PhotoSat survey for a portion of the oil sands mine site; continuously updated and delivered bi-monthly with survey update**

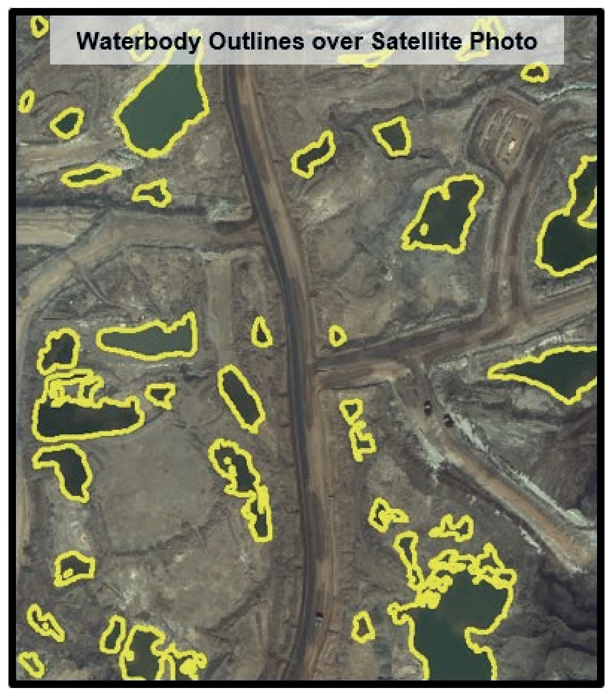

Figure 14. **Waterbody outlines derived from the precision satellite ortho photo**

Figure 15. Waterbody outlines derived from the precision satellite ortho photo

TAILINGS MONITORING

The survey team at the oil sands mine continuously monitors the large tailings ponds and provides water level information to PhotoSat corresponding to the date and time of each satellite image.

Beach lines of tailings ponds can be difficult to interpret from satellite images due to floating bitumen, so pond surface and beach slope elevations are used to determine the beach lines on each of the tailings ponds (Figure 16).

Volume & Dewatering Planning

The continuously updated satellite surveys are used by tailings engineers for volume planning at both the high-level and operational level; from annual budgeting to monthly, weekly, and daily volume planning.

The surveys provide accurate information on both the foundations and tops of the stockpiles, as well as the lift thicknesses of the tailings beaches and the dewatering cells. The up-to-date waterbody outlines form the basis for mine site dewatering plans.

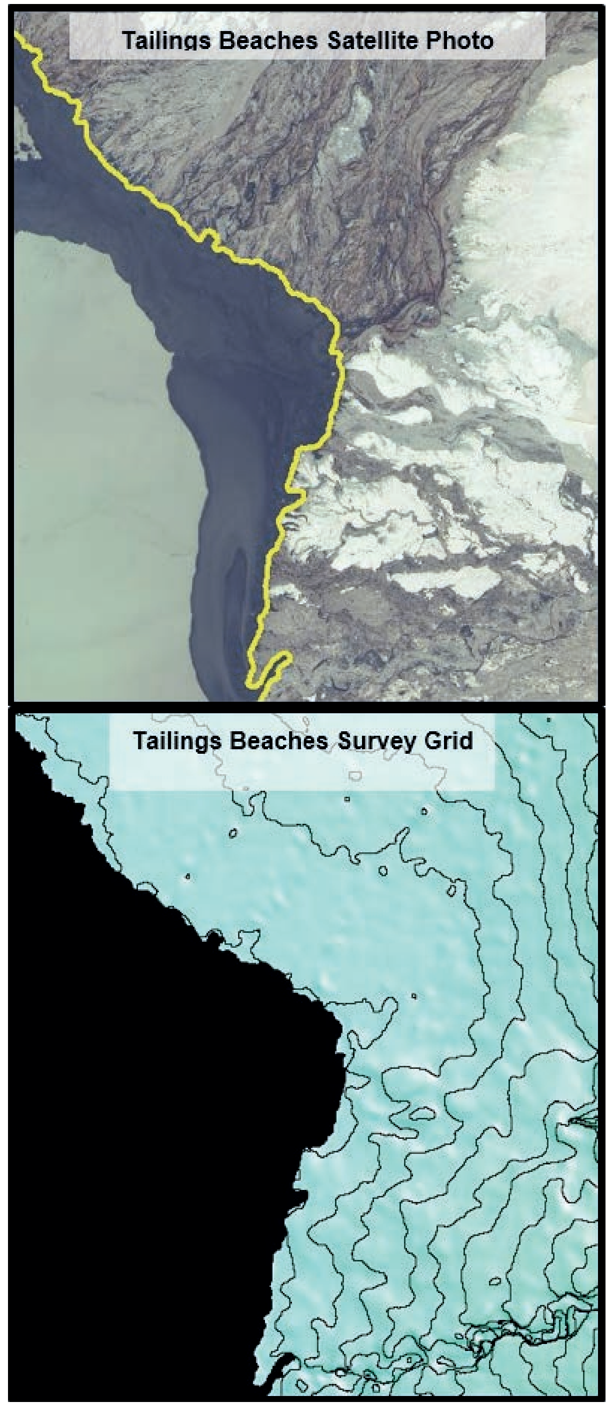

Figure 16. Satellite surveying of the oil sands Tailings Beaches

Roads & Dykes for Tailings

The surveys are also used by tailings engineers for road and dyke design, planning, and construction monitoring. They are useful for initial reconnaissance, design optimization, confirming regulatory compliance, and for cut and fill volume measurements. They also serve as "As-Built" surveys for future reference.

Reduction in Tailings Project Rework

Large reductions in time and cost associated with tailings project rework is one significant advantage of continuous satellite surveying. Often when work starts on a project, the actual ground surface is discovered to be different from the "As-Built" survey data, presumably due to the time that has passed since the "As-Built" was surveyed.

In these instances, construction is often suspended until the ground can be re-surveyed and the construction plans can be modified, which is usually also followed by physical reworking of the site.

Figure 17. Satellite Ortho Photo of Sand Dump

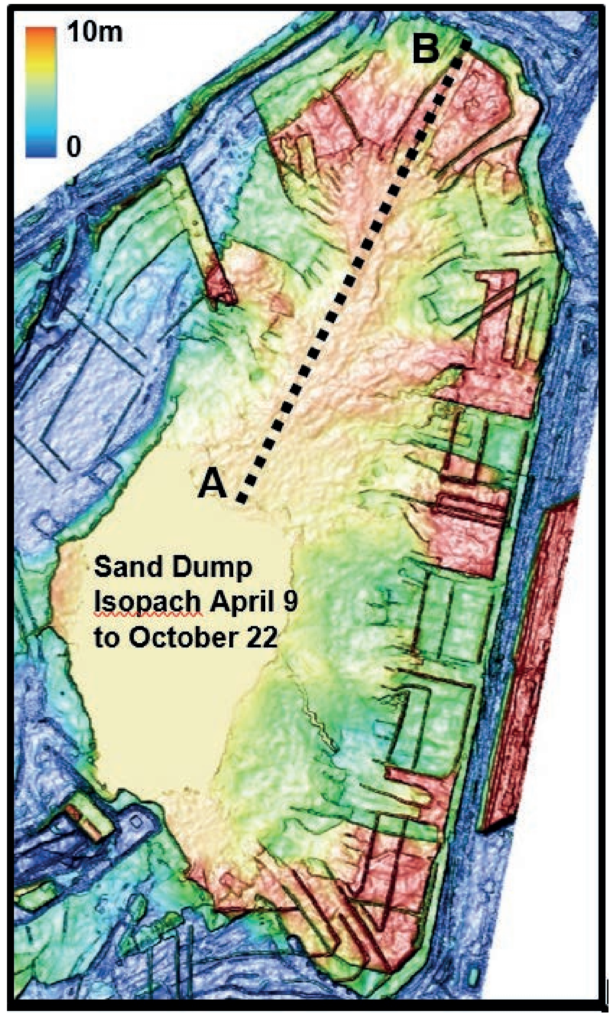

Figure 18. Sand Dump Isopach April 9 to October 22

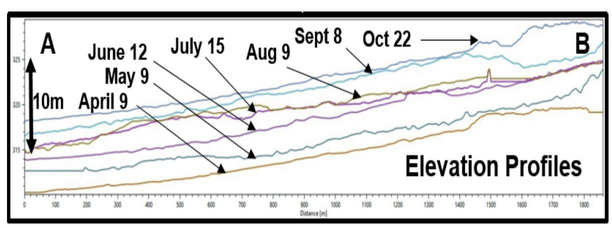

Figure 19. Monthly elevation profiles from cross-section in Figure 19 across one of the tailings plumes

Having machinery and operators on standby for these updates, modifications, and rework is costly. With continuous satellite surveying, engineers have confidence that they can plan projects anywhere on the mine site with accurate and up-to-date "As-Built" survey data.

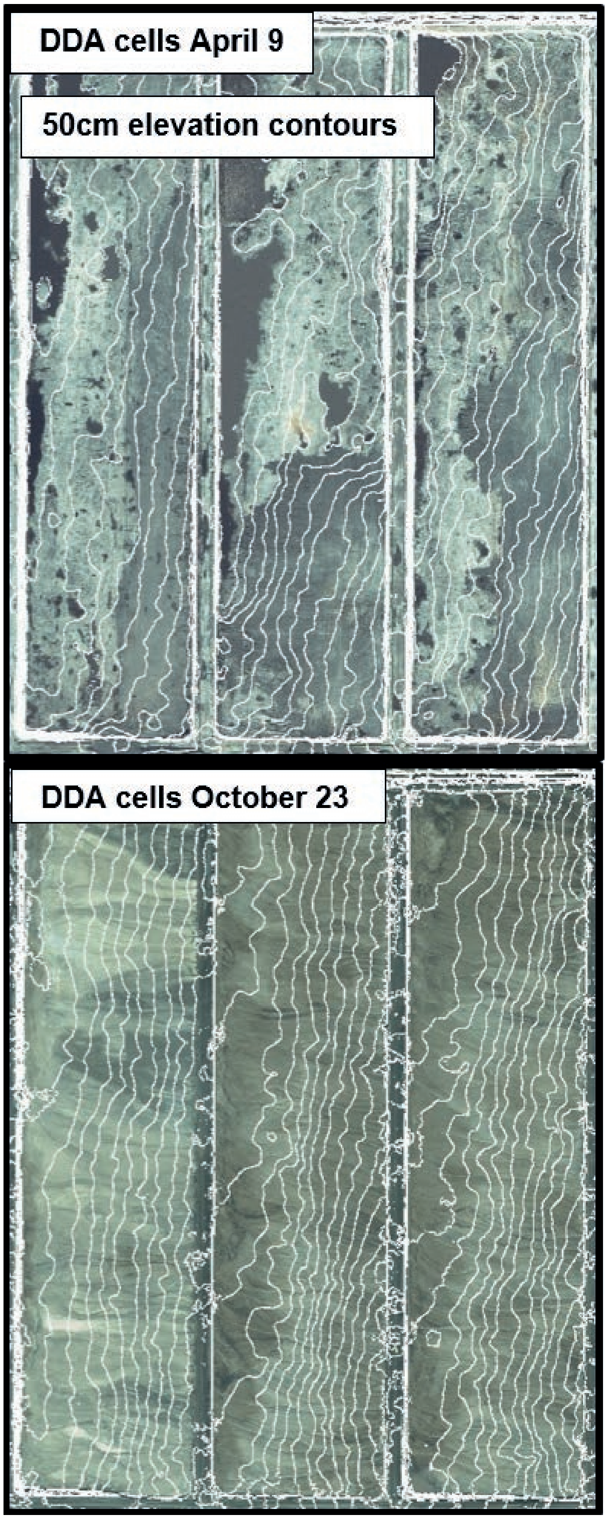

Figure 20. **Satellite photo of DDA cells April 9 and October 23 of the same year with 50cm elevation contours**

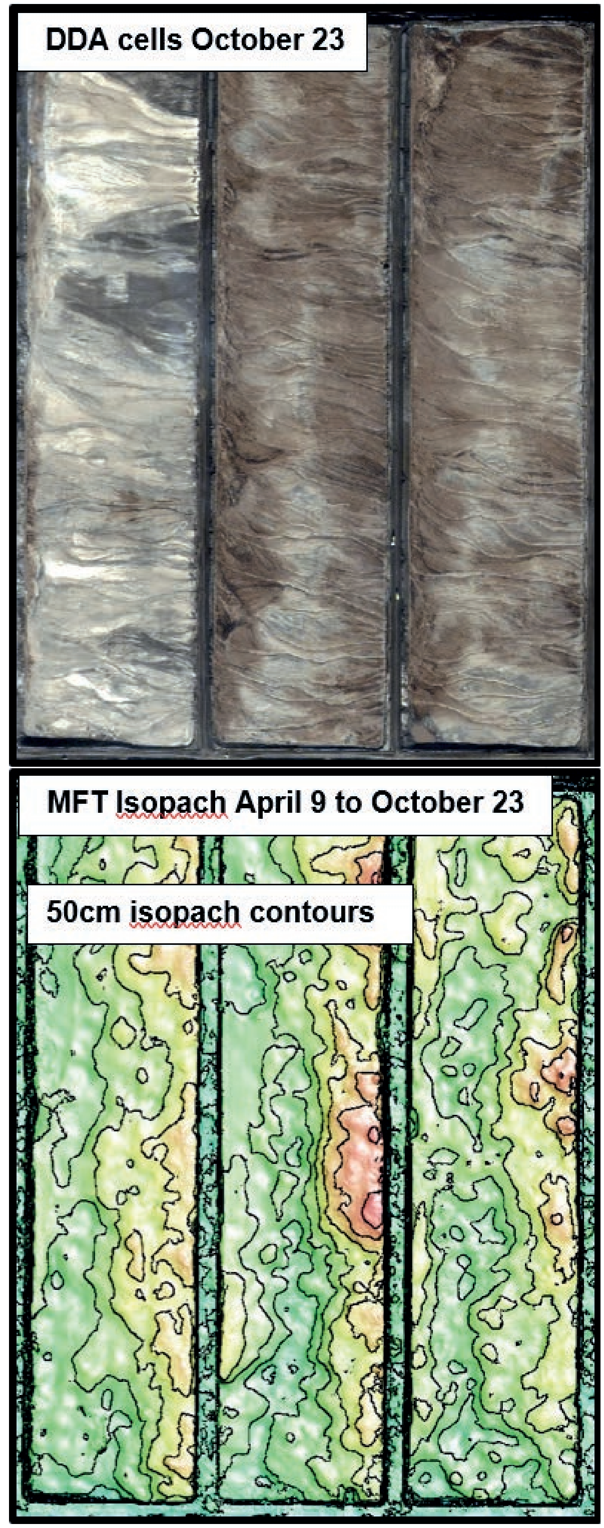

Figure 21. **Satellite photo of DDA cells above, Isopach of cumulative MFT thickness with 50cm contours, April 9 to October 23, below**

Sand Tailings

Planning and measuring tailings deposition in the sand dump is an important use of the continuous satellite surveys. Satellite surveying contributes to the following sand tailings processes:

- Analyzing beach slopes which generally slope at less than half a degree. Satellite surveying covers 100% of the beaches, while ground surveyors can only access the less than twenty percent that are consolidated.
- Planning future beach development to ensure beaches do not reach the floating barges that support the intake pipes for the water withdrawal system.
- Planning deposition locations eighteen months into the future.
- Generating volume inputs for the consolidated capture model, which consists of: ore volumes, processing volumes, and sand dump volumes.
- Producing tailings deposition projections to determine the required elevations of the sand dyke and the mine pit buttresses.

Mature Fine Tailings (MFT) of Oil Sands Mine

Planning for, and measuring deposition of, Mature Fine Tailings (MFT) in the Designated Drying Area (DDA) is an important use of the continuous PhotoSat surveys, which contribute to the following MFT and DDA processes:

- The base for the drying season is the surface surveyed in April, after excavation of the MFT over the winter and any modifications to the cells, and before the first pour.
- The surveyed base determines the total volume of MFT that can be accommodated by the DDA cells for the entire drying season.
- The thickness of each lift is estimated from the pour volumes. After approximately five pours the cumulative lift thicknesses for each DDA cell are measured using the continuous satellite surveying.
- Measuring the area of standing water in each of the cells.
- Measuring the area of utilization of each of the DDA cells to increase their effective drying areas; the effective drying areas increased by 20% from 2014 to 2015.
- Improved communication between the DDA tailings engineers and the operations engineers to maximize the effective areas and optimize the lift thicknesses.
- Monthly determination of the room that each cell has for additional MFT lifts.
- The surveyed surface at the end of the pouring season in October determines the volume of MFT and the amount of water within the MFT.
- The surveyed surface at the end of the drying season, after the last pour, is used to create the MFT excavation plans for the winter season.

SUMMARY

PhotoSat's continuous surveying of oil sands tailings has added significant value to mine operations in a number of ways. Up-to-date and accurate data and imagery have contributed to improved planning, and reduced rework across technical and operational oil sands mining teams.
Engineering teams are now equipped with products that are more easily imported, more accurately derived, and have confidence that their designs and plans are based on surveys that are no more than two weeks out-of-date with consistently high accuracy.

REFERENCES

Schmidt B, Malgesini M, Turner J, Reinson J. Satellite monitoring of a large tailings storage facility. In: *Proceedings of Tailings and Mine Waste 2015, 26-28 October 2015, Vancouver, BC.*

Lomond P, Turner J. *Session ID: GEO-6307 Mapping and Monitoring for Suncor's Oil Sands Tailings Reduction Operation process using GPS surveying and PhotoSat satellite topography. Trimble Dimensions 2014. 3-5 November 2014. Las Vegas, NV*

DigitalGlobe. WorldView-3 Spec Sheet: Available at: https://dg-cms-uploads-production.s3.amazonaws.com/uploads/document/file/95/DG_WorldView3_DS_forWeb_0.pdf

Mitchell G. *Highly Accurate Satellite Topographic Mapping Accuracy Study*. March 2015. Available at: http://photosat.ca/pdf/garlock-30cm-wv3-elevation-accuracy-report-mar2015.pdf

Mitchell G. *Highly Accurate Satellite Topographic Mapping Accuracy Study Eritrea.* July 2014 Available at: http://photosat.ca/pdf/eritrea_wv2_topographic_mapping_accuracy_report_july2014.pdf

AMPHIBIOUS ROBOT FOR ENVIRONMENTAL MONITORING OF OIL SANDS TAILINGS

Nicolas A. Olmedo, Stephen Dwyer, Jamie Yuen and Michael Lipsett
Copperstone Technologies Ltd., Calgary, Canada

ABSTRACT

An unmanned amphibious robot has been developed to improve soft tailings monitoring and characterization. There is a need for new technologies to collect low-risk and timely measurements of rheological and geotechnical properties of recently poured material. Current sampling and testing techniques require large manned vehicles that significantly disturb the deposit or are unable to access recently poured treated material. The paper describes the design and development of a screw-locomotion amphibious vehicle. A first prototype was commissioned and tested over a range of deposits including water, mud sloughs, snow, grass, and treated tailings. The system was instrumented for collecting subsurface samples and conducting standard cone penetrometer testing. In this paper we present the results from laboratory and outdoor trials and identify design improvements and opportunities for further research.

INTRODUCTION

Environmental monitoring of remote and difficult to access locations is a challenge for the mining industry. Advances in field robotics and remote sensing are key to improve how operators collect data, study, and understand the changes in environments affected by industrial operations. Mine waste, such as oil sands tailings deposits, need to be monitored for (i) improving the performance of mining processes (Lipsett, 2014), (ii) timely feedback to improve remediation efforts (Hold, 1993), (iii) environmental monitoring (Plumlee, 1994), and legislative compliance (Wills, 2016).

Bitumen extraction processes generate fluid tailings that take more than 30 years to settle. To further densify and consolidate the material, treatment is required for Mature Fine Tailings (MFT), which are partially consolidated fluids with approximately 30-35 %wt solids. Some common treatments include flocculants addition and centrifuging. The resulting material is deposited in drying cells or dedicated disposal areas. This deposits need continuous monitoring. Current characterization methods for mine waste are based on manual geotechnical sampling and measurement campaigns (Beier, 2013). The information and samples collected can help identify hazards, minimize long-term storage of material, and improve reclamation (Lipsett, 2009).

In many cases, manual geotechnical campaigns are limited to areas made accessible to workers, or areas that large manned vehicles can traverse. Equipment sinking and other risks to workers are possible in variable terrain and the nature of the operations. Current barge and boat techniques are intermittent, costly, and put personnel at risk. There is no or insufficient monitoring of areas inaccessible to workers. More geotechnical measurements are required to meet tightening regulations.

Robotic systems have been proposed to aid human workers in collecting samples and estimating soil properties (Olmedo, 2016). These systems have been field tested to collect oil sands tailings samples of deposits that have developed a crust. Unmanned vehicles can reduce the risk of injuries to workers, while permitting access to very rough terrains. A key limitation of the existing robotic solutions is the terrain bearing capacity necessary to support the mobile equipment. In many cases, the deposits that need to be studied have shear strengths less than 5kPa, to no bearing capacity at all.

Typically, operators need cone penetrometer test (CPT) and sampling of fine-grained lifts in tailings cells variously called centrifuge cake, dMFT/TRO, AFD, and NST. Tracked robotic systems such as the one described in Olmedo and Lipsett, 2016, use tracks to distribute the load of the vehicle, but still require a bearing capacity of 15kPa, to navigate without excessive sinkage.

This paper presents the design and preliminary field trials of an amphibious robot capable of traversing a range of deposits including water, mud sloughs, snow, grass and treated tailings.

DEVELOPMENT OF AN AMPHIBIOUS ROBOT FOR TAILINGS MONITORING

Copperstone Technologies developed an Amphibious Robot (CST-AR1) as part of a suite of remote monitoring technologies for oil sands tailings. The focus of these developments was to be able to collect geotechnical data from any location. Besides ground vehicles, the technology suite is composed of aerial robots to collect samples with no disturbance of sensitive surface crust and distributed sensor networks for continuous in-situ monitoring.

AR1 was developed to conduct geotechnical tests in challenging environments (Figure 1). The locomotion, control system, and payloads were designed and integrated to operate in the harsh environments typical of industrial operations.

The following subsections describe the main subsystems.

Figure 1. CST-AR1 field tests on a mud slough, Alberta, Canada

Locomotion System

The robot designed employs a twin-screw propulsion system. An aluminum frame supports a payloads tower in the centre of the chassis and two screws on the sides. Each screw comprises a sealed aluminum cylinder with welded helical blades. Each screw connects to two aluminum cones, which help displace material in front of the robot and reduce forward resistance. The aluminum cylinders provide sufficient material displacement to make the robot plus payloads neutrally buoyant in water (Figure 2). The overall mass of the system is 350 kg.

Two drive towers support each screw. Each tower has an internal drive mechanism connecting a DC motor and the screw with a chain and two sprockets. The gear ratio of the drives is adjustable. The robot has two drive towers per screw to double the available torque per side, while still using small lightweight electric DC motors. Additionally, having redundancy in the actuators of the system permits recovery of the platform even if one of the actuators fails.

Figure 2. AR1 field tests on a lake, Alberta, Canada

Control System

Two motor controllers drive the electric motors of the drive towers. A motor controller with two outputs is used for each screw. The motors can either be controlled in closed loop, with velocity feedback from optical encoders, or in open loop. Load balancing between the motors connected to each screw is necessary to prevent one of the motors from exceeding the limit current of the motor controller.

High-level control commands and set points are sent from an on-board Linux computer running the Robot Operating System (ROS) (Quigley, 2009). ROS nodes are implemented for high-level wireless tele-operation from a ground station using a joystick. A high-powered wireless 2.4GHz network sends control commands while receiving video and telemetry data from the robot. The wireless system was tested up to 2km without any noticeable communication signal strength loss. The control and communication nodes are designed to have fail-safe routines. In case of loss of communication, or loss of responsiveness of any of the software modules, the robot motors fail safe unpowered (although this would allow the machine to roll if on an incline). System health, state, status, and battery level indicators are made available to the user during operation through an operator ground station.

Power System

The applications of mobile robotic systems are typically limited by their run-time. AR1 is designed to carry two marine batteries with sufficient capacity to conduct operations in soft deformable material throughout an 8-hour shift, with perhaps a requirement for one battery change. In highly adhesive materials the run-time is expected to decrease because the locomotion system would require more power to move the platform.

Payloads

A payload tower deploys a standard core mud sampler or a standard cone penetrometer into the deposit to a depth of 3m. A design for a deeper achievable payload depth is also available but has not been tested. The payload tower consists of an aluminum frame supporting a rack-and-pinion mechanism (Figure 3). A geared DC motor rotates the pinion to lower the rack. Linear guides support the rack. The cone penetrometer or core sampler is attached to the rack through standard 8020 bolt connections. The data and power cables of wired instruments, such as the cone penetrometer, are routed through an inner tube of the rack to protect them during operation.

The payload deployment mechanism is controlled using a motor controller with built-in speed control. The DC motor used to rotate the pinion is instrumented with an optical encoder. This sensor is used to measure the position of the pinion, calculate the depth of the payload, and estimate its linear speed. The selected motor can move the cone penetrometer at the standard penetration rate of 2.0 cm/s over a wide range of resistance forces, up to the maximum weight of the vehicle.

The on-board Linux computer interfaces with a motor controller to actuate DC motor. A ROS node is implemented to send high-level control commands to the motor controller. The high level commands include a position set point and a velocity command. Low-level PID routines modulate the voltage input to the DC motor and use the optical encoder feedback to control the speed of the motor and move the rack to the commanded position. Limit switches are used to prevent movement of the rack beyond the operational limits. Over-current emergency cut-offs built in the motor controller prevent excessive loading on the motor.

Field demonstrations of CPT operations were conducted using a wired cone penetrometer developed by ConeTec (ConeTec, 2016). In manned operations, the cone penetrometer is typically deployed from large manned vehicles into the material using a hydraulic actuator. Using the payloads tower on AR1, the cone penetrometer was deployed up to a depth of 3m. A signal conditioning and acquisition box was interfaced with the cone penetrometer. An on-board Windows computer was used to communicate with data acquisition system and log data. The computer was remotely operated using a virtual desktop environment.

A standard mud sampler could be mounted on the payload drive to collect subsurface samples, The mechanism uses a one-way valve to allow material to flow into the sample container as the rack is lowered. Once the rack is retrieved, the one-way valve captures the material inside the container. The contained sample can be retrieved by an operator and stored for laboratory analysis.

During field trials, subsurface samples were collected using a standard mud sampler (Figure 3).

Figure 3. AR1 field tests on a lake, Alberta, Canada. Payloads deployment tower was deployed with a subsurface sampler.

PROTOTYPE DEMONSTRATIONS

A series of tests were conducted to test the feasibility of the system and analyze its performance. Four outdoor environments were tested: mud/slough, grass, water, and snow. Indoor tests demonstrated the feasibility of the system in treated MFT. The following subsections summarize the test results.

Outdoor Tests

AR1 was tested on hard ground and soft deformable terrain. Initial tests were conducted on hard topsoil with grass, in which the system performed well when side rolling both screws in the same direction (Figure 4). Rolling proved to be the best locomotion strategy on hard ground due to the low ground resistance observed. Forward motion, rotating the screws in opposite directions, consumed substantially more power. In that case, the friction resistance on the screws and the cutting forces of the hard soil surface with the blades could generate sufficient torque on the screws to stall the motors. For turning manoeuvres, one screw was rotated faster than the other, causing one of the screws to slide. These operations consumed substantial power when the blades of the screws are indented in hard soil.

Figure 4. AR1 field tests on a hard soil, Alberta, Canada

AR1 was tested on mud sloughs and snow (Figures 5 and 6). In both cases the robot traversed the material easily and with little resistance while turning. The best performance was achieved when the robot floated on the material. In that case the motors required less current to maintain a constant speed, compared to moving on hard ground, where frictional losses are significant. Snow tests also demonstrated the ruggedness of the system to freezing weather.

Water tests were conducted to demonstrate the buoyancy of the system and the stability while floating (Figure 3). A concern was that a high payload center of mass would make the robot unstable while floating, but lake tests were favourable and showed that the payloads expected do not risk tipping while floating. The locomotion of the robot behaved very similarly in mud and snow. In these cases, turning the screws in opposite directions rotated the robot on the spot, rather than rolling sideways as would happen in hard ground.

Figure 5. AR1 field tests on a mud slough, Alberta, Canada

Figure 6. AR1 field tests on a snow, Alberta, Canada

Indoor Tests

Two main tests were conducted on indoor tanks with treated MFT. The first test demonstrated the subsurface sample collection mechanism and the payloads tower (Figure 7). A subsurface sample was collected remotely and stored for analysis. The second test consisted of mobility tests on MFT. The tests were conducted on a large tank that provided several meters of forward travel. Initially the tests were conducted with a tether to pull out the robot in case of excessive sinkage or getting stuck. Adequate traction and mobility observations were recorded. Further untethered tests demonstrated the feasibility of the prototype traversing treated MFT to collect geotechnical data.

Figure 7. AR1 tank tests on treated MFT, Alberta, Canada

FUTURE WORK

Two main limitations were found on AR1. First, the locomotion on hard ground was limited by the twin-screw configuration. This configuration required the robot to use a large amount of power to perform turns. An improved locomotion configuration would be composed of two screws per side, which could be used as large wheels to turn the robot easily. A cleaning mechanism would improve screw performance in viscous, adhesive treated material. A second limitation is the depth of payload deployment. A necessary future improvement is an automated mechanism to connect drill string on the robot to reach larger depths. The technological challenges to connect and disconnect power and data cables to the payload at the end of the drill string still need to be addressed.

Long-term future work will include using the feedback of the locomotion system of AR1 to estimate soil properties. In that case, shear strength of the terrain can be estimated as the robot traverses the deposit. Autonomous operation of the robot can be incorporated to monitor large deposits with minimal operator supervision.

CONCLUSIONS

The design and development of an amphibious robot capable of deploying subsurface samplers and cone penetrometers was presented. We detailed the main subsystems and discussed the payloads used to conduct geotechnical studies. AR1 was demonstrated in a wide range of difficult terrains with favourable results. Future work to address the limitations of mobility on hard ground and depth of payload deployment were identified.

ACKNOWLEDGEMENTS

Technical support is gratefully acknowledged from ConeTec field engineers and shop-technicians during field trials. ElectroKinetic Solutions is also gratefully acknowledged for making the indoor tests possible.

REFERENCES

N. Beier, W. Wilson, A. Dunmola, and D. Sego, “Impact of flocculation-based dewatering on the shear strength of oil sands fine tailings,” Canadian Geotechnical Journal, vol. 50, no. 9, pp. 1001–1007, 2013.

ConeTec, “Geotechnical, Environmental and Marine Site Investigation”, www.conetec.com, Oct 1, 2016.

L. A. Holm, “Strategies for remediation,” in Geotechnical Practice for Waste Disposal, pp. 289–310, Boston, MA: Springer US, 1993.

M. Lipsett and S. Dwyer, “A robotic system to characterize soft tailings deposits,” in Proceedings of Mine and Tailings Waste Conference 2009, Banff Alberta, November 2009.

M. G. Lipsett, N. Olmedo, B. Rivard, and W. Wilson, “Robotic Systems for Measuring Properties of Tailings Deposits and Collecting Samples,” in Proceedings of the Fourth International Oil Sands Tailings Conference, (Lake Louise, AB), Dec. 2014.

N. A. Olmedo and M. G. Lipsett, “Design and field experimentation of a robotic system for tailings characterization,” J. Unmanned Vehicle Systems., Mar. 2016.

G. S. Plumlee, K. S. Smith, and W. H. Ficklin, “Geoenvironmental Models of Mineral Deposits, and Geology-based Mineral-environmental Assessments of Public Lands,” Tech. Rep. Open-File Report 94-203, 1994.

M. Quigley, K. Conley, B. P. Gerkey, J. Faust, T. Foote, J. Leibs, R. Wheeler, and A. Y. Ng, “Ros: an open-source robot operating system,” in ICRA Workshop on Open Source Software, 2009.

B. A. Wills and J. A. Finch, “Tailings Disposal,” in Wills’ Mineral Processing Technology, pp. 439–448, Elsevier, 2016.

DECANTING OF TAILINGS SUPERNATANT

Jeremy Boswell[1] and Stewart Bodtker[2]
[1]Thurber Engineering Ltd., Calgary, Canada
[2]Paterson & Cooke, Calgary, Canada

ABSTRACT

Removal of supernatant from Oil Sands tailings ponds has traditionally been achieved by using floating or barge based pumping solutions. Due to the operational and maintenance complexities of floating systems, an increasing focus over the past five years in the Oil Sands has been to consider shore-based or fixed decants for removal of supernatant.

This paper describes design conditions under which gravity or hybrid (combined gravity and pumped) decants may offer advantage over traditional Oil Sands recycle water methods. It presents the elements of a good decant design and lists some of the operational features and indirect benefits derived from the use of fixed decants, including:

- Reduction in the depth and area of pond.
- An increase in subaerial deposition or beach above water (BAW) and a reduction in areal extent of subaqueous deposition, or beach below water (BBW).
- A reduction in phreatic surface and associated improvement in tailings consolidation and slope stability.
- Reduced risk of tailings liquefaction.
- Reduced cost of recycling tailings supernatant.

This paper also presents design considerations unique to the Oil Sands industry such as year round operation in a northern climate, and dealing with bitumen and solids that are likely to end up in the supernatant.

INTRODUCTION

The decanting of water from Oil Sands tailings facilities has had to deal with a number of challenges that are somewhat unique from those typically encountered elsewhere in mineral tailings:

- Very large scale, and exceptionally large volumes of water.
- The presence of bitumen, sometimes in considerable quantities and concentration.
- A high percentage of clay and fine material in the tailings, leading to challenges with decant water quality.
- High levels of debris, typically woody vegetation, especially immediately after facility start-up.
- A relatively long and harsh northern winter climate, with a lack of solar radiation for evaporation and desiccation.
- Very weak dyke and dam foundation materials, and poor earthen construction materials for dyke design and construction.
- Levels of contamination from process affected water which limit options for water management.
- Rigorous environmental and regulatory control, also subject to ongoing revision.
- The need to keep process affected water separate from environmental or release water.

These factors have led to the development of Oil Sands tailings decanting systems which are necessarily most robust and flexible and which are able to deal with problems of bitumen clogging, harsh winter operating conditions, changing conditions and plans and other extremes. They have understandably been quite expensive.

The international mining industry has on the other hand, relied upon (typically gravity based) water decanting systems which have been simpler and less expensive. They have also been more helpful in more completely removing supernatant from tailings facilities.

Following the Mount Polley and Samarco tailings failures over the past two years, a renewed international focus on dam safety has generated a reconsideration of decanting processes, and what improvements in decant systems could offer in regard to improving dam safety.

A prolonged period of low oil price has generated considerable pressure on operators to cut costs and improve efficiencies. This theme is the subject of another paper at the conference by one of the authors, Boswell (2016). Decanting of supernatant is required to be efficient and affordable.

What improvements could be made to the decanting of water from Oil Sands tailings facilities?

THE CASE FOR FIXED DECANTS

State-of-the-art references regarding tailings decant design and operation are rare, and advance a case for increased publication to improve the quality of tailings management. Blight (2010) devotes about 20 pages to the design of elements of a gravity decant design. Jon Engels (2002) provides guidance on decant system design in a technical paper dedicated to water management considerations for conventional tailings storage. More comprehensive guidance on decant structures and methods may be found from the US Bureau of Mines, the US Bureau of Reclamation, the Ontario Ministry of the Environment and publications and resources developed in the water resources sector for water dam decant design.

Decant System Function & Key Elements

The primary purpose of a decant system is to collect and transport water and/or fluid tailings from inside a tailings disposal area to a point outside for further treatment (if necessary) and reuse. A well designed decant system enables the control of supernatant pond volume and elevation within a disposal area. (Ontario Ministry of the Environment)

Key elements of decant systems and their functions are described in the following sections. Different combinations of these key elements can be configured into a decant system suited for a specific application.

Decant Structures

Decant towers have been utilized for many years in various tailings storage applications globally. They can be constructed of a simple steel pipe (Figure 1) or a more complicated reinforced concrete structure with adjustable weir (Figure 2).

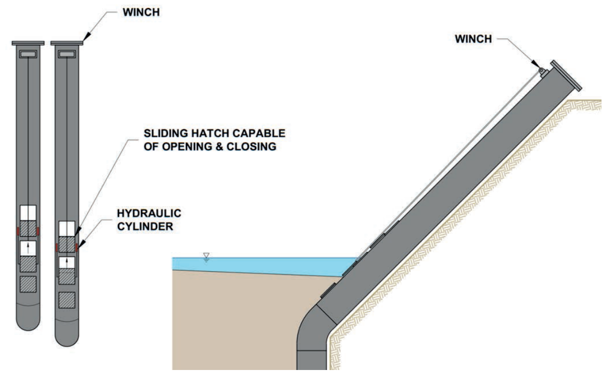

Figure 1. Inclined Steel Decant Pipe

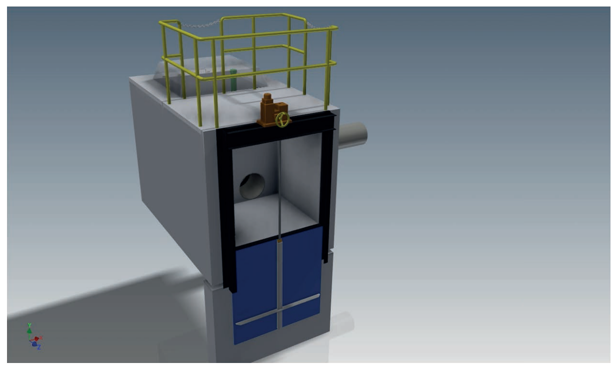

Figure 2. Reinforced Concrete Decant Structure

Depending on the original topography and design of the storage facility the tower can be oriented vertically with the tailings deposit forming around it and in other cases is installed on an incline (on original ground or in an embankment) and the deposit approaches from one side (Figure 3).

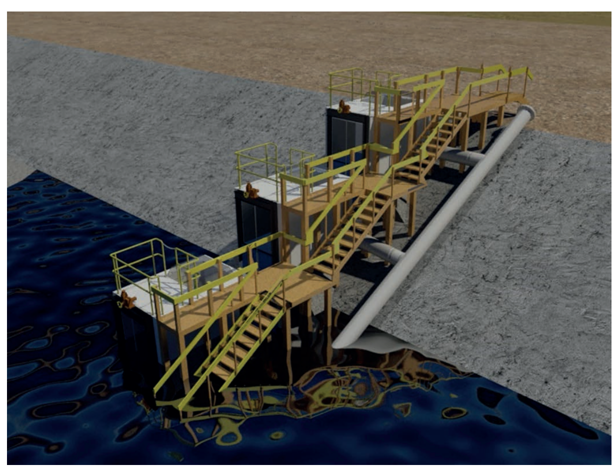

Figure 3. Decant Structure Installed on Incline

Decant towers (vertical or inclined) can be installed to their full height at the beginning of operation with openings (or slots) throughout their height to allow drainage of water and fluid tailings into the centre of the structure. As the deposit rises on the tower, the openings can be closed up to prevent excess solids from entering and plugging the system. The ability to open and close the intake slots enables flow control, operational flexibility and maintenance of the other decant components. The slots also facilitate the removal of water and fluid tailings below the deposit surface that are squeezed out as the coarse material consolidates under self-weight. Although care must be taken to prevent too high solids content material from entering and plugging the system.

Another approach is to incrementally raise the decant tower as the pond and deposit rises. This method can include openings throughout the height of the structure or only allow fluids to spill in from the top. With a vertical tower, precast reinforced concrete sections or pipe spools are added to the structure and raise the elevation of the inlet (Figure 4). With inclined structures, fluid enters from one side where stop logs are added or a weir plate is adjusted to raise the elevation of the spillway.

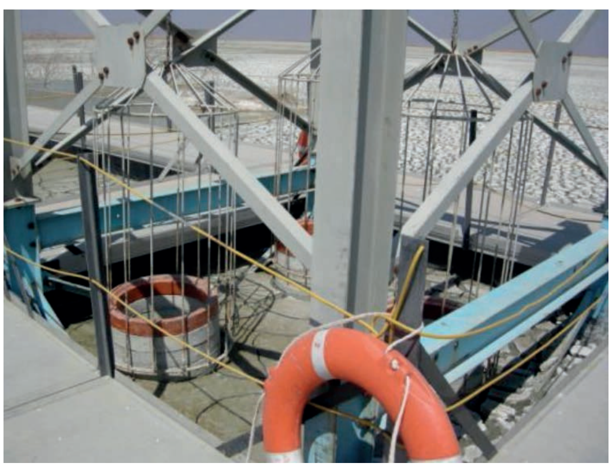

Figure 4. Vertical Tower Inlet Raised with Deposit

In all cases rock-fill or other protection surrounding the tower structure is necessary to protect the structure from floating debris and ice; rock-fill can also serve as a filter keeping coarse solids material from entering the central tower in the case of the slotted approach. Protection such as a steel gantry will also prevent stresses and possible crushing of the vertical tower as a result of downward sleeve friction imparted on the tower from settlement of the tailings.

Decant structure height, particularly in vertical configurations, is an important consideration. Depending on the storage container geometry multiple shorter towers installed at increasing elevations throughout the life of a facility may be more cost effective. Often times a new position for the intake within the deposit is better suited as the pond has migrated past or moved away from the original intake. It is difficult to manage the location of the supernatant pond, therefore, multiple intake structures throughout the life of a tailings facility provides operational flexibility – note it may not be necessary to construct all the towers in the initial phase of the facility. Shaping of original grade and construction of drainage channels which promote the flow of fluids towards intakes is good practice.

Decant Pipeline

Once the fluids have entered the decant tower, there are alternative approaches to transferring it out of the storage area.

Perhaps the simplest approach, from an operational perspective, the pipeline is connected to the base of the decant tower and installed with a sufficient slope to allow the decanted fluid to flow via gravity along the bottom of the tailings facility and through the embankment. There are commonly two main design challenges associated with this approach; the pipeline is exposed to the tremendous static and dynamic forces that result from the forming and shifting of the deposit above it and; the pipeline installed through the embankment can be the source of dam failure if not designed correctly. In other mining industries where original ground allows, gravity based systems avoid embankment penetration by constructing a tunnel in original ground around the dam structure. Topography in the Oil Sands industry does not accommodate tunneling around embankments. Perhaps there is opportunity to design and install decant pipelines within a trench in original ground under an embankment to limit the seepage around the pipeline and risk of subsequent failure. If a pipeline within or beneath a deposit is damaged or fails, it is not easily repaired and in some cases physically and economically impractical. To minimize this risk, decant pipelines within a tailings facility should be kept as short as possible (Ontario Ministry of the Environment).

Pumps

A pumping based approach is an alternative and avoids some of the embankment vulnerabilities associated with a gravity draining system. Floating pump barges are often utilized to reclaim fluids from storage facilities but need significant pond depth (which corresponds to a large pond area) to meet the minimum barge draft requirements. This paper focuses on fixed decant arrangements which strive to eliminate fluid storage within a tailings facility.

When utilizing pumps in a fixed decant arrangement, the decant structure serves as a sump for the equipment from which the fluids are lifted out of the deposit. Access to the pumping equipment is mandatory and there would typically be an electric power supply required; diesel powered pumps can also be used and provide back-up during emergency power outages.

Centrifugal slurry pumps provide the ability to handle fluid tailings that will inevitably reach the sump. Depending on the application, submersible (Figure 5), horizontal or vertical style centrifugal slurry pumps can be utilized. In high flowrate applications like seen in the oil sands industry, several large pump units in very large (or multiple) sumps would be needed; capital and operating costs are high in a pumped versus gravity pipeline based approach.

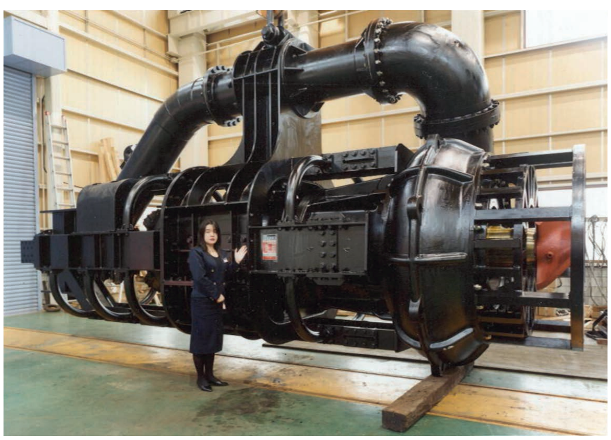

Figure 5. Toyo Submersible Slurry Pump (1000 HP, 5,000 m³/h)

Debris Screens

Screening is mandatory with fixed decants to keep debris from entering the system and creating blockages and/or operational problems with pumping equipment. Trash racks at the inlet to the decant sump are required at a minimum; floating boom mounted screens around the inlet can provide a double layer of protection for the decant system. Regardless of the screening system employed, there must be the ability to access the screen to clear debris.

De-icing System

In northern climates freezing conditions present further challenges in the design and operation of an effective decant system. If fluid is removed from the deposit quickly, in the case of a well-designed fixed decant, issues relating to ice formation can be minimized but likely not eliminated. Incorporating de-icing measures is a must and can be delivered in different forms. Recirculation of fluids in and around the intake through a dedicated piping manifold and nozzle arrangement is a common approach. Another technique is to introduce air bubbles below the surface to promote circulation of warmer fluid from lower in the pond upwards toward the surface; the benefits from this approach diminish with lower pond depths. Higher process water temperatures in the Oil Sands industry also helps mitigate ice formation and is an aspect that designers and operators of decant systems should consider.

GEOTECHNICAL BENEFITS OF GRAVITY (FIXED) DECANTS

Gravity decants have developed as the norm in the international tailings industry, for good reason. They are efficient and cost-effective. In addition, there are a number of substantial reasons why gravity or fixed decants off geotechnical benefit for hydraulic fill structures:

Reduction in the depth and area of pond

In cases where the beach deposition slope is low (less than 1%), it is important to keep the pond depth shallow, to avoid risks such as loss of freeboard, or the migration of the pond too close to the perimeter. In the diamond industry for example, fixed gravity decanting is able to reduce the pond depth to a few centimeters only.

Increase in BAW

There is a real benefit to increasing subaerial deposition or beach above water (BAW) and a reducing as far as possible the areal extent of subaqueous deposition, or beach below water (BBW). For BAW, environmental desiccative forces (solar radiation, wind drying) are mobilized and consolidation is advantaged.

Improved consolidation

A reduction in degree of saturation and a depression of the phreatic surface will always lead to an improvement in tailings consolidation and slope stability.

Reduced risk of tailings liquefaction

The findings from the investigation into the Samarco tailings failure, Morgenstern et al (2016), has reiterated to the international tailings community the importance of elimination of the risk of static liquefaction of tailings.

The key here is the reduction of void ratio to a point where the tailings dilate under shear rather than collapsing.

Reduced cost of recycling tailings supernatant

A well designed gravity decant will save much on electrical pumping and power costs, especially when measured over the operating life of a decant system.

FUNDAMENTAL PRINCIPLES OF DECANT DESIGN

Emergency Decant

Emergency or secondary decant systems should be in place in the event the primary decant system requires maintenance, repairs or fails altogether. A common decant malfunction is due to debris blockage at the intake or in the pipeline, therefore it is important to design a system which enables safe maintenance access so screens and pipelines can be monitored and cleaned on a regular basis. When a decant structure is raised along with the deposit, the access road must be raised as well.

Location

The inlet(s) should be located strategically with respect to discharge points, to take advantage of sedimentation mechanisms and minimize the solids content of the fluid tailings reaching the decant system. In some situations, it may be appropriate to build new decant inlet structures as the deposit matures and the pond migrates; this is dependent on the original topography on which the storage facility is built.

Locating a decant tower within or close to an embankment is less desirable; for stability purposes it is best to keep water away from embankments all together.

Decant pipelines aligned through embankments can be problematic if not designed correctly. The pipeline should be designed with seepage collars to prevent migration of water along the outside of the pipe causing erosion which can ultimately lead to dam failure. (Ontario Ministry of the Environment)

Structural

The decant tower should have a sound foundation installed on bedrock (Ontario Ministry of the Environment) to withstand the stresses expected throughout its lifespan. In oil sand tailings facilities, it is not possible to install a decant tower on bedrock, therefore the foundation must be designed carefully and appropriately to prevent long term settling. Limiting the height and weight of decant structures will minimize the structural failure risks.

Sizing

A decant system should be sized to handle the maximum cumulative flows expected from:

- The tailings entering the facility
- The appropriate precipitation event
- Run-off/drainage from adjacent areas

An appropriate factor of safety and precipitation event that satisfies general and site specific regulatory requirements should be used as the design basis.

THREATS

Plugging

Plugging is a common failure of decant systems and can happen in any season. Plugging can occur at the inlet to the system or within it. Organic material and debris from the mine such as wood and garbage which float on the surface are common causes of blockages. In winter months' blockages are commonly caused by blocks of ice. (Ontario Ministry of the Environment) In oil sands operations bitumen accumulates in mats on the surface presenting further challenges; these mats can harden and freeze and become very problematic at decant intakes. The means to unplug a plugged screen or pipeline should be incorporated into the design of the system.

Excessive Force

During the winter months of the year, ice that forms on the surface of the pond can exert significant forces on decant structures. Ice forming on decant structures can create unanticipated forces or load conditions as pond levels fluctuate. In the spring thaw, large blocks of ice floating in the pond, under certain conditions, can collide repeatedly against unprotected decant structures. (Ontario Ministry of the Environment) In other months of the year large floating objects such as logs or hardened mats of bitumen can damage decant structures with impact through wave action.

Decant towers and outlet pipelines in most cases are subject to increasing pressures due to the rise of tailings and water in the storage facility. Further complicating the matter, the tailings may not be deposited and approach the structure evenly from all sides; this could create unexpected asymmetric forces on the decant tower and foundation.

Abrasion & Corrosion

Outlet pipeline wear can compromise a decant system; particularly where coarse particles are present and in gravity systems where pipeline velocities become excessive under increased static hydraulic head conditions. In the case where pumping equipment is utilized in a decant system, pump capacity must be monitored, operating efficiency will be reduced as the pump components in contact with solids will wear.

Depending on the ore body and reagents utilized in the extraction and treatment a decant system can be exposed to various corrosive conditions that can weaken or destroy components.

CONCLUSION

The key to geotechnical safety in the management of hydraulic fill structures is in the management of water. One of the components of an effective water management system in turn, is the decant system for supernatant and precipitation.

The international tailings community has provided us with many successful examples of gravity and fixed decants, which have been developed and successfully implemented over the past century. The design of decant systems is a well-established competence which contributes to the management of dam safety.

The design of a tailings decant system needs to be robust, efficient, fit-for-purpose, and cost effective. It may be that the ideal design is in fact a hybrid – leveraging the benefits of a number of alternatives.

ACKNOWLEDGEMENTS

The support offered by our colleagues at Thurber Engineering and Paterson & Cooke is gratefully acknowledged.

REFERENCES

Boswell, J.E.S. 2016. Cost Effective and Responsible Tailings Management. Paper submitted to IOSTC 2016. Lake Louise. December 2016.

Blight, G.E., 2010. Geotechnical Engineering for Mine Waste Storage Facilities. Leiden: Balkema, pp 339-358.

Morgenstern, N.E., Vick, S.G., Viotto, C.B. and Watts, B.D. 2016. Fundão Tailings Dam Review Panel. Report on the Immediate Causes of the Failure of the Fundão Dam. Aug 25, 2016.

Engels, J., 2002. Water Management Considerations for Conventional Storage. Tailings.info.

Decant System Design Considerations for Ontario Mining Operations, Ontario Ministry of the Environment, n.d.

Wagener, E.V., Jacobsz, S.W., 1999. Penstock failures on gold tailings dams in South Africa. Geotechnics for Developing Africa: Proceedings of the 12th regional conference for Africa on soil mechanics and geotechnical engineering. Durban, South Africa, October 1999.

PIPELINE TRANSPORT OF CENTRIFUGE PRODUCT

Michael Graham[1], Stewart Bodtker[2], Neil McMinn[3] and Chuck Wanstrom[4]
[1]Shell Canada Ltd., Calgary, Canada
[2]Paterson & Cooke Canada Inc., Calgary, Canada
[3]Newalta Corporation, Calgary, Canada
[4]Schwing Bioset, Inc., Somerset, WI, USA

ABSTRACT

Shell Canada Limited (Shell) began developing tailings centrifugation technology in 2012 to minimize fluid fine tailings (FFT) volume accumulation. Shell installed a commercial scale centrifuge facility at their Jackpine Mine (JPM) oil sands mining operation, which utilized extensive research and development work conducted in collaboration under Canada's Oil Sands Innovation Alliance (COSIA). The JPM facility consists of four units that were installed in 2013 and 2014. Shell developed a pumping and pipeline delivery system to transport material, which differed to the historical approach of using conveyors and haul trucks to transport centrifuge product to Dedicated Disposal Areas (DDAs). The system has been successfully implemented but faces some operational challenges and limitations when approaching centrifuge product densities close to 50% solids content (by mass).

A pump and pipeline system has many inherent advantages over conveyor and truck systems, including less required energy, less emissions, more reliability, more availability, and less operating maintenance, particularly in cold weather conditions. However, the design of a pump and pipeline system for high density centrifuged product presents many challenges. This is primarily due to the changing rheological properties resulting from pipeline friction. The objective of this paper is to review the operating data and experiences gained from the commercial scale operation with focus on pre-conditioning of centrifuge product prior to pumping, non-linear pipeline hydraulic gradients, plug flow behaviour, pumping equipment considerations, and hydraulic transient mitigation.

INTRODUCTION

Background

Centrifugation of FFT became an approved technology in the oil sands under the Alberta Energy Regulator's (AER) *Directive 074* (D074), *Tailings Performance Criteria and Requirements for Oil Sands Mining Schemes* (AER 2013). The subsequent directive, which detailed the requirements for recovering and treating FFT, came following nearly 10 years of research and the successful deployment of Syncrude Canada Limited's commercial demonstration plant. In 2013, Shell entered into a contract with Newalta Corporation to provide and operate a commercial scale mobile centrifuge pilot plant at Shell's JPM site, located about 85 km north of Fort McMurray, Alberta. The mobile pilot plant would consist of four Alfa Laval LYNX 1000 decanter centrifuges. To transport the centrifuge tailings to a DDA, Shell would use positive displacement pumps designed and manufactured by Schwing Bioset Inc. and pipelines designed by Paterson & Cooke Canada Inc. (P&C).

Construction of the first two centrifuge production units commenced in May 2013. Mechanical completion was achieved in October 2013 with commissioning of the units completed in November 2013. The two units ran continuously until December 2013, with the exception of a few minor FFT feed source issues that impacted production. The plant was transitioned into a state of hibernation in December 2013. This allowed a permanent power source to be connected to the plant and for the plant to be fully winterized. The plant was restarted in May 2014 and was subjected to plant operations trials that occurred over the months of June to August 2014. This marked the period when both units entered full-scale commercial production mode. By the end of 2014, the first two units had centrifuged approximately 375,000 dry tonnes of FFT solids.

The construction of the third and fourth centrifuge units commenced in September 2014 with mechanical completion achieved in December 2014. These units were subjected to a commissioning and start-up period that lasted about two months until they achieved commercial scale design output in March 2015. The total annual production of all four centrifuge units in 2015 was approximately 1,380,000 tonnes of FFT solids.

Technology Objectives

In order to minimize FFT accumulation and ensure that tailings areas are progressively reclaimed during the life of the project, the Government of Alberta issued the *Tailings Management Framework* (TMF) for Mineable Athabasca Oil sands in March 2015. This framework transformed the approach to tailings management significantly from the regulations set out in D074, with the key difference being that the TMF requires oil sands operators to manage their fluid tailings inventory, while D074 focused on fines capture and strength gained in one calendar year. Shell's primary tailings technology for reducing the growth of FFT inventory at their operations is currently centrifugation.

In order to manage FFT inventory with the aim of achieving closure design requirements, Shell dredges FFT from a tailings pond at an average of about 25% solids content. The centrifuge operation produces a treated tailings product with an average solids content of about 45%. The objective of the centrifuge operation is to convert FFT into a high fines deposit with physical properties that are on a trajectory to support reclamation and closure objectives.

System Configuration

Each of the four centrifuge systems is a discrete production unit or train, where Units 1 and 2 are independent of Units 3 and 4. Dredged FFT from a tailings pond is initially screened for the removal of deleterious materials and the screened slurry is sent to a common FFT surge pond. The FFT is pumped from the surge pond to two different feed tanks; one feed tank provides FFT to Units 1 and 2 while the other feed tank provides FFT to Units 3 and 4. An anionic polymer is injected into the FFT stream to promote flocculation of the FFT particles prior to centrifugation.

Each of the four decanter centrifuges has its own FFT feed, a shear mixer for pre-conditioning the FFT, dedicated positive displacement pumps, and a centrate (effluent) pump. Figure 1 provides a simplified process flow diagram of this process.

Each centrifuge system incorporates a fully automated process control system. Every component of each system is housed

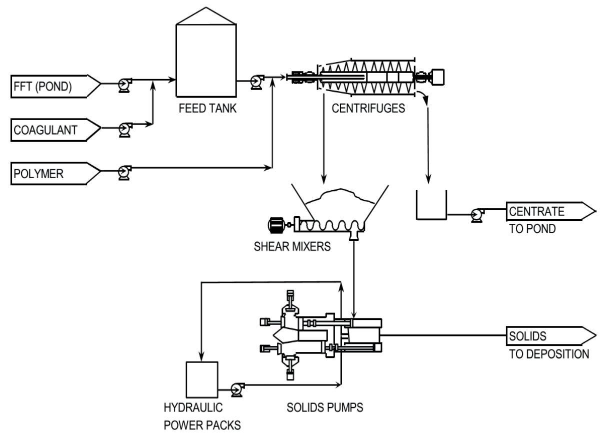

Figure 1. Process Flow Diagram

in fully winterized skids that are specially designed to be easily relocated. Each system also has the ability to apply a metered flow of coagulant solution to the FFT sent to the feed tank.

Ancillary facilities for each system include polymer make-down, coagulant preparation, and process water filtration systems.

PUMP EQUIPMENT DESIGN

Shear Mixer

The installation of a shear mixer between the centrifuge and the pump manipulates the rheology of the tailings to a more favourable state for pumping. The yield stress of the FFT is reduced through a shear thinning effect to more efficiently fill the pump chamber and increase throughput. Due to the cohesive nature of the tailings, a shear mixer with ribbon flighting was selected to prevent material accumulations on the shaft that might impede overall throughput. After shear mixing, the FFT is fed by gravity through a chute to the inlet ports of the pump.

Paste Pump

Previous test work and the preliminary system design led to the development of original pump specifications that required design operating conditions of 3,000 kPa and an output rate of 125 m^3/hr. The relatively low operating pressure allowed the pump and hydraulic power unit to be configured to minimize hydraulic oil flow requirements, allowing capital savings on the overall pump design, while still meeting project objectives. The positive displacement piston pump selected has a 3.1 m pumping stroke length and a 300 mm diameter material cylinder and is equipped with “poppet” valves for the suction and discharge systems. The poppet valves are hydraulically actuated check valves sequenced with pump operation. The poppet valves isolate the pump from the shear mixer feed hopper and the pressurized pipeline in sequence with the pump stroke. The poppet valve system is equipped with 280 mm diameter inlet valves and 250 mm outlet valves to allow for unrestricted flow of the FFT in and out of the pump.

As the project progressed, the detailed system design required a maximum operating pressure of 5,000 kPa and an output rate of 140 m^3/hr. The increase in pressure and output rate eliminated the design reserve in the pump system and the ability to use an internal pulsation dampening system to ramp pumping speeds up and down at the beginning and end of each pumping stroke. The ramp up and ramp down feature, termed “Ideal Control Circuit (ICC)” by the pump manufacturer, eliminated the abrupt material velocity changes in the pipeline and dampened out the water hammer effect commonly observed in fluid pumping systems. The increased maximum operating pressure required the pulsation dampening system that reduced pump output a small amount to be disabled in order to maximize production rates.

Hydraulic Power Unit

The hydraulic power unit for each centrifuge system includes a constant speed motor and variable displacement hydraulic pumps that enable individual output control of each hydraulic pump and variable speed control of the positive displacement piston pump.

The original pressure and output specifications yielded a motor requirement of 225 kW to operate simultaneously at the maximum pressure and output conditions. When the maximum operating pressure was increased, it was no longer possible to operate at the maximum output rate. To allow the pump system to operate at maximum pressure or maximum output, the pump manufacturer installed a proprietary Electronic Power Control (EPC) system that automatically reduces output capacity, should pressure requirements exceed the available power. This system prevents equipment overload, equipment stalling, and allows for continuous operations when approaching near the revised maximum specified conditions.

PIPELINE DESIGN

The rheology of the centrifuge product, particularly the yield stress, is of importance in pipeline design. Hydraulic models use rheological data to predict pipeline friction losses. The predicted friction losses allow for proper selection of pumps, pipeline, and valves.

Representative samples are typically collected for rheological characterization to facilitate system design. Representative samples were not available on this project; therefore, it was necessary to use prior P&C experience with pumping trials that involved slurries similar to Shell’s centrifuge product. In addition, it is known that centrifuge products are thixotropic slurries. Thixotropic slurries (also known as shear thinning slurries) experience a reduction in rheology as a result of shearing.

A major challenge in the design of pipelines for thixotropic slurries is this changing rheological nature. As a flocculated slurry is sheared, the structure of the flocs is broken down leading to a reduction in the slurry rheology. This causes non-uniform friction loss throughout the pipeline and complicates the design as typical models utilize one rheology along the length of a pipeline.

Knowing that the rheology will be reduced introduces questions as to the extent of reduction that can be expected for a given scenario. Another flow behaviour phenomenon that further complicates the design is the potential presence of a lubrication effect. This effect occurs when an un-sheared plug of high yield stress product is transported through an annulus of lower yield stress sheared product. Since the material in contact with the pipe wall is at a lower yield stress, the friction loss will be lower than that expected from the bulk yield stress of the material. Le et al. (2014) discuss this phenomenon in detail. P&C’s experience with similar slurries helped determine an estimated window of expected yield stresses for Shell’s centrifuge product. The average yield stress in the pipeline would be somewhere between its un-sheared yield stress (at the pump discharge) and its fully sheared yield stress (the point at which the yield stress no longer reduces with shear). Without prior test work measuring the relationship of rheology with applied energy, uncertainty in the average friction loss for Shell’s centrifuge pipeline had to be accounted for. A 200% safety factor was applied to the anticipated rheology established from P&C’s past experience.

The delivery pipeline was designed to handle centrifuge product from one or two operating pumps configured in parallel. Maintaining velocities in the pipeline below 1 m/s and above 0.5 m/s with one pump operating for flushing purposes was a consideration in the selection of the pipe diameter. A 12” carbon steel pipeline was selected based on this velocity consideration and the predicted pressure requirements.

Several other features were incorporated into the pipeline design for safety and operational monitoring purposes:

- Pressure transmitters were included to initiate pump trips in the event of over pressure events.
- Pressure transmitters were included along the pipeline for monitoring of pressure gradients and subsequent understanding of flow behaviour.
- Valves were included to enable manual pressure relief in the event of pipeline plugging.
- Flexible grooved couplings were included to absorb vibrations and thermal expansion/contraction and for ease in assembly/disassembly.
- Visual and audio alarm systems were incorporated to indicate over pressure events.
- Glycol heating units were utilized in the winter months for freeze protection.

The original pipeline design incorporated means to rotate the discharge point around multiple spigots to allow for strategic deposition of the centrifuge product. However, for operational simplicity purposes during the trial period, two fixed discharge points were utilized in the DDA. Shell continues to utilize this discharge strategy, with further consideration for revision based on results obtained from updated deposit performance outcomes.

OPERATIONAL EXPERIENCE

Operating Conditions

The JPM centrifuge plant operates year-round on a 24-hour basis and has better than 85% availability when FFT feed is available. Table 1 provides typical plant operating conditions.

Pre-conditioning of the FFT is considered essential to achieve efficient centrifugation performance. The current practice involves adding an anionic polymer inline immediately before the centrifuge to promote flocculation. A coagulant was used, along with an anionic polymer, to pre-condition the FFT in the trial period but there was no observed or measured benefit in terms of meeting the centrifugation performance target solids contents. However, it can be challenging at times to achieve the desired centrifuge performance, particularly when the FFT feed characteristics vary. There may be a benefit to adding a coagulant at these times, but there is currently no real time instrumentation or monitoring of the FFT feed characteristics in place to dictate when it would be required.

The centrifuge operation is also constrained by the practical limits of pumping the product. Periods of high variability in the pump discharge pressures result in some reduced throughput due to high pressure shutdown events.

Table 1. Typical Operating Conditions

Stream	Unit of Measure	Average Value	Range of Values
FFT	Solids Content by Mass (%)	29	26-33
Centrifuge Product	Throughput (dry tonnes/hr)	55	45-70
Centrifuge Product	Solids Content by Mass (%)	45	43-49
Centrate	Solids Content by Mass (%)	1.0	0.5-2.0
Pump Discharge	Pressure (kPa)	3,000	2,000-4,000

Material Characteristics

There are four characteristically different materials in the centrifugation operation: raw or untreated FFT, centrifuge cake, centrate, and the centrifuge product that ultimately ends up in the deposit.

A two-week sampling campaign performed in February 2016 yielded a subset of results that represents what is considered the typical material characteristics of the raw FFT, cake, and centrate. Table 2 provides a summary of the averages of these material characteristics. The centrate had an average bitumen content of 0.2% (by mass), an average solids content of 0.7%, and an average total suspended solids of 7,518 mg/L.

Table 2. Raw FFT and Cake Characteristics

Material	Characteristic			
	Fines Content (%)	Clay Content (%)	Bitumen Content by Mass (%)	Solids Content by Mass (%)
FFT	94.4	63.9	1.0	25.6
Cake	93.8	63.0	1.4	44.2

The results of the 2015 annual tailings investigation of the DDA1 centrifuge deposit indicated that the centrifuge product had an average fines content (<44 μm) of about 92.9%, an average clay content of about 45.7%, an average bitumen content of 1.6%, and an average solids content of 46.9%.

Fines content was determined by laser diffraction while the active clay content was determined utilizing a Methylene Blue Index test established by CanmetENERGY. Bitumen content and solids content were determined utilizing the Dean-Stark method.

Observations indicate that there is about 10% air entrainment in the centrifuge product. This is thought to occur due to both the centrifuging and shear mixing steps. The level of air entrainment not only increases the actual pumped volume over that expected, but also impacts the overall pumping characteristics. The entrained air is believed to affect variability in pump and pipeline pressures as well as flow behaviours.

Pump Unit Operation

Production demands require the pumping system to operate at or near maximum rated pressure and output capacities. As a result, some fatigue type failures have been observed in the hydraulic system. It is critical to adhere to the recommended preventative maintenance procedures when operating the pumps at their maximum duty points. Overall availability has been in excess of 85% with production goals being met. With three years of operating experience, a spare parts stocking program has been established and critical spare parts are now kept in inventory to minimize any potential delays in shipments, either from the manufacturer or as a result of importing equipment into Canada.

Pipeline Flow Behaviour

Observations at the pipeline discharge location support the theory that a high yield stress mixture travels through the pipeline as plug flow with an unsheared core of material in the central portion of the pipe and a narrow sheared annulus adjacent to the pipe wall. It is probable that the rheology of the mixture in the sheared annulus decreases locally through friction. Figure 2 depicts the discharge of centrifuge product at JPM.

Figure 2. Centrifuge Product Discharge

Pipeline Pressure Gradient

Over the course of several months, operating pressures were collected along the pipeline. Results from this effort indicate that a non-linear hydraulic gradient exists and that pipeline friction loss decreases with energy input. Upon further review, it is considered likely that this friction loss is associated with a reduction in the centrifuge product rheology in the sheared annulus adjacent to the pipe wall.

Deposition

Shell currently has one commercial centrifuge deposit at JPM located in a DDA within the External Tailings Facility. Deposition of centrifuge product has occurred in this location for approximately two years. This deposition strategy has resulted in a channel of centrifuge deposit that extends out into the DDA and eventually into the tailings pond. The centrifuge product, once it reaches the pond, appears to be displacing FFT as it progresses further into the pond.

Hydraulic Transient

Videos (and sound recordings) taken at the discharge of the pipeline indicate the presence of relatively significant transient pressures. The pumps most likely generate the transient pressures due to the pause in material flow at the completion of each pumping stroke. Continued operation under these transient conditions will increase maintenance requirements and reduce the life of the pipeline system.

The operator has observed large pressure fluctuations (spikes) at the pump discharge location, which is likely attributed to hydraulic transients. These pressure fluctuations become more pronounced with increasing solids content. When operating at high solids contents the pressure fluctuations trigger a reduced stroke rate due to high pressure conditions. To avoid exceeding the high pressure setpoint and pump shutdown, when pumping higher solids content material, the EPC system reduces the stroke rate of the pumps to enable operations at the higher pressures, but at lower throughput.

OPPORTUNITIES

Pre-conditioning with Variable Speed Mixer

While operation has shown that the shear mixer is capable of reducing the yield stress of the FFT, its true impact and capabilities are not yet fully understood. As the shear mixer is currently operated at a constant speed, retrofitting the unit with a variable frequency drive would allow further insight and optimization studies to determine if higher or lower revolutions per minute (rpm) provide additional benefit. It may be determined that the maximum shear thinning benefit is realized at some fraction of the current speed in consideration of shearing at the pipe annulus. If this is the case, long-term power consumption and equipment wear could be reduced by decreasing the shear mixer speed. In addition, further optimization of the shear mixer could lead to more efficient pump chamber filling, potentially resulting in lower hydraulic transients. Alternatively, increasing the shear mixer speed may reduce material yield stress allowing pump feed and pipeline pressures to be further reduced, resulting in the ability to pump the centrifuge product greater distances with the same power consumption.

Pump Specification and Design

Future piston pumps should be hydraulically configured such that the high pressure oil that drives the pump is applied to the piston side of the hydraulic cylinder. The current design, due to the originally planned lower operating pressures, was configured such that the high pressure oil was applied to the rod side of the hydraulic cylinder. Rod side connections have advantages in lower pressure pumping applications. They allow the use of smaller hydraulic pumps and smaller reservoirs, with the consequence of a less favourable hydraulic ratio that limits the operating pressure. Applying the oil on the piston side of the hydraulic cylinder would require more supply oil to be used, but this would also allow the pumps to operate at a higher pipeline pressures. This change would grant more flexibility when pressure requirements fluctuate, or are not well defined.

An additional opportunity exists to examine the end of pumping stroke sequencing and an alternate method of switching the inlet and discharge poppets. Ideal Switch (IS) technology is currently utilized at the end of the pumping stroke where the hydraulic oil pump displacement is adjusted to the “ideal” displacement for shifting the poppets. This value is adjustable based on the operating pressures and material rheology. However, in the case of a piston side configuration, the IS system may not be able to properly manage the oil flow at the end of the pumping stroke. Speed commands are given instantaneously, however, the oil pump is rotating at a high rpm and the desired IS oil displacement, for the short period of time required, may not be accurately controlled as the rotational momentum of the hydraulic pump causes excess oil to be supplied. To mitigate this, a twin hydraulic circuit configuration may be used. The twin circuit configuration will separate the poppet shifting from the pumping oil and allow the poppets to be shifted with their own hydraulic circuit so they are no longer influenced by the oil commands of the pumping system.

Hydraulic Transient Mitigation

Existing or future units could have the pump hydraulic power packs designed to higher operating pressure and capacity requirements. This would allow the use of the ICC circuit to reduce the abrupt material velocity changes that are likely generating the hydraulic transients within the pipeline. However, this should be done in conjunction with close monitoring of the FFT in the shear mixer to ensure high filling efficiency of the pump chamber. If a large fraction of the pump chamber is filled with air, the benefits of the ICC system will not be realized.

Additionally, the pump hydraulic system can be reconfigured such that operating pressures nearly twice the current design limitations can be attained. Enabling operation at higher pipeline pressures will afford pumping of FFT much greater distances. This, in conjunction with potential optimization of the shear mixer could allow the true limits of pumping distances to be discovered.

Transport Effects on Centrifuge Product

The primary purpose of the pipeline is to efficiently transport centrifuge product from the plant to the deposit. However, in doing so, a process that affects the properties of the product is inadvertently introduced.

Operational experience suggests this inadvertent process exists; effects are evident through visual observation and indirectly through non-linear hydraulic gradients as described previously. The degree to which the pipeline transport affects the material properties has not yet been quantified.

A better understanding of the centrifuge product rheological properties pre and post pipeline transport will provide additional insight into flow behaviour and the apparent lubrication effect at the pipe annulus. It will also provide valuable design information for scaling up to larger diameter centrifuge product pipeline transport systems.

Perhaps most importantly, a better understanding of the affects that the pipeline has, if any, on the water release and consolidation of the centrifuge product is needed. Evaluation of the product's ability to take on water (through precipitation or contact with water in the tailings pond) would be beneficial. As with most other tailings management technologies, the goal is to deposit a material that will continue to dewater and consolidate within an acceptable timeframe.

Increase Pipeline Diameter and/or Length

Pressure loss data from the 12" diameter pipeline, in conjunction with rheology measurements, will provide insight into the scale up of centrifuge product transport. A larger diameter pipeline serving more than two centrifuge units will likely decrease pipeline transport capital and operating costs per unit volume of centrifuge product.

There was uncertainty in the friction loss predictions in the original design of the pipeline; therefore, the pipeline pressure rating was conservatively selected. Operating data suggests that some of the design conservatism can be utilized to extend the pipeline. If the pressure spiking issues can be resolved, it is possible the existing pipeline can be extended an additional 500 m without exceeding the pipeline system pressure rating.

Multi-point Discharge Strategy

As opposed to the single point discharge strategy used to date, it is envisioned that a multi-point discharge strategy could be used to place the centrifuge product in the DDA. This could allow the centrifuge deposit to develop a desiccated surface crust because of exposure to atmospheric effects including evaporation and freeze/thaw. A better understanding of the hydraulic transient issue is necessary before the centrifuge pipelines can be extended and a multi-point discharge strategy can be implemented.

Process Optimization Considerations

Prior to centrifuging, an improved pre-treatment process could potentially be utilized to optimize the pumping, flow, and depositional behaviour of centrifuged product. For example, there is some early evidence to suggest that improvements to the pre-treatment of FFT prior to centrifugation may be beneficial when dealing with non-typical FFT feed characteristics. Investigations are ongoing to study the type of polymer used, the polymer addition strategy, and the addition of a coagulant with the objectives of improving both centrifugation performance and depositional behaviour.

SUMMARY

With guidance from prior pilot work, Shell developed a commercial scale centrifugation pilot facility at JPM to meet the tailings regulations at the time. The existing production units have now been in 24-hour service with greater than 85% availability for over three years. In this period, key learnings and knowledge have been gained regarding the rheological properties of the FFT, the design needs of the mechanical equipment, and the demands of the piping system that delivers the product. The centrifuged product deposited into the DDA appears to be displacing the resident FFT forming a peninsula into the pond.

Opportunities to further optimize the process and understand how the rheology of the FFT can be further manipulated, how the pumping system can be optimized to pump higher solids even greater distances, and how the piping system can evolve to best suit the next generation of operating conditions, will be looked at in future activities.

REFERENCES

Ahmed, M., Labelle, M., Brown, R. and Lahaie, R. (2009). Paste Pumping and Deposition Field Trials and Concepts on Syncrude's Dewatered MFT (Centrifuge Cake). Tailings and Mine Waste, University of Alberta Geotechnical Centre, Proceedings of the Thirteenth International Conference on Tailings and Mine Waste, 1-4 November 2009, Banff, Alberta, Canada, pp. 417-427.

H. D. Le, E. H. Kadri, S. Aggoun, J. Vierendeels, P. Troch, G. De Schutter (2015). Effect of lubrication layer on velocity profile of concrete in a pumping pipe. Materials and Structures 48:3991-4003.

Session G

Tailings Behaviour

DEWATERING BEHAVIOR OF FINE OIL SANDS TAILINGS: A SUMMARY OF LABORATORY RESULTS

Yutian Yao[1], A. Frits van Tol[1,2], Leon van Paassen[1] and Philip J. Vardon[1]
[1]Delft University of Technology, Delft, the Netherlands
[2]Deltares, Delft, the Netherlands

ABSTRACT

To evaluate the disposal technology for fine oil sands tailings, the appropriate engineering properties of the tailings should be ascertained. A laboratory study was conducted by Delft University of Technology (the Netherlands) on the geotechnical properties and dewatering behavior of the fine oil sands tailings (MFT, TT), obtained from Shell Canada's Muskeg River Mine. In this program, the tailings were characterized by performing various laboratory tests including index property tests, flocculation tests, column settling tests, oedometer tests, shrinkage and swelling tests, water retention tests, cracking tests and air drying tests. In this paper, a summary of the main tests results is presented. The data obtained for the MFT and flocculated MFT are compared to identify the effects of flocculation on the dewatering behavior.

INTRODUCTION

Fluid fine tailings resulted from the Alberta oil sands mining process are the major challenge facing the oil sands industry as they cannot be disposed economically due to poor engineering properties. The fluid fine tailings, mostly stored in ponds, must be dewatered before these ponds can be reclaimed by engineering methods. The existing tailings dewatering technologies involve making use of natural dewatering processes (e.g. self-weight consolidation, atmospheric drying, freezing and thawing) and physical/mechanical processes (e.g. filtration, centrifuge, prefabricated vertical drains) or using chemical treatment or mixing tailings with different materials and wastes to improve the tailings dewaterability (BGC, 2010). In order to evaluate the existing technologies or develop new techniques, the appropriate engineering properties of the tailings must be ascertained.

An experimental study has been conducted by Delft University of Technology, in the Netherlands. The main objective of the study was to determine the geotechnical properties of fine oil sands tailings and develop their dewatering behavior related to consolidation and drying processes. The research program consisted of a series tests relating to soil classification, flocculation behavior, sedimentation and consolidation behavior, drying and rewetting behavior and some benchmark dewatering tests. The research was aimed to provide experimental data to better understand the fine tailings dewatering process.

This paper presents a summary of the important results obtained from the experimental study. Detailed results and extensive discussions are available in a doctorate dissertation titled "Dewatering behaviour of fine oil sands tailings, an experimental study" which has been published by Delft University of Technology in 2016.

EXPERIMENTS AND RESULTS

Materials

The tailings used in this research were obtained from Shell Muskeg River Mine. Four barrels (180L each) of oil sands thickened tailings (TT) and three barrels of mature fine tailings (MFT) were delivered to Delft University of Technology. Two weeks after arrival, the tailings were mixed in barrels using a top entering mixer to re-homogenize the material. The mixed tailings were poured into a series of 20L buckets which were kept air tight in a room at 10°C. Samples used for the experiments were prepared from these materials. The homogenous TT and MFT suspensions had an initial solid content of about 35%.

Basic properties

Laboratory classification tests were performed to determine the basic geotechnical index properties. Figure 1 shows representative particle size distribution curves for TT and MFT samples. Table 1 summarizes the basic properties of each tailing.

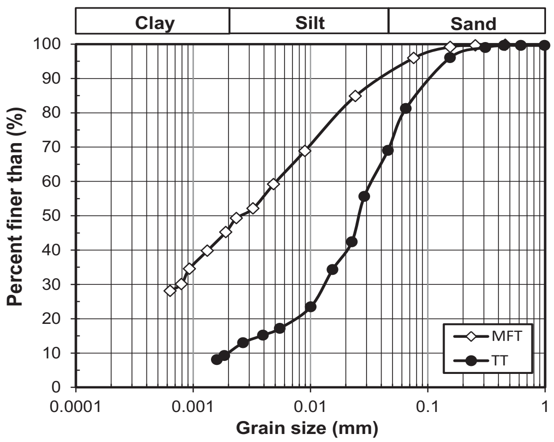

Figure 1. Particle size distributions of MFT and TT samples

Table 1. The basic properties of the MFT and TT used in this work

	MFT	TT
Specific gravity, G_s	2.3	2.3
Bitumen content (%)	2	1.8
Liquid limit (%)	55	48
Plastic limit (%)	28	22
Plasticity index (%)	27	26
Shrinkage limit (%)	16	12
Fines content (<44 μm%)	91	71
Clay content (<2 μm%)	48	14
USCS	CH	CL

Comparing these two tailings, TT had a lower fines and clay content than MFT. The difference is largely due to the fact that TT represents the chemically treated flocculated system while the MFT was non-treated. The particle size distribution and the Atterberg limits of the MFT were close to the values presented by Rima (2013) and Gholami (2014). The TT had a larger fines content than that presented by Innocent-Bernard (2013), however, the clay content values were comparable. It is hypothesized that the mixing process applied prior to sampling may affect the size of flocs in the TT but did not affect the amount of clay size particles.

Both the MFT and TT had a significantly larger fines and clay content values compared to those of different tailings (e.g. copper, gold, and coal wash tailings) presented by Qiu and Sego (2001). This implies that dewatering these fluid fine tailings is more challenging than conventional mine tailings due to low permeabilities. It was found that the particle size distributions and the plastic limit of the MFT were close to the very soft clay dredged from Rotterdam harbor (Limsiri, 2008).

Flocculation tests

In this study, a high molecular weight polymer (FLOPAM DPR 5285) was used to produce chemically amended tailings. To flocculate fine particles in MFT, the tailing suspension and the polymer were mixed in a glass beaker (88 mm in diameter) with a two-blade flat paddle impeller (60 mm in radius). In order to determine the optimum flocculation condition and the maximum dewaterability of the treated tailing, a series of flocculation tests were conducted by using various mixing parameters (e.g., mixing speed and time), polymer dosage and concentration of tailing. An inexpensive device was developed to monitor the impeller torque during mixing. The torque data were used to calculate the impeller power in each system. According to the results presented by Demoz and Mikula (2011), the mixing energy input played a critical role in the flocculation results.

Figure 2 shows the effect of the mixing variables on the flocculation. The flocculation outcome was presented by the volume of water released from 500 ml polymer treated MFT after a settling period of 24 hours. It can be seen that the MFT-polymer mixtures agitated at constant 200 rpm released the largest amount of water compared to other groups. The peak dewatering result was obtained after 3 min mixing and a total amount of 245 ml water was released. It suggests that under ideal condition up to 52% of the tailing water can be discharged from the treated tailings within one day after the deposition. The figures also show poor dewatering results for the group mixed at the speed of 100 rpm. This can be explained by that the turbulence created in the tank was too mild to distribute the added polymer, which caused local overdosing in some polymers rich areas while the whole tailing was still under-dosed and the flocculation was not complete. The results indicate that rapid mixing is desired for effective flocculation. However, based on the data, prolonged vigorous mixing created mediocre dewatering results since the high shear rate and stress destroyed the formed flocs forming smaller and micro flocs. It must be pointed out that the dewatering results for the over-mixed samples were still superior to the samples which were insufficiently mixed. Therefore, over-mixing would still be acceptable in engineering while insufficient mixing should be avoided.

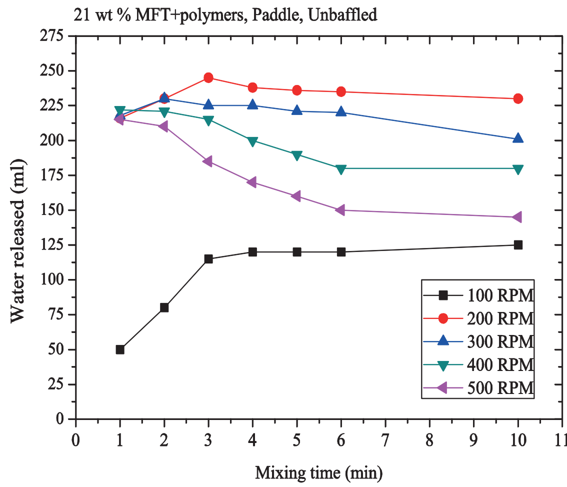

Figure 2. Volumes of water released by 500 ml polymer treated MFT produced under different mixing conditions

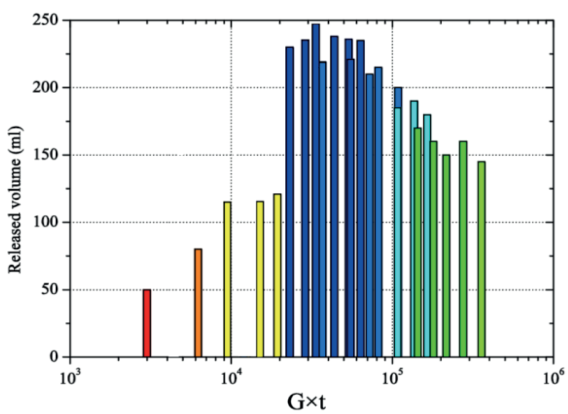

Figure 3. Dependence of dewaterability of FMFT (volume of water released in 24h) of FMFT on mixing energy input (G×t values)

In Demoz and Mikula (2012)'s work, the product of velocity gradient (G) and mixing time, G×t, was used as indicative of mixing energy input into each test and it may be used as a controlling parameter for the flocculation result. Figure 3 shows the dependence of the dewatering results on the measured G×t values obtained from above tests. It is apparent that the dewaterability data falling into the G×t range from 2×10^4 to 7×10^4 $s^{-1}\cdot s$ are obviously better than those in the rest of the test range, yielding the maximum volume of water released. This range is therefore considered to be the optimum operating envelop for the tailing in the current research.

Flocculation tests determined that the optimum polymer dosage was 1000g/t (1000 gram dry flocculant per 1 ton tailing solids). Increasing the dosage above the optimum did not improve the dewaterability but increased the fluid's resistance to settling. Table 2 suggests that using a higher solid content MFT will obtain a higher degree in the increase of the net water release (NWR) value after the flocculation. The NWR is given as follows

$$NWR = \frac{W_R - W_A}{W_0} \times 100\% \qquad [1]$$

where W_0 is the initial mass of water in the tailing, W_R is the mass of water released, and W_A is the mass of water added with the polymer solution into the tailing. Although the 32% solid content MFT had the largest degree (i.e. 12 times) in the increase of the NWR value after flocculation, the flocculated MFT material exhibited high yield strength, which is challenging for transportation of tailings via pipelines,. Therefore, in practice the original MFT should be prepared at a lower solid content before flocculation so that the generated flocculated tailings are easy to handle. By doing this, based on the optimum G×t values, the mixing energy required can also be reduced substantially.

Table 2. Dewaterability (NWR values) of the MFT samples and the optimum mixing energy (G×t values)

Soil content (%)	MFT NWR$_{24h}$ (%)	FMFT G×t ($s^{-1}\cdot s$)	FMFT NWR$_{24h}$ (%)
15	47.8	11,160	65.2
21	9.2	33,488	52.1
32	2.5	165,960	30.4

Column settling tests

The column settling tests were performed on the tailings (MFT, FMFT and TT) suspensions to investigate their settling behavior. The clay suspensions were well-mixed before they were transferred to a series of 500 ml cylinders. During settling the height of the mud in each column was recorded with time.

In order to create the hindered settling condition, the original MFT was diluted with tailing water to various solid content between 32% and 2%. Figure 4 shows the determined settling curves for one part of samples during the first 24h. The rest of the results are not presented for clarity. It can be seen that sample C4 (e_0 =15%) and C5 (e_0 =12%) showed a classic "S" shape which consisted of three primary stages referred to as flocculation, hindered sedimentation (zone settling) and self-weight consolidation. Unlike sample C4 and C5, C1 and C2 settled gradually at the significantly smaller rates.

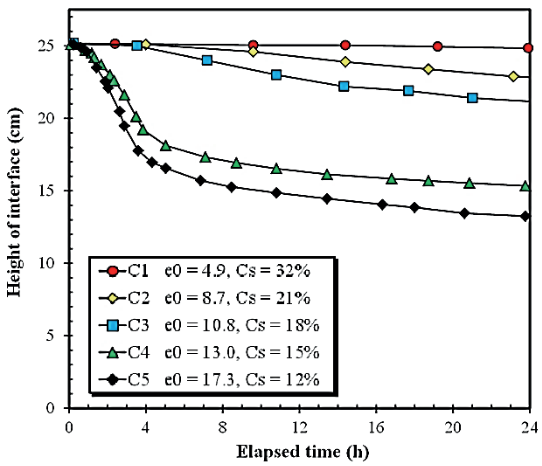

Figure 4. Settling curves for MFT suspensions at various initial solid content

The initial settling velocity of the fluid tailing was determined from the initial linear part of the settling curve. It was found that the tailings with a higher initial void ratio had larger initial settling velocity. The velocity dropped abruptly with initial void ratios between 10 and 11 (e.g. samples C4 and C5 in Figure 4). This void ratio is regarded as the boundary void ratio between hindered (zone) settling and consolidation and is designated as the soil formation void ratio, e_m. In most practical applications, e_m is about 7 times the void ratio at the liquid limit, e_L (Carrier,1983). For the MFT in this research, e_m was about 8.6 times e_L, this coefficient is close to that reported by Xu et al. (2012) for several dredged sludges (fine clays). Since the initial void ratio of the original MFT was lower than e_m, its settling behavior was controlled by consolidation.

Similar tests were performed on TT and polymer treated MFT samples. The setting transitioned from zone settling to consolidation when the initial void ratio decreased from 11.3 to 8.6. Newly prepared TT samples settled faster than TT that had been mixed intensively, indicating that the shear stress played a role in the floc size and hence influenced the settling rate.

The hydraulic conductivities of the tailing suspensions were calculated from the measured initial settling velocities using the equations proposed by Been (1980) and Pane and Schiffman (1997). For all the fluid fine tailings, the relationship between hydraulic conductivity and void ratio was highly non-linear. The results showed that use of polymer in flocculation of MFT greatly enhanced the hydraulic conductivity and therefore the settling rate. The initial hydraulic conductivity of the 21% solid content MFT was increased by 4 magnitudes after the treatment. For the optimally treated MFT, the flocs and aggregates settled rapidly during the first 1h, the settling rate then decreased sharply and became zero after 24h. Different from the non-flocculated MFT which settled continuously throughout the test, the FMFT did not settle when an equilibrium between the self-weight and the yield strength of the flocs was reached.

Oedometer tests

The purpose of the oedometer tests was to determine the consolidation behavior of the tailings over the effective stress range of 1–100 kPa which is operative in the majority of tailings management facilities (Qiu and Sego, 2001). To prepare the specimen, the fluid fine tailing was subjected to consolidation under self-weight and small pre-loading pressure to remove excess water. The specimen was consolidated by step loading method.

Figure 5 presents the experimentally determined compression curves (void ratio versus logarithm of effective stress plots) for the saturated samples of TT, MFT and FMFT. It can be seen that the compression data of the FMFT lay above that of the MFT while the TT is similar to the MFT. Table 3 shows the consolidation parameters calculated from the tests results for the MFT and the FMFT. According to the data, it is concluded that the FMFT was more compressible, more permeable and consolidated faster than the non-flocculated MFT. The differences are attributed to the floc structures formed in the tailing. The figure shows that with the increase of effective stress the compression curves of two tailings approach each other. It is hypothesized that the FMFT will exhibit similar behavior to the non-flocculated tailings at a high stress when all the flocs collapse.

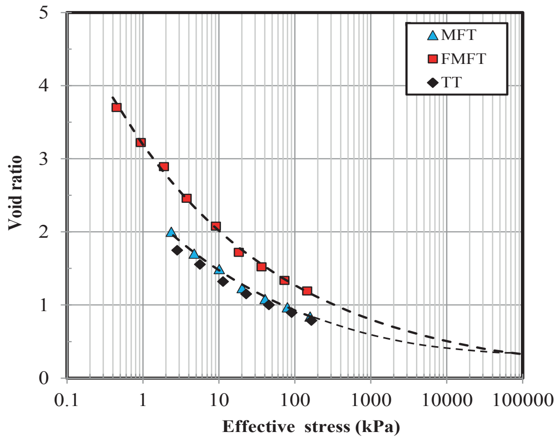

Figure 5. Relationship between initial settling velocity and void ratio

Table 3. Consolidation parameters of MFT and FMFT

	MFT	FMFT
Stress (kPa)	2.3 - 160	0.48 - 160
Void ratio	1.63 - 2.37	1.06 - 3.33
C_c	0.36 - 0.42	0.63 - 1.65
C_v (m^2/year)	0.05 - 0.28	0.13 - 0.52
M_v (m^2/MN)	0.8 - 30	1.5 - 249
K_s (m/s)	4.5×10^{-10} - 7.2×10^{-11}	7.2×10^{-8} - 1.4×10^{-10}

The compressibility and hydraulic conductivity data of MFT have been provided by many researchers in the open literature. In terms of TT and the polymer treated MFT, the available data were quite limited. The void ratio versus logarithm of effective stress plot of the MFT in current work was in good agreement with those presented by Pollock (1998) and Proskin (1998) for MFT over the effective stress range from 10 to 100 kPa. Some deviations occurring at small effective stresses may be due to different initial water content of the samples.

Shrinkage and swelling tests

The shrinkage and swelling tests were performed to determine the shrinkage curves of the fine tailings and their rewetting swelling behavior. The information is required to obtain a quantitative indication of how much volume changes in subaerial tailings disposal. The details about the tests were introduced in IOSTC 2014 (Yao et al., 2014). Figure 6 shows the shrinkage curves, presented as void ratio versus water content plots, for the MFT and three FMFT samples treated at different conditions. The shrinkage curves show a “J” shape consisting of three stages which are normal stage, residue stage and zero stage. The intersection between the saturation line and the horizontal asymptote of the curve when water content tended towards zero was considered as the real shrinkage limit (Fredlund et al., 2002). It can be seen that when the dosage of polymer increased from 0 (non-flocculated MFT) to 500g/t and then 1000g/t (the optimum), the shrinkage limit increased from 18% to 25% and 31%. Meanwhile, the minimum void ratio increased from 0.41 to 0.57 and 0.7. After drying, the over-mixed FMFT had smaller void ratio than the optimally mixed FMFT. Since there was no external pressure applied to the samples, varieties in the shrinkage curves were related to the different soil structures that were formed by flocculation. Based on the data, it is estimated that the volume of the desiccated FMFT is 25% larger than the non-flocculated MFT. This behavior should be considered in the design of the tailing disposal facility.

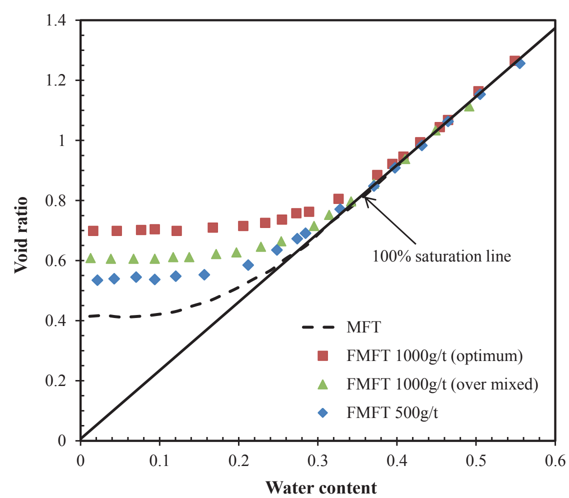

Figure 6. Shrinkage data of the MFT and the polymer treated MFT

Figure 7 is a schematic drawing of drying and rewetting curves of a fine tailing sample based on the test results. Point A is the minimum water content attained by the first drying. When the soil is rewetted from this point, the difference between the rewetting and drying path (hysteresis) is the largest. The linear part of the initial rewetting path AD is almost parallel to the 100% saturation line.

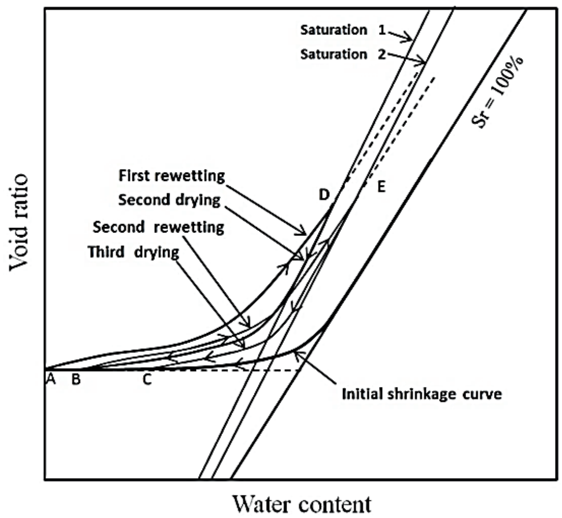

Figure 7. Schematic drawing of shrinkage and swelling paths during cyclic drying and rewetting

Once the second cycle starts at point D, the drying path will follow the saturation line 1 and may reach point B, which has the same void ratio as point A. The subsequent wetting path BE and the drying path EC are similar to the curve AD and DB, respectively. It was found that the difference between drying and wetting curve vanished after four successive drying-wetting cycles. This phenomenon reveals that for the tailing lifts in the atmosphere that undergo frequent drying and wetting processes, changes of bulk volume as function of changing water content are reversible. The obtained swelling results suggested that the fine oil sands tailings were not expansive soils.

Water retention characteristic tests

The water retention characteristic tests were used to assess the soil water retention curves (SWRC) of the fine tailings. Determination of SWRC of a soil requires measurement of suction at different water content. In principle, the traditional filter paper method can cover the whole suction range of fine tailing. This method was utilized in this work and the tests were conducted following the procedure described by ASTM D5298. Filter papers were placed in both contact manner (for matric suction) and non-contact manner (for total suction) with the tailing sample. At high suctions, filter papers come to equilibrium with soil only through vapor no matter being placed in contact or non-contact manner, and only total suction is measured. The SWRC at high suctions was determined using the WP4C dew point potentiometer (which is known for its distinct advantage in precisely and instantly determining the high total suction) and the result was combined with the filter paper result to establish the complete SWRC.

The difference between total suction and matric suction is regarded as osmotic suction. Osmotic suction is generated by the osmotic repulsion mechanism, arising from dissolved salts in the pore water. The results suggest that osmotic suction was major contributor to total suction for the fine tailings. This implies that the pore water in the fine oil sands tailings had relatively high salinity.

Figure 8 presents the SWRC assessed for different tailings. The figures show different water retention characteristics between the MFT and the FMFT. At the same water content, the FMFT had lower suction compared to the non-flocculated MFT. The cause of different behavior is related to changes in particle size and soil structures due to flocculation. It is noted that the TT shows over-consolidated characteristic, this is probably due to higher compaction degree of the sample. The SWRC of the MFT was compared to those reported by Fredlund et al. (2013) and Owolagba & Azam (2013) for different MFT samples. Despite some deviations in the lower suction range, these curves converge at above 1000 kPa.

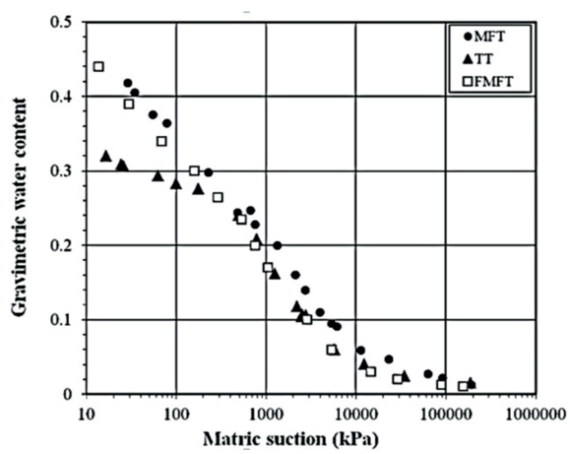

Figure 8. The soil water retention curves determined for different tailings

From the determined SWRC, it is difficult to determine the air entry value (AEV) since there is no distinct curvature in the region of low suctions. Fredlund and Houston (2013) proposed that the independent shrinkage curves should be used to properly interpret the SWRC. With the use of the shrinkage curve, the previously presented SWRCs are expressed as water content versus degree of saturation plots, as shown in Figure 9. From these plots, distinct air entry value (AEV) of each tailing can be identified by the break in the curvature of the curve at the 100% degree of saturation. For the FMFT, the AEV of SWRC was about 60kPa, which is significantly smaller than those of MFT (about 700kPa) and TT (about 800kPa). With the shrinkage data, the volumetric water content can be calculated based on the instantaneous volume measurements. The SWRC can thus be converted to the volumetric water content versus soil suction plot. This plot was used for the numerical work undertaken to simulate fine tailings drying, see the complementary paper presented in this conference (Vardon et al., 2016).

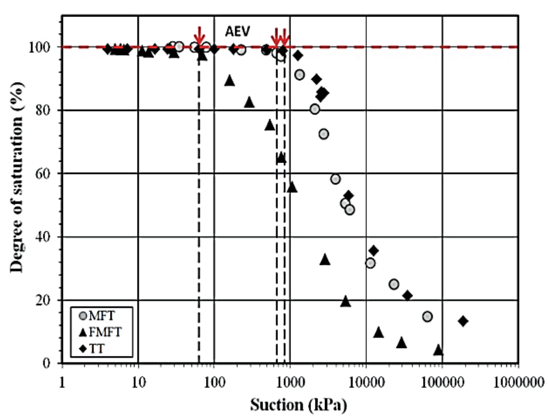

Figure 9. SWRCs presented as degree of saturation against suction

Cracking tests

Cracking tests were performed to investigate the cracking behavior of thin layers (~1 cm) of soft tailings. Homogenous fluid tailings or high water content clay paste was placed in a glass cup (98 mm diameter, 11 mm deep). The cup was placed on an electrical scale which was used to monitor the evaporative weight loss. The clay sample was dried by horizontal air flow created at constant rate above the tailing surface. A camera was fixed on top of the specimen to capture the images of the surface (Figure 10). The tests were performed in the climate controlled chamber where the temperature was maintained at 24°C.

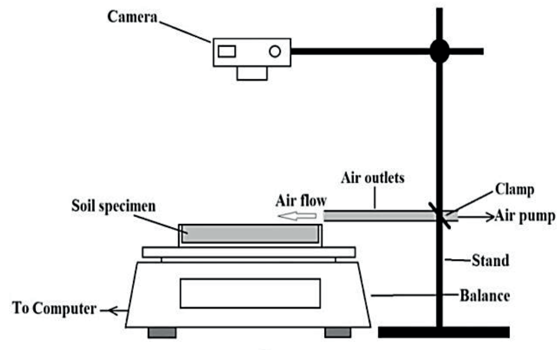

Figure 10. The set-up used for cracking tests

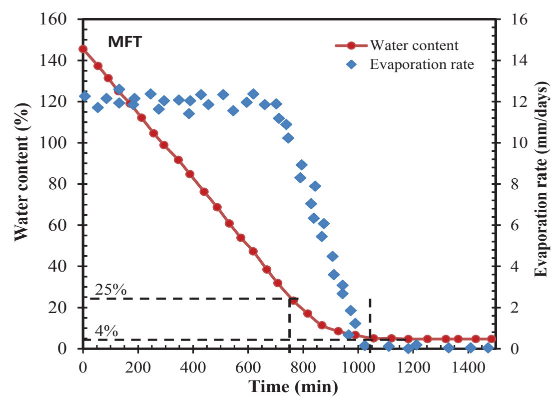

Figure 11. Water content and evaporation rate versus time curves for a MFT sample during drying

Figure 11 shows the monitored evaporation rates and the average water content of a 11 mm thick MFT sample during drying. It can be seen that variations of evaporation rate with decreasing water content can generally be divided into three stages: (1) the constant-rate stage at an average value of 12 mm/day (0 -700min); (2) the falling-rate stage (700-1000min) and (3) the low-rate stage (>1000min). The evaporation rate dropped rapidly at water content 25%, which was close to the plastic limit. At the end of test, the residual water content was about 4%.

Figure 12 illustrates how desiccation cracks occur and propagate on a 11 mm thick FMFT layer during drying. It can be seen that the first crack was initiated by connecting two tiny pits (surface defects) at a water content (52%). Another crack then occurred and small branches were born. The secondary cracks formed at the exiting primary cracks and terminated when they joined other cracks or extended to the rim of specimen. When the average water content decreased below the shrinkage limit, there was no change in the crack networks. According to the water contents reported in Figure 12 and the evaporation rate shown in Figure 11, the majority of cracks were formed in the constant evaporation rate stage.

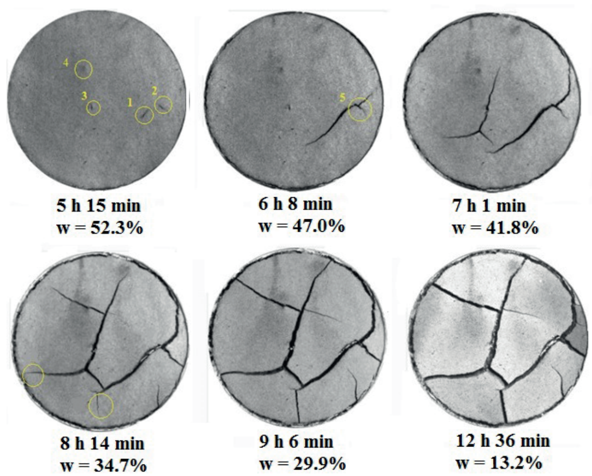

Figure 12. Formation and propagation of desiccation cracks on a thin FMFT

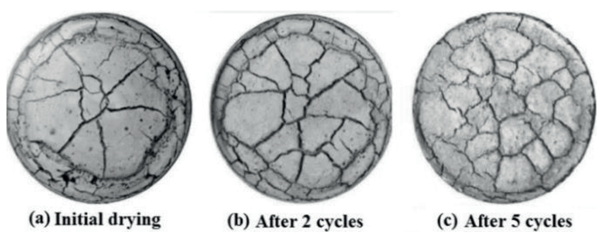

Figure 13. Changes of crack networks of MFT during multiple wetting-drying cycles

Unlike the FMFT, a large amount of clay in the MFT adhered to the glass wall during drying. This affected the formed crack pattern as some circumferential cracks were formed at the margin area of the surface (Figure 13a). The cracked sample was rewetted by soaking with water to allow most cracks close, then it was dried again. Figure 13 shows changes of the crack networks of a MFT sample after up to 5 drying-wetting cycles. It can be seen that with the increase number of cycles the number of cracks increased and the mean cell area reduced. This behavior has been previously observed for normal clayey soils (e.g. Yesiller et al., 2000, Tang et al., 2011). The cracked FMFT was also subjected to several wetting-drying cycles, but there was almost no change in the crack pattern. This different behavior suggests that FMFT has stronger particle bonds and tensile strength than non-flocculated MFT.

Air Drying Tests

A laboratory study on air drying of fluid TT was presented in IOSTC 2010 (Yao et al., 2010a). These preliminary results demonstrated that the TT can be effectively and efficiently dewatered by atmospheric drying. In order to obtain a deeper understanding of the tailings drying behavior and the specific measurements for numerical modelling and validation, a new experimental program was conducted. In this program, the fluid fine tailings (MFT and the FMFT at initially 35% solid content) were allowed to consolidate and desiccate in two layers in a series of PVC cylinders. The apparatus is shown in Figure 14. Air circulation was created above the tailing at constant rate (400 L/h) to accelerate the drying. The weight of the column was monitored throughout the test to determine the actual evaporation (AE) rate of the tailing. One cylinder was filled with water and placed in the same condition as the tailings to monitor the potential evaporation (PE) in laboratory conditions. All the tests were performed in the climate controlled environment. At regular intervals, the columns were scanned with the CT technique to identify the internal changes of the tailings during drying.

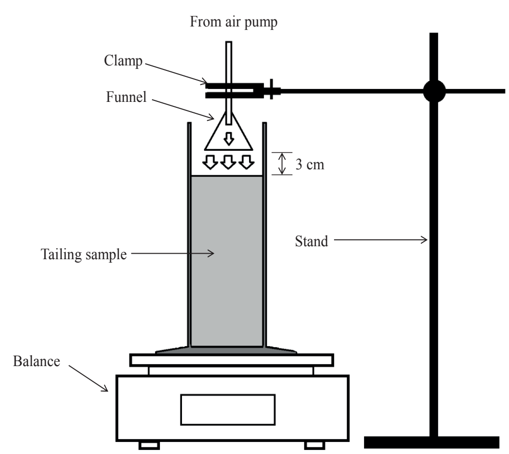

Figure 14. Set-up for column air drying tests

Due to the side wall adhesion, the height of the MFT was not always correctly measured. This effect also influenced the evaporation rate. Compared to the non-cracked tailing surface, the amount of evaporation from the cracked tailing and the suspended soils was significantly larger.

In the FMFT tests, settling of the tailing did not leave much material on the side wall while the whole soil column showed lateral shrinkage after the stagnant water was evaporated. Figure 15 shows the temporal change of the total height of the FMFT during drying. The diamonds on the graph stand for the total height of the material (mud + water) and the red squares represent the height of the mud surface. It can be seen the stagnant water completely evaporated by Day 11, this is the start of the desiccation of the sediment. The second layer was filled to an equivalent thickness of 19.1 cm, but it resulted in a height increase of 18.1 cm, indicating that about 1 cm slurry (about 61 cm^3) was filled to the shrinkage gap between the first layer and the side wall. At Day 40 the final height of the tailing was 16.3 cm.

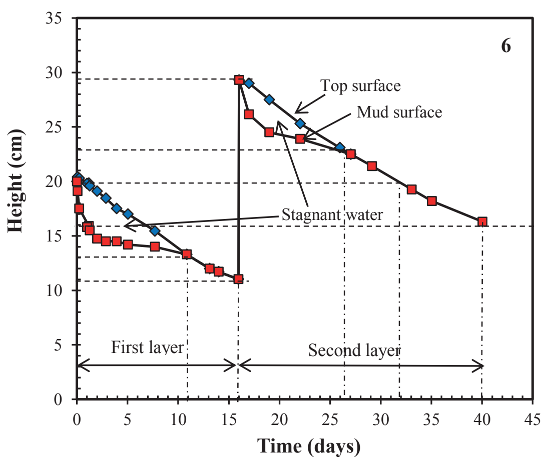

Figure 15. Changes of the height of the FMFT during drying

The measured evaporation rates suggest an average AE/PE ratio of 0.7 for the FMFT shortly after the supernatant water vanished. This value was slightly lower than the average monthly AE/PE ratio (0.75) reported by Kolstad et al. (2012) for a newly deposited FMFT in field tests. It is assumed that the lower AE/PE ratio was caused by a bitumen film remaining on the surface (as there was no run-off mechanism for supernatant water) and the salinity of pore water which suppresses evaporation by developing high osmotic suctions. Above assumptions are made based on the observed bitumen and salt crystals on the desiccating tailing surface, as shown in Figure 16.

Figure 16. The surface of the FMFT column showing bitumen and salt crystals

The CT scanning results for the FMFT are presented in Annex 1. These images were calibrated and processed in Matlab and the real bulk density values of the tailing were obtained. The bulk density profiles were derived from the x-ray images by plotting the average density values of the tailing with the height, as presented in Annex 2. The data show that a thin desiccated crust was formed on the top of the tailing and the thickness of the crust increased as drying progressed. One day after the filling of the second layer, the peak density of the first layer decreased from 1680 to 1550 kg/m^3. It indicates that the wet upper layer exerted a rewetting effect on the dried lower layer. Based on the images, no significant rewetting swelling was identified from the first layer. This highlights the potential advantage of depositing the tailing in layers.

Through the x-ray images, some gas bubbles were identified in the lower part of the tailing at the later stage of drying. The production of gas bubbles may be the result of decomposition of organic matter. In the previous test, it was found that a larger quantity of gas was released by fresh TT during the settling (Yao et al., 2010a). The gas bubbles formed in the FMFT were relatively small according to what they appear on the image (i.e. at average radius of 2mm).

CONCLUSIONS

A series of laboratory tests were performed to study the dewatering behavior of fine oil sands tailings. The main conclusions are summarized as follows:

- The developed properties (e.g. basic properties, compressibility, shrinkage property, water retention characteristic) of the MFT in current study were in general close agreement with the data reported in the open literature for the MFT. The TT showed different behavior to the reported, in particular the particle size and the settling behavior. One possible reason is that the flocs were destroyed by laboratory mixing and sampling process prior to the tests.

- Flocculation tests showed that an initial rapid mixing was desired for efficient flocculation. Prolonged vigorous mixing destroyed the flocs and led to mediocre dewatering results. There was an optimum range of mixing energy for the MFT-polymer system. The original MFT should be to some extent diluted before the flocculation to ensure the pumpability of the flocculated tailings.
- Upon deposition, the MFT experienced different settling processes depending on the initial void ratio. Transition from sedimentation to consolidation occurred at a void ratio which was about 8.5 times the void ratio at the liquid limit. Flocculation of MFT greatly accelerated the settling of the tailing slurry. The initial hydraulic conductivity of a 21% solid content MFT was increased by 4 magnitudes after flocculation.
- Flocculation of MFT affected the compressibility of the tailing. Oedometer tests suggest that the FMFT were more compressible and permeable than the MFT. At the same effective stress, the FMFT had larger void ratio than the MFT due to larger voids in floc structures. The floc structure tended to collapse at high surcharge pressure.
- The shrinkage data of the saturated fine tailing showed a J-shaped curve in a progressive drying pattern consisting of three stages. Hysteresis existed in the swelling curve when the soil was rewetted., This effect vanished after the soil experienced four consecutive wetting-drying cycles. Flocculation affected the shrinkage curve. When there was no external pressure applied on the sample, drying FMFT sample resulted in a larger void ratio in the residual shrinkage stage compared to drying the original MFT.
- Changes of the rate of evaporation from a thin tailing sample can be divided into three stages: constant-rate, falling-rate and low-rate. Most of volumetric change and desiccation cracks occurred in the constant-rate stage. Desiccation cracks initiated when the clay matrix was still fully saturated.
- The flocculated MFT contained in a column experienced a 3-D deformation upon drying.
- The actual evaporation rates measured from the tailing were smaller than the evaporation rates measured from pure water even at the beginning of drying. Some bitumen and salts found at the surface may suppress the evaporation. Deposition of a fresh tailing rewetted the underneath layer but did not cause large vertical swelling.

ACKNOWLEDGEMENTS

The material for these tests and funding for the PhD project were provided by Shell Canada. This support is gratefully acknowledged.

REFERENCES

Beier, N., Wilson, W., Dunmola, A., & Sego, D. (2013). Impact of flocculation-based dewatering on the shear strength of oil sands fine tailings. Canadian Geotechnical Journal, 50(9), 1001-1007.

BGC Engineering Inc., 2010. Oil Sands Tailings Technology Review. OSRIN, University of Alberta, School of Energy and the Environment, Edmonton, Alberta. OSRIN Report No. TR-1. 136 pp.

Carrier, W.D. III, Bromwell, L.G. & Somogyi, F., 1983. Design capacity of slurried mineral wastes ponds. J. G. Eng. ASCE. 109(5): 699-716.

Demoz, A., & Mikula, R. J., 2011. Role of mixing energy in the flocculation of mature fine tailings. Journal of Environmental Engineering, 138(1), 129-136.

Fredlund, M. D., Wilson, G.W., & Fredlund, D.G., 2002, Representation and estimation of the shrinkage curve. In UNSAT 2002, Proceedings of the Third International Conference on Unsaturated Soils, 145-149.

Fredlund, D.G., & Houston, S.L. 2013. Interpretation of soil-water characteristic curves when volume change occurs as soil suction is changed. Advances in unsaturated soils. CRC Press, Boca Raton, FL, 15-31.

Gholami, M., 2014. Shear Behaviour of Oil Sand Fine Tailings in simple shear and triaxial devices (Doctoral dissertation, Carleton University Ottawa).
Innocent-Bernard, T., 2013. Evaporation, cracking, and salinity in a thickened oil sands tailings. M.Sc. Thesis. Carleton University, Ottawa, Ontario.

Kolstad, D., Dunmola, A., Dhadli, N., O'Kane, M., Song, J., & Masala, S., 2012. Towards the improvement in geotechnical performance of atmospheric fines drying (AFD) deposits at Shell's Muskeg River Mine. In Proceedings of the 3rd International Oil Sands Tailings Conference, Edmonton, Alberta.

Limsiri, C., 2008. Very soft organic clay applied for road embankment: Modelling and optimization approach. Ph.D thesis. Delft University of Technology, Delft, The Netherlands.

Owolagba, J., & Azam, S. 2013. Unsaturated soil properties of centrifuged oil sand fine tailings. In press Proceedings, 66th Canadian Geotechnical Conference.

Proskin, S.A., 1998. A geotechnical investigation of freeze-thaw dewatering of oil sands fine tailings. PhD thesis, University of Alberta, Department of Civil and Environmental Engineering, Edmonton, Alberta. 414 pp.

Pollock, G.W.,1988. Large strain consolidation of oil sand tailings sludge. MSc Thesis, University of Alberta, Civil and Environmental Engineering, Edmonton, Alberta. 276 pp.

Rima, U.S., 2013. Characterization and Centrifuge Dewatering of Oil Sands Fine Tailings. Doctoral dissertation, Faculty of Graduate Studies and Research, University of Regina.

Tang, C.S., Shi, B., Liu, C., Suo, W.B., & Gao, L., 2011. Experimental characterization of shrinkage and desiccation cracking in thin clay layer. Applied Clay Science, 52(1): 69-77.

Vardon, P.J., Yao, Y., van Paassen, L.A. & van Tol, A.F, Consolidation and atmospheric drying of fine oil sand tailings: comparison of blind simulations and field scale results. Submitted to IOSTC 2016, Proceedings of the 5th International Oil Sands Tailing Conference

Xu., G., Gao, Y., Ji, F. & Cao, Y., 2012. Permeability coefficients of dredged slurries at high void ratio. Applied Mechanics and Materials, 170-173, 1269.

Xu, Y., Dabros, T., & Kan, J. 2008. Filterability of oil sands tailings. Process Safety an Environmental Protection, 86(4): 268-276.

Yesiller, N., Miller, C. J., Inci, G., & Yaldo, K. 2000. Desiccation and cracking behavior of three compacted landfill liner soils. Engineering Geology, 57(1): 105-121.

Yao, Y., van Tol, A.F, van Paassen, L.A., Everts, H.J. & Mulder A. 2010a., Experimental research on mud farming of fine oil sands tailings. Second international oil sands tailings conference. Sego D & Beier N (eds.). Edmonton: University of Alberta Geotechnical Center, 59-68.

Yao Y., van Paassen, L.A., van Tol, A.F., Everts, H.J. & Mulder, A. 2010b. Experimental research on accelerated consolidation using filter jackets in oil sands tailings. Second international oil sands tailings conference. 77-85.

Yao, Y., van Tol, A.F., van Paassen, L. & Vardon P.J. 2014. Shrinkage and swelling properties of flocculated mature fine tailings. In: IOSTC 2014, Proceedings of the 4th International Oil Sands Tailing Conference, 27-35.

Annex 1. X-Ray images obtained from CT scanning for FMFT

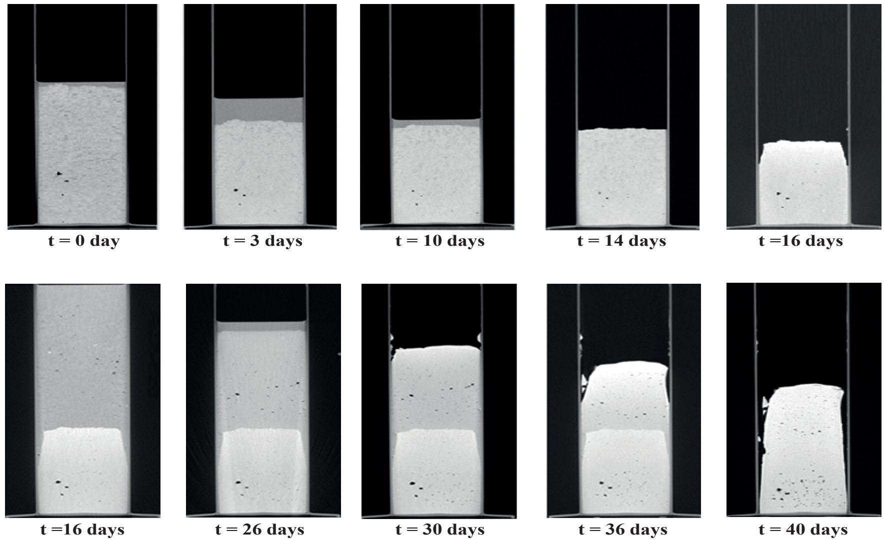

Annex 2. Soil density profiles derived from CT scanning

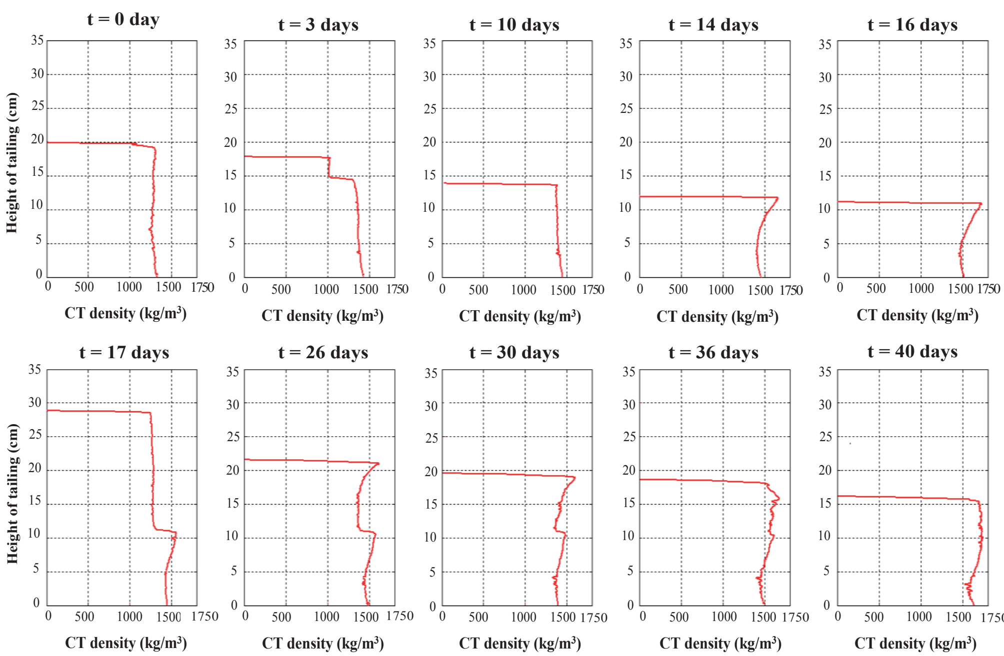

CONSOLIDATION CHARACTERISTICS OF FLOCCULATED MFT – EXPERIMENTAL COLUMN AND SICT DATA

Dobroslav Znidarcic[1], Dirk Van Zyl[2], Mario Ramirez[2], Kushagra Mittal[3] and Heather Kaminsky[4]
[1]University of Colorado
[2]University of British Columbia
[3] Coanda Research & Development
[4] Northern Alberta Institute of Technology

ABSTRACT

The paper presents the results of a comprehensive seepage induced consolidation and sedimentation column testing program on a single MFT, flocculated to five different conditions - optimally dosed-optimally mixed, optimally dosed-over mixed, optimally dosed - under mixed, over dosed-optimally mixed, and under dosed- optimally mixed. In addition to the time settlement relations the data provides an insight into fabric creation under different flocculation conditions. Both compressibility and permeability characteristics are measured and compared to the same characteristics of the untreated MFT. The results show significant fabric changes at effective stresses below 1 kPa and the corresponding increase in hydraulic conductivity at high void ratios.

INTRODUCTION

Disposal of oil sands tailings have posed major challenges for the oil sands industry over several decades. In search of acceptable and sustainable disposal strategies various methods are being explored and evaluated, including pre-deposition treatment by flocculating agents. The goals are: removal and recycling of process water, reduction of tailings volumes and reclamation of disposal areas. Upon field deposition tailings are subjected to sedimentation and consolidation processes that can be readily predicted using appropriate numerical models. The models require that sedimentation and consolidation properties are evaluated in appropriate experimental procedures and the model parameters are obtained by analyzing these experiments. The paper presents the results of a comprehensive seepage induced consolidation and sedimentation column testing program on a single MFT, flocculated to five different conditions.

SEDIMENTATION AND CONSOLIDATION TESTING

Seepage Induced Consolidation Test (SICT) was used to determine both compressibility and hydraulic conductivity characteristics for treated and untreated MFT. The testing procedure consists of three steps (Abu-Hejleh and Znidarcic, 1996). In the first step the void ratio at the effective stress zero is determined by allowing a slurry column about 0.05 m high to consolidate under its own weight. The average void ratio of the settled slurry is considered the void ratio at the effective stress of zero, or the void ratio at which the soil is formed and the consolidation theory, as opposed to the sedimentation theory, applies.

In the second step, seepage at a constant flow rate is applied through the soil by means of a flow pump and the sample is allowed to consolidate completely, i.e. until the steady state is reached. The steady state is determined from the pressure difference across the sample that is continuously monitored during the test. At steady state, the pressure difference and the final height of the sample are recorded. It is recognized that during this phase of the test the void ratio within the sample is non-uniform and this is correctly accounted for in the test analysis.

In the third step the sample is consolidated under the maximum desired stress level and the hydraulic conductivity is measured with the flow pump using a low flow rate to maintain sample uniformity during the test. At the end of the test the sample is dried and the total volume of solids is determined.

The analysis of the test is performed using the software package SICTA (Seepage Induced Consolidation Test Analysis). The procedure is based on the inverse problem solution approach and the theory used is compatible with the finite strain nonlinear consolidation theory (i.e. no simplifying or restrictive assumptions are made in the analysis). The input data for the SICTA program are all obtained from the described test. The output gives five parameters A, B, Z, C and D that define the consolidation properties for the sample. The compressibility and hydraulic conductivity relations with the five parameters are defined as:

Compressibility $\mathbf{e = A (\sigma' + Z)^B}$

Hydraulic Conductivity $\mathbf{k = C\, e^D}$

in which e is the void ratio, σ' is the effective stress, k is the hydraulic conductivity and A, B, Z, C and D are the model parameters. The application of the testing and analysis approach to oil sands tailings has been documented by Znidarcic et al (2011) and Esthepo et al (2013).

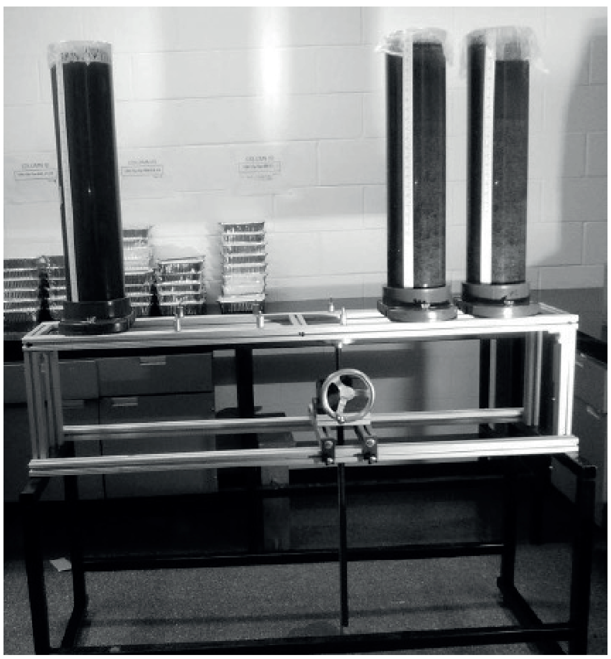

Figure 1. Settling columns arrangement at UBC

Settling columns testing

The settling column tests were performed to determine both the sedimentation properties of the treated and untreated MFT and to provide data of an independent verification of the consolidation properties obtained in the SICT. Several 0.6 m high and 0.152 m in diameter columns of identically prepared MFT were monitored for up to 60 days. Slurry settlement with time was continuously recorded by visual observations and the void ratio distributions were determined by sampling the columns at different preselected times to obtain density profile at different elapsed times. Each column included a sealed piston at the bottom that can be pushed up with a screw mechanism during the sampling procedure. Thus, the columns were sampled in vertical position with minimal disturbance of the material in the sampling process, Figure 1.

Both the consolidation and sedimentation characteristics were determined for a single MFT, but flocculated to five different conditions - optimally dosed-optimally mixed, optimally dosed-over mixed, optimally dosed - under mixed, over dosed- optimally mixed and under dosed- optimally mixed. In addition, the consolidation and settling column tests were performed on the untreated MFT for comparison.

The MFT used was part of a vac truck load sampled in August of 2015. The truck load was well mixed and decanted into totes and then into pails as required. Analysis of several subsamples was conducted by various laboratories and was deemed to be representative of the material tested in this study, the summary of the characteristics is shown in Table 1.

Table 1. MFT properties

Property	Average	Range
Bitumen wt%	2.2	1.9-2.4
Mineral wt%	40.3	39.8-40.9
Water wt%	56.8	55.8-57.4
MBI meq/100g	8.1	7.2-9
% Clay by MBI	58%	52-64%
% fines	80%	
TDS (g/L)	2.6	
pH	8.4	
Ca^{2+} (ppm)	7.7	
Na^{+} (ppm)	801.1	
K^{+} (ppm)	13.9	
Mg^{2+} (ppm)	5.2	
SO_4^{2-} (ppm)	85	
Cl^{-} (ppm)	655.4	
HCO_3^{-} (ppm)	991.2	
CO_3^{2-} (ppm)	15.7	

Flocculation technique

Flocculation was performed according to the Suncor Phase II flocculation protocol for a single injection of BASF flocculant ETD 7010 at a fixed rpm. Flocculation was performed by a single extremely well trained operator (Kushagra Mittal) in order to ensure consistency of the flocculation between experiments. Each flocculation test produced approximately 1 L of material and required almost 12 repeats to fill a column. Optimal dosage was gauged by visual observation and confirmed as the dose that gave the highest clay to water ratio after 24 hours. This dose was determined to be 2000g/t clay for the mixing conditions used. This resulted in a 24hr CWR of 0.58. Underdose was assessed as 1400g/t clay with a 24hr CWR of 0.47 for optimal mixing conditions, overdose was assessed as 2400 g/t clay with a 24hr CWR of 0.51 for optimal mixing conditions.

Overmix and undermix conditions were determined qualitatively. In undermix the optimal dosage was added but mixing was stopped before well defined flocs emerged. In overmixing the optimal dosage was added and mixing continued until the well defined floc structure was destroyed.

TEST RESULTS

Sample preparation results

Table 2 presents the data collected from the treated samples immediately after treatment and before they were placed in the SICT apparatus or in settling columns.

Table 2: Sample conditions before testing

Treatment Conditions	Mixing Void Ratio	Zero Effective Stress Void Ratio	24 h Void Ratio
Optimal dose-optimal mix	3.85	2.53	2.26
Optimal dose-undermix	3.85	3.06	2.69
Optimal dose-overmix	3.85	2.86	2.52
Underdose-optimal mix	3.73	3.20	2.80
Overdose-optimal mix	3.93	2.80	2.55

It is noted that the untreated MFT has an initial void ratio of 3.45. The addition of the flocculating agent increases this void ratio due to liquid addition, but the void ratio is then readily reduced by expelling water. The zero effective stress void ratio is higher than the 24h void ratio as in the SICT procedure a small (0.05 m) column is allowed to settle under its own weight while the 24 h test involves draining the material in a sieve, creating somewhat higher effective stresses in the sample.

Consolidation test results

Figure 2 presents the compressibility data for the untreated MFT and for all five treatment conditions while Figure 3 presents the hydraulic conductivity data for the same samples. Note that in the testing protocol in addition to performing the standard SIC test several step load increments were applied to the samples and direct hydraulic conductivity measurement was performed at each load. Table 3 lists the compressibility and permeability parameters determined in the Seepage Induced Consolidation Test Analysis (SICTA).

Table 3. Consolidation parameters obtained from SICTA

Treatment Conditions	A	B	Z (kPa)	C (m/day)	D
MFT	**2.46**	**-0.234**	**0.238**	**$9.64*10^{-6}$**	**2.73**
Optimal dose-optimal mix	**2.74**	**-0.277**	**1.34**	**$1.24*10^{-5}$**	**5.21**
Optimal dose-undermix	**3.30**	**-0.309**	**1.28**	**$1.16*10^{-5}$**	**4.14**
Optimal dose-overmix	**2.58**	**-0.216**	**0.614**	**$1.07*10^{-5}$**	**5.39**
Underdose-optimal mix	**2.67**	**-0.242**	**0.47**	**$1.03*10^{-5}$**	**4.45**
Overdose-optimal mix	**2.55**	**-0.266**	**0.708**	**$1.38*10^{-5}$**	**4.29**

Figures 4 and 5 present the compressibility and hydraulic conductivity relationships derived from the state parameters. They exhibit trends very similar to the data points obtained with direct measurements but the relationships derived from the SICTA show much less scatter. This is not surprising as the SICTA considers material variability within the sample, especially at low effective stresses where flocculated materials exhibit random structure of flocs and inter-floc pores.

Several conclusions for the consolidation behavior of treated MFT can be drawn from the presented results in Figures 2 and 4. It appears that the flocculation process does not affect the compressibility behavior of MFT significantly as all the curves are very close on both graphs. However, in the low effective stress range, less than 1 kPa, the data show significant scatter and even some points higher than the “zero effective stress" void ratio values. This is caused by the random nature of the floc structure where large flocs have sufficient strength and stiffness to resist deformation leaving wide open pores between them. It is hard to even collect a small "representative" sample from this material as one can never be sure to collect proper proportion of flocs and pore fluid for "zero effective stress void ratio" determination. This randomness is greatly reduced by the point where 1 kPa of effective stress is applied to the sample. It is interesting to note that the 24h void ratio values listed in Table 1 also correspond to the void ratio values at around 1 kPa on the presented curves. It could be argued that the randomness of the flocculated structure is essentially eliminated in the remolding process used to determine 24 h water release, or by the application of 1 kPa surcharge by the overlaying material or by other means.

The hydraulic conductivity relationships presented in Figures 3 and 5 show dramatic increase in hydraulic conductivity values for treated materials when compared to the untreated MFT. The optimally dosed samples show an increase in hydraulic conductivity of one order of magnitude, while the underdose and overdose samples show an increase of three to five times (i.e. less than one order of magnitude) the untreated MFT values. This shows the importance of proper dosage. Under mixing also appears to have a significant impact on the hydraulic conductivity whereas overmixing was shown to have no significant impact. This suggests that the initial formation of the flocs are critical in achieving optimal water release while destroying the apparent macrostructure is not critical.

The differences between treatments shrink rapidly and become insignificant above an effective stress of about 10kPa. What is even more important is the persistence of the flocculation effects vs. untreated MFT as the void ratio is reduced. The hydraulic conductivity of treated material remains substantially higher than for the untreated MFT until the void ratio is reduced to a value of one that corresponds to an effective stress of about 30 kPa. These findings will have significant repercussions on the consolidation behavior of tailings in field deposition and operation.

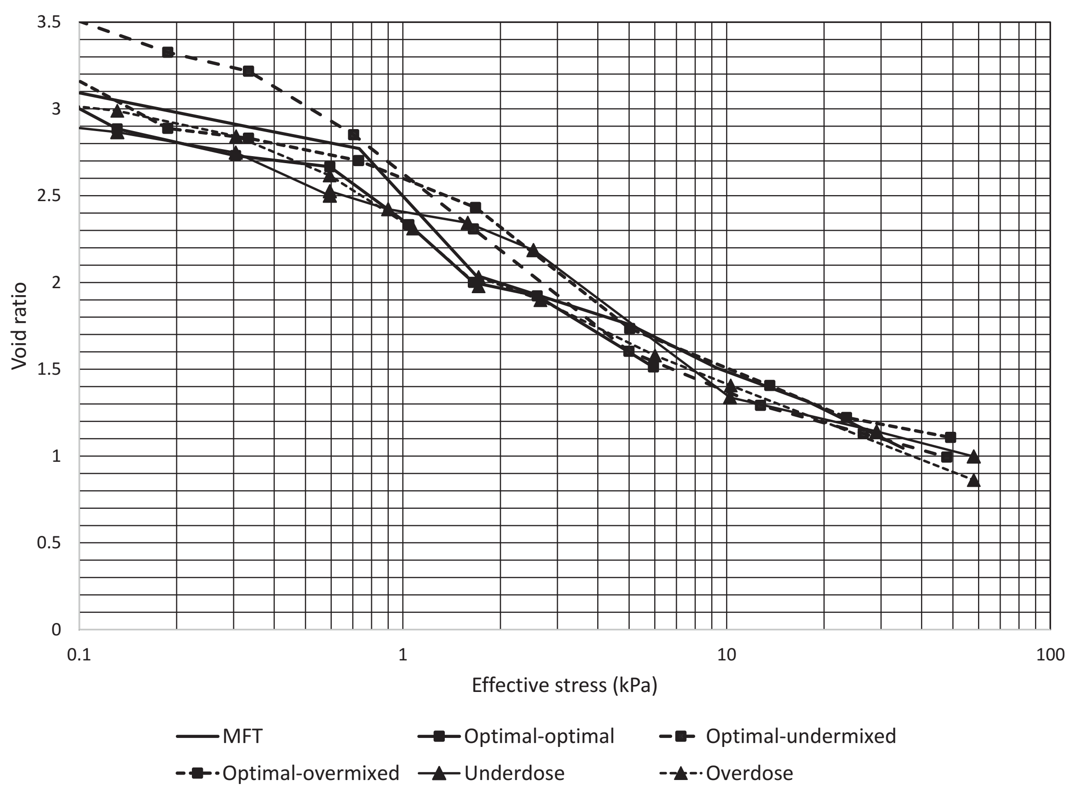

Figure 2. Compressibility data for SICTA tested samples

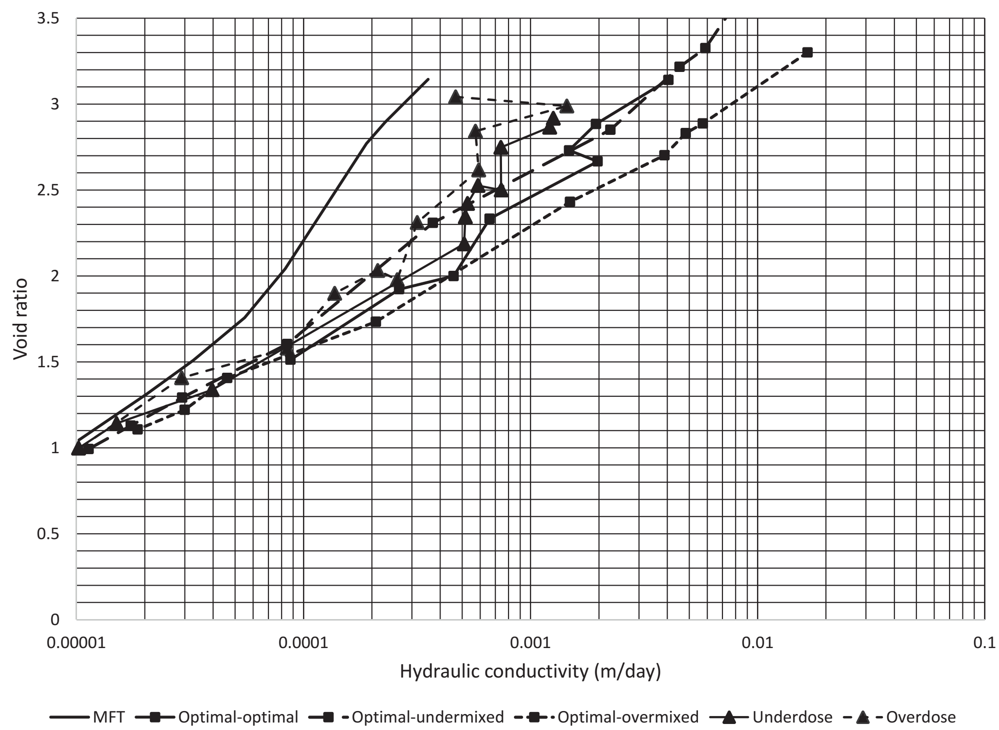

Figure 3. Hydraulic conductivity data for SICTA tested samples

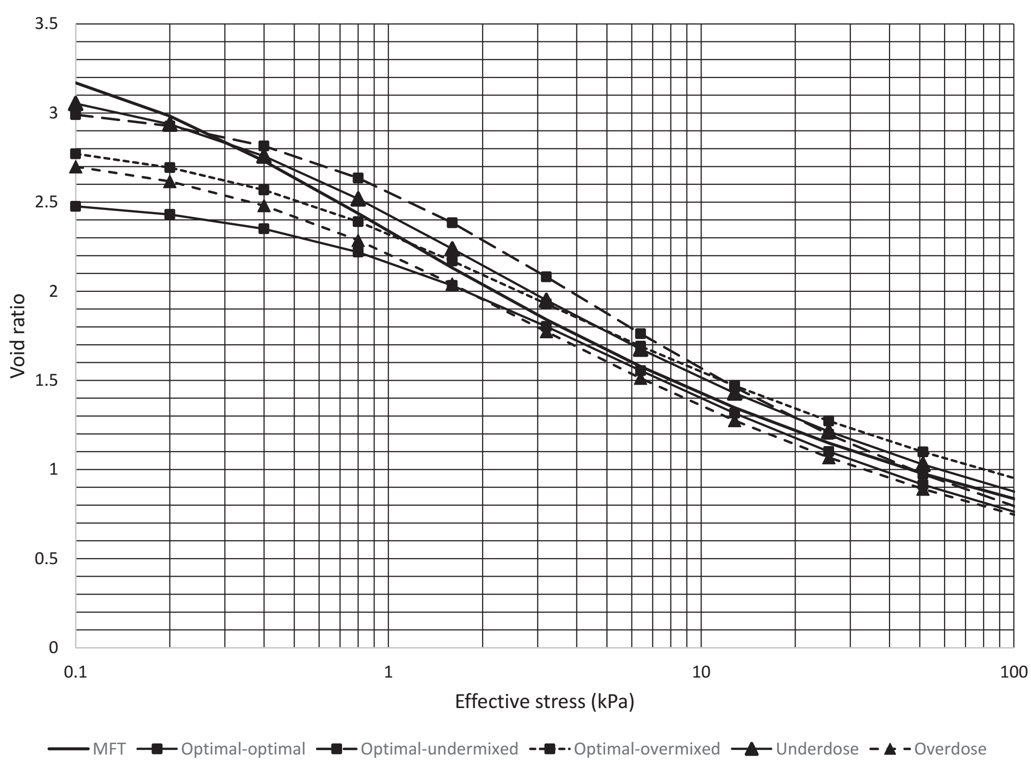

Figure 4. Compressibility relationships modeled from SICTA data

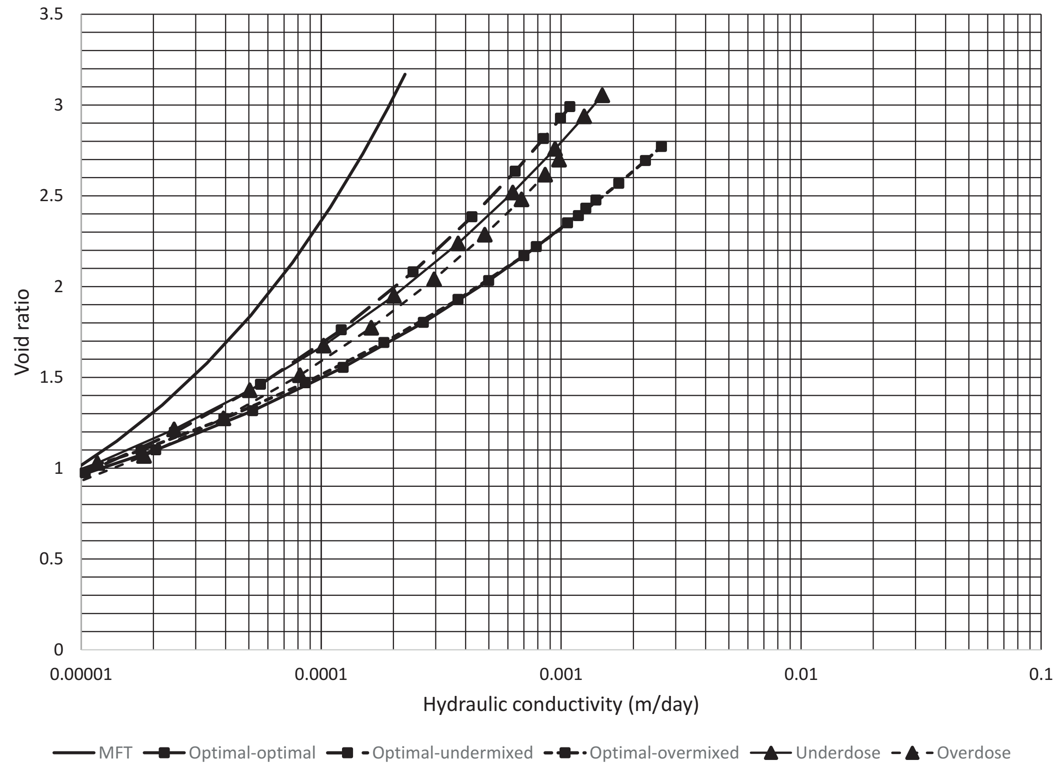

Figure 5. Hydraulic conductivity relationships modeled from SICTA

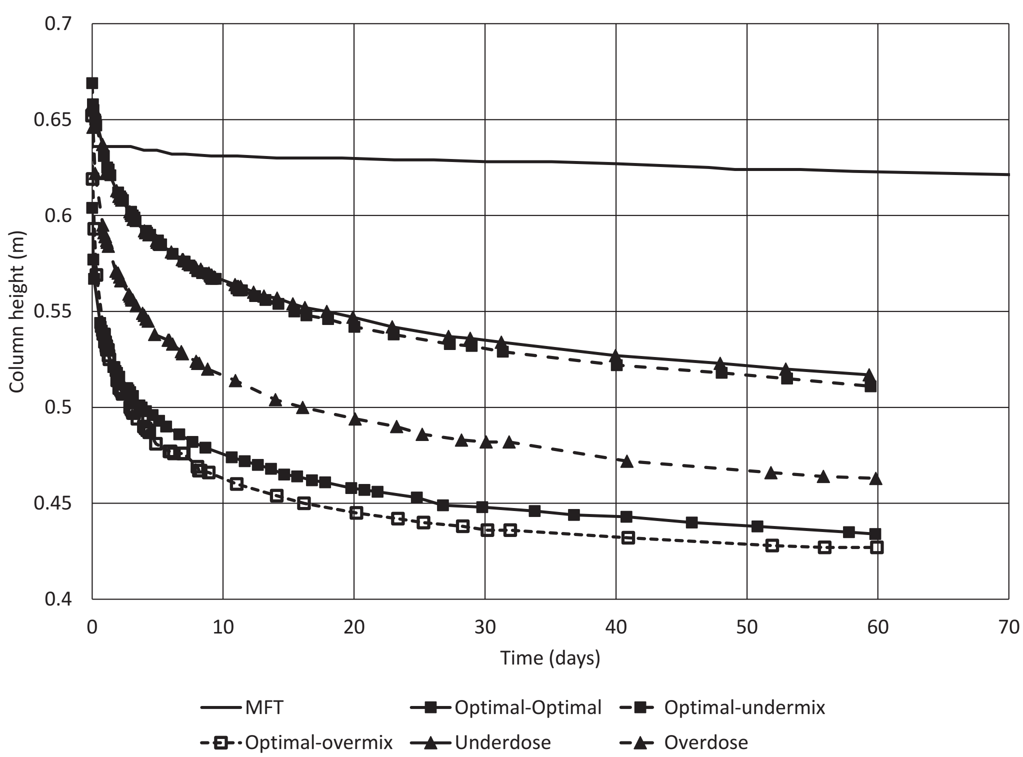

Figure 6. Settling columns settlement records

Settling columns test results

Figure 6 presents the time settlements records for an untreated MFT column and for five columns with various treatment conditions. The benefits of treatment is obvious from the results as the untreated MFT has hardly settled at all in the monitoring period. The amount of MFT in each column was the same and the differences in final heights illustrate the differences in compressibility characteristics for each column. It is noted that the maximum effective stress at the bottom of each column is around 2 kPa, so only the compressibility characteristics up to that stress level are relevant for interpreting these tests. As all treated materials exhibit somewhat random structure in that low stress range it is expected that the data will show quite a bit of scatter as well. For example Figure 7 presents the 30 days settlement records for several columns prepared with optimal dosage and optimal mixing conditions, however, decommissioned on different days. The difference between the curves indicates the extent to which the floc structures are different in otherwise identical samples.

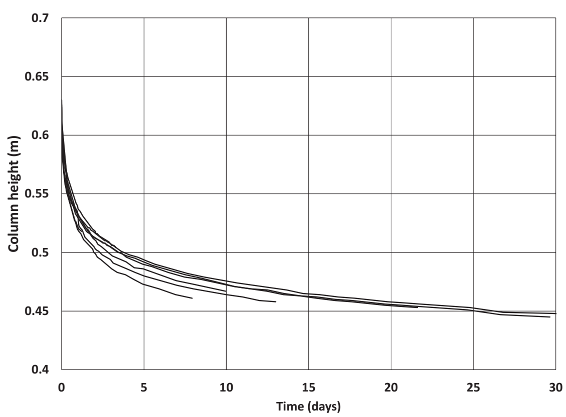

Figure 7. Settlement records for several columns with optimal dosage of the flocculent and optimal mixing

The initial slopes of settlement curves allow us to calculate the initial "apparent" hydraulic conductivity. The term apparent is used to indicate that in the early stage of settlement the treated material is in suspension and undergoes hindered settlement process rather than a consolidation process. To talk about hydraulic conductivity is not appropriate in this stage of the settling process. Nevertheless if such analysis were to be applied to the experimental data the hydraulic conductivity at the initial void ratio would be calculated to be an order of magnitude higher than the values measured in the consolidation tests.

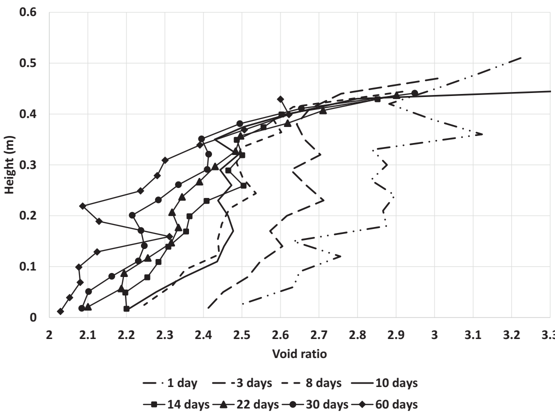

Figure 8. Void ratio distributions with time

Figure 8 presents the void ratio distributions measured at different times in the settling process for columns prepared at optimal dose of the flocculent and optimal mixing time. The results demonstrate that for the first 3 days the void ratio in the whole column, except at the very bottom, is higher than the void ratio of 2.5 corresponding to the void ratio at zero effective stress as determined in the consolidation tests. It takes additional 5 days for this consolidation front to reach the upper part of the column. The void ratio above the height of 0.39 m never drops below 2.5 indicating that at the top of the consolidating layer there will always be a portion of the material that doesn't consolidate but remains in a "fluffy" condition. The thickness of this layer at 60 days was about 0.07 m. The bottom portion of the column undergoing the consolidation process is accreting over time starting at about 3 days at the bottom and reaching the top at about 8 to 10 days. During that time the upper portion is undergoing a sedimentation process creating a need to model both processes simultaneously. A rational framework for modeling both sedimentation and consolidation processes simultaneously was developed by Pane (1985), but a working numerical model is not available at this point. In a companion paper we are presenting an approximate methodology of modeling the observed behavior.

Similar behavior was observed for all other columns with the exception of the untreated MFT column in which the material consolidates from the very beginning and the nonlinear finite strain consolidation theory can be used to predict column and field behavior.

CONCLUSIONS

Presented results support some important conclusions on the behavior of treated MFT. Treating MFT with flocculating agents is beneficial for field behavior of disposed tailings. The treatment facilitates faster release of the process water and speeds up the consolidation process of deposited materials. The beneficial effect of increased hydraulic conductivity persists even after the initial flocculated structure is lost and the macro pores are closed. The hydraulic conductivity of the flocculated material increases by up to one order of magnitude when compared to the untreated MFT. The compressibility characteristics are much less affected by the flocculation process and the final storage volume is not negatively affected, though there may be a significant impact of the difference during the initial fill.

The Seepage Induced Consolidation Testing methodology is appropriate for determining consolidation characteristics for both treated and untreated MFT. However, treated materials exhibit random compressibility behavior at low effective stresses and consolidation modeling in this zone is not appropriate as the slurry is not having soil like characteristics. Determining the effective stress or void ratio at which the material transitions from an open and random structure to a more slurry like homogeneous mixture is a critical step in any modeling effort. For the tested material and treatment methods that transition is taking place at about 1 kPa effective stress or a void ratio of about 2.5, depending on the treatment process.

For routine engineering applications the following procedure, similar to the one presented in the paper, can be implemented. Prepare the material in the lab with an appropriate dosage of the flocculating agent and mixing procedure that reflects mixing conditions in production. Perform a Seepage Induced Consolidation Test on a sample of the prepared material with an initial surcharge of 1 kPa. Complete the test with an applied load corresponding to the maximum effective stress the material will experience in the deposition process. Confirm the zero effective stress void ratio by testing a 0.5 m high column of the treated material and determining the void ratio distribution after about 7 to 10 days.

REFERENCES

Abu-Hejleh, A. N. and Znidarcic, D., 1996, Consolidation Characteristics of Phosphatic Clays, Journal of Geotechnical Engineering, ASCE, New-York, Vol. 122, No. 4. pp. 295-301.

Estepho, M., van Zyl, D., Znidarcic, D., and Revington, A., 2013, Seepage Induced Consolidation Testing of Mature Fine Tailings, Tailings and Mine Waste '13 conference proceedings, November 3-6, Banff, AB, Canada, ISBN: 978-1-55195-326-7, pp.101-109.

Pane, V., 1985, Sedimentation and Consolidation of Clays, PhD Dissertation, University of Colorado, Boulder

Znidarcic, D., Miller, R., van Zyl, D., Fredlund, M., and Wells, S., 2011, Consolidation Testing of Oil Sand Fine Tailings, Tailings and Mine Waste '11 conference proceedings, November 6-9, Vancouver, BC, Canada, ISBN: 978-0-88865-815-9, pp.251-257.

EFFECTS OF SHEARING AND SHEARING TIME ON DEWATERING AND YIELD CHARACTERISTICS OF OIL SANDS FLOCCULATED FINE TAILINGS

Babak Derakhshandeh[1], Abu Junaid[2] and Gavin Freeman[2]
[1]Coanda Research and Development Corporation, Burnaby, Canada
[2]Shell Canada Ltd., Calgary, Canada

ABSTRACT

This work presents a modeling study on the effects of pipeline shearing on dewatering and yield characteristics of Mature Fine Tailings (MFT) flocculated with different polymers. A 10 m^3/h capacity rig (4" pipe size) equipped with a 5" dynamic mixer (3.8" impellers) was used for in-line flocculation. To model the pipeline shearing, a large Couette device (bob diameter 11.255″ and cup inner diameter 12.368″), designed to satisfy the narrow gap assumption in rheometry while maintaining a wide gap to minimize floc disturbance, was used. Shear rates ranging from 8 to 63 s^{-1} were applied to predict the conditions experienced in fully sheared pipelines of commercial scale (24″ and 30″ diameter with flow rates of 662 and 2648 m^3/h). Each shear rate was applied for residence times corresponding to pipeline transport distances between 100 m to 10 km. Dewatering and yield characteristics of the samples were measured prior to and after the shearing by capillary suction time (CST), permeability index (PI), peak yield stress and 7-day water release tests to quantify the effects of shearing.

In general, it was found that the shearing increased the long-term water release of the samples while slightly negatively impacting the short-term water release and yield characteristics. The CST of the samples increased with shearing while their PI and yield stress decreased. However, the change in the yield stress was significant compared to the modest changes in the CST and PI values, which are indicators for short term water release. In contrast, the 7-day water release values of the sheared samples were higher than those of the non-sheared samples.

INTRODUCTION

Background

One of the most promising techniques developed to date for remediation of Mature Fine Tailings (MFT) is the flocculation of solid particles using a polymer flocculant (Wang et al. (2014). The polymer causes aggregation of colloidal particles within the MFT into flocs of different sizes and strength. Due to higher density, flocs settle in the suspensions over time, leading to separation of solids and water in tailings (Salam et al., 2016).

MFT Flocs formed by this process are generally sensitive to shear. If deformed under shear, flocculated MFT can lose its dewatering and settling capability, leading to an overall reduction in the performance of the treatment process. Therefore, the success of the flocculation process not only depends on the quality of mixing between polymer and MFT, but also on the transport conditions used to carry the flocculated MFT to disposal. In most cases, flocculated MFT is transported by a pipeline at laminar flow conditions to prevent any floc disturbance.

In a typical pipeline, flocculated MFT samples create a low viscosity layer at the wall (lubricated layer) that undergoes the majority of shear. At the same time, a core is formed at the center of the pipe where shear stress is lower than the material's yield stress (non-sheared core). This core is often transported with minimal disturbance due to the protection provided by the lubricated layers at the wall. Therefore, the flow regimes in pipeline transport of flocculated MFT can be divided into several broad categories based on the presence of lubrication (or lack thereof) and the symmetry of the material in the pipe, in particular referring to the top-to-bottom variations caused by the effects of gravity.

Given the shear sensitivity of the flocs and the ability to release water in a given geometry, proper design of a flocculated MFT transport system requires knowledge of the flow regimes, critical shearing conditions at which floc disturbance occurs, and the pipeline pressure drop. Laboratory-scale pipeline experiments can be performed to acquire such data and to develop correlations and models to predict flow regimes and the associated pipeline pressure drops. However, the relationships developed based on laboratory-scale data should be validated at larger field scales before they are used for design purposes. Clearly, acquiring such information requires a comprehensive study of pipeline transport of flocculated MFT at different scales and flow conditions which can be complex and challenging.

In this study, a more empirical approach is used to understand the effects of shearing on dewatering characteristics of the flocculated samples. This involved testing of flocculated MFT in a large Couette device designed to model shear conditions experienced in a fully-sheared pipeline at laminar flow conditions.

At fully sheared state, the lubricated layer and the non-sheared core are disrupted and the material is under shear everywhere across the pipe. This corresponds to the most intensive shearing condition that can exist in a given pipeline. Assuming laminar flow of Newtonian fluid, the pipe shear rates at fully sheared conditions were calculated and used to conduct experiments in the Couette device. Therefore, the experiments in this study mimicked the most intensive shearing conditions experienced in a field-scale pipeline.

EXPERIMENTAL PROCEDURE

Materials

Raw MFT (~30 wt% solids and MBI of ~7.3-7.6 meq/100 g solids) were procured from Shell's Albian Sands tailings storage facilities. The flocculated MFT samples were produced by mixing the raw Shell MFT with any of the following three flocculants: A (a partially hydrolyzed polyacrylamide), B (a polyethylene oxide) and C (a Ca-polyacrylamide) using a 10 m^3/h capacity (4" pipe size) mixing rig equipped with a inline dynamic mixer (5" diameter with 3.8" impellers). A range of mixing conditions was used to produce flocculated materials with different initial dewatering and yield characteristics.

Apparatus

The samples produced from the inline flocculation rig were sheared at different conditions in a large Couette apparatus (Figure 1), built to satisfy the narrow-gap assumption in rheometry to ensure uniform shear rate distribution across the gap. The bob and cup were baffled to prevent wall slip. With no baffles, due to the high apparent viscosity of the materials being tested and formation of depleted layers, a slip layer would form around the rotating bob resulting in the application of shear forces in a small layer without the bulk of fluid being sheared completely (Bennington et al., 1990).

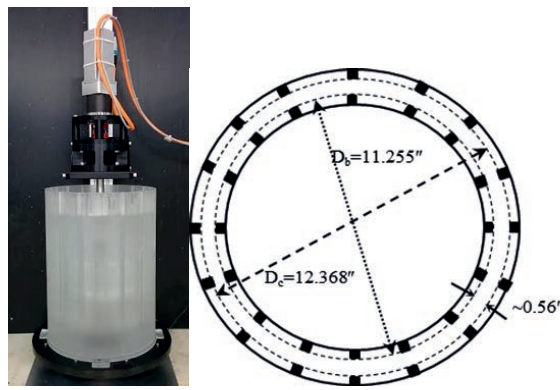

Figure 1. (Left) The Couette geometry used in this study (Right) Top view of the Couette geometry

The diameter of the Bob was 11.255″ (including baffles), the inner diameter of the cup was 12.368″ (including baffles), and the height of the Bob was 18.527″. The gap in the Couette apparatus, defined as the distance between the bob and cup baffles, was ~0.56″, large enough to accommodate the flocs while still satisfying the narrow gap assumptions used in rheometry (Barnes and Walters, 1989). In this geometry, the shear rate was calculated as:

$$\dot{\gamma} = \frac{N_B \times \overline{R}}{R_o - R_i} \tag{1}$$

$$\overline{R} = \frac{R_o + R_i}{2} \tag{2}$$

where N_B is the bob rotational speed in *rad/s*, R_o and R_i are the cup and the bob inner and outer radii including baffles. The flocculated MFT samples were sheared at pipeline conditions modeled by the shear rate, i.e., the bob rotational speed.

Procedure

Yield stress, CST, 7-day water release, and permeability index (PI) of the flocculated samples were measured prior to testing in the Couette. At fully sheared conditions and laminar flow, the shear rate in a pipe was estimated as *8U/D*, where *U* and *D* are the flow velocity and pipe internal diameter respectively. In the Couette, the flocculated MFT samples were sheared at rates corresponding to either 24″ or 30″ field-scale pipes. At two modelled flow rates of 662 m^3/hr and 2648 m^3/hr and pipe sizes of 24″ or 30″, four different nominal shear rates were calculated as 8U/D= ~8, ~16, ~32 and ~63 s^{-1}. Each of these shear rates was applied in the Couette and the variation of torque with time was recorded. The accuracy of the torque measurement was ~0.2% of the maximum torque applied.

Samples were collected for CST measurements at intervals equivalent to residence times corresponding to 100, 500, and 1000 m transport distances. At the end of the experiment, samples were also collected for the measurement of yield stress, PI, and CST to compare with those measured for the non-sheared samples. Generally, similar trends were observed in the change of dewatering and yield characteristics of the samples produced at different mixing conditions. This manuscript, however, reports the results from the well flocculated MFT samples only.

In order to understand the water release characteristics of the samples after prolonged shearing, additional experiments were conducted at the highest shear rate anticipated in the field-scale pipes at fully sheared laminar conditions (~63 s^{-1}) and residence times corresponding to long transport distances of 5 and 10 km. For these experiments, yield stress, CST, PI and 7-day water release of the samples were also measured prior and after shearing in the Couette.

RESULTS AND DISCUSSION

Variation of dewatering with shear

Generally, CST was found to increase with shear rate and duration. Figure 2 shows the variation of CST with shearing time at different shear rates for typical MFT samples flocculated with polymer A.. A higher CST value indicates poorer immediate dewaterability of a sample. At higher shear rates, the CST appeared to increase more significantly with time. At the highest shear rate and longest shearing time, the CST was found to increase between ~150% to ~200%. Generally, similar trends were observed for MFT samples flocculated with polymers B and C.

The post-sheared CST values, however, were within acceptable range for tailings treatment despite their increase with shearing. This implies that pipeline transportation of well-flocculated MFT samples will not affect the immediate dewaterability of the samples significantly. It should be noted that such variations in the CST values were measured at extreme shearing conditions, i.e. where the lubricated layer and the non-sheared core of the pipe are disrupted completely. In actual pipeline flow, the shearing of the flocculated MFT is expected to be less intense due to the existence of the lubricated layers at the wall, resulting in preserving the dewaterability of the tailings to some extent.

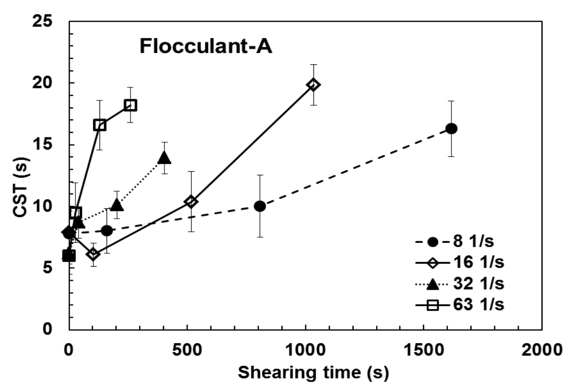

Figure 2. Variation of CST with time during shearing at different shear rates and residence times corresponding to 1 km transport for MFT samples flocculated with polymer-A. The error bars represent the standard deviation based on 5 different measurements.

Figure 3 shows the variation of permeability index (PI) of the MFT samples flocculated with polymers A and B at different shear rates. From this figure it is clear that the PI of the samples did not change significantly as a result of shearing which is consistent with the data presented in Figure 2. PI data for MFT flocculated with polymer C is not available.

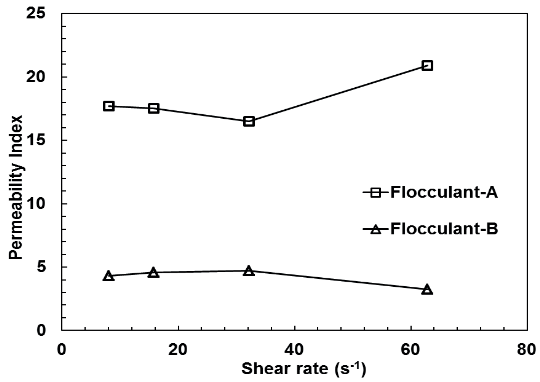

Figure 3. Variation of permeability index with shear rate for MFT samples flocculated with polymers A and B

Effects of prolonged shearing on dewatering

At long transport distances under intense shearing conditions the changes of the CST values of the samples were relatively moderate. Figure 4 shows the variation of CST of the flocculated samples after intensive shearing at $8U/D$=63 s^{-1} for long durations corresponding to 1, 5, and 10 km pipeline transport distances.. It is evident that the CST of the samples decreased only slightly. Similar behaviour was observed for the PI of the samples (data not shown here).

In addition to CST and PI measurements, samples were collected in graduated cylinders before and after shearing in the Couette to monitor their dewatering for 7 days (data shown in Figure 5). It is evident that shearing of flocculated MFT did not affect their long term dewatering. In fact, the dewatering of all the samples enhanced without exception as a result of shearing in the Couette.

Effects of prolonged shear on yield stress

The yield stress of the flocculated MFT is very shear sensitive. Figure 6 shows the change of yield stress of the MFT samples flocculated with different polymers after shearing at the highest rate (63 s^{-1}) for residence times corresponding to 1, 5, and 10 km modelled transport distances. In contrast to the dewatering characteristics, the yield stress of the samples was found to decrease significantly with shearing. This observation was consistent at all shearing conditions, even the mildest investigated in this study. However, the change of yield stress during actual pipeline transport can be significantly less than those measured in this study.

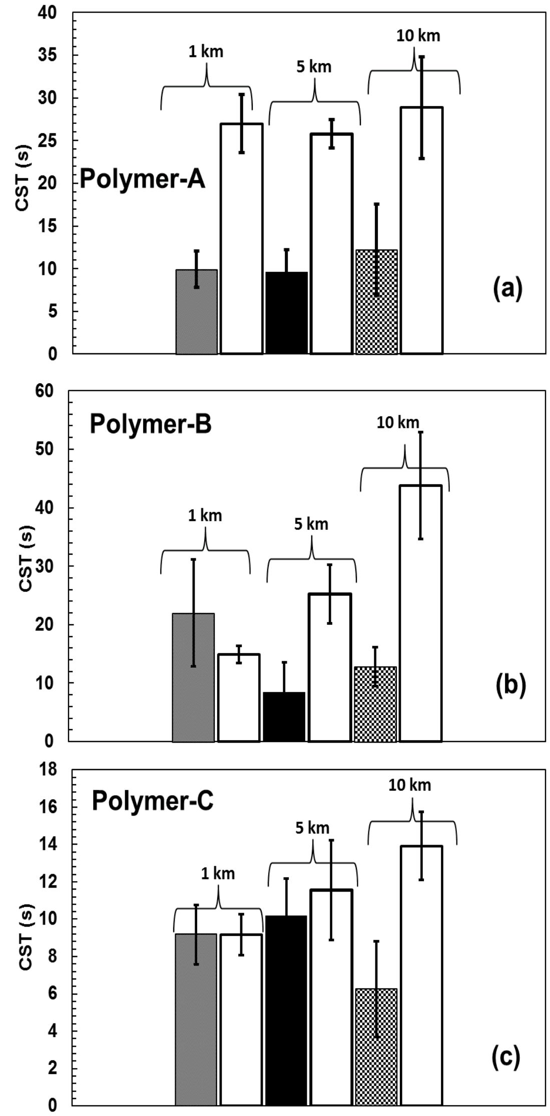

Figure 4. Effect of shearing at 63 s^{-1} for residence times corresponding to transport distances of 1, 5, and 10 km on CST of MFT samples flocculated with a) polymer-A, b) polymer-B, and c) polymer-C. The solid and white open bars indicate the CST of the non-sheared and sheared samples respectively.

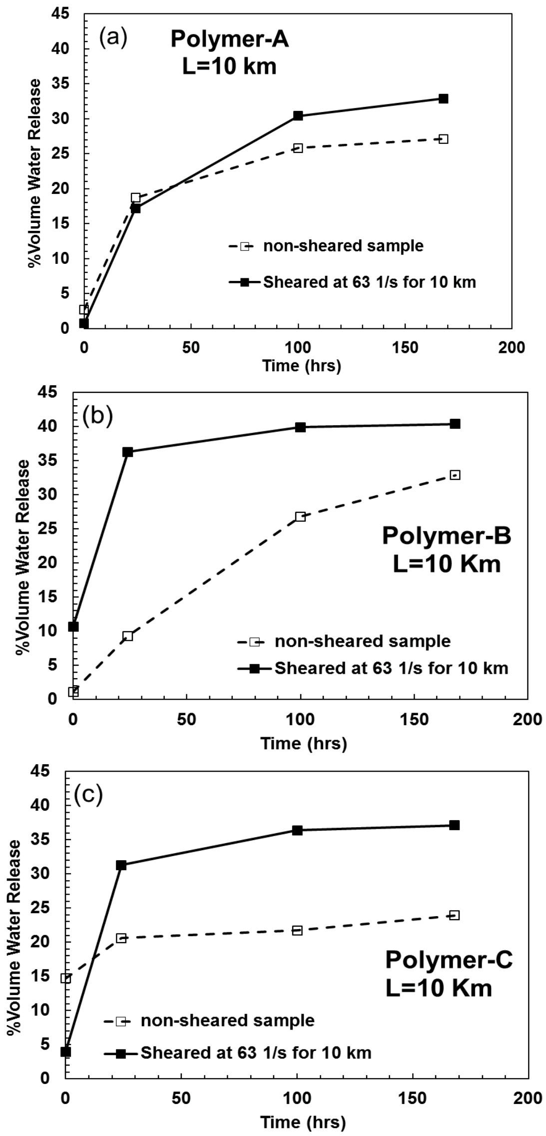

Figure 5. Effect of shearing at 63 s^{-1} for a residence time corresponding to transport distance of 10 km on 7-day water release of MFT samples flocculated with a) polymer-A, b) polymer-B, and c) polymer-C.

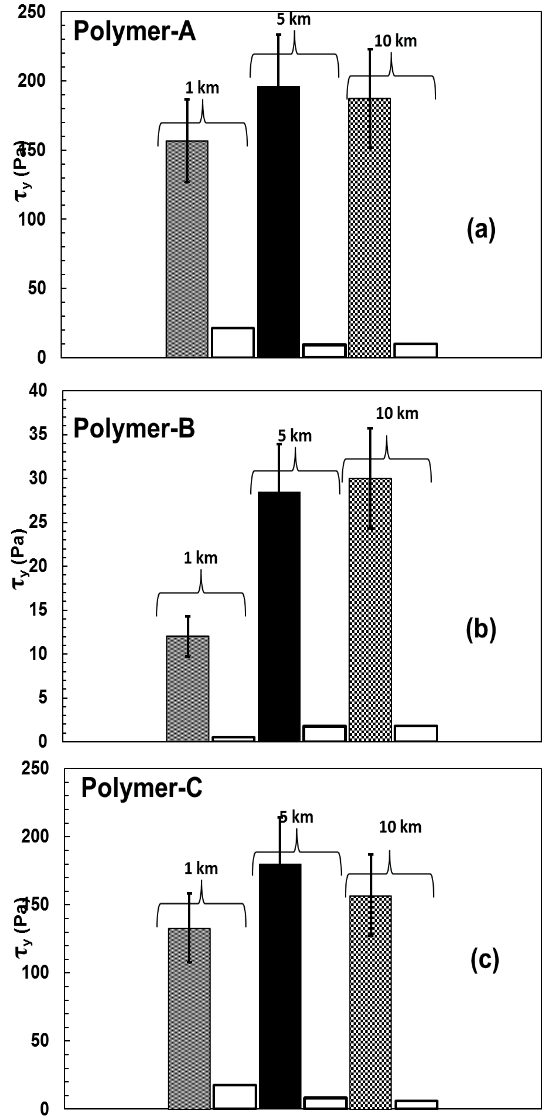

Figure 6. Effect of shearing at 63 s^{-1} for residence times corresponding to transport distances of 1, 5, and 10 km on yield stress of MFT samples flocculated with a) polymer-A, b) polymer-B, and c) polymer-C. The solid and white bars indicate the yield stress of the non-sheared and sheared samples respectively. The solid and white bars indicate the yield stress of the non-sheared and sheared samples respectively.

CONCLUSIONS

This study illustrates that pipeline shearing has only a slightly negative impact on the short-term dewatering of flocculated MFT, whereas the long-term dewatering actually increases. However, the yield stress of the MFT decreases significantly from the shearing. Therefore, based on these findings, it can be predicted within the boundaries of this model study that pipeline transportation produces a slightly less dewatered deposit with significantly reduced strength immediately following deposition, which then releases more water volume over time compared to non-pipeline sheared flocculated MFT.

REFERENCES

Barnes, H.A., Hutton, J.F., Walters, K. 1989. An Introduction to Rheology. Elsevier, Amsterdam.

Bennington, C.P.J., Kerekes, R.J., Grace, J.R. 1990. The yield stress of fibre suspensions. Canadian Journal of Chemical Engineering 68 (10), 748–757.

Salam, A.M., Ormeci, B., Simms, P.H. 2016. Determination of the optimum polymer dose for dewatering of oil sands tailings using UV–vis spectrophotometry. Journal of Petroleum Science and Engineering 147: 68-76.

Wang, C., Harbottle, D., Liu, Q., Xu, Z. 2014. Current state of fine mineral tailings treatment: A critical review on theory and practice. Minerals Engineering 58, 113-131.

MRM ETF NORTH POOL DEPOSIT PERFORMANCE

Monica Ansah-Sam and Karsten Rudolf
Shell Canada Ltd, Calgary, Canada

ABSTRACT

Co-deposition of thickened tailings (TT), coarse sand tailings, and the processed tailings from solvent recovery (TSRU tailings) was used to develop a fines enriched sand and sandy fines deposit within the External Tailings Facility (ETF) at Shell Canada's Muskeg River Mine (MRM). The deposit, designated as the North Pool Deposit (NPD) was separated in 2002 from the main pond of the ETF by a splitter dyke that created isolated disposal areas for TT and TSRU tailings. The splitter dyke was overtopped in 2005 and co-deposition of its constituent streams produced a mixed deposit. The co-deposition strategy has produced a deposit with enhanced fines capture while developing strengths that will support future capping or reclamation activities. This paper briefly summarizes the history of the NPD and describes the overall performance of the resulting deposit. Additionally, this paper includes discussions on the additional work being performed to support closure planning. This includes deposit strength, trafficability assessments and preliminary consolidation modelling.

INTRODUCTION

Since the start of operations in 2003, Shell Canada (Shell) has conducted annual tailings investigations to monitor the volume and material properties of fluid tailings in the MRM ETF and also to assess the geotechnical stability of the beaches (Esposito et al, 2012). The NPD is a deposit located within the ETF. The NPD was produced from the co-deposition of several tailings streams as a result of Shell's bitumen production process. This type of deposition strategy is not common in the oil sands industry. Shell has therefore put a significant effort into investigating and characterizing the NPD. Characterization of tailings deposits is a critical tool to support reclamation and closure design. The annual tailings investigations provided Shell with an understanding of the historic behavior and current conditions as well as the ability to predict the long-term behaviour of the deposit. This paper presents a summary of the characterization of the NPD and the geotechnical performance of the deposit up to 2015.

Background

The Muskeg River Mine is located about 70 km north of Fort McMurray, Alberta. Shell is the operator and majority shareholder of the Athabasca Oil Sands Project (AOSP); a joint venture between Shell Canada Limited (60%), Chevron Canada Limited (20%), and Marathon Oil Canada Corporation (20%). The AOSP consists of Shell's mining and extraction operations located north of Fort McMurray, the Scotford Upgrader, and the Quest Carbon Capture and Storage project that are both located north of Edmonton.

Mining operations include truck and shovel mining of bituminous oil sand and non-bituminous materials, typically referred to as mine waste (located above or interbedded within the oil sand deposit). Mine waste is removed and used to build dykes (when material specifications are met) and the remainder is placed in either external or in-pit mine waste dumps. The mined oil sand is transported to crushers where it is prepared for extraction.

The oil sand ore is mixed with warm water that is pH adjusted using an alkali salt (caustic) to separate the bitumen from the sand, silt, clay, and water. The mixture is then transported through a conditioning slurry line to primary separation cells (PSC). The bituminous froth from the PSC is further clarified in the high temperature and/or low temperature froth treatment (HTFT/LTFT) units. The final step in the extraction process is to recover the solvent from the froth in the tailings solvent recovery unit and the resultant bitumen is then transported via pipeline to the Scotford Upgrader and converted into synthetic crude oil.

Tailings are materials that remain after bitumen is extracted from the oil sands. As a result of primary extraction, whole tailings (WT) comprised of sand, silt, clay, water, and residual bitumen are produced. TSRU tailings comprised of sand, silt, clay, water and residual hydrocarbons (including asphaltenes) are produced as a result of froth treatment.

A portion of the WT stream is sent to hydro-cyclones where the underflow creates a tailings stream that has less water and fines than WT, referred to as coarse sand tailings (CST). The overflow is a high fines stream that is sent to the thickeners where it is flocculated to create a TT product and a warm water stream (overflow) that is returned to the plant. Tailings are transported hydraulically to tailings containment facilities within the mine.

Traditional deposition of tailings materials via slurry pipeline results in beaches within the tailings facilities. Larger and heavier materials drop out of the slurry creating a deposit with a lower proportion of fines (mineral solids less than 44 μm) compared to what was in the slurry. Some of the finer materials, with a lower sand-to-fines ratio (SFR), and the majority of the water flow along the beaches and into the pond. Over time, the fines settle in the pond creating fluid fine tailings (FFT) and a layer of water (clear water zone or CWZ). The CWZ is required for plant operation and is recycled back to the plant.

The ETF has CST slurry lines distributed around the facility that are used for construction of dykes and for development of conventional beaches. Thickened tailings and TSRU slurry lines are located on the northeast and eastern corner of the ETF. The pumping systems located on the north side of the ETF supply water to the recycle water pond and manage fluid containment.

The tailings slurries composing the deposit are of varying initial solids contents (includes bitumen). TSRU tailings are the lowest, with an average solids content of 22±2%. TT is slightly higher with a solids content of 24±5% and CST/WT sand is the highest of the three streams, with a solids content of 53±2%.

History

The deposit, designated as NPD, was separated from the main pond of the ETF in 2002 by the cross dyke, creating an isolated disposal area for TT and TSRU tailings (see Figure 1).

The intermediate dyke was overtopped in 2005 and co-deposition of its constituent streams produced a mixed deposit. Shortly after, the cross dyke was also overtopped (see Figure 2).

Infilling of the ETF with CST, TT, and TRSU are still ongoing within the facility (see Figure 3). WT are only deposited at times when there are plant upsets and/or pipeline maintenance is required. Depositional strategies are currently focused on optimization of tailings storage as the NPD is approaching its ultimate design elevation. The NPD which is approximately 50 m thick will eventually be capped and designed as part of the ETF landform for final closure.

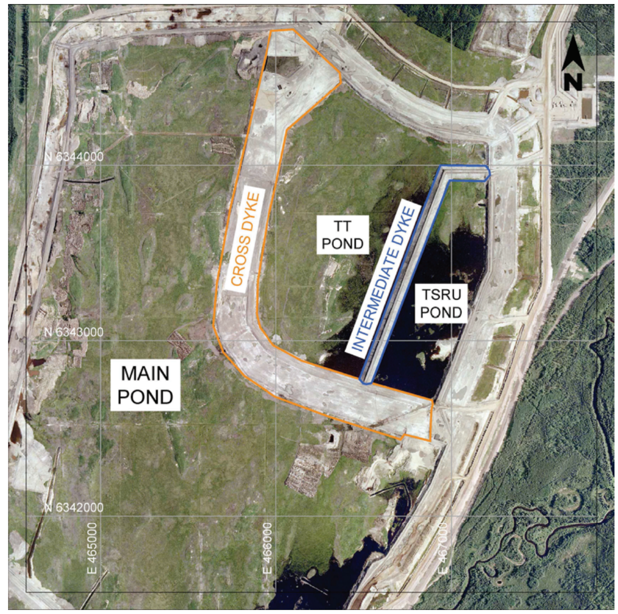

Figure 1. North Pool Deposit Area in 2002 – Initial Deposition

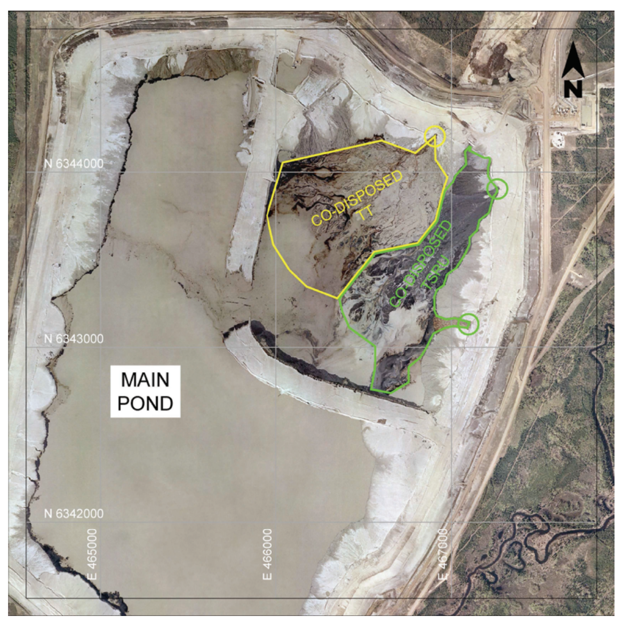

Figure 2. North Pool Deposit in 2005 – Dyke Overtopping

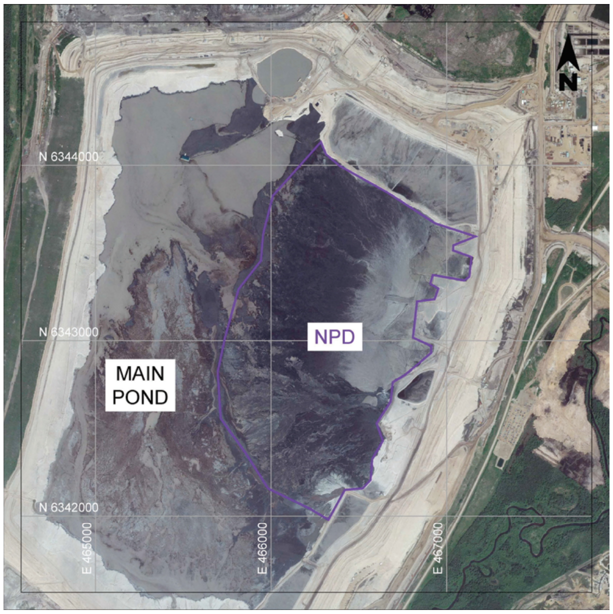

Figure 3. North Pool Deposit in 2016 – Current Deposit

CHARACTERIZATION

Characterization of tailings deposits serves two primary objectives; prediction and monitoring of geotechnical behaviour, and quantification of volumes and masses required for planning and reporting. Understanding the geotechnical properties of tailings deposits is an important component of the safe management of the facility. The oil sand industry, including Shell, incorporates cell construction, contained beaching and 'naturally' deposited tailings beaches in dyke designs. For operational reasons, Shell may occasionally require the deployment of equipment and infrastructure onto the tailings beaches. The strength and stability of the deposits is therefore an important component of tailings operations, reclamation and closure.

Ultimate closure and reclamation of tailings facilities considers stability and long-term consolidation behaviour of the final landform. Geotechnical strength, consolidation behaviour, geochemical properties, and many other factors will impact the final landform design. It is therefore important that the level of detail of the characterization of the individual deposits is appropriate for the closure design intent.

Cone Penetration Tests (CPTs) are performed during the annual tailings investigations to determine the stratigraphy and strength of the deposit. Samples are also collected during the investigations that are subjected to laboratory testing to determine solids/water/bitumen contents, particle size distribution, Atterberg limits, and Methylene Blue Index properties. In addition to the testing already outlined above, large strain consolidation, direct shear, and triaxial testing can also be performed. The results of these field tests are critical to confirm pilot or laboratory scale testing, and determine the sensitivity to scale, depositional environment, and geometry of the actual deposit. This testing can also support planning of similar deposits in future in pit facilities.

Regulatory reporting requires annual quantitative estimates of the volume and mass of solids in the deposits. These quantitative estimates also support mine planning in the development and calibration of planning models. To increase accuracy, current quantitative estimates are produced using "block modeling estimation" in a similar methodology that is traditionally used in resource estimation. This methodology incorporates the spatial variability of the data and allows for de-clustering of the data. De-clustering of the data is important in a tailings context as many investigations are designed to target specific zones of interest; and therefore any straight average of that data will be preferentially weighted to the characteristics of those zones of interest. The block models are used to describe compositional properties including bitumen content, solids content, water content, and fines content. The deposits are sampled and these characteristics are determined through laboratory testing; the results become inputs into the 3-D block model and an inverse distance weighted estimation algorithm is performed to estimate the properties of each individual "block" in the model. The model is then able to calculate the mass of solids, mass of fines, or any other secondary property of the block and provide summaries for desired zones in the model. Quantitative estimates for a variety of purposes are then easily produced as a model output. In addition, the visual outputs of the model can be assessed to better understand the spatial variability of individual properties.

General Composition

A convenient way to summarize the composition of a tailings deposit in a visual form is through the use of a ternary diagram (COSIA, 2012).

Figure 4 presents the ternary diagram of BAW NPD laboratory data obtained which indicates that the deposit is closer to the classification of fines enriched sand and sandy fines deposit. The deposit is composed mainly of sandy fines with some transition tailings.

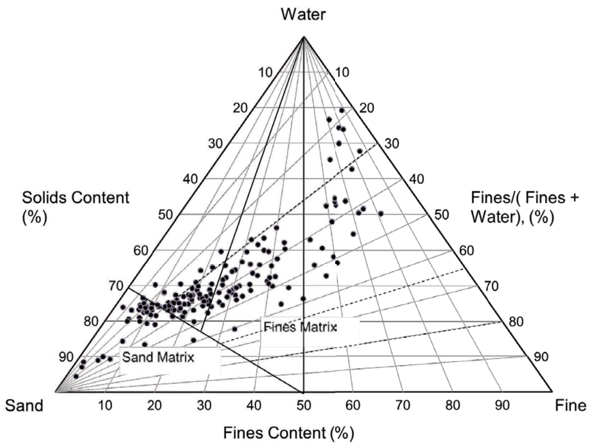

Figure 4. NPD Composition Ternary Diagram

Through the evaluation of laboratory, CPT, and hard bottom measurements conducted using the 'CT09' tool; the lateral and vertical extents of the NPD are identified on an annual basis and these extents are modelled as 3-D surface definitions. As described previously, the laboratory data is reviewed and used to populate the 3-D block model of the deposit within its defined extents. The model is then used to output overall averages for properties relevant to performance tracking. These average properties are presented in Table 1. The model is also used to estimate the total mass of solids contained within the deposit, and the incremental solids deposited between annual surveys. These annual values can then be compared with estimated slurry solids to determine capture rates, and used as a component of the site wide solids balance to validate the modelling.

Table 1. NPD Average Properties

Average Solids Content	71.1%
*Clay-Size Fraction (<2 μm)**	4.5%
*Fines Fraction (<44 μm)**	28.3%
Average Bitumen Content	3.6%
Average Water Content	25.3%
Average Dry Density (kg/m³)	1,341
Average SFR	2.5

*based on laser diffraction
*Includes BBW and BAW deposits

Variability and Areas of Interest

Beyond its ability to produce effective quantitative estimates, the block models can also be used as a tool to investigate the variability that exists within a deposit. The models easily allow for the integration of any variable that can be resolved as a surface definition. Additionally, the models can generate surface definitions to isolate zones based on input parameters; for example, the models can assess the fines content of a tailings material with a specific solids content range. In the case of the NPD, the block model also includes variables such as depositional period and beach length.

Age Dependant Variability

A useful tool in understanding the long-term behaviour of a deposit is the tracking of the material that was deposited over distinct periods of the deposit's life. The block modelling provides an advantage over simple comparison of year-on-year sampling by effectively combining multiple locations and averaging them. This accounts for clustering of the data. It can also help account for more complex deposit geometries; as long as the interval between surveys are appropriately selected to reflect the deposit growth and the estimation parameters are carefully selected to reflect the actual variability in the deposit.

Once the regions for each depositional period are defined and the average properties of the regions are determined, they can then be assessed in the context of age, historic loading, and the phreatic surface to better understand the deposit. Table 2 presents the characterization of the NPD in 2015, highlighting the distinct characteristics of each zone defined by a specific depositional period. The semi-solid, defined here as transition zone (TZ) material, that exists in the Beach-Below-Water (BBW) area of the NPD (see Figure 5) is not included in the averages presented in Table 2. This material could have been re-mobilized during deposition and therefore is challenging to associate to any specific depositional period. Zones in which sub-aqueous failures, mixing, and capture of weaker materials are expected can be tracked or monitored to ensure that these effects do not distort averages specifically produced to track behaviour over time. The densification of the material deposited early in the history of the NPD, compared to the 'fresher' material (less than a year) is apparent in these values. Assessing this trend appropriately, and comparing these values year-on-year for the same depositional periods can also help develop an overall understanding of the behaviour of the deposit.

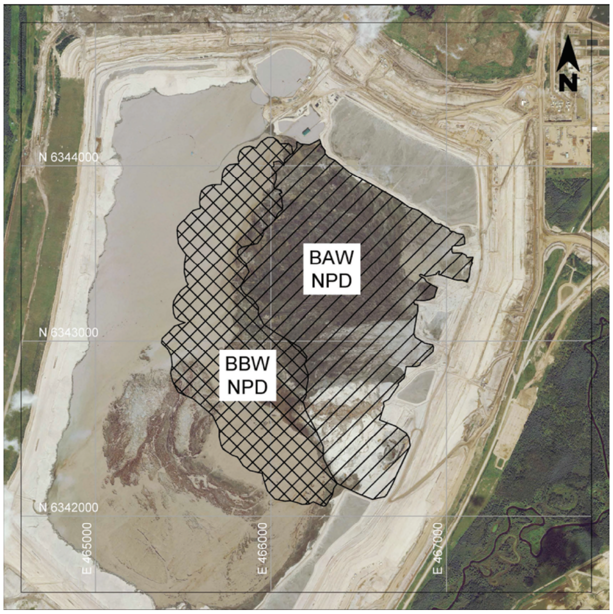

Figure 5. Extent of NPD used in the evaluation

Table 2. Tailings Properties vs. Depositional Period

Depositional Period	Pre - June 2010	June 2010 - June 2013	June 2013 - June 2014	June 2014 - June 2015
Average Solids Content	73.2%	69.3%	68.0%	67.7%
*Clay-Size Fraction (<2 μm)**	3.5%	5.65%	5.91%	5.54%
*Fines Fraction (<44 μm)**	23.6%	33.6%	35.1%	32.3%
Average Bitumen Content	3.3%	4.0%	4.4%	4.4%
Average Water Content	23.5%	26.6%	27.6%	27.9%
Average Dry Density (kg/m³)	1406	1291	1257	1247
Average SFR	3.2	2.0	1.8	2.1

**Based on laser diffraction*

Beach Length Variability

It is well understood that beach length has an impact on the characteristics of a deposit, with coarse particles settling closer to the discharge and finer particles settling further down the beach. This can lead to a deposit developing with distinct properties as a function of beach length. To appropriately design around this variability with beach length, it is important to be able to understand what natural variability exists in the deposit, zonate it appropriately for the specific requirements of the design, and then characterize each zone to determine appropriate values to feed into the design. To characterize the deposit, the block model can be used to create sections displaying the desired properties and their variability in 2-D along the section. Sections showing the variability in both solids content and fines content moving down the beach are included in Figure 6. The fines content is shown to increases with distance from the deposition point. This section can then be used to define reasonable distances for zonation and characterization to supplement future deposit design and/or closure design. In the specific example of the NPD it can also be seen that there exists a high fines zone behind the splitter dyke separating the pond from the treated tailings deposit. Using the block model, distinct zones, like this high fines zone, can be identified, isolated, and independently assessed to determine their impact on any future design. Table 3 provides example NPD properties as a function of beach length.

Table 3. Tailings Properties vs. Beach Length

Nominal Beach Length	0 m - 250 m	250 m - 500 m	500 m - 1000 m
Average Solids Content	73.8%	72.3%	68.5%
*Clay-Size Fraction (<2 μm)**	2.5%	3.2%	4.6%
*Fines Fraction (<44 μm)**	19.0%	23.4%	30.6%
Average Bitumen Content	3.1%	3.6%	4.7%
Average Water Content	23.2%	24.2%	26.9%
Average Dry Density (kg/m³)	1421	1379	1276
Average SFR	4.3	3.3	2.3

*Based on laser diffraction

The NPD is contained by the ETF dykes on the north and buttressed by the FFT pond on the western portion of the deposit. The NPD was produced through sub-aerial and sub-aqueous tailings deposition. These two depositional environments can produce characteristically different deposits. Assessment of the impact of sub-aqueous or sub aerial deposition is usually done by a classification of the deposit as beach-above-water (BAW) or beach-below-water (BBW). This involves a thorough review of beach and pond development, identifying the pond edge throughout the history of the deposit. The contents downstream of the pond edge are then classified as BBW and upstream of this edge as BAW. An alternative classification was used to determine this boundary for the NPD. Some treated tailings materials (TT and TSRU tailings) were identified based on CPT results and sampling. These treated tailings exhibit some fluid properties and so the extent of these materials needed to be established for performance tracking/monitoring. Data obtained from the BBW slope of the NPD was assessed and used to construct a boundary surface for this zone. This zonation was necessary because the semi-solid nature of this zone required it to be estimated as a separate domain from the rest of the deposit. The benefit of this approach is that the BBW material can be assessed, independent of the rest of the deposit, to support future design.

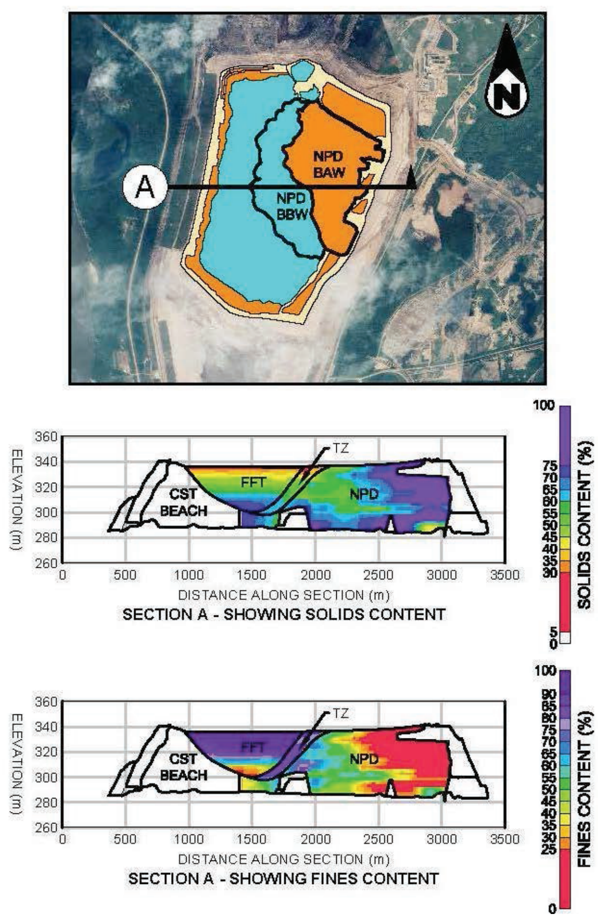

Figure 6. Solids Content and Fines Content Sections

Strength

The NPD is characterized in terms of strength primarily through the evaluation of CPT testing and laboratory testing. The NPD is a heterogeneous deposit, containing intermediate to high fines zones as well as sandy zones. In sandy zones a drained friction angle (φ') is calculated from the CPT, while in the areas with more fines, undrained shear strength (s_u) is a more appropriate parameter. Reconciling this heterogeneity requires careful assessment and is approached on a case-by-case basis in combination with engineering judgment. One useful tool used to support interpretation of the strength in such a heterogeneous deposit is a strength distribution plot. This presents a clearer picture of the variation in strength and informs parameter selection and design of sensitivity analyses. Figures 7 and 8 show the strength distribution observed for the NPD BAW and BBW (based on a vertical division at the current pond edge). These plots allow for parameters to be selected for stability analyses of the ETF for landform design and closure.

Future work to build on this assessment may include specific distribution plots of design critical areas, and the inclusion of friction angle within the distribution to better understand the distribution of sandier zones.

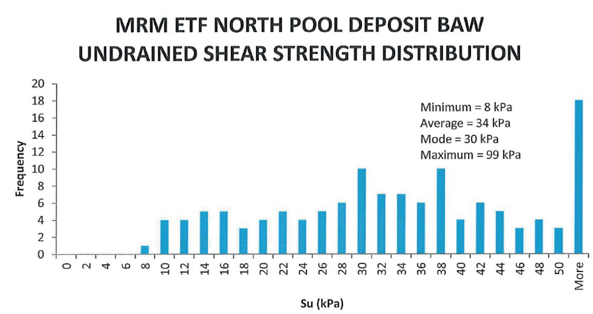

Figure 7. BAW Undrained Shear Strength Distribution

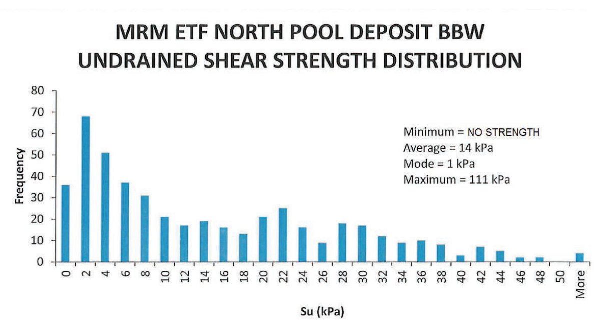

Figure 8. BBW Undrained Shear Strength Distribution

Strength Development

To further understand the development of strength in the deposit over time, a straightforward approach of comparing CPTs along a set section that has been investigated annually was used. The results are assessed annually and zones of strength gain are outlined. These strength gains are quantified and used to support projections of long-term strength. Figure 9 shows an example of annual strength gain in a specific CPT location over several years.

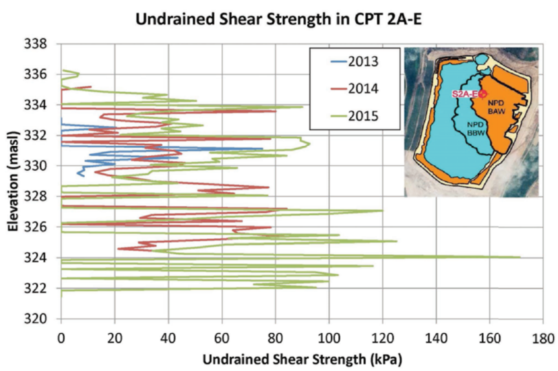

Figure 9. Historic Strength Gain at CPT S2A-E

As demonstrated in Figure 9, a general trend towards increased strength can be observed from 2013 to 2015. However, the variability in the strength profile in certain zones within the NPD requires careful interpretation.

Preliminary Consolidation Modelling

Consolidation is an important component for tailings planning since it impacts predictions of total tailings deposition growth and the resultant tailings containment required. At Shell, tailings planning does account for consolidation of FFT and sandy deposits (CST and WT). If the deposit consolidation is expected to occur quickly (within 1-2 years) then the deposit density is adjusted to reflect an average condition of the deposit. For high fines deposits and beaches, consolidation is not used in the operational time frame to ensure conservative estimates for overall tailings containment. A critical component of the successful design of closure landscapes and the long-term behaviour of the closure landscapes will be the expected consolidation behaviour of the underlying tailings deposits. Surface water management design can be undermined if differential settlement produces local depressions that can begin to impound water, which can impact stability, reclamation design, and many other aspects of the overall closure design. To support the consolidation analysis that will be done as a component of the closure design, preliminary assessments were conducted using the data collected through the annual tailings investigations. The strategy for the NPD is to develop a high level consolidation model for the deposit and validate it with historic data.

Initial compressibility and permeability curves were developed through a back-analysis of the current deposit conditions using first principles, similar to the approach described by Masala et al. (2014). This methodology integrated pore pressure dissipation tests performed during the CPT investigations and the average void ratio with depth (determined through sampling and lab testing). These were used to produce a 1-D consolidation model of the NPD to predict settlement during the initial years of operation. This model was then validated using two independent methods: monitoring of a distinct layer and comparison of actual performance throughout the development of the deposit with the predictions of the 1-D consolidation model. The first method involved tracking the elevations of discrete layers over time. Points at similar depths were tracked in the 1-D analysis and a comparison was used to validate the model. This was possible due to the fact that the NPD is heterogeneous and independent layers can be identified and recorded year-on-year. The model was additionally validated by a second method, in which the development of the deposit was modeled using the estimated compressibility and permeability curves. The predicted solids content and pore pressures in the model were then compared to the values measured in the most recent investigation.

For the detailed design of an entire deposit, a zoned approach that groups areas of similar consolidation characteristics should be considered. Zones can be determined based on the landform design and the final deposit characterization allowing a detailed consolidation map to be developed. Initial stages of this approach have been carried out to produce the zonation map shown in Figure 10. This zonation was developed based on several factors. Zone 1 was isolated due to the fact that this area was mechanically compacted during cell construction. Zone 5 was isolated because the area was developed primarily from TT deposition. Zone 6 is currently used to store atmospheric fines drying tailings and will require special consideration during closure. Zones 2 through 4 were then divided based on assessments of the solids contents in each zone. Each zone can then be modelled with a similar approach to the preliminary 1-D model and a set of maps can be developed to understand the expected settlement and consolidation and project critical stages.

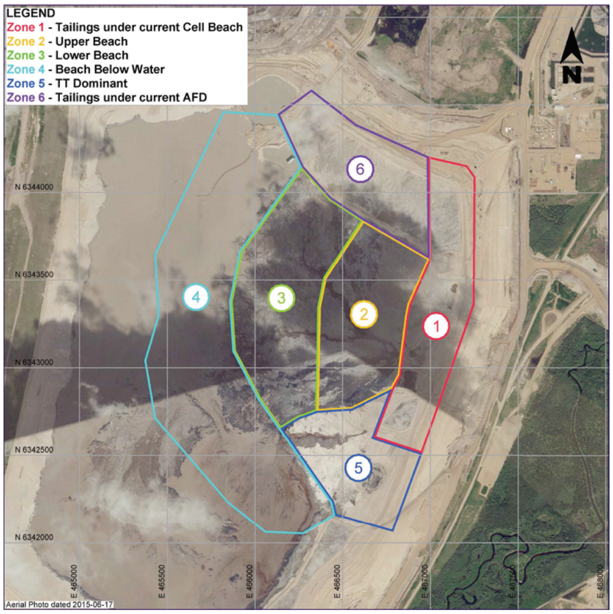

Figure 10. Proposed Zonation Map for NPD

Consolidation modelling is typically used as a guide and not expected to be exact. The main intent is to estimate settlement as much as possible to ensure that the overall material balance and closure design accounts for these areas of expected settlement as much as practicable.

The preliminary results of Shell's 1-D consolidation model indicate that majority of primary consolidation of the NPD will occur within ten years. This can be used as guidance in planning; however, as more detailed assessment progresses with the zonated approach described above, the detail required for closure planning will be developed. This is consistent with Esposito et al (2012) which estimated placement of final reclamation cover between 5 to 8 years.

Current assessment of the individual zones indicate Zones 1, 2, 5 and 6 are generally sandy and may not experience significant long term consolidation (some consolidation is still expected in high fines layers within the deposit). Consolidation in Zone 3 is expected to continue. Zone 4 however, will require further monitoring and additional characterization after infilling of the ETF pond is completed.

Trafficability Assessments

Trafficability of soils, in its definition, is the capacity of soils to support or permit the passage of vehicles. In mining and tailings operations, trafficability refers to the capacity of a deposit to support equipment, structures (tailings pipelines), and other soils (e.g., deposit capping with reclamation material). Generally, trafficability is a function of the bearing capacity and solids content of a given deposit. During mine operations, trafficability assessments are conducted to support construction activities requiring the deployment of assets onto tailings deposits, such as the extension of tailings pipelines. These assessments can sometimes be undertaken without having current geotechnical data within the area as in cases where the area was cell constructed.

Several trafficability assessments have been conducted on the NPD since 2015 in support of TRSU tailings pipeline extensions. Assessments have been conducted successfully up to approximately 200 m downstream of the discharge point, depending on the amount of time the deposit was allowed to 'drain'.

The NPD being 'trafficable' is an indicator that reclamation activities or mechanical capping can be achieved in certain areas of the deposit. Trafficability is considered a milestone activity since it indicates that some areas of the deposit can be transitioned into closure and reclamation activities.

Prior to any trafficability assessment, all relevant geotechnical data and the deposition history of the deposit should be evaluated, including field test data such as CPTs, vane shear, and plate bearing tests. A safety assessment and risk assessment in collaboration with key operations personnel is also required.

If berm construction or equipment traffic is required in an area within a sandy beach deposit, it is recommended that the deposit "drain" for a minimum four weeks and up to eight weeks after deposition ceases before the trafficability assessment is performed. This may vary depending on the geotechnical behaviour of the deposit. Any potential surface water management measures can also be implemented during this period to encourage strength development.

Once the deposit has sufficiently drained, a preliminary inspection of the area is performed.

This assessment includes a visual assessment and measurement of the crust thickness, (if being conducted on a soft, fines dominated deposit) and/or the depth of frost penetration (if being conducted in freezing temperatures). The visual inspection is performed by an experienced engineer familiar with the deposit. This inspection is intended to highlight potential soft zones due to surface water and identify clear indications of weak material such as excessive erosion and deep channelization. If applicable, the crust thicknesses and frost penetration should be compared with previous assumptions to confirm if there is any reduction of strength from the assumed surface conditions. In the absence of prior investigations and deposit specific experience, a crust/frost penetration thickness of about 10-15 cm is used as a guideline.

If the visual inspection indicates acceptable performance, an amphibious all-terrain vehicle (ATV) can be deployed for the initial survey. Survey points are placed at the final advance limit of the area to be trafficked. Once the area is clearly marked, the amphibious ATV is required to test the trafficability before a larger piece of trial equipment proceeds. The operator visually inspects the ground surface to ensure that it is safe for equipment to proceed. The operator observes and documents any ground deflections or load induced water release. On softer areas of the deposit, ground deflection may be deemed acceptable and reasonable failure criteria for the test may be surface cracking. As a guideline, 3 to 12 inches of 'roll' may occur prior to surface cracking. Once confirmation of a "successful pass" (reasonable ground deflection and no indication of potential failure or risk to equipment) is obtained from the operator, additional passes are repeated with equipment of increasing bearing pressure. Based on Shell's experience, the progression of amphibious ATV, to D4 dozer, to D6 Dozer is a practical approach. However, the exact equipment used in a trafficability study will be subject to the geotechnical behaviour of the deposit. For larger equipment it is recommended that support equipment be on hand that is capable of extracting the piece of trial equipment if it becomes stuck in a soft zone of the deposit.

The magnitude of observed deflection should be documented and compared to prior trafficability studies on similar deposits. As these studies are repeated, a tailings stream specific database can be developed to support this empirical approach; however, this methodology does initially rely on experienced operators and engineers being able to assess the surface behaviour of the deposit on these qualitative indicators.

If the trafficability assessment is deemed successful, only equipment with similar or lower bearing pressure to the final piece of trial equipment can be placed on the beach or deposit. In the case of an "unsuccessful pass", the specific bearing pressure of the trial equipment used during that pass can be then used in back-analysis, to support the calculation of an estimated bearing capacity. The geotechnical engineer may waive the trafficability assessment if in his/her professional opinion the tailings deposit is competent for traffic by the required equipment.

These trafficability assessments have proven useful in in understanding the risks when deploying assets onto sandy deposits and seem to be a good indicator as well for some high fines deposits that have gone through several cycles of freeze-thaw and wet-dry cycles. More work is still ongoing on high fines deposits.

SUMMARY AND CONCLUSION

A clear understanding of the composition, strength and consolidation behaviour of a tailings deposit are critical both during the operational phase of a deposit and to support closure design. Data from depositional history, CPT, and sampling were used to develop a broad understanding and detailed characterization of the NPD. This characterization provided the required inputs for regulatory reporting, operations support, deposit optimization, tailings planning and closure design. More work is required to include the development of a process which may effectively model the strength of the deposit in a 3-D block model.

Preliminary consolidation modelling has been done to compare consolidation in the deposit and will be used as a guide for similar deposits. For closure designs, further consolidation analysis will also be done, in which the current characterization is used to zonate the deposit. This could then be used to produce a consolidation map.

Trafficability assessments in certain areas of the deposit have been used as an indicator that the deposit is trafficable by certain types of equipment. More work is ongoing on high fines deposits. Environmental characterization will be included in future work.

ACKNOWLEDGEMENTS

Sincere appreciation and thanks to Adam Thompson of Shell Canada who provided input to the paper.

REFERENCES

COSIA. 2012. A technical guide for Fluid Fines Tailings Management

Esposito, G., Nik, R., 2012. Fines Capture in a Long Tailings Beach at the Shell Muskeg River Mine External Tailings Facility: Hydraulic and Depositional Aspects. IOSTC

Masala, S., Nik, R., Freeman, G., Mahood, R., 2014. Determination of field-representative consolidation properties of oil sand fine tailings by back-analysis of instrumented deposition trials. GEO Regina 2014, Regina, Saskatchewan.

A SHELL TAILINGS CONSOLIDATION CASING EXPERIMENTAL PILOT PROJECT (TCCEPP)

Jason Stianson[1], Robert Mahood[2], Dana Thomas[2], Jason Song[3] and Laura Li[3]
[1]Golder Associates Ltd.
[2]Shell Canada Energy
[3]O'Kane Consultants Inc.

ABSTRACT

The Tailings Consolidation Casing Experimental Pilot Project (TCCEPP) began in 2015 at the Shell Albian Sands (SAS) mine site located 65 km north of Fort McMurray, Alberta. The project has involved the design, construction, pouring of tailings and monitoring the initial performance of tailings in eight steel casings, each ~2.75 m in diameter and ~13 m in height. The casings were filled with approximately 10 m of oil sand fluid fine tailings (FFT) dredged from the Shell External Tailings Facility (ETF) and another Operator's facility, treated using different amendments with exception of one casing that was filled with untreated FFT. Construction of the casings and pouring of the treated and untreated FFT were completed over a four month period between July and October 2015. This paper presents the as-built conditions of the casing including instrumentation and sampling used to monitor the consolidation of the tailings. Early performance data is presented and provides an indication of how the tailings treatment methods have influenced the sedimentation and early consolidation behaviour of the tailings to influence commercial tailings technology selection.

INTRODUCTION

The Tailings Consolidation Casing Experimental Pilot Project (TCCEPP) was initiated in 2015 at the Shell Albian Sands (SAS) mine site, 65 km north of Fort McMurray, Alberta. The project involved the design, construction, pouring and initial performance monitoring of eight steel casings with a diameter of approximately 2.75 m and a height of approximately 13 m (Figure 1). The casings were filled with oil sand fluid fine tailings (FFT), treated by various methods. One casing was filled with untreated FFT. Construction of the casings and pouring of the treated and untreated FFT were completed over a four month period between July and October 2015. The eight steel casings are now installed vertically in the ground at the site location inside Shell mining oil sands Lease 13, within the Sharkbite Expansion Area.

This paper focuses on the TCCEPP design, planning, field execution, and initial performance data to the end of 2015. Detailed performance data, including consolidation, is not described in this paper, but will be reported after future performance assessments, which are being conducted annually, beginning in 2016 to influence commercial tailings technology selection. Results are being shared with Shell's partners through the Canadian Oil Sands Innovation Alliance (COSIA) within the Tailings Environmental Priority Area (EPA).

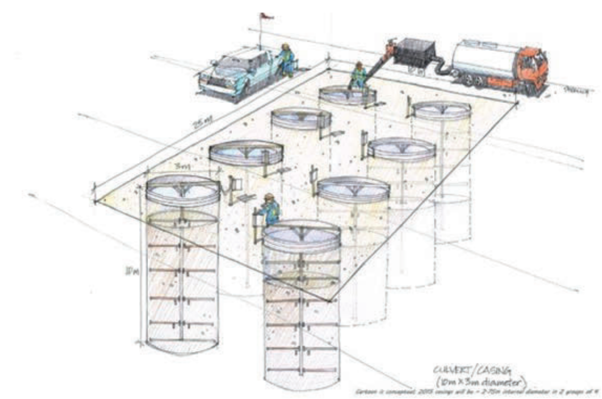

Figure 1. Overall view of the casing experimental pilot project

Project Objectives

The TCCEPP is an extension of previous projects such as the bench scale large strain consolidation tests (LSCs) and the geocolumns undertaken as part of the suite of Shell Technology Development projects (Figure 2).

The objective of the TCCEPP is to measure and analyze the sedimentation and self-weight consolidation behaviour of various tailings treatments and to use the measured data in combination with numerical modelling to contribute to the selection of an improved tailings management technology.

Figure 3 illustrates how the information obtained from the TCCEPP will influence the commercial tailings technology selection process.

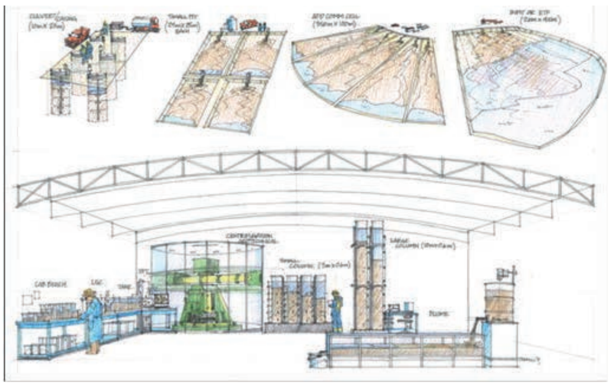

Figure 2. Scales of testing in a tailings technology evaluation program

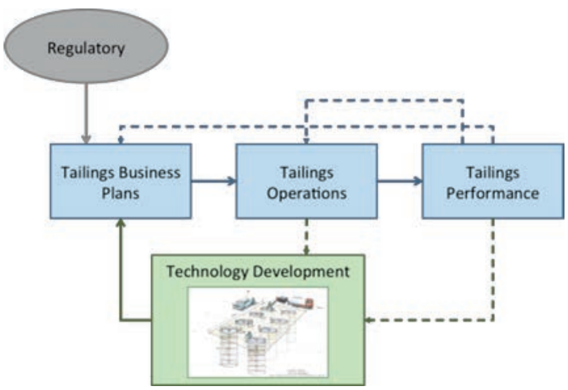

Figure 3. Technology evaluation and the business flowchart

DESIGN OF THE TCCEPP CASING SYSTEM

The TCCEPP design involved a multi-disciplinary team of Shell and technical consultants described below:

- Shell is the owner and operator of the TCCEPP and was responsible for coordinating and approving the overall design,
- BGC Engineering Inc., (BGC) designed the pad and casings, prepared "Issued for Construction" (IFC) drawings for the earthworks and casing installation, and also provided engineering support during the construction phase, including instrumentation installation,
- Gygax Engineering Associates Ltd., subcontracted through BGC, was responsible for the structural design of the casings,
- O'Kane Consultants Inc., was responsible for the design and monitoring of the casing instrumentation,
- Golder is responsible for data interpretation and back analysis modelling that will be undertaken as the consolidation of the tailings progresses,
- Shell Technology Development managed the process loop and integrated the above activities.

The main civil design component of TCCEPP was the eight steel casings, each ~2.75 m in diameter and ~13 m in height, used to contain the treated tailings (as well as one column of untreated tailings). A main design requirement was to minimize the likelihood of inward groundwater leakage and pore-fluids leakage out of the casings. A reinforced 16 mm thick steel plate, welded to the bottom of each casing, was included in the design to isolate the casing from the surrounding ground. Multiple grouting stages were used to further mitigate possible leakage and to overcome buoyancy effects during casing installation.

The design choice to locate the TCCEPP within the Sharkbite Expansion Area was made for the site's longevity, ground foundation conditions and lack of regulatory permitting requirements. Current plans are not to mine the area until the late 2030s. The foundation conditions consist of variable glacial Pleistocene sand and till, and Clearwater and rafted McMurray Formation till, all underlain by McMurray Formation oil sand bedrock. These ground conditions include a near-surface water table that reduces the likelihood of a significant hydraulic gradient between the filled casings and the surrounding ground if leakage were to occur.

Casing Construction

Construction and installation was completed over a four-week period from July to August 2015. Construction included an earthen pad, installation of the casings, construction of an access catwalk, and installation of the instrumentation.

An earth pad was constructed to provide a level well-draining working surface, provide sufficient bearing capacity for all construction equipment and the FFT tanks, and provide containment in the event of tailings spills on the pad. The earth pad consisted of a half-metre of gravel, underlain by approximately 2 m of lean oil sand (LOS), and surrounded by a LOS lined ditch.

The casings were fabricated off-site and delivered by truck. Each 13 m long steel casing was designed to have an outer diameter of 2.75 m and a wall thickness of 16 mm (5/8") resulting in an inside diameter of 2.72 m. Each casing included a reinforced 16 mm thick steel bottom plate welded to the bottom of the casing prior to installing in the auger hole. The casings were designed to be durable during the impacts and pressures associated with installation and avoid potential punctures or cracks that would allow water ingress or egress. The casings were also coated with Carbomastic® 15 FC, an epoxy mastic industrial coating, after being sand blasted. The coating was applied to prevent rust formation inside the casings and to reduce friction between the tailings and the casing sidewalls.

The casings were installed vertically in the ground using conventional civil engineering techniques, including multiple grouting stages, to a depth of ~11.75 m below the top of the pad for a stick-up distance of ~1.25 m. The stick-up allowed for safe and practical working access. The main installation steps are summarized below.

Figure 4. Drilling to final depth inside a temporary casing installed with a vibro hammer

- A Soilmec SR-70 drill rig and a 3.05 m auger with reaming teeth was used to drill a 3.2 m diameter open hole through pad material and loose wet sand to reach the underlying McMurray Formation.
- A Manitowoc 230 T crawler crane, hoisted a 3.2 m outer diameter (OD) open-ended steel pipe (temporary casing) into the open hole. A crane and a vibratory driver, or "vibro hammer" (APE model 200-6), advanced the temporary casing as far as possible into the McMurray Formation, to maintain the stability of the auger hole and to prevent the ingress of water into the auger hole.
- A SR-70 rig and a 3.05 m auger without reaming teeth, advanced the auger hole to a final depth of ~12.25 m (Figure 4).
- A cement grout base 0.4 m thick was poured to provide a level surface on which to set the permanent casing. (Water that had accumulated in the bottom of the hole was removed with a vacuum truck before the base was poured.)
- The casing was hoisted using the 230 T crane and placed 0.1 m into the still-wet cement grout and ensured to be plumb. The weight of the permanent casing was supported with the crane until the cement grout had cured to sufficient strength (Figure 5). A water ballast was added inside the casings to a height of 8 m to overcome buoyant forces of the annulus grout.
- A small diameter tremie pipe was used to pour grout in the annulus between the temporary and permanent casing. Stage 1 grout was poured to a height of 3 m and allowed to cure to a sufficient strength so that it no longer exerted a buoyant force on the casing. Stage 2 grout was poured to fill the annulus to the top of the permanent casing to provide head pressure when pulling out the temporary casing.
- The crane was used to remove the temporary casing and the water ballast was removed once the annulus grout reached sufficient strength. A 0.75 m thick, self-leveling cement bentonite grout plug was poured via gravity feed chute into the bottom of the casing. The grout plug created a second hydraulic seal at the bottom of the casing.
- Catwalks consisting of steel walkways (Figure 6) were placed over the installed casings to allow for safe access to the casings, a mounting platform to affix the leads for the geotechnical

instruments and to allow for subsequent sampling and testing.

Two 150-m^3 FFT tanks, a supporting pump and flow loops were installed in August 2015 in parallel with the above activities. An earth science crew, composed of both Shell and consultant staff, installed internal geotechnical instrumentation strings consisting of:

- basal total pressure cells,
- piezometers at one-metre intervals,
- thermistors in the upper two metres of each casing,
- a sonic ranger to record the fluid surface and a pressure probe mounted on a mud-plate to record the height of the top of the tailings (i.e. designed to float at the mudline due to contrasting water and tailings density), and
- data loggers and cellular communication infrastructure relying on solar panels and batteries.

Figure 5. Hoisting a permanent casing into place

Instrumentation and Monitoring

Performance monitoring is supported by instrumentations (e.g., vibrating wire piezometers, total pressure cells, near-infrared (NIR), and ultrasonic probes), wireline density profile surveys, and sampling to be conducted throughout the multi-year program. The resulting data will be used in combination with numerical modeling to refine current assumptions regarding consolidation behaviour.

Figure 6. Installed casings and catwalks

Key measurements include fluid levels, mudline, pore-water pressure, total stress and density (Figure 7 and Figure 8).

The TCCEPP's multi-year evaluation provides an opportunity for de-watering with under-drains, wicks or other methods, and for the application of surcharges, all of which will be evaluated at a later date, after sufficient self-weight consolidation has occurred.

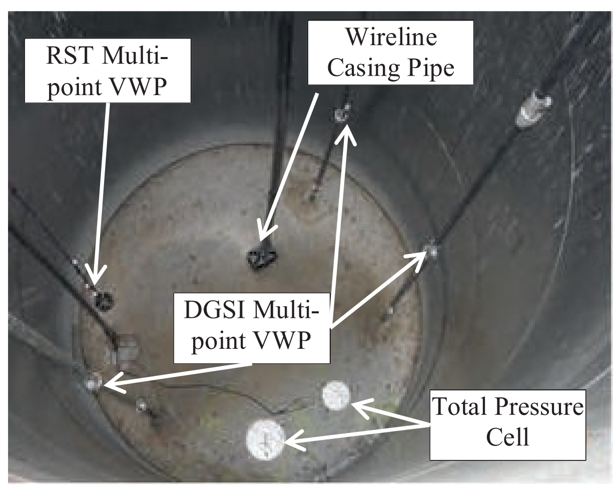

Figure 7. Installation of monitoring instrumentation

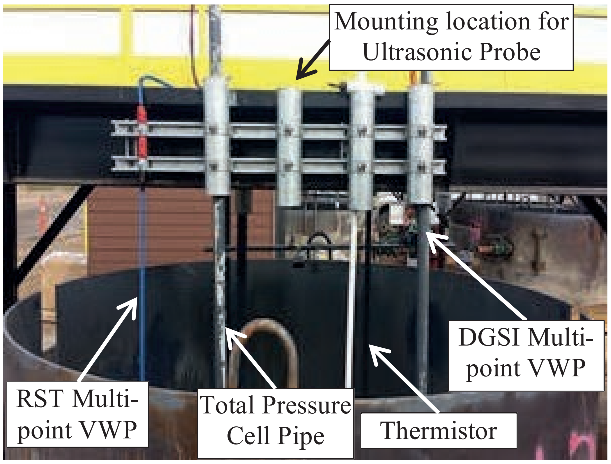

Figure 8. Installed instrumentation strings

Figure 9. Mudline monitoring device fabrication

A mudline monitoring device was constructed for the casing project consisting of a modified mud plate with an OTT PLS pressure probe (Figure 9). This device, similar to the COSIA mud plate (Alberta Energy Regulator 2016), was successfully used to remotely monitor the mudline as shown in Figure 10. The pressure data from the mudline monitoring device allowed for continuous recording of the mudline although the team decided to supplant the readings with at least monthly manual checks while the automatic mudline measurement system was validated.

During the pour period, the instruments recorded data at a frequency of one reading every two minutes. About a week after the final pour, the frequency was decreased to one reading every four hours.

Within one week of the final pour, two separate sampling campaigns were conducted concurrently:

- a core sample campaign, in which a coring device was used to obtain samples at roughly half-metre intervals,
- a downhole wireline geophysical campaign, which measured natural gamma, spectral gamma, density, induction conductivity, and nuclear magnetic resonance (NMR) with raw and corrected data intervals varying between 0.01–0.25 m amongst the various probes.

A key focus during the winter months is monitoring the upper casing temperature to prevent the freezing of the overlying sacrificial water cap and, more importantly, the actual tailings. The prevention of freezing avoids freeze-thaw, desiccation or other

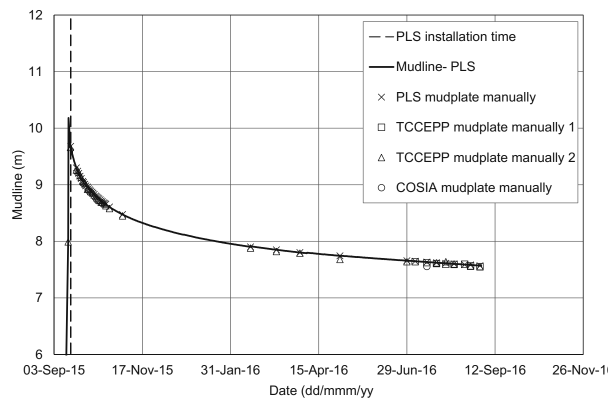

Figure 10. Mudline monitoring device data

environmental effects from complicating the consolidation of the tailings, thus allowing for a focused assessment of self-weight consolidation. Instruments were connected to data loggers and then to the cellular network allowing real-time monitoring. Although consolidation is a relatively slow process and does not require an intensive reading frequency, the remote monitoring system did allow real-time monitoring of instrument malfunctions and water cap temperature. The temperature monitoring was critical during winter months to avoid freezing of water, where the programming allowed text messages to be sent to staff located remotely, initiating a response to the near freezing conditions, which usually involved resetting of gensets at the site. The winter program includes a small generator running 24 hours/day for 4 months to provide constant power to floating commercial agricultural heaters in the water cap, insulated covers and real-time alarms sent by text to off-site team members.

The casings will be monitored for a minimum of five years leveraging the automated instrumentation and cellular data networks. The monitoring will focus on mudline settlement, excess pore-water pressure dissipation, solids content, tailings density and the water chemistry of the release water. An objective of the program was to minimize the annual monitoring and reporting resources by relying on remote telemetry and software macros to provide compiled data on demand with minimal staff input, other than a monthly manual check on mudlines and general site integrity.

Table 1. Summary of TCCEP Amendments and Pouring

Casing #	FFT Source	Amendment/ method	Target Flocculant Dosage (ppm)	Pour Duration	Tailings Thickness, Pour details
1	Shell MRM ETF[1]	FFT - none	-	Aug. 30, 2015	10 m, Poured from vacuum trucks directly into casing.
2	Shell MRM ETF	HPAM[5] - ILF[2]	950	Sep. 3-15, 2015	10 m, Five pours of ~3 m each
3	Shell MRM ETF	XUR - ILF	1500	Sep. 9-17, 2015	10 m, Five pours of ~3 m each
4	Shell MRM ETF	XUR 4A - ILF	1500	Sep. 4-16, 2015	10 m, Five pours of ~3 m each
5	Operator FFT[3]	HPAM[5] - ILF	1400	Sep. 24- Oct. 2, 2015	10 m, Five pours of 1-4 m each
6	Operator FFT	HPAM[5] - ILF	1500	Sep. 25- Oct. 1, 2015	10 m, Four pours of ~3 m each
7	-	-	-	-	Casing is empty.
8	Shell JPM Centrifuge Plant[4]	HPAM[5] - Centrifugation	1200	Sep. 24-26, 2015	10 m, Poured/"dumped" from several vacuum trucks directly into casing.

[1] MRM ETF = Muskeg River Mine-External Tailings Facility. The FFT did not reside in the tanks but was from a source identical to the other Shell MRM-ETF material

[2] ILF = Inline Flocculated

[3] Operator provided ~ 150 m^3 of FFT from another Operator via 10 m^3 vacuum trucks

[4] Shell's JPM centrifuge plant uses FFT feed from the JPM Sand Cell 1.

[5] HPAM treatments are not the same.

Tailings Pours

Seven of the casings contain a column of tailings approximately 10 m in height composed of various amendments and fluid fine tails sources. Casing 7 was deferred to a later date pending the performance of other casings. Table 1 details the FFT source, the amendment and method of amending, target flocculant dose, pour duration, and pour details.

The pouring of treated and untreated tailings was completed over a one month period from August 30 to October 2, 2015. Two 150 m^3 FFT tanks provided the raw tailings for six of the casings. All flocculants were prepared in one-cubic-metre totes, which were mixed off-site beforehand. Exceptions included Casing 1 which was filled with FFT and Casing 8 which was filled with centrifuge cake from Shell's Jackpine Mine, (JPM, centrifuge plant). Casings 2 through 6 were filled with inline flocculated tailings prepared using specialized mixing rigs. The mixing rigs consisted of FFT pumps, flocculant pumps, dynamic mixers, flowmeters, pressure gauges and data loggers. The mixing rigs produced inline flocculated tailings at a flow rate of approximately 10 USGPM with flocculant dosages ranging from 950–1500 ppm as detailed in Table 1.

The tailings were pumped to the bottom of the casings through a tremie diffuser at a discharge point 0.5 m to 2 m below the mudline (except for Casings 1 and 8 which were poured by gravity feed). The flow rate of 10 USGPM resulted in a vertical rate of rise of approximately 0.5 m per hour. The filling rate was selected as a compromise to allow the field execution to occur in a reasonable period of time rather than attempt to match the slower rate of rise in a typical commercial pond which can be on the order of 1 m per month.

During the last pour of each casing, the overlying release water that had accumulated over the preceding days was forced to the top by the rising underlying tailings. To maximize the amount of treated or untreated tailings in each casing, the release water was decanted by gravity via a diversion valve located a half-metre below the top of the casing. Pouring continued until the tailings were approximately 10 m thick with a water cap of approximately 0.5 m. The release water was collected in empty totes and weighed to provide input for subsequent mass balance determinations.

Laboratory Samples

Approximately 500 samples were taken for over 3,000 tests at all stages during the field program to be used for Key Performance Indicators (KPIs), index testing, sedimentation tests using graduated cylinders, and parallel large-strain consolidometer testing. KPIs focus on the treated tailings performance, which includes permeability index (PI), yield stress, capillary suction time (CST) and net water release.

Table 2. Summary of TCCEPP Tailings Index Properties

Casing	Solids Content (%)	Bitumen (%)	Specific Gravity	MBI	PSD < 44 μm (%)	Liquid Limit (%)	Plastic Limit (%)	Plasticity Index (%)
1	35	2.8	2.22	7.1	-	-	-	-
2	32	3.9	2.22	8.8	94	68	31	37
3	31	4.5	2.22	9.1	94	55	29	26
4	30	4.4	2.22	8.6	93	52	27	25
5	29	1.6	2.53	11.7	95	62	24	38
6	28	1.5	2.53	12.0	96	67	28	39
7	-	-	-	-	-	-	-	-
8	45	1.5	2.40	14.2	-	-	-	-

Figure 11. Near-infrared in-line instrument

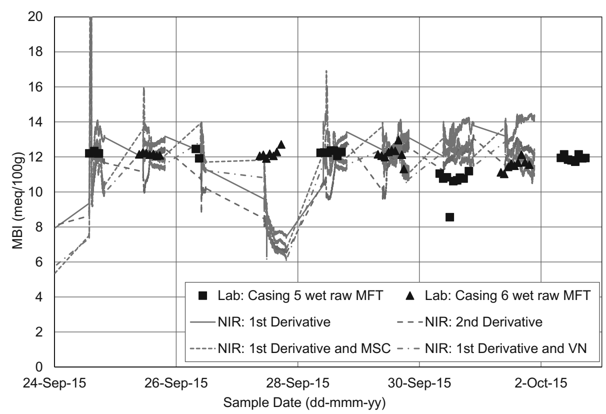

Figure 12. Comparison of real time near-infrared data with laboratory measurements on raw FFT

Typical index testing results on flocculated tailings samples are summarized in Table 2 including solids content, bitumen content (by Dean Stark), specific gravity, Methylene Blue Index (MBI), particle size distribution (PSD), and Atterberg limits.

Solids content (by weight) was determined by the oven method from samples taken during each pour (averaged over the pour height), where, solids content (%) = % mineral solids + % bitumen. MBI values for Casings 2–8 are the non-weighted average MBI values from grab samples collected during pouring. For Casing 1, the results are the non-weighted average MBI values from core samples collected from the casing after pouring.

Near-infrared (NIR) was also evaluated as a real time tailings instrument, as NIR technology offers the opportunity to characterize tailings as a proxy for MBI, and indirectly clay activity. The NIR (Figure 11) could allow for real-time amendment dosage optimization. Preliminary field evaluation from this pilot, completed as an incidental add-on, provides encouraging results as illustrated in Figure 12. Further work is required at both field pilot and commercial scale as with other instruments in oil sand tailings, bitumen fouling remains a challenge.

INITIAL PERFORMANCE

A typical comparison of the bulk unit weight inferred from NMR water content, oven dried solids content, and wireline measurements from Casing 2 is provided in Figure 13. The measurements from the gamma-gamma wireline tool show a lower unit weight through the water cap, a transition to a higher relatively consistent value through the middle of the tailings followed by a gradual increase in unit weight to the bottom of the casing. There appears to be relatively good agreement between the unit weight inferred from NMR water content and that calculated from oven dried solids content and specific gravity. The relationships remain under review and will be calibrated as the potential range in index properties is understood (e.g., specific gravity).

The wireline tool requires additional calibration to investigate lower than known unit weights for the supernatant water and a substantial increase in unit weight near the base of the casing. The marked increase in unit weight at the base of the casing may be due to the influences of a steel block that was used to anchor the empty wireline casing to overcome buoyancy during installation. Improvements in wireline tools continue to offer a non-invasive investigative technique.

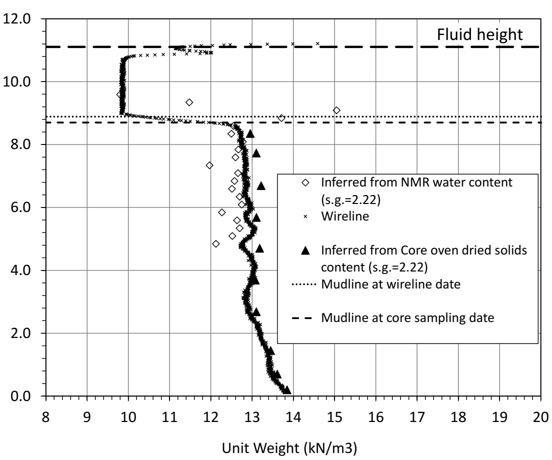

Figure 13. Typical unit weight comparison for Casing 2

A comparison of settlement and calculated average solids content (estimated from settlement records) over the first 200 days of monitoring is provided in Figure 14 and Figure 15, respectively. The following observations are made based on the initial monitoring data:

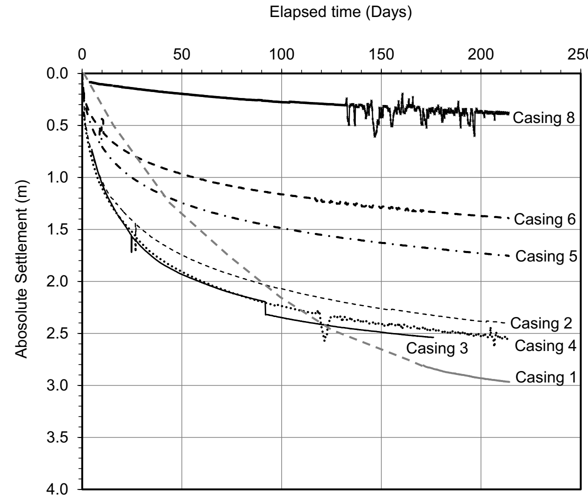

Figure 14. Comparison of Tailings Settlement

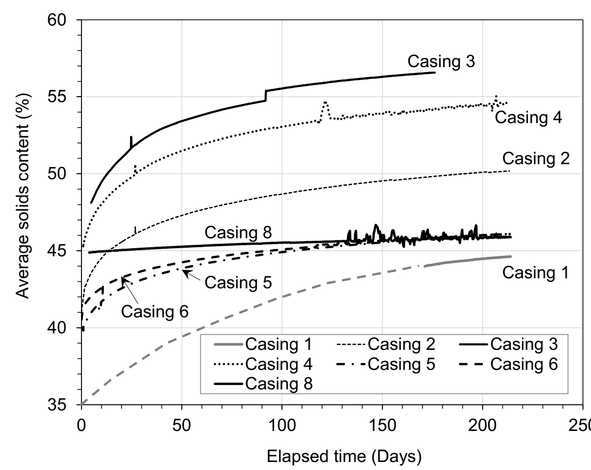

Figure 15. Comparison of Average Tailings Solids Content (i.e., computed from settlement)

- The centrifuge tailings settled less than 0.5 m resulting in a marginal increase in average solids content from 45% to about 46%. It should be noted that mechanical effort was used to increase the solids content to 45% prior to placement in the casing and the FFT source is different.
- The tailings in Casings 5 and 6 with another Operator’s FFT combined with HPAM treatments settled by about 1.6 m and 1.3 m, respectively. The solids content is estimated to have increased to about 46% over the first 200 days for both tailings treatment methods balanced by the difference in initial solids content at the time of pouring.

- The tailings in Casing 2, 3, and 4 settled between 2.4 m and 2.6 m and resulted in the highest increase in solids content. Casing 2 solids content increased from 32% to about 50% (18% increase), Casing 4 solids content increased from 30% to 54% (24% increase), and Casing 3 solids content increased from 31% to nearly 57% (26% increase).Casing 1 displayed surprisingly high rates of settlement, settling by nearly 3 m in the first 200 days, but at these lower initial solid content, the estimated increase in solids content is only from 35% to 45% (increase of 10%).

LIMITATIONS

Figure 2 illustrates some of the many scales of testing that are involved in a successful tailings technology evaluation program. No single scaled evaluation can test all the components of a commercial operation. The scale of the TCCEPP is large compared to typical bench scale tests but is still subject to a number of scale-up limitations:

1. A relatively homogenous FFT supply was used as compared to that found in a commercial scale operation.
2. Flowrates of about 10 USGPM are lower than a commercial scale operation by a factor between 200 to 1,000 times.
3. A vertical fill rate of 0.5 m per hour is rapid compared to the deposit rise rates found in commercial operations.
4. The use of tremie-deposition followed by a quiescent period between tailings pours in TCCEPP is different from the actual dynamic situation used in a commercial tailings pond

The above limitations require consideration when estimating the uncertainties involved in an actual commercial scale operation.

CONCLUSIONS

Through COSIA, and with input from Syncrude based on their prior experience with pilots, Shell was able to design and execute the TCCEPP project in less than ten months on an aggressive schedule. Several conclusions can be made regarding the overall design and application of the TCCEPP project to evaluate the consolidation behavior of tailings treatment technologies.

The present TCCEPP project:

- Allowed for increased tailings thicknesses and larger tailings volumes to evaluate consolidation at stress states approaching those experienced in the field;
- Provided data to evaluate scale-up of tailings mixing systems beyond the laboratory scale;
- Designed with instrumentation that can be monitored remotely providing a consistent data record even when site access may be interrupted (e.g., during the fires that swept through the Fort McMurray area in the spring of 2016.); and,
- Designed with features that allow the future evaluation of multiple drainage and/or loading scenarios.

Conclusions regarding the performance of the different tailings treatments for a commercial scale operation are premature and remain under evaluation, *particularly given the three different sources of FFT*. However, the initial comparison of settlement and solids content data suggests that the inline flocculated XUR product may provide more favorable sedimentation and possibly consolidation behavior when compared to the other tailings treatment options, for these specific pilot conditions, but follow up with equivalent FFT source is required.

The consolidation behavior will continue to be measured in terms of mudline settlement, excess pore-water pressure dissipation, and profiles of solids content. These measurements will be used in combination with numerical modelling to back analyze representative consolidation properties for the tailings treated with different amendments. The consolidation parameters will also be used to conduct both scale up modelling as well as input to future field evaluations at the commercial scale.

ACKNOWLEDGEMENTS

The authors would like to extend special thanks to the following individuals who provided support to the TCCEPP project.

Shell Albian Sands Operations staff including Ken Kieley, Clayton Bennett, and Sheri Wilson for the many short-notice support items.

Ian Mountain, Shell Technology Development Technologist, who acted as site manager during the pouring, and Sophie Kessler of O'Kane Consultants and Davan Russell of BGC Engineering, who

executed a cooperative effort to ensure efficient installation and programming of the instrumentation.

REFERENCES

Alberta Energy Regulator (2016) Directive 085, Fluid Tailings Management for Oil Sands Mining Projects, July 14, 2016

The Oil Sands Tailings Research Facility (OSTRF) was established in 2003 as a direct response to the global need for improved tailings management. Through extensive interaction and collaboration with other distinguished research groups, the OSTRF provides the novel research required to develop environmentally superior tailings disposal options. With the flexibility to support concurrent interdisciplinary research projects, the facility attracts the brightest minds in the field and trains early-career, technically competent scientists and engineers—the future leaders, consultants and regulators for the oil sands industry. The OSTRF is pioneering the way to innovative, environmentally conscientious solutions for future generations.

Drs. David C. Sego, Nicholas A. Beier and G. Ward Wilson, through the OSTRF, lead instrumental initiatives to bring together academia, industry and government agencies to find environmentally sustainable solutions for oil sands development. One such initiative is the International Oil Sands Tailings Conference (IOSTC), which is held every two years, and provides a forum for mine waste managers, engineers, regulators and researchers to present new ideas and to discuss the latest developments in the field.

The Fifth International Oil Sands Tailings Conference (IOSTC'16) offers the most recent developments in oil sands tailings and management through invited speakers and select technical presentations. The presentations and conference proceedings will provide documentation on the oil sands industry's research efforts since the issuing of the Government of Alberta's Tailings Management Framework for Mineable Athabasca Oil Sands in 2015. IOSTC'16 will also feature research from the NSERC/COSIA Senior Industrial Research Chair (IRC) in Oil Sands Tailings Geotechnique held by Dr. G. Ward Wilson with assistance from Dr. Nicholas Beier, the current Principal Investigator of the OSTRF. The IRC enables the oil sands industry to combine its efforts with those of leading researchers at the University of Alberta to develop novel technologies and methods to manage oil sands tailings in Alberta.

For more information about the University of Alberta Geotechnical Centre's current oil sand tailings research projects and initiatives, including the NSERC/COSIA IRC in Oil Sands Tailings Geotechnique or Oil Sands Tailings Research Facility, please visit www.ostrf.com or http://geotechnical.ualberta.ca.

International Oil Sands Tailings Conference

The UofA Geotechnical Centre

Proceedings cover photo courtesy of Syncrude Canada Ltd.